**UNIVERSIDAD POLITÉCNICA DE MADRID**
Escuela Técnica Superior de Ingeniería Agronómica, Alimentaria y de Biosistemas


# An integrative analysis of root adaptation to multiple environmental soil conditions

## DOCTORAL THESIS

Submitted for the degree of Doctor by:

**María Sánchez Bermúdez**
MSc in Plant Biotechnology

Madrid, 2025

UNIVERSIDAD POLITÉCNICA DE MADRID
Escuela Técnica Superior de Ingeniería Agronómica,
Alimentaria y de Biosistemas

**Doctoral Degree in Biotechnology and Genetic Resources of Plants and Associated Microorganisms**

# An integrative analysis of root adaptation to multiple environmental soil conditions

## DOCTORAL THESIS

Submitted for the degree of Doctor by:

**María Sánchez Bermúdez**
MSc in Plant Biotechnology

Under the supervision of:
Dr. Mónica Pernas Ochoa
Dr. Juan Carlos del Pozo Benito

Madrid, 2025

Title: An integrative analysis of root adaptation to multiple environmental soil conditions

Author: María Sánchez Bermúdez

Doctoral Programme: Biotechnology and Genetic Resources of Plants and Associated Microorganisms

Thesis Supervision:

Dr. Mónica Pernas Ochoa, Researcher CSIC-INIA, Centro de Biotecnología y Genómica de Plantas, CBGP (UPM-INIA/CSIC)

Dr. Juan Carlos del Pozo Benito, Research Professor, Centro de Biotecnología y Genómica de Plantas, CBGP (UPM-INIA/CSIC)

External Reviewers:

Thesis Defense Committee:

Thesis Defense Date:

This thesis has been partially supported by a Ph.D. contract (PRE-2019-088076), funded by the "Severo Ochoa Program for Centres of Excellence in R&D" (SEV-2016-0672, 2017-2021) from the "Agencia Estatal de Investigación" of Spain granted to the CBGP.

# Abstract

Climate change is a global threat for agriculture and has a strong impact on food security worldwide. The current increases in the global mean temperature and increased frequency of other climatic stresses have a negative impact on crop production. Roots play an essential role in plant growth and adaptation under different climatic environments. Most research on root responses to abiotic stress has focused on single stresses, but in natural environments, plants suffer the effects of several stresses simultaneously. Thus, a better understanding of the root responses to abiotic stress combinations is required to improve crop tolerance to climate change. With this aim, we studied the phenotypic variation in the root responses to combined warm temperature and nutrient (nitrogen / phosphate) deficiencies in a collection of *Brassica napus* varieties. We have observed significant variation on root architecture in response to combined warm temperature and nutritional stress between the varieties. Our results indicate that the combination of warm temperature and N deficiency produced a compensatory effect with an intermediate phenotype in several root traits like network width, distribution, and lateral root density compared to the individual stresses, whereas the combination of warm temperature and Pi deficiency caused a detrimental additive effect on overall root growth. Next, we selected varieties that showed differential responses among the different stress treatments to study their transcriptomic response through RNA-sequencing analysis in roots and shoots under the applied stresses. Based on these data, we identified a set of genes and Arabidopsis mutants to analyse the effects of combined warm temperature or heat stress and N deficiency as proof of concept.

Our RNA-sequencing results showed that the variety Wesway, which has an enhanced root growth under the combination of warm temperature and N deficiency, increased the expression of genes related to oxidoreductase activity, hormonal regulation and N metabolism and transport in roots, and genes related to peptide signalling in shoots. Wesway also showed a greater shoot biomass and C/N ratio under combined N deficiency and heat stress when grown in soil. On the other hand, our RNA-sequencing results revealed that combined warm temperature and Pi deficiency caused a strong suppression of the primary root growth via alteration of genes related to Fe-mediated signalling, auxin signalling and ubiquitin activity. These changes were accompanied by a repression of genes related to phenylpropanoid, lignin and anthocyanin synthesis in shoots.

Furthermore, warm temperatures strongly repressed genes related to the Pi starvation response, suggesting a direct regulatory interaction between both stresses. Finally, we studied the function of BnPHR1 and BnSPX1, two proteins involved in the Pi starvation response in *B. napus*, and confirmed that the interaction as well as the transcriptional regulation between both proteins was conserved. Finally, our results in Arabidopsis showed differences between the root responses to warm temperature and high temperature combined with N deficiency. Thus, high temperatures altered the root responses to N deficiency by causing changes in lateral root density and decreasing the expression of the *NRT2.4* transporter. In summary, this thesis has provided new insights into the root responses to combined elevated temperatures and nutrient deficiencies. Our research provides new information on the root responses to different abiotic stress combinations in *B. napus*, a crop with high economic importance, and uncovers different molecular processes that seem to be involved in their regulation.

# Resumen

El cambio climático constituye una amenaza para la agricultura y produce un un fuerte impacto en la seguridad alimentaria global. El constante aumento de las temperaturas y la mayor frecuencia de estreses climáticos tienen un impacto negativo en la productividad de los cultivos. Las raíces juegan un papel esencial en la adaptación de las plantas a diferentes condiciones climáticas. Las investigaciones actuales sobre la respuesta de las raíces a los estreses abióticos se centran en el estudio de estos estreses por separado, mientras que en la naturaleza, las plantas están expuestas a diferentes estreses de forma simultánea. Por lo tanto, es necesario estudiar la respuesta de las raíces a estreses abióticos en combinación. Con este objetivo, hemos estudiado la variación fenotípica en la respuesta de las raíces a la combinación de altas temperaturas y deficiencia de nutrientes (nitrógeno / fosfato) en una colección de variedades de *Brassica napus*, y hemos encontrado variabilidad en la respuesta a estos estreses. Nuestros resultados indican que la combinación de altas temperaturas y deficiencia de nitrógeno (N) produce un efecto compensatorio, con un fenotipo intermedio causado por el efecto de los estreses individuales en varios caracteres radiculares como el ancho y distribución del sistema radicular y la densidad de raíces laterales. De lo contrario, la combinación de altas temperaturas y deficiencia de fosfato (Pi) produjo un efecto perjudicial en el crecimiento de la raíz, con un efecto aditivo de los estreses individuales. Después, seleccionamos variedades con una respuesta diferencial a los estreses aplicados y realizamos un análisis de secuenciación masiva de RNA en raíz y parte aérea para estudiar sus respuestas transcriptómicas. Identificamos un set de genes diferencialmente expresados y seleccionamos determinados mutantes de Arabidopsis para analizar los efectos de la combinación de altas temperaturas y deficiencia de N.

Nuestros resultados indican que la variedad Wesway, capaz de mantener la longitud de las raíces laterales bajo la combinación de altas temperaturas y deficiencia de N, aumentó la expresión de genes relacionados con la actividad oxidorreductasa, regulación hormonal y metabolismo de N en raíces, y genes relacionados con la señalización por péptidos en parte aérea. Wesway también mostró una mayor biomasa de parte aérea y C/N ratio bajo la combinación de estrés por calor y deficiencia de N creciendo en suelo y aplicando estos estreses de forma prolongada. Por otro lado, la combinación de altas temperaturas y deficiencia de Pi

causó una supresión del crecimiento de la raíz principal mediante la alteración de genes relacionados con la señalización por Fe, auxinas y la ubiquitinación en raíz, además de una supresión de genes relacionados con la síntesis de fenilpropanoides, lignina y antocianinas en la parte aérea. Además, las altas temperaturas individualmente causaron una supresión de genes relacionados con la respuesta a deficiencia de Pi, lo que sugiere una directa interacción entre las respuestas a ambos estreses. Finalmente, hemos estudiado la función de BnPHR1 y BnSPX1, dos proteínas relacionadas con la respuesta a deficiencia de fosfato en *B. napus*, y hemos confirmado que tanto la interacción como la regulación transcripcional de ambas está conservada. Por último, nuestros resultados en Arabidopsis mostraron diferencias entre la respuesta radicular a altas temperaturas y estrés por calor combinadas con deficiencia de N. El estrés por calor alteró la respuesta a la deficiencia de N, causando cambios en la densidad de raíces laterales y reduciendo la expresión del transportador de nitrato *NRT2.4*. En resumen, esta tesis aporta nueva información sobre la respuesta de las raíces a diferentes combinaciones de altas temperaturas y deficiencia de nutrientes en *B. napus*, un cultivo de alta importancia económica, y revela diferentes procesos moleculares implicados en la regulación de esta respuesta.

# Table of Contents

# List of Figures

# List of Tables

# Abbreviations and Acronyms

| | |
|---|---|
| +N | Optimal nitrogen |
| +P | Optimal phosphate |
| -N | nitrogen deficiency |
| -P | phosphate deficiency |
| *A. thaliana* | *Arabidopsis thaliana* |
| *A. tumefaciens* | *Agrobacterium tumefaciens* |
| ABA | Abscisic acid |
| ABF | Abscisic acid responsive elements-binding factor |
| AC columna | Adsorption column |
| ACC | 1-amino-cyclopropane-1-carboxylic acid |
| ACO | ACC oxidase |
| ACP | Acyl carrier protein |
| ACS | ACC synthase |
| ACS | Cysteine synthetase |
| ACT | Actin |
| AD | Activation domain |
| AHK | Arabidopsis Histidine kinase |
| AIP | Actin-interacting protein |
| AL | ALFIN-like |
| ALMT | Aluminium activated malate transporter |
| AMT | Ammonium transporter |
| ANOVA | Analysis of variance |
| ANR | Arabidopsis nitrate regulated |
| AOC | Allene oxide cyclase |
| AOX | Alternative oxidase |
| APL | Altered phloem development |
| APX | Ascorbate peroxidase |
| ARF | Auxin response factor |
| ARR | Type-A Arabidopsis Response regulator |
| ASN | Asparagine synthetase |
| ATG4 | Autophagy protein |

| | |
|---|---|
| ATL | Arabidopsis tóxicos en levadura |
| ATPT | *Arabidopsis thaliana* phosphate transporter |
| AUX | Auxin |
| AUX1 | Auxin resistant 1*Brassica napus* |
| *B. napus* | *Brassica napus* |
| *B. oleracea* | *Brassica oleracea* |
| *B. rapa* | *Brassica rapa* |
| BD | Binding domain |
| BHLH | Basic helix-loop-helix |
| BIFC | Bi-molecular fluorescence complementation |
| BIN | Brassinosteroid-insensitive |
| BKI | Brassinosteroid kinase inhibitor |
| BLAST | Basic Local Alignment Search Tool |
| BLGU | Beta-glucosidase |
| BnIR | *Brassica napus* multi-omics information resource |
| bp | Base pairs |
| BR | Brassinosteroids |
| BR6OX | Brassinosteroid-6-oxidase |
| BRAD | Brassica database |
| BZR | Brassinazole resistant |
| C | Carbon |
| CAF | CCR4-associated factor |
| CAM | Calmodulin |
| CASP | Casparian strip membrane domain protein |
| CAT | Catalase |
| CBGP | Centro de Biotecnología y Genómica de Plantas |
| CC | Coiled-coiled |
| CCD | Carotenoid cleavage dioxygenase |
| CCS | Copper chaperone for SOD1 |
| cDNA | Complementary DNA |
| CEP | C-terminally encoded |
| CEPD | C-terminally encoded peptide downstream |
| CEPR | C-terminally encoded peptide receptor |
| CESA | Cellulose synthase |
| CIPK | CBL-interacting protein kinase |
| CK | Cytokinin |

| | |
|---|---|
| CKA | Casein kinase II alpha chain |
| CKB | Casein kinase II beta chain |
| CLE | CLAVATA3/ESR-related |
| CNB | Centro Nacional de Biotecnología |
| CoIP | Co-immunoprecipitation |
| Col-0 | Columbia-0 |
| ConvA | Network convex area |
| CPK | Calcium-dependent protein kinase |
| CRA | Compact root architecture |
| CRD | Copper response defect |
| CRK | Cysteine-rich RLK |
| CRY | Cryptochrome |
| CSIC | Consejo Superior de Investigaciones Científicas |
| CSLC | Cellulose synthase-like |
| CTL | Chitinase-like protein |
| CYP707A | Cytochrome P450 family 707 subfamily A polypeptide |
| DCL | Dicer-like |
| DEG | Differentially expressed gene |
| Dim | Dimension or component of the PCA |
| DIM | Diminutia |
| DIR | Dirigent protein |
| DIT | Dicarboxylate transporter |
| DL | Dynamin-like protein |
| DMSO | Dymethylsulfoxide |
| DNA | Deoxyribonucleic acid |
| DOB medium | Dropout base for synthetic defined dropout medium |
| DOF | DOF zinc finger protein |
| DRB | dsRNA-binding protein |
| DREB | Dehydration-responsive element binding |
| DRM | Domains rearranged methyltransferase |
| D-root | Dark-root |
| DRP | Dynamin related protein |
| dsDNAse | Double-strand DNA endonuclease |
| dTTP | 2'deoxytimidine-5'-triphosphate |
| DTX | Detoxification efflux transporter |
| dUTP | 2'-deoxyuridine-5'-triphosphate |

| | |
|---|---|
| DWF | Dwarf |
| *E. coli* | *Escherichia coli* |
| E2P2 | Enclosed Ecosystem Phenotyping Platform |
| EARatio | Ellipse axes ratio |
| EBF | EIN3-binding F box protein |
| EDTA | Ethylenediaminetetraacetic acid |
| EIL | Ethylene-insensitive-like |
| EIN | Ethylene-insensitive |
| ENDO | Endonuclease |
| ERD | Endoplasmic reticulum retention defective |
| ERF | Ethylene response factor |
| ESR | Enhancer of shoot regeneration |
| ET | Ethylene |
| ETC | Enhancer of triptychon and caprice |
| EXP | Expansin |
| FD | Ferredoxin |
| FDR | False discovery rate |
| FK | FACKEL |
| FNR | Ferredoxin oxidoreductase |
| FRD | Ferric reductase defective |
| FSD | Fe superoxide dismutase |
| FW | Forward primer |
| GDH | Glutamate dehydrogenase |
| GFP | Green fluorescent protein |
| GL | GLABRA |
| GLN | Glutamine synthetase |
| GO | Gene ontology |
| GOLS | Galactinol synthase |
| GPX | Glutathione peroxidase |
| GR | Glutathione reductase |
| GST | Glutathione-S-transferase |
| GUS | ß-glucuronidase |
| H2A | Histone A2 |
| H2B | Histone B2 |
| HB | Homeobox protein |
| HISAT | Hierarchical Indexing for Spliced Alignment of Transcripts |

| | |
|---|---|
| HOS | High expression of osmotically responsive genes |
| HPR | Hydroxypyruvate reductase |
| HSF | Heat shock factor |
| HSP | Heat shock protein |
| HTA | Histone H2A |
| HTR | Histone |
| HY5 | Elongated hypocotyl |
| HYH | HY5 homolog |
| IAA | Indole-3-acetic acid |
| INIA | Instituto Nacional de Investigación y Tecnología Agraria y Alimentaria |
| InsP | Inositol pyrophosphate |
| IPS | Induced by phosphate starvation |
| IPT | Isopenthenyl transferase |
| JA | Jasmonic acid |
| JAL | Jacalin-associated lectin |
| JAZ | Jasmonate ZIM-domain protein |
| JOX | Jasmonic acid oxidase |
| K | Potassium |
| KIN | Kinase |
| LAC | Laccase |
| LatR | Number of lateral roots |
| LatR/cm | Number of lateral roots / cm or lateral root density |
| LB | Left border primer |
| LB medium | Luria-Bertani broth medium |
| LBD | LOB domain containing protein |
| LDOX | Leucoanthocyanidin dioxygenase |
| LHCB | Light-harvesting chlorophyl b-binding |
| LHW | Lonesome highway |
| LOB | Lateral organ boundaries-domain |
| LOG | Lonely guy |
| Log2FC | Logarithm of fold change |
| LOX | Lipoxygenase |
| LP | Left primer |
| LPR | Low phosphate root |
| LR | Lateral root |

| | |
|---|---|
| LRD | Lateral root density |
| LRP | Lateral root primordium |
| LRRLK | Leucine-rich receptor-like kinases |
| LUC | Luciferase |
| MajA | Major ellipse axis |
| MAPK | Mitogen activated protein kinase |
| MATE | Multi-drug and toxic compound extrusion |
| MaxR | Maximum number of roots |
| MCM | Minichromosome maintenance |
| MedR | Median number of roots |
| MES | 2-(N-morpholino)ethanesulfonic acid |
| MinA | Minor ellipse axis |
| miRNA | microRNA |
| mRNA | messenger RNA |
| MS | Murashige & Skoog |
| MUFA | Monounsaturated fatty acid |
| MYB | MYB domain protein |
| MYR | MYB-related protein |
| N | Nitrogen |
| *N.benthamiana* | *Nicotiana benthamiana* |
| Narea | Network area |
| Nbush | Network bushiness |
| NCBI | National Center for Biotechnology Information |
| Ndepth | Network depth |
| NIGT | Nitrate-inducible GARP-type transcriptional repressor |
| NIR | Nitrite reductase |
| NLA | Nitrogen adaptation limitation |
| NLDist | Network length distribution |
| Nlength | Network length |
| NLP | NIN-like protein |
| NO | Nitric oxide |
| Nper | Network perimeter |
| NRT | Nitrate transporter |
| Nsolid | Network solidity |
| Nsurf | Network surface area |
| Nvol | Network volume |

| | |
|---|---|
| Nw/d | Network width to depth ratio |
| Nwidth | Network width |
| $O_3$ | Ozone |
| OD | Optical density |
| OMT | O-methyltransferase |
| P | Phosphorous |
| P1BS | PHR1-binding site |
| P4H | Prolyl-4-hydroxylase |
| P5C | Pyrroline-5-carboxylate |
| P5CS | Delta1-P5C synthase |
| PAO | Polyamine oxidase |
| PAP | Purple acid phosphatase |
| PBS | Pre-branch sites |
| PCA | Principal Component Analysis |
| PCR | Polymerase chain reaction |
| PECP | Phosphoethanolamine / phosphocholine phosphatase |
| PER | Peroxidase |
| PEX | Peroxin |
| PEX6 | Peroxisome biogenesis protein 6 |
| PGX | Peroygenase |
| pH | Hydrogen potential |
| PHL | PHR1-like |
| PHO1/2 | Phosphate 1 / 2 |
| PHR | Phosphate response |
| *PHR1_C* | C-terminal region of *PHR1* |
| PHT | Phosphate transporter |
| Pi | Phosphate |
| PIF | Phytochrome interacting factor |
| PIN | PIN-formed |
| PLC | Phospholipase |
| POD | Guaiacol peroxidase |
| PROC | P5C reductase |
| PRP | Pre-mRNA processing factor |
| PSI | Pi-starvation response |
| PSY | Phytoene synthase |
| PUFA | Poly-unsaturated fatty acid |

| | |
|---|---|
| PUMP | Uncoupling protein |
| PUP | Phosphatase underproducer |
| PYL | PYR-like |
| PYR | Pyrabactin resistance |
| qPCR | Quantitative PCR |
| RAB | RAB GTPase homolog |
| RAP | Related to AP |
| RBOH | Respiratory burst oxidase homolog |
| RHD | Root hair defective |
| RHS | Root hair specific |
| RLI | RNAse L inhibitor protein |
| RLK | Receptor-like protein kinase |
| RNA | Ribonucleic acid |
| RNA-seq | RNA sequencing |
| ROS | Reactive oxygen species |
| RP | Right primer |
| RPL | Large ribosomal protein |
| rpm | Revolutions per minute |
| RPS | Small ribosomal protein |
| RSA | Root system architecture |
| RSL | Root hair defective-like |
| RT-qPCR | Real time quantitative PCR |
| RV | Reverse primer |
| *S. cerevisiae* | *Saccharomyces cerevisiae* |
| SA | Salicylic acid |
| SAL | IT4 phosphatase-associated protein |
| SALK | Salk Institute for Biological Studies |
| SCL | Scarecrow-like |
| SCR | Scarecrow |
| SDE | Silencing defective |
| SDG | Set domain group |
| SDS | Sodium dodecyl-sulphate |
| SDS-PAGE | Sodium dodecyl-sulphate polyacrylamide gel electrophoresis |
| SHR | Shortroot |
| siRNA | Small interfering RNA |
| SLR | Solitary root |

| | |
|---|---|
| SOD | Superoxide dismutase |
| SPX | SPX domain protein |
| *SPX1.1p* | Promoter region of *SPX1.1* |
| SR | Homogeneous temperature in shoot and root |
| STOP | Sensitive to proton rhizotoxixity |
| SUS | Sucrose synthase |
| TAIR | The Arabidopsis Information Resource |
| TCP | TCP domain protein |
| T-DNA | Transfer DNA |
| TE | Tris/EDTA |
| TF | Transcription factor |
| TGA | TGACG sequence-specific binding protein |
| TGRooZ | Temperature Gradient in the Root Zone |
| TIFY | TIFY domain protein |
| TIR | Transporter inhibitor response |
| TSPO | Outer membrane tryptophan-rich sensory protein |
| t-test | t-Student test |
| Tukey HSD | Honestly-significant-difference Tukey method |
| UBC | Ubiquitin conjugating enzyme |
| UDG | Uracil-DNA-glycosylase |
| UNE | Unfertilized embryo SAC |
| UPM | Universidad Politécnica de Madrid |
| UV light | Ultraviolet light |
| VRN | Reduced vernalization response |
| VTE | Vitamin E deficient |
| WB | Wash buffer |
| WHP | Weihenstephaner |
| WOX | Wuschel related homeobox |
| WRKY | WRKY DNA binding protein |
| YFP | Yellow fluorescent protein |
| ZIP | Zinc transporter precursor |
| Zn | Zinc |

# 1. INTRODUCTION

One of the main challenges for agriculture is to increase crop production to feed a constantly increasing human population, while at the same time minimizing agricultural production losses and its environmental impact. Climate change is having a severe impact on natural ecosystems, causing negative effects on agricultural production (Watts *et al.*, 2021). The accumulation of $CO_2$ and other greenhouse gases in the atmosphere has been constantly increasing in the past years, leading to global warming (Chaudhry & Sidhu, 2021). This is causing an increase in the frequency of extreme weather events, such as heat-waves, drought, changes in the frequency of precipitations, floods, and altered freezing patterns, which are having a profound impact on agriculture and global food security (Dempewolf *et al.*, 2014). Furthermore, climate change is affecting soil N availability due to many factors, including erosion, leaching and N gasification (García-Díaz *et al.*, 2017; Dai *et al.*, 2020.), resulting in an increased use of N fertilizers (Swarbreck *et al.*, 2019). Additionally, the increasingly low availability of soluble phosphate (Pi) in soils has led to continuous P-fertilization. Furthermore, predictions show that the natural sources of phosphorous (P) will be consumed soon due to the higher demand for fertilizers (Pandey *et al.*, 2013; Goncalves *et al.*, 2020). This continuous decrease in P availability, combined with the poor capacity of most crops to acquire and utilize immobilized phosphate, will negatively impact crop productivity (Johnston *et al.*, 2014). Therefore, the development of sustainable solutions to obtain crops that are more adapted to changing climatic conditions without compromising productivity is essential to ensure global food security (St. Clair & Lynch, 2010).

## 1.1. The root system as a key to identify traits to improve tolerance to abiotic stresses.

Roots are crucial organs for plant growth and development. They perform vital functions such as anchoring the plants to the soil, absorbing water and nutrients, and establishing beneficial relationships with the soil microbiota (Shekhar *et al.*, 2019). Since roots are in direct contact with the soil, they are considered the primary sensors of various abiotic stresses, such as drought, salinity, and waterlogging, and they are the first organs to activate several signalling pathways

to adjust their responses to these stresses (Wells & Eissenstat, 2002; Davies & Bacon, 2003; Khan *et al.*, 2016). Although there are different root architectures depending on the plant species, a typical root system consists of a primary or seminal root and an indeterminate number of postembryonic secondary or lateral roots (LRs) that emerge from the primary root (Fitter, 2002). Depending on the emerging angle and the number of LRs, plants can extend their root system in search for nutrients, water or to respond to external changes in the rhizosphere. These LRs can also develop tertiary roots that form an angle with respect to the secondary root, thus forming a complex network of lateral branches that extends the root system into the soil (Catlin, 1996). Both, primary root and LRs can grow with elongation rates of several cm a day (Klepper, 1992). The primary or seminal root is the first root to develop in both monocots and dicots and is composed of several concentric tissue layers: epidermis, exodermis, cortex, endodermis, and the stele, which is composed of pericycle, xylem, phloem and vascular cells (Figure 1.1; Smith & De Smet, 2012). Root growth depends on the combination of cell division at the root meristem, cell elongation and cell differentiation. The root apical meristem is located at the tip of the primary root and contains a group of undifferentiated cells that rarely divide, called quiescent centre, that send signals to organize and maintain the surrounding stem cells. These stem cells actively divide in the meristem to give rise to all root cell types and to sustain root growth (Dolan *et al.*, 1993). The cell division rate is influenced by genetic signals but also by environmental signals, such as nutrient levels, salinity or water availability (Bernstein & Kafkafi, 2002; West *et al.*, 2004; Linn *et al.*, 2017; Verslues & Longkumer, 2022). After leaving the meristem, the root cells increase their length in the elongation zone and later differentiate into various cell types in the differentiation zone (Fisher & Sozzani, 2016).

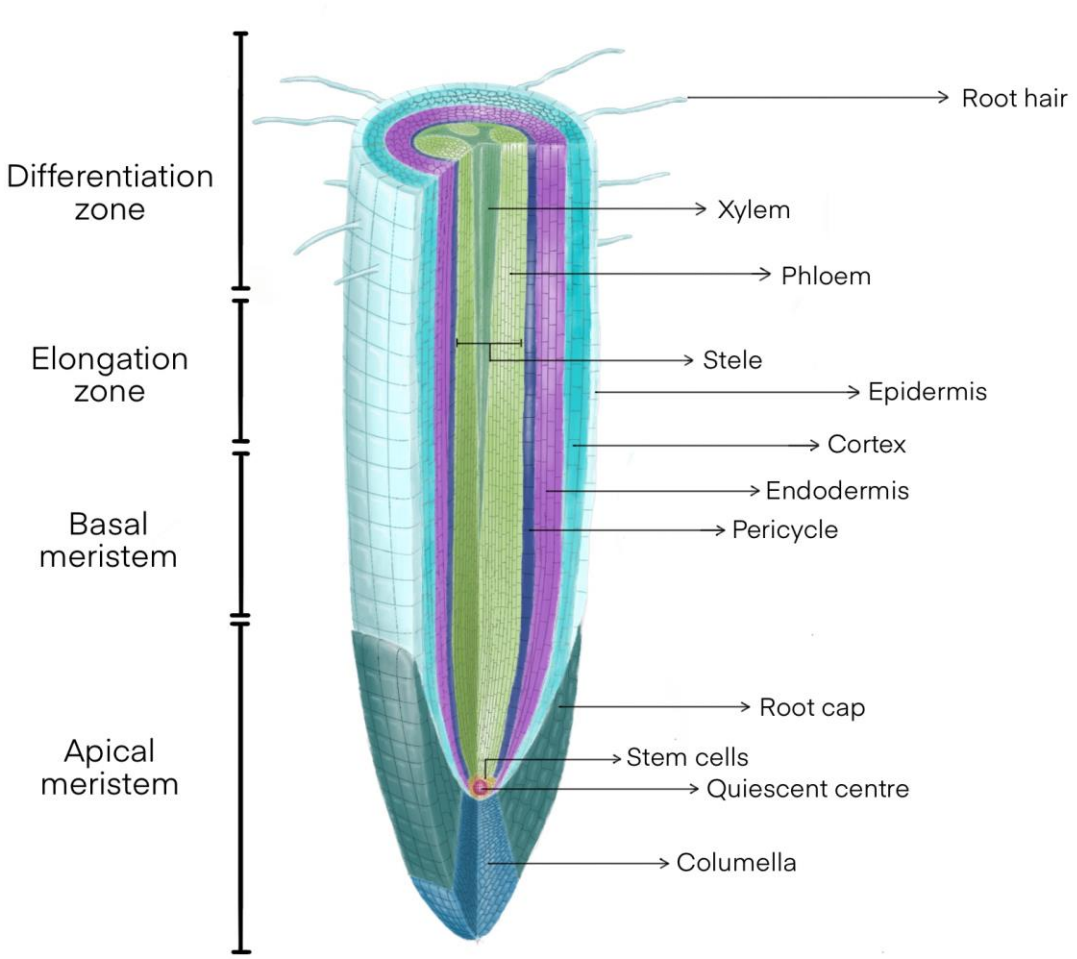


Figure 1.1: Schematic representation of a longitudinal cross section of the Arabidopsis root. Different cell types are disposed in layers surrounding the stele. The stele is composed by xylem, phloem and vascular cells, all surrounded by the pericycle. The external layers constitute the ground tissue (endodermis and cortex) and epidermis. Cell division occurs at the root apical meristem, which contains a group of undifferentiated cells called the stem cells surrounding the quiescent centre. Later, cells expand and differentiate to form all root tissue layers.

In Arabidopsis, LRs emerge from the primary root forming an angle and are originated from the pericycle cells (Dubrovsky *et al.*, 2001). In the basal meristem, the coordination of auxin-dependent signalling and root-clock dependent expression prime a group of pericycle cells to form the pre-branch sites, which are later transformed into the founder cells to become the precursors of lateral roots. These founder cells divide anticlinally and periclinally to develop a lateral root primordium, which will eventually give rise to an emerged lateral root (Sabatini *et*

*al.*, 1999; De Smet *et al.*, 2008). Later, tertiary lateral branches appear on LRs, expanding the surface of the root system into the soil.

Root development is highly plastic and can adopt several strategies to respond to different environmental stresses (Karlova *et al.*, 2021). For example, under mild drought or salinity stress, roots develop a longer root system, avoiding the top areas of the soil, where the drought or salinity is higher (Comas *et al.*, 2013; Gandullo *et al.*, 2021). Furthermore, under drought stress, lateral root branching changes and more LRs are formed in areas with more water availability (Orosa-Puente *et al.*, 2018). In Arabidopsis and several crops, in response to mild heat stress, the primary and secondary roots tend to enlarge to search for areas of the soil with lower temperatures (McMichael & Burke, 1998; Yang *et al.*, 2017). In *Brassica napus*, high temperatures can increase the angle between the primary root and the LRs, resulting in a greater extension of the root system (Nagel *et al.*, 2009).

Nevertheless, despite the critical role of roots in the plant responses to abiotic stresses, the effects of these stresses on the root system have been less studied than on the aerial parts of the plant (Koevoets *et al.*, 2016; Calleja-Cabrera *et al.*, 2020). This is largely due to the challenges associated to the study of the root system in the field (Franco *et al.*, 2015; Atkinson *et al.*, 2019). As a result, the analysis of the root system is often conducted under controlled laboratory conditions, which do not fully replicate the climatic conditions found in the field (Voss-Fels *et al.*, 2018; Qiao *et al.*, 2019). The development of experimental conditions that facilitate root phenotyping is crucial to study root responses to different stresses. In fact, most studies focused on root biology have been performed with the root system grown in the presence of light. The exposure of the root system to light can cause alterations in root development, affecting the growth of the primary root and lateral roots at a physiological and molecular level (Sassi *et al.*, 2012; Moni *et al.*, 2015; Navas-Silva et al., 2015; Navas-Silva et al., 2017). At the same time, light also worsens the response to different stresses due to an increase in the production of reactive oxygen species (ROS), which affects root system architecture (RSA; Yokawa *et al.*, 2011; Manzano *et al.*, 2014; Passaia *et al.*, 2014; Silva-Navas *et al.*, 2019). Therefore, our lab has developed different devices to optimize root phenotyping in both Arabidopsis and crop plants. Recently, we have engineered the D-Root, a cultivation device where plants maintain their roots in the dark while shoots grow under a normal photoperiod, simulating the natural conditions (Figure 1.2; Silva-Navas *et al.*, 2015). Recently, our lab has also

set up the Pouch and Wick system to improve root phenotyping in crops. The Pouch and Wick system allows the seedlings to grow vertically by disposing the roots between two pieces of moisturized germination paper, coated by two vertical covers to provide support, creating a "sandwich" disposition where the root system grows in the dark (Figure 4.1). This arrangement allows the roots to grow vertically in a two-dimensional system, facilitating root phenotyping (Atkinson *et al.*, 2015; Boter *et al.*, 2023).

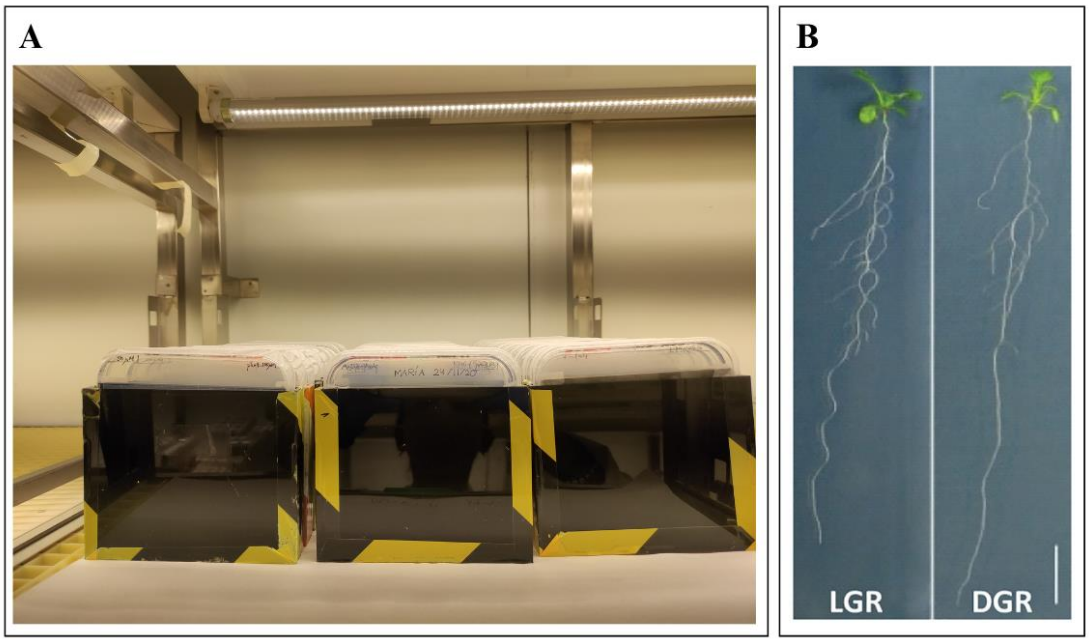


Figure 1.2: A) Arabidopsis (Col-0) seedlings grown vertically in Petri dishes with MS medium in the D-root system. B) Examples of 12-day old Arabidopsis (Col-0) seedlings grown with the roots exposed to light (LGR) or in the dark (DGR). Adapted from: Silva-Navas *et al.*, 2015.

## 1.2. Root responses to abiotic stresses: shared and specific responses.

Abiotic stresses can have a strong impact on the root system, altering root development and functionality, impairing the uptake of water and nutrients as well as its interactions with the microbiome (Koevoets *et al.*, 2016; Choi *et al.*, 2021). In turn, these changes can have negative effects on the above-ground parts of the plant, altering physiological and developmental processes like stomatal conductance, photosynthesis or carbon allocation, thereby compromising crop productivity (Ghosh & Xu, 2014; Khan *et al.*, 2016). Different abiotic stresses can cause shared or specific responses in the root system. Shared responses are those

that are common among most abiotic stresses, such as changes in the root system architecture like variations in the formation and elongation of LRs, modifications in root hair development, or adjustments in the allocation of carbon and nutrients (DoVale and Fritsche-Neto, 2015). Other shared responses in roots include metabolic changes, such as the accumulation of osmoprotectants (Figure 1.3). Thus, several abiotic stresses, such as drought, salinity, heat stress, flooding and heavy metal toxicity can cause the accumulation of osmoprotectants inside the cell to reduce the water potential and prevent cellular damage (Hossain *et al.*, 2022). Accumulation of reactive oxygen species (ROS) is also a well-known response to most abiotic stresses, including drought, salinity, temperature stresses, nutrient deficiencies, $O_3$ stress or hypoxia (Moller *et al.*, 2007; Foyer & Noctor, 2009). ROS are extremely reactive molecules derived from cellular stress that can interact with DNA, proteins and lipids and cause potential damage (Lamb & Dixon, 1997; Ashraf, 2009). Plant cells have antioxidant compounds and enzymes that prevent excessive ROS accumulation and manage the oxidative stress response. These compounds include carotenoids, glutathione, and ascorbate, and enzymes such as CATALASE (CAT), SUPEROXIDE DISMUTASE (SOD) and ASCORBATE PEROXIDASE (APX; Desikan *et al.*, 2004). The release of these compounds by roots has been reported as a response to several stresses, such as drought, heat, salinity or nutrient deficiencies (Medici *et al.*, 2004; Selote & Khanna-Chopra, 2010; Maksimović *et al.*, 2013; Liu *et al.*, 2018; Wang *et al.*, 2023c). Another typical reaction to abiotic stress is the elevation of cytosolic $Ca^{2+}$ levels due to the activation of $Ca^{2+}$ channels triggered by increased levels of ROS (Ranty *et al.*, 2016; Figure 1.3). These changes in $Ca^{2+}$ influx signal the initiation of various phosphorylation and dephosphorylation cascades by MITOGEN ACTIVATED PROTEIN KINASES (MAPKs) activated by $Ca^{2+}$. These cascades then transmit the stress signal to downstream targets, including specific families of transcription factors (TFs) that regulate the plant's overall stress response (Kumar *et al.*, 2020). The processes described above are responses that are shared between many abiotic stresses, but every abiotic stress can also trigger specific responses. Examples of specific responses are the increase in LR number and their elongation caused by phosphate deficiency (Waidmann *et al.*, 2020), as well as the suppression of LR growth in areas with low N availability to promote LR growth in areas with higher N (Poitout *et al.*, 2018). Another example is the sequestration of $Na^+$ and $Cl^-$ ions in vacuoles to ameliorate the effects of salinity stress in the cell, accompanied by an increase in the size of those vacuoles (Mansour, 2023).

Various plant hormones, including abscisic acid (ABA), jasmonic acid (JA), ethylene (ET), and salicylic acid (SA), play crucial roles in mediating (single or combined) abiotic stress responses in roots (Figure 1.3). ABA acts as an intermediary molecule in the root response to drought, heat, and salinity in plants such as wheat, rice, quinoa, and cucumber (Talanova *et al.*, 2003; Trapeznikov *et al.*, 2003; Jacobsen *et al.*, 2009; Ding *et al.*, 2016). Additionally, genes involved in the ABA biosynthetic pathway are activated to mediate root growth under various abiotic stresses (Tuteja, 2007). JA also contributes to root responses to abiotic stresses like salinity, drought, and thermal stress (de Ollas *et al.*, 2013; Habibi *et al.*, 2019; Ali *et al.*, 2020). ET mediates the root responses to salinity in tomato, heat in artichoke, and cold stress in tomato (Karni *et al.*, 2010; Klay *et al.*, 2014; Shinohara *et al.*, 2017). Similarly, SA is induced in response to drought in barley (Bandurska, 2005), and exogenous application of SA enhances tolerance to salinity, chilling, and heavy metal stress in barley, rice and tomato, respectivily (Metwally *et al.*, 2003; Stevens *et al.*, 2006; Guo *et al.*, 2009). Other hormones, such as cytokinins, brassinosteroids, auxins, and gibberellins, are also involved on the root response to abiotic stresses (Peleg & Blumwald, 2011). For example, different barley cultivars overexpressing a gene encoding for a cytokinin dehydrogenase in roots exhibit increased drought tolerance (Pospíšilová *et al.*, 2016), and the application of auxin to salt-stressed strawberry seedlings helps to maintain proper root growth (Zhang *et al.*, 2021).

Furthermore, abiotic stresses can cause extensive changes in the root transcriptome. Numerous molecular studies have compared the transcriptome of many crops under different abiotic stresses and identified overlapping transcriptional patterns in crops such as soybean, rice, and barley (Ozturk *et al.*, 2002; Yun *et al.*, 2012; Kidokoro *et al.*, 2015). Several families of transcription factors (TFs) have shown to be involved in the root responses to these stresses (Figure 1.3). For example, members of the MYB family are activated by stresses like drought, UV light, and cold in various crops (Vannini *et al.*, 2007; Schenke *et al.*, 2011; Seo *et al.*, 2011). The NAC family of TFs plays an important role in the response to drought, salinity, cold, and dehydration in wheat and rice (Fujita *et al.*, 2004; Nakashima *et al.*, 2007; Seo *et al.*, 2010; Xia *et al.*, 2010). Some members of the *ETHYLENE RESPONSE FACTOR* (*ERF*) family of TFs play a role in the response to drought, salinity, and cold in rice, soybean, and tobacco (Guo *et al.*, 2004; Cao *et al.*, 2006; Zhang G. *et al.*, 2009). The WRKY family is involved in the response to drought and heat stress in rice (Qiu and Yu, 2009; Peng *et al.*, 2011),

while the *DEHYDRATION-RESPONSIVE ELEMENT BINDING* (*DREB*) family is linked to drought, salinity, and cold stresses in crops like wheat, barley, rice, and soybean (Shen *et al.*, 2003; Li *et al.*, 2005; Wang *et al.*, 2008; Xu *et al.*, 2009). *HEAT SHOCK FACTORS* (*HSFs*) are critical TFs in the response to multiple abiotic stresses. They regulate several *HEAT SHOCK PROTEINS* (*HSPs*) that act as molecular chaperones, which are involved in the protection and stabilization of essential proteins to prevent protein denaturation during stress (Atkinson & Urwin, 2012). Specific HSPs are activated under different abiotic stress conditions, and their functional diversity enables plants to respond to a wide variety of stresses (Rizhsky *et al.*, 2004). The role of HSPs on the regulation of abiotic stress responses has been studied in several crops, including wheat, tomato and soybean (Mishra *et al.*, 2002; Zhu *et al.*, 2006; Xue *et al.*, 2014).

Finally, recent works have revealed that epigenetic mechanisms can influence the regulation of the root responses to abiotic stresses. DNA methylation and histone modifications play a crucial role on the response to salinity, drought, and temperature stress (Ashapkin *et al.*, 2020; Miryeganeh, 2021). In rice, the gene *DOMAINS REARRANGED METHYLTRANSFERASE 2 (DRM2)*, which encodes for a DNA demethylase, is upregulated under salinity stress in tolerant varieties (Ferreira *et al.*, 2015), and the histone marker H3K4me3 has been linked to the response to drought stress (Zong *et al.*, 2020). Cold stress triggers the expression of genes encoding for histone deacetylases, resulting in widespread modifications of the H3 and H4 histones in maize (Hu *et al.*, 2011). Furthermore, small non-coding RNAs, such as microRNAs (miRNAs) and small interfering RNAs (siRNAs) have shown to be involved in the response to various abiotic stresses (Sunkar *et al.*, 2007). These small RNAs can regulate gene expression through post-transcriptional gene silencing or DNA methylation mechanisms (Waititu *et al.*, 2020). The expression of many miRNAs can be induced by the exposure to stresses like drought, salinity, and heat, in crops such as barley, maize, and rice (Wei *et al.*, 2009; Sailaja *et al.*, 2014; Deng *et al.*, 2015). In rice, siRNAs involved on the regulation of genes that participate in oxidation, reduction and proteolysis have been associated with the response to drought stress (Jung *et al.*, 2016). Additionally, several heat-responsive siRNAs have been identified in *Brassica rapa* (Yu *et al.*, 2013).

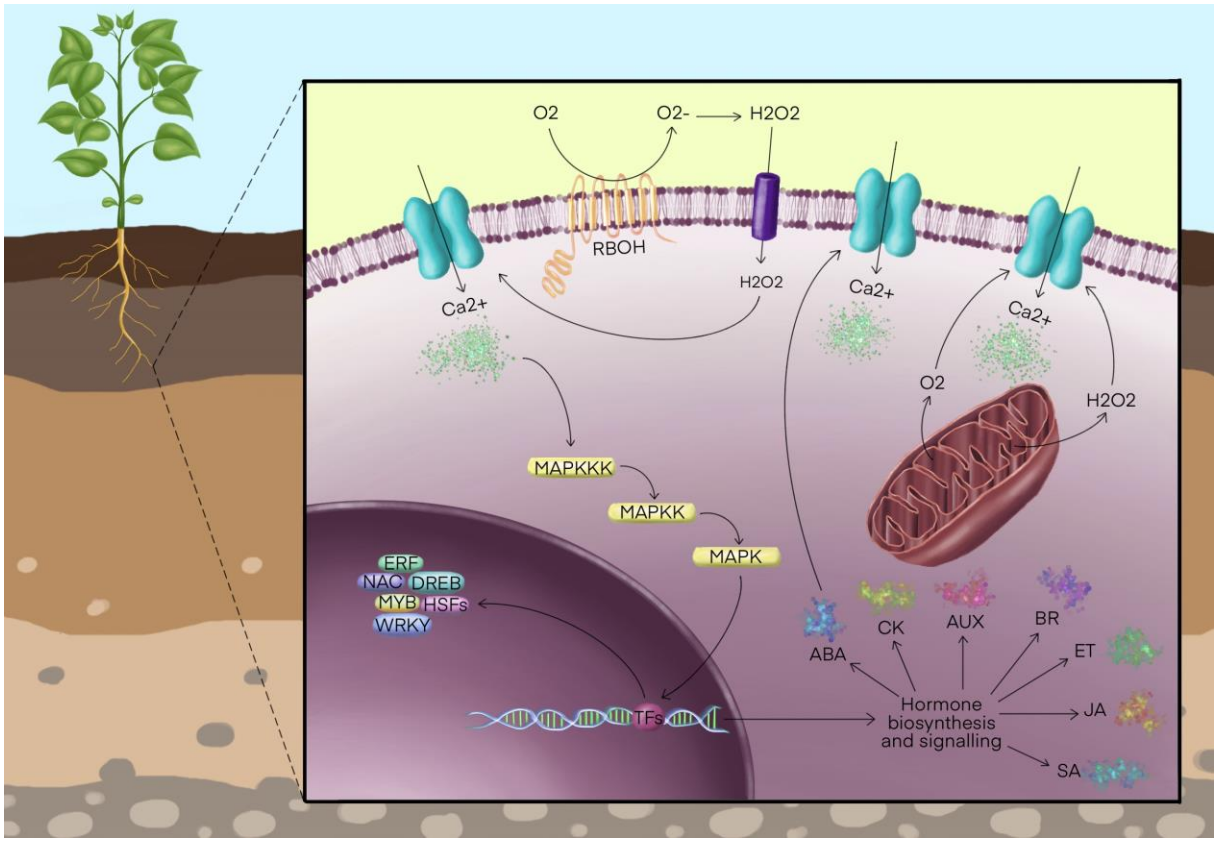


Figure 1.3: Schematic representation of several molecular responses that are shared in response to most abiotic stresses in the root system. Most abiotic stresses cause damage to the plasma membrane and lead to alterations in osmotic homeostasis, leading to the production of reactive oxygen species (ROS). The production of ROS is mediated by NADPH oxidases (RBOHs) in the plasma membrane. These ROS can enter the cell and trigger the activation of $Ca^{2+}$ channels, leading to an increase in cytosolic $Ca^{2+}$. This can lead to the activation of calcium-dependent protein kinases (MAPKs) and of other MAPKs, triggering a phosphorylation signalling cascade of that ends up with the activation of TFs and gene expression in the nucleus. These TFs belong to several families such as WRKY, DREB, MYB, NAC, ERF and HSFs, and regulate the expression of genes related to the biosynthesis of secondary metabolites and hormones like ABA, cytokinins (CKs), brassinosteroids (BRs), ethylene (ET), jasmonic acid (JA), salicylic acid (SA) and auxin (AUX). These hormones consequently trigger various signalling pathways that coordinate the response to different abiotic stresses. Adapted from: Sánchez-Bermúdez *et al.*, 2022.

Whereas some of the root adaptation responses are shared across different stresses, plants can also activate specific responses to a particular stress combination (Pandey *et al.*, 2015). Consequently, predicting plant responses to combined stresses is challenging, especially when most research has focused on studying abiotic stresses individually (Zandalinas *et al.*, 2021). Additionally, the presence of a second abiotic stress can either supress or exacerbate the negative effects of the first stress (Suzuki *et al.*, 2014). Thus, understanding root responses

to specific stress combinations is crucial to develop strategies to improve plant growth and yield under the changing environmental conditions driven by climate change.

## 1.3. Crops confront a combination of abiotic stresses in the field.

The changes in the frequency of extreme weather events are causing abiotic stresses to become more frequent and severe, leading to significant yield losses in crop production (Mittler, 2006; Chaudhry and Sidhu, 2021). For example, crops such as wheat, rice, maize, and soybean, which provide two-thirds of the world's food supply and are essential to guarantee food security, are predicted to experience yield reductions between 3 and 6 % for each 1°C rise in the global mean temperature (Zhao *et al.*, 2017). Traditionally, most of the studies have focused on studying the impact of individual abiotic stresses on plants. However, in natural conditions, abiotic stresses tend to occur in combination rather than individually (Suzuki *et al.*, 2014). Several studies have shown that the effect of combined abiotic stresses on crop productivity can differ from the effects of individual abiotic stresses. For instance, the global wheat and maize yields have declined due to the effect of high temperatures, and these reductions have been more severe in regions that also experience drought periods (Matiu *et al.*, 2017).

Plants have developed intricate mechanisms to adapt to abiotic stresses that begin with the detection and transmission of the stress signals, triggering various signalling pathways and ultimately leading to an adaptive response. Although some of the root responses are shared across different abiotic stresses, different stress combinations can trigger specific root responses (Pandey *et al.*, 2015). Furthermore, the physiological and molecular response of plants to a particular abiotic stress can differ from the responses to the same stress when applied in combination with other stresses (Pandey *et a*l., 2015; Mittler, 2006). Interestingly, the combination of some abiotic stresses can activate signalling pathways in plants that cause synergistic or antagonistic responses (Atkinson and Urwin, 2012). For instance, during heat stress, plants open their stomata to lower the leaf temperature, but when heat stress is combined with drought, the stomata remain closed to avoid water loss, thus impairing the regulation of the leaf temperature (Reynolds-Henne *et al.*, 2010). On the other hand, some abiotic stress combinations might activate synergistic signalling pathways. For instance, salinity stress alone

can disturb water absorption by roots since a high accumulation of salt in the root zone can impair water uptake. This effect is similar to the response to drought stress, which produces a reduction in water absorption (Roy *et al.*, 2014). Thus, root responses to the combination of drought and salinity can be more detrimental than the responses to the individual stresses (Zhang *et al.*, 2013a).

Antagonistic or synergistic responses to the simultaneous occurrence of two abiotic stresses can either worsen or ameliorate the effects of those abiotic stresses when applied individually (Suzuki *et al.*, 2014). While most stress combinations have a cumulative negative effect (Ahmed *et al.*, 2013; Alhdad *et al.*, 2013; Sales *et al.*, 2013), some combinations, such as drought combined with an excess of atmospheric ozone ($O_3$), or salinity combined with high $CO_2$ can interact positively, reducing the negative effects of the individual stresses (Iyer *et al.*, 2013; Pérez-López *et al.*, 2013). For instance, when drought stress is applied in combination with high $O_3$ levels, the production of ROS is lower than under drought stress alone (Iyer *et al.*, 2013). At the same time, elevated $CO_2$ could prevent high concentrations of salt to accumulate at the root surface, and thus reduce salt uptake by roots (Munns *et al.*, 1999). On the other hand, elevated $CO_2$ could cause an increase in the activity of antioxidant enzymes in roots grown under salinity stress (Yi *et al.*, 2018). Therefore, it is challenging to predict the root responses to combined stresses based solely on the root responses to the individual ones (Zandalinas *et al.*, 2021). Even though some research has focused on abiotic stress combinations, there is still a significant gap in our knowledge regarding the effects of combined abiotic stresses in crops. Addressing the effects of abiotic stress combinations rather than individual stresses in crops can help farmers and breeders to develop successful strategies to overcome their negative effects on crop production. Therefore, understanding the potential mechanisms that confer tolerance to different stress combinations is crucial for the development of crops that are better adapted to climate change.

## 1.4. *Brassica napus* as a model to study root responses to abiotic stress combinations in crops.

*Brassica napus* L., commonly known as oilseed rape/rapeseed or canola (short for Canadian oil low acid), is an allotetraploid crop originated about 7500 years ago by the spontaneous hybridization between *B. rapa* and *B. oleracea* (Chalhoub *et al.*, 2014; Lu *et al.*, 2019). It is an annual crop and contains winter, semi-winter and

spring varieties (Gulden *et al.*, 2008). *B. napus* has been extensively cultivated in many parts of the world under different climatic environments, leading to the development of a high number of different varieties (Khanzada *et al.*, 2020).

*B. napus* belongs to the *Brassicaceae* family and is closely related to *Arabidopsis thaliana*, with more than 86% of their protein sequences conserved (Cavell *et al.*, 1998). *B. napus* is part of the *Brassica* genus, which contains several species that evolved from a common ancestor and present a high level of similarity in their genomes (Wang *et al.*, 2011). Several hybridization events have occurred within the *Brassica* genus giving rise to some of the most common *Brassica* species. Different combinations of hybridizations between the species *B. rapa*, *B. oleracea* and *B. nigra* have led to the generation of the species *B. carinata*, *B. juncea* and *B. napus*, generating the so-called U's triangle model. *B. napus* emerged through a hybridization between the diploid species *B. rapa* (2n=20, AA) and *B. oleracea* (2n=18, CC), generating the allotetraploid *B. napus* containing both genomes (2n=38, AACC). Genomic studies have shown that the A and C genomes from *B. napus* are highly homologous (Chalhoub *et al.*, 2014). However, different *B. napus* genotypes might present alterations in their sub-genomic evolution and recombination frequencies, and variations in chromosome structures (Hu *et al.*, 2021). As mentioned above, other hybridization events have happened among the *Brassica* genus, generating some of the current *Brassica* species. For instance, the hybridization between *B. rapa* (2n=20, AA) and *B. nigra* (2n=16, BB) originated *B. juncea* (2n=36, AABB), whereas the hybridization between *B. oleracea* (2n=18, CC) and *B. nigra* (2n=16, BB) led to the generation of *B. carinata* (2n=34, BBCC) (Nagaharu *et al*, 1935). The genomic information about *B. napus* has been constantly increasing in the past few years. Different *B. napus* varieties have been sequenced, resulting in high quality reference genomes and an increase in the availability of annotations and genomic information from different databases (Hu *et al.*, 2021). Moreover, there is an extensive amount of germplasm resources stored in some of the major germplasm banks across the world (Bancroft, 2011; Li *et al.*, 2020a).

Oilseed rape is a versatile crop with a high socioeconomic importance due to its oil, which has an elevated nutritional value for humans and animals and has also been used for biodiesel production. In terms of vegetable oil production, *B. napus* is the second-highest yielding oil crop worldwide, producing 12% of all the vegetable oil production (Chew, 2020; Zheng & Liu, 2022). The *B. napus* seeds contain high quality oil that is rich in monounsaturated fatty acids (MUFAs) and poly-

unsaturated fatty acids (PUFAs), having many benefits for human health (Jahreis & Schäfer, 2011). Many studies demonstrate the beneficial effects of MUFAs in human health, such as reducing the risk of atherosclerosis and cardiovascular diseases (Kris-Etherton, 1999; Galassetti & Pontello, 2006). PUFAs could reduce the risks of coronary diseases, could be beneficial for the immune system and could also improve cognition (Kris-Etherton *et al.*, 2003; Hardman, 2007; Duda *et al.*, 2009; Fetterman & Zdanowicz, 2009). Furthermore, *B. napus* oil is low on saturated fatty acids (SFA) compared to other oils used for human feed, such as sunflower, corn or soybean oil, and is rich in vitamin E, vitamin K and tocopherols (Raboanatahiry *et al.*, 2021). SFAs are known to increase lipid levels in the blood, and given that the consumption of SFAs should be limited to less than 10% of the daily calories (Trumbo *et al.*, 2002), *B. napus* oil is a suitable option to meet this requirement compared to other oils. *B. napus* has many applications, since is used for different purposes (Raboanatahiry *et al.*, 2021). *B. napus* seeds oil has been proposed for industrial applications as well, such as the production of biofuels, reducing up to 90% of the greenhouse emission gases compared to the use of fossil fuels (Finco *et al.*, 2012; Del Gatto *et al.*, 2015). Moreover, *B. napus* oil is biodegradable, reducing the potential impact to the environment (Raboanatahiry *et al.*, 2021). The residual products from the *B. napus* oil extraction process can be used for human consumption and animal feed, being a source of high-quality proteins (Pastuszewska *et al.*, 2000). *B. napus* has also potential for the non-edible sector as a source of bioplastics with several purposes, such as the formation of capsules for drugs, polymer films (Bandara *et al.*, 2018; Zhang *et al.*, 2018b) and in the cosmetic industry, due to its high content in hydrolysates, which can have anti-aging properties (Rivera *et al.*, 2015).

The use of *B. napus* for human and animal consumption still presents some limitations. The *B. napus* oil has an elevated content of erucic acid, a fatty acid that has been labelled as potentially toxic (Wallace *et al.*, 2016). Erucic acid, when ingested, is assimilated into the blood stream and distributed to the different tissues, where undergoes ß-oxidation to acquire energy. However, the ß-oxidation rate of erucic acid is low, resulting in an accumulation of erucic acid in cardiac tissues, leading to potential coronary diseases (Wani *et al.*, 2022). However, *B. napus* varieties with a low content of erucic acid have been recently developed (Nath *et al.*, 2016). Another limitation in the use of *B. napus* for human and animal consumption is the high content of glucosinolates that are present in the rapeseed meal (Bhardwaj & Hamama, 2003). Glucosinolates, when ingested, can be

degraded into by-products that are toxic and can result in health problems (Lee *et al.*, 2020). However, glucosinolates are only toxic when they are degraded into by-products by the enzyme myrosinase, which is present in the rapeseed meal (Mawson *et al.*, 1993). Fortunately, myrosinase can now be easily eliminated from the rapeseed meal and glucosinolates can be safely ingested (Borgen *et al.*, 2010).

Many abiotic stresses such as heat, drought, salinity and nutrient deficiencies negatively affect *B. napus* and its productivity (Bybordi & Tabatabaei, 2009; Han *et al.*, 2017; Rashid *et al.*, 2018; Batool *et al.*, 2022). Research shows that *B. napus* cultivation is highly sensitive to temperature changes and shifts in global temperature could make *B. napus* cultivation unsuitable in the current production areas (Borges *et al.*, 2023). Thus, a better understanding of the responses of *B. napus* to abiotic stresses such as temperature-related stresses are crucial to develop solutions for this challenge. For this reason, and due to the high economic importance of *B. napus*, its closeness to Arabidopsis and other *Brassica* species, and to the increasing availability of genomic information and resources in this crop, we selected *B. napus* as a model to study the root responses to abiotic stress combinations in crops.

## 1.5. Effects of elevated temperature in the root system.

Climate change has led to a constant increase in the global mean temperature in the past few years, and many models predict that the temperatures will keep increasing, with rises of about 4.4ºC by the year 2100 (Masson-Delmotte, *et al.*, 2021). High temperatures have shown to produce a strong negative impact on crop yields (Ortiz-Bobea *et al.*, 2019). Several studies highlight the potential negative impact of high temperatures on the global yield of the four major staple crops: wheat, maize, rice and soybean (Zhao *et al.*, 2017; Wang *et al.*, 2020c). Other crops, such as cotton, cassava, pulses, millet and oats are predicted to suffer dramatic yield losses with only 1ºC increase in the global temperature (Agnolucci *et al.*, 2020). Moreover, high temperatures can alter seed quality and reduce the linolenic acid content in the oil of many oilseed crops, such as oilseed rape, sunflower, flax and castor (Canvin, 1965).

High temperature directly affects plant cells by producing changes in the permeability of cell membranes, reducing cell water content and leading to decreases in cell size, increases in the size of xylem vessels and causing damage to the mesophyll cells, as well as causing protein denaturation and in some cases

provoking cell death (Figure 1.4; Figure 1.7; Hasanuzzaman *et al.*, 2013; Shaheen *et al.*, 2016). High temperature can impact plant growth and development at various physiological levels. During seed germination, high temperatures have shown to reduce germination rates and reduce seedling growth and vigour (Bita & Gerats, 2013). Heat stress negatively affects photosynthesis, altering chloroplast size, position and efficiency (Wahid & Shabbir, 2005). During the vegetative and reproductive stages, high temperature enhances evapotranspiration leading to increased water loss, which in many cases is combined with reduced water uptake by roots, resulting in dehydration and reduced plant growth (Fahad *et al.*, 2017). During the reproductive phase, heat stress alters flower and fruit production, reduces pollen viability and causes alterations in pollen release due to alterations in the disposition of endothelial cells present in the anther (Hasanuzzaman *et al.*, 2013; Lohani *et al.*, 2020; Parthasarathi *et al.*, 2022).

In the case of the root system, the responses to heat stress can vary depending on the level of the temperature and the type of soil. Whereas mild heat stress tends to cause an enlargement of the primary root and an increase in the size of the root system, severe heat stress can cause the opposite effect and supress root growth (Fonseca de Lima *et al.*, 2021; González-García *et al.*, 2023). Severe heat stress has shown to modify root architecture by reducing root growth in Arabidopsis, tomato and rice (Giri *et al.*, 2017; Kilasi *et al.*, 2018; González-García *et al.*, 2023). In *Brassica campestris*, heat stress has shown to produce a negative impact in several root traits, like root depth, surface area and volume in a sensitive cultivar compared to a tolerant cultivar (Yuan *et al.*, 2016a). Studies in *Agrostis* species show that low protein content in roots is strongly associated with heat sensitivity, and tolerant species showed a higher root protein content that correlates with an increase in root growth. This effect seems to be mediated by the activation of several stress-related proteins like GLUTATHIONE-S-TRANSFERASE (GST), SOD, PEROXIDASE (PER), CAT and HSPs that function as ROS-scavenging enzymes and play a role in maintaining protein conformation (Xu & Huang, 2008; Huang *et al.*, 2012; Xu *et al.*, 2015). Furthermore, heat stress can affect the uptake of essential nutrients like nitrogen, phosphorous or potassium as well as other microelements. Normally, heat stress reduces nutrient uptake, which has been correlated with low protein content, decreased expression of nitrogen and phosphorous transporters and antioxidant enzymes (Rennenberg *et al.*, 2006; Giri *et al.*, 2017).

At a cellular level, heat stress enhances the production of ROS in root cells, causing damage to nucleotides and proteins (Shi *et al.*, 2019). In *Brassica campestris*, ROS production produces alterations in the structure of the plasma membrane and nuclear membrane. Consequently, heat-tolerant cultivars display a better capacity to maintain a thick cell wall, protecting the integrity of the membrane (Yuan *et al.*, 2016a). Heat stress also alters the potential of the plasma membrane in root cells, modifying membrane fluidity and leading to the activation of $Ca^{2+}$ channels (Figure 1.4). The increase in cytosolic $Ca^{2+}$ leads to the activation of a downstream signalling cascade involving MAPKs that ends in the activation of heat-responsive genes such as HSPs and ROS-scavenging enzymes (Figure 1.7; Kotak *et al.*, 2007; Mittler *et al.*, 2012). The transcriptional response to heat stress varies among different types of root cells (Teves & Henikoff, 2011). Thus, cell types that are directly more exposed to heat stress, such as root hairs and cells from the epidermis and cortex present more changes in gene expression compared to cells from more internal layers like the stele cells (Jean-Baptiste *et al.*, 2019). In soybean, root hairs expressed a higher number of genes related to heat stress after six hours of treatment compared to other cell types, and showed a high enrichement of the expression of HSFs and WRKY transcription factors (Valdés-López *et al.*, 2016).

At the phytohormone level, auxin, ethylene, abscisic acid, cytokinins, salicylic acid, gibberellins and brassinosteroids have shown to play a role in the root responses to heat stress (Li *et al.*, 2021). Excessive high temperature can cause decreases in ABA, cytokinins, JA and auxin in root tissues in Arabidopsis (Prerostova *et al.*, 2020). Even though heat stress causes a general decrease in auxin levels in the root system, the root meristem can locally enhance auxin biosynthesis to maintain root growth under heat stress (Brumos *et al.*, 2018). In tobacco, overexpression of several auxin-related genes, including *NtYUCCA 6/8P, PIN-FORMED 1/2 (NtPIN1/2)* and *AUXIN RESPONSE FACTOR 1/2 (NtARF1/2)* increases root growth under heat stress (Song *et al.*, 2019). Exogenous application of cytokinins has shown to enhance root growth and development under heat stress in bentgrass and barley (Liu *et al.*, 2002; Berka *et al.*, 2020). ABA is activated in response to heat stress, leading to an increase in the production of ROS-scavenging enzymes and to the activation of many HSPs (Hu *et al.*, 2010a; Zhu, 2016). In Arabidopsis, the enhanced root growth as a response to heat stress has been related to an increase of ABA in root tissues (Figure 1.4; Larkindale *et al.*, 2005).

Epigenetic modifications, like DNA-methylation, chromatin remodelling, histone modifications and small RNAs have shown to play a role in the root responses to

heat stress (Liu & He, 2020; Tiwari *et al.*, 2021). HSFs are known to be crucial components of the responses to heat stress, and together with changes in DNA methylation can also be involved in the activation of transposable elements (TEs) and mediate epigenetic modifications (Quadrana, 2020). In soybean, root cells of heat stressed plants showed a different DNA methylation profile than root cells of plants grown under optimal conditions (Hossain *et al.*, 2017). Histone acetylation has also shown to play a role in the root response to heat stress in maize and has been related to the inhibition of LR primordia formation and development in response to this stress (Zhang *et al.*, 2018a).

In *B. napus*, warm temperatures can increase the extent and size of the root system among different genotypes (Table 1.1; Boter *et al.*, 2023). However, the exposure to long-term heat stress leads to a decrease in root length, root surface area and volume, and a significant suppression of LR development (Wu *et al.*, 2020b). Heat stress in *B. napus* has also shown to produce root exudation of N and C compounds (Delamare *et al.*, 2023). Recently, our lab has identified significant phenotypic variation in the root response to warm temperatures among different *B. napus* genotypes in terms of the capacity to develop an extended root system under warm conditions (Boter *et al.*, 2023). These differential responses were correlated with changes in root cell division and elongation. Furthermore, the transcriptional response of two different *B. napus* genotypes in response to warm temperatures revealed different root adaptation strategies to warm temperature, correlating with differences in the expression of genes related to hormone signalling, such as ABA, ethylene, cytokinin, brassinosteroids or gibberellins, as well as genes related to oxidative stress and the heat-shock response (Table 1.1; Boter *et al.*, 2023).

In nature, due to the geothermal properties of the soil, during high temperature periods, the soil temperature is lower than the air temperature, with higher values in the top parts of the soil and gradually decreasing to lower values in deeper areas, forming a temperature gradient (Shen *et al.*, 2018). Thus, roots experience a higher temperature in the top parts, whereas the bottom parts of the root system are exposed to a lower temperature. For that reason, under mild high temperature stress, roots tend to elongate to reach zones of the soil with lower temperatures (Illston & Fiebrich, 2017). Despite this, most studies focused on root and shoot responses to high temperature stress use the same high temperature in both parts. Thus, our lab has engineered the TGRooZ (Temperature Gradient in the Root Zone), a device that allows root phenotyping under heat stress, by creating a temperature gradient in the root-zone with higher temperatures in the top parts

of the root system and lower temperatures in the deeper parts, mimicking natural soils (González-García *et al.*, 2023). Remarkably, while Arabidopsis seedlings homogeneously heat-stressed in root and shoot showed arrested root growth, heat-stressed Arabidopsis seedlings grown in the TGRooZ were able to maintain root growth and functionality (González-García *et al.*, 2023). Furthermore, seedlings grown in the TGRooZ showed a different gene expression profile in shoots than seedlings grown at a homogeneous high temperature stress, although the shoot temperature was similar. They also showed differences in cell division in the root apical meristem, having a larger meristem size and a higher number of dividing cells. Finally, the root-zone temperature also influenced the diversity of the microbial communities in the rhizosphere and root-associated microbiome under heat stress, which are essential for proper plant growth and development (González-García *et al.*, 2023).

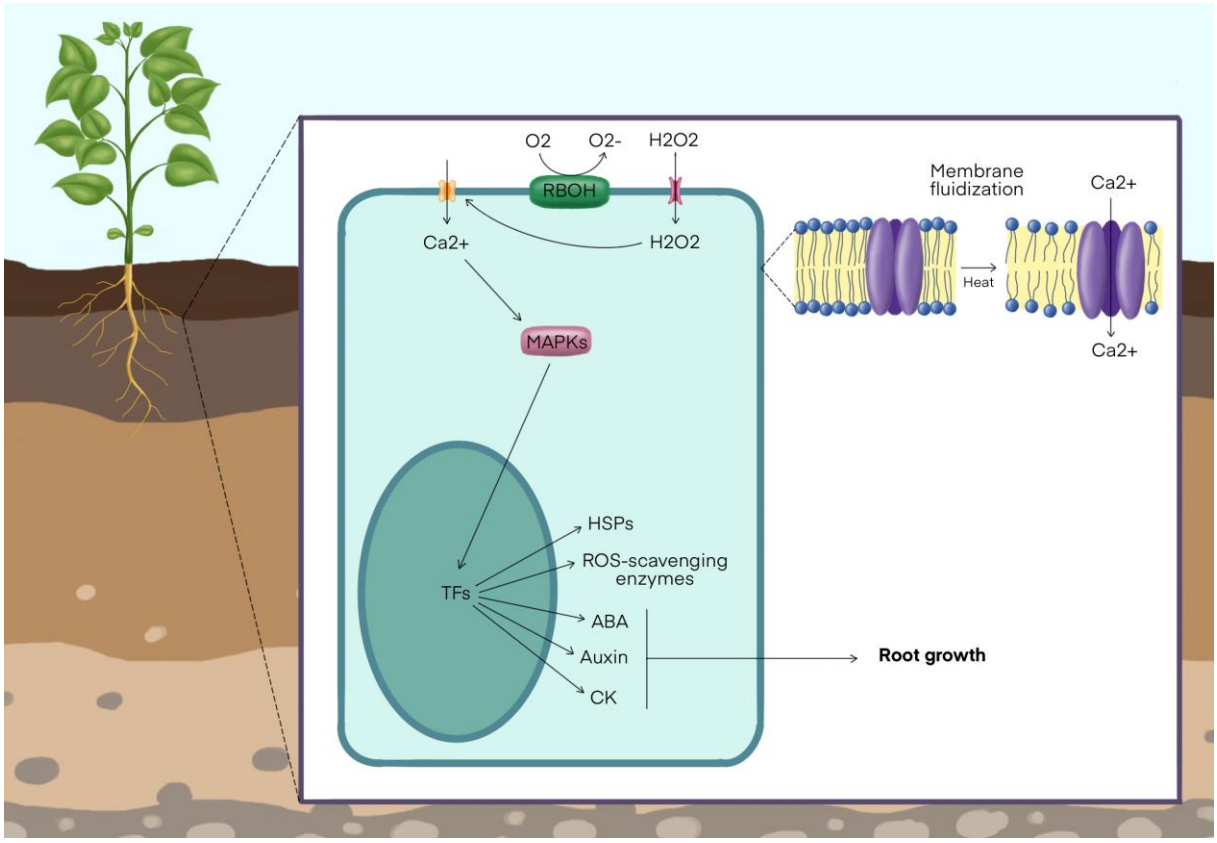


Figure 1.4: Overview of the molecular responses of root cells to elevated temperatures. Elevated temperature changes the fluidity and permeability of the plasma membrane, leading to the activation of $Ca^{2+}$ channels and increase in ROS formation, which causes an accumulation of cytosolic $Ca^{2+}$. This activates a signalling cascade involving MAPKs that ends up with the induction of several genes in the nucleus. These genes trigger different adaptation responses to cope with heat stress and some of them include HSPs and ROS-scavenging enzymes that can mitigate the negative effects of ROS. The changes in gene expression also lead to the activation of different hormonal signalling pathways, involving

ABA, auxin and cytokinins that contribute to enhance root growth in order to search for cooler zones in the soil.

## 1.6. Effects of nitrogen deficiency in the root system.

Nitrogen (N) is one of the essential macronutrients for plant growth and development and has a strong impact on agricultural production (Jiao *et al.*, 2016). It is crucial for the biosynthesis of amino acids, nucleic acids and secondary metabolites (Kusano *et al.*, 2011). An adequate N availability in soils is crucial to increase agricultural productivity (Maheswari *et al.*, 2017). For this reason, low N availability in soils has led to the use of N fertilizers to increase crop production. During the past 40 years, the use of N fertilizers has been dramatically increasing with the increase in the global population and the higher agricultural demand (Gastal *et al.*, 2015). However, this is causing negative effects on the environment, producing eutrophication and soil acidification, and aggravating the impact of agriculture in the environment (Zheng *et al.*, 2015). Thus, developing crops with improved N use efficiency is essential to reduce the use of N fertilizers and to promote a sustainable agriculture in the scope of climate change. Several studies have reported an increase in the size of the root system under mild N deficiency in Arabidopsis, but severe N deficiency has shown to cause a significant inhibition of root growth (Figure 1.7; Gruber *et al.*, 2013; Giehl & von Wirén, 2014; Conesa *et al.*, 2020). Increases in root growth have also been reported in crops such as maize and rice as a consequence of N deficiency (Shi *et al.*, 2015; Sun *et al.*, 2020). In maize, mild N deficiency causes a reduction in the number of lateral roots but an increase in the length of the upper lateral roots and crown roots (Gao *et al.*, 2015; Li *et al.*, 2015a). In barley, comparative analyses of a tolerant and a sensitive cultivar showed that several traits related to root architecture, including root length, area and volume were significantly enhanced in the tolerant cultivar under low N availability (Gao *et al.*, 2023). Moreover, carbohydrate metabolism in roots is altered by N deficiency, causing a decrease in the concentration of sucrose and an increase in starch and hexoses (Aloni *et al.*, 1991).

Plants adapt their root system architecture to find areas of the soil with an adequate N supply, producing local changes in LR number and elongation (Liu & von Wirén, 2017). Nitrate ($NO_3^-$) acts a signalling molecule that regulates LR growth locally and systemically by controlling meristematic activity in the lateral root tip. $NO_3^-$ promotes root elongation via the nitrogen receptor NITRATE TRANSPORTER 1 (NRT1.1/NPF6.3), which has a dual function, suppressing LR

growth in N-starved zones and promoting LR growth in zones with higher N (Krouk *et al.*, 2010; Vidal *et* al., 2010; Mounier *et al.*, 2014; Vidal *et al.*, 2014). Under N deficiency, the transporter NRT1.1 acts as an auxin transporter reducing auxin levels in the lateral root tips and suppressing lateral root elongation. At the same time, in zones with higher N, the transcription factor ARABIDOPSIS NITRATE REGULATED 1 (ANR1) is activated, initiating a signalling cascade that promotes lateral root growth in those zones (Bouguyon *et al.*, 2016). Furthermore, roots grown under N deficiency accumulate C-TERMINALLY ENCODED (CEP) peptides, which are transported to the shoot where they bind to the C-TERMINALLY ENCODED PEPTIDE RECEPTOR 1 and 2 (CEPR1 and CEPR2), leading to the activation of signalling cascades involving the CEP DOWNSTREAM (CEPD) polypeptides, CEPD1 and CEPD2, that are directed towards the up-regulation of nitrate transporter genes in roots (Taleski *et al.*, 2018; Figure 1.5). Heterogeneous N availability in the soil can trigger the accumulation of CEP peptides in the N-starved areas of the root system. Then, these peptides trigger signalling cascades to activate nitrate transporters in the N-rich areas of the soil and restrict root growth in the poor N areas, thus ensuring an adequate N uptake for the whole plant (Tabata *et al.*, 2014; Taleski *et al.*, 2018; Roy *et al.*, 2022). Exogenous application of CEP peptides has shown to increase nutrient uptake and induce the expression of hundreds of genes, including many nitrogen transporters, LEUCINE-RICH RECEPTOR-LIKE KINASES (LRRLK) and many transcription factors (Roy *et al.*, 2022). In *M. truncatula*, exogenous application of MtCEP1 caused a suppression of lateral root growth mediated by COMPACT ROOT ARCHITECHTURE 2 (CRA2), a CEPR1 ortholog (Mohd-Radzman *et al.*, 2016). Trans-zeatin has also shown to act as a signalling molecule that controls lateral root growth in areas with a higher N supply (Poitout *et al.*, 2018). Under low N, ISOPENTHENYL TRANSFERASES (IPTs) mediate the accumulation of trans-zeatin in roots and translocation from roots to shoots, activating a signalling cascade from shoots to roots that promotes lateral root elongation in the N-rich areas of the soil (Jia & von Wirén, 2020).

Hormonal regulation plays a role in the root responses to low N availability as well. Although the mechanisms underlying the increases in root elongation under N deficiency are not well known, several plant hormones have shown to participate in the process, such as auxin, ABA, ethylene, cytokinin, brassinosteroids and strigolactones (Figure 1.5; Takatsuka & Umeda, 2014; Pacifici *et al.*, 2015; Steffens & Rasmussen, 2016). For example, an increase in auxin transport from shoot to

root under N deficiency has been reported in maize (Caba *et al.*, 2000; Liu *et al.*, 2010). Auxin is involved in many processes related to root growth and development, including cell division and elongation in the root tip and LR formation in Arabidopsis (Du & Scheres, 2018). Furthermore, in Arabidopsis, oscillatory gene patterns regulated by auxin accumulation and the root clock prime a group of cells along the primary root that constitute the initiation sites for lateral roots (Moreno-Risueño *et al.*, 2010). This oscillatory expression pattern is controlled by the auxin transcription factors ARF7, IAA18 and IAA28 (Perianez-Rodriguez *et al.*, 2021). Then, apart from the meristem, auxin mediates the degradation of the IAA14/SOLITARY ROOT (SLR) repressor to trigger the activation of cell division in founder cells to initialize the formation of lateral root primordia (Guseman *et al.*, 2015). In response to N deficiency, auxin has also shown to be synthesized in roots or transported from shoots to roots, where interacts with other hormones and triggers complex signalling pathways that contribute to root elongation (Sun *et al.*, 2020). Another mechanism of response to N deficiency involves the nitrate transporter NITRATE TRANSPORTER 2 (NRT2.1), that can bind the auxin transporter PIN-FORMED 7 (PIN7) and antagonize its activity to regulate the primary root elongation (Wang *et al.*, 2023e). Increased auxin levels can also stimulate the production of NITRIC OXIDE (NO), which increases the production of strigolactones, leading to an accelerated cell division (Sun *et al.*, 2020). High N has also shown to produce an increase in cytokinins, which can antagonize auxin signalling, and this auxin/cytokinin balance ultimately modulates LRs formation and root growth (Mi *et al.*, 2008; Tian *et al.*, 2005). Increases in ethylene have shown to correlate with a reduction in root elongation in several crops (Alarcón *et al.*, 2009; Ma *et al.*, 2014; García *et al.*, 2015). In Arabidopsis, high N increases the production of ethylene due to an increase in the expression of the genes encoding for ACC OXIDASE (ACO) and ACC SYNTHASE (ACS), leading to a strong reduction of root growth (Tian *et al.*, 2009). Furthermore, the same study demonstrated that ethylene can reduce nitrate uptake by roots, since ethylene can negatively regulate the expression of the nitrate transporters *NRT1.1* and *NRT2.1* in Arabidopsis. Increased cytokinins caused by high N can also stimulate the production of ethylene and contribute to the suppression of root growth (Sun *et al.*, 2020). In Arabidopsis and *Medicago truncatula*, nitrate increases ABA levels in roots and positively regulates root elongation by enhancing cell division in the meristem (Morere-Le Paven *et al.*, 2011; Ondzighi-Assoume *et al.*, 2016). In Arabidopsis, N deficiency led to variations in the transcript levels of *DWARF 1 (DWF1)*, a gene involved in brassinosteroid

biosynthesis and increase the transcript levels of other brassinosteroid-related genes like *DWARF 4 (DWF4)* and *BRASSINOSTEROID-6-OXIDASE 2* (*BR6OX2*) (Jia *et al.*, 2020). Moreover, exogenous application of brassinosteroids increases the number and length of lateral roots under N deficiency (Al-Mamun *et al.*, 2024). This study also demonstrated that plants with mutations in the transcription factors *BRASSINAZOLE-RESISTANT 1 (BZR1)* and *BRASSINAZOLE-RESISTANT 2 (BES1/BZR2)*, which regulate brassinosteroid signalling, showed larger meristems with a higher number of meristematic cells under N deficiency.

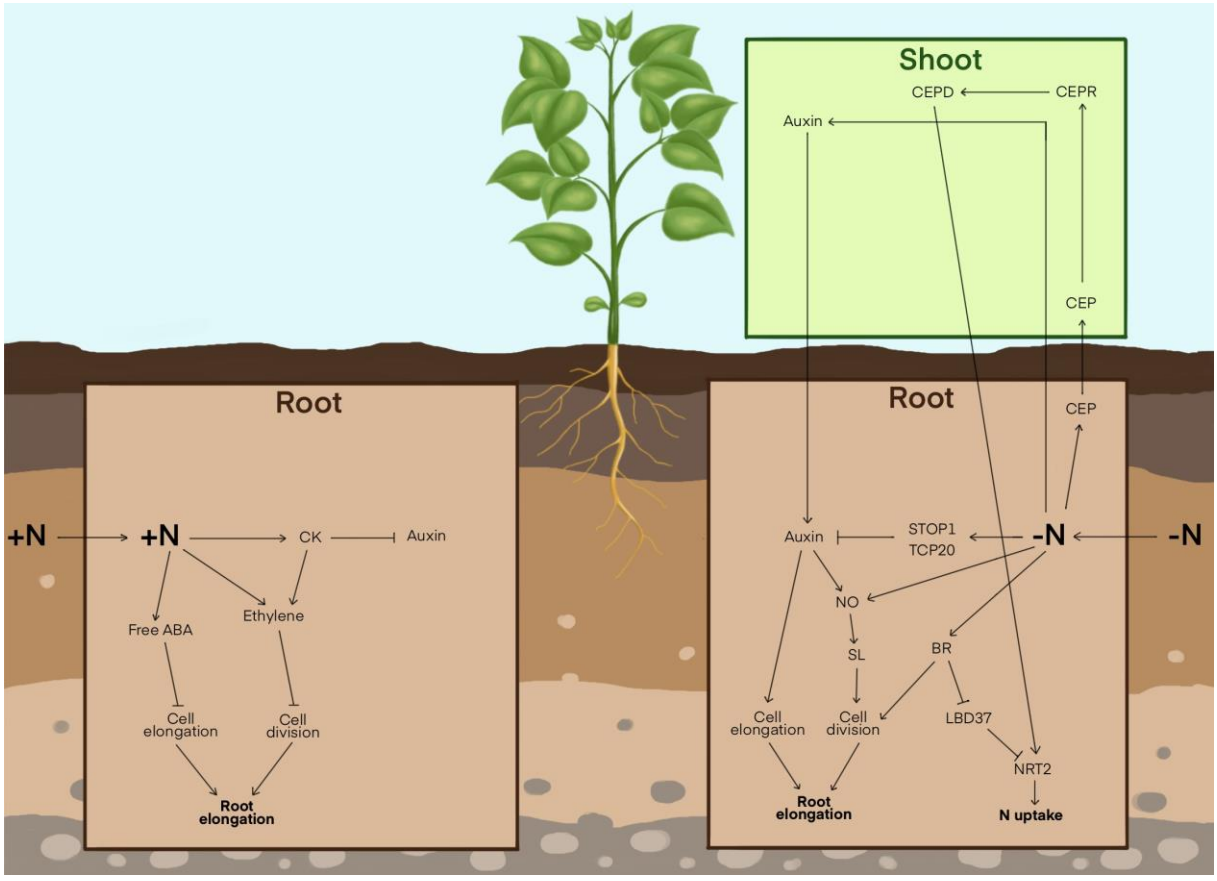


Figure 1.5: Hormonal signalling under high N (left) and N deficiency (right) in roots. High N can stimulate the production of abscisic acid (ABA), ethylene and citokinins (CK), leading to a suppression of root elongation. N deficiency causes the accumulation of CEP peptides in roots, which are transported to shoots and bind to CEPR receptors. This activates a signalling cascade involving CEPD polypeptides that ends up activating nitrate transporters such as NRT2 in roots. Low N availability also leads to decreased N status in shoots, which triggers auxin transport from shoots to roots. Auxin interacts with many other hormonal pathways in roots, involving nitric oxide (NO) and strigolactones (SL), contributing to root elongation. Low N availability can also stimulate brassinosteroid (BR) and nitric oxide (NO) signalling, which ultimately contribute to root elongation.

Several transcription factors have been associated to the root responses to N deficiency. LATERAL ORGAN BOUNDARY DOMAIN (LBD) transcription factors such as *LBD37*, *LBD38* and *LBD39*, as well as NIN-LIKE PROTEIN (NLP) transcription factors like *NLP6* and *NLP7* are implicated in the activation of N transporter genes (Rubin *et al.*, 2009; Marchive *et al.*, 2013; Konishi & Yanagisawa, 2013). The transcription factors *SENSITIVE TO PROTON RHIZOTOXICITY 1 (STOP1)* and *TCP DOMAIN PROTEIN 20 (TCP20)* have shown to regulate the expression of *NRT1.1* in response to N deficiency and ultimately affect lateral root growth (Tokizawa, *et al.*, 2023). In poplar, the NAC transcription factor *PtaNAC1* and the ERF transcription *factor RELATED TO AP2.11 (PtaRAP2.11)* are important for the regulation of the root responses to N deficiency (Dash *et al.*, 2015). In rice, the transcription factors *ZINC TRANSPORTER 11 PRECURSOR (OsbZIP11)* and *RNASE L INHIBITOR PROTEIN 1 (OsRLI1)* play a relevant role on the regulation of the root responses to N deficiency (Ueda *et al.*, 2020b). Conversely, a mutation in rice *SHORTROOT 2 (OsSHR2)* causes an increase in the sensitivity to N deficiency, with reductions in root growth and root meristem size, accompanied by changes in N distribution and a strong reduction in yield (Hu *et al.*, 2024). In Arabidopsis, *NITRATE-INDUCIBLE GARP-TYPE TRANSCRIPTIONAL REPRESSOR 1 (NIGT1)* and *DOF ZINC FINGER PROTEIN 1.7 (DOF1.7)* regulate the expression of nitrogen transporters like *NRT2.1*, *NRT2.4* and *NRT2.5* under N deficiency (Zhou *et al.*, 2024).

Root responses to N deficiency are also epigenetically regulated. This regulation includes DNA methylation, histone modifications and regulation by small RNAs. Histone modifications play a role in the regulation of N uptake in dicot plants, like methylations on the histone H3 (H3K36me3 or H3K27me3; Li *et al.*, 2015b; Zhang *et al.*, 2023a). Modifications in H3K36me3 lead to the activation of genes involved in N metabolism under N deficiency, thus enhancing N uptake, whereas methylation of H3K27me3 downregulates *NRT2.1* in Arabidopsis under high N (Zhang *et al.*, 2023a). The Arabidopsis histone methyltransferase SET DOMAIN GROUP 8 (SDG8) has shown to trigger N-dependent transcription reprogramming, regulating the expression of genes like *NRT2.1*, *NRT1.5* and *GLN1.4* (Li *et al.*, 2015b). miRNAs also play a role in root responses to low N availability. In Arabidopsis, *miRNA169* is down-regulated under N deficiency, and this indirectly down-regulates *AtNRT2.1* (Zhao *et al.*, 2011). In rice, N deficiency leads to the accumulation of *miR444a,* which causes a reduction on lateral root

growth via binding to the transcription factor ANR1 (Yan *et al.*, 2014). In dicots, high N induces the activity of several miRNAs involved on root elongation and N uptake, such as *miR393* (Vidal *et al.*, 2010), *miR167* (Gifford *et al.*, 2008) and *T5120* (Liu *et al.*, 2019a).

Additionally, the nitrogen transporters *AMMONIUM TRANSPORTER (AMT) AtAMT1;1* and *AtAMT1;3* can be post-translationally regulated by phosphorylation, which supresses the activity of these transporters under high N supply (Yuan *et al.*, 2013). Conversely, *AtNRT1.1/NPF6.3* is phosphorylated in response to low N, increasing the affinity of the transporter (Ho *et al.*, 2009). Under high N supply, AtNRT2.1 can also be post-translationally inactivated by phosphorylation, C-terminal cleavage or dimer disruption (Wirth *et al.*, 2007; Yong *et al.*, 2010; Engelsberger & Schulze, 2012).

In *B. napus*, N deficiency has shown to cause an overall increase in root depth due to an increase in cell division and cell expansion in the primary root (Qin *et al.*, 2019; Vazquez-Carrasquer *et al.*, 2021; Table 1.1). Louvieaux *et al.* (2020) found variation in the root responses to N deficiency among different *B. napus* genotypes and observed increases in the length of the primary root and lateral roots but not in the lateral root density. Further proteomic analysis showed that N deficiency causes an increase in the expression of cell-wall related proteins such as EXPANSINS (EXPs) and proteins involved in the synthesis of cellulose and chitin of cell walls, such as CELLULOSE SYNTHASE 1 and 3 (CESA1 and 3) and CHITINASE-LIKE PROTEIN 1 (CTL1/POM1), and a decrease in the expression of many peroxidases (Qin *et al.*, 2019). N deficiency also increases the accumulation of flavonoids and sugars in roots and decreases the amount of some phytohormones such as salicylic acid and zeatin (Shen *et al.*, 2022). Transcriptomic analysis revealed that genotypes with higher N use efficiency tend to increase the expression of several N transporters in roots, especially *BnNRT2.1* (Li *et al.*, 2020b). Furthermore, they found variations in the expression profiles of several glutamine synthetase (*BnGLN1*) genes. *B. napus* contains 16 *BnGLN1-like* genes that encode for different isoforms of glutamine synthetase, and the exposure to different N levels in the medium induce the expression of different *BnGLN1* isoforms in different tissues (Orsel *et al.*, 2014). For example, *BnGLN1.2* is induced by high N in roots, whereas *BnGLN1.4* is induced under N starvation in both root and shoot. In Arabidopsis, *AtGLN1.4* is known to be expressed in the root pericycle upon N deficiency (Ishiyama *et al.*, 2004). Finally, ethylene seems to play a role on N uptake by roots in *B. napus*. Inhibition of ethylene biosynthesis causes an

increase in root elongation, accompanied by an increase in N uptake, whereas treatment with ACC, a precursor of ethylene biosynthesis, severely suppresses root growth. Interestingly, an increase in N uptake is also observed after treatment with ACC as a compensatory mechanism for the reduction in root growth, by increasing the expression of the nitrogen transporters *BnNRT1.1* and *BnNRT2.1* (Lemaire *et al.*, 2013).

## 1.7. Effects of phosphate deficiency in the root system.

Phosphorous (P) is an essential macronutrient for plant growth and development, and is necessary for the biosynthesis of nucleic acids, ATP or phospholipids among other molecules (Crombez *et al.*, 2019). Inorganic phosphate (Pi) is the only form of phosphate that can be assimilated by plants. Due to mineralization and precipitation events, the amount of free Pi in cultivated soils is usually low for plant growth and development and consequently, many agricultural systems rely on massive exogenous Pi fertilization (López-Arredondo *et al.*, 2014). However, the efficiency of Pi fertilization is low since most of the supplied Pi is not absorbed by the plant, causing a rapid Pi immobilization and transformation into different salt forms, or consumption by the soil microbiota (Johnston *et al.*, 2014). Thus, improving crops to enhance tolerance to Pi deficiency or to achieve a higher Pi absorption and utilization efficiency is essential for agricultural productivity.

The root system is highly plastic to Pi availability, and roots can trigger various signalling pathways to adapt to different levels of this nutrient (López-Arredondo *et al.*, 2014), including the suppression of the primary root growth in favour of promoting LR formation and growth (Crombez *et al*, 2019). In Arabidopsis, Pi starvation tends to cause a significant reduction of the primary root growth, accompanied by a reduction in cell division and an impairment of the function of the quiescent centre (Sánchez-Calderón *et al.*, 2005; Reymond *et al.*, 2006). Despite of the reduction in the length of the primary root, an induction in lateral root growth has been commonly observed as an adaptation response to Pi deficiency in Arabidopsis (Dong *et al.*, 2017; Jia *et al.*, 2017). Genotypes that are able to promote LR formation under Pi starvation show higher Pi uptake rates due to an increase in the number of lateral root tips, which are crucial regions for Pi uptake and absorption (Figure 1.7; Lynch, 2011; Kanno *et al.*, 2016), and tend to improve their overall fitness under Pi starvation.

PHOSPHATE RESPONSE (PHR) transcription factors belong to the MYB-CC family of transcription factors, which are characterized by having two domains: the MYB domain, which is involved on DNA binding, and the coiled-coiled (CC) domain, which is involved on dimer formation (Bustos *et al.*, 2010; Zhou *et al.*, 2021; Wang *et al.*, 2024b). These TFs play a central role in the root response to Pi starvation (Rubio *et al.*, 2001; Bustos *et al.*, 2010). In Arabidopsis, PHR1 can activate the transcription of Pi-starvation responsive (PSI) genes by binding to the PHR1-binding site (P1BS) sequence in the promoter of those genes (Castrillo *et al.*, 2017). Under Pi sufficiency, SPX DOMAIN GENE 1 (SPX1) interacts with PHR1, forming a complex that blocks the transcriptional activity of PHR1 (Figure 1.6). This interaction is favoured by inositol pyrophosphate 8 (InsP8), a metabolite that acts as a molecular glue for both proteins. Under Pi deficiency, the levels of InsP8 drop, leading to the release of PHR1, which consequently activates the transcription of PSI genes (Dong *et al.*, 2019). This mechanism has also been described in rice, where OsSPX1 binds OsPHR2, and this binding is mediated by InsP6. Under Pi starvation, the reduction of InsP6 levels releases the complex, and PHR2 proteins form dimers that bind the promoter sequences of PSI genes to activate their transcription (Zhou *et al.*, 2021).

The Pi-starvation dependent increase in LR growth has been correlated with an increase in auxin signalling in the primary root tip and lateral root primordia (Figure 1.6). This higher auxin activity is mediated by an increase in the expression of *TRANSPORT INHIBITOR RESPONSE 1 (TIR1)*, an auxin receptor that is a gene target for PHR1 (Pérez-Torres *et al.*, 2008; Castrillo *et al.*, 2017). *TIR1* is involved in the activation of several ARFs and Aux/IAA proteins that contribute to LR initiation. Moreover, several ARF transcription factors, such as *ARF7* and *ARF19,* which are involved in LR initiation, are PHR1 targets (Castrillo *et al.*, 2017). These data suggest that the initiation of LR growth triggered by Pi starvation is auxin dependent. PIN transporters are crucial for auxin distribution and play an important role in the proper development and patterning of the primordium during lateral root formation (Xu *et al.*, 2005), and they have shown to be important in the root response to Pi deficiency, ensuring a correct lateral root development. Consequently, some of them have shown to be PHR1 targets (Wang *et al.*, 2009; Castrillo *et al.*, 2017). This increase in LR number constitutes an adaptative response to increase Pi uptake, since it magnifies the root surface area in the upper parts of the soil where Pi tends to accumulate.

In addition, Pi starvation increases the level of the Pi transporters PHOSPHATE TRANSPORTER 1;1 and 1;4 (PHT1;1 and PHT1;4) in the epidermis and in the lateral root caps (Figure 1.6). Interestingly, these transporters are highly expressed in the lateral root caps, a region located in the tips of the lateral roots that has shown to be particularly effective for Pi uptake (Shin *et al.*, 2004; Nussaume *et al.*, 2011). Whereas the increase in LR formation caused by Pi deficiency is dependent on PHR1, the decrease in the growth of the primary root caused by Pi deficiency does not seem to be PHR1-dependent (Svistoonoff *et al.*, 2007). Thus, Pi deficiency seems to alter Fe homeostasis in roots, causing the conversion from $Fe^{2+}$ to $Fe^{3+}$ via the LOW PHOSPHATE ROOT1 and 2 (LPR1 and LPR2) oxidases, which in turn causes the accumulation of $Fe^{3+}$ in the stem cell niche and leads to an increase in ROS production and the cessation of the meristematic activity (Figure 1.6). This effect disturbs the activity of SHR and SCARECROW (SCR), which results in a decreased expression of *WUSCHEL RELATED HOMEOBOX 5 (WOX5)*, leading to a suppression of the primary root growth (Crombez *et al.*, 2019). The molecular mechanisms described above are only present under Pi starvation, but not under optimal Pi and high Fe, thus constituting a response that is exclusive to Pi starvation (Muller *et al.*, 2015). Pi starvation can also induce the ALUMINIUM-ACTIVATED MALATE TRANSPORTER (ALMT1) and MULTI-DRUG AND TOXIC COMPOUND EXTRUSION (MATE), which are malate and citrate efflux channels that secrete organic acids to the apoplast to solubilize insoluble forms of Pi (Mora-Macías *et al.*, 2017). Because malate can form a complex with $Fe^{3+}$, the formation of ROS is also favoured by an accumulation of malate in the apoplast of the cells that are located in the inner layers of the root, thus contributing to the inhibition of the primary root growth (Figure 1.6). Furthermore, STOP1, a Cys2His2-type zinc finger transcription factor (Iuchi *et al.*, 2007), has shown to directly regulate the expression of *LPR1* and *LPR2*, constituting a new PHR-independent signalling pathway for the root responses to Pi starvation (Balzergue *et al.*, 2017; Mora-Macías *et al.*, 2017).

Apart from Fe-mediated signalling, other mechanisms also play a role in the inhibition of the primary root growth under Pi starvation, such as hormonal signalling. For instance, cytokinins have shown to be repressors of *WOX5* and *SCR* (Zhang *et al.*, 2013b), and in turn, some cytokinin-related genes involved on root growth have shown to be PHR1 targets, such as *RESPONSE REGULATOR 12 (ARR12*; Crombez *et al.*, 2019). Ethylene is another hormone that seems to play a

role on the suppression of the primary root growth. Interestingly, ethylene inhibitors can reverse the primary root growth inhibition caused by Pi deficiency (Chacón-López *et al.*, 2011). Some ethylene related genes, such as *ERF1* and *ETHYLENE-INSENSITIVE3-LIKE 1 (EIL1)* are PHR1 targets (Figure 1.6; Castrillo *et al.*, 2017), suggesting that PHR1 might also play a role in the inhibition of the primary root growth (Crombez *et al.*, 2019). Additionally, Fe accumulation in the primary root tip has shown to induce the BRASSINOSTEROID KINASE INHIBITOR 1 (BKI1), which inhibits BZR1, and BZR1 acts as a regulator of *LPR1*, suggesting a role of brassinosteroids on the Fe-dependent inhibition of the primary root growth under Pi deficiency (Singh *et al.*, 2018). Lastly, exogenous gibberellin treatment has shown to further enhance the primary root growth inhibition under Pi starvation (Jiang *et al.*, 2007).

Finally, Pi starvation has shown to induce root hair growth by increasing the number of trichoblasts and enhancing root hair length (Janes *et al.*, 2018). Furthermore, Pi starvation induces *ROOT HAIR DEFECTIVE 6-LIKE 4 (RSL4)*, a transcription factor involved in root hair formation, and the expression of *RSL4* depends on LPR1 and LPR2, suggesting a Fe-dependent regulation of these genes (Figure 1.6; Yi *et al.*, 2010; Datta *et al.*, 2015). Some *PHR1* gene targets have also shown to participate in root hair development, such as *ROOT HAIR DEFECTIVE 2 (RHD2)* and *ROOT HAIR SPECIFIC 19 (RHS19)*, suggesting that PHR1 also regulates root hair development under Pi-starvation (Won *et al.*, 2009; Salazar-Henao, *et al.*, 2016). Auxin has shown to play an important role on the Pi-starvation induced root hair development. For instance, several auxin response factors, like ARF5, ARF7, ARF8 and ARF19 can induce *RSL4* as well (Velasquez *et al.*, 2016; Mangano *et al.*, 2017). Moreover, ARF7 and ARF19, which are expressed in root hair cells, are major PHR1 targets and can induce both *RSL2* and *RSL4* under low Pi (Figure 1.6; Pacheco *et al.*, 2023). Ethylene-dependent signalling increases as a response to Pi deficiency, activating the transcription factor ETHYLENE-INSENSITIVE 3 (EIN3), which in turn induces *RSL4* and other genes involved in root hair growth (Song *et al.*, 2016). The transcription factor GLABRA2 (GL2) is crucial for root hair development and its down-regulation triggers *RHD6*, thus inducing *RSL4* and contributing to the formation of root hairs (Balcerowicz *et al.*, 2015). Pi starvation could induce *ALFIN-LIKE 6 (AL6)*, which downregulates *ENHANCER OF TRIPTYCHON AND CAPRICE1 (ETC1)*, leading to the downregulation of *GL2* and contributing to root hair development (Figure 1.6; Crombez *et al.*, 2019).

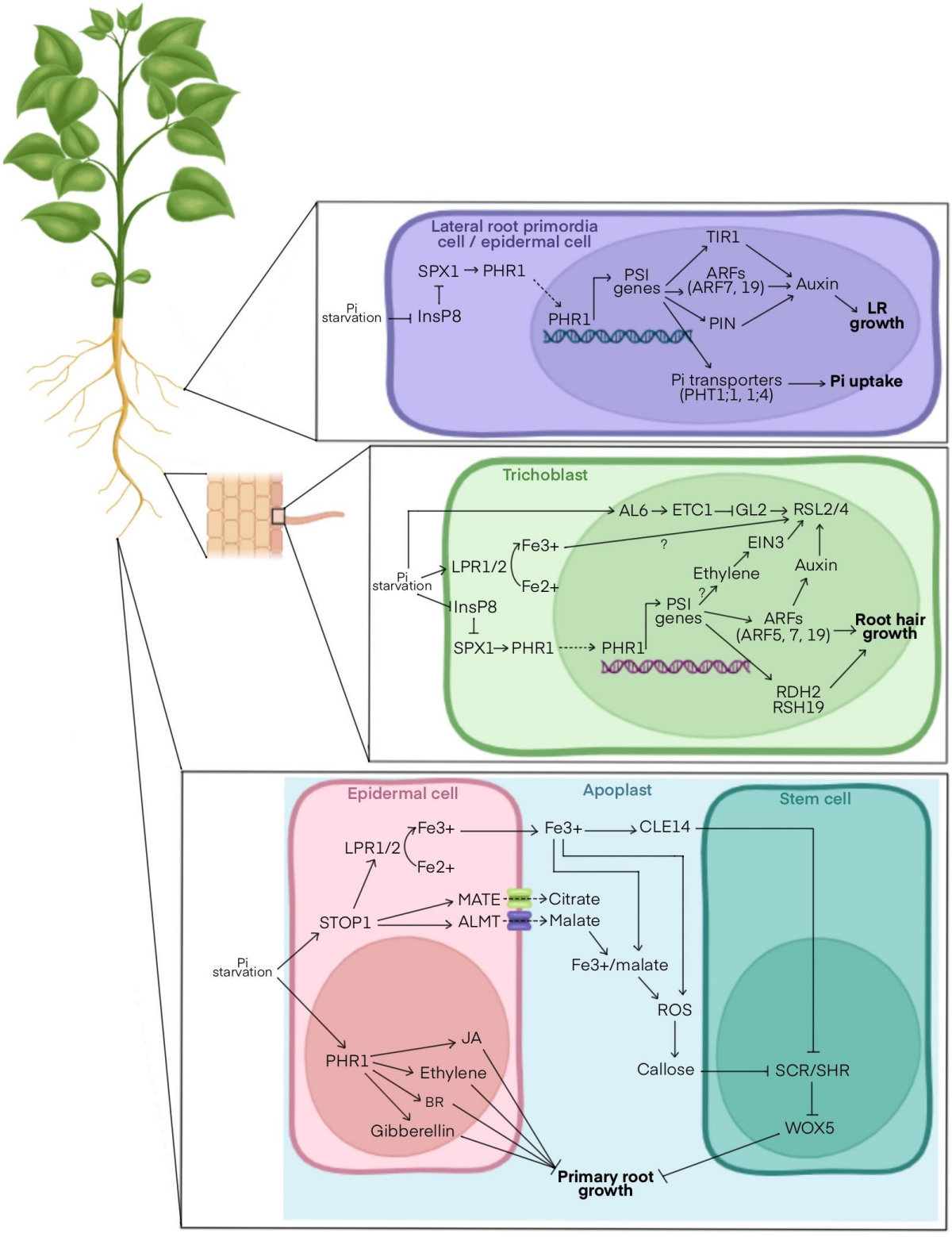


Figure 1.6: Overview of the main signalling pathways controlling the root responses to Pi deficiency. The model summarizes the three most important mechanisms contributing to root adaptation to Pi deficiency: increased lateral root growth (upper box), increased root hair development (middle box) and reduction of the primary root growth (bottom box). The molecular pathways contributing to each of these mechanisms are described at a cellular level.

In *Brassica napus*, reductions in the primary root growth have been observed under Pi deficiency, and they are accompanied by an increase in the root/shoot ratio, due to the distribution of carbohydrates to roots (Table 1.1; Yuan *et al.*, 2016b; Duan *et al.*, 2020). Furthermore, roots from *B. napus* plants grown under low Pi tend to secrete more acid phosphatase to solubilize organic phosphate and organic acid to solubilize insoluble forms of phosphate than plants grown at optimal Pi (Duan *et al.*, 2020; Zhang *et al.*, 2024). They also tend to have an increased activity of antioxidant enzymes such as CAT, SOD, APX, GLUTATHIONE PEROXIDASE (GPX) and GLUTATHIONE REDUCTASE (GR) to mitigate the damaging effects of excessive ROS levels (Chen *et al.*, 2015a). Moreover, variation in the response to Pi deficiency has been described among different *B. napus* genotypes, with the more Pi use-efficient genotypes developing more and longer lateral roots and reducing their lipid peroxidation activity (Hu *et al.*, 2010b; Chen *et al.*, 2015b). Pi use-efficient genotypes tend to grow a larger root system, with more efficient Pi uptake, a higher ATPase activity and greater exudation of carboxylates than Pi-inefficient genotypes (Zhang *et al.*, 2011). Pi deficiency also causes a decrease in the concentration of several ions in roots of *B. napus*, but an increase in the amount of Fe (Wang *et al.*, 2020a). Overexpression of the *B. napus* transporter *BnPHT1;4* in Arabidopsis roots has shown to increase Pi uptake and modify root architecture (Ren *et al.*, 2014). Pi starvation caused an induction of several JA-related genes in *B. napus* roots, including *JASMONATE-ZIM-DOMAIN PROTEIN (JAZ)* and *LIPOXYGENASE (LOX)* genes, as well as an induction of many ABA-related genes and genes related to sugar metabolism (Li *et al.*, 2022b). JA has also shown to induce the expression of many Pi starvation-induced genes in *B. napus,* suggesting a role of this hormone in the root responses to Pi deficiency (Li *et al.*, 2023). Interestingly, the PHR1-dependent Pi starvation response characterized in Arabidopsis and rice described above might be conserved in *B napus*. Thus, a total of 69 *SPX* genes have been recently identified and characterized, which contain a PB1S sequence in their promoters and are induced by Pi starvation (Du *et al.*, 2017). Furthermore, one PHR member has been recently identified as a transcription activator that seems to be involved in the Pi deficiency response in roots of *B. napus*, and its overexpression in Arabidopsis leads to the activation of many PSI genes, such as *ACYL CARRIER PROTEIN 5 (ACP5)*, *INDUCED BY PHOSPHATE STARVATION 1 (IPS1)*, *ARABIDOPSIS THALIANA PHOSPHATE TRANSPORTER 1* and *2 (ATPT1* and *ATPT2*; Table 1.1; Ren *et al.*, 2012).

## 1.8. Effects of elevated temperatures combined with nutrient (nitrogen or phosphate) deficiency in the root system.

Climate change is affecting soil fertility and the ability of plants to acquire and utilize nutrients, worsening the already existing challenges for crop production (St. Clair & Lynch, 2010). Even though some works have shown that heat stress reduces nutrient content in plant tissues and diminishes the activity of enzymes involved in nutrient metabolism (Klimenko *et al.*, 2006; Heckathorn *et al.*, 2013; Hungria & Kaschuk, 2014), there is limited information concerning the effects of elevated temperatures combined with nutrient deficiencies on root growth and development. In Norway spruce, heat stress leads to changes in the distribution of the root system, and reduces root diameter and growth, leading to decreased nutrient uptake (Lahti *et al.*, 2005). However, the impact of high temperature on nutrient uptake varies depending on the type of nutrient and the crop. High temperatures usually impair the ability of the plant to acquire and utilize nitrogen (Figure 1.7). In tomato, increases in soil temperature limit root growth and nitrogen absorption, and cause a reduction in the activity of nitrogen uptake-related proteins in roots (Tindall *et al.*, 1990; Giri *et al.*, 2017). Heat stress also reduces nitrogen fixation in alfalfa root nodules (Munns *et al.*, 1977), while nitrogen deficiency alone increases the expression of genes encoding for HSPs in poplar (Song *et al.*, 2019). Conversely, exogenous application of nitrogen can alleviate heat stress symptoms in bentgrass, increasing the activity of antioxidant enzymes like SOD, APX and GUAIACOL PEROXIDASE (POD) in roots (Wang *et al.*, 2012). Further research in this species shows that the combination of nitrogen deficiency and elevated temperatures increases the synthesis of HSPs more significantly than high temperature stress alone (Wang *et al.*, 2014a). Higher root-zone temperatures combined with nitrogen deficiency in pepper cause an increase in the amount of phenolic compounds, a decreased activity of nitrate reductase, and a reduced leaf photosynthetic capacity (Sheibanirad *et al.*, 2023). In *B. napus*, a field study showed that temperature has a strong impact on N absorption and mineralization, having different effects along the year (Villar *et al.*, 2019). However, the effects of the combination of high temperatures and nitrogen deficiency in crops, including *B. napus*, are still limited (Figure 1.7).

Table 1.1: Effects of high temperature, N deficiency and Pi deficiency in the root system of *B. napus*.

| Effects of high temperature stress | Effects of N deficiency | Effects of Pi deficiency |
|---|---|---|
| ○ Short term heat stress increases the length, size and extension of the root system (Boter *et al.*, 2023).<br>○ Long term heat stress decreases root length, area, volume, and supresses lateral root growth (Wu *et al.*, 2020b).<br>○ Increases in N and C exudation by roots (Delamare *et al.*, 2023).<br>○ Variation in the response among different genotypes: differences in root growth and development, changes in cell division and elongation rates and differences in gene expression (Boter *et al.*, 2023). | ○ Increase in root elongation due to enhanced cell division (Qin *et al.*, 2019).<br>○ Increase in the amount of flavonoids and sugars (Shen *et al.*, 2022).<br>○ Reduction in ethylene that mediates the elongation of the root system and enhances N uptake (Lemaire *et al.*, 2013).<br>○ Variation in N use efficiency among different genotypes: a better N use efficiency is correlated with higher activities of NRT2.1 and GLN1 (Orsel *et al.*, 2014). | ○ Reduction in the elongation of the primary root (Yuan *et al.*, 2016b; Duan *et al.*, 2020).<br>○ Increase in the distribution of carbohydrates to the root (Yuan *et al.*, 2016b; Duan *et al.*, 2020).<br>○ Increase in the activity of antioxidant enzymes (CAT, SOD, APX, GPX and GR; Chen *et al.*, 2015a).<br>○ Increase in the amount of Fe (Wang *et al.*, 2020a).<br>○ Induction of several JA- related genes (JAZ and LOX), ABA-related genes and genes related to sugar metabolism (Li *et al.*, 2022b).<br>○ Conservation of the PHR1-dependent response to Pi starvation (Ren *et al.*, 2012; Du *et al.*, 2017).<br>○ Variation in the response among different genotypes: tolerant genotypes displaying more and longer lateral roots, enhanced Pi uptake and lower levels of lipid peroxidation (Hu *et al.*, 2010b; Chen *et al.*, 2015b). |

The effects of elevated temperatures combined with phosphate deficiency in roots are largely unknown as well. In barley, heat stress causes a strong down-regulation of many PSI genes in roots such as *PHT1;1*, *PHT1;4*, *PHT1;6*, *PHOSPHATE 1* and *2 (PHO1* and *PHO2)* and several *SPX* genes (Figure 1.7). However, despite this down-regulation of Pi transporters, the levels of free cellular Pi in roots are unaltered, possibly due to the down-regulation of *PHO1* and *PHO2*, which are responsible for Pi transport from roots to shoots (Pacak *et al.*, 2016). Furthermore, overexpression of the wheat *TaHsfA2d* in Arabidopsis worsens the root responses to Pi deficiency by suppressing LR growth and reducing Pi uptake. This suggests that *TaHsfA2d* can cause a negative regulation of the Pi starvation responses, thus enhancing the sensitivity to Pi starvation (Zhao *et al.*, 2022). In

maize, high temperatures cause a slight reduction in the uptake of several nutrients, including phosphorous (Bravo-F and Uribe, 1981; Bassirirad, 2000). In Arabidopsis, heat stress causes changes in the expression of genes related to the plant ionome, some of them involved on Pi acquisition and transport, such as *PHT1;1*, *PHT1;4*, *PHT1;5* and *PHT1;9*, as well as the down-regulation of the transcription factors *PHR1*, *PHR1-LIKE 1 (PHL1)* and *PHO2*, which regulate Pi transport to the xylem (González-García *et al.*, 2023). The same study demonstrated that high temperatures can cause a reduction in the levels of free cellular Pi in shoots and roots (Figure 1.7).

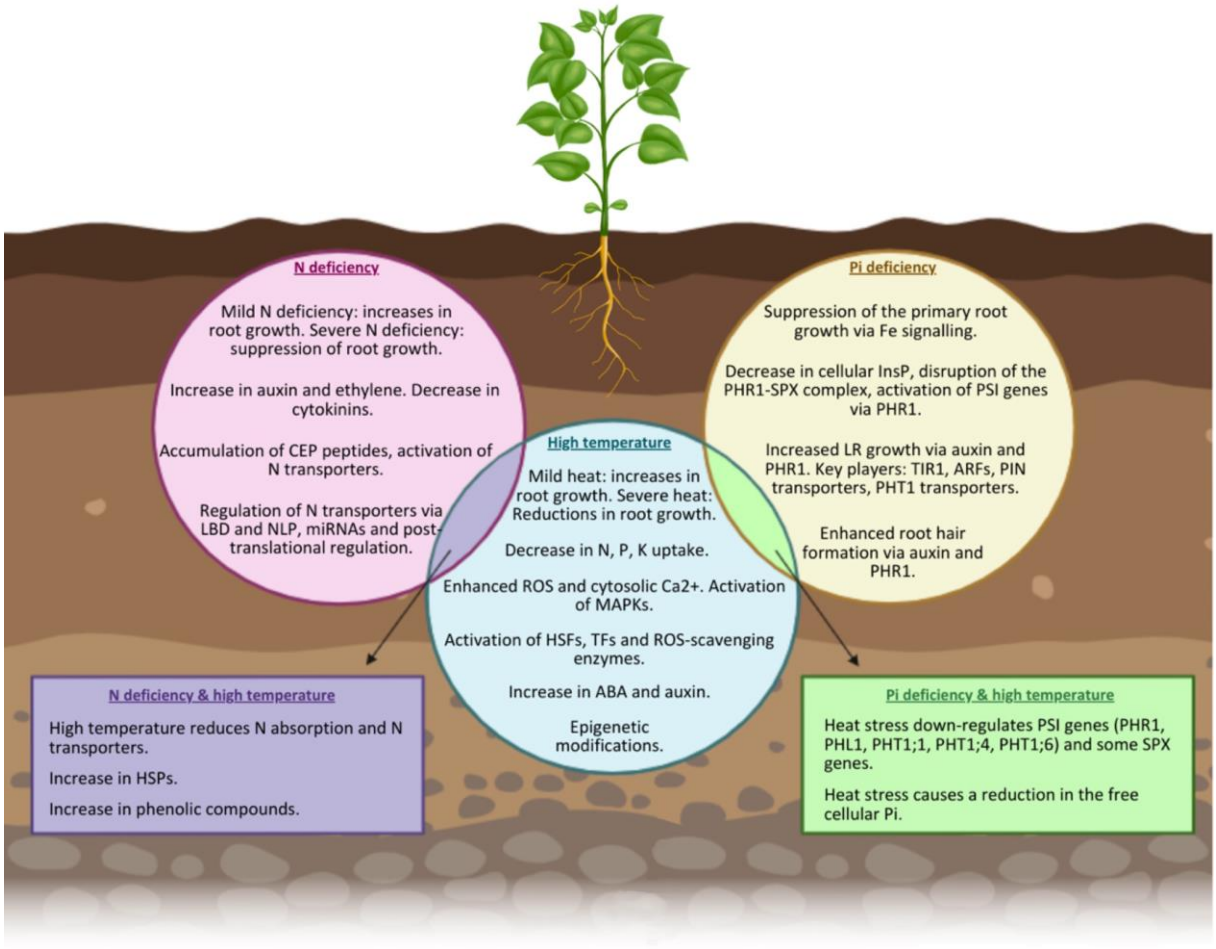


Figure 1.7: Overview of the effects of individual abiotic stresses and stress combinations studied in this thesis in the root system.

Given that most arable land is nutrient-poor and temperatures are expected to continue increasing in the coming years, crops are likely to face both heat stress and nutrient deficiencies simultaneously in the future. Therefore, it is crucial to deepen our understanding of the plant responses to this stress combination to

address this emerging challenge effectively. Furthermore, since most research has focused on shoot responses to abiotic stresses, our approach focused on the study of the root system could provide novel solutions for adaptation to abiotic stress combinations.

# 2. OBJECTIVES

The increase in the frequency of abiotic stresses caused or exacerbated by climate change constitutes a threat to crop productivity and food security. Furthermore, many models predict that global temperatures will continue increasing in the next years, worsening the effects of climate change on crop production. In the past years, research has been focused on the effects of abiotic stresses on plants. However, most studies have considered the effects of abiotic stresses individually, whereas in the field abiotic stresses tend to happen in combination. Furthermore, most works have studied the effects of abiotic stresses on the above-ground parts of the plant, ignoring the role of roots in the plant responses to abiotic stresses and the potential of root improvement to enhance plant tolerance. Therefore, this research focuses on studying root responses to the combination of warm temperatures and nutrient (nitrogen or phosphate) deficiencies, using *Brassica napus* as a model, due to its high economic importance for both dietary and industrial purposes. Thus, this work has three main objectives:

1. To analyse the root responses to the combination of warm temperatures and nutritional deficiency (nitrogen and phosphate) in *B. napus*.
2. To identify *B. napus* genotypes with differential root responses to the combination of warm temperatures and nutrient (nitrogen and phosphate) deficiency and to study the effects of this variation on shoot performance.
3. Identification of gene regulatory networks underlying root and shoot responses to the combination of warm temperatures and nutritional deficiency (nitrogen and phosphate) in *B. napus*.

# 3. MATERIAL AND METHODS

## 3.1. Plant material.

### 3.1.1. *Brassica napus*.

In this work, *Brassica napus* (oilseed rape / rapeseed) was used as a model crop and a total of 12 different *B. napus* spring varieties were analysed. The 12 varieties from different geographical regions and contrasting environments were a gift from Dr. Rod Snowdon (Justus Liebig University, Giessen, Germany). The names of the varieties, together with their genotype codes and countries of origin are shown in Supplementary Table 1A.

### 3.1.2. *Arabidopsis thaliana*.

We also used *Arabidopsis thaliana* as an experimental model for specific assays as indicated. We used seedlings from the ecotype Columbia (Col-0) as well as from different mutant and reporter lines. The line *pNRT2.4*::*GUS* was provided by Dr. del Pozo's lab (CBGP, Madrid, Spain. Conesa *et al.*, 2020). The DR5::LUC seedlings were provided by Dr. Miguel Ángel Moreno Risueño (CBGP, Madrid, Spain. Moreno-Risueño *et al.*, 2010). We also used five mutant lines obtained from NASC (Nottingham Arabidopsis Stock Center): *aco1* (SALK_127963C), *hb52* (GK-058A12.04), *lbd37* (SALK_057939), *nrt1.1* (SALK_138710C) and *nrt2.1-2* (SALK_035429). Additionally, we used two Arabidopsis mutant lines provided by Prof. Mingguang Lei (Shanghai Center for Plant Stress Biology, Shanghai, China): *spx3* (SALK_035262C) and *spx1spx2*, created by genetic cross between *spx1* (SALK_092030) and *spx2* (SALK_080503).

## 3.2. Growth conditions and stress treatments.

### 3.2.1. Growth conditions of *B. napus* seedlings.

*B. napus* seedlings from the 12 spring varieties were surface sterilized using a solution of 15% bleach and 0.1% Tween-20 for 15 minutes and then treated with 100% ethanol for 2 minutes, followed by three washes with sterilized water. After

that, they were sown in Petri dishes with ¼ MS medium (Murashige & Skoog medium including vitamins from Duchefa Biochemie) with 0.05% MES, pH=5.8 and plant agar 6 g/L, and posteriorly stratified at 4ºC in the dark for 3 days. Then, they were germinated at 21ºC with a 16 h photoperiod for other 3 days.

Three-day old *B. napus* seedlings were then transferred to the Pouch and Wick system (Figure 4.1), where roots were positioned between two slices of germination paper (previously submerged in medium), leaving the shoots uncovered. The two slices of germination paper were covered with two polypropylene flat covers to provide support and darkness to the root system, and the germination paper and the covers were clipped together, conforming a pouch that enables the roots to grow in a flat surface. The flat pouches were placed in rectangular pots containing 1.5L of medium (either full nutrient solution or medium with N deficiency or Pi deficiency) at the bottom. The pots with the flat pouches submerged in media were placed in two growth chambers with different temperatures (either 21ºC or 29ºC), a relative humidity of 40% and a 16h photoperiod for 7 days.

The liquid nutrient solution used in the experiments contained ¼ MS medium lacking N, P and K (Murashige & Skoog basal salt mixture without N, P and K from Phyto Technology Laboratories), supplemented with vitamins (Murashige & Skoog vitamin mixture from Duchefa Biochemie), 2mM MES and 0.312 mM of KCl (from a 0.5M KCl stock solution) as a source for potassium and the pH was adjusted to 5.8. Then, for the control treatment with optimal nitrogen and phosphate, this basal nutrient solution was supplemented with 9.84 mM of nitrogen by adding 4.69 mM of $KNO_3$ and 5.15 mM of $NH_4NO_3$ (added from a 0.5M stock solutions), and 0.312 mM of phosphate by adding $KH_2PO_4$ (from a 0.5M stock solution). The N deficiency medium was obtained by complementing the basal solution with 0.1 mM of nitrogen (0.05 mM of $KNO_3$ and 0.05 mM of $NH_4NO_3$) and 0.312 mM of phosphate ($KH_2PO_4$). The Pi deficiency medium was done by complementing the basal solution with 9.84 mM of nitrogen (4.69 mM of $KNO_3$ and 5.15 mM of $NH_4NO_3$) and 0.0025 mM of phosphate ($KH_2PO_4$).

### 3.2.2. Soil experiments in *B. napus*.

*B. napus* seedlings from the varieties Westar and Wesway were surface sterilized with a solution of 15% bleach and 0.1% Tween20 for 15 minutes, and then treated with 100% ethanol for 2 minutes, followed by three washes with sterilized water. Later, they were sown in Petri dishes on top of a sheet of filter paper previously

moisturized with 2 ml of sterilized water, and the Petri dishes were then secured with Parafilm. The seeds were stratified during 3 days in the dark and were subsequently germinated at 21ºC with a 16h photoperiod for 5 days.

Five-day old *B. napus* seedlings were transferred to pots containing different types of soil: either full fertilized soil (optimal amount of all nutrients) or N deficient soil. The basal soil was composed by a mixture of a poor substrate (unfertilized blond peat turf from Floratorf) sand and vermiculite nº3 (Projar) in a 6:2:1 proportion. The soil with optimal N was obtained by adding a fertilizer containing potassium and phosphate (from Select MKP) to achieve a concentration of 0.312 mM of phosphate and 0.312 mM of potassium and posteriorly complemented with 9.84 mM of N (ammonium nitrate from ArgiPlus). The soil with N deficiency was obtained by adding the fertilizer with potassium and phosphate (from Select MKP) to achieve the concentrations described above and with no additional nitrogen.

For soil experiments using the TGRooZ system, 3.5 L pots were placed in different chambers with a 16h photoperiod and different temperatures: either 22ºC in both root and shoot, 36ºC in both root and shoot or 36ºC in shoot with a root-zone temperature gradient in the root achieved with the TGRooZ system. The TGRooZ system creates a decreasing temperature gradient of 1.1ºC/cm as indicated by Gonzalez-Garcia *et al.* (2023).

For quantification of the total N and C content in leaves, plants were grown in 5 L pots in the CBGP's Enclosed Ecosystem Phenotyping Platform (E2P2) under different temperatures (either 24ºC or 34ºC) in chambers with 40% of relative humidity and 16h of daylight for 4 weeks.

### 3.2.3. Growth conditions of Arabidopsis lines.

For the initial experiments to assess the effects of combined elevated temperatures and N deficiency on morphological root traits, 30 individual Col-0 seedlings were grown in Petri dishes (10 seedlings each) for each temperature and N treatment as indicated for each experiment. To analyse the expression of *pNRT2.4::GUS*, 18 seedlings (6 seedlings per Petri dish) were used for each temperature and N treatment, and then were stained to check the GUS activity. For the experiments with Arabidopsis mutants (*aco1*, *hb52*, *lbd37*, *nrt1.1*, *nrt2.1-2*, *spx3* and *spx1spx2*), three Petri dishes were used for each mutant in each temperature and N treatment, and each Petri dish consisted of six mutant seedlings together with six Col-0 seedlings (18 mutant and Col-0 seedlings in total for each treatment).

Seeds from Arabidopsis Col-0, *pNRT2.4::GUS* and Arabidopsis mutants (*aco1*, *hb52*, *lbd37*, *nrt1.1*, *nrt2.1-2*, *spx3* and *spx1-2*) were surface sterilized using a 50% bleach solution for 5 minutes, followed by three washes with sterilized water. The seeds were subsequently sown in square Petri dishes with ½ MS (Murashige & Skoog basal salt mixture without nitrogen, phosphorous and potassium from Phyto Technology Laboratories), supplemented with vitamins (Murashige & Skoog vitamin mixture from Duchefa Biochemie), 0.05% MES, 1% sucrose, 10 g/L of plant agar, 0.625 mM of KCl (from a previously prepared 0.5M KCl stock solution) as a source for potassium and 0.625 mM of $KH_2PO_4$ as a source of phosphate (from a previously prepared $KH_2PO_4$ stock solution). The pH was adjusted to 5.8. The medium with optimal N was complemented with 2.5 mM of N (1.25 mM of $KNO_3$ and 1.25 mM of $NH_4NO_3$). The N deficiency medium was complemented with 0.05 mM of N (0.025 mM of $KNO_3$ and 0.025 mM of $NH_4NO_3$). The Petri dishes were then placed at 4ºC in the dark during 3 days for seed stratification. Later, the Petri dishes were transferred to the D-root system and placed at 21ºC with a 16h photoperiod for germination. After 4 days, the Petri dishes were transferred to different chambers for the different temperature treatments: 22ºC, 29ºC or 32ºC, and they were either incubated at constant root temperature or transferred to the TGRooZ system to generate a root-zone temperature gradient (from 32ºC in the surface to 24ºC in the bottom of the plate).

### 3.2.4. Growth conditions of Arabidopsis DR5::LUC seedlings.

For measurements of morphological root traits and quantification of DR5::LUC expression, 18 DR5::LUC seedlings were used for each temperature and N treatment (six seedlings per petri dish). Arabidopsis DR5::LUC seeds were surface sterilized with 50% bleach for 5 minutes followed by three washes with sterilized Milli-Q water. Consequently, seeds were sown in Petri dishes containing ½ MS without N (Murashige & Skoog modified basal salt mixture without nitrogen from Phyto Technology Laboratories), supplemented with vitamins (Murashige & Skoog vitamin mixture from Duchefa Biochemie), 0.05% MES, 1% sucrose, 10 g/L of plant agar and 0.625 mM of $KH_2PO_4$ as a source of phosphate (from a previously prepared $KH_2PO_4$ stock solution). The pH was adjusted to 5.8. The medium with optimal N concentration (2.5 mM) was completed with 2.5 mM of $KNO_3$ and 6.4 mM of KCl. The medium with mild N deficiency (0.2 mM) was completed with 0.2 mM of $KNO_3$ and 7.2 mM of KCl. The medium with mild N deficiency (0.1 mM) was completed with 0.1 mM of $KNO_3$ and 7.3 mM of KCl. The medium with

extreme N deficiency (0.05 mM) was completed with 0.05 mM of $KNO_3$ and 7.4 mM of KCl. The seeds followed a 3-day stratification at 4ºC in the dark, were transferred to the D-root system for germination, and placed in a chamber at 21ºC and 16h photoperiod for 4 days. Finally, the Petri dishes were transferred to different chambers for the temperature treatments: 22ºC or 32ºC, and were either left at constant root and shoot temperature or transferred to the TGRooZ system to generate a root-zone temperature gradient (from 32ºC in the surface to 24ºC in the bottom of the plate).

## 3.3. Microbiological material.

### 3.3.1. *Escherichia coli*. Transformation and growth conditions.

We used *Escherichia coli* (strain DH5α) for the production and selection of plasmid constructs in several experiments. For bacterial transformation, we used a heat shock protocol adapted from Inoue *et al.* (1990). Briefly, about 100-500 ng of plasmid material were added to 100 µL of competent DH5α cells and incubated on ice for 10 minutes. Then, they were heat shocked by incubation at 42ºC in a water bath for 30 seconds. After chilling on ice for 2 minutes, they were incubated on 700 µL of LB medium [1% (w/v) of tryptone, 0.5% (w/v) of yeast extract and 0.5% (w/v) of NaCL] at 37ºC in agitation for 30 minutes. After that, the culture was centrifuged at 5000 rpm for 1 minute to remove excess medium and was consequently plated in a Petri dish containing LB medium with the corresponding antibiotics for plasmid selection. Finally, the plate with the culture was incubated at 37ºC overnight to allow for colony formation.

### 3.3.2. *Agrobacterium tumefaciens*. Transformation and growth conditions.

*Agrobacterium tumefaciens* (strain GV3101) was used to transform different constructs into *N. benthamiana* leaves. For transformation of *A. tumefaciens* with the plasmids of interest, we used a heat shock protocol adapted from Lang *et al.* (2015). Briefly, about 100-500 ng of plasmid material were added to 100 µL of competent *A. tumefaciens* (GV3101) cells and incubated on ice for 10 minutes. Then, the cells followed a freeze treatment with liquid nitrogen for 30 seconds and a consequent incubation at 37ºC in a water bath for 5 minutes. After chilling on ice for 2 minutes, the cells were incubated on 600 µL of LB medium [1% (w/v) of

tryptone, 0.5% (w/v) of yeast extract and 0.5% (w/v) of NaCl] at 28ºC in agitation for 2 hours. After that, the culture was centrifuged at 5000 rpm for 1 minute and consequently plated in a petri dish containing rifampicin (50 µg/mL), necessary for growth and selection of transformed *A. tumefaciens*, and the corresponding antibiotic of the introduced plasmid. Finally, the plate was incubated at 28ºC for 2 days to allow for colony formation.

### 3.3.3. *Saccharomyces cerevisiae*. Transformation and growth conditions.

We used *Saccharomyces cerevisiae* (strain AH109) to test protein to protein interactions in a yeast-two hybrid experiment. For yeast transformation, 500 ng of each plasmid (1 µg of DNA in total) were added to *S. cerevisiae* (AH109), together with 10 µL of carrier DNA. The cells were transformed with two plasmids simultaneously, in different combinations (see Material and methods: 3.13.2). Then, the yeasts were incubated with 350 µL of polyethylene glycol/lithium acetate solution (LiAc 1x; TE 1x; ssDNA 5 µL; PEG 1x). Then, 40 µL of Dimethylsulfoxide (DMSO) were added to the reaction and the yeasts were incubated at 42ºC in a water bath for 15 minutes. After chilling on ice and centrifugation, the yeast cells were resuspended in 500 µL of Tris/EDTA (TE) and plated in Petri dishes with DOB medium (MP Biomedicals) -Trp/-Leu to select for transformants and grown for 3 days at 28ºC. Then, colonies were grown in liquid -Trp/-Leu medium for 3 days and plated in Petri dishes with selective DOB medium -Trp/-Leu/-His/-Ade and grown at 28ºC. After two weeks, the colonies were checked and photographed.

## 3.4. Vectors and primers.

### 3.4.1. Plasmid material.

A list of the plasmid material used in this thesis is summarized in Table 3.1. The antibiotic resistance or auxotrophy for selection in bacteria, yeast or plant for each plasmid are also depicted in the table, as well as the experimental procedures where the plasmid was used in this thesis.

Table 3.1: List of vectors used in this thesis, with their respective selection resistance in bacteria or plant/yeast, their procedures and references.

| Vector | Selection in bacteria | Selection in plant / yeast | Procedure | Reference |
|---|---|---|---|---|
| pCAMBIA1300-35S-C-cYFP | Kanamycin | Hygromycin | Expression in plant and detection of YFP signal | Duan *et al.*, 2017 |
| pCAMBIA1300-35S-C-nYFP | Kanamycin | Hygromycin | Expression in plant and detection of YFP signal | Duan *et al.*, 2017 |
| pCAMBIA1305.1-35S-TMΩ-FLAG | Kanamycin | Hygromycin | Expression in plant and immunoprecipitation and detection | New England Biolabs |
| pCAMBIA1305.1-35S-TMΩ-eGFP | Kanamycin | Hygromycin | Expression in plant and immunodetection | New England Biolabs |
| pGBKT7-BD | Kanamycin | Tryptophan | Expression in yeast | Clontech |
| pGADT7-AD | Ampicillin | Leucin | Expression in yeast | Clontech |
| pGREENII-0800-LUC | Kanamycin | Kanamycin | Expression in plant and detection of LUC signal | Hellens *et al.*, 2005 |

## 3.4.2. Primers.

A list of all the primers used for RT-qPCR analyses in *B. napus* is depicted in Table 3.2.

Table 3.2: List of primers used for RT-qPCR experiments in *B. napus*.

| Primer | Sequence (5' – 3') |
|---|---|
| BnPSY1 (FW) | CAAGTCCAAAGCAACGACCG |
| BnPSY1 (RV) | CTTCGCCAACGTCTCTGAGT |
| BnPER71 (FW) | TACACGTGAACTCGTCGTCC |
| BnPER71 (RV) | GATGCATCACCGTTTTGGGG |
| BnPER59 (FW) | GGGAGGACATGTGCTGCTTA |
| BnPER59 (RV) | GGCTTAGCTGTGCCCTAACA |
| BnACO1 (FW) | GGTCCAGAAGGTCCAGCTTT |
| BnACO1 (RV) | GACCAGGCACTTGATCATCCT |
| BnACO1 (FW) | CCAGCTGGGGATGCCATAAT |
| BnACO1 (RV) | GCGATGCATCCTAGACGGAA |
| BnHB52 (FW) | ACAAGTCGCAGTCTGGTTCC |
| BnHB52 (RV) | TGCTTCAAGCTTGGACTGGA |
| BnNRT2.1 (FW) | GGTTTGCTGAGAACGCCAAG |
| BnNRT2.1 (RV) | TCTTGACAGATCATCGGTGTGA |
| BnLBD37 (FW) | CTCCGCTGTACCGGAATCTC |
| BnLBD37 (RV) | AGAAGCTCAGGGATCGGTCT |
| BnNIA1 (FW) | ACTACACCTGGTCACGAAGAG |
| BnNIA1 (RV) | CCTCTCAACGTGTACGGCTT |
| BnSPX3 (FW) | TACAAGAGTCGTTGCCGGAG |

| | |
|---|---|
| BnSPX3 (RV) | GCAATTCCTTGTGGTGGATG |
| BnSPX1 (FW) | CGAGGATCCTACGGTTACTGC |
| BnSPX1 (RV) | TGTGGAGGCTCTCCATGAAC |
| BnPECP2 (FW) | AGATGTTGACTAGTGCGGAG |
| BnPECP2 (RV) | AGAAACTCGAAGAGCACGGG |
| BnPHO1 (FW) | TCTCGTAAACCAAAACCCGC |
| BnPHO1 (RV) | GGTCGAAAAGAGATCGGCCA |
| BnACT7 (FW) | TGGGTTTGCTGGTGACGAT |
| BnACT7 (RV) | TGCCTAGGACGACCAACAATACT |

The primers used to generate the constructs for the different experiments are shown in Table 3.3, together with the restriction enzymes used to produce each construct.

Table 3.3: List of primers used for cloning the *B. napus* sequences of *BnPHR1, BnSPX1, BnPHR1_C* (C-terminal region of *BnPHR1*) and *BnSPX1.1p* (the promoter region of *BnSPX1.1*) and the restriction enzymes used to generate each construct. Capital letters show the region binding to the DNA. Lowercase letters indicate the adapter region. Bold letters indicate the restriction enzyme sites.

| **Primer** | **Sequence (5' - 3')** | **Restriction enzymes** | **Construct** |
|---|---|---|---|
| BnPHR1 (FW) | gagaacacgggggac**gagctc**ATGGAAGCTCGTCCGGTTC | SacI | pCAMBIA1300-35S-BnPHR1-cYFP |
| BnPHR1 (RV) | tgggtacatgtcgac**tctaga**GTTATCGGTTTTGGGGCGC | Xba1 | |
| BnSPX1.1 (FW) | gagaacacgggggac**gagctc**ATGAAGTTCGGTAAGAGCCTG | SacI | pCAMBIA1300-35S-BnSPX1-nYFP |
| BnSPX1.1 (RV) | ttgctccatgtcgac**tctaga**TTTGGCTTCTTGCTCCAACAAC | XbaI | |
| BnPHR1_C (FW) | tatggccatggaggcc**gaattc**ATGCCTTCTCCTTCTGTGTCTG | EcoRI | pGBKT7-BD-BnPHR1_C |
| BnPHR1_C (RV) | tatgcggccgctgca**ggtcgac**TCAGTTATCGGTTTTGGGGC | SalI | |
| BnSPX1.1 (FW) | ggccatggaggccagt**gaattc**ATGAAGTTCGGTAAGAGCCTG | EcoRI | pGADT7-AD-BnSPX1.1 |
| BnSPX1.1 (RV) | gattcatctgcagctc**gagctc**CTATTTGGCTTCTTGCTCCAAC | SacI | |
| BnPHR1 (FW) | acaattacatttaca**attacc**ATGGAAGCTCGTCCGGTTC | NcoI | pCAMBIA1305.1-35S-TMVΩ-BnPHR1-GFP |
| BnPHR1 (RV) | tcaccatcgcctgagg**gagctc**GTTATCGGTTTTGGGGCGC | SacI | |
| BnSPX1.1 (FW) | tacaattacatttaca**attacc**ATGAAGTTCGGTAAGAGCCTG | NcoI | pCAMBIA1305.1-35S-TMVΩ-BnSPX1.1-FLAG |
| BnSPX1.1 (RV) | gcttgcatgcctgca**ggtcgac**TTTGGCTTCTTGCTCCAACAAC | SalI | |

| | | | |
|---|---|---|---|
| BnSPX1.1p (FW) | ggtcgacggtatcgat**aagctt**GTATTGGTCATGCGACAATGTC | HindIII | pGreenII0800-BnSPX1.1p::LUC |
| BnSPX1.1p (RV) | ttatgtttttggcgtc**ttccat**GCTTTTCTTCTTCTTCTTCTTC | NcoI | |

The primers used to check positive transformants by colony PCR and by sequencing all the constructs are shown in Table 3.4.

Table 3.4: Primers used to check the presence of the fragment of interest in each construct by qPCR and sequencing.

| **Primer** | **Sequence** | **Construct** |
|---|---|---|
| M13 (FW) | 5'-GTAAAACGACGGCCAG-3' | pCAMBIA1300-35S-BnPHR1-cYFP |
| BnPHR1 (RV) | GTTATCGGTTTTGGGGCGC | |
| M13 (FW) | 5'-GTAAAACGACGGCCAG-3' | pCAMBIA1300-35S-BnPHR1-nYFP |
| BnSPX1 (RV) | TTTGGCTTCTTGCTCCAACAAC | |
| T7 | 5′-TAATACGACTCACTATAGGG-3′ | pGBKT7-BD-BnPHR1_C |
| BnPHR1_C (RV) | TCAGTTATCGGTTTTGGGGC | |
| T7 | 5′-TAATACGACTCACTATAGGG-3′ | pGADT7-AD-BnSPX1.1 |
| BnSPX1 (RV) | CTATTTGGCTTCTTGCTCCAAC | |
| M13 (FW) | 5'-GTAAAACGACGGCCAG-3' | pCAMBIA1305.1-35S-TMVΩ-BnPHR1-GFP |
| BnPHR1 (RV) | GTTATCGGTTTTGGGGCGC | |
| M13 (FW) | 5'-GTAAAACGACGGCCAG-3' | pCAMBIA1305.1-35S-TMVΩ-BnSPX1.1-FLAG |
| BnSPX1 (RV) | TTTGGCTTCTTGCTCCAACAAC | |
| M13 (FW) | 5'-GTAAAACGACGGCCAG-3' | pGreenII0800-BnSPX1.1p::LUC |
| BnSPX1p (RV) | GCTTTTCTTCTTCTTCTTCTTC | |

Table 3.5 shows the primers used to genotype Arabidopsis mutants obtained from SALK.

Table 3.5: Primers used to genotype Arabidopsis mutant lines.

| Primer | Sequence (5' – 3') |
|---|---|
| aco1 (LP) | CTTTCCCAATCTGCATCTGAG |
| aco1 (RP) | AACACAACACCACGCATATCC |
| lbd37 (LP) | GGGCTCTCTCTCTGTGTCATG |
| lbd37 (RP) | GAAGCATCTGAGATCTGCACC |
| nrt1.1 (LP) | AGGAGCAATTTGAACTCCCTC |
| nrt1.1 (RP) | TTGGAAACCTGGATTGTTGAC |
| nrt2.1-2 (LP) | GCAAGCGACTATCATCACTCC |
| nrt2.1-2 (RP) | GTTCTCCATGAGCTTCGTGAG |
| spx3 (LP) | TCAACAAGAACAATCGCTCTG |
| spx3 (RP) | AGAAATAAAAGGACTGGGCCC |
| spx1 (LP) | AACCTCTTCCCCCTCTCTTTC |
| spx1 (RP) | TGCTCCAACAATGGAATCTTC |
| spx2 (LP) | AATTACATGACTCGCGCTCTG |
| spx2 (RP) | TTGATCCCAAATCATCAAACC |
| LBb1.3 | ATTTTGCCGATTTCGGAAC |

## 3.5. Molecular biology techniques.

### 3.5.1. Generation of constructs by restriction enzyme digestions.

For the Bi-molecular fluorescence complementation assay (BiFC) assay, the coding sequence of *BnPHR1* was cloned into pCAMBIA1300-35S with a cYFP tag, whereas the coding sequence of *BnSPX1.1* was cloned into pCAMBIA1300-35S with the nYFP tag. To generate these constructs, the expression vectors pCAMBIA1300-35S-cYFP and pCAMBIA1300-35S-nYFP were digested with the restriction enzymes SacI and XbaI in a double digestion reaction (Table 3.3). For the yeast two hybrid assay (see Material and methods: 3.13.2.), the C-terminal region of *BnPHR1* and the full coding sequence of *BnSPX1.1* were cloned into the expression vectors pGBKT7 (containing the binding domain) and pGADT7 (containing the activation domain), respectively. First, the vectors pGBKT7-BD (with resistance to kanamycin) and the vector pGADT7-AD (with resistance to ampicillin) were digested with the restriction enzymes EcoRI and SalI (for pGBKT7) or EcoRI and SacI (for pGADT7) in a double digestion reaction (Table 3.3). For the CoIP (see Material and methods: 3.13.3.), the full coding sequence of *BnPHR1* was cloned into pCAMBIA1305.1-35S-TMVΩ with a GFP fluorescence

tag, whereas the coding sequence of *BnSPX1.1* was cloned into pCAMBIA1305.1-35S-TMVΩ with a FLAG tag. To obtain the constructs, the expression vectors pCAMBIA1305.1-35S-TMVΩ-GFP and pCAMBIA1305.1-35S-TMVΩ-FLAG were digested with the restriction enzymes NcoI and SacI, or NcoI and SalI, respectively (Table 3.3). Finally, for the trans-activation assay (see Material and Methods: 3.13.4.), the promoter region of *BnSPX1.1* was cloned into the expression vector pGREENII 0800 fused to the luciferase (LUC) gene. The empty vector pGREENII 0800-LUC was digested with the restriction enzymes HindIII and NcoI.

Restriction enzyme digestions were done by incubating each plasmid with their respective restriction enzymes in a double incubation (Table 3.3), which consisted of a first incubation at 37ºC for 2 hours, followed by a second incubation at 65ºC for 20 minutes to stop the reaction. Then, gel-purified PCR products of the genes of interest were ligated to the digested vectors using 5x DNA Assembly Mix Plus (ShareBio). The ligation product was transformed into *Escherichia coli* (DH5α strain). Positive transformants were confirmed by colony PCR and plasmid DNA was isolated from the positive transformants using the PurePlasmid DNA Mini Extraction Kit (Adamas Life). The constructs were then sequenced to confirm the positive transformants.

### 3.5.2. DNA amplification by PCR.

To generate the different constructs described in the previous section, total RNA was extracted from roots of *B. napus* 3-day old seedlings (variety Wesway) grown in agar plates in ¼ MS media, using the HiPure Plant RNA Mini Kit from Magen (see Material and methods: 3.6.1.). The RNA concentration was determined using NanoDrop One (Thermo Scientific). First-strand cDNA synthesis was done with 1µg of RNA, using the First Strand cDNA synthesis Kit from Yeasen, according to the manufacturer guidelines. The obtained cDNA was used for PCR-amplification of the sequences of *BnPHR1*, *BnSPX1* and *BnPHR1_C* (C-terminal region of *BnPHR1*). PCR-amplification of *BnSPX1.1p* (the promoter region of *BnSPX1.1*) was done on genomic DNA obtained from 3-day old *B. napus* seedlings (see Material and methods: 3.5.3.). All PCRs were done using the Phanta Max Super-Fidelity DNA Polymerase P505 (Cellagen Technology), according to the manufacturer guidelines. The following program was used for PCR-amplification:

| Steps | Temperature | Time | Cycles |
|---|---|---|---|
| Pre-denaturation | 95ºC | 30 seconds | 1 |
| Denaturation | 95ºC | 15 seconds | 32 |
| Annealing | 56ºC | 15 seconds | |
| Extension | 72ºC | 1 minute | |
| Final extension | 72ºC | 5 minutes | 1 |

The PCR-products were run in an agarose (1%) gel and their respective bands were isolated and purified using the Omega Biotek Gel Extraction Kit (Omega).

Colony PCR was used to select positive transformants of the different constructs, *E. coli* colonies grown at 37ºC overnight in LB medium with antibiotics were collected from the petri dish and diluted in 9 µL of water. Then, 1 µL of the dilution was used for PCR. The pair of primers used for colony PCR are depicted in Table 3.4. For each construct, we used the forward primer of the insert of interest and a reverse primer that binds to the sequence of the vector. We performed the PCR amplification reaction with the 2xHieff PCR Master Mix (With Dye) from Yeasen, according to the manufacturer's guidelines. The following program was used:

| Steps | Temperature | Time | Cycles |
|---|---|---|---|
| Pre-denaturation | 94ºC | 3 minutes | 1 |
| Denaturation | 94ºC | 30 seconds | 29 |
| Annealing | 56ºC | 30 seconds | |
| Extension | 72ºC | 1 minute | |
| Final extension | 72ºC | 5 minutes | 1 |

The PCR products were run in an agarose (1%) gel to select for positive transformants. Then, positive transformants were sent to Tsingke Biotech (Shanghai, China) for sequencing.

### 3.5.3. DNA extraction, purification and analysis.

To obtain genomic DNA from *B.napus*, root tissue was collected in a 1.5 mL tube containing glass beads and immediately frozen in liquid nitrogen, and then homogenized with a tissue disruptor (Ventura Mix 2) with three cycles of 10 seconds each. Then, the sample was incubated with SDS DNA extraction buffer [50 mM of Tris-HCl pH 8; 100 mM of NaCl; 10 mM of EDTA pH 8; 1% SDS] at 65ºC for 30 minutes, followed by centrifugation at 13000 rpm for 10 minutes. Then, the supernatant was incubated with isopropanol at -20ºC for 30 minutes and was

centrifuged at 13000 rpm for 10 minutes. The pellet was then washed with ethanol 75%. Samples were dried at 65ºC to remove excess ethanol and resuspended in 50 µL of water.

To isolate and purify genetic material from PCR products we used the Gel Purification Kit from Bioteke Corporation. Briefly, the PCR fragments of interest were isolated from an agarose (1%) gel under UV light using a clean blade. Then, the isolated bands were transferred to a clean 1.5 mL tube and incubated in three volumes of DB binding solution in a 42ºC water bath for 10 minutes to fully dissolve the agarose. Then, they were mixed with 1 volume of isopropanol and transferred to an AC adsorption column and consequently centrifuged at 12000 rpm for 1 minute. After discarding the supernatant, samples were washed with 700 µL of wash buffer (WB) containing ethanol and centrifuged at 12000 rpm for 1 minute. Then, they followed a second wash with 500 µL of WB followed by centrifuging the empty columns for 2 minutes to remove excess ethanol. Then, samples were eluted with 50 µL of elution buffer by incubating them at room temperature for 2 minutes and centrifugation at 12000 rpm for 1 minute.

To isolate plasmid DNA from transformed *E.coli* bacterial cultures, we used the PurePlasmid DNA Mini Extraction Kit (from Adamas Life). Briefly, 5 mL bacterial cultures grown overnight at 37ºC in agitation were centrifuged at 5000 rpm for 8 minutes. After discarding the supernatant, the pellet was resuspended in 250 µL of buffer P1 containing RNAse A and vortexed thoroughly. Then 250 µL of buffer P2 were added to the same tube, and the tubes were inverted 6-8 times to lyse the cells. After that, the cells were treated with 350 µL of buffer P3 and immediately mixed by inverting the tubes 6-8 times and then centrifuged at 12000 rpm for 10 minutes. The supernatant was transferred to a spin column AC and centrifuged at 12000 rpm for 60 seconds. Afterwards, the tubes were treated with 500 µL of buffer PE and centrifuged at 12000 rpm for 30 seconds. Then, the tubes were washed twice with washing buffer containing ethanol and centrifuged at 12000 rpm for 30 seconds, and then the empty tubes were centrifuged at 12000 rpm for 2 minutes to remove excess ethanol. Finally, DNA was eluted by adding 100 µL of pre-heated Elution Buffer to the column membrane and incubating at room temperature for 2-5 minutes, followed by centrifugation at 12000 rpm for 1 minute.

### 3.5.4. Arabidopsis mutant genotyping.

Arabidopsis mutants obtained from NASC (see Material and methods: 3.1.2.) were genotyped by PCR to check the presence of the T-DNA insertion into the corresponding gene in two steps: a first PCR amplification to check the presence of the T-DNA insertion (LB + RP reaction) and a second PCR to screen for the absence of the wild type gene (LP + RP reaction). For the LB + RP reaction, we used the LBb1.3 primer, which is a primer binding to the left border of the T-DNA insertion, and the RP primer, which is specific for the gene of interest (Table 3.5). For the LP + RP reaction, we used the LP and RP primers, which are specific for the gene of interest and bind to sequences that are flanking the T-DNA insertion (Table 3.5). For genotyping the different mutants, we used gDNA extracted from mutant seedlings and Col-0 seedlings as a negative control. For PCR amplification, we used the NZYTaq II 2x Green Master Mix (NZYtech). The program used for PCR amplification is shown below:

| Steps | Temperature | Time | Cycles |
|---|---|---|---|
| Pre-denaturation | 95ºC | 3 minutes | 1 |
| Denaturation | 95ºC | 30 seconds | 35 |
| Annealing | 55ºC | 30 seconds | |
| Extension | 72ºC | 1 minute | |
| Final extension | 72ºC | 10 minutes | 1 |

Then, the PCR products were run in an agarose (1%) gel to check the sizes of the obtained bands.

## 3.6. Gene expression analyses.

### 3.6.1. RNA extraction and sequencing.

RNA extraction for massive RNA-sequencing analyses and for RT-qPCR expression analyses was performed in whole roots and shoots of *B. napus* seedlings, with three independent biological replicates per treatment. *B. napus* seedlings from the varieties Westar and Wesway were grown in the Pouch and Wick system under different temperature and N conditions. In a separate experiment, *B. napus* seedlings from the varieties Industry and Wesway were grown in the Pouch and Wick system under different temperature and Pi conditions. Seven days after the start of the treatments, whole shoots and roots were collected from three

independent biological replicates per treatment. For each biological replicate, whole roots or shoots from four different seedlings were collected together in a 1.5 mL tube containing glass beads and immediately frozen in liquid nitrogen. Samples were homogenized with a tissue disruptor (Ventura Mix 2) with three cycles of 10 seconds each. RNA extraction was performed with the RNeasy Plant Mini Kit from Qiagen according to the manufacturer's guidelines. The RNA concentration was measured with a NanoDrop One (Thermo Scientific). After RNA extraction and determination of the RNA concentration, RNA sequencing was performed by BGI Genomics (Beijing, China).

The stranded mRNA library used for sequencing was generated by DNBSEQ Eukaryotic Stranded Transcriptome library preparation. The mRNA library was constructed as follows: first, mRNA was enriched and purified using oligo dT beads to enrich mRNA with a poly A tail. Then, RNA was fragmented, and first strand cDNA was synthesized using random N6-primed reverse transcription, followed by a second-strand cDNA synthesis with dUTP instead of dTTP. The synthesized cDNA was subjected to end-repair and then was 3' adenylated. Adaptors were ligated to the ends of these 3' adenylated cDNA fragments. Prior to PCR amplification, the dUTP-marked strand was selectively degraded by Uracil-DNA-Glycosylase (UDG). The remaining strand was amplified to generate a cDNA library suitable for sequencing. Many rounds of PCR amplification were performed to enrich the purified cDNA template. PCR products were denatured by heat and the single stranded DNA was cyclized by splint oligo and DNA ligase. Sequencing was performed on the DNBSEQ (DNBSEQ Technology) platform, and the length of the resulting reads was 150 bp. The analysis of transcriptomic data is described below (see Material and Methods: 3.10).

### 3.6.2. RNA expression analysis by RT-qPCR.

For RT-qPCR, three independent biological replicates per treatment were used. Each biological replicate was composed of four whole roots or four whole shoots pooled together. Samples were immediately frozen in liquid nitrogen and RNA was extracted with the RNeasy Plant Mini Kit from Qiagen (see Material and methods: 3.6.1.). The RNA concentration was determined in each sample using NanoDrop One (Thermo Scientific). First-strand cDNA synthesis was done with 1µg of RNA, using the Maxima First Strand cDNA Synthesis Kit with dsDNase (Thermo Scientific) according to the manufacturer guidelines. Consequently, cDNAs were diluted 1/20 and 2 µL of diluted cDNA were used for RT-qPCR with a final volume

of 12 µL. RT-qPCR was done with the Light Cycler FastStart DNA Master SYBR Green I (Roche), according to the manufacturer's guidelines. The program used for RT-qPCR is shown below:

| Steps | Temperature | Time | Cycles |
|---|---|---|---|
| Pre-denaturation | 95ºC | 5 minutes | 1 |
| Denaturation | 95ºC | 10 seconds | 40 |
| Annealing | 60ºC | 20 seconds | |
| Extension | 72ºC | 20 seconds | |
| Dissociation | 95ºC | 15 seconds | 1 |
| | 60ºC | 30 seconds | |
| | 95ºC | 1 second | |

Primers used for RT-qPCR in *B. napus* are displayed in Table 3.2. The expression levels of each gene were normalized to the expression levels of *BnACT7*.

## 3.7. Root and shoot phenotyping.

### 3.7.1. Analysis of morphological root traits in *B. napus*.

*B. napus* seedlings from 12 varieties were grown in the Pouch and Wick system for 7 days, with the roots covered by a flat pouch that allows the roots to grow in two dimensions in the dark. After 7 days, the flat pouches were opened, displaying the two-dimensional disposition of the root system, and photographed with a Canon PC2152. For each treatment and variety, 4 independent seedlings from 5 biological replicates were photographed. The pictures were adjusted with photoshop to remove stains in the background and uploaded to the GiaRoots software for root trait analyses. The trait "Number of lateral roots (LatR/LR)" was measured by hand by counting the number of lateral or secondary roots emerging from the primary root, and the trait "Lateral root density (LatR/cm)" was obtained by dividing the number of lateral roots by the Network Depth. All the remaining 17 root traits were measured with the GiaRoots software. The names of the traits, as well as their respective abbreviations, description and categories are shown in Table 4.1 and Supplementary Table 1B.

### 3.7.2. Shoot phenotyping in *B. napus*.

*B. napus* plants from the varieties Westar and Wesway were grown in pots under different temperatures (22ºC, 36ºC and 36ºC with the TGRooZ) and N conditions (optimal N or N deficiency) for two weeks (see Material and methods: 3.2.2.). Afterwards, entire shoots from 6 independent biological replicates per temperature and N treatment were collected and consequently photographed in a white background with a Canon PC2152. Then, the hypocotyl length and total leaf area were measured with ImageJ. Shoot fresh weight was immediately determined after harvesting. For dry weight, shoots were dried at 60ºC for 24 hours.

*B. napus* plants from the varieties Westar and Wesway grown in pots in the CBGP's E2P2 platform (see Material and methods: 3.2.2.) were photographed with the High Throughput system (LemanTec Co) after four weeks.

### 3.7.3. Analysis of morphological root traits in Arabidopsis.

Arabidopsis seedlings from Col-0, *pNRT2.4*::GUS, DR5::LUC and mutant lines (*aco1*, *hb52*, *lbd37*, *nrt1.1*, *nrt2.1-2*, *spx3* and *spx1spx2*) grown under different temperatures and N conditions for 10 days were scanned using an EPSON GT-1500 scanner. Afterwards, the primary root length was measured using ImageJ, and the number of lateral roots or secondary roots emerging from the primary root was counted. Then, the lateral root density was calculated as the number of lateral roots divided by the length of the primary root.

## 3.8. Biochemical analyses.

### 3.8.1. Quantification of nitrate content in roots and shoots of *B. napus*.

*B. napus* seedlings were grown in the Pouch and Wick system under different temperatures (21ºC or 29ºC) and N treatments (optimal N or N deficiency). After 7 days, whole roots and shoots of two replicates, containing eight seedlings pooled together, were collected and frozen in liquid nitrogen. Total nitrate content was measured following the protocol from Hachiya & Okamoto (2017) with a few adaptations. Briefly, nitrate was extracted by adding 10 volumes of Milli-Q water to each sample and boiling them at 100ºC in a water-bath for 20 minutes. For nitrate quantification, 10 µL of the supernatant were mixed with 40 µL of 0.05% (w/v) salicylic acid in sulfuric acid, and incubated at room temperature for 20

minutes. Then, 1 mL of 8% (w/v) NaOH in Milli-Q water was added to the same tubes. After mixing thoroughly, the OD was measured at 410 nm with a spectrophotometer. The nitrogen concentration (as µg/g) was calculated using a standard calibration curve and adjusted to the fresh weight of the samples.

### 3.8.2. Quantification of phosphate content in roots and shoots of *B. napus*.

*B. napus* seedlings from 12 varieties were grown in the Pouch and Wick system under different temperatures (21ºC or 29ºC) and different Pi conditions (optimal Pi and Pi deficiency). After 7 days, whole shoots and roots were collected and frozen in liquid nitrogen. Phosphate content was measured in three independent experiments with four seedlings pooled together in each experiment, following the protocol by Ames *et al.* (1966) with a few adaptations. First, phosphate was extracted by submitting the samples to four freeze-thaw cycles in 1 mL of 0.1% acetic acid, using liquid nitrogen and a 60ºC stove. For Pi quantification, 60 µL of the supernatant (root samples) or 30 µL of the supernatant (shoot samples) were mixed with 0.1% acetic acid to a volume of 300 µL. Then, samples were treated with 700 µL of ascorbic acid/ ammonium molybdate buffer, and incubated at 37ºC for 1 hour. Finally, the OD was measured at 820 nm using a spectrophotometer. The Pi concentration (as nmoles/mg) was calculated using a standard calibration curve and adjusted to the fresh weight of the samples.

### 3.8.3. Quantification of total nitrogen (N) and carbon (C) content in shoots of *B. napus*.

*B. napus* plants from the varieties Westar and Wesway were grown in pots in the CBGP's Enclosed Ecosystem Phenotyping Platform (E2P2) under different temperatures (either 24ºC or 34ºC) and N treatments (see Material and methods: 3.2.2.). After four weeks, entire shoots were harvested and the total N content and C content of five different plants were measured using an elemental analyser (ThermoQuest Flash EA 1112) at Universidad de La Coruña, Spain (https://www.sai.udc.es/es/unidades/UTIA). The N and C contents were given as percent (%) of N and C to the total dry weight of the sample.

## 3.9. Histochemical analyses.

### 3.9.1. GUS-staining for the analysis of *NRT2.4::GUS* expression in Arabidopsis roots.

Arabidopsis *NRT2.4::GUS* seedlings were germinated for 4 days and then grown at different temperatures (21ºC, 29ºC, 29ºC TGRooZ, 32ºC or 32ºC TGRooZ) and different N conditions (optimal N or N deficiency) for 6 days (see Material and methods: 3.2.3.). After that, the GUS staining solution was directly applied in the Petri dish to detect the expression of *NRT2.4* in roots. One mL of GUS-staining solution [obtained by adding of 1 µL of X-Gluc substrate (15 mg/mL of powdered X-gluc from Thermo Scientific in dimethyl formamide) per mL of GUS buffer (GUS buffer 50mM with 0.2% triton and 0.2% acetone)] was added to each Petri dish containing 12 *pNRT2.4::GUS* seedlings. Then, the Petri dishes were incubated at 37ºC overnight and the roots were observed and photographed with a Leica MZ9.5 to visualize the GUS staining.

### 3.9.2. DR5::LUC fluorescence assay in Arabidopsis roots.

Arabidopsis DR5::LUC seedlings were grown under different temperatures (21ºC, 32ºC or 32ºC TGRooZ) and different N conditions (optimal N and N deficiency; see Material and methods: 3.2.4.). Plates containing 10-day old seedlings were sprayed with 1 mL of 2.5 mM potassium luciferine. After 2 minutes, the LUC signal was checked with a NightOwl II, Berthold LB 983 (exposure time = 300 µs) and photographed with a MetaMorph Image Analysis Software. The number of pre-branch sites (PBS) was quantified by manually counting the number of spots with accumulation of LUC fluorescent signal along the primary root.

## 3.10. Analysis of transcriptomic data.

### 3.10.1. Quality control, filtering, alignment to the reference genome and identification of DEGs.

Two independent RNA-sequencing experiments were performed for the *B. napus* varieties Westar, Wesway and Industry grown under different temperature and N or Pi conditions. For the first experiment, RNA was extracted from whole roots and shoots of *B. napus* seedlings from the varieties Westar and Wesway grown under

different temperature and N conditions in the Pouch and Wick system (see Material and methods: 3.6.1.). Quality control and filtering of the raw reads was done with the SOAPnuke software (Cock *et al.*, 2010). Filtering consisted in removing reads with adaptors, removing genes whose N content was greater than 5% and removing low quality reads. After quality control and filtering of the raw reads, the reads were aligned to the reference sequence (GCF_000686985.2_Bra_napus_v2.0, NCBI) using Hierarchical Indexing for Spliced Alignment of Transcripts (HISAT) software (Kim *et al.*, 2015). The clean reads were mapped to the reference transcriptome with Bowtie2 (Langmead & Salzberg, 2012), and the gene expression levels of each sample were calculated with RSEM (Li & Dewey, 2011). The differentially expressed genes (DEGs) were obtained for each comparison with the DEseq2 method (version 1.44.0; Love *et al.*, 2014).

For the second experiment, RNA was extracted from whole roots and shoots of *B. napus* individuals from the Industry and Wesway varieties grown under different temperature and Pi conditions (see Material and Methods: 3.6.1.). Quality control of the raw reads and filtering was done with FastQC version 0.11.8. Alignment of the reads to the reference genome was done with STAR version 2.5.2b. For the alignment, Fasta files (from Brassica_napus.AST_PRJEB5043_v1.dna.toplevel.fa) and gtf files (from Brassica_napus.AST_PRJEB5043_v1.58.gtf) downloaded from ENSEMBL FTP Plants were used. HTSeq-count version 2.0.5 was used to count the reads in features from the aligned reads. For differential expression analysis, DEseq2 was used (version 1.44.0; Love *et al.*, 2014).

### 3.10.2. Hierarchical clustering of DEGs and GO enrichment.

The following step-by-step workflow was used to select the differentially expressed genes (DEGs) in the two RNA-sequencing analyses of Westar and Wesway grown under different temperature and N conditions in roots and shoots, separately. For each of the two varieties, the gene expression under N deficiency (21ºC-N), high temperature (29ºC+N) and the combination of both stresses (29ºC-N) was compared to the gene expression under the control treatment (21ºC+N). Thus, for each variety, three comparisons were considered (six comparisons in total). DEGs with a $|\log2FC| > 1$ and a p-value < 0.05 in each comparison were considered for further analysis. Gene names were provided as NCBI identifiers by BGI Genomics (e.g. 106357621). We converted the NCBI identifiers to *B. napus* Darmor gene IDs (e.g. BnaA01g02940D) using the "biomaRt" package from Ensembl in Rstudio, with

the dataset "bnapus_eg_gene". We also obtained their respective *Arabidopsis thaliana* homologs using the dataset "athaliana_eg_gene". Volcano plots of DEGs for each comparison were done using DESeq2.

The following workflow was used to select the DEGs in the two RNA-sequencing analyses of Industry and Wesway grown under different temperature and Pi conditions in roots and shoots, separately. For both Industry and Wesway, the gene expression under P deficiency (21ºC-P), high temperature (29ºC+P) and the stress combination (29ºC-P) was compared to the gene expression under the control treatment (21ºC+P). Thus, for each variety, three comparisons were done (six comparisons in total). DEGs with a $|\log2FC| > 0.58$ and a p-value < 0.01 in each comparison were considered for further analysis. Volcano plots of DEGs were done in R studio using the package "EnhancedVolcano" from Bioconductor.

For all RNA-seq experiments, bar plots displaying the number of up-regulated and down-regulated genes for each comparison were done in Rstudio with the "ggplot2" package. Venn-diagrams of the up-regulated and down-regulated genes for each comparison were done in Venny 2.1 (CNB, CSIC). For hierarchical clustering, DEGs that were significant ($|\log2FC| > 1$; p-value < 0.05 for the first experiment; $|\log2FC| > 0.58$ and a p-value < 0.01 for the second experiment) in at least one of the six comparisons were used to build a dendrogram of the DEGs according to their expression profiles. For each DEG, the average of the normalized read counts from three replicates in each treatment was used to build the dendrogram. The dendrogram was built based on the distance between the different samples and the genes using the function "as.dist" and "hclust" from the "stats" package. The function "as.dendrogram" was used to visualize both dendrograms in a tree. The dendrogram of the DEGs, which orders the genes according to their expression profiles across the treatments, was used to build a heatmap. For the heatmap, normalized read counts were transformed to Z-scores. The Z-score of each sample and the heatmap were computed using the function "heatmap.2" from the gplots package. Posteriorly, hierarchical clustering was performed to identify clusters of genes with similar expression profiles across the treatments. For hierarchical clustering, dendrogram was cut at height (k) = 5. Then, Gene Ontology (GO) analyses were done for each cluster in Shiny GO (http://bioinformatics.sdstate.edu/go/), using the *B. napus* Darmor gene IDs.

### 3.10.3. Generation of molecular interaction networks.

We used the genes from the most relevant categories obtained in the GO analyses (see Material and methods: 3.10.2.) to build protein interaction networks. The *A. thaliana* homologs from the genes in the top enriched categories from the GO analyses were identified using the "biomaRt" package from Ensembl in Rstudio, with the dataset "athaliana_eg_gene", and subsequently searched against the STRING version 12.0 database (Szklarczyk *et al.*, 2015) to identify possible interactions between the input genes. The interaction score was set between 0.3 – 0.7 and for all other parameters the default settings were used. Clusters within each interaction network were calculated by k-means. The output provided a network of proteins that are known to interact with each other or to participate in the same molecular pathway.

## 3.11. Identification and characterization of the MYB-CC protein family in *B. napus*.

### 3.11.1. Identification and characterization of MYB-CC members in *B. napus*.

First, the amino acid sequence of *AtPHR1* (AT4G28610) was obtained from TAIR (The Arabidopsis Information Resource, https://www.arabidopsis.org) and used as query for a BLASTp search against the *Brassica napus* ZS11.v0 database. Proteins with a % identity of at least 35% were considered and obtained from the BnIR database (*Brassica napus* multi-omics information resource, https://yanglab.hzau.edu.cn/). Then, all protein sequences were checked through Pfam (http://pfam.xfam.org/) and Smart (http://smart.embl-heidelberg.de/) databases to confirm the presence of the Myb DNA-binding (PF00249) and CC LHEQLE (PF14379) domains. The molecular weight and isoelectric point of all proteins were calculated using the Compute pI/Mw tool from ExPASy (https://www.expasy.org/). The chromosomal positions, transcript length, number of exons and the start and end positions of each exon were retrieved using the JBrowser tool from BnIR. The *A. thaliana* homologs from each protein were obtained using the "biomaRt" package from Ensembl in Rstudio with the dataset "athaliana_eg_gene".

### 3.11.2. Phylogenetic tree construction.

For the phylogenetic tree, the *A. thaliana* amino acid sequences for *AtPHR1* (AT4G28610), *AtPHL1* (AT5G29000), *AtPHL2* (AT3G24120) and *AtPHL3* (AT4G13640) were obtained from TAIR. The *B. oleracea* amino acid sequence for *BolPHR1* (Bo8g054450) and *B. rapa* amino acid sequences for *BrPHR1* (Bra010355), *BrPHR2* (Bra024188), *BrPHR3* (Bra036469) and *BrPHR4* (Bra036679) were retrieved from BRAD (Brassica Database; http://brassicadb.cn). The amino acid sequences for *OsPHR1* (Os03g0329900) and *OsPHR2* (Os03g0343400) in *Oryza sativa*, *TaPHR1* (Traes_4AS_7220D33B3) in *Triticum aestivum*, *ZmPHR1* (Zm00001d029020) in *Zea mays* and *SlPHR1* (Solyc05g055940) in *Solanum lycopersicum* were retrieved from EnsemblPlants (https://plants.ensembl.org/index.html). The multiple sequence alignment was done with ClustalW in GenomeNet (https://www.genome.jp) using the default parameters. The phylogenetic tree was done with ClustalW in GenomeNet, which performs a phylogenetic reconstruction using the function "build" from ETE3 3.1.2. (Huerta-Cepas *et al.*, 2016). The phylogenetic tree was constructed using FastTree v2.1.8 (Price *et al.*, 2010). The visualization of the phylogenetic tree was done in Itol (https://itol.embl.de/).

## 3.12. Identification and isolation of PHR1 and SPX1 in *B. napus*.

### 3.12.1. Identification of *BnPHR1* and *BnSPX1.1*.

For identification of *BnPHR1*, we used the PHR proteins obtained in the previous analysis (see Material and methods: 3.11.) and selected the proteins with the highest homology with *AtPHR1*. To identify *BnSPX1.1*, the amino acid sequence of *AtSPX1* from *A. thaliana* was obtained from TAIR (https://www.arabidopsis.org) and used as a query for a BLAST search in the *B. napus* ZS11.v0 database. The SPX proteins from *B. napus* with the highest percent of identity to *AtSPX1* were selected. Then, putative *AtPHR1* and *AtSPX1* homologues were used to perform a multiple sequence alignment with *AtPHR1* or *AtSPX1* using ClustalW in GenomeNet (https://www.genome.jp), and a consequent phylogenetic tree. The phylogenetic reconstructions and tree visualization were performed as previously described (see Material and methods: 3.11.2.).

### 3.12.2. Isolation of the *BnPHR1*, *BnPRH1_C*, *BnSPX1.1* and *BnSPX1.1p* sequences from *B. napus*.

PCR-amplification of *BnPHR1*, *BnSPX1.1*, *BnPHR1_C* was performed on cDNA synthesized form the previously extracted RNA (see Material and methods: 3.6.1.), whereas PCR-amplification of *BnSPX1.1p* was obtained by amplification from genomic DNA (see Material and methods: 3.5.3.), and both amplifications were performed as described on Material and methods: 3.5.2.

## 3.13. Protein-protein interaction analyses.

### 3.13.1. Bi-molecular fluorescence complementation assay (BiFC) in *N. benthamiana* leaves.

The constructs pCAMBIA1300-35S-BnPHR1-cYFP and pCAMBIA1300-35S-BnSPX1.1-nYFP were transformed into *Agrobacterium tumefaciens* in two independent transformation procedures. Agrobacterium-mediated transformation of both constructs was done as previously described (Material and methods: 3.3.2.). Positive transformants were grown in 10 mL of LB medium containing kanamycin and rifampicin and were incubated at 28ºC shaking for 1 day. Then, the cultures were centrifuged at 4000 rpm for 5 minutes, and cells were resuspended in 5 mL of agroinfiltration medium (MA supplemented with 10 mM of MES, 10 mM of MgCl2 and 150 μM of acetosyringone). *A. tumefaciens* containing the constructs were infiltrated in leaves of 3-week old *N. benthamiana* in different combinations: BnPHR1-cYFP : BnSPX1.1-nYFP (containing both constructs); BnPHR1-cYFP : 0-nYFP (negative control containing pCAMBIA1300-35S-BnPHR1-cYFP and the empty vector pCAMBIA1300-35S-nYFP); 0-cYFP : BnSPX1.1-nYFP (negative control containing the empty vector pCAMBIA1300-35S-cYFP and pCAMBIA1300-35S-BnSPX1.1-nYFP); and finally 0-cYFP : 0-nYFP (negative control with both empty vectors pCAMBIA1300-35S-cYFP and pCAMBIA1300-35S-nYFP). All combinations were mixed in a final volume of 5 mL of agroinfiltration medium with a $OD_{600}$ of 0.1. Two days after infiltration, the YFP fluorescence signal was checked using a fluorescence microscope (Leica Microsystems). The emission wavelength was set at 580 nm and the fluorescence was detected at 405-633 nm.

### 3.13.2. Yeast two hybrid assay.

The constructs pGADT7-AD-BnSPX1.1 and pGBKT7-BD-BnPHR1_C (see Material and methods: 3.4.) were transformed into *Saccharomyces cerevisiae* strain AH109 in different combinations: pGADT7-AD-BnSPX1.1 and pGBKT7-BD-BnPHR1_C (co-transformed together); pGADT7-AD-BnSPX1.1 and pGBKT7-BD-0 (negative control with the plasmid containing BnSPX1.1 and the activation domain and the empty plasmid containing the biding domain); pGADT7-AD-0 and pGBKT7-BD-BnPHR1_C (negative control containing the empty plasmid with the activation domain and the plasmid containing BnPHR1 with the binding domain); and pGADT7-AD-0 and pGBKT7-BD-0 (negative control containing both empty plasmids co-infiltrated together). Furthermore, a positive control was added by transforming pGADT7-AD-OsSPX1 and pGBKT7-BD-OsPHR2_C (containing *OsSPX1* and the C-terminal region of *OsPHR2* from rice). Yeast transformation was performed as previously described (see Material and methods: 3.3.3.). After selection of positive transformants, colonies were grown in liquid -Trp/-Leu medium for 3 days and plated in Petri dishes with selective DOB medium -Trp/-Leu/-His/-Ade and grown at 28ºC. After two weeks, colonies were checked and photographed.

### 3.13.3. Co-immunoprecipitation (CoIP) in *N. benthamiana* leaves and Western Blot.

The constructs pCAMBIA1305.1-35S-TMVΩ-BnPHR1-GFP and pCAMBIA1305.1-35S-TMVΩ-BnSPX1.1-FLAG (see Material and methods: 3.4.) were transformed into *Agrobacterium tumefaciens* separately. Agrobacterium-mediated transformation was performed as previously described (see Material and methods: 3.3.2.). Positive transformants were grown in 5 mL of LB medium containing kanamycin and rifampicin and were incubated at 28ºC shaking for 1 day. The cultures were then centrifuged at 4000 rpm for 5 minutes and were consequently resuspended in 5 mL of agroinfiltration medium (MA supplemented with 10 mM of MES, 10 mM of MgCl2 and 150 µM of acetosyringone). *A. tumefaciens* containing the constructs were infiltrated in leaves of 3-week old *N. benthamiana* in two different combinations: 35S::*BnPHR1-GFP* : 35S::*BnSPX1.1-FLAG* (the combination of pCAMBIA1305.1-35S-TMVΩ-BnPHR1-GFP and pCAMBIA1305.1-35S-TMVΩ-BnSPX1.1-FLAG) and 35S::*BnPHR1-GFP* : 0 (negative control containing the construct pCAMBIA1305.1-35S-TMVΩ-BnPHR1-GFP infiltrated

alone). Both combinations were prepared in a final volume of 2 mL of agroinfiltration medium with an $OD_{600}$ of 0.5.

Two days after co-infiltration, leaf material was collected in 2 mL tubes containing glass beads and immediately frozen in liquid nitrogen and consequently homogenized with a tissue disrupter. Then, homogenized leaf tissue was incubated with 750 µL of lysis buffer (NaCl 150 mM; $MgCl_2$ 5 mM; glycerol 10%; NP-40 0.1%; DDT 0.5 mM; protease inhibitor 1x; Tris-HCl 50 mM) in agitation at room temperature for 30 minutes. Then, the tubes were centrifuged at 13000 rpm at 4ºC for 10 minutes and the supernatant was transferred to new tubes and followed a second centrifugation at 13000 rpm for 10 minutes. Each sample was divided into two different sub-samples (called input and IP-FLAG) and one of them was incubated at 4ºC for 3 hours with Anti FLAG M2 Magnetic Beads (Sigma-Aldrich), which are beads that bind to the FLAG tag, which is fused to BnSPX1.1, thus enriching for the presence of 35S::*BnSPX1.1-FLAG* in the samples. Then, samples were transferred to new tubes and washed with 1 mL of washing buffer (NaCl 150 mM; $MgCl_2$ 5 mM; glycerol 10%; NP-40 0.01%; DDT 0.5 mM; protease inhibitor 1x; Tris-HCl 50 mM) three times. Finally, samples were mixed with 5x SDS loading buffer and pre-heated at 100ºC for 10 minutes. Then, samples were centrifuged at 13000 rpm for 10 minutes and 18 µL of each sample were separated into a 10% SDS-PAGE gel for 2 hours and transferred to a PDVF membrane. The membrane was incubated with Anti- GFP (Roch, 11814460001, 1:1000 dilution) or Anti-FLAG (Sigma, F1804, 1:4000 dilution) that have linked the peroxidase to detect the corresponding fusion proteins.

### 3.13.4. Trans-activation assay in *N. benthamiana* leaves.

The construct pGreenII0800-BnSPX1.1p::LUC (see Material and methods: 3.4.), containing the promoter region of *BnSPX1.1* fused to the luciferase (LUC) gene was transformed into *Agrobacterium tumefaciens*, as well as the constructs pCAMBIA1305.1-35S-TMVΩ-BnPHR1-GFP and pCAMBIA1305.1-35S-TMVΩ-BnSPX1.1-FLAG (used previously for CoIP assays; see Material and methods: 3.13.3.). Agrobacterium-mediated transformation was performed as previously described (see Material and methods: 3.3.2.). The transformed Agrobacterium cells were grown in LB medium with kanamycin and rifampicin at 28ºC in agitation for 1 day. The three cultures were centrifuged at 4000 rpm for 5 minutes and then resuspended in 5 mL of agroinfiltration medium (MA supplemented with 10 mM of MES, 10 mM of $MgCl_2$ and 150 µM of acetosyringone). *A. tumefaciens* containing

the constructs were infiltrated in leaves of 3-week old *N. benthamiana* in the following combinations:

| Combination | Components | Name of the constructs | Proportion |
|---|---|---|---|
| A | - *BnSPX1.1p::LUC* | - pGreenII0800-proBnSPX1.1-LUC | |
| B | - *BnSPX1.1p::LUC* | - pGreenII0800-proBnSPX1.1-LUC | 1 |
| | - 35S::*BnPHR1-GFP* | - pCAMBIA1305.1-35S-TMVΩ-BnPHR1-GFP | 2 |
| C | - *BnSPX1.1p::LUC* | - pGreenII0800-proBnSPX1.1-LUC | 1 |
| | - 35S::*BnPHR1-GFP* | - pCAMBIA1305.1-35S-TMVΩ-BnPHR1-GFP | 2 |
| | - 35S::*BnSPX1.1-FLAG* | - pCAMBIA1305.1-35S-TMVΩ-BnSPX1.1-FLAG | 1 |
| D | - *BnSPX1.1p::LUC* | - pGreenII0800-proBnSPX1.1-LUC | 1 |
| | - 35S::*BnPHR1.1-GFP* | - pCAMBIA1305.1-35S-TMVΩ-BnPHR1-GFP | 2 |
| | - 35S::*BnSPX1.1-FLAG* | - pCAMBIA1305.1-35S-TMVΩ-BnSPX1.1-FLAG | 3 |

All combinations were done in a final volume of 5 mL of agroinfiltration medium with an $OD_{600}$ of 0.5. Two days after infiltration, leaves were sprayed with 100 mM luciferin. After 2 minutes, the luciferase signal was photographed with a CCD camera (PyLoN1300B, Princeton Instruments).

## 3.14. Statistical analyses.

### 3.14.1. Correlation analysis of morphological root traits.

*B. napus* seedlings from 12 varieties were grown in the Pouch and Wick system under different temperatures (21ºC or 29ºC), N treatments (optimal N and N deficiency) or Pi treatments (optimal Pi and Pi deficiency; see Material and methods: 3.7.1.). After 7 days, 19 root traits (see Supplementary Table 1B) were measured in 960 *B. napus* individuals (20 individual biological replicates x 4 treatments x 12 varieties). The measurements obtained for the different root traits in all varieties and treatments were used to compute a multiple correlation analysis between all traits, and Pearson's correlation coefficients were calculated between all traits using Rstudio with the "stats" and "corrplot" packages (Wei *et al.*, 2021).

### 3.14.2. Principal component analysis and hierarchical clustering.

Principal component analysis (PCA) was done for the *B. napus* experiment combining different temperatures and N treatments and the experiment

combining different temperatures and Pi treatments (see Material and methods: 3.7.1.). The 19 measured root traits were used as quantitative variables for the PCA. Both PCAs were done in Rstudio using the "FactoMineR" and "factoextra" packages. Hierarchical clustering was performed with the function HCPC from the "FactoMineR" package in R studio, which performs an agglomerative hierarchical clustering between the individuals based on the results of the PCA. The optimal number of clusters was determined using K-means and the "average" method. Individuals were grouped according to their variety and treatment.

### 3.14.3. ANOVA and t-test.

Statistical analyses of root trait quantifications in *B. napus* were done in Rstudio using the "stats" package. For each of the 12 varieties, a two-way ANOVA was performed for each trait using temperature and treatment as qualitative factors, using the "res.aov2" function from the "stats" package in Rstudio. The two-way ANOVA tested the effects of two factors (temperature and nutrient treatment), as well as the interaction between them on each trait (p-value < 0.05). To obtain significant differences between groups, a pairwise comparison test was done with the Tukey HSD method using the "TukeyHSD" function from the "multcompView" package in Rstudio. For shoot traits measured in pot experiments in *B. napus*, and root traits measured in Arabidopsis Col-0, DR5::LUC and mutant lines (*aco1*, *hb52*, *lbd37*, *nrt1.1*, *nrt2.1-2*, *spx3* and *spx1spx2*), statistical analyses were done individually for each treatment with a t-test (p-value < 0.05) to compare the means between different groups using the "t-test" function from the "stats" package in Rstudio.

# 4. RESULTS

## 4.1. Characterization of the differential root responses to the combination of warm temperatures and nitrogen deficiency in *B. napus*.

### 4.1.1. The combination of warm temperature and nitrogen deficiency affects multiple root traits in *B. napus*.

To define the root responses to the combination of warm temperatures and nitrogen deficiency in *B. napus*, we performed a detailed characterization of the changes in 19 root traits in a collection of twelve different spring *B. napus* varieties coming from diverse geographical regions. The root traits measured are shown in Table 4.1 and Supplementary Table 1B**,** and include a set of root traits related with the extent, intrinsic size, distribution, and shape of the root networks. Seedlings from the different *B. napus* varieties (see Supplementary Table 1A) were grown under optimal (21ºC) or warm (29ºC) temperature and under optimal nitrogen (+N; 9.84 mM) or nitrogen deficiency (-N; 0.1 mM) using the pouch and wick system (Table 4.1A; B).

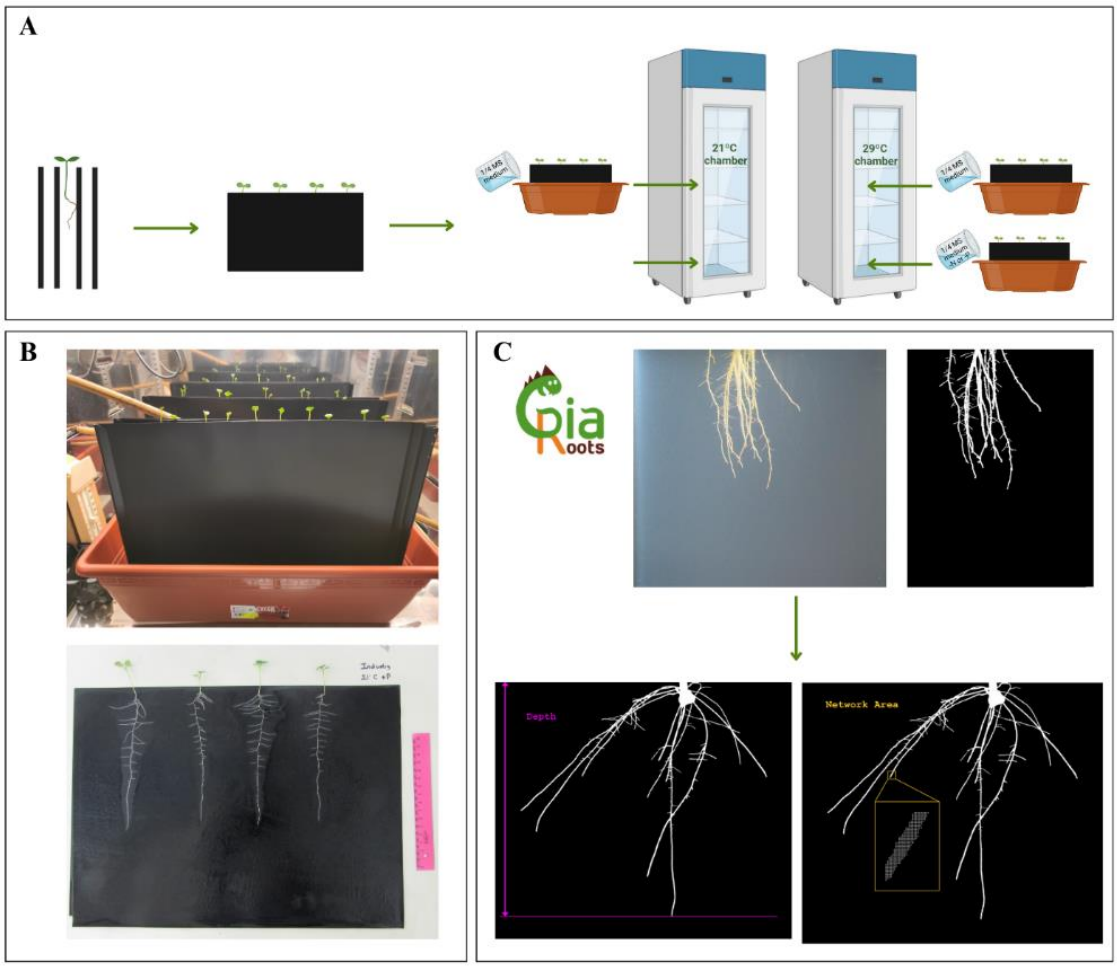


Figure 4.1: A) Schematic representation of the pouch and wick system. B) Pictures of *B. napus* seedlings grown in the pouch and wick system for 7 days. Top: *B. napus* seedlings growing inside the chambers of the system. Bottom: *B. napus* seedlings grown in the system during 7 days with the roots disposed in two dimensions and ready for phenotyping. C) Images of the GiaRoots software. Top: from left to right, an example of a root picture, and the same picture converted into black and white pixels and ready for analysis. Bottom: examples of two traits that are quantified by the GiaRoots software: network depth (left) and network area (right).

Table 4.1: All root traits measured in *B. napus* seedlings using the GiaRoots software, grouped by their respective categories.

| Abbreviation | Trait | Description | Category |
|---|---|---|---|
| Ndepth | Network Depth | The number of pixels in the vertical direction from the upper-most network pixel to the lower-most network pixel. | Traits related to extension |
| Nwidth | Network Width | The number of pixels in the horizontal direction from the left-most network pixel to the right-most network pixel. | |
| ConvA | Network Convex Area | The area of the convex hull that encompasses the image. | |
| MajA | Major Ellipse Axis | The length of the major axis of the best fitting ellipse to the network. | |
| MinA | Minor Ellipse Axis | The length of the minor axis of the best fitting ellipse to the network. | |
| Nlength | Network Length | The total number of pixels in the network skeleton | Traits related to size |
| Narea | Network Area | The number of network pixels in the image. | |
| Nper | Network Perimeter | The total number of pixels connected to a background pixel (using a 8-nearest neighbour neighbourhood). | |
| Nvol | Network Volume | The sum of the local volume at each pixel of the network skeleton, as approximated by a tubular shape whose radius is estimated from the image. | |
| Nsurf | Network Surface Area | The sum of the local surface area at each pixel of the network skeleton, as approximated by a tubular shape whose radius is estimated from the image. | |
| Nbush | Network Bushiness | The ratio of the maximum to the median number of roots. | Traits related to distribution |
| NLDist | Network Length Distribution | The fraction of network pixels found in the lower 2/3 of the network. The lower 2/3 of the network is defined based on the network depth. | |
| Nsolid | Network Solidity | The total network area divided by the network convex area. | |
| MaxR | Maximum Number of Roots | After sorting the number of roots crossing a horizontal line from smallest to largest, the maximum number is the 84th-percentile value (one standard deviation). | |
| MedR | Median Number of Roots | The result of a vertical line sweep in which the number of roots that crossed a horizontal line was estimated, and then the median of all values for the extent of the network was calculated. | |

| | | | |
|---|---|---|---|
| LatR or LR | Number of Lateral Roots | Number of secondary or lateral roots (LRs) emerged from the primary root. | Traits related to lateral / secondary roots |
| LR/cm or LRD | LR Density | The number of secondary or LRs emerged from the primary root divided by the value of the network depth. | |
| EARatio | Ellipse Axes Ratio | The ratio of the minor to the major axis of best fitting ellipse. | Traits related to shape |
| Nw/d | Network Width to Depth Ratio | The value of the network width divided by the value of the network depth. | |

After 7 days, 19 root traits were measured for each seedling using the GiaRoots software (Figure 4.1C). N deficiency caused significant changes in 9 traits out of 19 in most varieties, whereas 7 traits out of 19 were altered on average by warm temperatures. The combination of warm temperature and N deficiency caused significant alterations in 8 traits on average in most varieties, most of those traits were more influenced by warm temperature than by N deficiency. Among all other varieties, Line and Westar were the most responsive to -N, having 12 traits significantly increased, whereas Marnoo had the greatest reductions at -N (11 traits; Figure 4.2B). Under warm temperature, the varieties showing more significant reductions were Karat (12 traits), Dux (14 traits), Duplo (10 traits) and Westar (9 traits) whereas most varieties showed no significant increases (<3 traits). Finally, the stress combination, compared to the control treatment, caused significant increases in 8 root traits in WHP, and in 6 root traits in Line, and caused significant reductions in 12 traits in Fido, and in 9 traits in Marnoo.

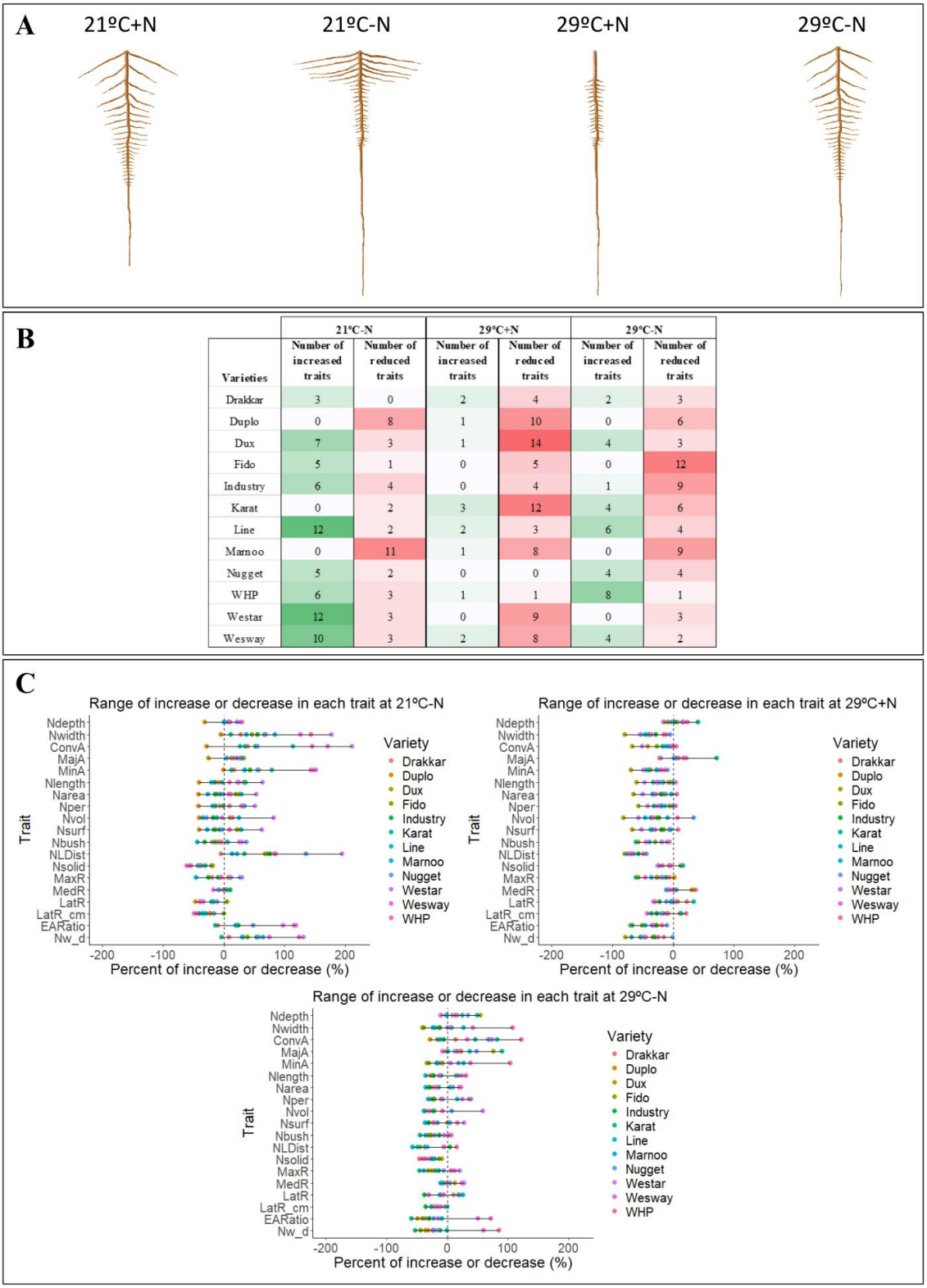


| Varieties | 21ºC-N | | 29ºC+N | | 29ºC-N | |
|---|---|---|---|---|---|---|
| | Number of increased traits | Number of reduced traits | Number of increased traits | Number of reduced traits | Number of increased traits | Number of reduced traits |
| Drakkar | 3 | 0 | 2 | 4 | 2 | 3 |
| Duplo | 0 | 8 | 1 | 10 | 0 | 6 |
| Dux | 7 | 3 | 1 | 14 | 4 | 3 |
| Fido | 5 | 1 | 0 | 5 | 0 | 12 |
| Industry | 6 | 4 | 0 | 4 | 1 | 9 |
| Karat | 0 | 2 | 3 | 12 | 4 | 6 |
| Line | 12 | 2 | 2 | 3 | 6 | 4 |
| Marnoo | 0 | 11 | 1 | 8 | 0 | 9 |
| Nugget | 5 | 2 | 0 | 0 | 4 | 4 |
| WHP | 6 | 3 | 1 | 1 | 8 | 1 |
| Westar | 12 | 3 | 0 | 9 | 0 | 3 |
| Wesway | 10 | 3 | 2 | 8 | 4 | 2 |

Figure 4.2: A) Graphical representation of the root responses to the different temperature and N treatments observed among most *B. napus* varieties. B) Number of significantly increased and reduced root traits in the 12 *B. napus* varieties under the three stress treatments (21ºC-N, 29ºC+N and 29ºC-N). C) Range of decrease or increase of each trait at 21ºC-N (top left), 29ºC+N (top right) and 29ºC-N (bottom) compared to the control conditions. Coloured dots represent each variety.

Next, we analysed in detail the effect of -N on the root system of our *B. napus* varieties. We found that most varieties, as a tendency, showed a deeper root system when grown at 21ºC-N with a few exceptions (e.g. Duplo; Figure 4.2). The values for network depth increased from 5% (e.g. Nugget) to 30% (e.g. Dux) at 21ºC-N compared with those grown at 21ºC+N (Figure 4.2C; Figure 4.3). This is consistent with previous findings, where the enlargement of the root system was described as a typical response of *B. napus* to nitrogen deficiency (Guo *et al.*, 2017; Qin *et al.*, 2019; Shen *et al.*, 2022). This enlargement of the root system in 21ºC-N seedlings was also accompanied by an increase in the width of the root system. Thus, the values for network width were higher in all varieties grown at 21ºC-N than 21ºC+N, with increases ranging from 11% in Karat to 177% in Westar (Figure 4.2C; Figure 4.3; Supplementary Table 2). Even though the depth and width of the root system were increased at 21ºC-N, other traits such as number of LRs and LR density (LRD) were decreased in most varieties (Figure 4.2C; Figure 4.3). However, their length was increased at 21ºC-N, represented by the significant increase in the network width of all varieties (Figure 4.3). Increases in the length of the LRs have been recently reported in Arabidopsis as a response to mild N deficiency (Zhu *et al.*, 2022). Interestingly in our analyses, most varieties showed an increase in the length of the LRs located in the upper areas of the root system, but this increase in LR length was less pronounced in the lower parts. These differences resulted in a significant increase in the network length distribution in 21ºC-N seedlings. Consistently, network solidity (Nsolid), a trait that provides information about the "density" of the root system by calculating the ratio between the area of the root system and the area of the background covered by the root system (network convex area), was decreased by N deficiency at 21ºC (Supplementary Figure 2; Supplementary Table 1B). This effect was mainly produced by an increase in the network convex area, thus reflecting the increase in the length of LRs located in the upper region of the root system, but not in the middle and lower regions (Supplementary Figure 1; Supplementary Table 2A; 2B). In summary, N deficiency increased the depth and width of the root system in most varieties and caused changes in the distribution of the lateral roots, with an increase in the length of the LRs in the upper parts of the root system and a decrease in the length of those located in the middle and lower regions. Together, these results suggest that roots modify part of their LR development, thus favouring the enlargement of the root system in the upper regions to search for zones in the soil with more nutrient availability.

Then, we analysed the effect of warm temperatures at optimal N levels (29ºC+N) on the root system of *B. napus* compared with 21ºC+N. We observed an overall increase in network depth in most of the varieties, with values ranging from 4% in Industry to 41% in Karat, but with some exceptions (e.g. Westar; Figure 4.2; Figure 4.3). The increase in the depth of the root system produced by warm temperatures has been recently reported in *B. napus* (Boter *et al.*, 2023). However, network width decreased, with values ranging from 4% to 79% (Figure 4.2C; Figure 4.3). This decrease in width was caused by a reduction in the LR length, especially in the areas close to the upper parts of the root system. This change in root architecture was consistently observed in all varieties, and contrary to the effects of N deficiency described above. Furthermore, the LRs in the middle and lower parts of the root were shorter at 29ºC+N than at 21ºC+N, producing a decrease in the network length distribution in all varieties (Supplementary Figure 2). Additionally, there was a significant decrease in LR number in these upper parts of the root. Consequently, LRD decreased at 29ºC in most varieties. These results might suggest that under warm temperatures plants developed a deeper primary root in search for cooler areas of the soil, and at the same time reduced the growth of the upper LRs to avoid their development in the superficial and warmer areas (Supplementary Table 2A; B).

Finally, we analysed the effects of the combination of warm temperatures and N deficiency in the root architecture of *B. napus*. Roots subjected to this stress combination responded with a general increase in network depth in most varieties, suggesting that both stresses had an additive effect in network depth. Previously, we mentioned that N deficiency caused a general increase in the length of the upper lateral roots (up to 177% increase in network width), whereas warm temperatures caused a decrease in the length of those upper lateral roots (up to 78% decrease in network width). But when warm temperature was applied together with N deficiency, the growth of the upper LRs was restored (values ranging from a 40% decrease to a 107% increase in network width), although they were shorter than at N deficiency (Figure 4.2C). These results indicate that the increase in LR length produced by N deficiency was, at least, partially sufficient to compensate the reduction provoked by warm temperatures (Figure 4.3). Similarly, this compensatory effect was observed with the network length distribution, which increased at 21ºC-N (up to 194% in Westar) and decreased at 29ºC+N (with decreases from 43% in Nugget to 79% in Dux), but showed an intermediate phenotype under the stress combination (29ºC-N) with some individual differences

between the varieties (32% decrease in Nugget compared to 15% increase in WHP). Interestingly, a similar tendency but with opposite effects was observed in the LRD. Thus, LRD decreased at 21ºC-N but slightly increased under 29ºC+N, whereas under the stress combination, most varieties displayed an intermediate phenotype, with decreases in LRD being less pronounced than under 21ºC-N (e.g. 11% decrease compared to 15% in Nugget or 13% compared to 48 % decrease in Westar). In summary, the combination of both stresses (warm temperature plus N deficiency) produced different root responses compared to the individual stresses, suggesting a complex and possible compensatory effect of both stresses in the root architecture of *B. napus*, demonstrating the plasticity of root responses to single or combined stresses. Thus, most traits showed a compensatory effect of the individual stresses, with the exception of network depth, that showed an additive effect.

To summarize, in response to N deficiency, *B. napus* seedlings developed a deeper root system accompanied by an increase in the length of the upper lateral roots. Warm temperatures also caused an increase in the depth of the root system, but LR length was reduced. On the other hand, the combination of warm temperatures and N deficiency caused an increase in the depth of the root system, but LR development is more complex and showed compensatory or opposite effects regarding LR length and density compared to the effects of the individual stresses.

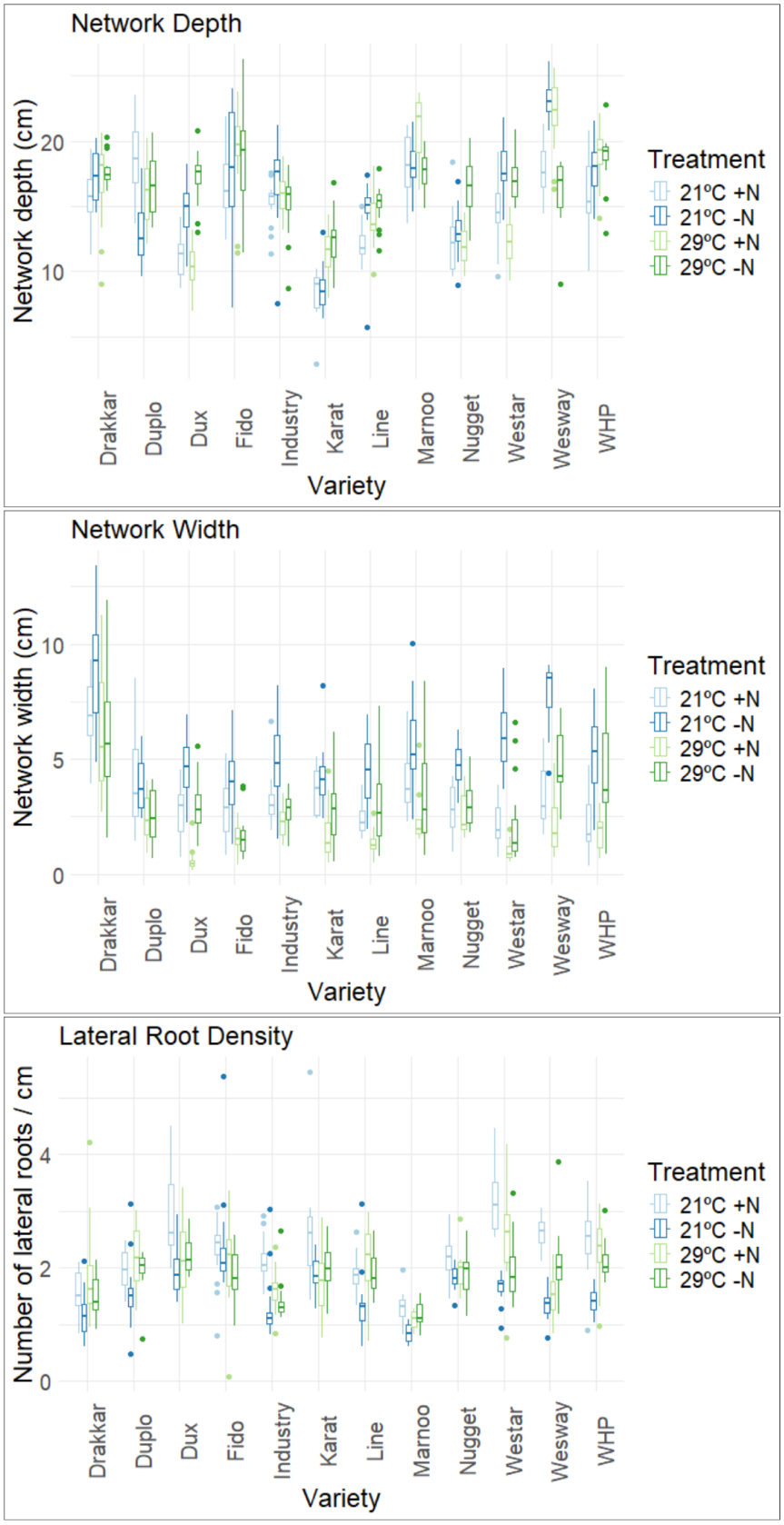


Figure 4.3: Boxplots showing the distribution of the mean values of three root traits (network depth, network width and LRD) across *B. napus* individuals from 12 different varieties grown under different temperatures (21 and 29°C) and/or nitrogen treatments

(+N and -N). The X-axis indicates the different varieties. The legend indicates the different colours corresponding to the treatments: 21ºC+N, 21ºC-N, 29ºC+N and 29ºC-N. Boxplots for the remaining root traits measured are shown in Supplementary Figure 1; 2.

### 4.1.2. Different *B. napus* varieties show differential root responses to the combination of warm temperature and nitrogen stress.

We have shown that the root responses to combined warm temperature and N deficiency are complex and differ from root responses to the individual stresses in the root system of *B. napus*. To extend this characterization and to identify the main differences between the varieties, we first calculated the correlation coefficients between the different traits. Some of the traits showed high correlation coefficients (Figure 4.4; Supplementary Table 3A), reflecting that their values displayed similar patterns across the different treatments and varieties. These correlation coefficients were higher among traits that belong to the same category. For instance, network width and minor ellipse axes were highly correlated (correlation coefficient of 0.95; Supplementary Table 3A), since both traits are related to the width of the root system. Other traits showed negative correlations, such as network solidity and network convex area, (correlation coefficient of -0.61) since those traits depend on each other: the higher the network convex area, the lower the network solidity (see Supplementary Table 1B). Under optimal temperature and N conditions, network depth would be expected to have a high correlation with network width, since a typical *B. napus* root system tends to grow similarly in both directions. However, we found that the correlation coefficient between both traits was low (0.17), reflecting that the different temperatures and N treatments caused the network depth to be less correlated with the network width. As we previously described, at 29ºC+N most varieties showed a deeper root system while reducing network width, thus lowering the correlation coefficient between both traits. The correlation coefficient between network width and LRD was -0.19, likely due to the fact that N deficiency caused an overall increase in network width but a decrease in LRD and that warm temperatures and the combination of both stresses caused significant decreases in network width, while LRD was unaltered in most varieties, thus causing a reduction in the expected correlation coefficient between these two traits.

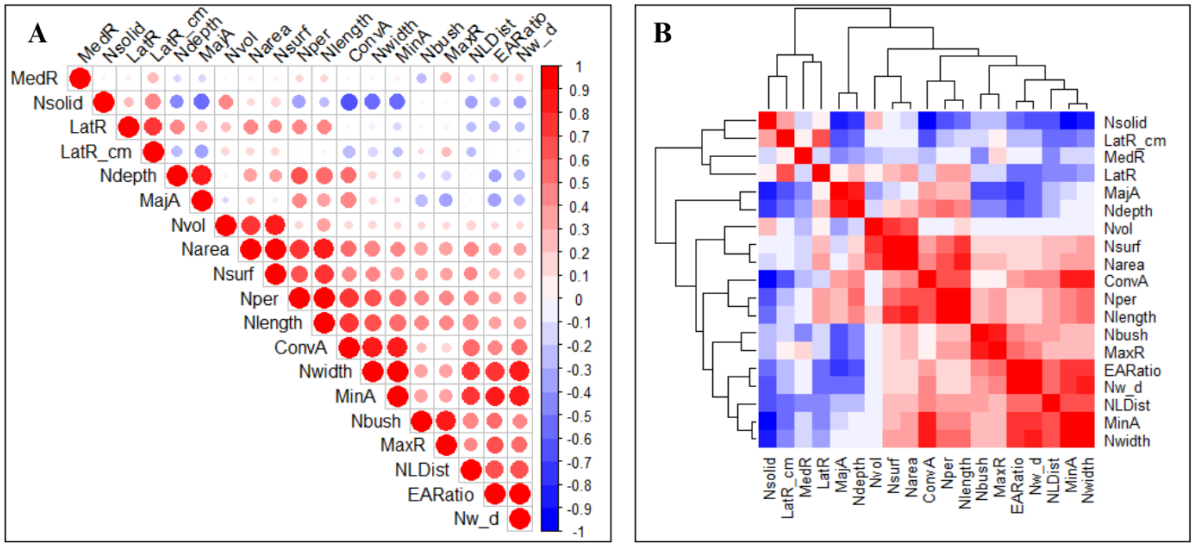


Figure 4.4: A) Graphical representation of the correlation coefficients between the different variables. B) Heatmap showing the correlation coefficients between the different variables. Variables are quantitative measurements of 19 root traits across *B. napus* individuals from 12 different varieties submitted to different temperature and nitrogen treatments: 21ºC+N, 21ºC-N, 29ºC+N and 29ºC-N. Red indicates a higher correlation coefficient, whereas blue indicates a lower correlation coefficient. A table with all the values for the correlation coefficients is provided in Supplementary Table 3A.

To capture the variability in the root responses between the varieties, a multivariate principal component analysis (PCA) was performed using all the traits described above as variables. The values for the contribution of each variable to the principal dimensions and the cos2 values for the quality of the representation are shown in Supplementary Table 3B and C, respectively. We observed that the first dimension (Dim1) was composed by multiple traits related to the network width and distribution, causing 40% of the variation within the dataset. Whereas the second dimension (Dim2) was formed by traits that were exclusively related to the network depth, such as network depth and major ellipse axis, being responsible for 18.5% of the variation (Figure 4.5A; B). In the PCA plot, we observed that most individuals from 21ºC+N and 29ºC-N were located close to the centre of the plot, whereas individuals from 29ºC+N and 21ºC-N were more separated to the left and right, respectively, indicating that the root responses to these two treatments were differential, which correlates with our previous observations where 21ºC-N and 29ºC+N caused opposite effects in most root traits (see Results: 4.1.1.; Figure 4.5C). This indicates that 29ºC-N individuals differed from those treated with 21ºC-N mainly in traits related to network width and distribution (see Figure 4.5A). This correlates with previous observations, where

network width was strongly increased at 21ºC-N in most varieties but was dramatically decreased at 29ºC+N, both compared to 21ºC+N (Figure 4.3). Furthermore, network length distribution increased in most varieties at 21ºC-N but decreased at 29ºC+N, all compared to 21ºC+N (Supplementary Figure 2). When we grouped the individuals according to their varieties, we observed that the varieties responded differently (Figure 4.5D). For example, individuals from Wesway tended to group around the centre of the plot, except for 29ºC+N samples, that located in the upper left of the plot, and 21ºC-N samples, which located in the upper right, showing differences regarding traits related to network width and distribution but also network depth between these two treatments (Figure 4.5E). The fact that the distributions from the different treatments were similar suggests that Wesway had fewer alterations in the root system in response to the treatments. In the case of Westar (Figure 4.5F), the differences in the distribution of the individuals from each treatment were much more pronounced than in Wesway, and individuals were spread along the horizontal axes of the plot, reflecting significant differences in the traits related to the width and distribution of the root system. All individuals from 29ºC+N were located towards the left of the plot, whereas individuals from 21ºC-N were located towards the right of the plot, indicating that they differed remarkably in the traits related to network width and distribution, whereas individuals from 21ºC+N and 29ºC-N displayed more similar responses. In summary, these results suggest that the root system of Westar was more responsive to the individual stresses. On the contrary, Wesway showed fewer differences in the distribution of the individuals from the different treatments, suggesting a better capacity to maintain root growth under these stresses.

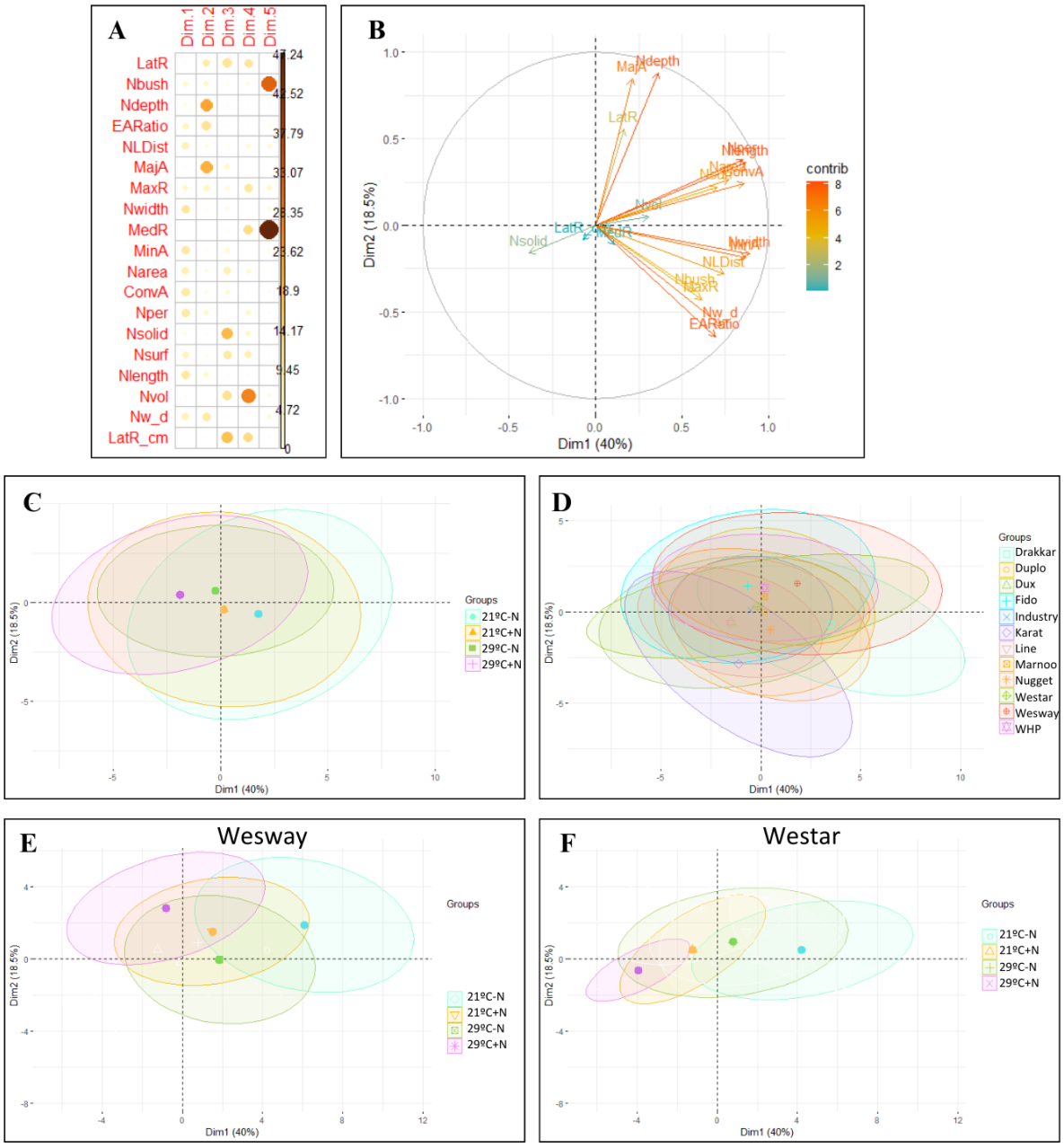


Figure 4.5: Principal component analysis (PCA) of the different root traits measured in *B. napus* individuals from different varieties and submitted to different temperature and N treatments. The different root traits were used as variables for the PCA. A) Schematic representation of the contribution of each variable to the first five components of the PCA. B) Plot of the contribution of each variable to the first two components of the PCA. X-axis indicates the first component (Dim 1), whereas Y-axis indicates the second component (Dim 2). C) Plot of the contribution of the individuals to the first two components of the PCA grouped by treatment: 21ºC+N, 21ºC-N, 29ºC+N and 29ºC-N. D) Plot of the contribution of the individuals to the first two components of the PCA grouped by variety. E) Plot of the contribution of the individuals from the variety Westar to the first two components of the PCA, grouped by treatment. F) Plot of the contribution of the individuals from the variety Wesway to the first two components of the PCA, grouped by treatment. In each plot, ellipses represent the distribution of the individuals in each group. Dots represent the mean values of the coordinates of all individuals in each group.

To group the varieties and treatments according to their responses, we performed a hierarchical cluster analysis of the mean values in each variety and treatment, based on the response across the principal components of the PCA. The different varieties and treatments were grouped in five clusters according to their distribution across the principal components. In general, the N treatment had a greater influence than the temperature treatment in the definition of the clusters. Thus, from left to right, the first and second clusters contained more individuals from 21ºC-N, whereas the other three clusters were more abundant in individuals grown at 29ºC+N. The second and third clusters were bigger than other clusters and contained most of the varieties and treatments, whereas the first, fourth and fifth clusters (from left to right) represented varieties and/or treatments that displayed root responses that deviated from the general response (Figure 4.6).

As mentioned above, two varieties showed a differential response to the treatments, Wesway and Westar. These differences were further dissected in this cluster analysis. Thus, the root response of Wesway was divided into two different clusters. One cluster grouped its response to N deficiency at both temperatures (21ºC-N and 29ºC-N) and the other cluster, showed their response to different temperatures at optimal N (21ºC+N and 29ºC+N), reflecting that the N treatment caused more differences in the root response than the temperature treatment. However, in Westar, roots treated with optimal N (21ºC+N and 29ºC+N) belonged to the same cluster, but samples treated with N deficiency at 21ºC or 29ºC belonged to different clusters, suggesting that their differences were more extreme. This is consistent with their distribution on the PCA plot across the first two principal components, where samples from 29ºC-N and 21ºC-N showed a differential distribution (Figure 4.5E).

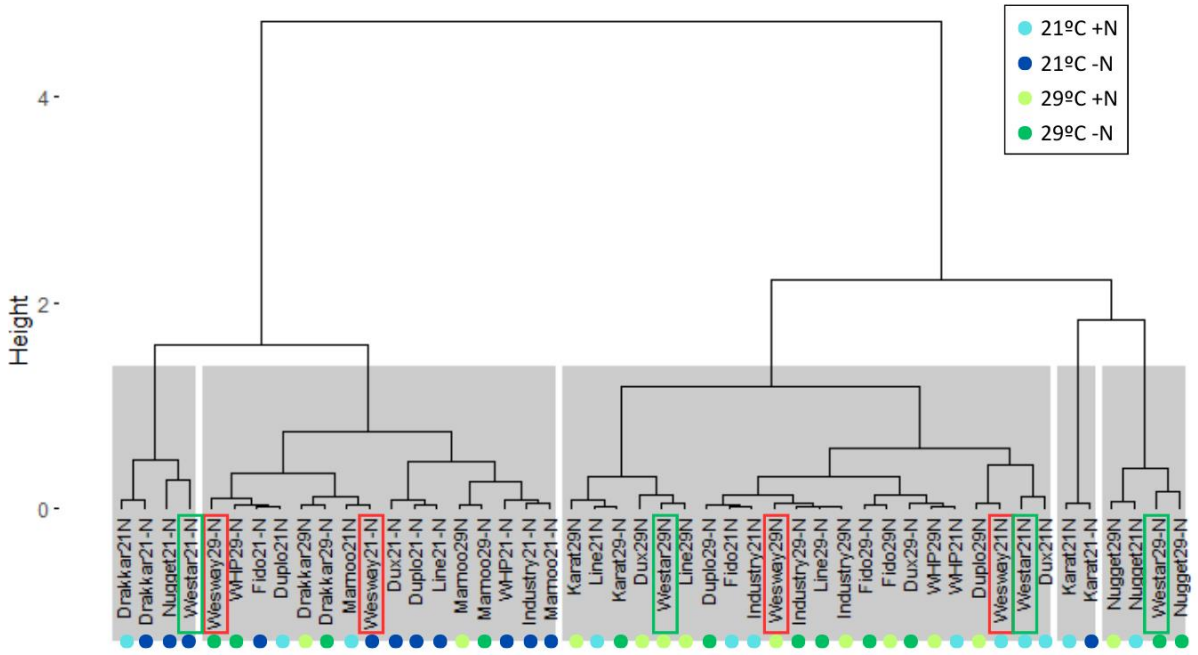


Figure 4.6: Dendrogram plot of hierarchical clustering analysis of the categorical variables on the principal components. Data from 12 different *B. napus* varieties and treatments: 21º C+N, 21ºC-N, 29ºC+N and 29ºC- N was used for the cluster analysis. Coloured circles at the bottom of the graph (light blue, dark blue, light green and dark green) were used to indicate the different treatments according to the legend in the upper right corner. The position of the varieties Westar and Wesway in the different clusters was highlighted with rectangles in green and red, respectively.

Since the varieties Westar and Wesway seemed to respond differently to the stress treatments, we analysed the individual root traits in those two varieties in more detail. In both varieties, network depth increased under N deficiency independently of the temperature. At 29ºC+N, network depth increased in Wesway but decreased in Westar, and under the stress combination (29ºC-N) both varieties showed a similar network depth to the control treatment (Figure 4.7A; B). The most remarkable difference between the root patterns in both varieties was the capacity of Wesway to increase the width of the root system under the stress combination (29ºC-N) compared to Westar, indicating an increase in the length of the LRs. Thus, in Wesway, there was a significant increase in Network Width (4.87 cm in Wesway vs. 2.16 cm in Westar; Figure 4.7; Supplementary Table 2B); network width to depth ratio (0.3 cm in Wesway vs. to 0.12 cm in Westar; Figure 4.7; minor ellipse axis (3.8 cm in Wesway vs. 1.95 cm in Westar; Supplementary Figure 3), and ellipse axes ratio (0.23 cm in Wesway vs. 0.12 cm in Westar; Supplementary Figure 4). Regarding traits related to the size of the root system, such as network area, network volume and network surface area (Supplementary

Figure 3; 4), Wesway behaved similar to the control treatment when grown at 21ºC-N, 29ºC+N or 29ºC-N. This suggests that Wesway was able to maintain the size of the root system under all stress treatments compared to 21ºC+N. Conversely, in Westar, traits related to the network size, such as network area, volume, and surface area were significantly increased at 21ºC-N (53%, 82% and 63%, respectively) and decreased at 29ºC+N (49%, 56% and 52%, respectively), indicating that Westar suffered more alterations in the size of the root system as a consequence of the treatments. Finally, both varieties decreased their LRD at 21ºC-N, 29ºC+N and 29ºC-N. However, Wesway had higher LRD at 29ºC-N than at 21ºC-N or 29ºC+N (Figure 4.7B), suggesting a specific induction of LR formation under the stress combination that is not present under both stresses applied individually.

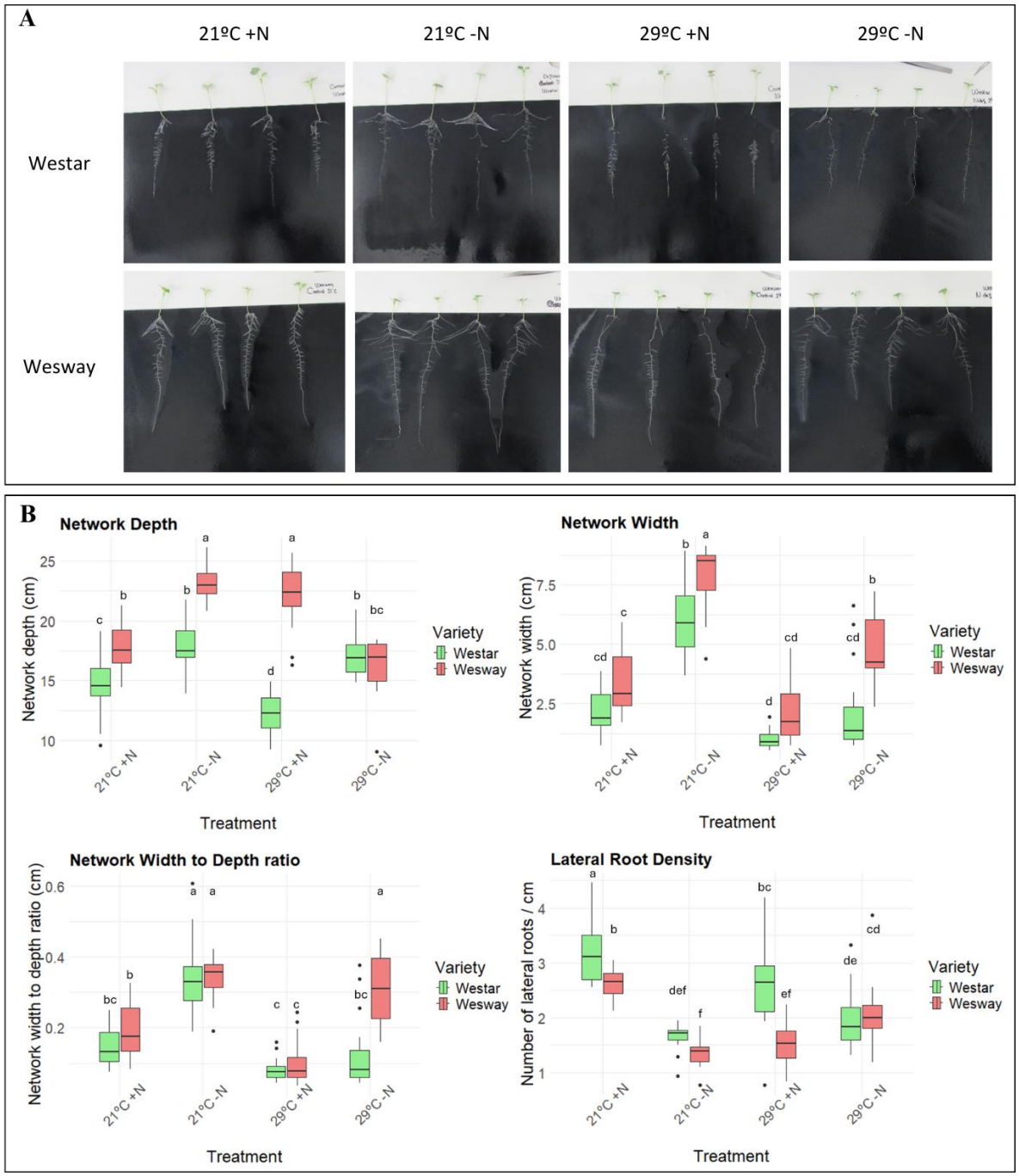


Figure 4.7: Main differences between the varieties Westar and Wesway in response to different temperature and N treatments. A) Images of roots from Westar (upper row) and Wesway (bottom row) seedlings grown in the pouch and wick system under different temperature and N treatments (from left to right: 21ºC+N, 21ºC-N, 29ºC+N and 29ºC-N) for 7 days. B) Mean values of different traits (network depth, network width, network width to depth and lateral root density) in *B. napus* seedlings grown in the pouch and wick system under different temperature and nitrogen treatments for 7 days. X-axis indicates the different treatments. The legend indicates the variety: Westar (green) and Wesway (red). Boxplots showing the values for Westar and Wesway in all the other measured root traits are shown in Supplementary Figure 3; 4. Letters indicate significant differences between groups ($p < 0.05$). Groups that are significantly different from each other do not share any letter.

In summary, we have characterized the variation in the root responses to warm temperatures, N deficiency and the combination of both stresses among different *B. napus* varieties and have identified specific root responses to the different treatments. Thus, in Westar these changes were very pronounced, whereas Wesway showed a more buffered response across the treatments. Furthermore, Wesway showed specific responses to the stress combination, such as an increase in the width of the root system due to the increase in the length of the lateral roots, and a higher LRD compared to the individual stresses.

### 4.1.3. Two *B. napus* varieties with different root responses to warm temperatures and N deficiency show differences in their nitrate content in roots and shoots.

We have previously characterized the phenotypic root response of 12 *B. napus* varieties under N deficiency, warm temperature or the combination of both stresses, and selected two varieties with contrasting responses, particularly under the stress combination. N deficiency causes alterations in root architecture, influencing N transport and assimilation, and in turn, changing the N content of the whole plant (Krouk *et al.*, 2010; Mounier *et al.*, 2014). To investigate whether the differential root responses to the temperature and N treatments between our selected two varieties, Westar and Wesway, contribute to improve or impair N availability in the plant, nitrate content was measured in whole roots and shoots from both varieties using the colorimetric method adapted from Hachiya & Okamoto (2017). Under optimal nitrogen conditions, Westar accumulated more nitrate in roots at 29ºC than at 21ºC (69.73 µg/g compared to 53.96 µg/g), whereas in Wesway this difference was not observed (66.96 µg/g compared to 64.24 µg/g) (Figure 4.8A). This correlates with our results observed in root traits, where Westar was more sensitive to warm temperatures than Wesway, changing several root traits (Figure 4.8). Interestingly, this increase in nitrate content in roots of Westar at 29ºC was not accompanied by an increase in nitrate content in shoots, since a reduction in nitrate content was observed in both varieties (Figure 4.8B). Under N deficiency, in both Wesway and Westar, accumulation of nitrate in roots was very low and similar under both temperatures (2.86 ug/g at 29ºC and 2.24 ug/g at 21ºC in Wesway, and 2.82 ug/g at 29ºC and 2.63 ug/g at 21ºC in Westar). However, in shoots under N deficiency, Wesway accumulated more N at 21ºC than at 29ºC (4.8 ug/g at 21ºC vs. 4.19 ug/g at 29ºC; Figure 4.8B), contrary to its behaviour in roots. Thus, nitrate content in roots and shoots of *B. napus* was

altered by the different temperature and N treatments. Under N deficiency, both varieties dramatically reduced their N content in roots independently of the temperature. However, in shoots, Wesway accumulated more nitrate than Westar, suggesting a complex regulatory process affecting nitrogen transport or metabolism in the whole plant under these stresses.

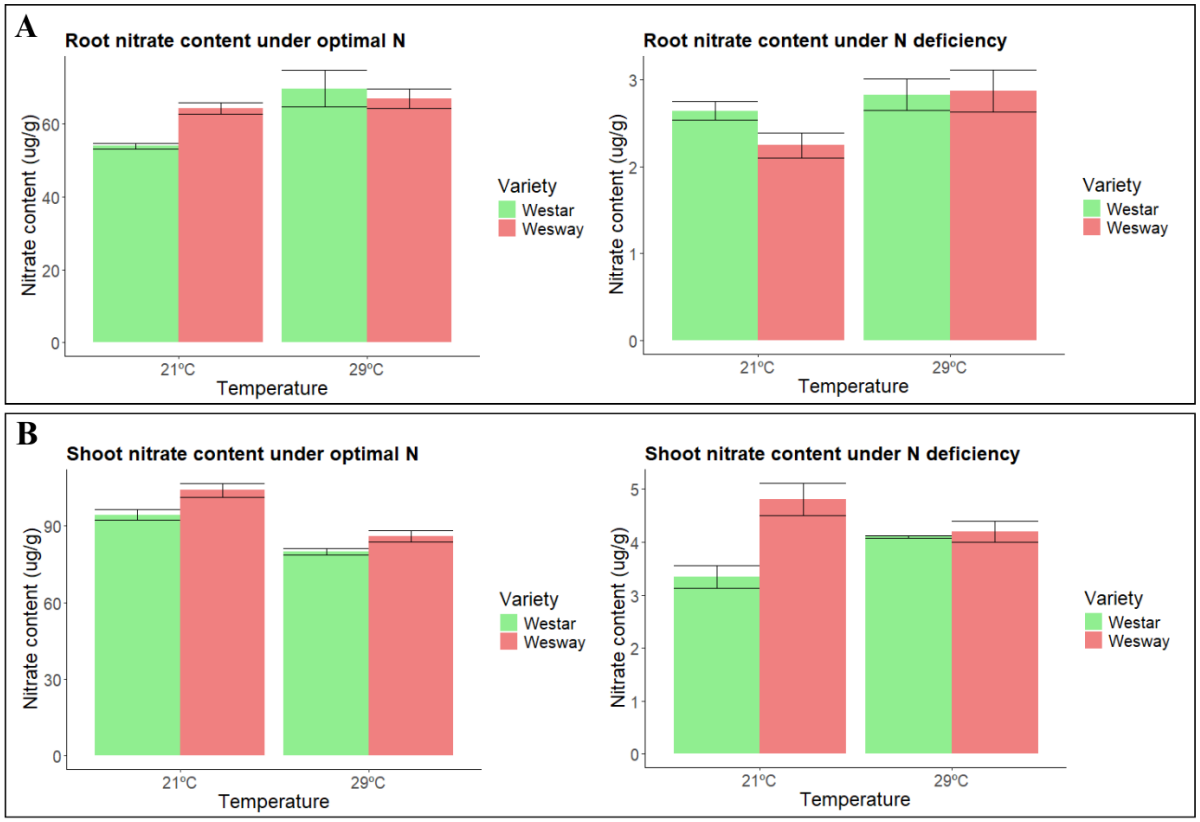


Figure 4.8: Nitrate content in whole roots and shoots of *B. napus* seedlings from two varieties: Westar and Wesway grown under different temperature and/or nitrogen conditions for 7 days. Error bars represent the standard deviation between the average nitrate content of two replicates containing 8 seedlings each. A) Nitrate content in whole roots (µg/g). B) Nitrate content in whole shoots (µg/g). X-axis indicates the different temperatures. Left: N content in seedlings grown under optimal N. Right: N content in seedlings grown under N deficiency.

## 4.2. Identification of the main transcriptional networks and biological processes underlying root responses to the combination of warm temperature and nitrogen deficiency in *B. napus*.

### 4.2.1. Transcriptional responses of two *B. napus* varieties with different root adaptation strategies to combined warm temperatures and nitrogen deficiency.

Since the varieties Westar and Wesway showed different root adaptation strategies to the stress treatments, we decided to compare the root transcriptional response of the two varieties to understand the genetic regulation of these differential responses. Thus, we performed an RNA sequencing analysis in whole roots and shoots of both varieties grown in the pouch and wick system under differential temperature and/or nitrogen conditions for 7 days. In this section, we focus on describing the transcriptional responses in roots.

In roots, the differentially expressed genes (DEGs) were calculated under the three stress treatments: N deficiency (21ºC-N), warm temperatures (29ºC+N) and the stress combination (29ºC-N), compared to the treatment with optimal N and temperature (21ºC+N) in each of the two varieties independently, performing six comparisons in total (Figure 4.9). We observed that the number of DEGs was much higher in response to warm temperatures (29ºC+N) or to stress combination (29ºC-N) than to N deficiency alone (21ºC-N) in both varieties, and the number of up-regulated and down-regulated genes was similar within each comparison (Figure 4.9A; B). Under N deficiency alone (21ºC-N), Wesway showed more up-regulated genes and less down-regulated genes than Westar, whereas at 29ºC+N and 29ºC-N the ratio between up-regulated and down-regulated genes was similar in both varieties (Figure 4.9C). Altogether, all these results suggest that both varieties have a differential transcriptomic response regarding not only the type (induction vs. repression) but also the intensity (higher or lower number of DEGs) of the changes.

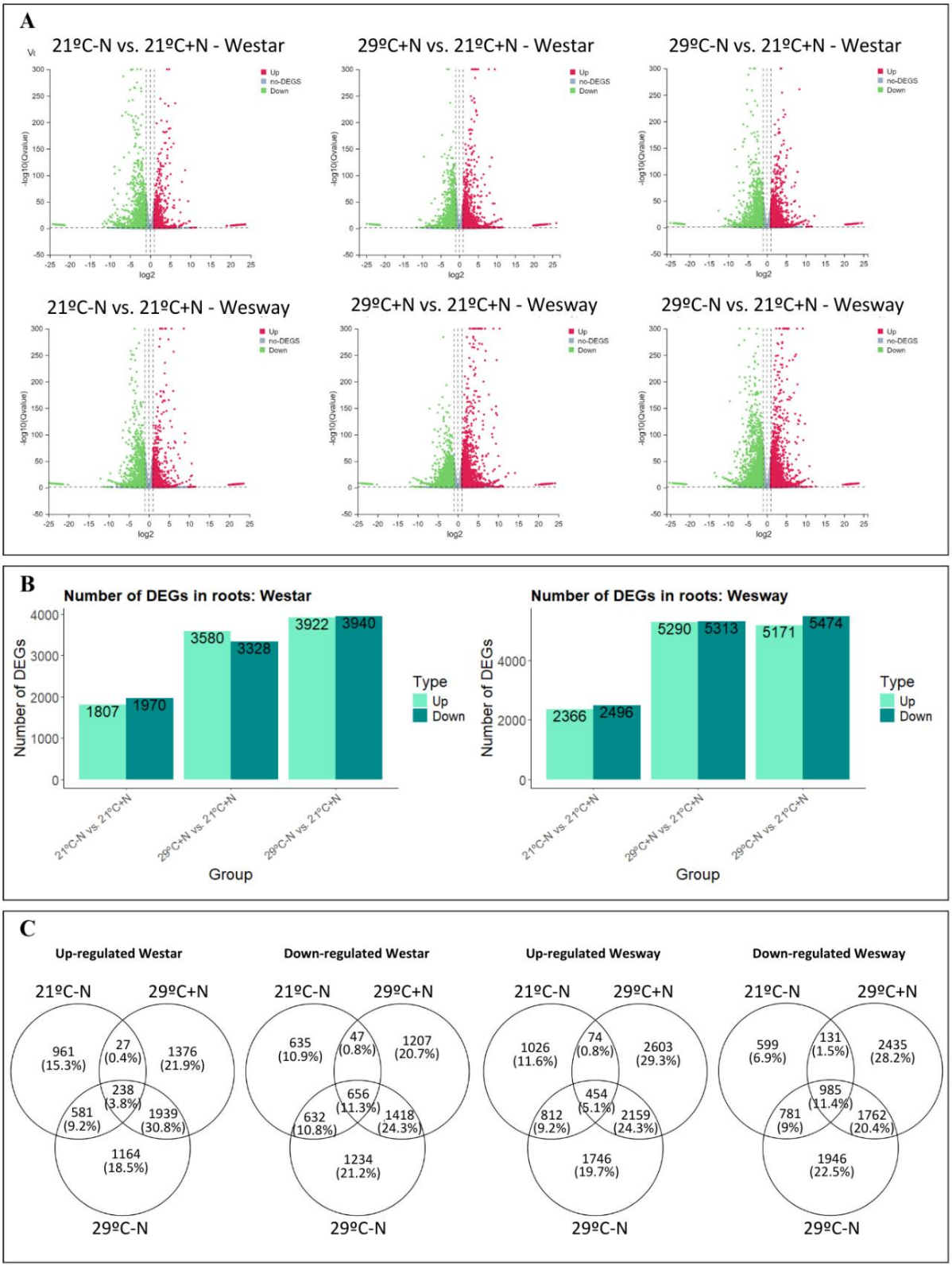


Figure 4.9: Effect of temperature and N content on gene expression in roots of Westar and Wesway. A) Volcano plots for the differentially expressed genes (DEGs) (|log2FC| > 1; p-value < 0.05) in roots under different temperature and nitrogen treatments compared to control conditions. The top row shows volcano plots for the variety Westar, whereas the plots in the bottom row correspond to Wesway. From left to right: DEGs in roots under

nitrogen deficiency (21ºC-N), DEGs in roots under warm temperature (29ºC+N) and DEGs in roots under the stress combination (29ºC-N), all of them compared to the control conditions (21ºC+N). B) Number of DEGs (|log2FC| > 1; p-value < 0.05) in roots of Westar (left) and Wesway (right) under different temperature and nitrogen treatments compared to control conditions. X-axis show the different comparisons: nitrogen deficiency (21ºC-N vs. 21ºC+N), warm temperature (29ºC+N vs. 21ºC+N) and the stress combination (29ºC-N vs. 21ºC+N). The legend indicates whether the genes are up-regulated or down-regulated. C) Venn diagrams showing the number of DEGs that are common between the three treatments (21ºC-N, 29ºC+N and 29ºC-N), all compared to the control treatment (21ºC+N). From left to right: Up-regulated genes in Westar, down-regulated genes in Westar, up-regulated genes in Wesway, down-regulated genes in Wesway.

To further identify the genes and molecular pathways involved in the differences in the root responses between these two varieties, we performed a cluster analysis. First, we took the DEGs from the six comparisons described above and used their normalized read counts in all treatments (the average of three replicates per treatment) to build a dendrogram of the DEGs according to their expression profiles. Then, normalized read counts were scaled to obtain the Z-score of each gene (-2.5 to 2.5). The Z-scores were visualized in a heatmap, and the genes in the heatmap were ordered according to the previously calculated dendrogram of the normalized read counts (Figure 4.10). Finally, the cluster analysis grouped the genes in five different clusters according to their expression profiles (Figure 4.10).

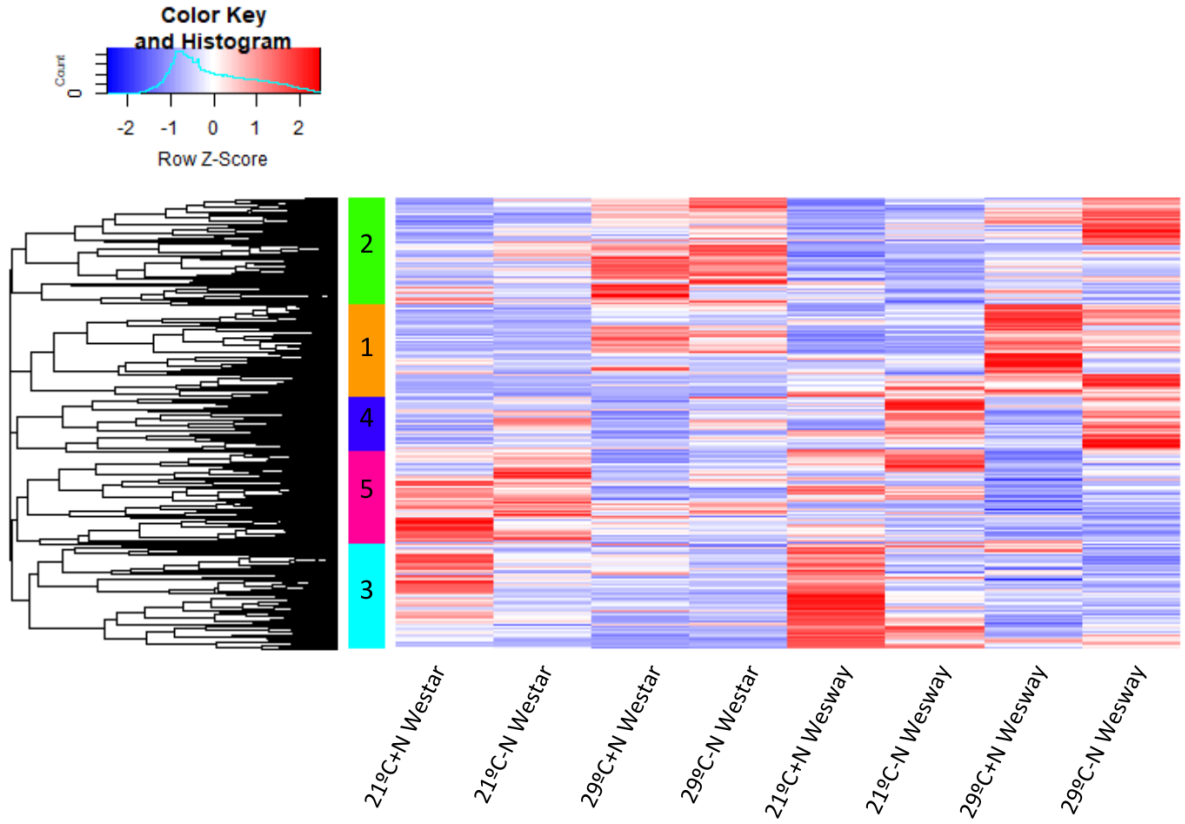


Figure 4.10: Heatmap visualization of DEGs in roots of *B. napus* individuals from two varieties (Westar & Wesway) and four temperature and nitrogen treatments (21ºC+N, 21ºC-N, 29ºC+N and 29ºC-N). The heatmap was built using Z-scores of the average of the normalized read count from three replicates per treatment. Only genes that were differentially expressed (|log2FC| > 1; p-value < 0.05) in at least one of the six comparisons between the treatments and/or varieties were considered. The genes were grouped in different clusters according to their expression profiles across the samples (k=5). The colour legend at the upper left corner indicates the Z-score values: blue (lower Z-score, lower expression); red (higher Z-score, higher expression). A table with the Z-scores of all DEGs for each treatment, with their respective log2FC for each comparison can be found in Supplementary Table 4A.

A gene ontology (GO) analysis was done for each of the five clusters mentioned above to identify the molecular pathways that are responsible for the differences in gene expression (Figure 4.11; Supplementary Table 4B). Cluster 1 represented a group of genes that showed high expression values under warm temperature and to a lesser extent, under the stress combination in both varieties, especially in Wesway (Figure 4.10). GO analysis of the genes found in Cluster 1 revealed several categories related to unfolded protein binding and protein self-association, containing genes encoding for heat shock proteins such as *BnHSP70-8* and *70-4*, *BnHSP26-5* and *BnHSP18.1*, that are related to the response to temperature stress (Figure 4.11; Supplementary Table 4B).

Cluster 2 contained genes with higher Z-score values under warm temperature and the stress combination, particularly in Westar. Interestingly, a subset of cluster 2 was strongly expressed under the stress combination in Wesway and less expressed in Westar (Figure 4.10). According to the GO analysis, one of the enriched categories was oxidoreductase activity, which showed a high log10FDR value (> 2.4) and contained many genes encoding for proteins that participate in the oxidative response, such as *PEROXIDASE 50, 51* and *71 (BnPER50, 51* and *71)*, *BnCAT1*, *POLYAMINE OXIDASE 2* (*BnPAO2*), *BnGPX2* and *ALTERNATIVE OXIDASE 1A, B* and *C (BnAOX1A, B* and *C)* (Figure 4.11; Supplementary Table 4B). Many of these genes related to the oxidative response belonged to the subset of genes that were strongly expressed under the stress combination in Wesway but not in Westar, suggesting a distinct activation of the oxidative response and peroxidase activity in Wesway under the stress combination.

Cluster 3 contained genes that generally showed a lower gene expression (Z-score < 0) under all the three stress treatments in both varieties (Figure 4.10), and it included a group of genes related to structural molecule activity, with many ribosomal genes, such as *LARGE RIBOSOMAL PROTEIN 32A (BnRPL32A)* and *SMALL RIBOSOMAL PROTEIN 24B (BnRPS24B)* and structural constituents of chromatin, with genes like *HISTONE 3.1 (BnHTR2)* and *HISTONE 3.3 (BnHTR4)* (Figure 4.11; Supplementary Table 4B). This suggests that the three stress treatments strongly down-regulated ribosomal activity in both varieties.

Genes in cluster 4 were highly expressed under N deficiency and in response to the stress combination in both varieties but the expression was much higher in Wesway (Figure 4.10). This cluster included gene categories like glutamate ammonia ligase activity, containing genes encoding for *GLUTAMINE SYNTHEASE 1*, like *BnGLN1-4* and *BnGLN1-5*, that play an important role in N assimilation in plants, (+)-abscisic acid 8-hydroxylase activity, with genes like *CYTOCHROME P450 FAMILY 707 SUBFAMILY A POLYPEPTIDE 3 (BnCYP707A3),* and DNA-binding transcription factor activity, with genes like *BnWRKY25, BnDREB2E, BnERF1A* or *BnERF13* (Figure 4.11; Supplementary Table 4B).

Finally, cluster 5 contained genes that showed a lower gene expression under warm temperature and under the stress combination in both varieties, being slightly more pronounced in Wesway than in Westar (Figure 4.10). Some of the enriched categories in cluster 5 were oxidoreductase activity, with genes related to

proline biosynthesis like *PYRROLINE-5-CARBOXYLATE (P5C) REDUCTASE (BnPROC1)* and *DELTA1-P5C SYNTHASE 1 (BnP5CS)*, as well as *GLUTAMATE DEHYDROGENASE (BnGDH3*; Figure 4.11; Supplementary Table 4B). Different N sources have shown to affect proline accumulation under high temperature stress (Rivero *et al.*, 2004).

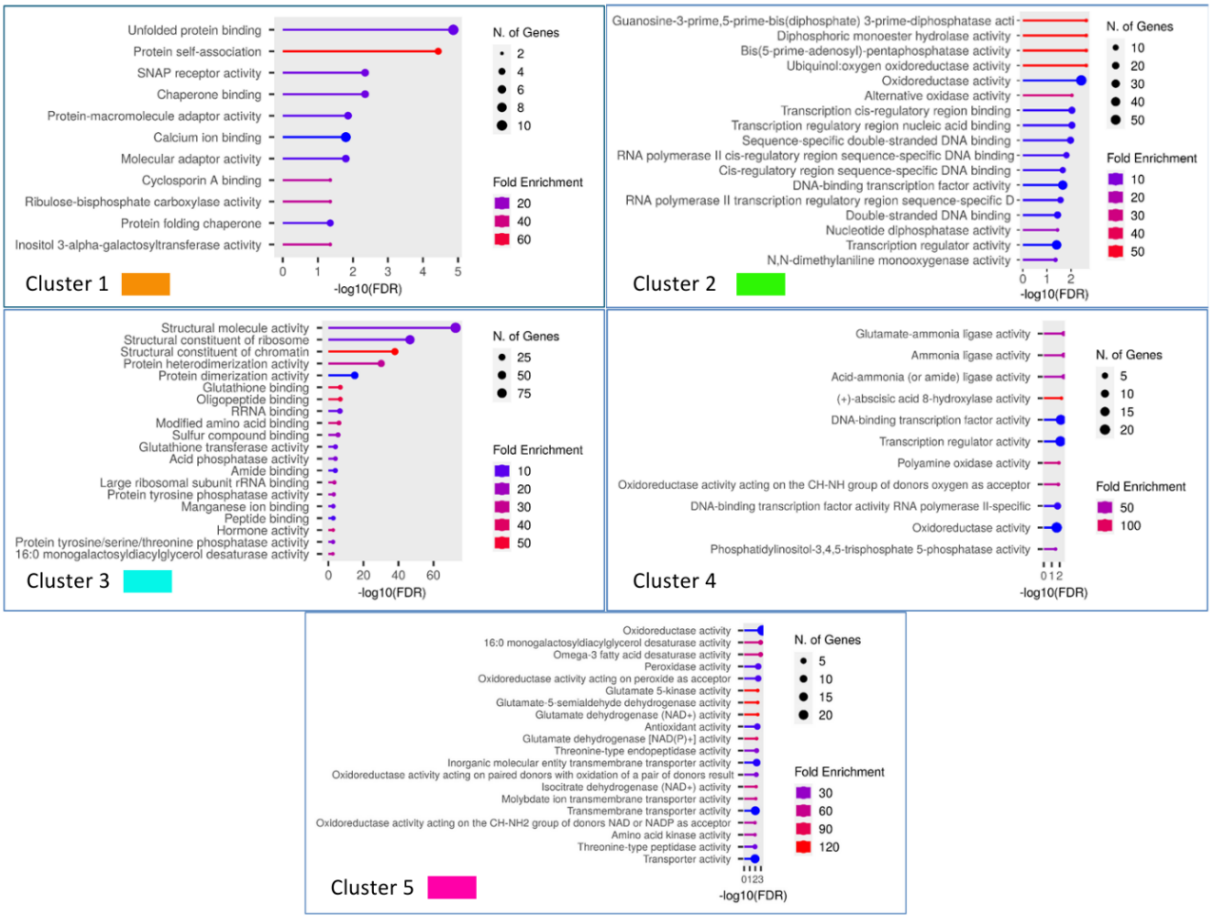


Figure 4.11: Gene ontology (GO) enrichment analysis of the differentially expressed genes (DEGs) in roots of *B. napus* individuals from two varieties (Westar & Wesway) and four temperature and nitrogen treatments (21ºC+N, 21ºC-N, 29ºC+N and 29ºC-N). The GO enrichment was done individually for each of the five gene clusters previously obtained according to the expression profile of the genes across the samples and was calculated using Shiny GO.

To gain additional insights into the most altered molecular pathways within each cluster, we obtained the *A. thaliana* homologous from the genes in the most relevant categories, and we searched for possible interactions between them using the STRING database (https://string-db.org/). Using this approach, we obtained different protein interaction networks (Figure 4.12). For cluster 1, we selected a subset of genes that were up-regulated (logFC > 1; p-value < 0.05) at 29ºC+N and

to a lesser extent at 29ºC-N in both varieties (Figure 4.12; Supplementary Table 4A). The obtained network contained proteins related to protein folding and response to heat stress, such as heat shock proteins (HSP18, 21, 22, 26 and 70) and proteins related to the stress response like GALACTINOL SYNTHASE 1 (GOLS1), indicating their role in the response to warm temperatures in roots. We also obtained a network related to response to dehydration, with proteins like NAC072 and PEROXYGENASE 3 (PGX3). NAC072, also called RD26, is a TF that usually participates in the response to dehydration via ABA, and negatively regulates root growth and root hair formation (Fujita *et al.*, 2004; Kamranfar *et al.*, 2021).

As previously described, cluster 2 had an overrepresentation of genes related to oxidoreductase activity. We selected a subset of genes that were up-regulated in both varieties at 29ºC-N, and found an interaction network containing genes related to hydrogen peroxide metabolism and many ROS-scavenging proteins, like PER50, PER51, GPX2 and PAO2 (Figure 4.12). Peroxidases are known to play a role in ROS mitigation under abiotic stresses (Kidwai *et al.*, 2020), and they are involved in LR emergence and elongation (Manzano *et al.*, 2023; Silva-Navas *et al.*, 2016), suggesting that they could play a role in the better capacity of Wesway to develop LRs at 29ºC-N.

For cluster 3, we selected a subset of genes that were significantly down-regulated (logFC < 1; p-value < 0.05) at 29ºC-N in both varieties (Supplementary Table 4A), and to a lesser extent at 21ºC-N and 29ºC+N. The first network contained proteins related to the cellular response to Pi starvation like SPX3, SPX1, PURPLE ACID PHOSPHATASE 17 (PAP17), LBD38 and TGACG SEQUENCE-SPECIFIC BINDING PROTEIN 1 and 4 (TGA1, 4; Figure 4.12). Interestingly, TGA1 is a TF that responds to nitrate and has shown to positively regulate lateral root elongation (Alvarez *et al.*, 2014), additionally, it interacts with LBD38, a known repressor of nitrate transporters in roots (Teng *et al.*, 2022). The down-regulation of TGA1 could be related to the reduced lateral root density observed at 21ºC-N and 29ºC-N, compared to control conditions. The second network was related to linolenic acid biosynthesis and jasmonic acid signalling, with proteins like ALLENE OXIDE CYCLASE 1, 2 and 4 (AOC1, 2 and 4), TIFY DOMAIN PROTEIN 9 (TIFY9) and PHYTOALEXIN DEFICIENT 4 (PAD4), suggesting a role of this hormonal pathway in the response to the stress combination. The third network contained proteins related to ribosomal activity (RPLs and RPSs): small ribosomal proteins (RPS5, 11, 13, 21, 27, 30) and large ribosomal proteins (RPL10, 21, 27, 32). In Arabidopsis, RPS5 is known to be involved in cold tolerance (Zhang *et al.*,

2016), whereas RPL10 has been involved in the response to UV light (Ferreyra *et al.*, 2010; Zhang *et al.*, 2020a) and down-regulation of *RPL32* under abiotic stresses has been reported in rice (Mukhopadhyay *et al.*, 2011).

For cluster 4, we selected a subset of genes that were up-regulated (logFC > 1; p-value < 0.05) in Wesway at 29ºC-N, and to a lesser extent in Westar, but not under the individual stress treatments (Supplementary Table 4A). Here, we highlighted two networks. One of them with proteins related to the cellular response to stress. Like AOX1A, UNCOUPLING PROTEIN 5 (PUMP5), CCR4-ASSOCIATED FACTOR 1-9 (CAF1-9), WRKY25 and ERF1A (Figure 4.12), and also the genes *DREB2E, CYP707A3* and *WRKY25* known to contribute to lateral root elongation under several abiotic stresses via ABA (Sakuma *et al.*, 2002; Li *et al.*, 2009; Deolu-Ajayi *et al.*, 2019; Li *et al.*, 2014; Wu *et al.*, 2020a), suggesting that Wesway could up-regulate mechanisms involved in the ABA-mediated response to stress at 29ºC-N. The second network contained proteins related to the response to N deficiency (AMT1-1, GLN1-4, GLN1-5). In *B. napus*, GLN1 has many isoforms, and the expression of different isoforms has been related to N remobilization to different parts of the plant (Orsel *et al.,* 2014). On the other hand, AMT1-1 is a high affinity ammonium transporter and is typically expressed under N deficiency (Zhu *et al.*, 2023).

For cluster 5, we selected genes that were down-regulated (logFC < 1; p-value < 0.05) at 29ºC+N and to a lesser extent 29ºC-N in both varieties (Supplementary Table 4A), and generated a protein interaction network that highlighted the function in proline biosynthesis (PROC1, P5CSA). This suggests that warm temperature could negatively affect proline biosynthesis in both varieties. We also obtained another network related to root cap activity, with proteins like JACALIN-ASSOCIATED LECTIN 9 and 10 (JAL9, 10; Figure 4.12). JAL9 and 10 are induced by salinity stress, and are expressed in root caps to positively contribute to root growth (Das *et al.*, 2023; Alagarasan, 2024). Since they were down-regulated at 29+N and not in the other treatments, they could be involved in the decrease in LR growth observed at 29ºC+N.

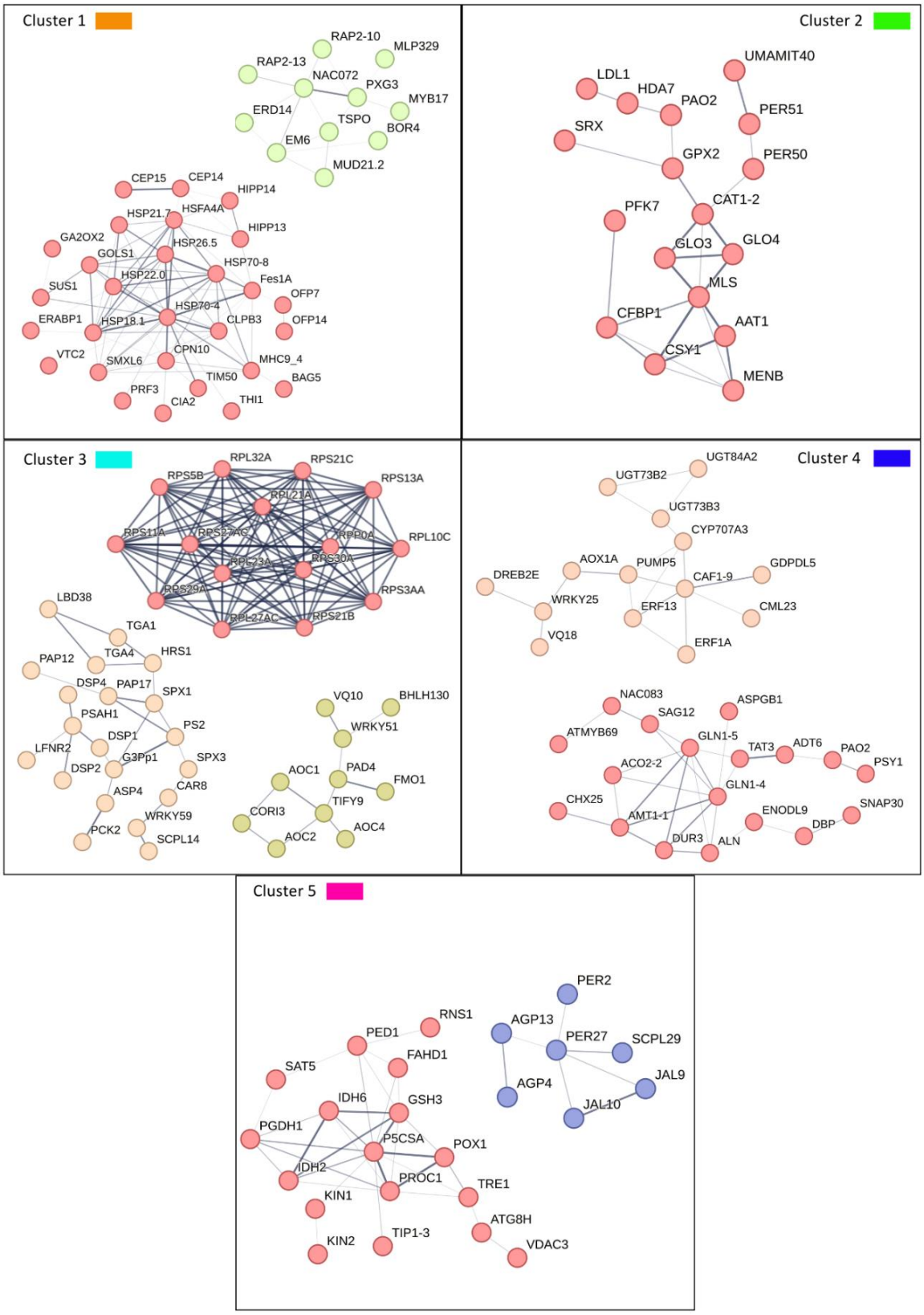


Figure 4.12: Interaction networks for each of the five clusters of DEGs in roots of *B. napus* individuals from two varieties (Westar & Wesway) and four temperature and nitrogen treatments (21ºC+N, 21ºC-N, 29ºC+N and 29ºC-N). The *A. thaliana* orthologs from the most relevant DEGs were considered.

These analyses allowed us to identify several clusters of genes that could underlie the effects of warm temperature, N deficiency or the stress combination in the root system. As mentioned above, cluster 2 and 4 contained several genes that were more expressed in Wesway than in Westar in response to the stress combination (Figure 4.10; Supplementary Table 4B). One of the categories that was enriched in both cluster 2 and cluster 4 was oxidoreductase activity (Figure 4.12). This category contained many genes related to the response to oxidative stress, including several peroxidases (*BnPER58*, *BnPER59*, *BnPER71*) and other enzymes such as polyamine oxidase (*BnPAO2*), alternative oxidase (*BnAOX1A*) and peroxygenases (*BnPGX4* or *BnPGX5*). Furthermore, these genes belonged to the subset of cluster 2 that were strongly expressed at 29ºC-N in Wesway (Figure 4.10). A closer look into the genes from this subset revealed that these peroxidase genes were up-regulated (logFC > 1; p-value < 0.05) by the stress combination in both varieties, but this up-regulation was more significant in Wesway (Supplementary Table 4A). We quantified the expression of two of these peroxidases, *BnPER59* and *BnPER71* by real time quantitative PCR (RT-qPCR) in roots of both Westar and Wesway treated under the four conditions (21ºC+N, 21ºC-N, 29ºC+N and 29ºC-N). *BnPER71* was more expressed in Westar than in Wesway in all treatments (Figure 4.13B), but both varieties showed a clear up-regulation of *BnPER71* under the stress combination compared to the other treatments (Figure 4.13A; B). A recent study has found that *AtPER71* was induced by different abiotic stresses, such as heat, cold and salinity in Arabidopsis roots (Eljebbawi *et al.*, 2022). Interestingly, *PER71* has previously shown to be activated by cold stress in the grass species *C. dactylon*, and this activation of *PER71* is mediated by ethylene response factors (Hu *et al.*, 2020). Accordingly, we observed an enhanced expression of these ethylene response factors in both varieties at 29ºC-N, including *BnERF11, BnERF13, BNERF112* and *BnERF118*, and some of them only in Wesway, such as *BnERF1A* (Supplementary Table 4A). All these evidence support the idea that *BnPER71* might be involved in the root response to combined warm temperature and N deficiency in *B. napus*. Regarding *BnPER59*, it was induced by N deficiency in both varieties, but the induction was higher under the stress combination. Furthermore, the induction of *BnPER59* in Wesway was higher than in Westar at 21ºC-N and 29ºC-N (Figure 4.13A; B). Thus, these results suggest that *BnPER59* might also be involved in the root responses to N deficiency and the combination of both stresses in *B. napus* roots. Due to the antioxidant and ROS-scavenging capacity of peroxidases, the higher induction of peroxidase genes in

Wesway under the stress combination (29ºC-N) might help this variety to adapt to N deficiency stress more efficiently than Westar.

**A**

| Gene name | A. thaliana ortholog | Protein | Westar 21°C +N | Westar 21°C -N | Westar 29°C +N | Westar 29°C -N | Wesway 21°C +N | Wesway 21°C -N | Wesway 29°C +N | Wesway 29°C -N |
|---|---|---|---|---|---|---|---|---|---|---|
| BnaC02g42930D | AT5G64120 | PER71 | -0.44896 | -0.3841 | **-0.6436** | **-0.084** | -0.1456 | -0.34675 | -0.38407 | **2.4373** |
| BnaC06g12560D | AT5G39580 | PER62 | -0.6333 | -0.6578 | **-0.1927** | **-0.046** | -0.25393 | 0.296763 | **-0.8169** | **2.3037** |
| BnaC02g42920D | AT5G64100 | PER69 | -0.16651 | -0.3449 | -1.05032 | 0.79237 | 0.068828 | 0.560122 | **-1.478** | 1.61843 |
| BnaC09g37740D | AT5G19890 | PER59 | -0.62734 | -0.7252 | -0.84399 | **0.386** | -0.6314 | **0.38258** | -0.10033 | **2.1597** |

**B**

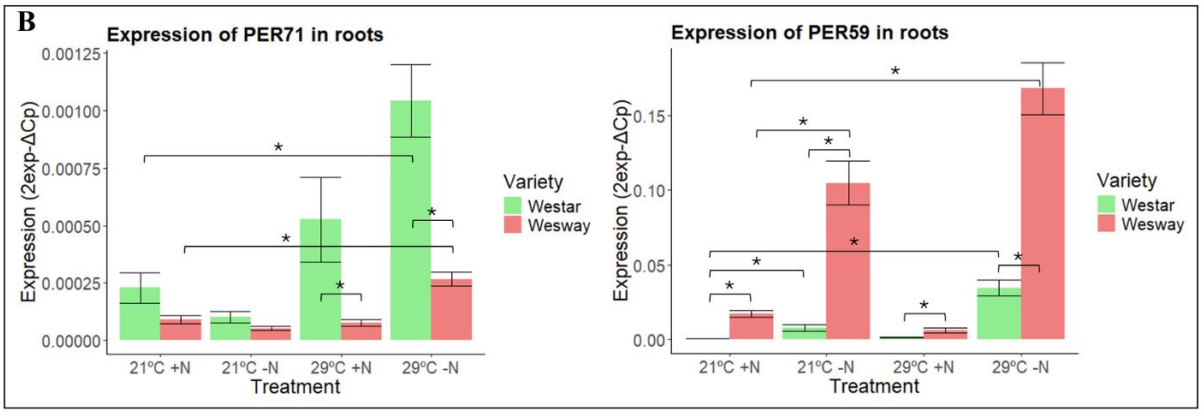


Figure 4.13: Expression of peroxidase genes in response to N deficiency (21ºC-N), warm temperature (29ºC+N) or the combination of both stresses (29ºC-N) in roots from *B. napus* varieties Westar & Wesway. A) Z-score values of different peroxidase genes quantified by RNA sequencing. Z-score values represent the average from three independent replicates per variety and treatment. Red indicates more expression while blue indicates less expression. Bold numbers indicate significant differences ($|log2FC| > 1$; p-value < 0.05) with the control treatment (21ºC+N) from each variety. B) Expression of *BnPER71* (*BnaC02g42930D*; left) and *BnPER59* (*BnaC09g37740D*; right) quantified by quantitative RT-PCR (qRT-PCR) in roots of *B. napus* individuals from two varieties (Westar & Wesway), grown under different temperature and N treatments: 21ºC+N, 21ºC-N, 29ºC+N and 29ºC-N. X-axis indicates the expression levels (2exp-ΔCp) normalized to the expression of the control gene *BnACT7*. Error bars show the variation between three independent biological samples (with three technical replicates each). Asterisks indicate significant differences between groups (p-value < 0.05).

Other genes in cluster 4 that were more expressed in Wesway than in Westar at 29ºC-N, were related to ABA metabolism, such as *BnCYP707A3*, which has previously shown to be up-regulated by ABA, salinity and drought (Umezawa *et al.*, 2006; Zhou *et al.*, 2007). The phytohormone ABA is known to promote carotenoid biosynthesis in roots under abiotic stress conditions via *PHYTOENE SYNTHASE (PSY)* genes in Arabidopsis (Li *et al.*, 2008; Maass *et* al., 2009; Bowman *et al.*, 2014) and rice (Welsch *et al.*, 2008). Accordingly, we observed a

strong up-regulation of *BnPSY1* in Wesway at 29ºC-N, and not in Westar (Figure 4.14A). We quantified the expression of *BnPSY1* by RT-qPCR in roots of both Westar and Wesway grown under the four conditions (21ºC+N, 21ºC-N, 29ºC+N and 29ºC-N). The RT-qPCR data indicated that *BnPSY1* was more expressed under the combination of warm temperature and N deficiency than under the individual stresses (Figure 4.14B). However, the RNA-seq data showed that the induction of *BnPSY1* under the stress combination was higher in Wesway than in Westar (Figure 4.14A), whereas the RT-qPCR showed a similar high induction in both varieties under the stress combination (Figure 4.14B).

**A**

| Gene name | A. thaliana ortholog | Protein | Westar 21ºC +N | Westar 21ºC -N | Westar 29ºC +N | Westar 29ºC -N | Wesway 21ºC +N | Wesway 21ºC -N | Wesway 29ºC +N | Wesway 29ºC -N |
|---|---|---|---|---|---|---|---|---|---|---|
| BnaC07g18360D | AT5G45340 | CYP707A3 | 0.6861816 | -0.651736 | -0.777672 | 0.47872 | -0.790031 | 0.482314 | -1.17162 | **1.74384** |
| BnaAnng05520D | AT5G45340 | CYP707A3 | 0.3937245 | -0.325874 | -0.409994 | 0.438951 | -1.306947 | **0.62302** | -1.13986 | **1.72698** |
| BnaC09g40730D | AT5G17230 | PSY1 | -0.506374 | -0.492954 | -0.660386 | -0.00933 | -0.450563 | -0.33837 | 0.061502 | **2.39648** |

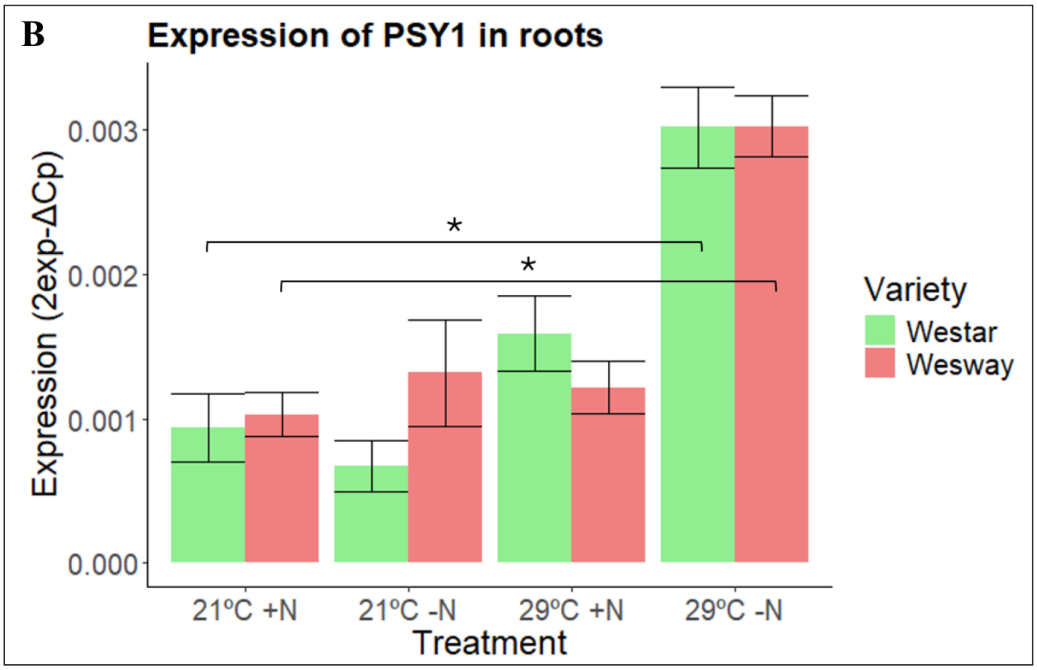


Figure 4.14: Differential expression of the *BnPSY1* gene in *B. napus* roots in response to N deficiency (21ºC-N), warm temperature (29ºC+N) or the combination of both stresses (29ºC-N). A) Z-score values of *BnPSY1* and other genes related to ABA catabolism quantified by RNA sequencing. Z-score values represent the average from three independent replicates per variety and treatment. Red indicates more expression while blue indicates less expression. Bold numbers indicate significant differences (|log2FC| > 1; p-value < 0.05) with the control treatment (21ºC+N) from each variety. B) Expression of *BnPSY1 (BnaC09g40730D)* quantified by quantitative PCR (qPCR) in roots of *B. napus* individuals from two varieties (Westar & Wesway), grown under different temperature and N treatments: 21ºC+N, 21ºC-N, 29ºC+N and 29ºC-N. X-axis indicates the expression levels (2exp-ΔCp) normalized to the expression of the control gene *BnACT7*. Error bars show the variation between three independent biological samples (with three technical replicates each). Asterisks indicate significant differences between groups (p-value < 0.05).

Thus, we identified several pathways that were more up-regulated in Wesway than in Westar at 29ºC-N, including oxidoreductase activity or genes related to the ABA-mediated response to stress. Interestingly, several of these genes are known to contribute to LR elongation, suggesting that these pathways might play a role on the better capacity of Wesway to develop LRs under the stress combination.

### 4.2.2. The ethylene gene network plays a role in the root responses to warm temperatures and nitrogen deficiency in *Brassica napus* and Arabidopsis.

Our analysis of RNA sequencing data in roots of Westar and Wesway grown under different temperature and N treatments (21ºC+N, 21ºC-N, 29C+N and 29ºC-) revealed changes in the expression of many genes related to hormone signalling. Among all these genes, we encountered significant differences in the expression of ethylene response factors (ERFs) between both varieties (Figure 4.15). Ethylene is known to play a crucial role on LR development (Negi *et al.*, 2008; Lewis *et al.*, 2011), and increased production of ethylene has shown to inhibit LR growth in Arabidopsis under high N (Tian *et al.*, 2009). Furthermore, in *B. napus*, inhibition of ethylene biosynthesis is known to promote root elongation and increase N uptake under N deficiency (Lemaire *et al.*, 2013). Thus, we aimed to investigate the role of ethylene in the differences in LR elongation observed between Westar and Wesway under the stress combination.

| Gene name | A. thaliana ortholog | Protein | Westar 21°C +N | Westar 21°C -N | Westar 29°C +N | Westar 29°C -N | Wesway 21°C +N | Wesway 21°C -N | Wesway 29°C +N | Wesway 29°C -N |
|---|---|---|---|---|---|---|---|---|---|---|
| BnaCnng36390D | AT5G07580 | ERF106 | 0.604062 | 1.58926 | -1.01573 | -0.2461 | -0.91706 | **1.18499** | -0.43761 | -0.7618 |
| BnaA09g27300D | AT1G28370 | ERF11 | -0.8808 | -0.9031 | -0.50172 | **0.8585** | -0.7916 | **0.70241** | **-0.2787** | **1.795** |
| BnaCnng05370D | AT2G33710 | ERF112 | -1.06472 | **0.3255** | -0.78042 | **0.677** | -0.84791 | **0.87086** | -0.7901 | **1.6098** |
| BnaAnng20260D | AT1G68550 | ERF118 | -0.64385 | 0.00928 | 1.022854 | **1.6063** | -1.24104 | -1.05943 | -0.20027 | **0.5061** |
| BnaA06g33270D | AT3G25890 | ERF119 | -1.00071 | -0.8691 | **1.2562** | 0.81476 | -0.87792 | -0.88111 | **1.1259** | 0.43203 |
| BnaC04g49870D | AT2G44840 | ERF13 | -0.88975 | **-0.056** | -0.96771 | **0.1627** | -0.29723 | 0.59154 | -0.64027 | **2.0962** |
| BnaC06g00880D | AT1G44830 | ERF14 | -0.84712 | **-0.345** | -0.61424 | **0.4921** | -0.83889 | **0.52892** | **-0.4612** | **2.0852** |
| BnaCnng05080D | AT4G17500 | ERF1A | -0.07414 | 0.43174 | -0.77191 | 0.92018 | -0.84168 | **0.20497** | **-1.4522** | **1.5831** |
| BnaA01g23940D | AT3G23240 | ERF1B | 0.012183 | -0.7621 | 1.24764 | -0.5215 | 1.590201 | -0.30423 | 0.13461 | **-1.397** |
| BnaA08g24660D | AT1G12630 | ERF27 | 2.043796 | 0.84418 | **-0.2666** | **-0.267** | 1.18E-15 | -0.62202 | **-1.0663** | **-0.666** |
| BnaCnng77210D | AT4G16750 | ERF39 | -1.4183 | -0.4036 | -0.52152 | **1.5272** | -0.19018 | -0.39502 | -0.02285 | 1.4242 |
| BnaC09g20100D | AT5G47230 | ERF5 | -0.44017 | -0.2953 | -0.84476 | -0.6974 | 1.303042 | 1.732602 | **-0.8947** | 0.13674 |
| BnaA09g18210D | AT5G47230 | ERF5 | -0.89054 | -0.8748 | -0.71767 | -0.2305 | 1.41438 | 1.435334 | **-0.702** | 0.56575 |
| BnaAnng29660D | AT2G20880 | ERF53 | -0.42227 | -0.3395 | **2.19555** | **0.6399** | -0.8758 | -0.77316 | **-0.1086** | **-0.316** |
| BnaA08g13860D | AT4G28140 | ERF54 | -0.54649 | -0.7056 | **1.50818** | 0.04006 | -0.8961 | -0.74501 | **-0.2399** | **1.5848** |
| BnaA03g54460D | AT4G39780 | ERF60 | -0.21429 | -0.7719 | -0.16683 | -0.2024 | -0.82526 | -0.62951 | **2.1999** | **0.6102** |

Figure 4.15: Z-score values of genes encoding for ethylene response factors (ERF) quantified by RNA sequencing. Z-score values represent the average from three independent replicates per variety and treatment. Red indicates more expressed, blue indicates less expressed. Bold numbers indicate significant differences ($|log2FC| > 1$; p-value < 0.05) with the control treatment (21°C+N) from each variety.

We observed that gene expression of some key genes in the ethylene biosynthetic pathway (like *BnACO1 and BnACS9*) were significantly repressed in both varieties by N deficiency independently of temperature (21°C-N and 29°C-N; Figure 4.16A). To confirm these changes in gene expression, we quantified the expression of *ACC OXIDASE 1* (*BnACO1*), a key enzyme in ethylene biosynthesis, by RT-qPCR (Figure 4.16B). We observed that both varieties repressed the expression of *BnACO1* at 21°C-N and 29°C-N, but this repression was stronger in Wesway that in Westar, compared to the control treatment (21°C+N). Since ethylene is known to be a negative regulator of LR development under high N (Tian *et al.*, 2009), the stronger repression of *BnACO1* in Wesway could be related to the capacity of this variety to develop longer LRs at 29°C-N. We also observed increased expression of *BnACO1* in Westar than in Wesway at 29°C+N in the RNA-sequencing data (Figure 4.16A), which correlates with the stronger suppression of LR elongation and consequent reduction in network width in Westar at 29°C+N. Another gene related to ethylene regulation is *HB52*, a member of the HD-ZIP family of

transcription factors that participates in the ethylene-mediated suppression of root growth (Xu *et al.*, 2020). Our RNA-seq data showed that the expression of *BnHB52* increased in Westar at 29ºC+N and 29ºC-N (Figure 4.16A), whereas the expression of *BnHB52* in Wesway was unaltered, while in the RT-qPCR results both varieties induced *BnHB52* at 29ºC+N and 29ºC-N (Figure 4.16B), suggesting a possible role of HB52 in the regulation of the LR elongation observed in both varieties.

**A**

| Gene name | A. thaliana ortholog | Protein | Westar 21°C +N | Westar 21°C -N | Westar 29°C +N | Westar 29°C -N | Wesway 21°C +N | Wesway 21°C -N | Wesway 29°C +N | Wesway 29°C -N |
|---|---|---|---|---|---|---|---|---|---|---|
| BnaA09g44060D | AT2G19590 | ACO1 | 1.371997 | -0.5142 | 0.089934 | **-0.726** | 1.232595 | **-1.0849** | 0.69665 | **-1.066** |
| BnaC08g36640D | AT2G19590 | ACO1 | 0.986712 | **-1.096** | 0.453561 | **-0.91** | 0.997747 | **-0.8566** | 1.2052 | **-0.78** |
| BnaCnng67880D | AT2G19590 | ACO1 | 1.833482 | 0.46411 | 0.910649 | **-0.012** | -0.74376 | -0.92105 | -0.86376 | -0.6678 |
| BnaCnng33000D | AT2G19590 | ACO1 | -0.48873 | **-1.084** | **1.69602** | -0.1499 | 0.977522 | **-1.2313** | 0.4367 | -0.1561 |
| BnaC07g31520D pro | AT3G49700 | ACS9 | 0.419525 | **-0.557** | 0.05128 | 0.03665 | 2.219132 | **-0.7019** | **-0.6455** | **-0.822** |
| BnaA02g09950D | AT5G53980 | HB52 | -1.20761 | **-0.242** | **0.72457** | **1.6907** | -0.24152 | 0.724569 | -1.20761 | -0.2415 |

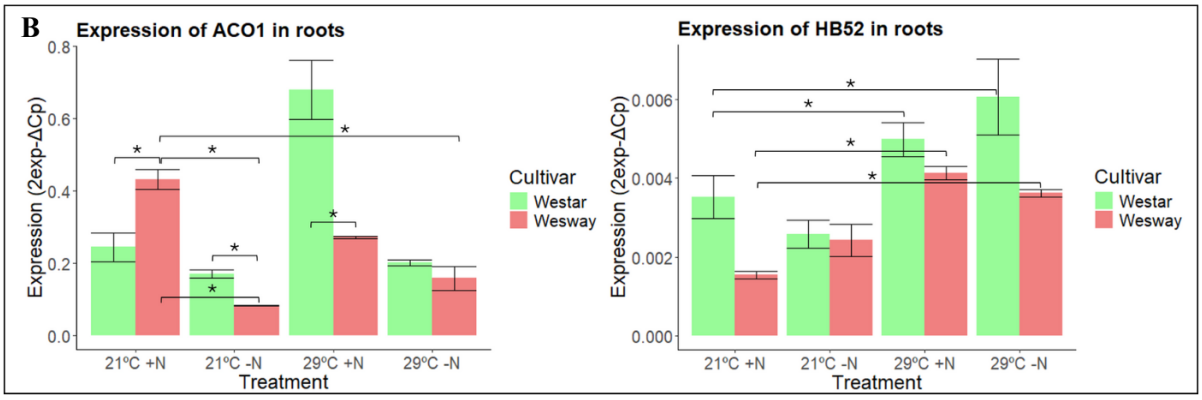


Figure 4.16: Expression of genes related to ethylene biosynthesis and signalling in roots of *B. napus* individuals from two varieties (Westar & Wesway) in response to different temperature and N treatments: 21ºC+N, 21ºC-N, 29ºC+N and 29ºC-N. A) Z-score values of genes related to ethylene biosynthesis and signalling quantified by RNA sequencing analysis. Z-score values represent the average from three independent replicates per variety and treatment. The table shows the Z-score values of normalized read counts from three independent replicates per variety and treatment. Red indicates higher expression, blue indicates lower expression. Bold numbers indicate significant differences ($|\log2FC| > 1$; p-value < 0.05) compared to the control treatment (21ºC+N) from each variety. B) Expression of *BnACO1* (*BnaA09g44060D, BnaC08g36640D, BnaCnng67880D* & *BnaCnng33000D*; left) and *BnHB52* (*BnaA02g09950D* & *BnaCnng64030D*; right) quantified by quantitative PCR (qPCR) in roots of *B. napus* individuals from two varieties (Westar & Wesway), grown under different temperature and N treatments: 21ºC+N, 21ºC-N, 29ºC+N and 29ºC-N. X-axis indicates the expression levels (2exp-ΔCp) normalized to the expression levels of the control gene *BnACT7*. Error bars show the variation between three independent biological samples (with three technical replicates each). Asterisks indicate significant differences between groups (p-value < 0.05).

To confirm the putative role of ethylene biosynthesis and signalling in the root responses to warm temperature, N deficiency and their combination, we obtained Arabidopsis lines carrying T-DNA insertions that led to loss of function of the genes *AtACO1* and *AtHB52*. Then, we grew these mutants, *aco1* (SALK_127963C) and *hb52* (GK-058A12.04), in petri dishes with ½ MS medium containing an optimal N supply (+N) or N deficiency (-N), and under optimal temperature (21ºC) or warm temperature (29ºC) to study their response to these stresses. Our results indicate that *aco1* had a longer primary root compared to Col-0 seedlings in all treatments (Figure 4.17A), indicating that the lack of *ACO1* leads to enhanced root growth independently of the temperature and N conditions. In the case of *hb52*, the primary root length was greater in the mutant than in Col-0 seedlings (Figure 4.17A) in all treatments except for 29ºC-N, indicating that the lack of *HB52* could have a function in the response to the stress combination. This response correlates with our results in *B. napus* where the expression of *BnHB52* was higher under the stress combination than under the individual stress treatments in the case of Westar (Figure 4.16). The lateral root density was also greater in *hb52* than in Col-0 at 21ºC, but at 29ºC the lateral root density was similar between *hb52* and Col-0 (Figure 4.17B). This suggests that *HB52* could regulate LRD in response to N deficiency, but this effect is counteracted by warm temperatures.

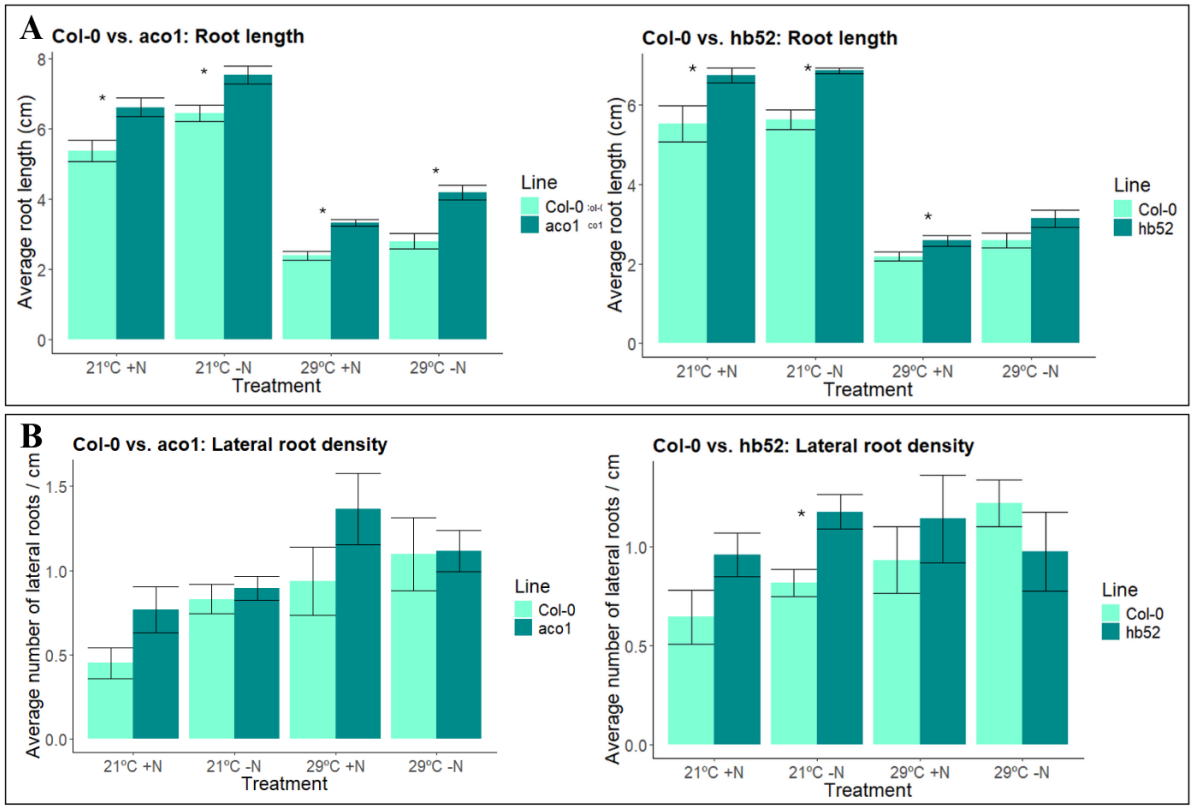


Figure 4.17: Quantification of root traits in Arabidopsis Col-0, *aco1* and *hb52* seedlings grown under different temperature and N conditions (21ºC +N, 21ºC -N, 29ºC +N and 29ºC -N) for 10 days. A) Quantification of root length in Col-0 vs. *aco1* seedlings (left) and in Col-0 vs. *hb52* seedlings (right). B) Quantification of LRD in Col-0 vs. *aco1* seedlings (left) and in Col-0 vs. *hb52* seedlings (right). Error bars represent the standard deviation between 18 seedlings. Asterisks indicate significant differences between the mutant and Col-0 within each treatment (p-value < 0.05).

These results suggest that a reduction in the expression of *BnACO1* and a consequent reduction in ethylene biosynthesis could be involved in the enhanced root elongation observed in *B. napus* at 21ºC-N and 29ºC-N. Our results also indicate that the expression patterns of *BnHB52* do not fully correlate with those of *BnACO1*, indicating that the expression of *BnHB52* might depend on other factors apart from ethylene.

### 4.2.3. Genes involved in N transport play a role in the root responses to warm temperatures and nitrogen deficiency in Arabidopsis and *Brassica napus*.

Quantifications of nitrate content in roots and shoots of the varieties Westar and Wesway suggested an alteration of N transport under the different stresses (see Results: 4.1.3). Additionally, in our RNAseq, a closer look at the genes identified in cluster 4 revealed genes not only related to N metabolism such as *BnGLN1-4*, *BnGLN1-5* and *BnAMT1-1*, but also to N transport. Thus, we observed contrasting responses in the expression patterns of *BnNRT2.1* and *BnNRT1.1* under the different treatments (Supplementary Table 4A; Figure 4.18). *NRT1.1* and *NRT2.1* encode for nitrate transporters that are known to participate in the root responses to N deficiency and in the auxin-mediated regulation of LR development (Léran *et al.*, 2013; Bouguyon *et al.*, 2016; Wang *et al.*, 2023e). *AtNRT2.1* and *AtNRT1.1* have shown to present opposite transcriptional responses in Arabidopsis in response to N. High levels of N induce the expression of *AtNRT1.1* while at the same time reduce the expression of *AtNRT2.1* (Tian *et al.*, 2009). Conversely, *NRT2.1* is induced by N starvation (Cerezo et al., 2001; Gansel et al., 2001). In Westar, the expression of *BnNRT2.1* was down-regulated by N deficiency independently of the temperature (Figure 4.18A; B), whereas the expression of *BnNRT1.1* showed a different response, being up-regulated at 29ºC independently of the N deficiency (Figure 4.18A), suggesting a specific effect of these stresses in the regulation of *BnNRT1.1*. In Wesway, on the contrary, *BnNRT2.1* was significantly up-regulated by N deficiency and also by the stress combination to a lesser extent (Figure 4.18A; B). Furthermore, in Wesway *BnNRT1.1* and some transporters from the NPF family were also up-regulated under the stress combination (Figure 4.18A). Expression of *AtNRT1.1* in Arabidopsis is known to be involved in nitrate signalling to enhance LR growth in nitrate-rich areas (Bouguyon *et al.*, 2016. Thus, the specific up-regulation of *BnNRT1.1* in Wesway could explain the enhanced LR growth observed at 29ºC-N when compared to Westar.

**A**

| Gene name | A. thaliana ortholog | Protein | Westar 21°C +N | Westar 21°C -N | Westar 29°C +N | Westar 29°C -N | Wesway 21°C +N | Wesway 21°C -N | Wesway 29°C +N | Wesway 29°C -N |
|---|---|---|---|---|---|---|---|---|---|---|
| BnaA06g04560D | AT1G08090 | NRT2.1 | -0.61145 | **-0.24** | -0.63976 | **-0.183** | -0.62894 | **2.17279** | -0.6418 | **0.7727** |
| BnaC08g43380D | AT1G08090 | NRT2.1 | -0.54407 | **-0.211** | -0.49034 | **-0.331** | -0.53667 | **2.37717** | -0.54116 | **0.2779** |
| BnaA09g49050D | AT1G08090 | NRT2.1 | -0.39557 | **-0.363** | -0.39584 | **-0.362** | -0.35568 | **2.46788** | -0.41979 | **-0.176** |
| BnaA06g04570D | AT1G08090 | NRT2.1 | -0.55694 | **-0.195** | **-0.4934** | **-0.314** | -0.55678 | **2.37114** | -0.54315 | **0.2877** |
| BnaC05G0059600ZS | AT1G08090 | NRT2.1 | -0.35796 | **-0.785** | -0.3604 | -0.3636 | -0.36052 | **2.21365** | **-0.6872** | **0.7009** |
| BnaA08G0300800ZS | AT1G08090 | NRT2.1 | -0.5854 | **-0.477** | -0.57434 | **-0.427** | -0.53518 | **1.84473** | **-0.6084** | **1.363** |
| BnaA08g24900D | AT1G12110 | NRT1.1/NPF6.3 | 1.274084 | **-1.758** | 1.290154 | 0.35264 | -0.62151 | -0.13528 | -0.12393 | -0.2782 |
| BnaCnng61860D | AT1G12110 | NRT1.1/NPF6.3 | -1.00946 | -0.9333 | **0.85709** | **0.5904** | -1.16184 | **0.43807** | **-0.3238** | **1.5428** |
| BnaA07g24080D | AT1G69870 | NRT1.7/NPF2.13 | -0.67473 | 0.3819 | 1.114553 | 1.25013 | **-1.69792** | -0.78775 | **0.1582** | **0.2556** |
| BnaC06g30920D | AT1G69870 | NRT1.7/NPF2.13 | -1.02696 | -0.8378 | **0.02673** | **0.5094** | -0.87612 | -0.58045 | **1.3895** | **1.3957** |
| BnaA07g24560D | AT1G68570 | NPF3.1 | -1.17678 | -0.1423 | 0.075305 | **1.433** | -1.10664 | 0.168368 | -0.62604 | **1.375** |
| BnaC06g30180D | AT1G68570 | NPF3.1 | -0.93244 | -0.2534 | -0.55698 | **0.4074** | -0.93521 | **-0.2292** | **0.3728** | **2.127** |
| BnaC03g20920D | AT2G37900 | NPF5.6 | -0.31922 | -0.696 | **-0.8893** | **-1.018** | 0.019724 | -0.12038 | **1.5249** | 1.49861 |
| BnaA03g17480D | AT2G37900 | NPF5.6 | -0.56722 | -0.939 | -0.88244 | -0.9051 | 0.201175 | 0.264415 | **1.625** | 1.20322 |
| BnaA09g54940D | AT3G53960 | NPF5.7 | -0.80272 | -0.3804 | -0.42024 | -0.3223 | -0.43146 | 0.144334 | -0.17329 | **2.3861** |
| BnaA09g30560D | AT1G22550 | NPF5.16 | 0.414996 | -0.0686 | **-0.97** | **-1.082** | 1.925034 | 0.461387 | **-0.8699** | 0.18919 |

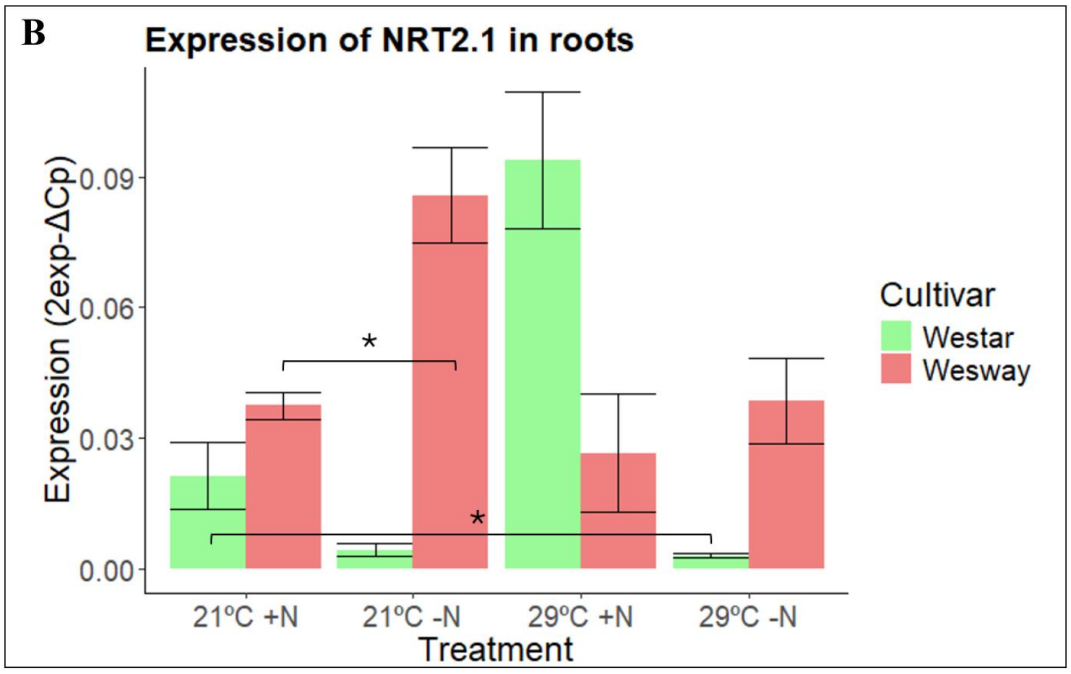


Figure 4.18: Differential expression of nitrogen transporter genes in response to different temperatures and N treatments. A) Expression of genes related to nitrate acquisition and transport quantified by RNA sequencing analysis in roots from *B. napus* individuals from two varieties (Westar & Wesway), grown under different temperature and N treatments: 21ºC+N, 21ºC-N, 29ºC+N and 29ºC-N. The table shows the Z-score values of normalized read counts from three independent replicates per variety and treatment. Red indicates up-regulated, blue indicates down-regulated. Bold numbers indicate significant differences (|log2FC| > 1; p-value < 0.05) compared to the control treatment (21ºC+N) from each variety. B) Expression of *BnNRT2.1* (*BnaA06g04560D* & *BnaC08g43380D*) quantified by quantitative RT-qPCR (qPCR) in roots of *B. napus* individuals from two varieties (Westar & Wesway), grown under different temperature and N treatments:

21ºC+N, 21ºC-N, 29ºC+N and 29ºC-N. X-axis indicates the expression levels (2exp-ΔCp) normalized to the expression of the control gene *BnACT7*. Error bars show the variation between three independent biological samples (with three technical replicates each). Asterisks indicate significant differences between groups (p-value < 0.05).

To understand the relationship between nitrate transporters and LR growth under warm temperatures and N deficiency, we identified loss of function T-DNA Arabidopsis mutants for the genes *AtNRT2.1* and *AtNRT1.1*. The mutants *nrt2.1-2* (SALK_035429) and *nrt1.1* (SALK_138710C) were grown in petri dishes with ½ MS medium with an optimal N supply (+N) or N deficiency (-N), and under optimal temperature (21ºC) or warm temperature (29ºC) to study their response to these stresses. Both the *nrt2.1-2* and *nrt1.1* mutants had a higher root length than Col-0 in all treatments (Figure 4.19A), indicating that the lack of these transporters could enhance root length independently of the temperature and N conditions. LR density was higher in both mutants than in Col-0 seedlings at 21ºC, but at 29ºC both mutants had a similar LR density than Col-0 (Figure 4.19B). This suggests that the lack of these transporter genes could lead to enhanced LR density independently of the N content under optimal temperature conditions. However, under warm temperature the lack of these transporters did not enhance LR density, suggesting a different role of these transporters on LR growth under warm temperature.

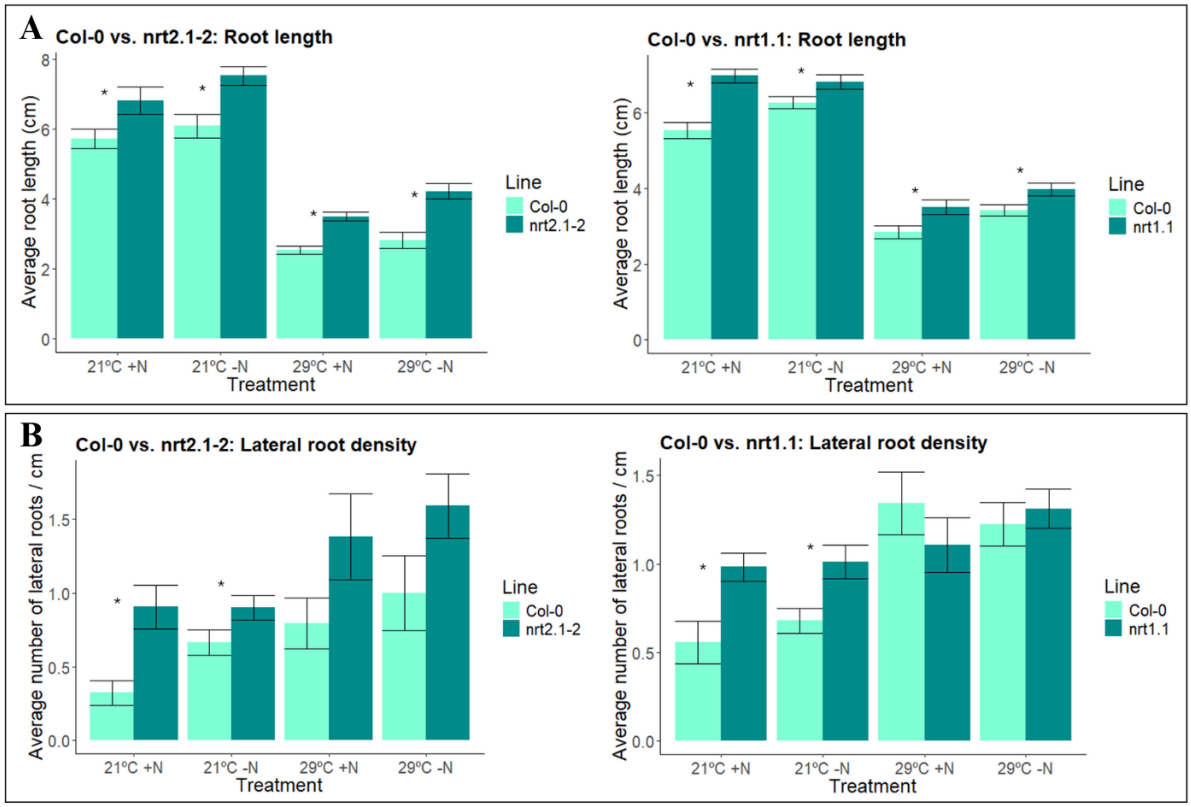


Figure 4.19: Quantification of root traits in Arabidopsis *nrt2.1-2* and *nrt1.1* seedlings grown under different temperature and N conditions (21°C +N, 21°C -N, 29°C +N and 29°C -N) for 10 days. A) Quantification of root length in Col-0 vs. *nrt2.1-2* seedlings (left) and in Col-0 vs. *nrt1.1* seedlings (right). B) Quantification of LRD in Col-0 vs. *nrt2.1-2* seedlings (left) and in Col-0 vs. *nrt1.1* seedlings (right). Error bars represent the standard deviation between 18 seedlings. Asterisks indicate significant differences between the mutant and Col-0 within each treatment (p-value < 0.05).

LOB DOMAIN-CONTAINING proteins such as LBD37, LBD38 and LBD39, are known to down-regulate the expression of *NRT1.1* and *NRT2.1* in Arabidopsis (Chai *et al.*, 2022). We observed the transcript levels of the orthologous genes, *BnLBD37, 38* and *39*, and found that all of them were strongly down-regulated by N deficiency independently of the temperature in both varieties (Figure 4.20A; B), which correlates with the previously observed up-regulation of *BnNRT2.1* and *BnNRT1.1* in Wesway (Figure 4.18A; B), but not in Westar. This suggests that the down-regulation of *BnNRT2.1* and *BnNRT1.1* in Westar in response to N deficiency is independent on *LBD37* and other factors must play a role in such regulation.

**A**

| Gene name | A. thaliana ortholog | Protein | Westar 21°C +N | Westar 21°C -N | Westar 29°C +N | Westar 29°C -N | Wesway 21°C +N | Wesway 21°C -N | Wesway 29°C +N | Wesway 29°C -N |
|---|---|---|---|---|---|---|---|---|---|---|
| BnaA07g37360D | AT5G67420 | LBD37 | 0.469457 | **-0.99** | 0.824294 | **-0.887** | 0.228318 | **-0.6324** | **1.7963** | **-0.81** |
| BnaC02g16720D | AT5G67420 | LBD37 | -0.66841 | **-0.921** | -0.67884 | **-0.857** | 1.471802 | **0.09139** | 1.52738 | **0.0352** |
| BnaAnng05130D | AT5G67420 | LBD37 | 0.334223 | **-1.344** | 0.698972 | 0.22024 | 0.21352 | -1.22457 | 1.64471 | -0.5433 |
| BnaCnng56620D | AT5G67420 | LBD37 | 0.580922 | **-0.96** | 1.189529 | **-0.813** | 0.112153 | **-0.6828** | **1.5158** | **-0.942** |
| BnaC09g07260D | AT5G67420 | LBD37 | 1.128192 | **-1.028** | 1.158964 | **-0.687** | 0.509293 | **-0.7861** | 0.83571 | **-1.131** |
| BnaA09G0094400ZS | AT5G67420 | LBD37 | 1.29644 | **-1.073** | 0.827844 | **-1.018** | 0.722848 | **-0.4076** | 0.74683 | **-1.096** |
| BnaC07g31610D | AT3G49940 | LBD38 | 0.997981 | **-1.164** | 0.812055 | **-0.963** | 0.309282 | -0.20669 | 1.31153 | **-1.098** |
| BnaA03g40660D | AT3G49940 | LBD38 | 0.187276 | **-0.634** | 0.941296 | **-1.025** | -1.02463 | **-0.1955** | **1.8769** | **-0.126** |
| BnaA09G0467700ZS | AT3G49940 | LBD38 | 1.767691 | **-0.868** | 0.67286 | **-0.774** | 0.654011 | **-0.8395** | 0.30561 | **-0.92** |
| BnaC08g21490D | AT3G49940 | LBD38 | 1.497078 | **-0.834** | 1.129781 | **-0.826** | 0.31101 | **-0.9238** | 0.56176 | **-0.916** |
| GSBRNA2T00043279001 | AT3G49940 | LBD39 | 1.144704 | **-0.888** | 1.767381 | **-0.702** | -0.40483 | **-0.8808** | **0.3968** | -0.4335 |
| BnaA03g0157560 | AT3G49940 | LBD39 | 1.365838 | **-0.888** | 0.119415 | **-0.885** | 1.296957 | **-0.8958** | 0.67046 | **-0.784** |
| BnaC07g0834720 | AT3G49940 | LBD39 | 0.325876 | -0.9063 | 0.200874 | **-0.924** | 0.611595 | **-1.4242** | 1.57608 | 0.54017 |
| BnaC01g0426250 | AT3G49940 | LBD39 | 1.647057 | **-0.954** | 0.938137 | **-0.79** | 0.530647 | **-0.8286** | 0.34362 | **-0.887** |

**B**

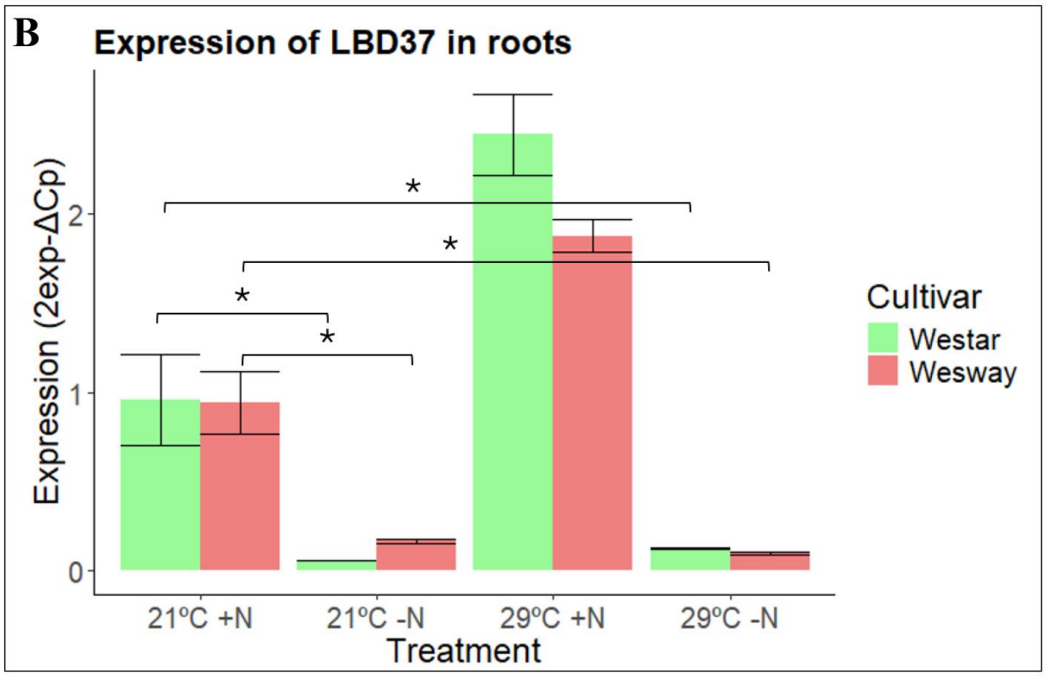


Figure 4.20: Differential expression of *BnLBD37, 38* and *39* in response to different temperatures and N treatments. A) Expression of *BnLBD37, 38* and *39* quantified by RNA sequencing analysis in roots from *B. napus* individuals from two varieties (Westar & Wesway), grown under different temperature and N treatments: 21ºC+N, 21ºC-N, 29ºC+N and 29ºC-N. The table shows the Z-score values of normalized read counts from three independent replicates per variety and treatment. Red indicates up-regulated, blue indicates down-regulated. Bold numbers indicate significant differences ($|\log2FC| > 1$; p-value < 0.05) compared to the control treatment (21ºC+N) from each variety. B) Expression of *BnLBD37 (BnaA07g37360D* & *BnaCnng56620D)* quantified by quantitative PCR (qPCR) in roots from *B. napus* individuals from two varieties (Westar & Wesway), grown under different temperature and N treatments: 21ºC+N, 21ºC-N, 29ºC+N and 29ºC-N. X-axis indicates the expression levels (2exp-ΔCp) normalized to the expression of the control gene *BnACT7*. Error bars show the variation between three independent biological samples (with three technical replicates each). Asterisks indicate significant differences between groups (p-value < 0.05).

We quantified the root length and LRD in the Arabidopsis T-DNA mutant *lbd37* (SALK_057939) compared to Col-0 under different temperature and N conditions. We observed that root length increased under all treatments except for under 21ºC-N, and LRD increased at 21ºC, but not at 29ºC, suggesting a possible interactive effect of the warm temperature and N deficiency in the expression and function of *AtLBD37* (Figure 4.21).

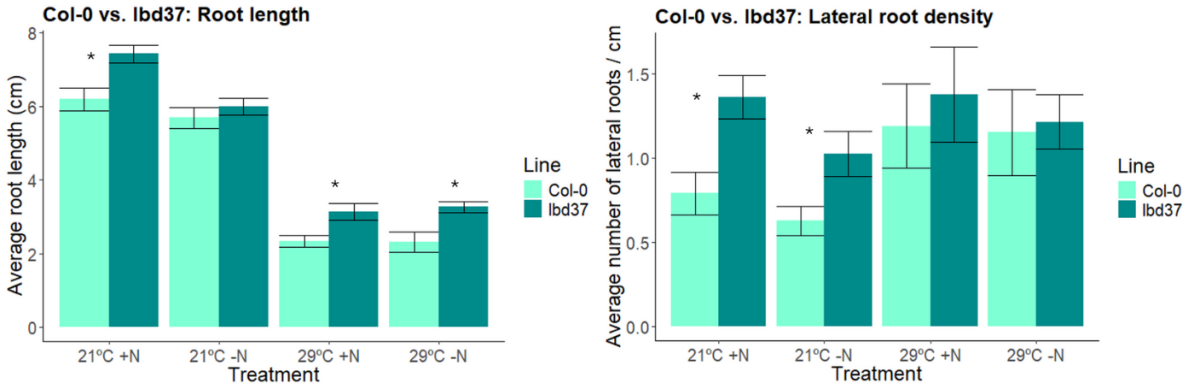


Figure 4.21: Quantification of root traits in Arabidopsis *lbd37* seedlings grown under different temperature and N conditions (21ºC +N, 21ºC -N, 29ºC +N and 29ºC -N) for 10 days. Error bars represent the standard deviation between 18 seedlings. Asterisks indicate significant differences between the mutant and Col-0 within each treatment (p-value < 0.05).

All these results suggest that N deficiency, warm temperatures and the stress combination regulate *BnNRT2.1*, *BnNRT1.1* and *BnLBD37* differentially. However, the root responses of the loss of function mutants suggest a complex role of N transport under these conditions.

## 4.3. Elevated temperature alters the root responses to N deficiency in Arabidopsis.

### 4.3.1. Root responses to N deficiency in Arabidopsis are altered by warm temperatures.

To compare the effects of combined warm temperature and N deficiency between *Brassica napus* and Arabidopsis, we grew Arabidopsis Col-0 seedlings at an optimal temperature (21ºC) or warm temperature (29ºC) and under optimal nitrogen (+N) or nitrogen deficiency (-N). After 10 days, the length of the primary root was shorter in -N seedlings than +N seedlings when plants were grown at 21ºC (Figure 4.22A). This contrasts our previous results in *B. napus*, where N deficiency caused an increase in network depth in most varieties (see Results: 4.1.1.). The reason behind this result could be the severity of the N deficiency treatment, since Arabidopsis seedlings grew under a more severe N deficiency (0.05 mM vs. 0.1 mM previously used for *B. napus*). Previous studies show that plants tend to increase the size of their root system under mild N deficiency, whereas a strong suppression of root growth is observed under severe N deficiency (Gruber *et al.*, 2013; Giehl & von Wirén, 2014). While N deficiency reduced the length of the primary root in Arabidopsis at 21ºC, when plants were submitted to warm temperature (29ºC), the length of the primary root was similar between +N and -N seedlings, indicating that warm temperature attenuated the effects of N deficiency on root length. Regarding LR density, N deficiency caused a reduction at 21ºC, being consistent with our results in *B. napus* (see Results: 4.1.1.). At 29ºC we also observed a reduction in LR density, which contrasts our previous results in *B. napus*, where LR density was less reduced at 29ºC-N than at 21ºC-N. Again, this seems to be caused by the difference in the severity of the N deficiency treatment, since we used a more severe N deficiency in this experiment than in our previous experiments in *B. napus*.

To investigate how warm temperature can alter the effects of N deficiency, we observed the expression of *NRT2.4* using Arabidopsis lines expressing *NRT.4::GUS*. NRT2.4 is a high affinity nitrate transporter located in the epidermal cells of the lateral roots, and it is known to be induced by N deficiency, participating in nitrate uptake and loading into the phloem (Kiba *et al.*, 2012). Since high temperatures have previously shown to induce the expression of nitrogen transporters, such as *NRT2.1*, in Arabidopsis roots (Zheng *et al.*, 2013),

we aimed to study the expression of *AtNRT2.4* under the combination of high temperature and N deficiency in Arabidopsis roots. *NRT2.4::GUS* Arabidopsis seedlings were grown under N sufficiency (+N) or N deficiency (-N) and under two different temperatures: 21ºC or 29ºC. After 10 days, N deficiency caused an increase in the GUS staining signal in seedlings grown at 21ºC (Figure 4.22B). However, when seedlings were grown at 29ºC and N deficiency, the GUS staining signal was less intense than at 21ºC, suggesting that elevated temperature could suppress the expression of *NRT2.4* even under N deficiency.

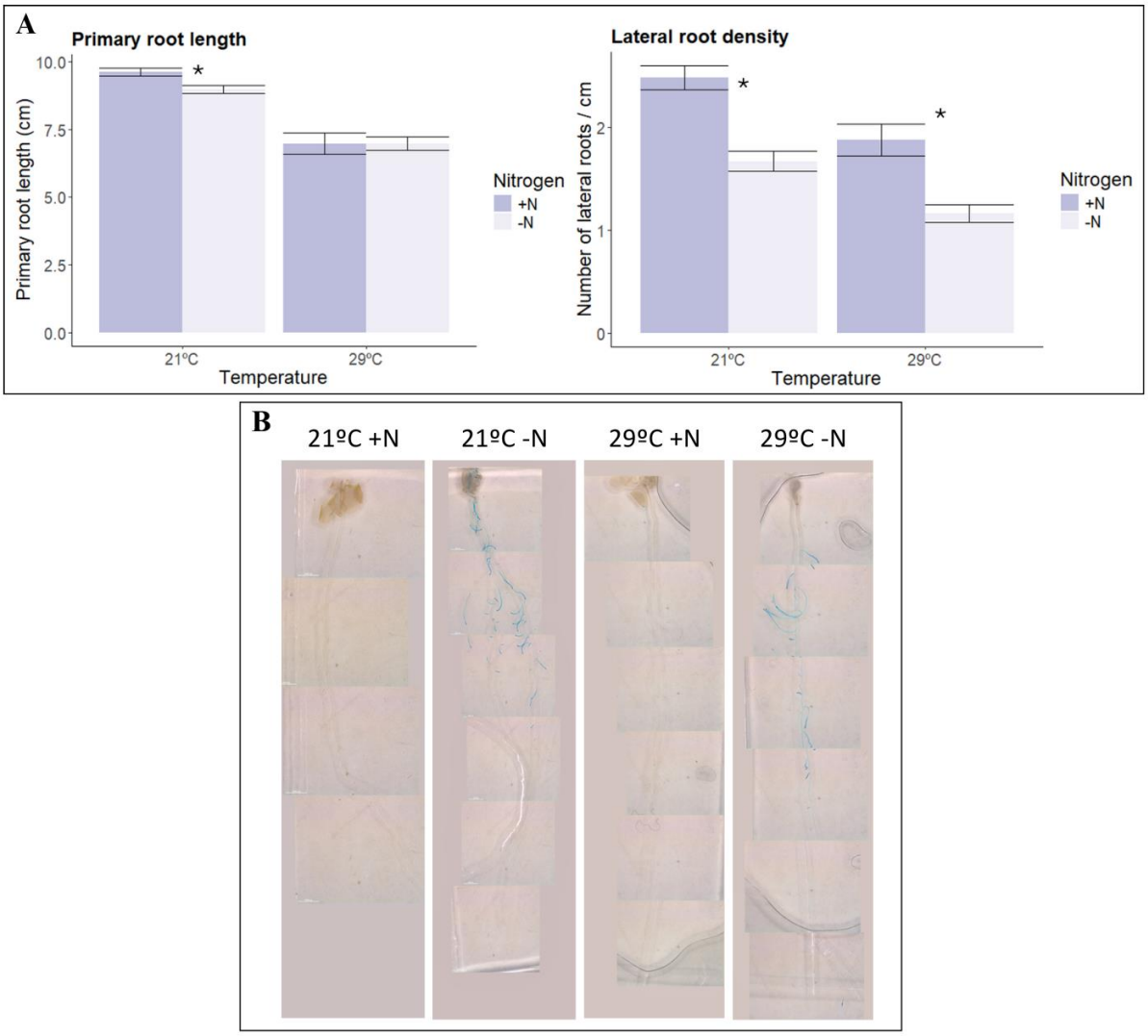


Figure 4.22: A) Quantification of root traits (primary root length and lateral root density) in Arabidopsis Col-0 seedlings grown under different temperature and nitrogen treatments for 10 days. X-axis indicates the different temperature treatments. The legend at the right of each graph shows the two nitrogen treatments. Error bars show the standard deviation between 24 individual seedlings. Asterisks indicate significant differences ($p < 0.05$). B) GUS staining of 10-day old *NRT2.4::GUS* seedlings grown under different temperature and nitrogen treatments: 21ºC+N, 21ºC-N, 29ºC+N and 29ºC-N.

### 4.3.2. Heat stress alters root architecture and reduces the expression of the *NRT2.4* transporter under N deficiency.

To confirm the hypothesis that an elevated temperature could suppress the expression of *NRT2.4* and potentially attenuate the root responses to N deficiency, we performed similar experiments applying heat stress instead of warm temperature. Thus, we grew Col-0 Arabidopsis seedlings under optimal temperature (21ºC) or heat stress (32ºC) and under N sufficiency (+N) or N deficiency (-N). Previous studies from our lab have shown that an elevated temperature of 32ºC applied homogeneously in both shoot and root completely suppresses plant growth and does not represent the conditions present in nature, since the soil buffers the high atmospheric temperature (González-García *et al.*, 2023; Supplementary Figure 5). Natural soils, due to its geothermal properties, form a temperature gradient with a higher temperature in the top parts of the soil and a lower temperature in deeper areas. For that reason, our lab has recently developed the TGRooZ, a device that generates a temperature gradient in the root zone while keeping the roots in the dark, thus mimicking the natural conditions (González-García *et al.*, 2023). The TGRooZ can be used for cultivation in in vitro plates or in pots with soil. Thus, in this experiment, we grew the plants under a temperature gradient in the root zone using the TGRooZ to apply heat stress in a more realistic scenario.

Seedlings grown under optimal temperature in both root and shoot (21SR) showed a shorter primary root at -N compared to +N (Figure 4.23A). However, when plants were grown under high temperature (32TGRooZ), the length of the primary root was similar between +N and -N seedlings. This is consistent with our previous results observed under warm temperature combined with N deficiency and again suggests that an elevated temperature could attenuate the effects of N deficiency in the root system. Furthermore, the lateral root density of +N seedlings was significantly reduced at 32TGRooZ compared with 21SR, whereas the lateral root density of -N seedlings was similar between 21SR and 32TGRooZ (Figure 4.23A), supporting this hypothesis. In accordance, the GUS staining signal was evidently induced by N deficiency, but this signal was lower at 32TGRooZ (Figure 4.23B). This again suggests that elevated temperatures could decrease the expression of *NRT2.4* under N deficiency conditions and supports the idea that elevated temperatures can inhibit the response to N deficiency.

To further study the molecular responses to combined heat stress and N deficiency, we analysed the expression of *DR5* by a luciferase fluorescence assay. DR5::LUC is an auxin response reporter that shows spots along the primary root where auxin accumulates, constituting the pre-branch sites (PBS), that are sites of origin for future lateral roots (Moreno-Risueño *et al.*, 2010). Thus, we used DR5::LUC seedlings grown at different temperatures and different nitrogen concentrations to monitor the auxin response and LR formation by observing the luciferase activity and quantifying the number of spots with DR5 signal along the primary root, which correspond to pre-branch sites (PBS). After 10 days, we did not observe significant differences between +N and -N seedlings in the intensity of the LUC signal or the PBS density under both temperatures (Figure 4.23C; D). This contrasts our previous results, where lateral root density was smaller at -N than at +N (Figure 4.23A). This suggests that under N deficiency, Arabidopsis seedlings form less LR per cm of root (LR density), but still develop a similar number of lateral root primordia, which can develop as LR later if the plant requires to give the proper response.

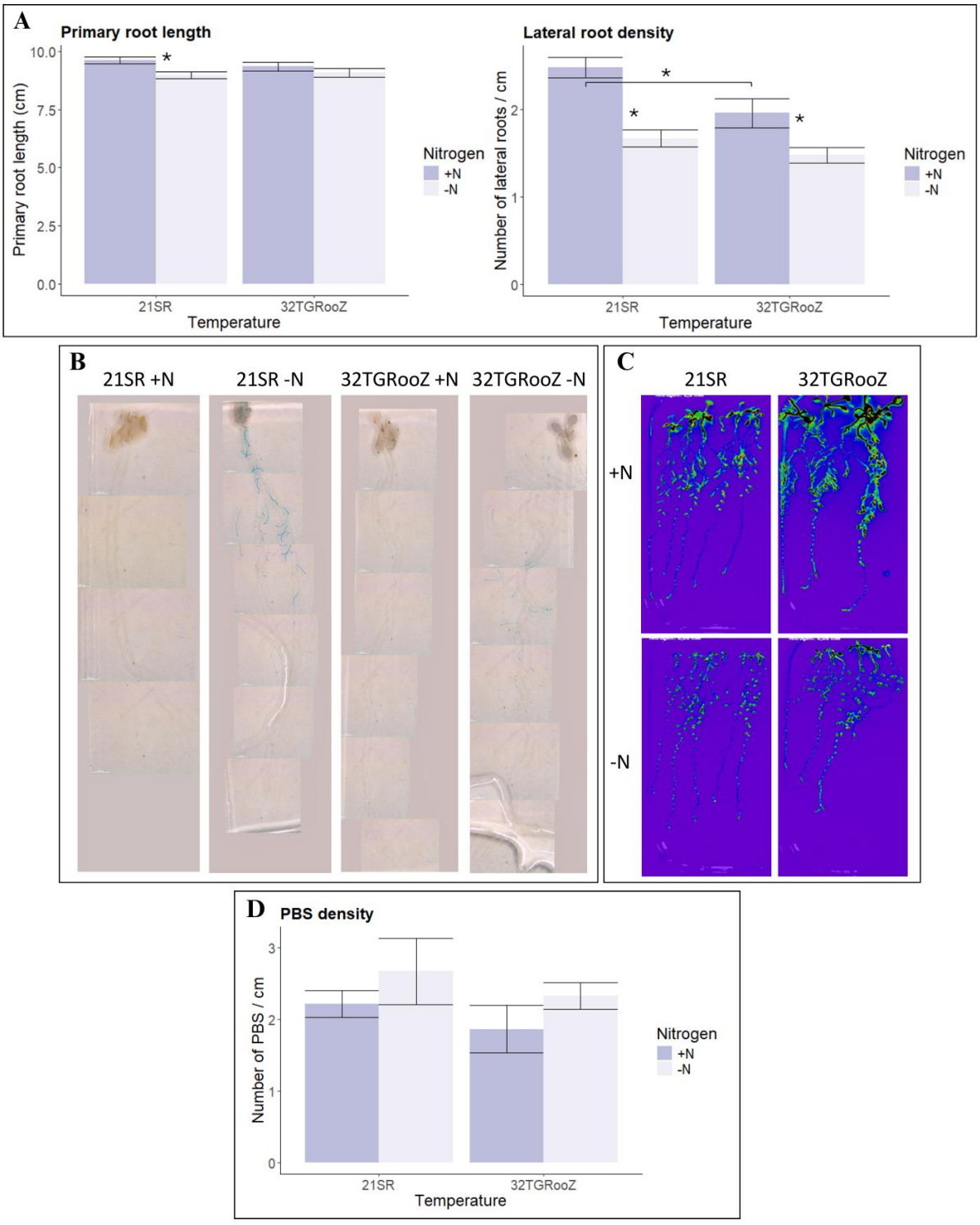


Figure 4.23: A) Quantifications of root traits (primary root length and lateral root density) in Arabidopsis Col-0 seedlings grown under different temperature and nitrogen treatments for 10 days. X-axis indicates the different temperature treatments. The legend at the right of each graph shows the two N treatments. Error bars show the standard deviation between 24 individual seedlings. Asterisks indicate significant differences between groups ($p < 0.05$). B) GUS staining of 10-day old *NRT2.4::GUS* seedlings grown under different temperature and nitrogen treatments: 21SR +N, 21SR -N, 32TGRooZ +N and 32TGRooZ -N. C) DR5::LUC signal in roots of 10-day old DR5::LUC Arabidopsis

seedlings grown under different nitrogen and temperature treatments. D) Number of pre-branch sites (PBS) in roots of 10-day old DR5::LUC Arabidopsis seedlings grown under different nitrogen and temperature treatments. X-axis indicates the temperature treatments. The legend indicates the N treatment. Asterisks indicate significant differences between groups ($p < 0.05$).

Altogether, these results suggest that warm temperature alters the root responses to N deficiency, and these alterations are even more pronounced under heat stress, causing changes in root architecture and in the expression of N deficiency-related genes.

## 4.4. Characterization of differential root responses to the combination of warm temperature and phosphate (Pi) deficiency in *B. napus*.

### 4.4.1. The root architecture of *B. napus* is significantly altered by the combination of warm temperatures and low phosphate (Pi) availability.

To analyse the effect of phosphate deficiency and warm temperatures in *B. napus*, seedlings from the same 12 *B. napus* varieties previously analysed (see Supplementary Table 1A) were grown in the Pouch and Wick system under two different temperatures, standard (21ºC) and warm (29ºC) temperature, and two different concentrations of inorganic phosphate (Pi) in the medium, either optimal Pi (+P, 625 µM) or Pi starvation (-P, 2.5 µM) for 7 days. Then, the same root traits previously described were quantified again using the GiaRoots software (Table 4.1; Supplementary Table 1B). We observed that as previously mentioned, warm temperatures (29ºC) caused significant changes in several traits in most varieties, with Dux and Karat (14 and 12 traits negatively altered out of 19) being again the most affected by warm temperatures (Figure 4.24). The effects of Pi deficiency on root architecture were less pronounced than those observed in response to warm temperature, and Drakkar was the most affected variety, with 13 traits significantly altered out of 19, whereas the varieties Dux, Industry and Marnoo did not show any altered trait under -P alone. Even though the effects of 21ºC-P were not very strong in most varieties, the combination of warm temperatures and Pi deficiency (29ºC-P) caused significant alterations in most traits in all varieties, even more than warm temperatures alone, with Line and Marnoo being the less altered varieties (10 traits negatively changed; Figure 4.24; Supplementary Table 5A; B).

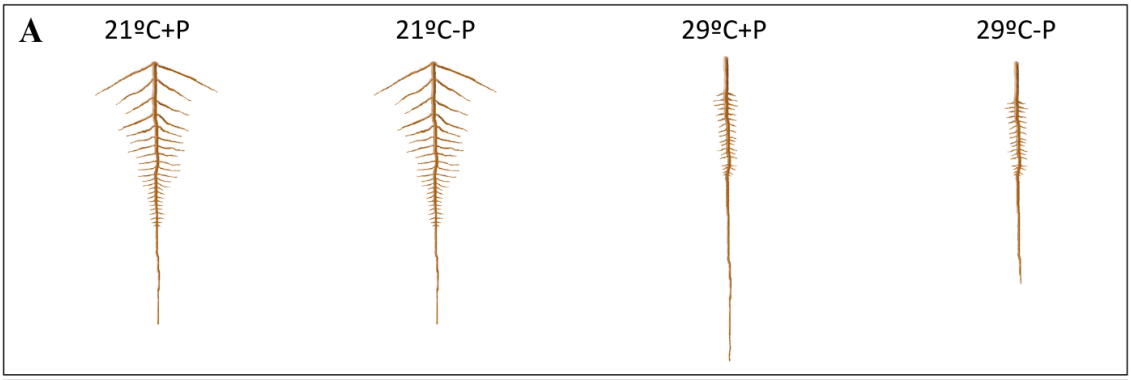


B

| Varieties | 21°C-P | | 29°C+P | | 29°C-P | |
|---|---|---|---|---|---|---|
| | Number of increased traits | Number of reduced traits | Number of increased traits | Number of reduced traits | Number of increased traits | Number of reduced traits |
| Drakkar | 0 | 13 | 2 | 4 | 1 | 17 |
| Duplo | 0 | 6 | 1 | 10 | 0 | 16 |
| Dux | 0 | 0 | 1 | 14 | 1 | 17 |
| Fido | 0 | 2 | 0 | 5 | 0 | 15 |
| Industry | 0 | 0 | 0 | 4 | 0 | 16 |
| Karat | 1 | 4 | 3 | 12 | 2 | 16 |
| Line | 0 | 4 | 2 | 3 | 0 | 10 |
| Marnoo | 0 | 0 | 1 | 8 | 0 | 10 |
| Nugget | 1 | 8 | 0 | 0 | 0 | 17 |
| WHP | 1 | 11 | 1 | 1 | 1 | 16 |
| Westar | 0 | 12 | 0 | 9 | 0 | 17 |
| Wesway | 0 | 11 | 2 | 8 | 0 | 17 |

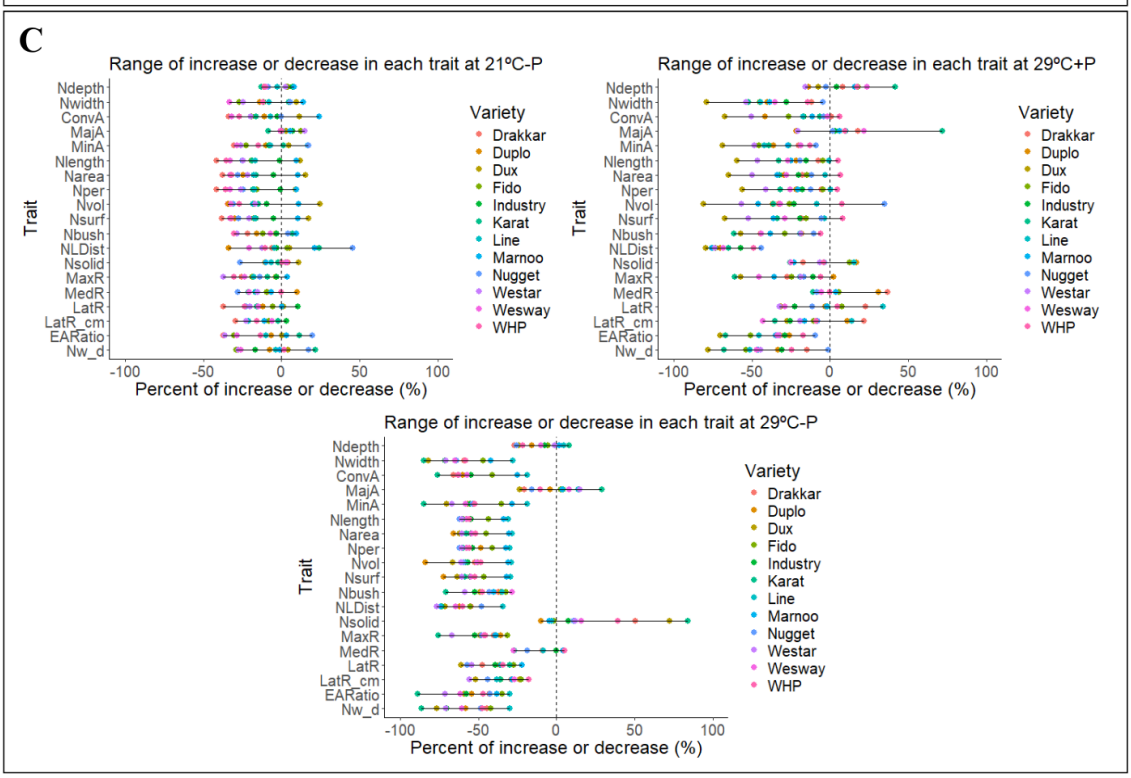


Figure 4.24: A) Graphical representation of the root responses to the different temperature and Pi treatments observed among most *B. napus* varieties. B) Number of significantly increased and reduced root traits in the 12 *B. napus* varieties under the three stress treatments (21ºC-P, 29ºC+P and 29ºC-P). C) Range of decrease or increase of each trait at 21ºC-P (top left), 29ºC+P (top right) and 29ºC-P (bottom) compared to control conditions (21ºC+P). Coloured dots represent each variety.

The effects of Pi deficiency (21ºC-P) in network depth were subtle and had similar values to those in the control treatment, ranging from a 12% decrease in Karat to a 11% increase in Drakkar (Figure 4.24C). Consequently, most varieties did not experience significant changes in network depth at 21ºC-P (Figure 4.25). The effects of -P on network width were slightly more pronounced (Figure 4.25), with values ranging from a 33% decrease in Drakkar to a 14% increase in Marnoo, compared to 21ºC+P (Figure 4.24C). The distribution of the root system was also altered in response to Pi deficiency, with changes in network solidity (from a 26% decrease in Nugget to a 10% increase in Dux) and network length distribution (from a 33% decrease in Duplo to a 45% increase in Nugget; Figure 4.24C; Supplementary Figure 7). Finally, some varieties showed a reduction in lateral root density at 21ºC-P (e.g. a reduction of 29% in Drakkar), whereas others (E.g. Dux, Industry and Marnoo) displayed a lateral root density similar to the control treatment (Figure 4.24C; Figure 4.25; Supplementary Figure 6; 7).

The effects of warm temperature were similar to those previously described (see Results: 4.1.1.). Whereas Pi deficiency led to slight alterations or no significant changes in network depth, network width or traits related to lateral roots or the distribution of the root system, the combination of Pi deficiency and warm temperatures caused noticeable changes in the root system. Network depth decreased in most varieties to levels up to 27% decrease in Drakkar or 25% in Nugget (Figure 4.24C; Figure 4.25). Furthermore, we observed that the growth of the upper lateral roots remained suppressed as observed under warm temperature alone, causing a strong reduction in network width (up to 84%) and lateral root density (up to 55%) in all varieties (Figure 4.24C; Supplementary Figure 6; 7).

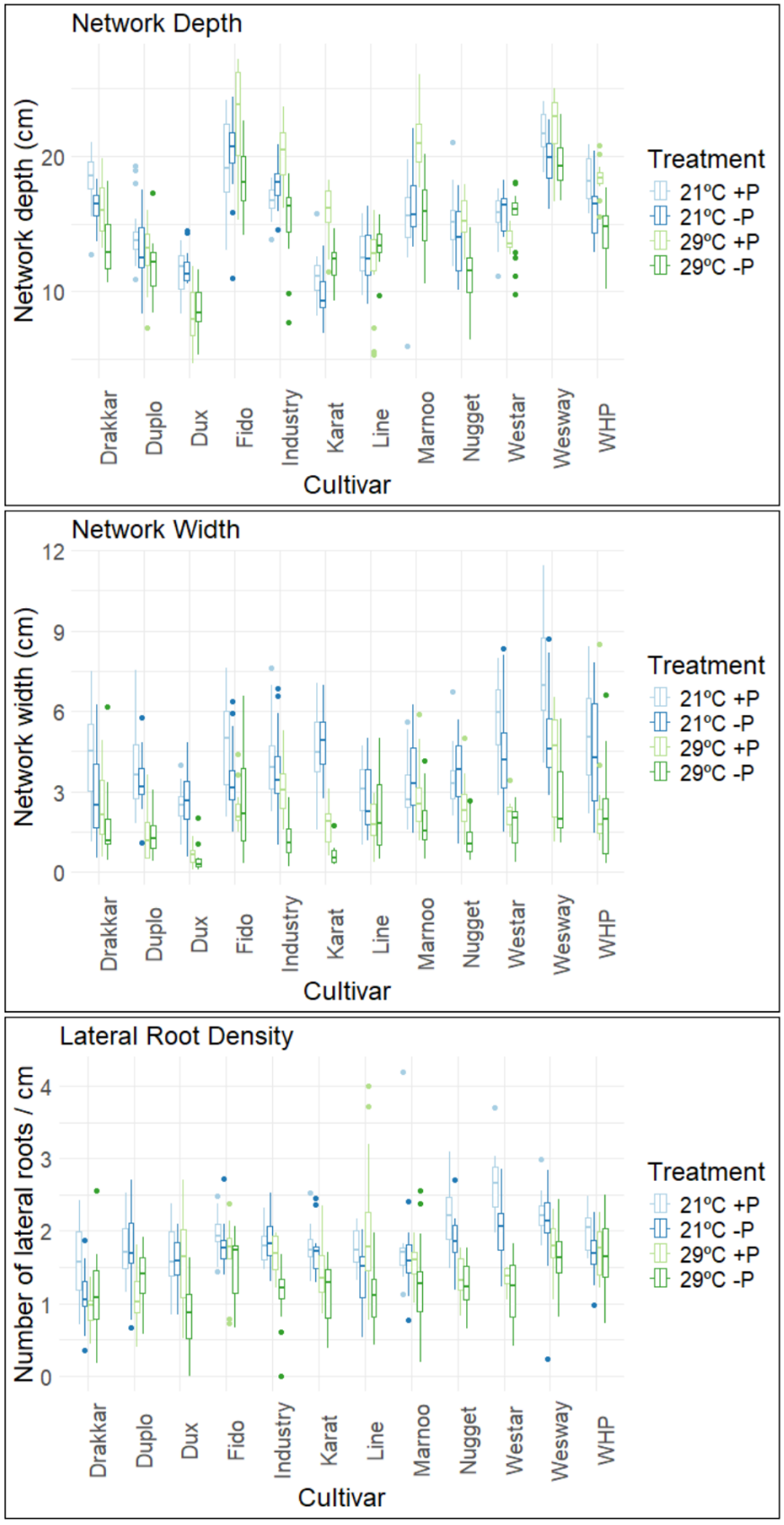


Figure 4.25: Boxplots showing the distribution of the values from three root traits (network depth, network width and LRD) across *B. napus* seedlings submitted to different

temperature and phosphate (Pi) treatments. The X-axis indicates the different varieties. The colour legend shows the different temperature and Pi treatments: 21ºC+P, 21ºC-P, 29ºC+P or 29ºC-P. Boxplots for the remaining measured root traits are displayed in Supplementary Figure 6; 7.

### 4.4.2. Different *B. napus* varieties show different root adaptation strategies to the combination of warm temperatures and low Pi availability.

We have analysed the general tendencies in the root responses to combined warm temperatures and Pi starvation in *B. napus*, and we detected variation in the response across different varieties. To identify concrete differences, we first calculated the correlation coefficients between all traits (Figure 4.26; Supplementary Table 6A). We observed that network solidity was negatively correlated with several traits, especially those related to extension, since network solidity is negatively related to the network convex area, and network convex area is positively correlated with most traits. A lower network solidity indicates that those plants developed a more expanded root system but less dense, whereas a higher network solidity indicates a denser root system but less expanded (Supplementary Table 1B). Whereas network depth is expected to be highly correlated with network width under optimal conditions due to the normal development of the root system, in our experiment the correlation coefficient between both was only 0.32 (Supplementary Table 6A). This low correlation coefficient suggests that the effect of the treatments caused changes in the relationship between network width and network depth, in this case due to the effects of warm temperature, since network depth increased but network width strongly decreased in most varieties at 29ºC+P, causing a decompensation in those traits, and thus reducing their correlation coefficient. Furthermore, under the stress combination (29ºC-P) both traits decreased in all varieties but decreases in Network Width (up to 84% in Karat) were much stronger than decreases in Network Depth (up to 27% in Drakkar), reducing the correlation coefficient even further.

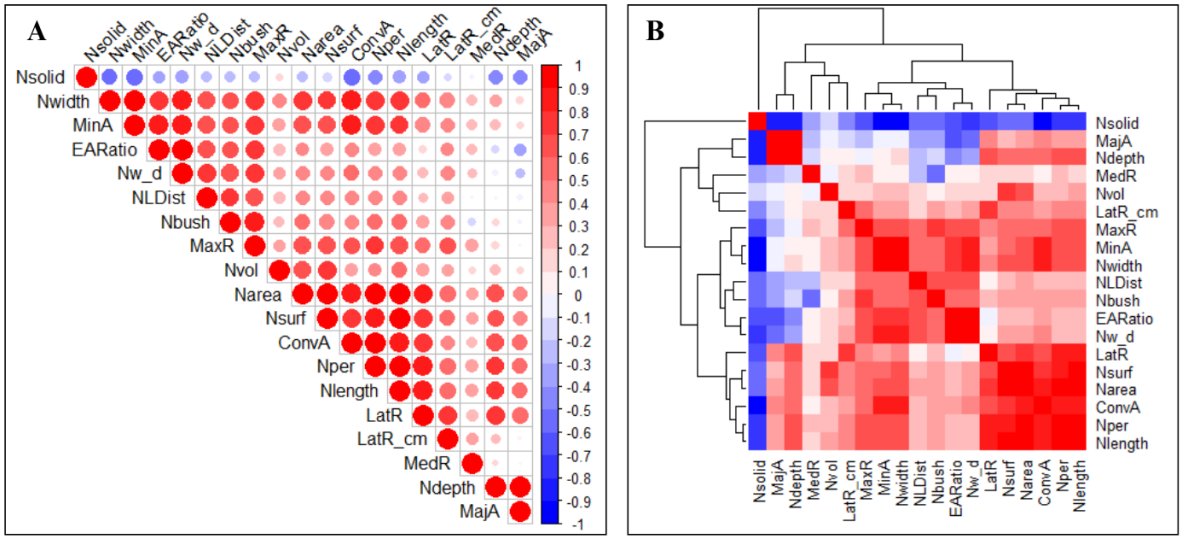


Figure 4.26: A) Graphical representation of the correlation coefficients between the different variables. B) Heatmap representing the correlation coefficients between the different variables. Variables are quantitative measurements of the different root traits across *B. napus* individuals from 12 different varieties submitted to different temperature and phosphate treatments. Red indicates a higher correlation coefficient, whereas blue indicates a lower correlation coefficient.

These results indicate that the root architecture of *B. napus* slightly changed in response to Pi deficiency in our conditions. However, root morphology was significantly altered by the combination of Pi deficiency and warm temperature, indicating a possible additive effect of the individual stresses.

To define the variability in the root responses to the different treatments among the different varieties, we performed a principal component analysis (PCA) using the different root traits as variables. The first dimension of the PCA (Dim1) was responsible for the 54.3% of the variation and was composed by traits that are related to network size and distribution (Figure 4.27A; B). The second dimension (Dim2) explained the 17.9% of the variation and was composed by traits related to the depth of the root system, such as network depth and major ellipse axis (Supplementary Table 6B). In the PCA plot, samples grown at 21ºC were located close to the centre of the plot, whereas individuals grown at 29ºC were disposed towards the left side of the plot indicating that they differ in traits related to Dim1, that are related to the size and distribution of the root system (Figure 4.27C). As previously observed, these data suggest that the temperature treatment had greater effects than the Pi treatment in most individuals (e.g. reductions in network length distribution were up to 72% at 29ºC+P and were up to 76% at 29ºC-

P, whereas at 21ºC-P network length distribution was unaltered, compared to 21ºC+P). When the individuals were grouped according to their variety, some of them were located towards the centre of the plot, indicating that the treatments did not cause remarkable effects in their root responses. Other varieties were distributed along the horizontal axis (Dim1) of the PCA, suggesting that the treatments caused stronger alterations on the measured root traits (Figure 4.27D). In some varieties, such as Wesway (Figure 4.27E), individuals treated with -P (21ºC-P), warm temperature (29ºC+P) and the stress combination (29ºC-P) showed a similar distribution across the PCA plot, indicating that these stresses had similar effects on their root architechture. However, other varieties, such as Industry (Figure 4.27F), showed a differential distribution. Individuals grown at 29ºC-P in Industry were separated from individuals from the other three treatments, suggesting that the stress combination caused significant alterations in the root system.

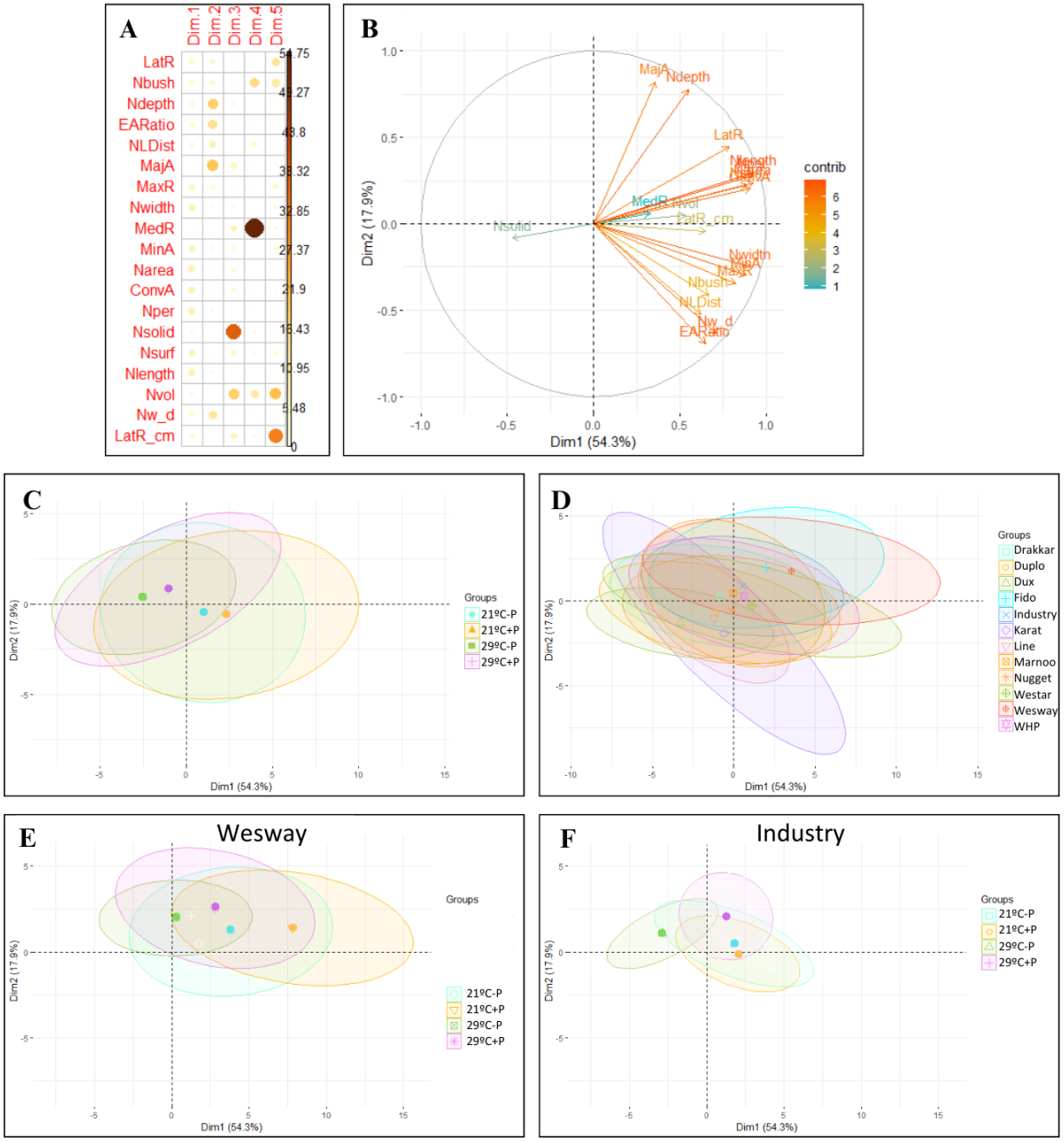


Figure 4.27: Principal component analysis (PCA) of the different root traits measured across *B. napus* individuals from different varieties submitted to different temperature and Pi treatments. The different root traits were used as variables for the PCA. A) Schematic representation of the contribution of each variable to the first five components of the PCA. B) Plot of the contribution of each variable to the first two components of the PCA. X-axis indicates the first component (Dim 1), whereas Y-axis indicates the second component (Dim 2). C) Plot of the contribution of the individuals to the first two components of the PCA grouped by treatment: 21ºC+P, 21ºC-P, 29ºC+P and 29ºC-P. D) Plot of the contribution of the individuals to the first two components of the PCA grouped by variety. E) Plot of the contribution of the individuals from the variety Wesway to the first two components of the PCA, grouped by treatment. F) Plot of the contribution of the individuals from the variety Industry to the first two components of the PCA, grouped by treatment. In each plot, ellipses represent the distribution of the individuals in each group. Dots represent the mean values of the coordinates of all individuals in each group.

To further analyse the differences in the root response across the varieties and treatments, we performed hierarchical clustering on the mean values of all varieties and treatments, according to their distribution on the PCA (Figure 4.28). Hierarchical clustering showed a clear separation between seedlings grown at 21ºC and at 29ºC, regardless of the Pi treatment. From left to right, the first cluster contained individuals grown mainly at 29ºC (+P and -P treatments), whereas the fourth cluster was exclusively composed by seedlings grown at 21ºC (21ºC+P and 21ºC-P), indicating a stronger influence of the temperature treatment than the Pi deficiency in the definition of the clusters. The second cluster contained only individuals from Westar and Wesway grown at 21ºC+P, indicating a differential root growth of these two varieties compared to the other varieties at 21ºC+P. The third cluster contained a mixture of all the treatments and was mainly composed by individuals from Fido and Wesway. Wesway samples grown at 21ºC-P, 29ºC+P or 29ºC-P belonged to the same cluster, but 21ºC+P samples belonged to a different cluster, suggesting that the three stress conditions caused similar effects on root traits compared to 21ºC+P (Figure 4.28). On the other hand, in the case of Industry, seedlings treated with 21ºC+P and 21ºC-P were grouped in the same cluster, whereas seedlings treated with 29ºC+P belonged to a different cluster. This result suggests that temperature stress alone caused greater effects than Pi deficiency alone in Industry. Furthermore, seedlings grown under the stress combination (29ºC-P) belonged to a different cluster than those grown at 29ºC+P in Industry, confirming that Pi deficiency together with warm temperatures caused major alterations in root traits in this variety, being consistent with our previous results in individual traits (16 significantly reduced traits out of 19).

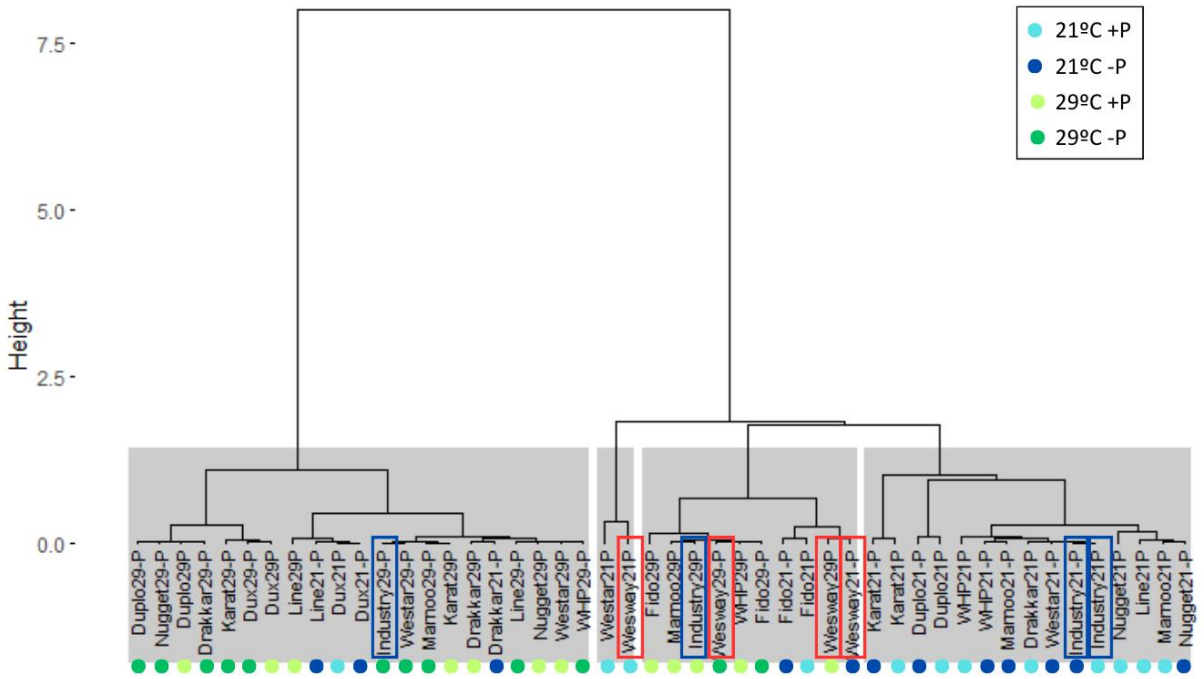


Figure 4.28: Hierarchical clustering (HC) analysis of the categorical variables on the selected principal components. Data from the 12 different *B. napus* varieties was used for the HC, and each variety was divided in 4 groups according to their treatments: 21ºC+P, 21ºC-P, 29ºC+P and 29ºC-P. Coloured circles at the bottom of the graph (light blue, dark blue, light green and dark green) were used to indicate the different treatments according to the legend in the upper right corner. The position of the varieties used for further analyses, Industry and Wesway, was highlighted with rectangles in blue and red, respectively.

In Industry, Pi deficiency alone did not cause significant alterations in any trait, suggesting that the root system of Industry was insensitive to this stress or had better P usage and, therefore, reduced its responses to Pi deficiency. Warm temperature alone caused an increase in network depth in Industry, but most traits related to network width and distribution were not altered. However, when Industry was challenged by the combination of Pi deficiency and warm temperatures (29ºC-P), a decrease of 35% in lateral root density was observed, as well as decreases in most traits related to network size (54% decrease in network area, 53% decrease in network perimeter or 56% decrease in network volume, and 71% decrease in network width due to an inhibition of lateral root elongation (Figure 4.29; Supplementary Figure 8; 9). All these results suggest that Industry was more sensitive to Pi deficiency under warm temperatures than under optimal temperature. In the case of Wesway, Pi deficiency caused reductions in network depth, network width and traits related to network size, compared to seedlings grown at 21ºC+P (Figure 4.29; Supplementary Figure 8; 9). Remarkably, the

combination of both stresses (29ºC-P) reduced network depth and most traits related to size, although these changes were softer than in Industry. These data suggest that the root system of Wesway might be more affected by Pi deficiency at 21ºC, but showed less changes at 29ºC-P compared to Industry.

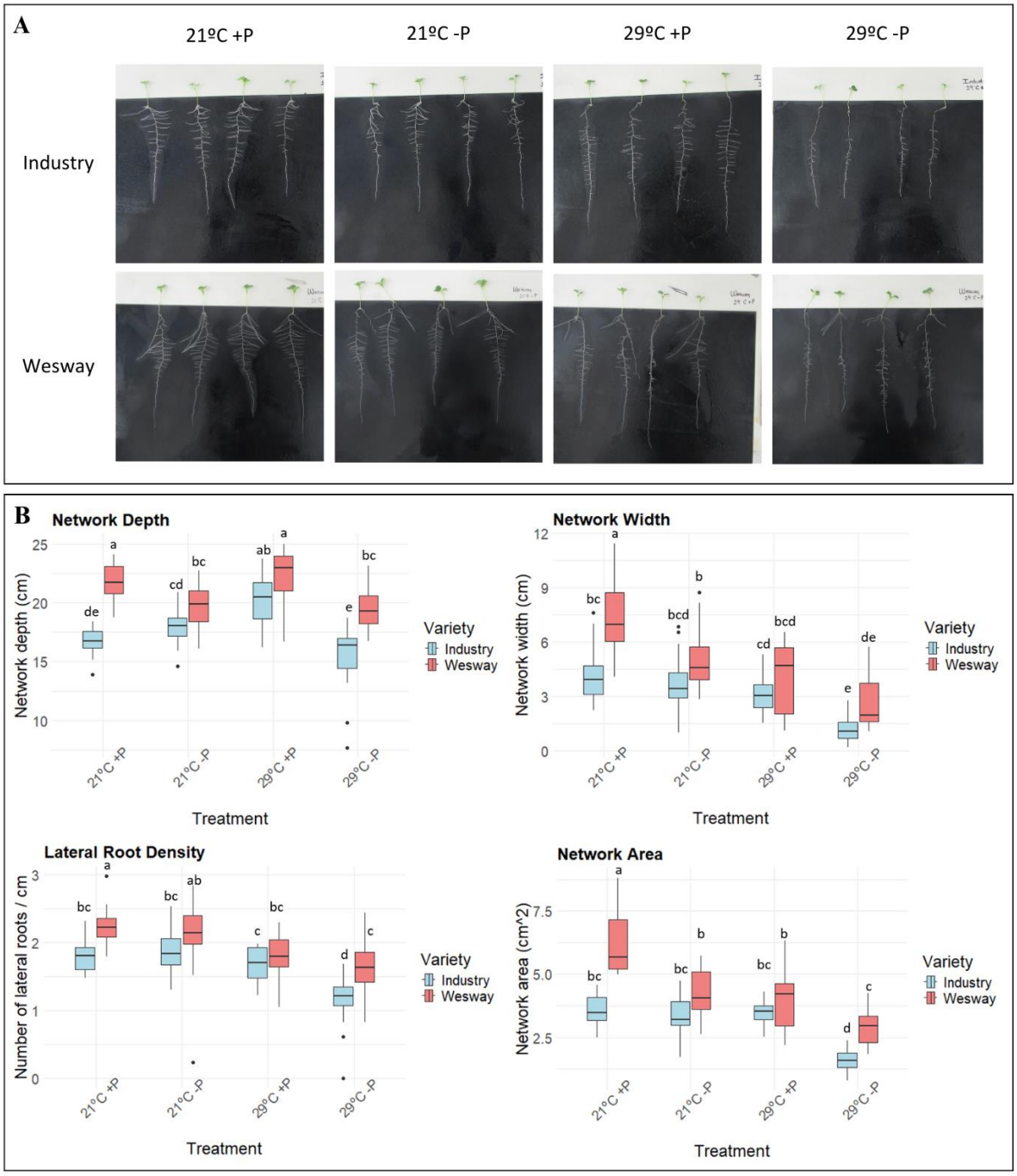


Figure 4.29: Summary of the main differences between the varieties Industry and Wesway in response to the different temperature and Pi treatments. A) Seedlings from Industry (upper row) and Wesway (bottom row) grown in the Pouch and Wick system under different temperature and Pi treatments (from left to right: 21ºC+P, 21ºC-P, 29ºC+P and 29ºC-P) for 7 days. B) Mean values of different traits (network depth, network width, LRD and network area) in *B. napus* seedlings grown in the Pouch and Wick system under different temperature and Pi treatments for 7 days. X-axis indicates the different treatments. The legend at the right indicates the variety (Industry and Wesway). Boxplots showing the values for Industry and Wesway in all the other measured root traits are displayed in Supplementary Figure 8; 9. Letters indicate significant differences between groups ($p < 0.05$). Groups that are significantly different from each other do not share any letter.

In summary, our results show significant variation in the root responses to combined warm temperatures and Pi deficiency among different *B. napus* varieties. These differential responses are highlighted in two varieties: Industry and Wesway. Whereas the root system of Industry was less affected by Pi deficiency alone, it suffered significant alterations under the combination of warm temperature and Pi deficiency. On the other hand, Wesway was less affected by the combination of both stresses than Industry.

### 4.4.3. Different *B. napus* varieties show differential Pi accumulation in roots and shoots under warm temperatures and low Pi availability.

We have previously characterized the root responses to the combination of warm temperatures and Pi starvation in *B. napus* and observed changes in several root traits. Furthermore, we observed variation in this response across several *B. napus* varieties. Since changes in root architecture could be associated to changes in Pi uptake and transport (Crombez *et al.*, 2019), we wanted to quantify the Pi content in roots and shoots of *B. napus* under the different temperature and Pi treatments. Thus, we measured the free cellular Pi content in both roots and shoots of all the 12 *B. napus* varieties grown in the Pouch and Wick system under different temperature and/or Pi conditions (21ºC+P, 21ºC-P, 29ºC+P and 29ºC-P) (Supplementary Figure 10).

We observed that several varieties accumulated less Pi in roots and shoots in response to P deficiency (e.g. Duplo contained 0.33 nmoles/mg in roots and 0.48 nmoles/mg in shoots at 21ºC-P compared to 0.58 nmoles/mg in roots and 0.84 nmoles/mg in shoots at 21ºC+P; Supplementary Figure 10) whereas others showed a similar Pi content (e.g. Drakkar; Supplementary Figure 10). This suggests that some varieties might trigger differential responses to maintain Pi levels in roots. However, most varieties accumulated more Pi at 29ºC than at 21ºC in both roots and shoots, independently of the Pi supply, suggesting an effect of the warm temperature in Pi uptake or mobilization from organic compounds (Supplementary Figure 10). Moreover, when warm temperatures and P deficiency were applied together, we observed that most varieties accumulated more Pi in shoots than in roots. In barley, Pacack *et al.* (2016) observed that Pi content was not decreased in roots grown under high temperature and Pi starvation, compared to control conditions, and they suggested that this happened due to a down-regulation of

*PHO1* and *PHO2* produced by high temperature. *PHO1* and *PHO2* are responsible for Pi transport from roots to shoots, and down-regulation of these genes would cause Pi accumulation in roots at 29ºC-P. This observation is contrary to our findings, since we observed Pi accumulation in shoots at 29ºC-P suggesting that other factors could contribute to Pi accumulation in roots at 29º-P. In Industry, Pi accumulated in shoots at 29ºC-P (Figure 4.30), which could be explained by a more active Pi translocation to the shoot or by Pi mobilization from organic-P compounds to free Pi in shoots. On the other hand, in Wesway, Pi content in roots was similar in individuals grown at 21ºC-P and 21ºC+P, but in shoots, Pi content was higher at 21ºC-P, suggesting that the plant might prioritize Pi transport from roots to shoots to favour shoot growth rather than Pi accumulation in roots.

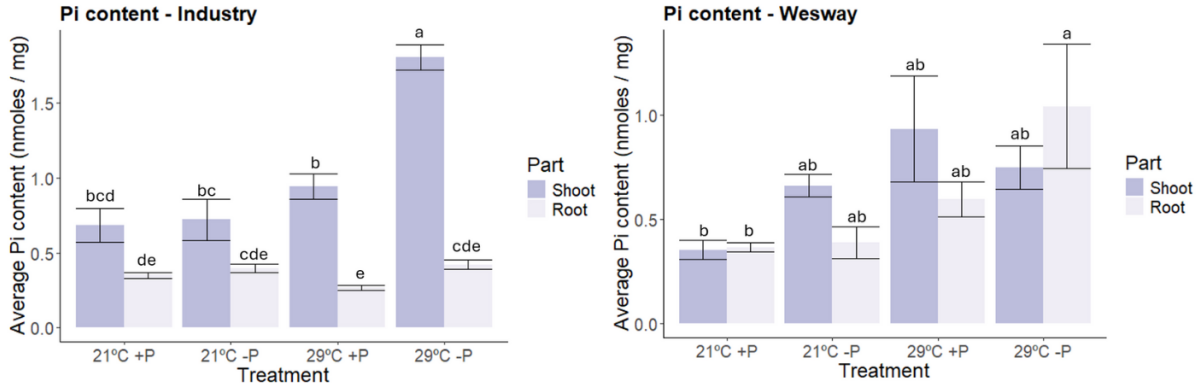


Figure 4.30: Phosphate (Pi) content in whole roots and shoots of *B. napus* seedlings from two varieties: Industry (left) and Wesway (right) grown under different temperature and/or Pi conditions for 7 days. X-axis indicates the different treatments: 21ºC+P, 21ºC-P, 29ºC+P and 29ºC-P. The colour legend indicates the sample type: either root or shoot. Error bars represent the variation between three different pools of 4 seedlings each and three technical replicates per pool. Letters indicate significant differences between groups ($p < 0.05$). Groups that are significantly different from each other do not share any letter. Pi content in whole roots and shoots of seedlings from the 10 remaining *B. napus* varieties is shown in Supplementary Figure 10.

To summarize, the combination of warm temperature and Pi deficiency can influence Pi accumulation and transport in roots and shoots in *B. napus*, and we have found variation in this response among different *B. napus* varieties. Industry seems to accumulate Pi in shoots under the combination of both Pi deficiency and warm temperature, whereas in Wesway, the amount of Pi in roots and shoots is more balanced at 29ºC-P. These data suggest the use of different strategies for Pi utilization under combined temperature and nutrient stress between different *B. napus* varieties.

## 4.5. Identification of a conserved regulatory mechanism of the Pi starvation response, involving BnPHR1 and BnSPX1, in *B. napus*.

### 4.5.1. Identification and characterization of the MYB-CC protein family in *B. napus*.

The interaction between PHR and SPX proteins has recently shown to be a crucial mechanism to regulate Pi homeostasis in Arabidopsis and rice (Dong *et al.*, 2019; Zhou *et al.*, 2021). Under Pi starvation, PHR proteins can directly activate the transcription of Pi-starvation induced (PSI) genes by binding to their promoters, whereas under Pi sufficiency, SPX proteins bind to PHR proteins, blocking their activity and inhibiting the consequent activation of PSI genes. Here, we aimed to study the interaction between SPX proteins and PHR proteins in *B. napus* as a potential conserved regulatory mechanism that participates in the Pi-starvation response.

In Arabidopsis, the MYB-CC family contains 15 members in total, including AtPHR1, AtPHL1, AtPHL2 and AtPHL3 (Rubio *et al.*, 2001). Characterization of the MYB-CC family in other species has identified 12 MYB-CC members in rice, 18 in maize, and 14 in sorghum (Xu *et al.*, 2018).We wanted to characterize the MYB-CC protein family in *B. napus*, to identify MYB-CC proteins that share high homology with AtPHR1. Thus, using bioinformatic tools (see Material and methods: 3.11.), we identified 58 MYB-CC proteins in the *B. napus* genome that contained both the MYB and coiled-coiled (CC) domains, characteristic of the MYB-CC family. We only considered proteins that showed at least 35% of homology with AtPHR1 (AT4G28610) in their amino acid sequences. The MYB-CC members were identified through BLAST searches in the ZS11 *B. napus* genome database using the amino acid sequence of AtPHR1 as a query, and then consequent BLAST searches using the amino acid sequences of other three Arabidopsis MYB-CC members: AtPHL1, AtPHL2 and AtPHL3. The proteins were named in order according to their chromosomal positions (Table 4.2). Additional information such as the number of exons of each gene and the coding sequence start and end positions for each exon can be found in Supplementary Table 7.

Table 4.2: Information of the MYB-CC members identified in *B. napus*, including their gene names, gene IDs from the ZS11 database and the Darmor database, chromosomal locations, transcript length, isoelectric point (pI), molecular weight (MW) of the proteins and their respective Arabidopsis homologs. Additional information such as the number of exons in each gene and the coding sequence start and end positions for each exon can be found in Supplementary Table 7.

| Name | Gene ID (ZS11) | Gene ID (Darmor) | chr. location | Transcript length (bp) | pI | MW (Da) | A. thaliana homolog |
|---|---|---|---|---|---|---|---|
| *BnMYB-CC1* | BnaA01G0084300ZS | BnaA01g08300D | A01:4739668..4741509 | 2084 | 6.08 | 45950.72 | PHR1 |
| *BnMYB-CC2* | BnaA01G0286300ZS | BnaA01g23320D | A01:26769040..26772967 | 690 | 5.46 | 26152.13 | PHL2 |
| *BnMYB-CC3* | BnaA01G0362900ZS | BnaA01g30110D | A01:32655904..32657950 | 2297 | 5.75 | 48643.16 | GAMMAMYB2 |
| *BnMYB-CC4* | BnaA01G0365100ZS | BnaA01g30340D | A01:32782779..32784031 | 1072 | 6.9 | 26916.35 | -- |
| *BnMYB-CC5* | BnaA01G0404900ZS | - | A01:36064488..36066162 | 1675 | 8.73 | 44725.46 | -- |
| *BnMYB-CC6* | BnaA02G0023600ZS | BnaAnng01860D | A02:1494117..1496501 | 1128 | 6.69 | 42283.01 | -- |
| *BnMYB-CC7* | BnaA02G0182500ZS | BnaA02g14410D | A02:11154907..11156430 | 1257 | 6.29 | 36771.36 | -- |
| *BnMYB-CC8* | BnaA02G0237500ZS | - | A02:15440631..15442180 | 1550 | 7.83 | 38720.59 | APL |
| *BnMYB-CC9* | BnaA02G0311300ZS | - | A02:28208939..28211001 | 2063 | 5.54 | 34220.24 | -- |
| *BnMYB-CC10* | BnaA03G0025400ZS | BnaA03g55680D | A03:1198168..1200488 | 1119 | 7.2 | 42063.01 | -- |
| *BnMYB-CC11* | BnaA03G0331200ZS | - | A03:17450237..17452794 | 2558 | 5.49 | 50691.54 | GAMMAMYB2 |
| *BnMYB-CC12* | BnaA03G0377600ZS | BnaA03g37160D | A03:20180473..20182204 | 1035 | 6.2 | 32195.22 | PHL2 |
| *BnMYB-CC13* | BnaA03G0506300ZS | BnaA03g58920D | A03:28199062..28200539 | 2321 | 8.34 | 40884.81 | PHR1 |
| *BnMYB-CC14* | BnaA06G0000900ZS | BnaA06g00030D | A06:202105..203700 | 1095 | 5.92 | 40365.02 | GAMMAMYB2 |
| *BnMYB-CC15* | BnaA06G0413200ZS | - | A06:46557414..46558799 | 1386 | 5.69 | 31142.59 | -- |
| *BnMYB-CC16* | BnaA06G0429600ZS | BnaAnng05640D | A06:47360698..47362248 | 843 | 8.54 | 31236.12 | -- |
| *BnMYB-CC17* | BnaA07G0003300ZS | BnaA07g00280D | A07:179648..181303 | 1017 | 6.01 | 37838.63 | PHL4 |
| *BnMYB-CC18* | BnaA07G0071500ZS | BnaA07g05970D | A07:12132817..12134685 | 1022 | 9.75 | 31444.68 | PHL2 |
| *BnMYB-CC19* | BnaA07G0231100ZS | BnaA07g20350D | A07:23143190..23144759 | 1169 | 8.76 | 38292.21 | APL |
| *BnMYB-CC20* | BnaA07G0270900ZS | BnaA07g24220D | A07:25436313..25437803 | 966 | 6 | 36838.51 | -- |
| *BnMYB-CC21* | BnaA07G0310800ZS | BnaA07g28130D | A07:27860539..27862051 | 1344 | 6.19 | 37985.79 | -- |
| *BnMYB-CC22* | BnaA07G0382600ZS | BnaA07g34920D | A07:31937454..31939096 | 1348 | 8.4 | 39630.56 | APL |
| *BnMYB-CC23* | BnaA08G0054000ZS | BnaA08g05130D | A08:5057976..5059138 | 861 | 8.82 | 29061.96 | UNE16 |
| *BnMYB-CC24* | BnaA08G0162100ZS | BnaA08g13620D | A08:20459314..20462004 | 2357 | 5.75 | 43731.26 | PHR1 |
| *BnMYB-CC25* | BnaA09G0125900ZS | BnaA09g10270D | A09:7565451..7567114 | 1513 | 5.13 | 35908.38 | PHL4 |
| *BnMYB-CC26* | BnaA10G0189400ZS | BnaA10g16590D | A10:21286874..21288652 | 1680 | 5.91 | 44300.48 | MYR1 |
| *BnMYB-CC27* | BnaA10G0265100ZS | BnaA10g24150D | A10:24825440..24827869 | 1125 | 7.65 | 42259.33 | -- |
| *BnMYB-CC28* | BnaC01G0090400ZS | - | C01:5614942..5618350 | 3409 | 5.05 | 39478.92 | PHL1 |
| *BnMYB-CC29* | BnaC01G0102600ZS | BnaC01g09850D | C01:6751625..6753389 | 1844 | 6.03 | 44256.62 | PHR1 |
| *BnMYB-CC30* | BnaC01G0351000ZS | BnaC01g30350D | C01:40197514..40201686 | 693 | 5.33 | 26281.25 | PHL2 |
| *BnMYB-CC31* | BnaC01G0453000ZS | BnaC01g38060D | C01:52031766..52034984 | 2582 | 5.63 | 48633.04 | GAMMAMYB2 |
| *BnMYB-CC32* | BnaC01G0455700ZS | - | C01:52363049..52364304 | 1256 | 6.9 | 26950.37 | -- |
| *BnMYB-CC33* | BnaC01G0510400ZS | - | C01:57421240..57422928 | 1689 | 7.27 | 44520.04 | -- |
| *BnMYB-CC34* | BnaC02G0025500ZS | BnaC02g01850D | C02:1814045..1816482 | 1131 | 6.72 | 42385.1 | -- |
| *BnMYB-CC35* | BnaC02G0239900ZS | BnaC02g19330D | C02:21869364..21870883 | 1257 | 7.13 | 37761.68 | -- |
| *BnMYB-CC36* | BnaC02G0319400ZS | - | C02:31345265..31346826 | 1562 | 7.83 | 38758.66 | APL |
| *BnMYB-CC37* | BnaC02G0421500ZS | - | C02:51843233..51845257 | 2025 | 5.95 | 30758.27 | -- |
| *BnMYB-CC38* | BnaC02G0494400ZS | BnaC02g39280D | C02:59870888..59872712 | 1048 | 5.08 | 45238.19 | PHL1 |

| | | | | | | | |
|---|---|---|---|---|---|---|---|
| *BnMYB-CC39* | BnaC03G0031000ZS | - | C03:1587927..1590294 | 2368 | 7.22 | 42125.98 | -- |
| *BnMYB-CC40* | BnaC03G0397300ZS | BnaC03g73670D | C03:26954264..26956020 | 2512 | 5.63 | 47150.68 | GAMMAMYB2 |
| *BnMYB-CC41* | BnaC03G0462400ZS | BnaC03g43430D | C03:32958722..32960763 | 1135 | 6.41 | 32237.26 | PHL2 |
| *BnMYB-CC42* | BnaC05G0475400ZS | BnaC05g40460D | C05:52283105..52284295 | 696 | 7.23 | 26542.02 | -- |
| *BnMYB-CC43* | BnaC05G0555400ZS | BnaC05g47520D | C05:56960739..56962502 | 1298 | 6.51 | 41833.12 | -- |
| *BnMYB-CC44* | BnaC06G0093500ZS | - | C06:16276306..16277914 | 1609 | 6.04 | 39424.12 | GAMMAMYB2 |
| *BnMYB-CC45* | BnaC06G0249500ZS | BnaC06g19840D | C06:35825993..35827560 | 1358 | 8.76 | 38387.3 | APL |
| *BnMYB-CC46* | BnaC06G0306200ZS | BnaC06g25290D | C06:41018729..41021055 | 1059 | 5.65 | 40205.17 | -- |
| *BnMYB-CC47* | BnaC06G0361200ZS | BnaC06g28050D | C06:46236759..46238261 | 1344 | 6.77 | 37681.51 | -- |
| *BnMYB-CC48* | BnaC06G0450000ZS | BnaC06g39850D | C06:51988496..51990092 | 1345 | 8.4 | 39659.55 | APL |
| *BnMYB-CC49* | BnaC07G0009300ZS | BnaC07g00540D | C07:1791153..1792773 | 1023 | 5.59 | 38331.08 | PHL4 |
| *BnMYB-CC50* | BnaC07G0110500ZS | BnaC07g07340D | C07:22291918..22294996 | 1758 | 6.09 | 56315.28 | PHL2 |
| *BnMYB-CC51* | BnaC07G0242100ZS | BnaC07g18520D | C07:38662463..38663995 | 843 | 7.72 | 31234.19 | -- |
| *BnMYB-CC52* | BnaC07G0263500ZS | - | C07:40771050..40772430 | 1381 | 5.6 | 31143.58 | -- |
| *BnMYB-CC53* | BnaC07G0484600ZS | BnaC07g41450D | C07:57051490..57054010 | 2210 | 6.02 | 42939.26 | PHR1 |
| *BnMYB-CC54* | BnaC08G0071200ZS | BnaC08g08750D | C08:9236856..9238342 | 849 | 7.09 | 31016.14 | UNE16 |
| *BnMYB-CC55* | BnaC08G0179600ZS | BnaC08g13160D | C08:28733213..28735787 | 2283 | 6.21 | 31220.39 | PHR1 |
| *BnMYB-CC56* | BnaC09G0041100ZS | BnaC09g02840D | C09:2591776..2593509 | 1236 | 5.73 | 45904.72 | PHL1 |
| *BnMYB-CC57* | BnaC09G0132300ZS | BnaC09g10430D | C09:9712854..9714467 | 1688 | 5.43 | 36745.23 | PHL4 |
| *BnMYB-CC58* | BnaC09G0483100ZS | BnaC09g54190D | C09:59518674..59520495 | 1536 | 6 | 44222.36 | MYR1 |

The amino acid sequences of each MYB-CC member in *B. napus* were used to build a phylogenetic tree based on a multiple sequence alignment, together with the *A. thaliana* MYB-CC members: AtPHR1 (AT4G28610), AtPHL1 (AT5G29000), AtPHL2 (AT3G24120) and AtPHL3 (AT4G13640). The MYB-CC members from other species that are orthologs of AtPHR1 according to TAIR (https://www.arabidopsis.org/) were included in the phylogenetic tree: BrPHR1 (Bra010355), BrPHR2 (Bra024188), BrPHR3 (Bra036469) and BrPHR4 (Bra036679) from *Brassica rapa*, BolPHR1 (Bo8g054450) from *Brassica oleracea*, OsPHR1 (Os03g0329900) and OsPHR2 (Os03g0343400) from *Oryza sativa*, TaPHR1 (Traes_4AS_7220D33B3) from *Triticum aestivum*, ZmPHR1 (Zm00001d029020) from *Zea mays* and SlPHR1 (Solyc05g055940.2) from *Solanum lycopersicum* (Figure 4.31).

The phylogenetic tree revealed the *B. napus* MYB-CC members that were most closely related to AtPHR1, and were BnMYB-CC1, BnMYB-CC13 and BnMYB-CC29, that also showed high homology with BrPHR2 from *B. rapa*. Other PHR members from *B. napus* such as BnMYB-CC38 and BnMYB-CC56 showed a higher homology with AtPHL1, whereas others such as BnMYB-CC2, BnMYB-CC30 and BnMYB-CC50 showed high homology with AtPHL2, or BnMYB-CC23 and BnMYB-CC54 with AtPHL3. Furthermore, PHR members from rice, maize and

wheat were distant from PHR members in *A. thaliana*, *B. napus*, *B. oleracea* and *B. rapa*, as expected (Figure 4.31).

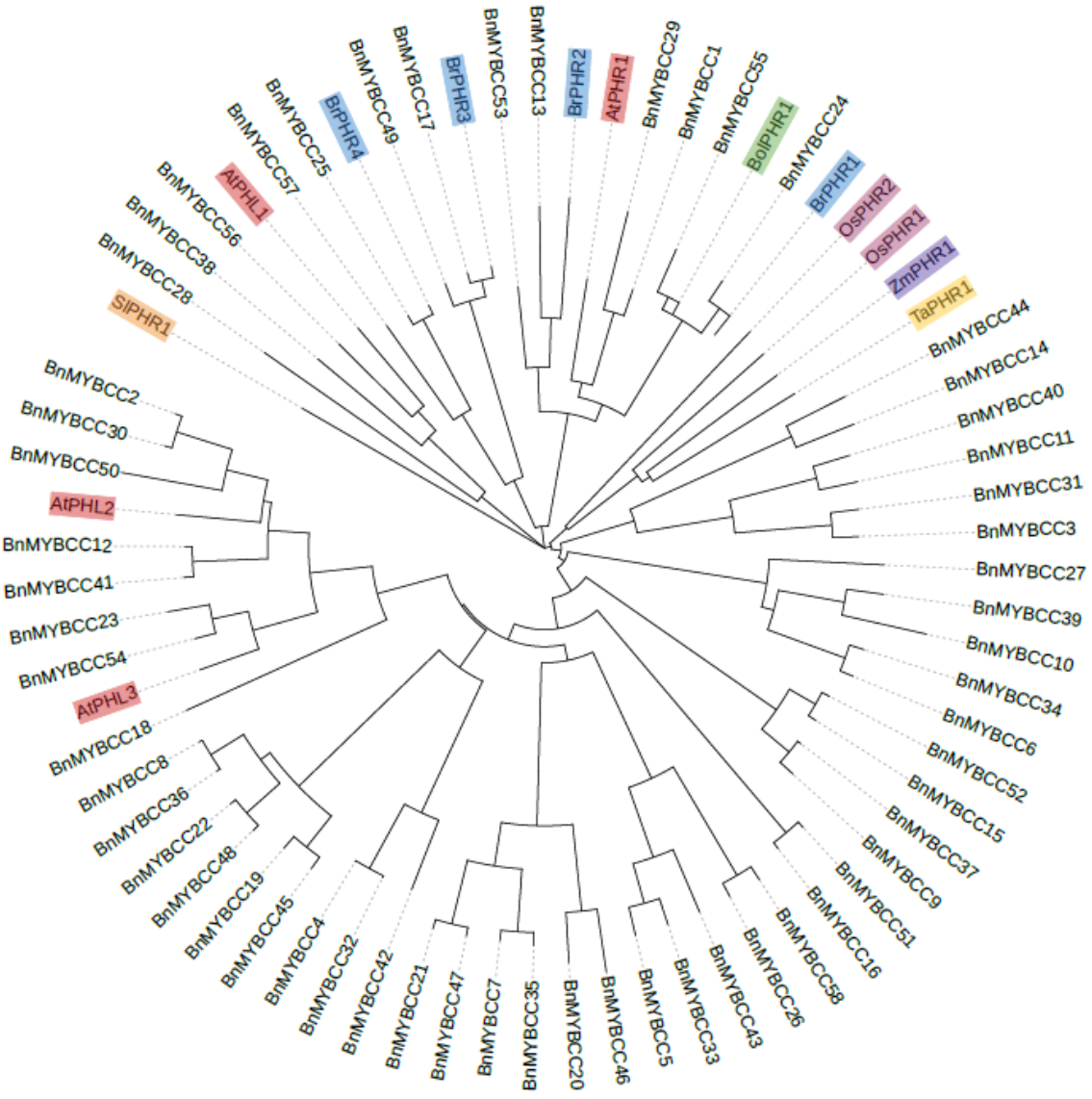


Figure 4.31: Phylogenetic tree of the MYB-CC members of *B. napus*. Some of the main MYB-CC proteins from other species were included and labelled in different colors: *Arabidopsis thaliana* in red (AtPHR1, AtPHL1, AtPHL2 and AtPHL3), *Brassica rapa* in blue (BrPHR1, BrPHR2, BrPHR3 and BrPHR4), *Brassica oleracea* in green (BolPHR1), *Oryza sativa* in pink (OsPHR1 and OsPHR2), *Zea mays* in purple (ZmPHR1), *Triticum aestivum* in orange (TaPHR1) and *Solanum lycopersicum* in brown (SlPHR1). The multiple sequence alignment and the phylogenetic tree were constructed using ClustalW. The phylogenetic tree was visualized using the Itol software.

In summary, we have identified 58 different MYB-CC members and characterized their gene structure and protein sequence in *B. napus*. The MYB-CC members from BnMYB-CC1 to BnMYB-CC27, belonging to chromosomes A1 to A10, are

derived from the *B. rapa* genome, whereas the MYB-CC members from BnMYB-CC28 to BnMYB-CC58 found in chromosomes C1 to C9 derive from the *B. oleracea* genome (Table 4.2). The phylogenetic tree revealed the putative homologs of each known MYB-CC member in Arabidopsis. The higher number of MYB-CC members in *B. napus* compared to other crops is likely due to the complexity of its genome.

### 4.5.2. Identification of the *B. napus* AtPHR1 and AtSPX1 orthologs.

To identify the most closely related AtPHR1 homologs in *B. napus*, we generated a new phylogenetic tree using previous phylogenetic information (Table 4.2; Figure 4.32). According to this phylogenetic tree, we found that BnMYB-CC1 and BnMYB-CC29 had the highest homology with AtPHR1. Recently, a study has confirmed the ability of BnMYB-CC1 (BnaA01g08300D) to bind the promoter of *BnPHT1;2*, a Pi-starvation induced (PSI) gene, and showed that the overexpression of *BnMYB-CC1* in Arabidopsis enhanced the development of lateral roots and increased Pi concentration (Liu *et al.*, 2023). Furthermore, previous research has shown that overexpression of *BnMYB-CC29 (BnaC01g09850D)* in both Arabidopsis and *B. napus* induces the expression of many Pi- starvation induced (PSI) genes, triggering the Pi-starvation response (Ren *et al.*, 2012). This suggests that both BnMYB-CC1 and BnMYB-CC29 are functional orthologs of AtPHR1, with *BnMYB-CC1* belonging to the A genome (derived from *B. rapa*) and *BnMYB-CC29* belonging to the C genome (derived from *B. oleracea*). We decided to choose BnMYB-CC1 for further analysis and gave it the name of BnPHR1.

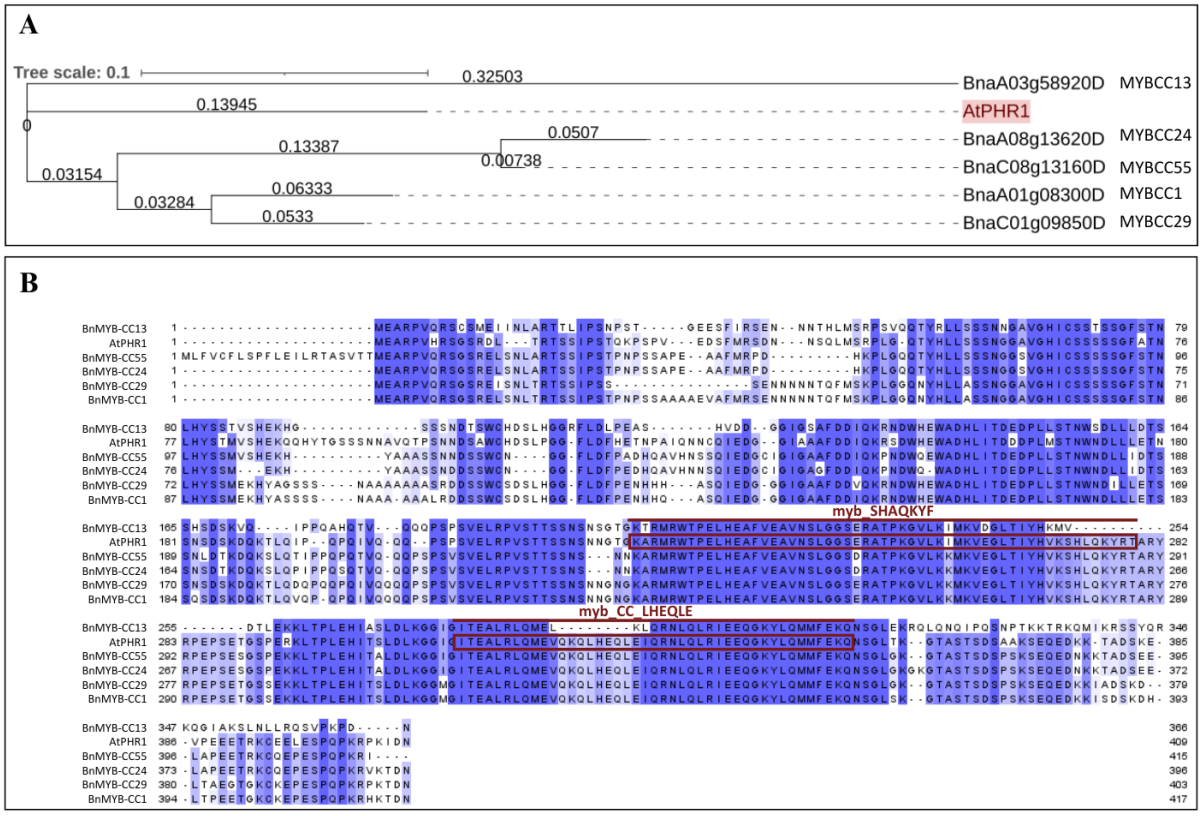


Figure 4.32: A) Phylogenetic tree of AtPHR1 (highlighted in red) and the *B. napus* MYB-CC proteins that are most closely related to AtPHR1 (BnMYB-CC1, BnMYB-CC13, BnMYB-CC24, BnMYB-CC29 and BnMYB-CC55). The phylogenetic tree was built in ClustalW and visualized using the Itol software. B) Multiple sequence alignment of the amino acid sequences of BnMYB-CC1, BnMYB-CC13, BnMYB-CC24, BnMYB-CC29, BnMYB-CC55 and AtPHR1. The colour gradient indicates the level of conservation (dark purple = identical residues; light purple = less conserved residues; white = not conserved residues). The regions belonging to the myb (myb_SHAQKYF) and CC (myb_CC_LHEQLE) domains are highlighted in red. The multiple sequence analysis was built in ClustalW and visualized in Jalview (version 2.11.3.3).

Even though those PHR proteins have shown to induce the expression of some PSI genes in *B. napus*, the role of SPX proteins as regulators of the activity of PHR proteins has not been studied in *B. napus* yet. Thus, we identified the most closely related AtSPX1 homologs in *B. napus* through BLAST searches in the *B. napus* ZS11 database, using the amino acid sequence of AtSPX1 as a query (Figure 4.33). BnaA03g07930D was identified as the putative ortholog of AtSPX1 and was called BnSPX1.1 and selected for further analysis.

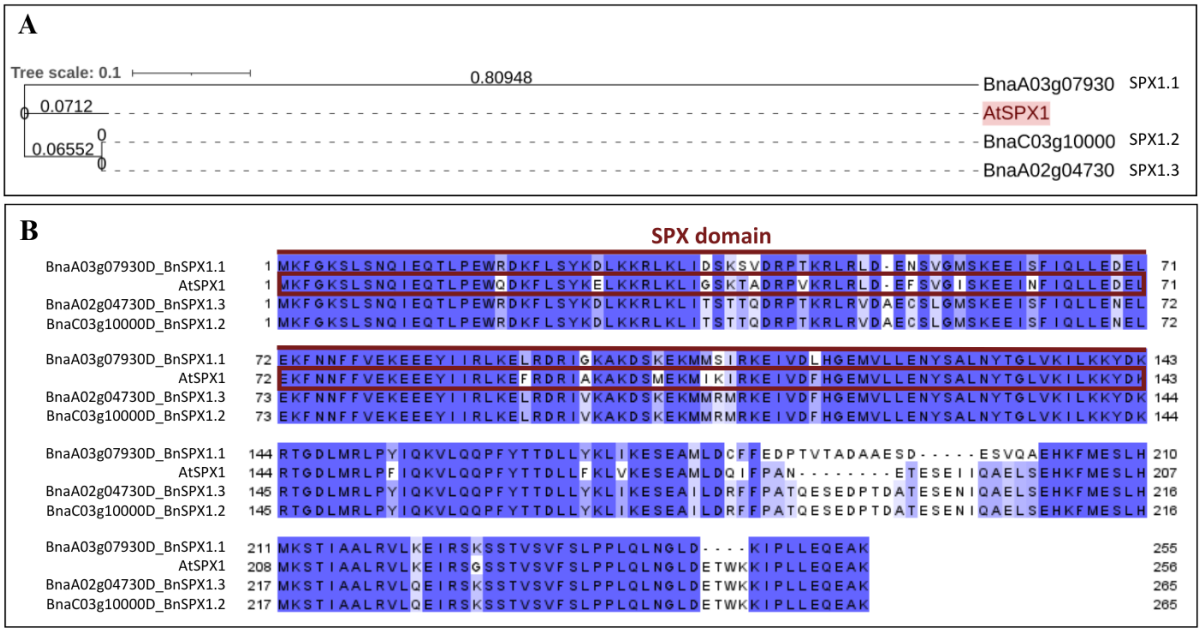


Figure 4.33: A) Phylogenetic tree of AtSPX1 (highlighted in red) and the *B. napus* SPX proteins that are most closely related to AtSPX1. The phylogenetic tree was built in ClustalW and visualized in Itol. B) Multiple sequence alignment of AtSPX1 and the *B. napus* proteins that are most closely related to AtSPX1. The colour gradient indicates the level of conservation (dark purple = identical; light purple = less conserved residues; white = not conserved residues). The region containing the SPX domain in AtSPX1 is highlighted in red. The multiple sequence alignment was built in ClustalW and visualized in Jalview (version 2.11.3.3).

Therefore, both BnPHR1 and BnSPX1.1 were selected for further analysis at the molecular level.

### 4.5.3. The *B. napus* proteins PHR1 and SPX1.1 interact in the nucleus.

First, we tested the interaction between PHR1 and SPX1.1 in *B. napus* through a BIFC assay. The coding sequences of *BnPHR1* and *BnSPX1.1* were amplified from cDNA from *B. napus* (variety Wesway) roots, and fused to c-YFP or n-YFP tag, respectively. Afterwards, both constructs were co-infiltrated in *N. benthamiana* leaves and the YFP fluorescence signal was observed two days after infiltration. The YFP fluorescence signal was observed in leaves co-infiltrated with both *BnPHR1* and *BnSPX1.1*, while this signal was absent in leaves co-infiltrated with the negative control or only with one of the constructs (Figure 4.34A). Remarkably, this interaction was observed exclusively in the nucleus where both proteins are known to interact in Arabidopsis and rice (Dong *et al.*, 2019; Zhou *et al.*, 2021).

To confirm this interaction by a different approach, we carried out a co-immunoprecipitation (CoIP) assay. The coding sequences of *BnPHR1* and *BnSPX1.1* were fused to a GFP or FLAG tag, respectively, and these constructs were co-infiltrated into *N. benthamiana* leaves. The construct containing 35S::*BnPHR1-GFP* was also infiltrated alone as a negative control. After 2 days, total proteins were extracted and incubated with anti-FLAG beads to immunoprecipitate 35S::*BnSPX1.1-FLAG*. Finally, the proteins were separated in an SDS-PAGE gel and submitted to immunoblot analysis using an anti-FLAG or anti-GFP antibodies, to identify 35S::*BnSPX1.1-FLAG* or 35S::*BnPHR1-GFP*, respectively. Incubation with anti-GFP showed a band corresponding to the size of 35S::*BnPHR1-GFP* in samples containing both 35S::*BnPHR1-GFP* and 35S::*BnSPX1.1-FLAG* and immunoprecipitated with 35S::*BnSPX1.1-FLAG*. However, this band was absent in samples containing only 35S::*BnPHR1-GFP* and immunoprecipitated with 35S::*BnSPX1.1-FLAG* (Figure 4.34C). Incubation with the anti-FLAG antibody as a positive control in both samples confirmed the correct immunoprecipitation of 35S::*BnSPX1.1-FLAG*. This confirms the interaction between BnPHR1 and BnSPX1.1 in *planta*.

Finally, we did a yeast-two hybrid assay to test whether there is a direct interaction between BnPHR1 and BnSPX1.1. Research shows that the C-terminal region of *BnPHR1* interacts with SPX1 and SPX2 in rice (Wang *et al.*, 2014b), while the N terminus contains a transactivation domain that is active in yeast (Zhou *et al.*, 2008; Bustos *et al.*, 2010). For this reason, we cloned only the C-terminal region of *BnPHR1* into the bait expression vector pGBKT7, containing the GAL4 DNA-binding domain (BD). Furthermore, the full coding sequence of *BnSPX1* was cloned into pGADT7, which contains the activation domain (AD). Both plasmids were then used in a yeast two-hybrid (Y2H) assay. Transformations of the empty vectors or single transformations of *BnPHR1_C* or *BnSPX1.1* were used as negative controls, while *OsSPX1.1* and *OsPHR2_C* (C-terminal) constructs from rice were co-infiltrated as a positive control (Wang *et al.*, 2014b). After one week, all construct combinations were able to grow in selection medium, indicating that transformation was successful (Figure 4.34B). However, when transformed yeasts were grown in medium to select for the interaction, only the positive control was able to grow, indicating that the BnPHR1 and BnSPX1.1 proteins were unable to directly interact in the two hybrid system. Recently, the interaction between SPX proteins and PHR proteins has shown to be dependent on the levels of inositol pyrophosphate (InsP), which is necessary to mediate this interaction (Zhou *et al.*,

2021). However, the positive control, which consists of the rice *OsPHR2_C* and *OsSPX1.1* was able to grow on yeast selective media, indicating that this might not be the limiting factor in our experiments. Given that our previous assays showed a clear interaction between *BnPHR1* and *BnSPX1.1*, another component is possibly needed to promote the interaction between *BnPHR1* and *BnSPX1.1* in yeast. Alternatively, it is possible that *B. napus* proteins fused to the AD and DB domains did not fold correctly in yeast, preventing their interaction.

Altogether, these results indicate that BnPHR1 and BnSPX1.1 interact in the nucleus in planta, reinforcing the hypothesis that this regulatory mechanism of the Pi starvation response is conserved in *B. napus.*

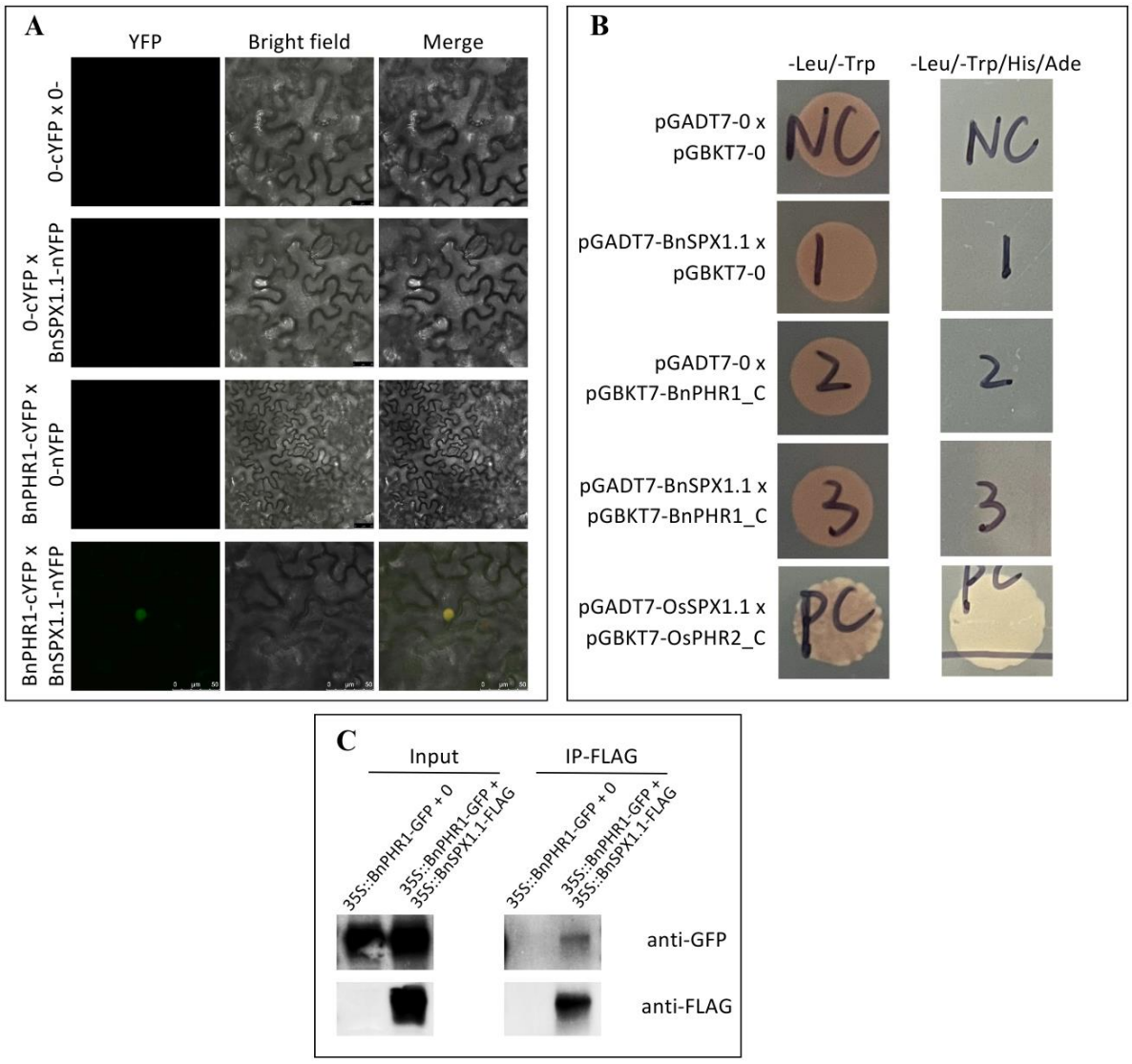


Figure 4.34: Analysis of the interaction between BnPHR1 and BnSPX1.1. A) Bimolecular fluorescence complementation assay (BIFC) in tobacco leaves showed the interaction between BnPHR1 and B.SPX1.1 in the nucleus. The full length of the coding sequences of BnPHR1 and BnSPX1.1 were fused to cYFP and nYFP, respectively. The YFP fluorescent

signal was observed two days after infiltration. B) Yeast-two-hybrid assay of BnPHR1 and BnSPX1.1. The full length of BnSPX1.1 and the C-terminal region of BnPHR1 were cloned into pGADT7 (AD)and pGBKT7 (BD), respectively. The empty vectors were used as a negative control. The C-terminal region of OsPHR2 and the full length of OsSPX1 were used as positive control. C) Co-IP assay of the interaction between BnPHR1 and BnSPX1.1 in tobacco leaves. Input samples contain the total proteins, whereas IP-FLAG samples contain immunoprecipitated 35S::*BnSPX1.1-FLAG* samples after a 3-hour incubation with FLAG beads. 35S::*BnPHR1-GFP* + 0 indicates proteins extracted from leaves infiltrated only with 35S::*BnPHR1-GFP*, whereas 35S::*BnPHR1-GFP* + 35S::*BnSPX1.1-FLAG* indicate proteins extracted from leaves co-infiltrated with both constructs 35S::*BnPHR1-GFP* and 35S::*BnSPX1.1-FLAG*.

### 4.5.4. BnPHR1 activates the transcription of *BnSPX1* and the overexpression of *BnSPX1.1* suppresses the transcriptional activation effects of BnPHR1.

To study the effects of BnPHR1 as a transcriptional activator of Pi-starvation induced (PSI) genes, we did a transactivation assay in tobacco leaves. Since *SPX1* is known to be a PSI gene in Arabidopsis (Secco *et al.*, 2012), we cloned the promoter region of *BnSPX1* fused to the LUC (*BnSPX1.1p::LUC*) gene to monitor the possible activation of this gene by BnPHR1. Thus, we carried out a transient expression analysis in *Nicotiana benthamiana* leaves infiltrated with this construct alone, in combination with 35S::*BnPHR1-GFP*, or in combination with both 35S::*BnPHR1-GFP* and 35S::*BnSPX1.1-FLAG*, and the LUC signal was checked after two days (Figure 4.35). We observed the presence of the LUC fluorescent signal when we used the *BnSPX1.1* promoter alone (*BnSPX1.1p::LUC)*, indicating that this construct is functional in *planta*. When the *BnSPX1.1p::LUC* was co-infiltrated together with 35S::*BnPHR1-GFP*, the intensity of the fluorescent signal was higher, indicating that BnPHR1 induced the transcription of *BnSPX1.1*. Moreover, when *BnSPX1.1p::LUC* was co-infiltrated with 35S::*BnPHR1-GFP* and with 35S::*BnSPX1.1-FLAG* in a triple infiltration, the fluorescent signal was less intense, indicating a repression in the transcription of *BnSPX1.1* mediated by a negative loop.

Thus, BnPHR1 is able to induce the transcription of *BnSPX1.1*, a PSI gene. Furthermore, BnSPX1.1 might sequester BnPHR1, blocking the induction of its own transcription.

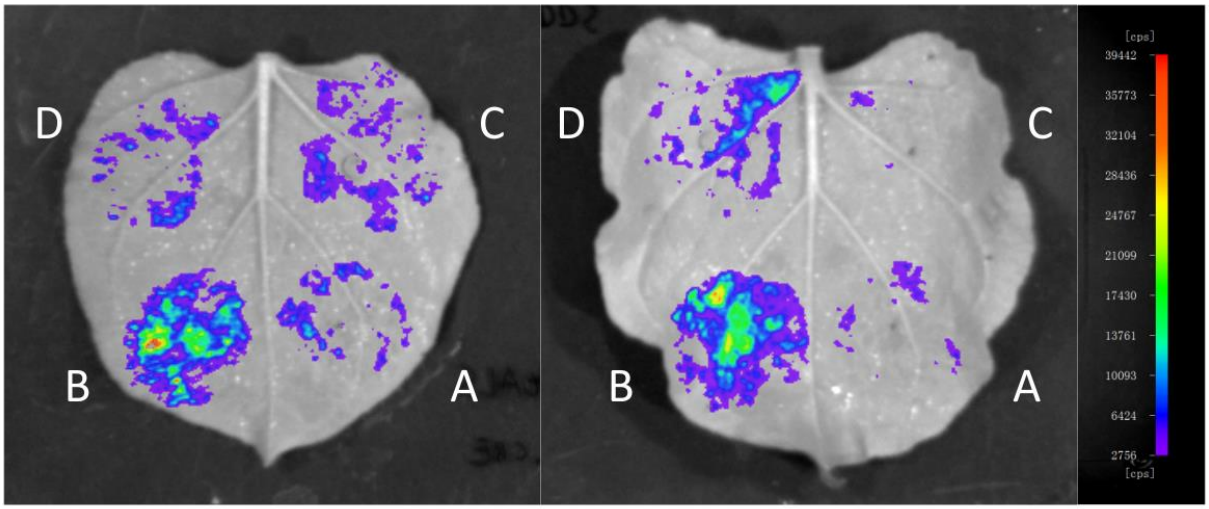


**A:** *BnSPX1.1p::LUC.*
**B:** *BnSPX1.1p::LUC* x 35S::*BnPHR1-GFP.*
**C:** *BnSPX1.1p::LUC* x 35S::*BnPHR1-GFP* x 35S::*BnSPX1.1-FLAG* (1:2:1).
**D:** BnSPX1.1p::LUC x 35S::*BnPHR1-GFP* x 35S::*BnSPX1.1-FLAG* (1:2:3).

Figure 4.35: Transactivation assay in tobacco leaves showing the transcription activation effects of BnPHR1 in the promoter of *BnSPX1.1*. The promoter region of *BnSPX1.1* was fused to the LUC gene and infiltrated in tobacco leaves alone (A) or co-infiltrated with 35S::*BnPHR1-GFP* (B) or with 35S::*BnPHR1-GFP* and 35S::*BnSPX1.1-FLAG* in a 1:2:1 ratio (C) or in a 1:2:3 ratio (D). The LUC signal was observed two days after infiltration. The colour legend at the right indicates the intensity of the luminescent signal. The two different images represent two independent biological replicates.

In this section, we aimed to study the conserved mechanism that involve the capacity of SPX1 to interact and block the activity of PHR1 in *B. napus*. We have identified the AtPHR1 and AtSPX1 orthologs in *B. napus* and confirmed their interaction in the nucleus. Moreover, we confirmed the capacity of BnPHR1 to activate the transcription of *BnSPX1.1*, as well as the repressor activity of BnSPX1.1, blocking the activation of its own transcription.

## 4.6. Identification of transcriptional networks and biological processes that regulate the root responses to combined warm temperature & phosphate deficiency in *B. napus*.

### 4.6.1. The expression of PSI genes in roots of *B. napus* under combined warm temperatures and Pi starvation is time dependent.

We have previously characterized the root responses of *B. napus* to the combination of warm temperatures and Pi starvation, and we have identified variation in the response among different genotypes. Most varieties showed few alterations in their root organization as a consequence of Pi deficiency alone, but had significant alterations under the stress combination (see Results: 4.4.1.). Particularly, Industry was severely affected under the stress combination (29ºC-P, with 16 traits significantly reduced) but not under the individual stresses (21ºC-P and 29ºC+P), whereas Wesway was less affected by the stress combination (Figure 4.29; Supplementary Figure 8; 9; Supplementary Table 5A; B). To gain additional insights into the regulation of the root responses to combined warm temperatures and Pi starvation in this variety, we aimed to study the expression patterns of several well-known PSI genes over time. Thus, we performed a time-course experiment using *B. napus* seedlings (variety Wesway) grown in the Pouch and Wick system under the same different temperature and/or Pi treatments previously used (21ºC+P, 21ºC-P, 29ºC+P and 29ºC-P). Then, we measured the expression levels of several PSI genes (*BnSPX3*, *BnSPX1*, *BnPECP2* and *BnPHO1*) by RT-qPCR in roots at different time points: 6 hours, 9 hours, 24 hours or 7 days after the start of the treatments.

Quantification by RT-qPCR shows that the expression of *BnSPX3*, *BnPECP2*, *BnPHO1* and *BnSPX1* reached its peak after 7 days when seedlings were grown at 21ºC+P (Figure 4.36). The expression levels of these genes increased under Pi deficiency, reaching its maximum at 7 days as well, except for *BnSPX1*, which showed an initial induction peak after 6 hours of Pi starvation. Remarkably, warm temperature (29ºC+P) caused a strong repression of all PSI genes, with their expression levels being even lower than under control conditions after 7 days. When warm temperature was combined with Pi starvation, the expression levels were still repressed, but to a lesser extent than under warm temperature alone (Figure 4.36). These results suggest that warm temperatures can reduce the expression levels of some PSI genes, even in combination with Pi deficiency.

Taken together these data seem to indicate that warm temperatures have a negative effect on the expression of PSI genes, which could negatively affect the response to Pi deficiency.

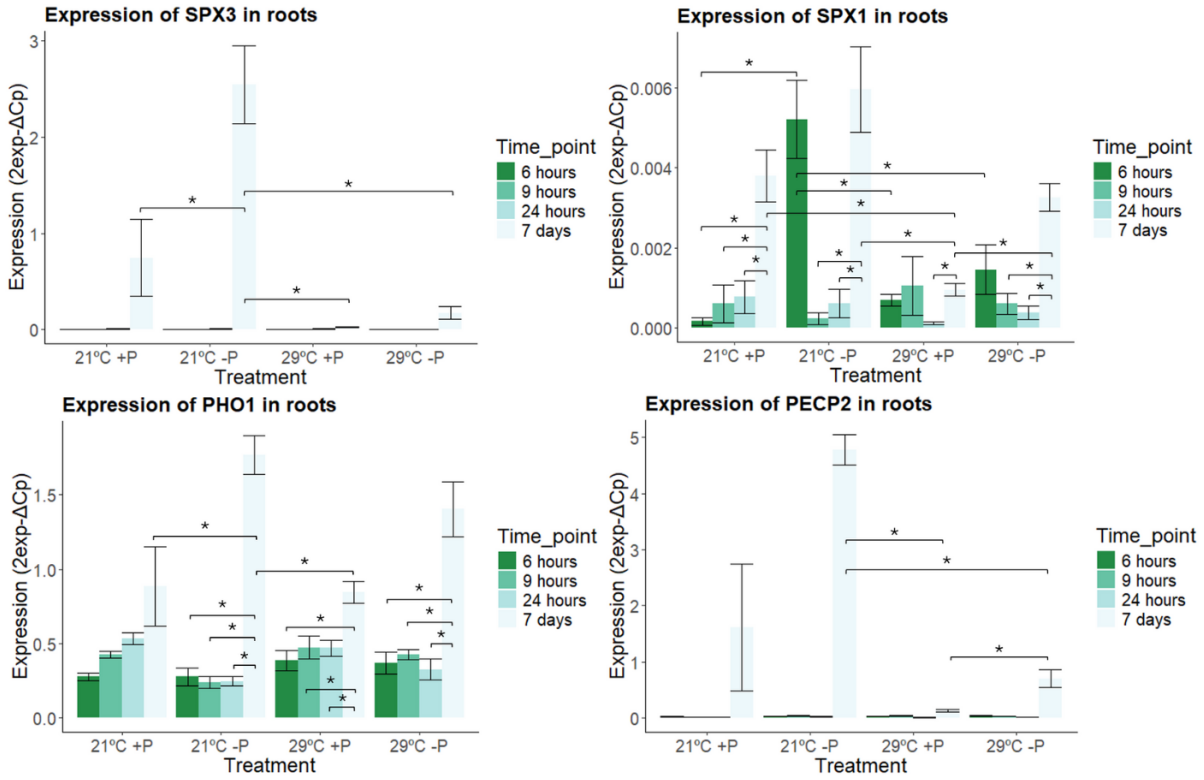


Figure 4.36: Expression of *BnSPX3 (BnaC04g50120D* & *BnaA03g21050D), BnSPX1 (BnaA03g07930D), BnPHO1 (BnaC01g30780D* & *BnaA01g23840D)* and *BnPECP2 (BnaA02G0204200ZS)* quantified by RT-qPCR in roots of *B. napus* plants (variety Wesway) grown under different temperature and/or phosphate treatments and sampled at different time points after the start of the treatments. X-axis shows the different treatments: 21ºC+P, 21ºC-P, 29ºC+P and 29ºC-P. The colour legend indicates the different time points: 6 hours, 9 hours, 24 hours and 7 days after the start of the treatments. X-axis indicates the expression levels (2exp-ΔCp) normalized to the expression levels of the control gene *BnACT7*. Error bars show the variation between three independent biological samples (with three technical replicates each).

### 4.6.2. Two *B. napus* varieties with different root adaptation strategies to combined warm temperatures and Pi deficiency show differences in their transcriptional response.

The previous characterization of the root responses of *B. napus* to the combination of warm temperatures and Pi starvation has helped us to identify the variability in this response among different varieties. The root system of several varieties such as Dux, Industry and Marnoo was unaltered as a consequence of Pi starvation, but was severely affected by the stress combination (29ºC-P). On the

other hand, other varieties displayed alterations in their root system at 21ºC-P and also at 29ºC-P. Two varieties that exemplify these different adaptation strategies were Industry and Wesway. Whereas Industry did not have any traits significantly altered at 21ºC-P, the stress combination (29ºC-P) caused significant changes on root morphology. In Wesway, the root system was altered at 21ºC-P, and at 29ºC-P, but the effects at 29ºC-P were less pronounced than in Industry. Thus, to understand the molecular basis underlying these differences, we performed RNA-sequencing in roots and shoots of these two cultivars grown on the Pouch and Wick system for 7 days under different treatments (21ºC+P, 21ºC-P, 29ºC+P and 29ºC-P).

The differentially expressed genes (DEGs) were calculated for the three stress treatments, Pi starvation (21ºC-P), warm temperature (29ºC+P) and the stress combination (29ºC-P), all compared to the control treatment (21ºC+P) in each of the two varieties. The number of DEGs at 21ºC-P was much lower than at 29ºC+P or 29ºC-P in both varieties (Figure 4.37A; B), indicating that the Pi starvation alone (21ºC-P) had a much softer effect on gene expression than the other two treatments (29ºC+P and 29ºC-P) in both varieties. These molecular differences correlate with the effects caused on root traits by the different stresses (see Results: 4.4.1. and 4.4.2.). Even though at 21ºC-P the number of DEGs was lower in both varieties, it was higher in Industry than in Wesway (731 up-regulated genes and 328 down-regulated genes in Industry vs. 43 up-regulated genes and 61 down-regulated genes in Wesway; Figure 4.37B). This observation could be related to the higher capacity of Industry to maintain root growth and development at 21ºC-P, compared to Wesway. Moreover, in both varieties, the number of up-regulated and down-regulated genes shared between 29ºC-P and 29ºC+P was higher than the number of genes shared between 29ºC-P and 21ºC-P (Figure 4.37C), reinforcing our previous observation that the effects of warm temperature caused a greater effect than the Pi starvation in both varieties also at the transcriptional level.

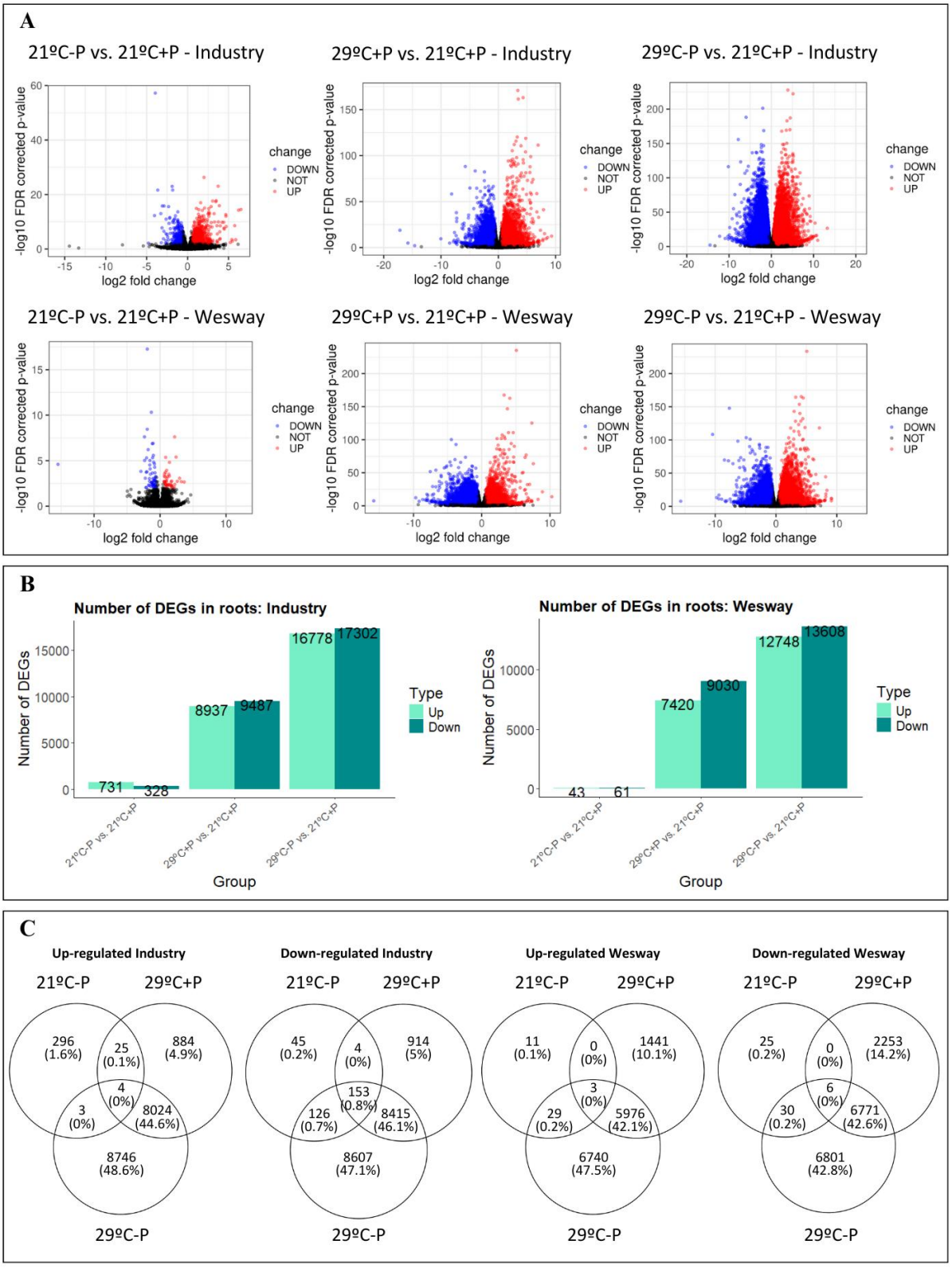


Figure 4.37: Analysis of gene expression detected by RNAseq in roots of the *B.napus* varieties Westar and Wesway grown under different temperature and phosphate (Pi) treatments. A) Volcano plots for the differentially expressed genes (DEGs; |log2FC| > 0.58; p-value < 0.01) in roots under different temperature and Pi treatments compared to control conditions. The top row shows volcano plots for Industry, whereas the plots at the

bottom row correspond to Wesway. From left to right: DEGs in roots under Pi deficiency (21ºC-P), under warm temperature (29ºC+P) and under the stress combination (29ºC-P), all of them compared to the control conditions (21ºC+P). B) Number of DEGs (|log2FC| > 0.58; p-value < 0.01) in roots of Industry (left) and Wesway (right) under different temperature and Pi treatments compared to control conditions. X-axis shows the different comparisons: Pi deficiency (21ºC-P vs. 21ºC+P), warm temperature (29ºC+P vs. 21ºC+P) and the stress combination (29ºC-P vs. 21ºC+P). The colour legend indicates whether the genes are up-regulated or down-regulated. C) Venn diagrams showing the number of DEGs that are common between the three stress treatments (21ºC-P, 29ºC+P and 29ºC-P), all compared to the control treatment (21ºC+P) expressed in roots under the four treatments: 21ºC+P, 21ºC-P, 29ºC+P and 29ºC-P. From left to right: Up-regulated genes in Industry, down-regulated genes in Westar, up-regulated genes in Industry, down-regulated genes in Wesway.

We have detected the major transcriptional changes in roots of the varieties Industry and Wesway caused by the different stress treatments (21ºC-P, 29ºC+P and 29ºC-P). Furthermore, we detected some differences in the number of DEGs between the two varieties across the different treatments. To identify the molecular mechanisms underlying these differences in gene expression, we performed the following bioinformatic analyses. For the analyses, only DEGs from at least one of the six comparisons described in the previous section were considered. First, the average of the normalized read counts from three biological replicates per treatment and variety was used to build a dendrogram of the DEGs according to their expression profiles. This dendrogram divided the DEGs into 5 different clusters according to their expression profiles across the treatments. To visualize the dendrogram and clusters, normalized read counts were scaled to Z-scores (-2.5 to 2.5) and plotted in a heatmap (Figure 4.38).

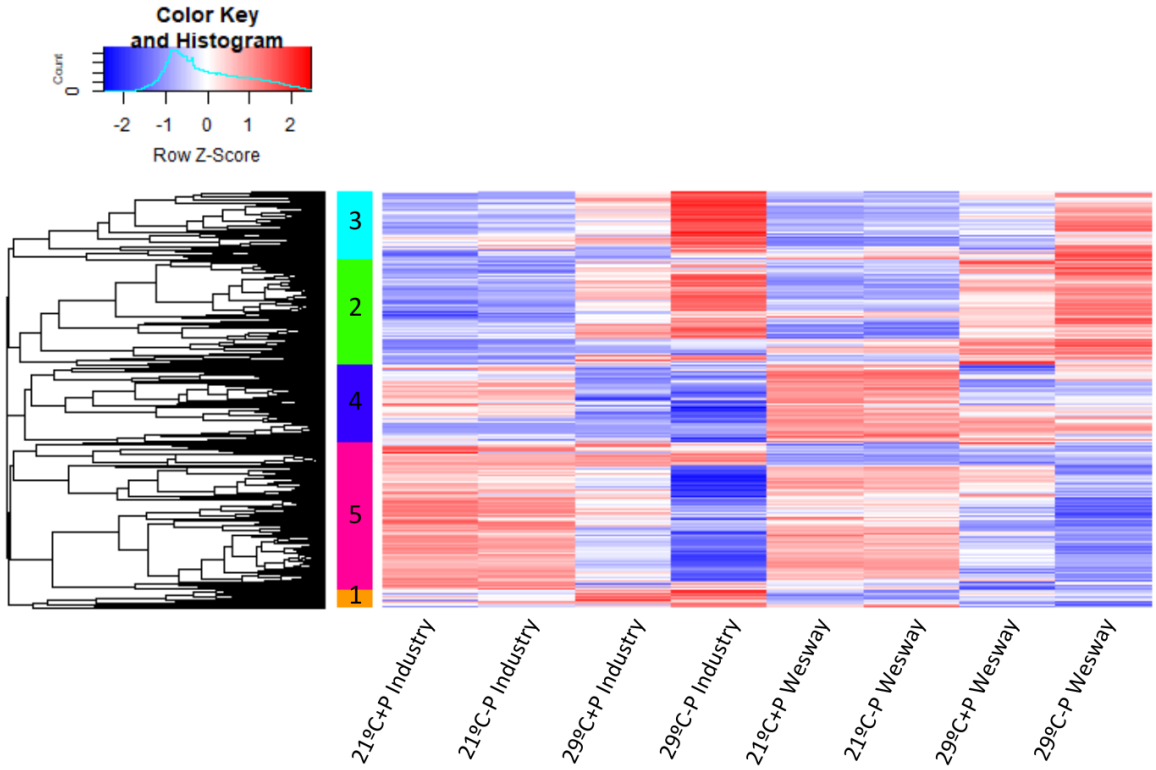


Figure 4.38: Heatmap of differentially expressed genes (DEGs) in roots of *B. napus* individuals from two varieties (Industry & Wesway) and four temperature and Pi treatments (21ºC+P, 21ºC-P, 29ºC+P and 29ºC-P). The heatmap was built using Z-scores of the average of the normalized read count from three replicates per treatment. Only genes that were differentially expressed ($|\log2FC| > 0.58$; p-value < 0.01) in at least one of the six comparisons between the treatments and/or varieties were considered. The genes were grouped in different clusters according to their expression profiles across the treatments (k=5). The colour legend at the upper left corner indicates the Z-score values: blue (lower Z-score, lower expression); red (higher Z-score, higher expression). A table with the Z-scores of the DEGs for each treatment, with their respective log2FC for each comparison is shown in Supplementary Table 8A.

Then, we performed a GO analysis of the genes found in each cluster to identify the molecular pathways that are responsible for these differences in gene expression (Figure 4.39). Cluster 1 contained a group of genes that were highly expressed in Industry at 29ºC+P and 29ºC-P but poorly expressed in Wesway under those treatments (Figure 4.38). Some of the gene categories with a high -log10FDR in cluster 1 include chlorophyl binding, with genes like *BnLHCB1.1*, *BnLHCB1.2* and *BnLHCB1.3*, and hormone binding, with genes like *PYRABACTIN RESISTANCE 1 (BnPYR1), PYR1-LIKE 2, 4* or *5 (BnPYL2, 4* or *5*) (Figure 4.39; Supplementary Table 8B).

Cluster 2 contained genes that were highly expressed in both varieties under warm temperature, and even more expressed under the stress combination (Figure 4.38). GO analysis identified several enriched categories related to ubiquitin activity, suggesting that protein degradation through the ubiquitin pathway might be relevant for the response to the stress combination (Figure 4.39). These ubiquitin-related categories included many genes encoding for proteins from the RING/U-box superfamily, and zinc-finger family, which are E3 proteins involved in target recognition for subsequent degradation (Supplementary Table 8B). Several enriched categories in cluster 2 were also related to transcription factor activity, containing many transcription factors, some of them induced in both varieties at 29ºC-P, but not at 21ºC-P or 29ºC+P. Some examples of TFs that were exclusive for the stress combination were *BnWRKY20, BnERFs, BnDREB2, BASIC HELIX-LOOP-HELIX 30, 36 (BnBHLH30, 36)* and *BnMYB3*.

Cluster 3 contained genes that were exclusively expressed under the stress combination, and this expression was higher in Industry than in Wesway (Figure 4.38). GO enrichment analysis of genes from cluster 3 revealed the category DNA-binding transcription factor activity as highly enriched, as well as the category transcription regulator activity (both with a -log10FDR > 30; Figure 4.39). Both categories contained many heat shock factors, as well as transcription factors from the WRKY, ERF, DREB, MYB and PHL families, among others, and genes related to ethylene signalling (*BnEIN3*, *BnEIL1*, *BnERF1*, *BnERF2* or *BnERF3*). Some of them, such as *LATERAL ROOT PRIMORDIUM 1* (*BnLRP1*), which is induced by auxin and related to reductions in LR growth (Singh *et al.*, 2020), or *SCARECROW-like 3 (BnSCL3)*, involved in the inhibition of the primary root growth (Crombez *et al.*, 2019), were specifically induced by the stress combination in both varieties, and not at 21ºC-P or 29ºC+P (Supplementary Table 8B). Interestingly, the category transition metal ion binding contained many genes related to Fe metabolism, some of them, like *FERREDOXIN 1 (BnFD1), FE SUPEROXIDE DISMUTASE 3 (BnFSD3), PROLYL 4-HYDROXYLASE 4* and *5 (BnP4H4* and *BnP4H5*) were highly expressed in both varieties at 29ºC-P and others only in Industry at 29ºC-P, like *BnLPR1*. Fe metabolism is involved in the inhibition of the primary root growth in response to Pi starvation (Crombez *et al.*, 2019). The enzyme LPR1 mediates the conversion of $Fe^{2+}$ and $Fe^{3+}$, leading to an accumulation of $Fe^{3+}$ in the apoplast, which in turn forms a complex with malate and citrate, and leads to the accumulation of peptides like CLE14, ultimately leading to the inhibition of the primary root growth (Crombez *et al.*, 2019).

Accordingly, we observed an increased expression of malate and citrate transporters in both varieties at 29ºC-P, such as *BnALMT1, 2* and *3, DETOXIFICATION EFFLUX TRANSPORTER (BnDTX) 9, 10, 11, 12, 13, 14, 21, 43, 44, 53* and *56*, as well as increased expression of the peptide *CLE14*. Some of the genes related to Fe metabolism were highly expressed only in Industry at 29ºC-P and not in Wesway, like *LPR1, COPPER RESPONSE DEFECT 1 (BnCRD1), FERREDOXIN OXIDOREDUCTASE 2 (BnFNR2)* and Fe dependent oxygenases like *JASMONIC ACID OXIDASE 2* (*BnJOX2*), as well as *BnSTOP1*, the transcription factor that regulates the expression of *LPR1*. Since Industry was more severely affected by the stress combination than Wesway, the higher expression of those genes suggests that Industry might activate transcriptional responses directed towards the inhibition of the primary root growth to a greater extent than Wesway at 29ºC-P.

The genes in cluster 4 were poorly expressed by warm temperature, independently of the Pi level in both varieties, but to a greater extent in Industry (Figure 4.38). The gene categories with the highest -log10FDR were related to transmembrane transporter activity (Figure 4.39). These categories were rich in genes related to Pi transport (*BnPHO1*, *BnPHT1*, *BnPHT1*-3, *BnPHT1-8*, *BnPHT4*, *BnPIN2*) or the transport of other nutrients like nitrogen (*BnNRT2.1*, *BnNPF1.1*, *BnNRT1.1/NPF6.3*, *BnNPF6.4*; Supplementary Table 8B). Since warm temperature is known to reduce nutrient uptake, this suggests that warm temperature caused a reduction of nutrient uptake at 29ºC-P, and this reduction was stronger in Industry. Some of those poorly expressed genes related to Pi transport are crucial in the Pi starvation response, suggesting that warm temperatures could suppress the Pi starvation response, thus increasing the sensitivity to Pi deficiency. Accordingly, we also observed lower expression of other PSI genes like *BnSPX1,2* and *3* at 29ºC+P and 29ºC-P in both varieties. The category phosphoric ester hydrolase activity contained genes related to inositol phosphate, and some of them were down-regulated at 29ºC-P (*BnPLC1, BnSAL2*; Supplementary Table 8A; B). Since Pi starvation is known to produce a decrease in the inositol levels (Dong *et al.*, 2019), this suggests that Pi starvation signalling was triggered at 29ºC-P and not at 21ºC-P. These results suggest that Pi starvation was enhanced at 29ºC-P than at 21ºC-P, likely because warm temperatures reduced the expression of some genes involved in Pi homeostasis, exacerbating the effects of the Pi deficiency.

Finally, cluster 5 contained genes that showed lower expression under the stress combination in both varieties, being even lower in Industry than in Wesway (Figure 4.38). GO analysis identified the categories structural molecule activity and structural constituent of ribosome as highly enriched (-log10FDR > 150; Figure 4.39), and both categories contained many genes encoding for ribosomal proteins, suggesting a strong reduction in the ribosomal activity caused by the stress combination in both varieties.

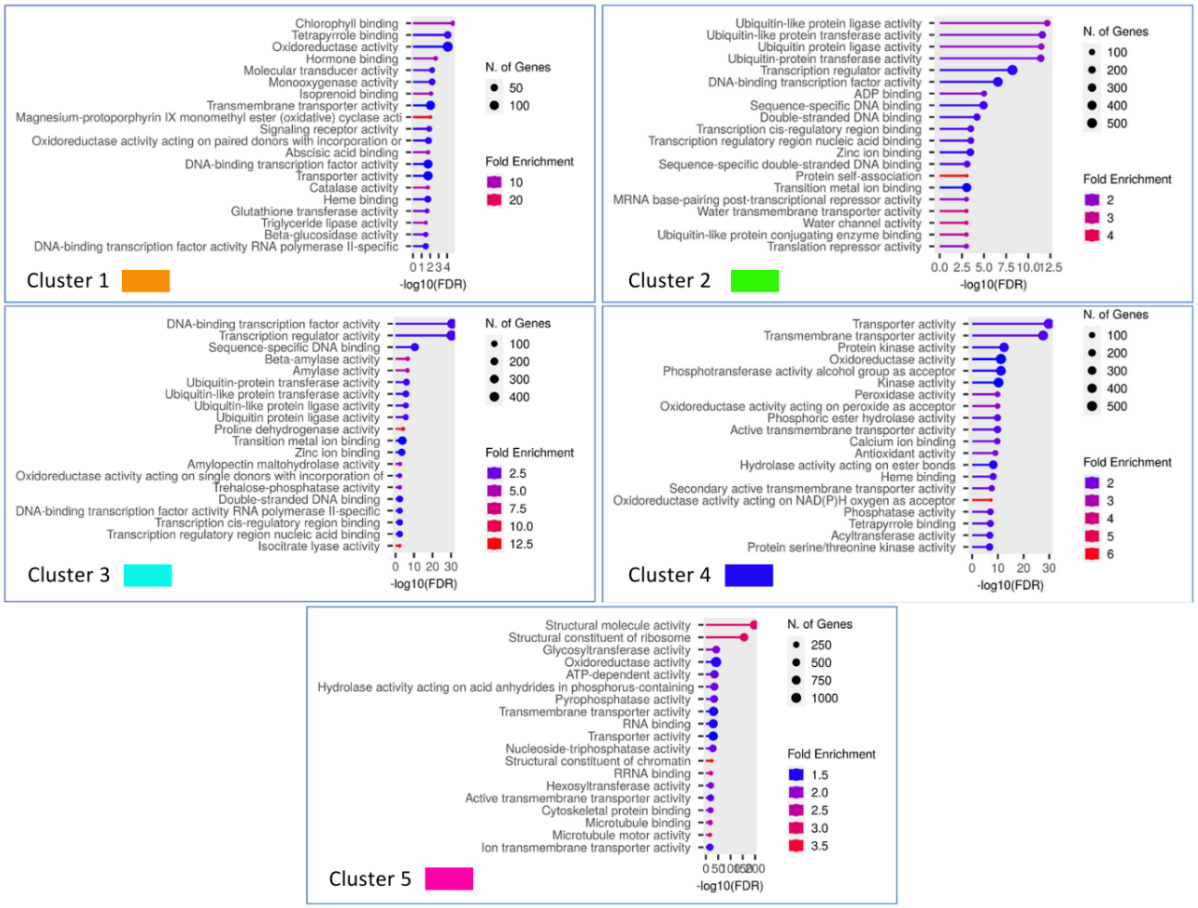


Figure 4.39: GO enrichment analysis of DEGs in roots of *B. napus* individuals from two varieties (Industry & Wesway) and four temperature and Pi treatments (21ºC+P, 21ºC-P, 29ºC+P and 29ºC-P). The GO enrichment was done individually for each of the five clusters of DEGs previously obtained using Shiny GO.

This analysis allowed us to identify the main molecular pathways that are altered by Pi starvation and by the combination of warm temperature and Pi starvation in *B. napus* roots and allowed us to identify the key differences in the transcriptional response between two varieties that respond differently to the stress combination.

To identify the molecular pathways that are more representative of these differences, we identified the *A. thaliana* orthologs of the genes present in each cluster. Later, using the STRING software (https://string-db.org/) we analysed the possible interactions between them. For each cluster, we built networks of proteins that are known to interact with each other (Figure 4.40). For cluster 1, we selected a subset of genes that were up-regulated (log2FC > 0.58; p-value < 0.01) in Industry at 29ºC+P and 29ºC-P and not in Wesway (Supplementary Table 8A). The first network was related to carotenoid biosynthesis, with proteins like CYP707A3, BETA GLUCOSIDASE 18 (BGLU18), and CAROTENOID CLEAVAGE DIOXYGENASE 4 (CCD4), and the second network was related to vitamin E biosynthesis, with proteins like VITAMIN E DEFICIENT 4 and 6 (VTE4, 6).

For cluster 2, we selected a subset of genes in cluster 2 that were specifically up-regulated (log2FC > 0.58; p-value < 0.01; Supplementary Table 8A) under 29ºC-P in both varieties, and obtained several networks, one of them related to the cytokinin signalling pathway, with proteins like ARR1, HISTIDINE KINASE 3 (AHK3) and LONESOME HIGHWAY (LHW; Figure 4.40). LHW is known to be expressed in the root apical meristem, regulating vascular development in roots, and can increase the levels of auxin and cytokinins (Ohashi-Ito *et al.*, 2019). Cytokinins have shown to be repressors of *WOX5* and *SCR* (Zhang et al., 2013b), thus contributing to the inhibition of the primary root growth. This suggests that cytokinins could play a role on the reductions in root depth observed in both varieties at 29ºC-P (see Results: 4.4.2.). We also obtained a network related to ubiquitin activity, with proteins like UBIQUITIN-CONJUGATING ENZYME 7, 11, 14, 17 (UBC7, 11 14, 17), and another network related to the ubiquitin E3 ligase, with proteins like CASEIN KINASE II ALPHA CHAIN 4 (CKA4), CASEIN KINASE II BETA CHAIN 4 (CKB4) and ARABIDOPSIS TOXICOS EN LEVADURA (ATL78). This ubiquitin ligase complex has shown to be involved on Pi uptake in Arabidopsis (Iglesias *et al.*, 2013; Rojas-Triana *et al.*, 2013; Pan *et al.*, 2019; Sun *et al.*, 2022). The last network was related to the regulation of gene expression and contained proteins like DSRNA-BINDING PROTEIN 1 (DRB1), DICER-LIKE 3 (DCL3), SILENCING DEFECTIVE 5 (SDE5), WRKY39 and 45 (Figure 4.40).

In cluster 3, we selected a subset of genes that were specifically up-regulated at 29ºC-P in both varieties (Supplementary Table 8A), and we obtained three networks (Figure 4.40). The first network contained proteins related to peptide

signalling under nutrient starvation (CLE14, 42). The second network had proteins related to malate and citrate transport (ALMT1, 2, DTX43, 56). Many of these proteins are involved in the Fe dependent inhibition of the primary root growth. This suggests that Pi could induce the Fe dependent inhibition of the primary root growth at 29ºC and not at 21ºC. Furthermore, the up-regulation of those genes was more significant in Industry than in Wesway (Supplementary Table 8A). This is consistent with our previous results, where both varieties reduced their network depth at 29ºC-P, but this reduction was more pronounced in Industry compared to the individual stresses (see Results: 4.4.2.). The third network in cluster 3 was related to auxin signalling and had proteins related to the Pi starvation induced auxin response, like TIR1, ABSCISIC ACID RESPONSIVE ELEMENTS-BINDING FACTOR 3 (ABF3), IAA2, 4, 26, 30 and the ethylene response, like EIN3-BINDING F BOX PROTEIN 2 (EBF2) and ENHANCER OF SHOOT REGENERATION 2 (ESR2). This suggests an activation of the Pi starvation response at 29ºC-P in both varieties. EBF2 is an EIN3-binding protein (Wang *et al.*, 2023b), and EIN3 is known to participate in root hair development (Crombez *et al.*, 2019). Furthermore, *GL2* was down-regulated in both varieties at 29ºC-P (Supplementary Table 8A), and down-regulation of GL2 has shown to contribute to root hair development under Pi deficiency (Balcerowicz *et al.*, 2015), suggesting a possible induction of root hair formation at 29ºC-P.

For cluster 4, we selected a subset of genes that were specifically down-regulated at 29ºC-P in both varieties (Supplementary Table 8A), and not at 21ºC-P or 29ºC+P. We obtained a network related to phenylpropanoid biosynthesis and cell wall organization, containing LACCASE 17 (LAC17), DIRIGENT PROTEIN 6, 9, 10, 16, 18 and 25 (DIR6, 9, 10, 16, 18 and 25) and CASPARIAN STRIP MEMBRANE DOMAIN PROTEIN 1, 2, 3 and 5 (CASP1, 2, 3 and 5; Figure 4.40). Finally, we obtained a network related to lipid biosynthesis, with proteins like DIMINUTIA (DIM) and FACKEL (FK). FK is crucial for cell division and elongation, contributing to root growth (Schrick *et al.*, 2000), whereas DIM influences the formation of the secondary cell wall in Arabidopsis roots (Hossain *et al.*, 2012). These results suggest that the stress combination could affect cell wall organization, negatively influencing root growth, which is consistent with our results in root traits, where both varieties reduced root growth at 29ºC-P (see Results: 4.4.2.).

Finally, for cluster 5 we selected a subset of genes that were down-regulated only in Industry at 29ºC-P, and not in Wesway (Supplementary Table 8A), and we obtained a network of proteins related to lateral root development induced by Pi starvation, mediated by auxin and ethylene transport and signalling (Figure 4.40). Some of these proteins included AUXIN RESISTANT 1 (AUX1), PIN3, MYB77, ERF6, suggesting that Industry could suppress lateral root growth at 29ºC-P by modulating these hormonal pathways. This correlates with our previous results, where Industry reduced its lateral root density and network width at 29ºC-P more than under warm temperature alone, and in Wesway this reduction was less pronounced and was similar between 29ºC-P and 29ºC+P (see Results: 4.4.2.).

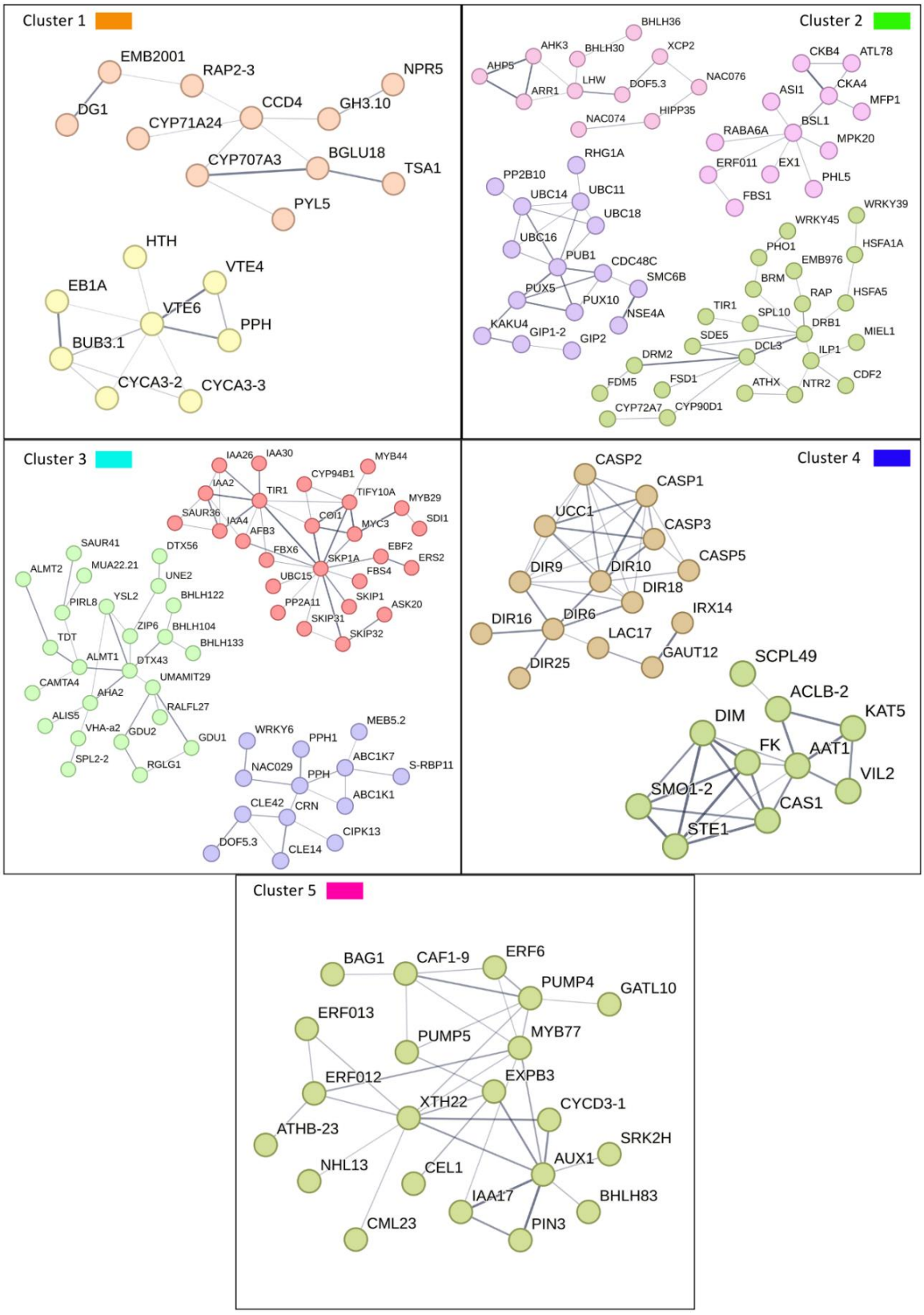


Figure 4.40: Interaction networks for each of the five clusters of DEGs in roots of *B. napus* individuals from two varieties (Industry & Wesway) and four temperature and Pi treatments (21ºC+P, 21ºC-P, 29ºC+P and 29ºC-P). The *A. thaliana* orthologs from the most relevant DEGs were considered.

These results suggest that the combined stress (29ºC-P) had a stronger impact on gene expression than the individual stresses (21ºC-P or 29ºC+P). Interestingly, this impact was even stronger in Industry than in Wesway. In addition, these results also indicate that the stress combination induced the expression of genes related to ubiquitin activity, as well as genes involved in the Fe dependent inhibition of the primary root growth, and reduced the expression of genes involved in the synthesis of phenylpropanoids and cell wall organization. Finally, the induction of genes involved in the inhibition of the primary root growth at 29ºC-P was stronger in Industry than in Wesway, which could be related to the stronger inhibition of the primary root growth observed in Industry under the stress combination compared to the individual stresses. At the same time, Industry down-regulated several genes involved in the auxin-mediated induction of LR growth at 29ºC-P. These results correlate with our previous results, where LR density and network width were more reduced at 29ºC-P than under the individual stresses in Industry, whereas in Wesway these reductions were similar between the stress combination and the individual stresses.

## 4.7. Analysis of the integrative responses to nutrient (nitrogen and phosphate) deficiencies in the root system of *B. napus* under high temperatures.

### 4.7.1. N deficiency, warm temperature and the combination of both stresses suppress Pi-starvation related genes.

Research has shown that N deficiency reduces nutrient uptake, including Pi uptake, in *B. napus* (Yin *et al.*, 2015). We have previously quantified the expression of several Pi-starvation induced (PSI) genes by RT-qPCR in *B. napus* seedlings grown under warm temperature, Pi deficiency or the combination of both stresses (see Results: 4.6.1.). Our results suggest that warm temperatures (29ºC) suppressed the expression of PSI genes. Furthermore, our RNA-sequencing results in *B.* napus roots show that some PSI genes such as *BnSPX3*, *BnSPX1*, *BnPHO1*, *BnIPS3*, as well as phosphatases involved in the Pi starvation response, like *BnPECP2*, *BnPAP7*, *BnPAP17* were down-regulated under N deficiency (21ºC-N), warm temperature (29ºC+N) and the combination of both stresses (29ºC-N; Figure 4.41).

| Gene name | A. thaliana ortholog | Protein | Westar 21ºC +N | Westar 21ºC -N | Westar 29ºC +N | Westar 29ºC -N | Wesway 21ºC +N | Wesway 21ºC -N | Wesway 29ºC +N | Wesway 29ºC -N |
|---|---|---|---|---|---|---|---|---|---|---|
| BnaA03g21050D | AT2G45130 | SPX3 | 0.0671602 | -0.45659 | -0.4269 | -0.4549 | 2.4351792 | -0.4664 | -0.28995 | -0.4076 |
| BnaC04g50120D | AT2G45130 | SPX3 | 1.9965345 | -0.53238 | -0.4325 | -0.5439 | 1.1560319 | -0.5845 | -0.46469 | -0.5946 |
| BnaA04g26060D | AT2G45130 | SPX3 | 2.1038139 | -0.53947 | -0.3359 | -0.5453 | 0.973892 | -0.6137 | -0.4804 | -0.5628 |
| BnaA03g07930D | AT5G20150 | SPX1 | 2.1933241 | -0.55565 | -0.1819 | -0.6091 | 0.7373196 | -0.6502 | -0.27446 | -0.6594 |
| BnaA02g04730D | AT5G20150 | SPX1 | 1.253186 | -0.66663 | -0.6042 | -0.7099 | 1.9056782 | -0.4447 | -0.27248 | -0.4609 |
| BnaC02G0099900ZS | AT5G20150 | SPX1 | 2.4643124 | -0.19733 | -0.294 | -0.2842 | -0.347181 | -0.4288 | -0.45478 | -0.458 |
| BnaC02g18430D | AT1G68740 | PHO1 | 0.6692844 | -0.58157 | -0.3751 | -0.5173 | 2.2503727 | -0.5459 | -0.31107 | -0.5887 |
| BnaA07g24450D | AT1G68740 | PHO1 | 1.1895011 | -0.76263 | -0.834 | -0.6082 | 0.7281729 | -0.834 | 1.5813058 | -0.4602 |
| BnaA07g27390D | AT1G68740 | PHO1 | 1.3388919 | -0.67877 | -0.9597 | -1.3079 | 1.2833316 | -0.15404 | 0.6452624 | -0.1671 |
| BnaC06g30370D | AT1G68740 | PHO1 | 1.7192938 | -0.3925836 | -1.0262 | -0.9062 | 1.2877401 | -0.16209 | 0.0529848 | -0.57293 |
| BnaA02g35630D | AT1G68740 | PHO1 | 0.1738689 | -0.56208 | -0.5128 | -0.4167 | 2.3847306 | -0.5378 | -0.03986 | -0.4894 |
| BnaAnng30500D | AT1G73010 | PECP2 | 1.9943041 | -0.62806 | -0.4293 | -0.5534 | 1.1108162 | -0.6358 | -0.17333 | -0.6852 |
| BnaA06g34460D | AT2G01880 | PAP7 | 1.7538939 | -0.1723164 | -0.584 | -0.22249 | 1.2908316 | -0.25628 | -1.16394 | -0.6457 |
| BnaC01g34650D | AT3G17790 | PAP17 | 1.4112028 | -0.86371 | -0.3732 | -0.8086 | 1.401661 | -0.7069 | 0.6780149 | -0.7385 |
| BnaC02g00460D | AT5G10170 | IPS3 | 1.8766512 | 1.0849781 | -0.1952 | -0.0341 | -0.170464 | -0.69811 | -0.996721 | -0.86711 |

Figure 4.41: Z-score values of of Pi-starvation induced (PSI) genes quantified by RNA sequencing analysis in roots of *B. napus* individuals from two varieties (Westar & Wesway), grown under different temperature and N treatments: 21ºC+N, 21ºC-N, 29ºC+N and 29ºC-N. The table shows the Z-scores of the gene expression from the average of three

independent replicates per variety and treatment. Red indicates more expressed; blue indicates less expressed. Bold numbers indicate significant differences (|log2FC| > 1; p-value < 0.05) with the control treatment (21ºC+N) from each variety.

### 4.7.2. Pi-starvation related genes are involved on root adaptation to warm temperature and N deficiency in Arabidopsis.

Given the expression patterns of some PSI in response to the combination of warm temperature and N deficiency, we aimed to further investigate the role of these genes in the root responses to these stresses. Thus, we obtained different Arabidopsis loss of function mutant lines of some of these well-known PSI genes: *spx3* (SALK035262C) and *spx1spx2*, obtained by genetic crossing of *spx1* (SALK092030) and *spx2* (SALK080503). Then, we grew these mutants and Col-0 seedlings in Petri dishes under different N treatments: 2.5 mM of N (+N) or 0.5 mM of N (-N) and under optimal temperature (21ºC) or warm temperature (29ºC). After 10 days, the total root length and lateral root density were measured (Figure 4.42).

First, we observed that Col-0 plants reduced their root growth at 29ºC. This reduction was not observed in previous studies, likely because in those studies the roots were exposed to light, and we used the D-Root system, which keeps the roots in the dark. In our conditions, the *spx1spx2* double mutant had a similar root length to Col-0 under optimal temperature (21ºC), suggesting that the absence of *SPX1* and *SPX2* did not cause significant differences at optimal conditions. However, at 29ºC+N or 29ºC-N, the root of *spx1spx2* was longer than that of Col-0 (Figure 4.42A). Similarly, we observed that the lateral root density at 29ºC+N and 29ºC-N was higher in *spx1spx2* than in Col-0 and this difference was not present at 21ºC-N (Figure 4.42B). These results indicate that at 29ºC, the absence of both *SPX1* and *SPX2* led to increased root length and lateral root density, suggesting that both genes participate in the repression of root growth under warm temperatures. In *B. napus*, our previous results show that both Westar and Wesway repressed *BnSPX1* at 29ºC+N and 29ºC-N (Figure 4.41), which correlates with the enhanced network depth observed in Wesway at 29ºC+N and the increased network width observed in the same variety at 29ºC-N, but both varieties suppressed lateral root density (Figure 4.7). This suggests that even though both varieties repressed those genes, other factors might contribute to the suppressions in root growth observed at 29ºC.

On the other hand, the *spx3* mutant was able to grow a longer primary root than Col-0 under all treatments (Figure 4.42A), which suggests that *SPX3* acts a repressor of root growth independently of the N content or the temperature. Regarding lateral root density, *spx3* had a higher lateral root density than Col-0 at 21ºC+N, 21ºC-N and 29ºC+N (Figure 4.42B). However, under the stress combination (29ºC-N), the lateral root density of *spx3* and col-0 was similar, suggesting that *SPX3* does not control LR density under the stress combination or that Col-0 could down-regulate *SPX3* specifically under the stress combination.

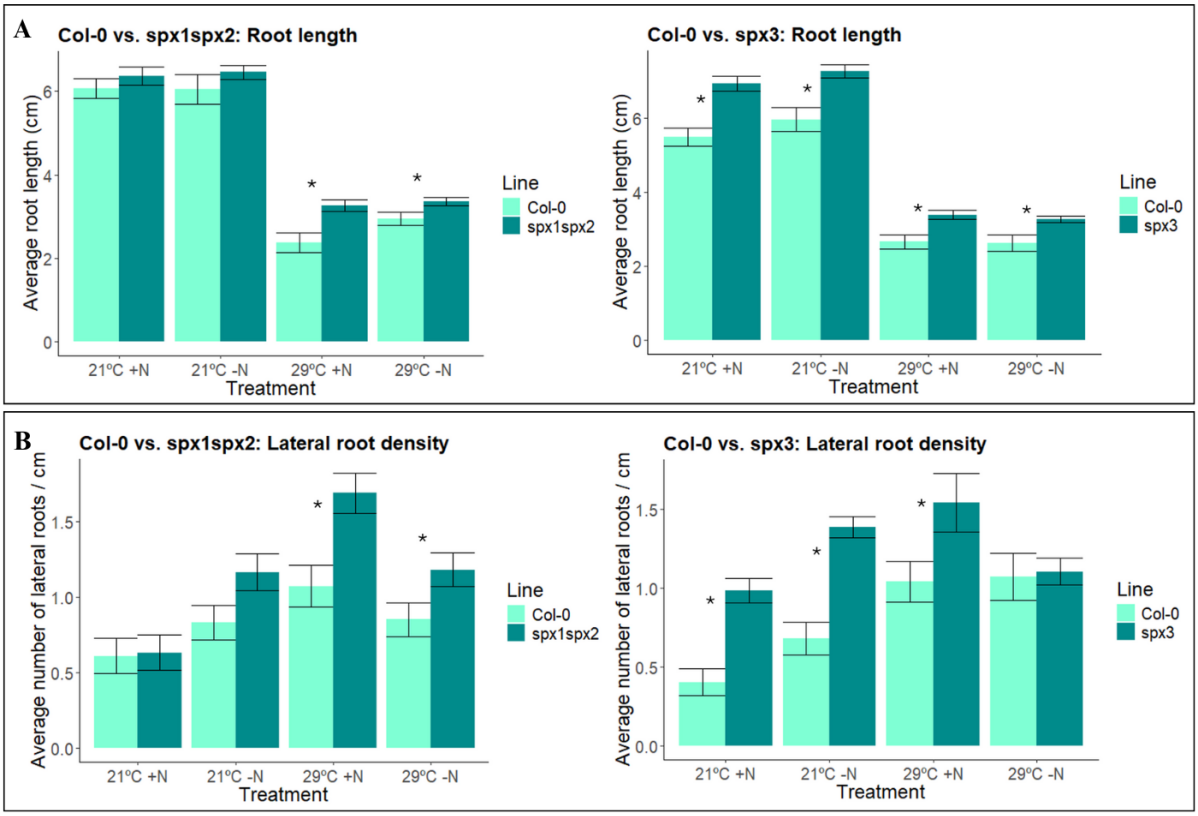


Figure 4.42: Quantification of root length (A) and lateral root density (B) in Arabidopsis Col-0 or mutant seedlings grown under different temperature and N treatments for 10 days. X-axis indicates the different treatments: 21ºC+N, 21ºC-N, 29ºC+N and 29ºC-N. The colour legend indicates the different lines: Col-0, *spx3* or *spx1spx2* double mutant. Error bars show the standard deviation between 18 individual seedlings per treatment and line. Asterisks indicate significant differences (p-value < 0.05) between the mean of each mutant and the mean of Col-0 seedlings in each treatment.

### 4.7.3. Pi-starvation related genes are also involved in the root responses to combined heat stress and N deficiency.

We have previously shown that PSI genes play a role in the root responses to warm temperature, N deficiency and the combination of both stresses. To further study

the dynamics of these genes under temperature stress and N deficiency, we aimed to study the response of these genes to the combination of heat stress and N deficiency in Arabidopsis. Thus, we grew Arabidopsis Col-0, *spx3* and *spx1spx2* under two different temperatures: 22ºC (optimal temperature) or 32ºC (heat stress); and under different N conditions: 2.5 mM of N (+N) or 0.5 mM of N (-N). Since a homogeneous temperature of 32ºC is too high for the development of the root system and does not represent the conditions present in nature (González-García *et al.*, 2023), we used the TGRooZ to create a temperature gradient in the root zone and thus grow the plants in conditions that are more realistic and similar to nature.

After 10 days, the total root length and lateral root density were quantified (Figure 4.43). In the case of *spx1spx2*, there were not significant differences in root length or lateral root density between *spx1spx2* and Col-0 under any of the treatments (Figure 4.43). This contrasts our previously obtained results (see Results: 4.7.2.), where *spx1spx2* had a greater root length and lateral root density than Col-0 at 29ºC. These results suggest that the application of a temperature gradient in the root zone softened the temperature stress, thus obtaining a similar phenotype than under optimal temperature. Alternatively, we can speculate that *SPX1* and *SPX2* do not participate in the response to heat stress.

Conversely, the *spx3* mutant showed a greater primary root growth and LRD than Col-0 at 22TGRooZ, but not at 32TGRooZ. This result is similar to the observed in the previous section (see Results: 4.7.2.), where *spx3* grew a longer primary root under all treatments and had higher LRD under all treatments except for the stress combination, but in this case, the differences observed at 32TGRooZ +N were not significant (Figure 4.43). These results suggest that *SPX3* does not participate in the root responses to heat stress but plays a role in the response to warm temperature.

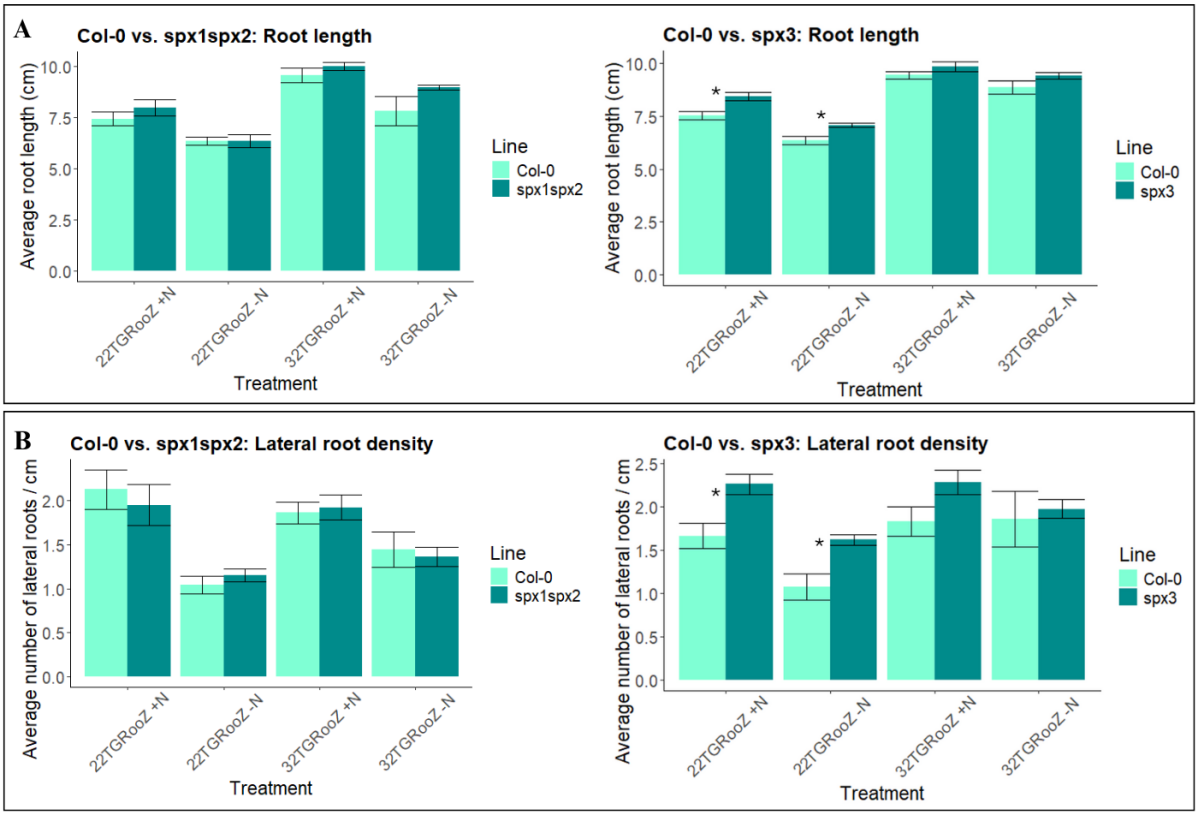


Figure 4.43: Quantification of root length (A) and lateral root density (B) in Arabidopsis Col-0 or mutant seedlings grown under different temperature and N treatments for 10 days. X-axis indicates the different treatments: 22TGRooZ +N, 22TGRooZ -N, 32TGRooZ +N and 32TGRooZ -N. The colour legend indicates the different lines: Col-0, *spx3* or *spx1spx2* double mutant. Error bars indicate the standard deviation between 18 individual seedlings per treatment and line. Asterisks indicate significant differences (p-value < 0.05) between the mean of each mutant and the mean of Col-0 seedlings in each treatment.

These results suggest that *SPX3* acts a repressor of root growth and plays a role in the response to warm temperature when combined with N deficiency in Arabidopsis, and could connect the Pi starvation response or Pi cellular homeostasis with the response to high temperatures and low N availability. Finally, as commented before, the use of the TGRooZ is necessary to study the effects of combined heat stress and nutrient deficiencies correctly.

## 4.8. Analysis of shoot responses to the combination of elevated temperatures and nitrogen deficiency in *B. napus*.

### 4.8.1. Two *B. napus* varieties with different root adaptation strategies to the combination of warm temperature and N deficiency show a differential transcriptional response in shoots.

We have previously characterized the variability in the root responses of *B. napus* to N deficiency (21ºC-N), warm temperature (29ºC+N) or the combination of both stresses (29ºC-N (see Results: 4.4.1.) and selected two varieties (Westar & Wesway) that showed different root adaptation strategies to the combination of these stresses. Whereas Westar was more prone to modify its root architecture under warm temperature and N deficiency, the root system of Wesway showed fewer alterations. Among these changes, one interesting difference was that Wesway developed longer LRs at 29ºC-N than Westar, reflected by its increase in network width. Due to the essential functions of roots, changes in root architecture might affect the aerial part of the plants, altering shoot morphology and growth (Shekhar *et al.*, 2019). In this section, we will explore the shoot responses to these stresses at the transcriptional, physiological and morphological level.

First, we performed an RNA-sequencing analysis in whole shoots of Westar and Wesway grown as previously described (see Material and methods: 3.2.1.). DEGs were calculated in three comparisons for each variety: N deficiency (21ºC-N), warm temperature (29ºC+N) and the stress combination (29ºC-N), all compared to the control treatment (21ºC+N). In the case of Westar, the number of DEGs was higher at 21ºC-N than at 29ºC+N or 29ºC-N (Figure 4.44A; B), indicating a more significant effect of the N deficiency alone on gene expression in shoots. This contrasts our previous results in roots, where both varieties had more DEGs at 29ºC-N and 29ºC+N than at 21ºC-N. On the contrary, our analyses on Wesway shoots retrieved a higher number of DEGs at 29ºC-N, suggesting a greater effect of the stress combination. In the case of Westar, the number of down-regulated genes was higher that the number of up-regulated genes in response to warm temperatures, independently of the N level (Figure 4.44B). Both varieties had DEGs shared between the different stress treatments, but an elevated number of DEGs was specific to 29ºC-N, indicating a specific gene expression response under the stress combination (Figure 4.44C).

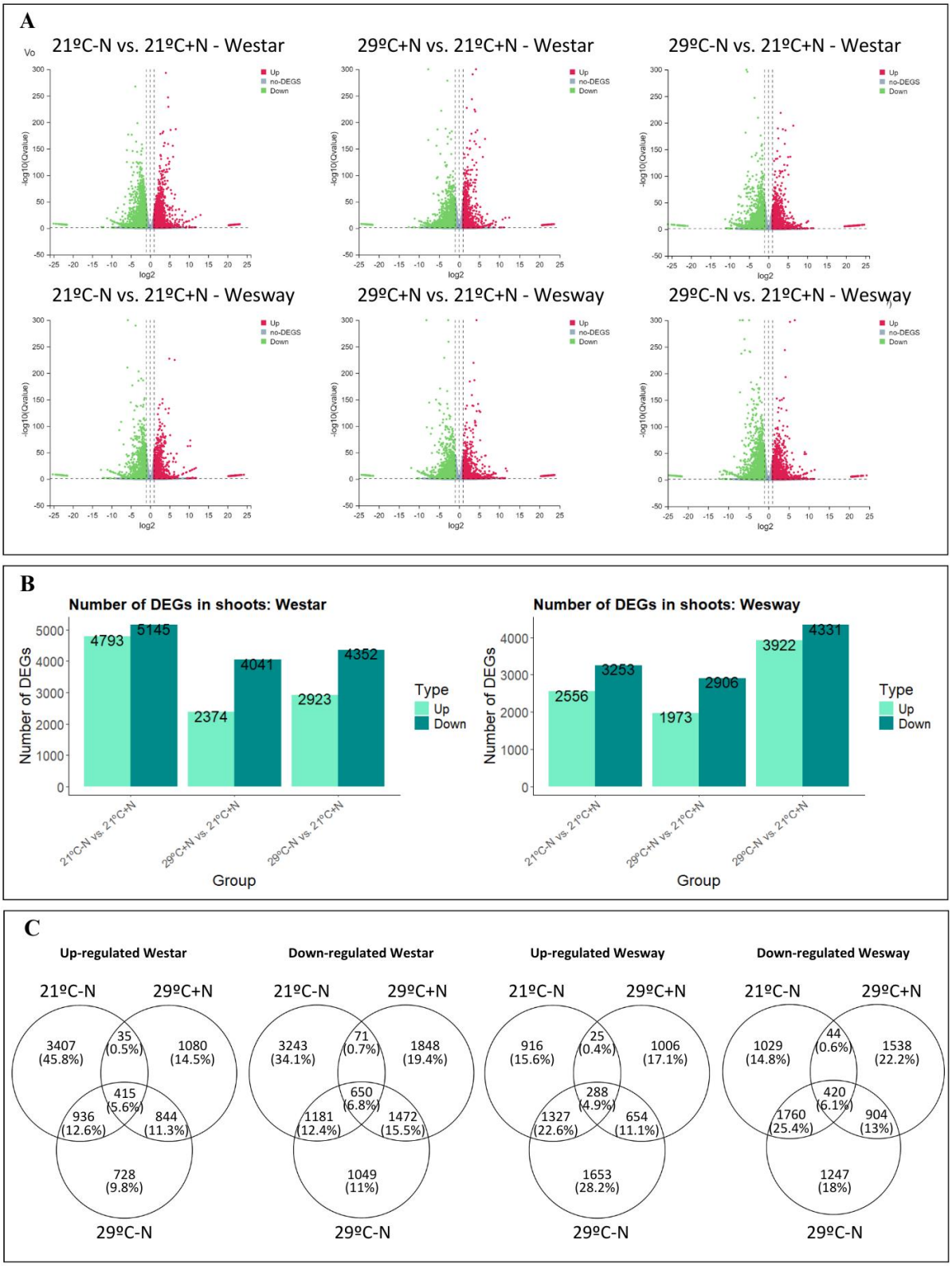


Figure 4.44: Analysis of gene expression performed by RNA-sequencing in shoots of the *B. napus* varieties Westar and Wesway grown under different temperature and N treatments. A) Volcano plots for DEGs (|log2FC| > 1; p-value < 0.05) in shoots under different temperature and nitrogen treatments compared to control conditions. The top row shows volcano plots for the cultivar Westar, whereas the plots in the bottom row

belong to Wesway. From left to right: DEGs in shoots under nitrogen deficiency (21ºC-N), under warm temperature (29ºC+N) and under the stress combination (29ºC-N), all of them compared to the control conditions (21ºC+N). B) Number of DEGs (|log2FC| > 1; p-value < 0.05) in shoots of Westar (left) and Wesway (right) under different temperature and nitrogen treatments compared to control conditions. X-axis show the different comparisons: nitrogen deficiency (21ºC-N vs. 21ºC+N), warm temperature (29ºC+N vs. 21ºC+N) and the stress combination (29ºC-N vs. 21ºC+N). The legend indicates whether the genes are up-regulated or down-regulated. C) Venn diagrams for Westar (left) and Wesway (right) showing the number of genes that are commonly expressed in shoots under the four treatments: 21ºC+N, 21ºC-N, 29ºC+N and 29ºC-N. From left to right: Up-regulated genes in Westar, down-regulated genes in Westar, up-regulated genes in Wesway, down-regulated genes in Wesway.

We have identified differences in the transcriptional response in shoots between the varieties Westar and Wesway grown under N deficiency (21ºC-N), warm temperature (29ºC+N) or the combination of both stresses (29ºC-N). To identify the molecular pathways underlying these differences in gene expression, we first calculated a dendrogram of the DEGs according to their expression profiles across the different varieties and treatments that divided them in five clusters. For the dendrogram and heatmap analysis, we only considered DEGs that were significant (|log2FC| > 1; p-value < 0.05) in at least one of the six comparisons described above. Normalized read counts were obtained for these selected DEGs in each treatment, and those normalized read counts were posteriorly scaled to obtain Z-scores that were used to visualize the expression of these genes across the different treatments in a heatmap (Figure 4.45). Then, we performed a GO analysis of the genes from each cluster.

Cluster 1 contained genes that were more expressed under N deficiency (21ºC-N) and under the stress combination (29ºC-N) in Wesway but not in Westar (Figure 4.45). GO enrichment highlighted categories related to calcium ion binding, with genes such as *BnCAM2* and *BnCAM3* (Figure 4.46; Supplementary Table 9B). Other enriched categories included superoxide dismutase copper chaperone activity and hormone binding, with genes like *COPPER CHAPERONE FOR SOD1* (*BnCCS*) and *PYRABACTIN RESISTANCE 1-LIKE 9* (*BnPYL9*), which is involved in the perception of ABA (Figure 4.46; Supplementary Table 9B). Interestingly, genes that were up-regulated (log2FC > 1; p-value > 0.05) in Wesway at 29ºC-N but not in Westar included the peptide CEP6 (*BnCEP6*; Supplementary Table 9A; B). CEP peptides are important regulators of the systemic response to low N availability and trigger a shoot to root signal that enhances the expression of nitrate transporters in roots (Taleski *et al.*, 2018; Aggarwal *et al.*, 2020; Taleski *et*

*al.*, 2024). Interestingly, other genes that were up-regulated in Wesway at 29ºC-N but not in Westar include CLE peptides as well (*BnCLE26 and BnCLE43*; Supplementary Table 9A). Expression of *AtCLE26* in *B. napus* has previously shown to modulate root architecture by inhibiting the growth of the primary root and enhancing lateral root growth (Czyzewicz *et al.*, 2016). This is consistent with our previous results, where both Westar and Wesway developed longer lateral roots at 21ºC-N, but only Wesway developed longer lateral roots at 29ºC-N. This suggests that the mechanisms involved in the regulation of root architecture via long distance signalling are more activated in Wesway than in Westar at 29ºC-N and could be related to the enhanced expression of *BnNRT1.1* and *BnNRT2.1* transporters in roots of Wesway at 29ºC-N (see Results: 4.2.3.).

Cluster 2 contained genes that were more expressed in Westar under optimal N (21ºC+N and 29ºC+N), but that were not altered or less expressed under N deficiency, independently of temperature (Figure 4.45) and in Wesway were poorly expressed under all treatments. GO enrichment identified highly enriched categories like structural molecule activity (-10logFDR > 40) and structural constituent of chromatin (-log10FDR > 30), containing many genes related to the ribosome (*BnRPL4, 7, 12, 13, 17, 21, 22, 23, 27, 34* and *BnRPS5, 6, 7 13, 16, 19, 21, 24, 28, 29*), indicating that ribosomal activity is altered in response to N deficiency independently of the temperature.

Cluster 3 contained genes that showed lower expression in response to the three stress treatments (Figure 4.45). GO enrichment identified the categories structural molecule activity and structural constituent of ribosome as highly enriched (-log10FDR > 150 and (-log10FDR > 100, respectively), containing many genes encoding for ribosomal proteins similar to those found in cluster 2, such as *BnRPL15, 24, 26, 29, 31* and *BnRPS3, 10* and *15* (Figure 4.46; Supplementary Table 9B), reinforcing the idea that ribosomal activity is widely altered under the three stress treatments, which is similar to the previously observed response in roots (see Results: 4.2.1).

Cluster 4 contained genes that were highly expressed at 21ºC-N and less expressed under the stress combination and these differences were more remarkable in Westar than in Wesway (Figure 4.45). The GO enriched categories for this cluster include GTPase activity and GTP binding, containing genes genes such as *BnRABB1*, *BnRABC1* or *BnRABC2* (Figure 4.46; Supplementary Table 9). RAB proteins are involved in intracellular trafficking and are known to play a role in

abiotic stress responses (Tripathy *et al.*, 2021). Cluster 4 was also enriched in genes related to metabolic processes, such as peroxygenases, which are involved in cutin and wax biosynthesis (*BnPGX4,5*), alternative oxidases (*BnAOX1A*) or ubiquitin conjugating enzymes (*BnUBC4, BnUBC6*).

Finally, cluster 5 contained genes that were more expressed at 29ºC+N and 29ºC-N in both varieties, but to a greater extent in Wesway than in Westar (Figure 4.45). The enriched categories in cluster 5 corresponded to unfolded protein binding, containing heat shock proteins (*BnHSP26.5*, *BnHSP70-4* and *BnHSP70-8*; Supplementary Table 9B), and inositol 3-alpha galactosyltransferase activity, containing key genes in the heat shock response like *BnGOLS1* (Figure 4.46).

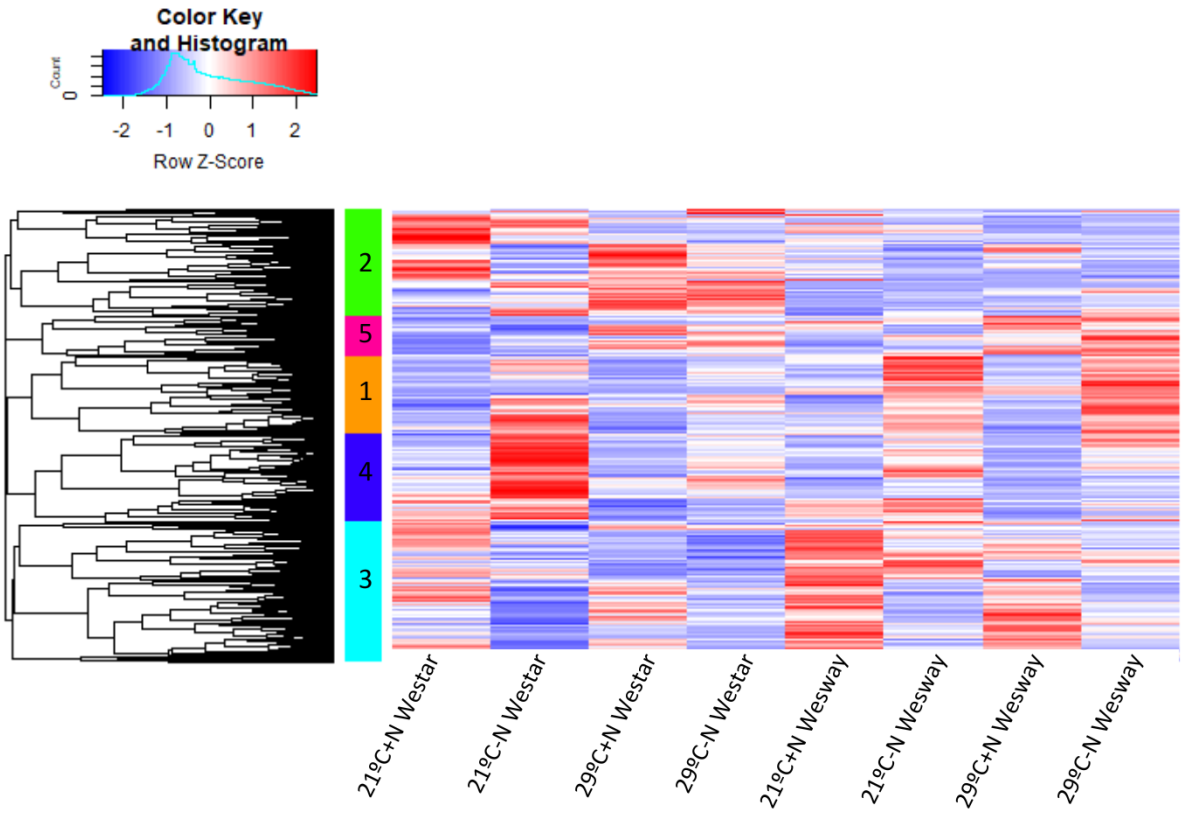


Figure 4.45: Heatmap of DEGs in shoots of *B. napus* individuals from two varieties (Westar & Wesway) and four temperature and nitrogen treatments (21ºC+N, 21ºC-N, 29ºC+N and 29ºC-N). The heatmap was built using Z-scores of the average of the normalized read counts from three replicates per treatment. Only genes that were differentially expressed ($|log2FC| > 1$; p-value < 0.05) in at least one of the comparisons between the treatments and/or varieties were considered. The genes were grouped in different clusters according to their expression profiles across the samples (k=5). A table with the Z-score values of each gene and their respective log2FC for each comparison can be found in Supplementary Table 9A.

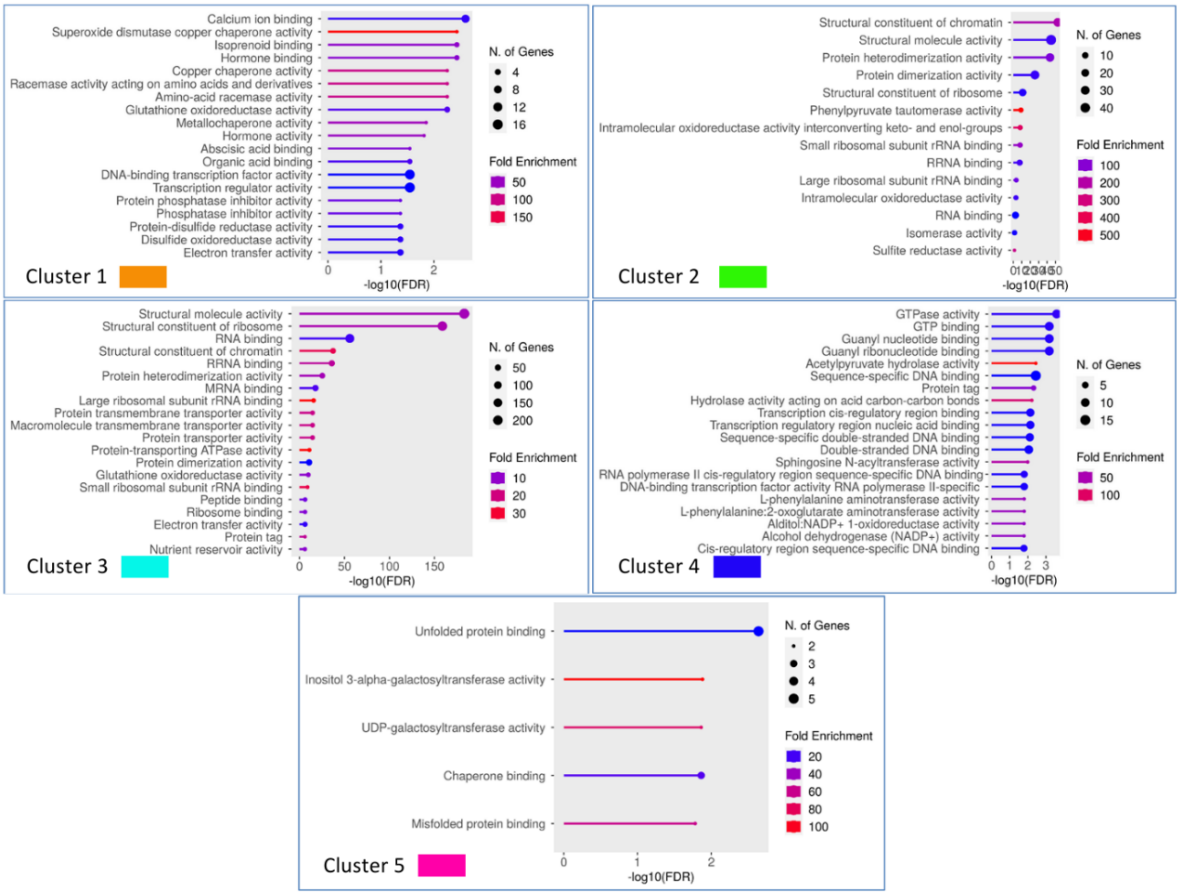


Figure 4.46: GO enrichment analysis of DEGs in shoots of *B. napus* individuals from two varieties (Westar & Wesway) and four temperature and nitrogen treatments (21ºC+N, 21ºC-N, 29ºC+N and 29ºC-N). The GO enrichment was done individually for each of the five clusters of genes previously obtained and was calculated using Shiny GO. A list with all the genes within each GO category is displayed in Supplementary Table 9B.

After performing our cluster and GO enrichment analysis, we identified the main interaction networks for each cluster. Thus, we selected the *A. thaliana* orthologs from some of the genes present in each cluster and used them to build a protein network using the STRING software (Figure 4.47).

For cluster 1, we selected a subset of genes that were up-regulated ($|\log2FC| > 1$; p-value < 0.05) in Wesway at 29ºC-N but not in Westar (Supplementary Table 9A), and obtained a network of proteins related to calcium ion binding (CAM2, CAM3) and a group of transcription factors (ERF5, 104, WRKY33, 40), as well as a small network related to flavonoid biosynthesis (LDOX, OMT1, MYB4, HOS3) (Figure 4.47). CAM2 has been related to tolerance to abiotic stresses such as drought and aluminium toxicity (Yoo *et al.*, 2019; Zhu *et al.*, 2022), whereas CAM3 has been related to drought and salinity tolerance (Zheng *et al.*, 2022: Hau *et al.*, 2024).

Furthermore, the transcription factors WRKY33 and WRKY40 have been related to stress tolerance in cassava (Freeborough *et al.*, 2021). At the same time, accumulation of flavonoids has shown to enhance tolerance to combined heat and salinity stresses (Jan *et al.*, 2021). This suggests that Wesway but not Westar could activate distinct pathways related to the response to stress tolerance at 29ºC-N.

For cluster 2, we first selected a subset of genes that were down-regulated (log2FC < 1; p-value < 0.05) in both varieties at 29ºC-N (Supplementary Table 9A), and obtained a network of proteins involved in ribosomal activity (RPS5, 7, 16, 24, 29, RPL4, 23, 27, 34; Figure 4.47). The second network was built using genes that were down-regulated only in Westar at 29ºC-N, and not in Wesway, and the network contained other proteins related to ribosomal activity (RPS6, 13, 21, 30, RPL12, 13, 17), as well as ACONITASE 2 (ACO2) and 6-PHOSPHOGLUCONOLACTONASE 5 (PGL5). Aconitase has shown to be important in the response to oxidative stress, suggesting that Westar could be more affected by oxidative stress at 29ºC-N (Moeder *et al.*, 2007). Ribosomal activity has previously shown to participate in the response to stress (Fakih *et al.*, 2023). This suggests that the stress combination could alter ribosomal activity, suggesting a possible role of post-transcriptional modifications in the response of both varieties to 29ºC-N.

For cluster 3, we generated two networks. First, we selected a subset of genes that were down-regulated at 29ºC+N and 29ºC-N only in Westar (Supplementary Table 9A), and we obtained a network of proteins related to nucleosome activity (Figure 4.47), containing histones (HTA6, 13, HTR2) and HY5-HOMOLOG (HYH). The bZIP transcription factor HYH is a homolog of HY5 and is essential for nitrogen assimilation via regulating NITRITE REDUCTASE 1 (NIR1) (Jonassen *et al.*, 2008). Under N deficiency, HY5 triggers a shoot to root signal to up-regulate nitrate transporters (Xuan *et al.*, 2017). The *HYH* gene was down-regulated in Westar at 29ºC+N and 29ºC-N, suggesting that warm temperature had a negative effect on the expression of *HYH* in Westar, possibly affecting long distance signalling and having negative consequences in the response to N deficiency. This could be related to the lower expression of nitrate and ammonium transporters observed in Westar at 29ºC-N, compared to Wesway. The second network was built using a set of genes down-regulated in both Westar and Wesway at 29ºC-N (Supplementary Table 9A), and contained proteins related to the N response: NIR1, ASPARAGINE SYNTETHASE 2 (ASN2), DICARBOXYLATE

TRANSPORTER 2-1 (DIT2-1; Figure 4.47), suggesting a negative regulation of amino acid biosynthesis and a reduction in N metabolism in both varieties at 29ºC-N.

The networks from cluster 4 were built with a subset of genes that were up-regulated at 29ºC-N only in Wesway (Supplementary Table 9A). We obtained a network related to the citrate cycle and to malate, citrate and iron transport, containing proteins such as SUCCINATE DEHYDROGENASE 2-1 (SDH2-1), AOX1A, ACO3, ACETOACETYL-COA THIOLASE 1 (AACT1); DTX17, DTX43 and FERRETIN 1 (FER1; Figure 4.47). This is consistent with our results in roots, where we also observed increased expression of AOX1A in Wesway at 29ºC-N. AOX1A is involved in the response to oxidative stress and the lack of AOX1 can lead to increased sensitivity to combined stresses such as drought and light stress, reducing root and shoot growth, suggesting that AOX1A could play a role in the enhanced LR growth observed in Wesway at 29ºC-N compared to Westar (Clifton *et al.*, 2006; Giraud *et al.*, 2008). Another network was related to calcium-mediated ABA signalling, with proteins like CALMODULIN-LIKE 24 (CML24), CALCIUM-DEPENDENT PROTEIN KINASE 32 (CPK32), PHOSPHATE UNDERPRODUCER 4 (PUP14) and LONELY GUY 7 (LOG7), which is again consistent with the results obtained in roots, where genes related to the ABA-mediated response to stress were up-regulated in Wesway at 29ºC and not in Westar.

Finally, the interaction network obtained in cluster 5 was built using genes up-regulated by 29ºC+N and 29ºC-N in both varieties (Supplementary Table 9A), and the network contained proteins related to the response to temperature stress, with heat shock proteins (HSP26.5, HSP70-4 and HSP70-8) and other proteins related to stress tolerance like GOLS1 and OUTER MEMBRANE TRYPTOPHAN-RICH SENSORY PROTEIN (TSPO; Figure 4.47) and proteins related to the ABA-mediated response to stress like KINASE 1, 2 (KIN1, KIN2) and ERD10.

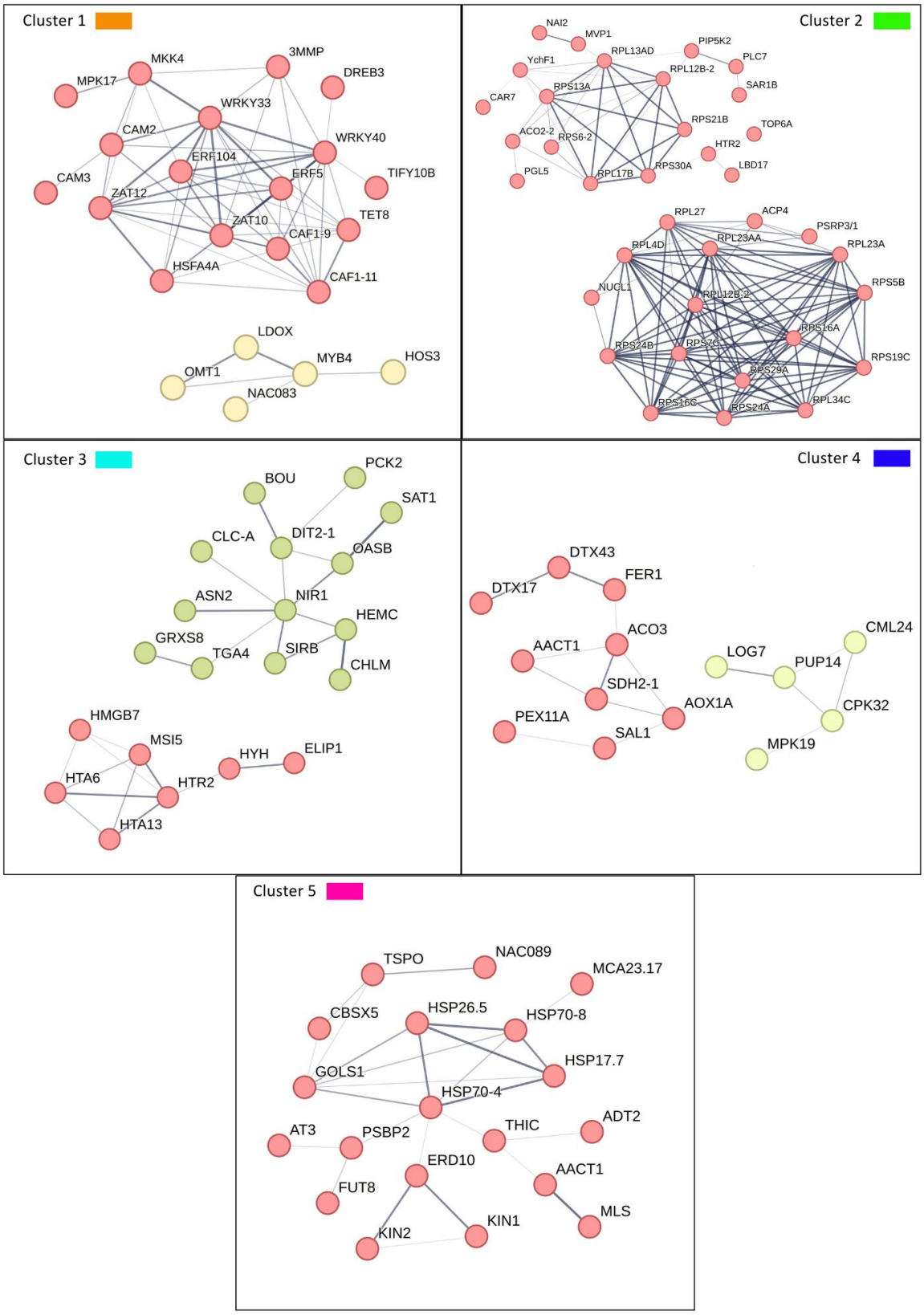


Figure 4.47: Interaction networks for each of the five clusters of DEGs in shoots of *B. napus* individuals from two varieties (Westar & Wesway) and four temperature and nitrogen treatments (21ºC+N, 21ºC-N, 29ºC+N and 29ºC-N). The *A. thaliana* orthologs from the most relevant genes were considered.

Our previous results in roots indicate that peroxidases were strongly up-regulated in roots of both *B. napus* varieties, Westar and Wesway, when grown at 29ºC-N (See Results: 4.2.1.), suggesting that they could contribute to the response mechanisms to warm temperatures under N deficiency in *B. napus*. We explored the possibility that these peroxidases could also be involved in the shoot responses to these combined stresses by analysing our RNA-seq results and performing RT-qPCR (Figure 4.48A). We observed that, contrary to our previous observations in roots, most peroxidases were significantly down-regulated at 29ºC-N in shoots of both varieties. RT-qPCR quantification confirmed that *BnPER71* was down-regulated in Westar at 21ºC-N, and more significantly at 29ºC+N and 29ºC-N, whereas in Wesway the expression levels of *BnPER71* were only reduced at 29-N (Figure 4.48B). Class III peroxidases, are involved in the lignification of cell walls and are important components in the oxidative stress response, reducing the $H_2O_2$ levels. For this reason, they have been proposed as key enzymes for tolerance to biotic or abiotic stresses (Kidwai *et al.*, 2020). This induction of peroxidase genes in roots and repression in shoots has also been observed as a response to drought stress in alfalfa (Kang & Udvardi, 2012), suggesting that this differential regulation between different organs might contribute to the correct response and adaptation of plants to different stresses.

**A**

| Gene name | A. thaliana ortholog | Protein | Westar 21°C +N | Westar 21°C -N | Westar 29°C +N | Westar 29°C -N | Wesway 21°C +N | Wesway 21°C -N | Wesway 29°C +N | Wesway 29°C -N |
|---|---|---|---|---|---|---|---|---|---|---|
| BnaC02g42930D | AT5G64120 | PER71 | 0.66183 | 1.76517 | -0.4909 | **-1.125** | 0.649845 | 0.143646 | -0.4789 | **-1.125** |
| BnaAnng19770D | AT4G36430 | PER49 | 1.0922 | 0.56663 | 0.172453 | **-0.879** | -1.01008 | **-0.4845** | **1.5521** | -1.0101 |
| BnaA06g16150D | AT3G49110 | PER33 | 1.724502 | **-0.075** | **-0.941** | **-1.119** | 0.867295 | 0.199965 | 0.33285 | **-0.99** |
| BnaC04g47720D | AT2G41480 | PER25 | 0.372005 | 0.15635 | -0.6847 | **-1.202** | 1.795326 | 0.673921 | 0.00539 | **-1.116** |
| BnaAnng16310D | AT1G05260 | PER3 | 2.101131 | **-0.646** | **-0.408** | **-0.786** | 0.225069 | **-0.7333** | 0.742 | **-0.495** |
| BnaA09g53760D | AT4G08770 | PER37 | 1.581433 | **-0.359** | 0.39406 | **-0.965** | 1.078827 | 0.125485 | **-0.4914** | **-1.365** |
| BnaA03g54060D | AT4G37520 | PER50 | -0.1706 | 0.26222 | **-1.1283** | **-0.991** | 1.238704 | 1.569869 | 0.02385 | **-0.805** |
| BnaA03g17000D | AT2G37130 | PER21 | 0.091818 | 0.07293 | **-1.2641** | **-0.999** | 0.497587 | 1.514355 | **-0.9179** | 1.00388 |
| BnaA04g29190D | AT2G37130 | PER21 | -0.66783 | **1.1553** | **-1.4433** | -0.7826 | 0.353499 | 0.573768 | -0.52724 | 1.33847 |
| BnaC09g24040D | AT4G11290 | PER39 | 0.77672 | 0.5084 | -0.05598 | **-1.4** | -0.20881 | 0.084229 | **1.5761** | **-1.281** |

**B**

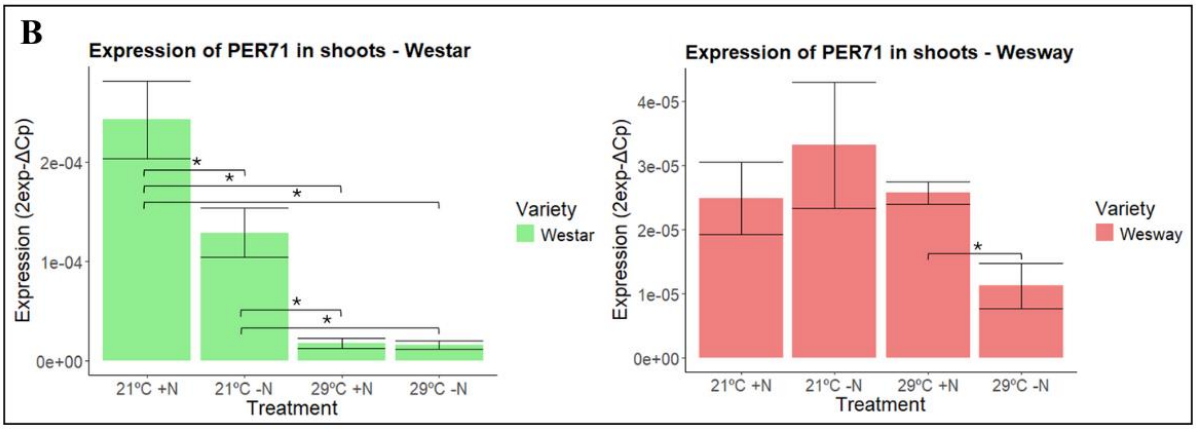


Figure 4.48: A) Z-score values of the expression of different genes encoding for peroxidases quantified by RNA sequencing analysis in shoots of *B. napus* individuals from two varieties (Westar & Wesway), grown under different temperature and N treatments: 21ºC+N, 21ºC-N, 29ºC+N and 29ºC-N. The table shows the Z-score values calculated from the average of the normalized read counts from three independent replicates per variety and treatment. The table shows the gene names from *B. napus*, as well as the *A. thaliana* orthologs. Red indicates more expressed, blue indicates less expressed. Bold numbers indicate significant differences (|log2FC| > 1; p-value < 0.05) with the control treatment (21ºC+N) from each variety. B) Expression of *BnPER71 (BnaC02g42930D)* quantified by quantitative PCR (qPCR) in shoots of *B. napus* individuals from two varieties (Westar & Wesway), grown under different temperature and N treatments: 21ºC+N, 21ºC-N, 29ºC+N and 29ºC-N. Error bars show the standard deviation between three independent biological samples (with three technical replicates each) that are different from those used for the RNA sequencing analysis. Asterisks indicate significant differences between groups (p-value < 0.05).

These results provide insights into the shoot responses of both varieties to N deficiency, warm temperature or the combination of both stresses. We identified several differences in the transcriptional responses in shoots between both varieties, with Westar showing a stronger transcriptional response to the different

treatments than Wesway in response to N deficiency. Furthermore, we identified some molecular pathways that might explain these differences. Particularly, Wesway expressed more genes related to long distance peptide signalling, calcium signalling and ABA signalling at 29ºC-N, compared to Westar. Our results also indicate that both varieties repressed the expression of peroxidase genes in shoots under the stress combination (29ºC-N), but not under the individual stresses. Since class III peroxidases are crucial components in redox homeostasis, cell elongation, carbon allocation and cell wall lignification (Veljović *et al.*, 2018), these data suggest that the stress combination could negatively impact shoot growth and development more than the individual stresses.

### 4.8.2. Two varieties with differential root responses to combined warm temperature and N deficiency show differences in their shoot performance under N deficiency combined with heat stress.

We have studied the root and shoot responses to warm temperatures combined with N deficiency in two different *B. napus* varieties. Our previous data indicate that Wesway might have a better root adaptation to combined higher temperatures and N deficiency than Westar. To test this, we decided to analyse the effects of heat stress combined with N deficiency in plants grown in soil using the TGRooZ to mimic the natural soil conditions as much as possible, and to compare the responses when seedlings are grown in the TGRooZ system or at a constant high temperature in root and shoot. Thus, individuals from the previous selected *B. napus* varieties Westar and Wesway were grown in pots under different temperatures: optimal homogeneous shoot/root temperature (22ºC), high homogeneous shoot/root temperature (36ºC) and high shoot temperature with a temperature gradient in the root-zone (36ºC TGRooZ), creating a gradient from 36ºC in the top parts of the soil to approximately 24ºC at the bottom of the pot. Furthermore, *B. napus* plants from Westar and Wesway were grown under two different N concentrations: 9.84 mM of N (indicated as +N) or total absence of N in the soil (indicated as -N).

After two weeks, we observed that Westar developed a larger hypocotyl (15.5 cm on average) and more expanded leaves (80.06 $cm^2$ of total leaf area on average) than Wesway (11.1 cm and 47.1 $cm^2$, respectively) under optimal conditions (22ºC+N; Figure 4.49). However, under N deficiency (22ºC-N), the total leaf area, shoot fresh weight and dry weight decreased in Westar (60.6 cm, 3.01 g and 0.2 g,

respectively) compared to 22ºC+N (80.06 $cm^2$, 3.74 g and 0.29 g, respectively). On the contrary, Wesway increased its total leaf area, shoot fresh weight and dry weight at 22ºC-N (70.2 $cm^2$, 3.04 g and 0.21 g) compared to 22ºC+N (47.1 $cm^2$, 1.96 g and 0.17 g), confirming that both varieties have different responses to N deficiency in the aerial parts as well. Altogether, our data suggest that Wesway has a better capacity to maintain shoot development under N deficiency than Westar. Under high temperature (36ºC+N) or the combination of high temperature and N deficiency (36ºC-N), both varieties showed a strong reduction in hypocotyl length, total leaf area and shoot weight compared to 22ºC, indicating a strong suppression of shoot growth in both varieties (Figure 4.49). As expected in accordance to published data (Gonzalez-Garcia, *et al.* 2023), plants grown at 36ºCTGRooZ did not reduce their shoot growth as much as plants grown at 36ºC. Remarkably, Wesway plants grown at 36TGRooZ developed more expanded leaves than Westar. Thus, at 36TGRooZ, Wesway had a higher total leaf area than Westar under both N conditions (+N: 12.08 $cm^2$ vs. 1.5 $cm^2$) or (-N: 13.7 $cm^2$ vs. 1.3 $cm^2$) (Figure 4.49B). Moreover, the shoot fresh weight and dry weight of Wesway at 36TGRooZ-N (0.84g and 0.056g on average) were significantly greater than in Westar (0.46g and 0.016g on average; Figure 4.49).

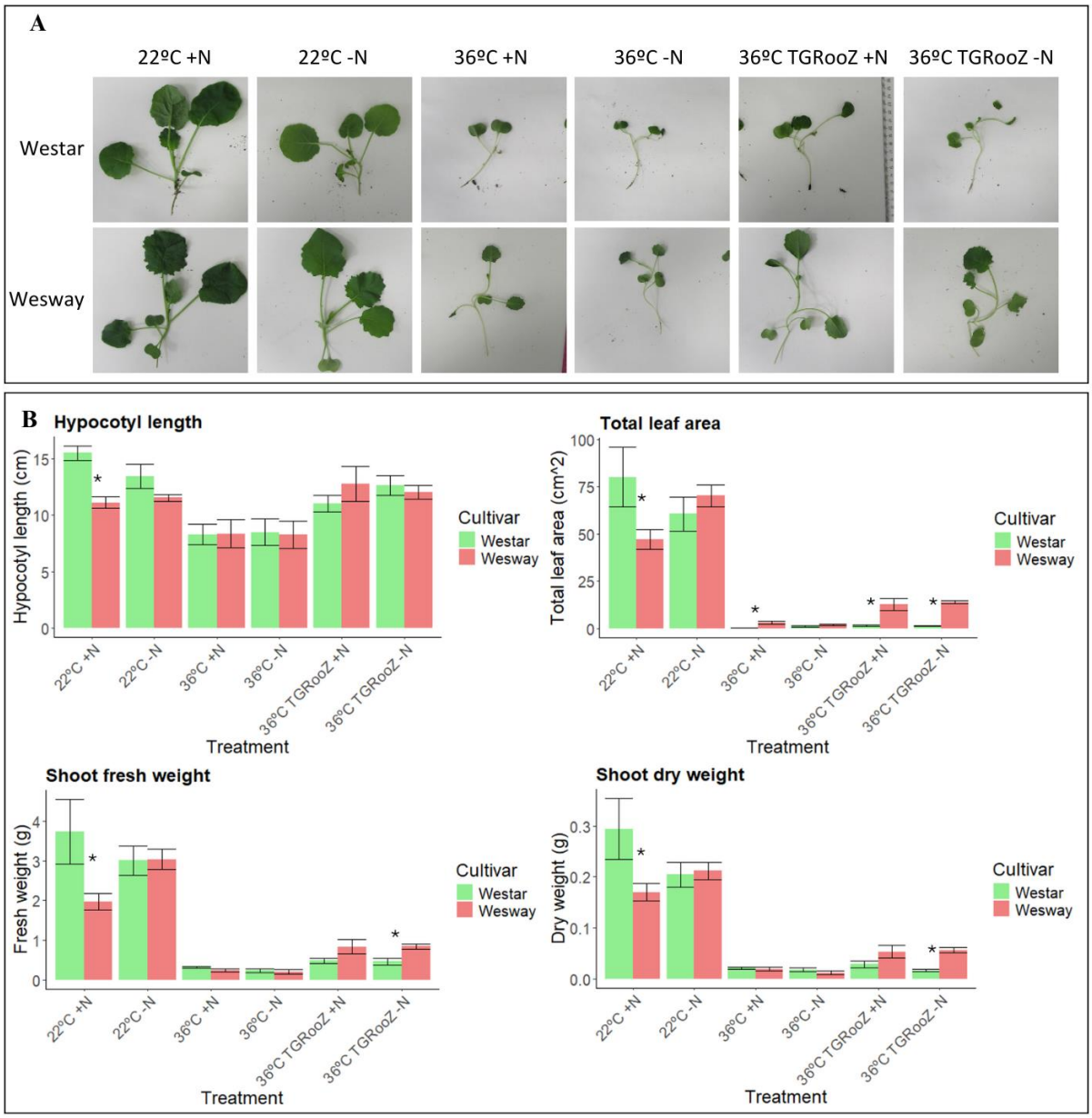


Figure 4.49: Shoot phenotyping in *B. napus* seedlings from two varieties (Westar & Wesway) grown in pots submitted to different temperature and nitrogen treatments for 2 weeks. A) Shoot images from Westar (upper row) and Wesway (lower row) after two weeks. B) Quantification of morphological shoot traits (hypocotyl length, total leaf area, shoot fresh weight and shoot dry weight). Error bars represent the standard deviation between six independent biological replicates. X-axis indicates the different temperature and nitrogen treatments. The legend at the right of each graph indicates the variety. Asterisks indicate significant differences between both varieties in each treatment ($p < 0.05$).

In this section, we selected two *B. napus* varieties with different root adaptation responses to the combination of warm temperature and -N, and studied their shoot performance under severe high temperature combined with -N, growing them either in the TGRooZ or at a homogeneous temperature in shoot and root. Our

results indicate that Wesway can maintain its hypocotyl length and leaf size in response to low N, whereas Westar reduced those traits. Furthermore, Wesway developed a longer hypocotyl and bigger leaves under the stress combination than Westar. Our previous results under warm temperature and N deficiency showed that Wesway could develop longer lateral roots than Westar at 29ºC-N, and more lateral roots at 29ºC-N compared to the individual stresses (see Results: 4.1.2.). Altogether, our results indicate that Wesway can grow better under -N and the combination of elevated temperatures and -N, compared to Westar and, most importantly, confirm that varieties with stronger roots systems seem to be more prepared to respond to the combination of nutrient and temperature stresses. Additionally, since the shoot responses of *B. napus* to homogeneous high temperature and -N are significantly different when plants are grown under a root zone temperature gradient than under homogeneous temperature, systems such as the TGRooZ should be taken into account for future experiments to provide conditions more similar to nature and thus facilitate the search for more adapted varieties.

### 4.8.3. Two varieties with different root responses to combined warm temperatures and N deficiency show a different C/N ratio under combined N deficiency and heat stress.

We have found differences in the shoot responses to the combination of high temperatures and N deficiency between the varieties Westar and Wesway after two weeks of treatments in soil (see Results: 4.8.2.). We have previously measured the nitrate concentration in roots and shoots of both Westar and Wesway under the different treatments: 21ºC+N, 21ºC-N, 29ºC+N and 29ºC-N using the pouch and wick system (see Results: 4.1.3.) and found that both varieties had differential responses. Wesway accumulated less nitrate in roots than Westar at 21ºC-N, but more in shoots. However, at 29ºC+N and 29ºC-N the accumulation of nitrate in roots and shoots was similar in both varieties. We wanted to analyse the shoot responses to combined high temperatures and N deficiency, including measurements of the N and C content in the aerial parts of both varieties grown in soil under a longer period of stress treatments. Thus, we performed an experiment under different temperatures and N conditions with plants grown in pots with soil for four weeks. Since the previous application of a homogeneous high temperature of 36ºC resulted in a suppression of shoot growth in both varieties, we reduced the heat stress to 34ºC to allow further shoot development. Seedlings from

the *B. napus* varieties Westar and Wesway were grown in pots with soil containing two different N concentrations: 9.84 mM of N (+N) or total absence of N (-N). The pots were disposed in different chambers to apply the temperature treatments: optimal temperature (22ºC) or high temperature (34ºC).

Four weeks later, both varieties showed symptoms of early senescence due to the N deficiency (22ºC-N; Figure 4.50A). Under high temperature (34ºC+N) the leaves of both varieties showed dehydration symptoms such as reduced leaf turgor. Finally, under the stress combination (34ºC-N) shoots were smaller and showed more signs of senescence and dehydration than in the individual stress treatments (22ºC-N or 34ºC+N) in both varieties. Total N content was dramatically reduced by N deficiency in both varieties, but Wesway had more N than Westar at 22ºC-N. However, at 34ºC+N and 34ºC-N the total N content was higher in Westar than in Wesway, indicating that N content in shoots in Wesway was sensitive to high temperature. Total C content was similar between both varieties at 22ºC+N, 22ºC-N and 34ºC+N, but was significantly higher in Wesway than in Westar under the stress combination (34ºC-N; Figure 4.50B). Since Wesway had less N content under this condition, this effect at 34ºC-N was reflected in a dramatic increase in the C/N ratio compared to Westar. High C/N ratios in leaves are a typical response to different abiotic stresses and are a reflection of enhanced sugar accumulation in leaves to provide osmotic protection against dehydration (Chen *et al.*, 2015c; Wang *et al.*, 2022b).

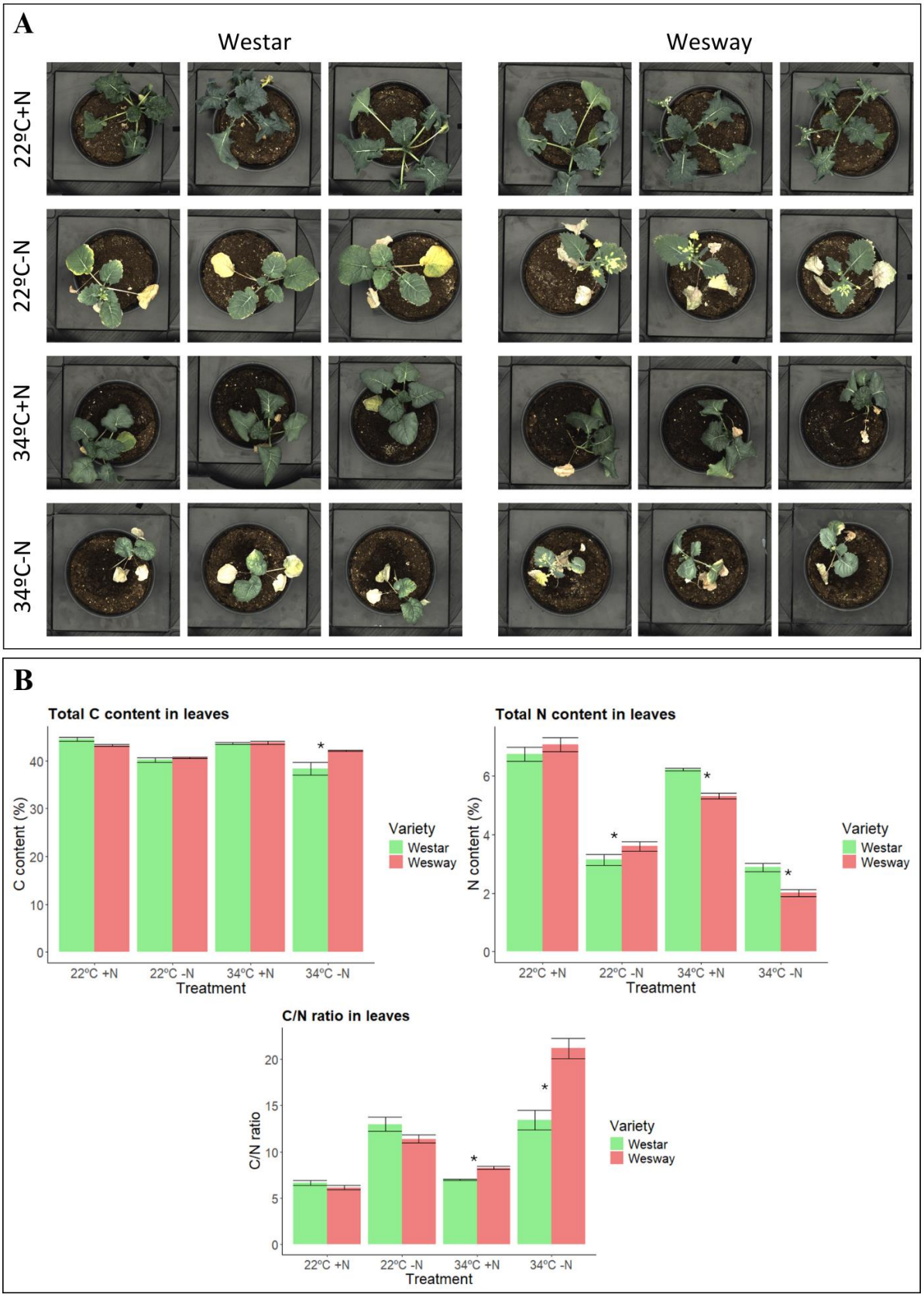


Figure 4.50: The *B. napus* varieties Westar and Wesway were grown in pots under different temperature and/or N treatments 22ºC+N, 22ºC-N, 34ºC+N and 34ºC-N for four weeks. A) Images of shoots from three biological replicates of Westar (left) and Wesway

(right) after four weeks. Different rows indicate the different treatments. B) Nitrogen (N) content, carbon (C) content and C/N ratio in leaves of Westar (green) and Wesway (red) after four weeks. X-axis indicates the different treatments. Error bars represent the standard deviation between five different biological replicates. Asterisks represent the significant differences between the mean values from each variety within each treatment (p-value < 0.05).

In this section, we provided new insights into the differential shoot responses of two *B. napus* varieties to the combination of high temperatures and N deficiency. We observed that N deficiency as well as the combination of high temperature and N deficiency caused senescence symptoms in both varieties. We also observed a significant increase in the C/N ratio in Wesway at 34ºC-N. These results suggest that Wesway could accelerate its life cycle at -N and the combination of -N and high temperatures, compared to Westar.

## 4.9. Analysis of shoot responses to the combination of warm temperatures and Pi deficiency in *B. napus*.

### 4.9.1. Different root adaptation strategies to combined warm temperature and Pi deficiency are correlated with differences in the transcriptional response in shoots.

We have previously characterized the root responses to Pi deficiency, warm temperature and the combination of both stresses in *B. napus* (see Results: 4.4.1.) and observed two major tendencies. Some varieties did not show significant alterations in the root system at 21ºC-P, but were negatively affected at 29ºC-P. On the other hand, other varieties suffered alterations under both 21ºC-P and 29ºC-P. Therefore, we selected two varieties that represent these two responses, Industry and Wesway, to analyse their shoot responses to the combination of warm temperatures and Pi deficiency, and the possible relationship with their root responses. Industry did not show alterations in the root system at 21ºC-P, but was negatively affected at 29ºC-P, whereas Wesway suffered alterations under both stresses.

Thus, we performed an RNA-sequencing analysis in whole shoots of seedlings from Industry and Wesway grown in the Pouch and Wick system during 7 days under different temperature and Pi conditions: 21ºC+P, 21ºC-P, 29ºC+P and 29ºC-P. The number of DEGs in both varieties was calculated for the three stress treatments compared to the control treatment (21ºC+P) in each variety. The number of DEGs at 21ºC-P was very low compared to the other two stress treatments: 29ºC+P and 29ºC-P (Figure 4.51A; B) in both varieties. In Industry, we found 489 up-regulated and 478 down-regulated genes at 21ºC-P, whereas in Wesway those numbers were even lower, having only 3 up-regulated and 4 down-regulated genes at 21ºC-P (Figure 4.51B). These reduction in the number of genes was also observed in the RNA-sequencing analysis performed in roots (see Results: 4.6.2.), even though in shoots the number was much lower, suggesting that in our conditions, the Pi deficiency alone had a softer effect on gene expression compared to the other stress treatments. The number of DEGs at 29ºC+P or 29ºC-P was much higher in both varieties. Interestingly, we detected, a greater number of down-regulated than up-regulated genes in both treatments (Figure 4.51B). This was also observed in previous results in shoots (see Results 4.8.1), and is likely caused as a response to warm temperature. In both varieties, most DEGs at 29ºC-P were shared with

29ºC+P, indicating that the changes in gene expression at 29ºC-P are much more influenced by the warm temperature than by the Pi deficiency (Figure 4.51C). However, the number of genes that are specific of 29ºC-P was also high, indicating a specific response to the stress combination that was not present under the individual stresses.

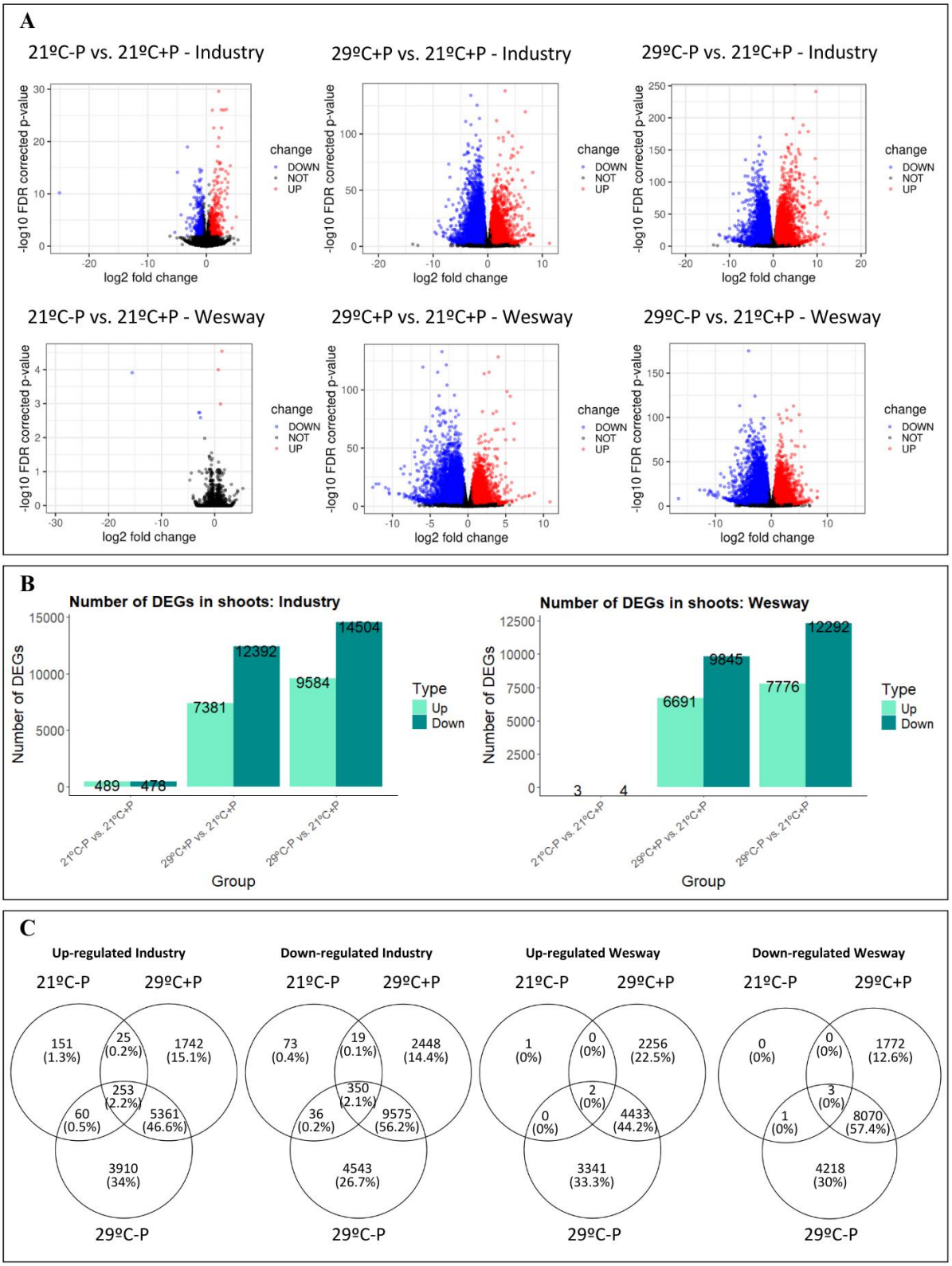


Figure 4.51: Analysis of gene expression detected by RNAseq in shoots of the *B.napus* varieties Industry and Wesway grown under different temperature and Pi treatments. A) Volcano plots of DEGs (|log2FC| > 0.58; p-value < 0.01) in shoots under different temperature and Pi treatments compared to control conditions. The top row shows volcano plots for the cultivar Industry, whereas the plots in the bottom row belong to Wesway.

From left to right: DEGs in shoots under Pi deficiency (21ºC-P), DEGs in shoots under high temperature (29ºC+P) and DEGs in shoots under the stress combination (29ºC-P), all of them compared to the control conditions (21ºC+P). B) Number of DEGs (|log2FC| > 1; p-value < 0.01) in shoots of Industry (left) and Wesway (right) under different temperature and Pi treatments compared to control conditions. X-axis show the different comparisons: Pi deficiency (21ºC-P vs. 21ºC+P), warm temperature (29ºC+P vs. 21ºC+P) and the stress combination (29ºC-P vs. 21ºC+P). The legend indicates whether the genes are up-regulated or down-regulated. C) Venn diagrams of Industry (left) and Wesway (right) showing the number of genes that are commonly deregulated in shoots under the four treatments: 21ºC+P, 21ºC-P, 29ºC+P and 29ºC-P. From left to right: Up-regulated genes in Industry, down-regulated genes in Industry, up-regulated genes in Wesway, down-regulated genes in Wesway.

After determining the major changes in gene expression in shoots of Industry and Wesway under Pi starvation (21ºC-P), warm temperature (29ºC+P) and the combination of both stresses (29ºC-P), we wanted to identify the main molecular pathways underlying these transcriptomic changes. Thus, we used the average of the normalized read counts of three biological replicates to build a dendrogram of the genes according to their expression profiles across the different treatments and varieties, and we obtained five different clusters of genes. Z-score were calculated from the normalized read counts and used to visualize their expression patterns in a heatmap (Figure 4.52).

Then, to identify the mayor molecular processes that define each cluster, we performed a GO analysis for each cluster. Cluster 1 contained genes that were less expressed at 29ºC+P and 29ºC-P compared to 21+P and 21-P in Wesway but less expressed in Industry under all treatments (Figure 4.52), and GO analysis identified several highly enriched categories such as protein kinase activity (-log10FDR > 30) and phosphotransferase activity alcohol group as acceptor (-log10FDR > 20), containing many genes encoding for protein kinases (Figure 4.53; Supplementary Table 10B), such as *CYSTEINE-RICH RLK (RECEPTOR-LIKE PROTEIN KINASE) 11, 36, 38 (BnCRK11, 36, 38), BRASSINOSTEROID-INSENSITIVE 2 (BnBIN2), CBL-INTERACTING PROTEIN KINASE 7, 10 (BnCIPK7, 10)* and *RLP15.* Several categories were also related to the transport of several nutrients like N, P and Fe, with genes like *BnPHO1, BnNPF6.3, BnNRT2.1, BnAMT2, FERRIC REDUCTASE DEFECTIVE 3 (BnFRD3),* and *BnDTX27, 37, 43, 49*.

Cluster 2 contained genes that were less expressed in response to warm temperatures, independently of the Pi level (less expressed at 29ºC+P and 29ºC-P

in both varieties compared to 21ºC+P and 21ºC-P; Figure 4.52). Gene ontology analysis identified several highly enriched categories, such as catalytic activity acting on DNA and DNA helicase activity, with genes involved in DNA replication, like *MINICHROMOSOME MAINTENANCE 2, 7 (BnMCM2, 7*; Figure 4.53). Several categories in cluster 2 were also related to microtubule and cytoskeleton formation, containing genes like *BnKIN4, 10, DYNAMIN RELATED PROTEIN 1 (BnDRP1)* and *DYNAMIN-LIKE PROTEIN 1 (BnDL1)*.

The genes in cluster 3 represented the opposite pattern of Cluster 2, where genes were more expressed at 29ºC+P and 29ºC-P compared to 21ºC+P y 21ºC-P in both varieties (Figure 4.52). GO analysis identified ubiquitin protein transferase activity as highly enriched, as well as other categories related to the ubiquitin process (Figure 4.53), such as *BnUBC4, BnUBC11,* or *BnUBC14*.

Cluster 4 contained genes that were more expressed in Industry but less expressed in Wesway under all treatments (Figure 4.52), and the most enriched categories corresponded to protein heterodimerization activity and structural constituent of chromatin, containing genes encoding for histones and histone modifiers like *BnHTA4, HISTONE B2 (BnH2B*; Figure 4.53*)*. Other categories included sucrose synthase activity, with *SUCROSE SYNTHASE 5 (BnSUS5)*, and glucosyltransferase activity, with *BnGOLS2, CELLULOSE-SYNTHASE LIKE 4 (BnCSLC4)* and *HYDROXYPYRUVATE REDUCTASE (BnHPR)*, suggesting that sugar metabolism could be negatively affected by warm temperature, -P and the combination of both.

Finally, cluster 5 had genes that were more expressed at 29ºC-P than under the other treatments (Figure 4.52), and GO analysis identified DNA binding transcription factor activity as a highly enriched category (Figure 4.53), with *BHLH* transcription factors (*BnBHLH3, BnBHLH93*), as well as *SCARECROW-like* TFs (*BnSCL1, 5, 13*). Furthermore, a GO category related to Zinc ion binding was enriched as well, and Zn nutrition has recently shown to be important for heat stress tolerance (Ullah *et al.*, 2019).

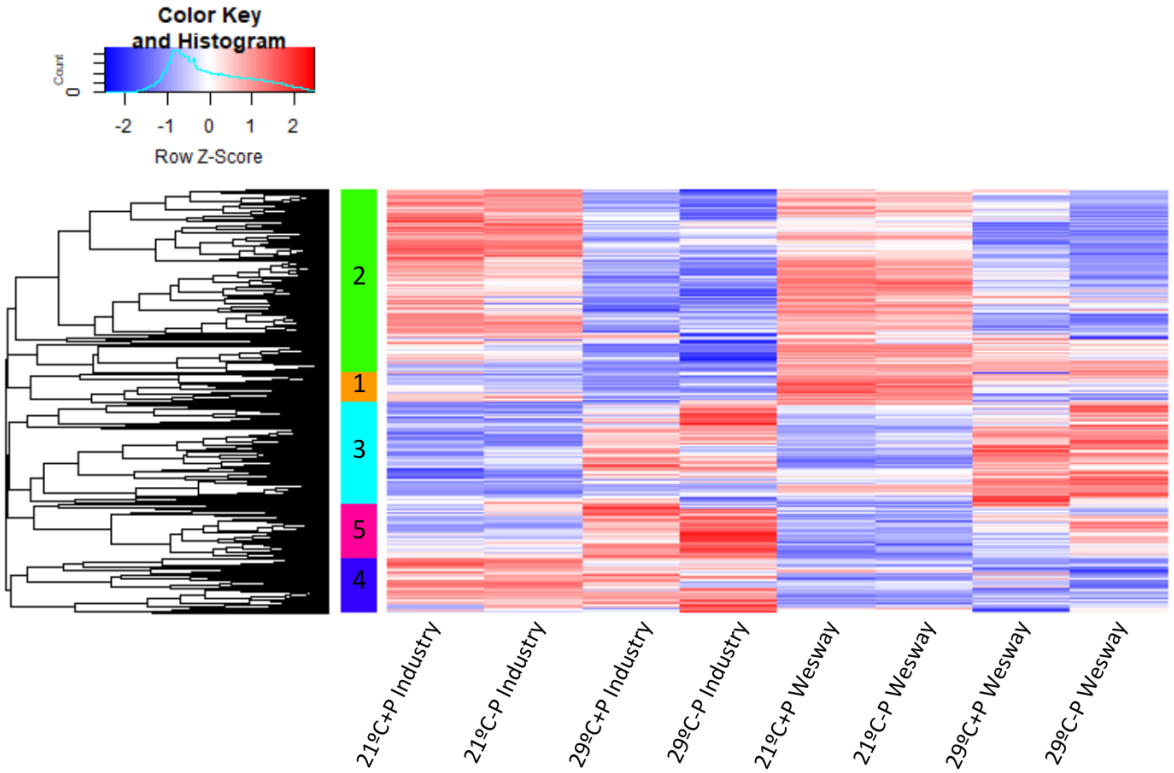


Figure 4.52: Heatmap of DEGs in shoots of *B. napus* individuals from two varieties (Industry & Wesway) and four temperature and Pi treatments (21ºC+P, 21ºC-P, 29ºC+P and 29ºC-P). The heatmap was built using Z-scores of the average of the normalized read counts from three replicates per treatment. Only genes that were differentially expressed ($|log2FC| > 0.58$; p-value $< 0.01$) in at least one of the comparisons between the treatments and/or varieties were considered. The genes were grouped in different clusters according to their expression profiles across the treatments (k=5). A table with the Z-score values of the DEGs for each treatment, with their respective log2FC for each comparison can be found in Supplementary Table 10A.

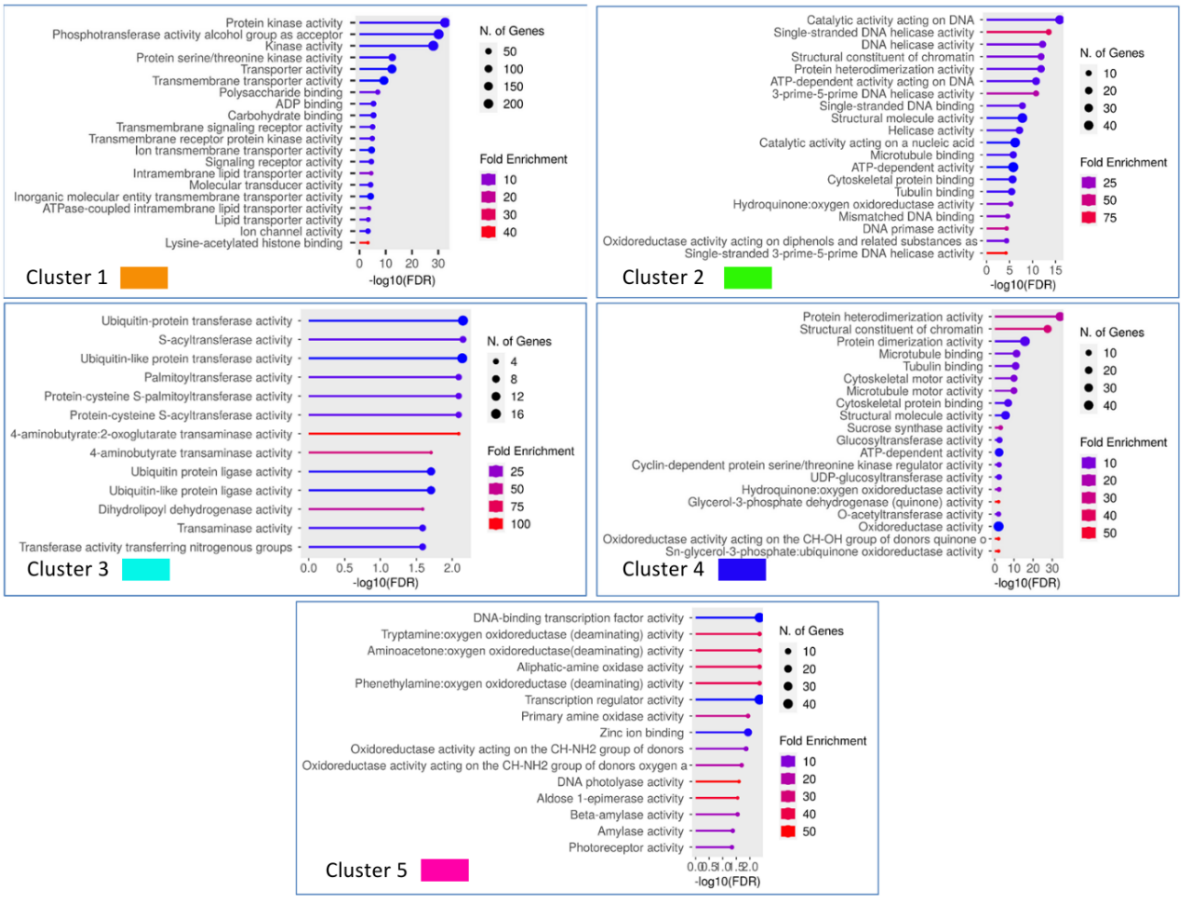


Figure 4.53: GO enrichment analysis of the DEGs in shoots of *B. napus* individuals from two varieties (Industry & Wesway) and four temperature and Pi treatments (21ºC+P, 21ºC-P, 29ºC+P and 29ºC-P). The GO enrichment was done individually for each of the 5 gene clusters previously obtained and was calculated using Shiny GO. A list with all the genes within each GO category is displayed in Supplementary Table 10B.

To identify protein networks that were representative of each cluster, we followed the same protocol as previously described (see Results: 4.2.1.). In cluster 1, we highlighted a network of proteins related to phosphate transport (PHT1-4, PHT1-8, PHT4-4, PHO1, PECP1) and nitrogen transport and assimilation (NRT2.1, NPF6.3, AMT1-3), whose genes were strongly down-regulated (log2FC < 0.58; p-value < 0.01) at 29ºC+P and 29ºC-P in both varieties (Figure 4.54; Supplementary Table 10A). This is consistent with our results in roots, where warm temperatures down-regulated genes related to the Pi starvation response, even at -P conditions, and genes related to N transport and assimilation (Supplementary Table 8A).

For cluster 2, we selected a subset of genes that were down-regulated at 29ºC-P in both varieties, but not under the individual stresses (21ºC-P or 29ºC+P; Supplementary Table 10A), and obtained a network of proteins related to

phenylpropanoid metabolism, with proteins like LDOX, LACCASE 10, 11, 17 (LAC10, 11, 17), PER50, PER51 (Figure 4.54), and proteins related to microtubule and cytoskeleton formation with several protein kinases (KIN4, 5, 8, 14). LDOX has shown to participate in anthocyanin accumulation mediated by Pi starvation in Arabidopsis and tomato (Liu *et al.*, 2022; Wu *et al.*, 2023), whereas LAC11 and LAC17 participate in lignin production, and the absence of those genes can cause severe disruptions in shoot growth (Khandal *et al.*, 2020).

For cluster 3, we selected a subset of genes specifically up-regulated at 29ºC-P (log2FC > 0.58; p-value < 0.01), and obtained a network of proteins related to the ubiquitin process like UBC4, 11, 14, PEROXIN 10, 13 (PEX10, 13; Figure 4.54; Supplementary Table 10A).

For cluster 4, we selected a network of proteins whose genes were down-regulated at 29ºC-P (log2FC < 0.58; p-value < 0.01), and not under the individual stresses, and contained proteins related to starch and sugar metabolism, as well as auxin signalling, such as AUX1, PIN3, ISOPENTENYLTRANSFERASE 3 (IPT3), SUS5, ENDONUCLEASE 1 (EDNO1), EXPANSIN 1 (EXPA1; Figure 4.54). Carbohydrate and sugar metabolism has shown to be important for the Pi starvation response, and altered expression of key genes in carbohydrate metabolism has shown to increase the sensitivity to Pi starvation (Karthikeyan *et al.*, 2007).

Finally, for cluster 5 we selected a subset of genes that were up-regulated (log2FC > 0.58; p-value < 0.01) only in Industry at 29ºC-P and not in Wesway, and we highlighted two networks, one of them involved in the Cul4-RING E3 ubiquitin ligase complex, with proteins like PRE-mRNA PROCESSING FACTOR 19B, 40C (PRP19B, 40C), ACTIN-INTERACTING PROTEIN 1-2 (AIP1-2), AUTOPHAGY PROTEIN 4A, 5 (ATG4A, 5), PEROXISOME BIOGENESIS PROTEIN 6, 7 (PEX6, 7). The second network was related to the circadian clock and photo-lyase activity, with proteins like CRYPTOCHROME 1, 2 (CRY1, 2), HIGH EXPRESSION OF OSMOTICALLY RESPONSIVE GENES 1, 15 (HOS1, 15), PHYTOCHROME INTERACTING FACTOR 3 (PIF3) or REDUCED VERNALIZATION RESPONSE 1 (VRN1; Figure 4.54). HOS1 has been related to enhanced thermotolerance (Han *et al.*, 2020) and is known to be a negative regulator of ABA signalling under drought stress (Ali & Yun, 2020).

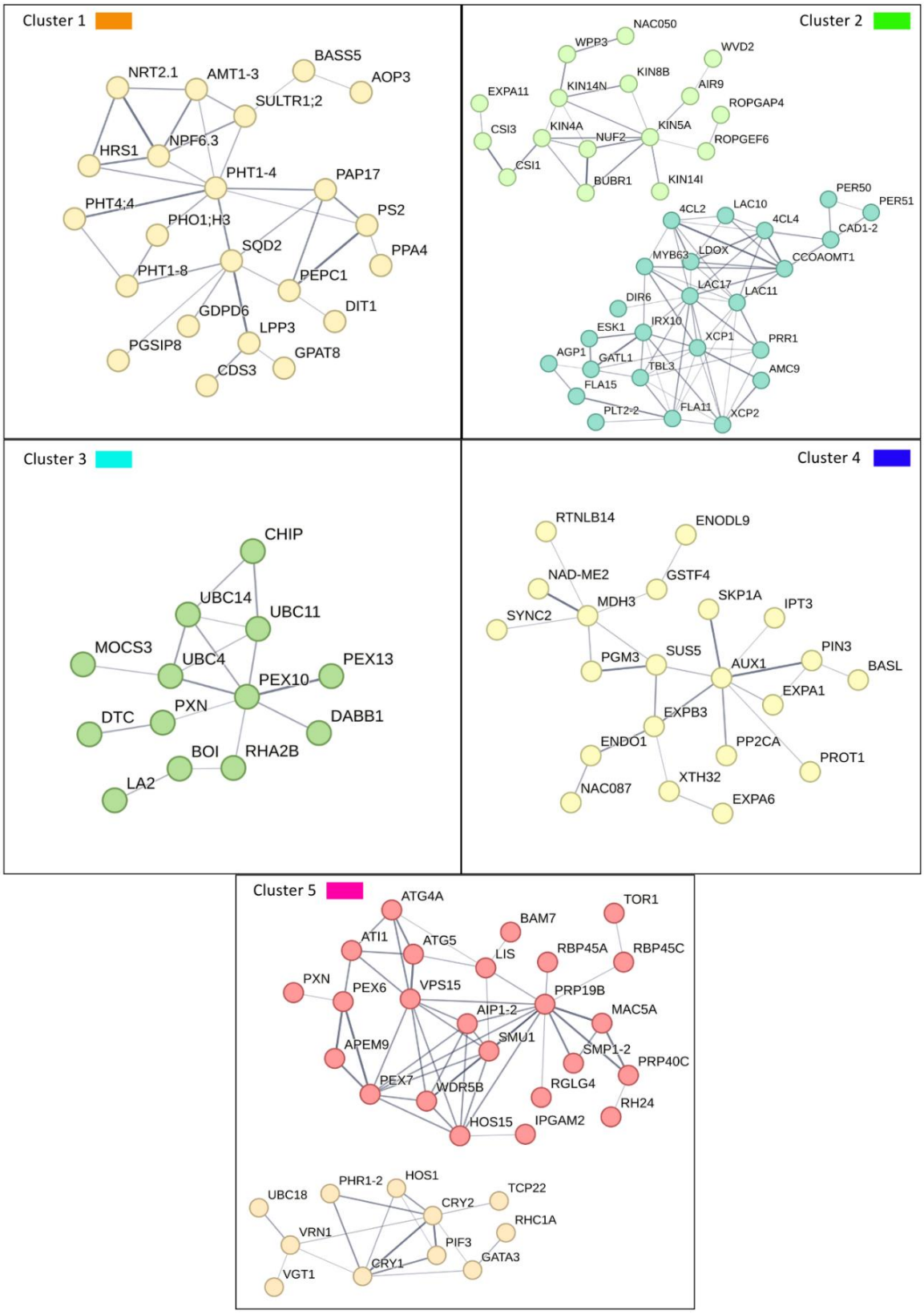


Figure 4.54: Interaction network analysis for each of the five clusters of DEGs in shoots of *B. napus* individuals from two varieties (Industry & Wesway) and four temperature and Pi treatments (21ºC+P, 21ºC-P, 29ºC+P and 29ºC-P). The *A. thaliana* orthologs from the most relevant DEGs were considered.

In this section we obtained insights into the shoot responses to the combination of warm temperature and Pi deficiency in *B. napus*. Our results suggest that warm temperatures could alter Pi homeostasis, enhancing the sensitivity to Pi starvation when plants are exposed to the combination of both stresses.

# 5. DISCUSSION

## 5.1. The combination of warm temperature and N deficiency produces a compensatory effect on root traits in *B. napus*.

One of the goals in this thesis has been to analyse the root responses to the combination of warm temperatures and nitrogen deficiency in *B. napus*. To do this, we have performed an extensive characterization of the root architecture in different *B. napus* varieties under warm temperature, N deficiency and the combination of both stresses. Our results indicate that under N deficiency, *B. napus* showed a general tendency to develop a deeper root system, accompanied by an increase in the length of the lateral roots. We also observed changes in the distribution of the lateral roots, and the formation of longer lateral roots in the upper parts of the root system and shorter lateral roots in the deeper parts. Regarding the effects of warm temperature, we observed a general increase in the depth of the root system, that might be explained by the need to search for deep and cooler areas, accompanied by a strong suppression on lateral root growth, leading to very short and scarce lateral roots. When *B. napus* seedlings were grown under the combination of warm temperature and N deficiency, we observed a compensatory effect on LR growth, with LRs having an intermediate length. Moreover, other traits (such as network width, area, or lateral root density) also showed intermediate phenotypes compared to the opposite effects of the individual stresses. Network depth was the only trait that seems to maintain its increase under the stress combination. This compensatory effect in most traits suggests that both stresses produce opposite responses in the root system in terms of lateral root development, and the stress combination triggers both responses leading to an intermediate phenotype. In this context, some varieties showed a phenotype more similar to the response to warm temperature, and other varieties had more N deficiency symptoms.

Our results regarding the effect of N deficiency alone are consistent with previous findings. Increases in root depth have been previously observed in *B. napus* (Guo *et al.*, 2017; Qin *et al.*, 2019; Shen *et al.*, 2022), in Arabidopsis (Gruber *et al.*, 2013; Giehl & von Wirén, 2014; Conesa *et al.*, 2020), and in other crops like wheat, rice and maize (Li *et al.*, 2016; Hsieh *et al.*, 2018; Tian *et al.*, 2020). On the other hand,

longer lateral roots have been observed in *B. napus* under N deficiency (Shen *et al.*, 2022), but this expansion was usually accompanied by an increase in the lateral root density, that was not observed in our experiments. This discrepancy could be caused by the different conditions used in this work, since Shen *et al.* (2022) used a hydroponic culture that applies different growth conditions than the pouch and wick system used in our work. Furthermore, Guo *et al.*, (2017) observed that *B. napus* tends to develop longer lateral roots and a higher lateral root density when seedlings are grown under a moderate N deficiency (0.5 mM), but both traits are reduced under extreme N deficiency (0 mM). The level of the N deficiency treatment applied in our experiments could be considered as "intermediate", and might cause some of the observed differences. In soil, many studies described that the root system of plants grown under N deficiency tends to respond in a local manner, generating longer lateral roots in patches with higher N content while suppressing lateral root growth in zones with lower N availability (Krouk *et al.*, 2010; Mounier *et al.*, 2014; Liu & von Wirén, 2017). This suggests that in our conditions, more N could be accumulated in the top parts of the pouch and wick system, likely due to the diffusion-saturation of the medium in these top parts, and consequently promoting LR growth in this area. Consistently, in natural soils, total nitrogen is known to accumulate in the top parts of the soil rather than in the bottom parts (You *et al.*, 2024).

Regarding the effects of warm temperature in *B. napus*, our results are also consistent with prior findings. A previous work in our lab showed that warm temperature produced an increase in root depth in *B. napus* (Boter *et al.*, 2023), and similar results have been reported in Arabidopsis (Hanzawa *et al.*, 2013; Wang *et al.*, 2016; Martins *et al.*, 2017) and crops like maize, soybean and rice (Xia *et al.*, 2021; Lee *et al.*, 2024). Since higher temperatures tend to correlate with low water content in the soil, the increase in root length could be related to the need to explore deeper soils areas in search for water (M'hamdi *et al.*, 2023). Warm temperature has also shown to produce a decrease in lateral root length in *B. napus* (Wu *et al.*, 2020b), being consistent with our results. This reduction could be explained as a strategy to reduce root growth in the top areas where water is scarce.

When we evaluated the morphological root responses to N deficiency among the different *B. napus* genotypes, we observed high uniformity in the root response to N deficiency. This effect could be due to the process of selection, since N use efficiency is one of the most relevant traits searched by crop breeders. However, regarding the effects of warm temperature alone, we have observed more

variability among the different *B. napus* genotypes. Variability in the root responses to warm temperatures has been previously reported in *B. napus* (Boter *et al.*, 2023). This might be due to the adaptations of each variety to different environments, since they come from different geographical regions with different climatic conditions.

Even though several works have studied the effects of temperature stress or N deficiency individually, few studies have focused on the effects of warm temperature combined with N deficiency simultaneously and, to our knowledge, none has been performed in roots. As indicated above, our results suggest a compensatory effect of both stresses on root architecture, since most traits are not significantly reduced by the stress combination and show an intermediate phenotype. This suggests that the activation of opposite adaptation responses to the individual stresses caused a mixed phenotype. Other stress combinations have also shown to produce a potential compensatory effect on each other, such as the combination of drought and $O_3$ stress (Suzuki *et al.*, 2014). In this context, we know that N deficiency induces the expression of genes related to the heat shock response (Song *et al.*, 2019; Wang *et al.*, 2014a), pointing out to a possible interconnection between N levels and the response to temperature changes. This idea seems to be supported by a study showing that exogenous application of nitrogen can alleviate heat stress symptoms (Wang *et al.*, 2012). The compensatory effects on root traits observed under the stress combination suggest that elevated temperatures caused by climate change could modify the responses to N deficiency. These data are relevant and should be taken into consideration when designing new fertilization plans. In addition, since excessive N fertilization can cause negative effects on the environment, the selection of varieties that can maintain their N use efficiency under the combination of warm temperatures and N deficiency is essential to design new sustainable agricultural practices. In this thesis, we have identified different genotypes that can maintain the adaptive responses to N deficiency under warm temperature, such as elongation of the lateral roots (Wesway), whereas others reduce their adaptive response to N deficiency under warm temperatures (Westar). This information could be useful for breeding programs trying to select and/or develop varieties that are more tolerant to the combination of warm temperatures and N deficiency. Therefore, identifying the genetic and molecular determinants of this adaptation is crucial to achieve this goal.

Finally, warm temperatures produced a decrease in nitrate content in shoots of both varieties (Wesway and Westar), whereas in roots nitrate content was unaltered in Wesway and slightly increased in Westar. Reductions in nitrate content in shoots as a consequence of warm temperatures have also been reported in Arabidopsis, rice and soybean (Lee *et al.*, 2024) and in tomato (Tindall *et al.*, 1990; Giri *et al.*, 2017), indicating that warm temperatureshave a clear effect on N usage. On the other hand, these varieties experience a strong decrease in nitrate content in both roots and shoots when they are grown under N deficiency alone and under the stress combination. This reduction in root nitrate content as a consequence of N deficiency has been observed in *B. napus*, wheat, citrus and poplar (Liu *et al.*, 2019b; Song *et al.*, 2019; Tian *et al.*, 2020; Huang *et al.*, 2021). However, in shoots, this reduction in nitrate content was less pronounced in Wesway than in Westar, suggesting that the better capacity of Wesway to develop longer lateral roots under N deficiency could increase the surface area resulting in increased nutrient absorption. It is worth to mention that *B. napus* varieties with more expanded root systems under N deficiency tend to accumulate more nitrate in roots and shoots than varieties with smaller root systems (Ye *et al.*, 2010), highlighting the crucial role of roots in the response to these stresses.

## 5.2. Oxidoreductase activity, hormonal regulation and increased N transport as key factors for better root adaptation to warm temperature and N deficiency in *B. napus*.

As mentioned before, one of our aims in this Thesis is to identify the main components that regulate the root responses to the combination of warm temperatures and N deficiency in *B. napus.* Two examples of genotypes with differential root responses to the combination of warm temperatures and N deficiency are Westar and Wesway. Westar shows dramatic alterations in response to N deficiency or to warm temperature alone, whereas Wesway seems to be less responsive to the individual treatments. Interestingly, under the stress combination, Wesway develops a higher number and longer lateral roots than under the individual treatments, whereas lateral root elongation is severely affected in Westar. To identify the key genes that are involved in these responses, we performed a transcriptomic analysis in roots and shoots of these two selected varieties. Transcriptomic analysis in roots revealed that in Westar, the differential

gene expression englobed a higher number of genes under the stress combination than under warm temperature or N deficiency alone, being N deficiency the stress condition with a lower number of deregulated genes. In Wesway, the transcriptional response is also softer under N deficiency alone, but is similar to warm temperature or the stress combination. Remarkably, in both varieties, these DEGs are not the same at 29ºC+N and 29ºC-N, as the stress combination treatment deregulates many genes that are different than those deregulated by the individual stress treatments, indicating that the response is specific for the stress combination. Taken together, these data seem to indicate that the combination of warm temperature and N deficiency produces a distinct transcriptional response compared to the individual stresses that could underlie the compensatory effects observed on root traits.

Transcriptional analyses allowed us to identify several processes whose genes are more expressed under the stress combination than under the individual treatments. Remarkably, this enrichment is more significant in Wesway than in Westar, indicating a differential molecular adaptative response. Thus, we found enrichment of processes such as oxidoreductase activity, containing genes encoding for Class III peroxidases such as *BnPER62*, *BnPER59*, *BnPER69* and *BnPER71*, as well as genes involved on antioxidant activity, such as *BnGPX2, BnPAO2, BnAOX1a, BnPSY1* and *BnCAT1-2* (Figure 5.1). Peroxidases are part of the molecular mechanisms directed to mitigate the negative effects of ROS on plant cells under a vast majority of stresses (Kidwai *et al.*, 2020). Class III peroxidases are also involved on the regulation of cell walls and several studies demonstrate that they contribute to root hair elongation by triggering modifications in the cell wall and promoting expansin activity, which leads to enhanced root growth (Vijayakumar *et al.*, 2016; Martinez Pacheco *et al.*, 2021; Marzol *et al.*, 2022). Interestingly, our analyses show that Wesway expresses higher levels of expansin-related genes (*BnEXPLB1*, *BnBEE3*, *BnEXPA5* and *BnEXPA1)* than Westar under the stress combination, correlating with an enhanced lateral root elongation in our conditions. Studies from our lab and others have shown that ROS and peroxidase activity play an important role on LR emergence and the elongation of the primary root (Manzano *et al.*, 2014; Orman-Ligeza *et al.*, 2016; Silva-Navas *et al.*, 2016; Campos-García *et al.*, 2021). We also observed that *BnAOX1* increased its expression in Wesway in response to warm temperature (29ºC). *AOX1* is expressed in different tissues, including roots, and plays a role in the oxidative response to stress (Clifton *et al.*, 2006; Figure 5.1). Similarly, higher AOX1 activity

correlates with reduced oxidative stress under N deficiency in Arabidopsis and rice (Ji *et al.*, 2023; Otomaru *et al.*, 2024), suggesting a conserved functional response of this gene in different species. All these results suggest a correlation between the ability of Wesway to develop a wider root system with longer lateral roots under the stress combination and the increased activity of peroxidases and antioxidant enzymes. Thus, increased activity of these enzymes, which can alleviate the negative effects of ROS, in Wesway might favour the elongation of the lateral roots in response to the combination of warm temperatures and N deficiency. Interestingly, one of the enriched peroxidases, *PER59,* is also induced under salinity stress in Arabidopsis roots via ethylene response factors and contributes to its tolerance (Vaseva *et al.*, 2021). On the other hand, *PER71* has been related to cold tolerance in citrus (He *et al.*, 2020) and is induced in Arabidopsis roots under heat, cold, salinity and different combinations of these stresses (Eljebbawi *et al.*, 2022), suggesting that could play a role in the responses to multiple and combined stresses. Moreover, increased expression of *PER71* seems to improve the tolerance to cold stress in bermudgrass, and in this case, its expression is regulated by *ERF1,* an ethylene response transcription factor (Hu *et al.*, 2020). Interestingly, our transcriptomic analysis also shows increased expression of several ERFs under the combination of N deficiency and warm temperature. Particularly, *BnERF1A* is significantly induced in Wesway under the stress combination, but not in Westar, suggesting that an increased expression of *BnPER71* could be mediated via *BnERF1A* in this variety, being similar to the response to cold stress. Furthermore, *BnERF11* and *BnERF13* are up-regulated in both Westar and Wesway. *ERF11* and *ERF13* participate in the root responses to several abiotic stresses (Liu *et al.*, 2020; Lv *et al.*, 2021; Yu *et al.*, 2024), mostly by down-regulating lateral root development. As *ERF11* and *ERF13* were up-regulated in both Westar and Wesway when combining warm temperature and low N, and both varieties reduce their lateral root density at 29ºC-N, it is possible that these two TF regulate LR formation and development in *B. napus* in response to the combination of both stresses (Figure 5.1).

Other genes that are related to the response to N deficiency, such as *GLN1-4, GLN1-5* and *AMT1-1,* are up-regulated under the stress combination in both varieties (Figure 5.1), but their expression is significantly higher in Wesway than in Westar. Previous research in *B. napus* shows that different cultivars with differential N use efficiency show changes in the expression of several *BnGLN1* genes (Li *et al.*, 2020b). *GLN1* has many isoforms in *B. napus* that are expressed

in different tissues in response to different N availability levels (Orsel *et al.*, 2014). For instance, *AtGLN1-4* is expressed in roots and its expression increases under N deficiency. *AMT1-1* is a high affinity ammonium transporter that is typically expressed under N deficiency (Zhu *et al.*, 2023). Thus, the induction of this gene suggests that in *B. napus*, the combination of both stresses could enhance the uptake of ammonium-based compounds (Figure 5.1). We also observe significant differences in the expression of genes related to nitrate acquisition and transport between both varieties. *NRT1.1*, also called *NPF6.3*, is a nitrate transporter of the NRT1 family that participates in nitrate root to shoot transport (Léran *et al.*, 2013), whereas *NRT2.1* belongs to the NRT2 family and is involved in nitrate uptake from the soil and in the auxin-mediated regulation of LR development in response to different N levels (Wirth *et al.*, 2007; Wang *et al.*, 2023e). The expression patterns of *BnNRT2.1* are different from those of *BnNRT1.1* within the same variety under N deficiency. In our experiments, *BnNRT2.1* was strongly suppressed in Westar at 21ºC-N and 29ºC-N, but strongly induced in Wesway under those treatments, especially at 21ºC-N, suggesting that this differential response contributes to differences in N accumulation between both varieties. This expression pattern is similar to the N-dependent expression changes previously reported by Tian *et al.* (2009), who observed that high N up-regulates *AtNRT1.1* and down-regulates *AtNRT2.1*. Furthermore, *B. napus* cultivars with better N use efficiency have a higher expression of *BnNRT2.1* in roots than sensitive cultivars (Li *et al.*, 2020b). Additionally, *NRT2.1* is known to promote lateral root initiation under low N (Remans *et al.*, 2006), which correlates with the better capacity of Wesway to maintain lateral root growth at 29ºC-N. The expression of *BnNRT1.1*, on the contrary, is significantly induced at 29ºC-N in both varieties, but this induction is higher Wesway than in Westar. Remarkably, the expression of *BnNRT1.1* in response to N deficiency alone is different in Westar than in Wesway, being down-regulated or up-regulated respectively. The role of *NRT1* in nitrate root to shoot transport is consistent with our results, since we observed higher levels of nitrate in Wesway shoots at 21ºC-N, compared to Westar. *NRT1.1* can either negatively or positively regulate lateral root development via different pathways. High expression of *NRT1.1* decreases auxin levels in the lateral root tips, ultimately leading to a reduction on lateral root growth in areas of the soil with low N (Krouk *et al.*, 2010), but *NRT1.1* can also stimulate lateral root growth in areas with more N availability by inducing *ANR1* and *ABF3* (Maghiaoui *et al.*, 2020; Figure 5.1). Interestingly, *BnABF3* was significantly up-regulated in both varieties at 29ºC-N, suggesting a possible role of *NRT1.1* on the stimulation of

lateral root development by modulating auxin signalling. These results suggest that the increased expression of these transporters in Wesway, compared to Westar, plays a role on its capacity to grow longer lateral roots in response to the combination of warm temperatures and N deficiency.

Our results show that many genes related to ethylene biosynthesis are repressed by the effect of N deficiency in a temperature-independent manner, especially in Wesway. In Arabidopsis, ethylene, which is induced under high N, mediates the negative regulation of lateral root development (Tian *et al.*, 2009). In *B. napus*, previous research shows that inhibition of ethylene biosynthesis causes an increase in root elongation that is accompanied with an increase in N uptake (Lemaire *et al.*, 2013). This suggests that the stronger repression of genes related to ethylene biosynthesis at 29ºC-N in Wesway could be related to the better capacity of this variety to develop longer lateral roots compared to Westar. Contradictorily, we observed that several ERF transcription factors, such as *BnERF1*, or *BnERF11*, which are known to be regulated by ethylene (Huang *et al.*, 2016), have an increased expression at 29ºC-N. This suggests that these transcription factors are activated by ethylene-independent pathways in our conditions. In fact, different works have shown that other hormones, such as ABA or JA, can also induce the activation of *ERF* transcription factors (Li *et al.*, 2011; Zhang *et al.*, 2023b). For example, *ERF11,* which reduces ethylene biosynthesis by repressing the expression of *ACC synthases,* is activated by ABA (Li *et al.*, 2011; Figure 5.1). The phytohormone ABA plays a role in the root responses to heat stress, contributing to the regulation of root growth (Larkindale *et al.*, 2005; Zhu, 2016). We observed an up-regulation of *BnERF11* in both varieties at 29ºC-N, suggesting a possible involvement of this TF in the repression of ethylene biosynthesis during the stress combination. Furthermore, our results also show that the expression of *BnHB52* was significantly increased at 29ºC-N in Westar, but unaltered in Wesway. HB52 is a member of the HD-ZIP family of TFs and mediates the suppression of root growth via ethylene (Miao *et al.*, 2018). Since genes related to ethylene biosynthesis are repressed in *B. napus* in response to warm temperature combined with N deficiency, the induction of *HB52* in Westar should be dependent on other factors different than ethylene. Taken together, our data suggest that ethylene signalling plays an important role in the adaptation of *B. napus* to N deficiency and the combination of warm temperature and N deficiency (Figure 5.1).

We also observe an up-regulation of genes involved in the ABA-mediated response to stress, such as *BnCYP707A3, BnWRKY25* and *DREB2E,* in Wesway, but not in Westar in response to combined warm temperatures and N deficiency. *CYP707A3* is involved in ABA catabolism and is involved in the ABA-mediated response to salinity and drought (Umezawa *et al.*, 2006; Zhou *et al.*, 2007). The transcription factor *WRKY25* has been related to early root responses to heat, salinity and micro-nutrient deficiency stresses, contributing to root elongation (Li *et al.*, 2009; Deolu-Ajayi *et al.*, 2019; Wu *et al.*, 2020a). *WRKY25*, which is mainly expressed in roots, is activated by oxidative stress or by the excess of ROS caused by heat stress (Li *et al.*, 2009). This suggests that Wesway might have a better capacity to mitigate the damage caused by oxidative stress and ROS, being consistent with our previous results that show that Wesway increases the expression of genes encoding for peroxidases and antioxidant enzymes. Furthermore, induction of *DREB2* transcription factors has been related to tolerance to several abiotic stresses, and they are up-regulated by ABA in Arabidopsis roots (Sakuma *et al.*, 2002). In tobacco, increased expression of *DREB2* results in enhanced LR elongation under drought, salinity or heat stress (Li *et al.*, 2014). This suggests that increased expression of *DREB2* in Wesway at 29ºC-N could be related to its capacity to elongate the LRs under this condition and suggests a possible involvement of ABA in this process. PSY1 is a crucial enzyme in the carotenoid biosynthetic pathway (Lopez-Emparan *et al.*, 2014). As *BnPSY1* is up-regulated in both varieties at 29ºC-N, but more significantly in Wesway (Figure 5.1), we can speculate that differences in carotenoid accumulation might contribute to the differential responses observed between both varieties. Furthermore, ABA also plays a role in triggering carotenoid biosynthesis in roots under abiotic stresses via PSY1 (Li *et al.*, 2008; Welsch *et al.*, 2008). Carotenoid biosynthesis has been related to enhanced LR growth, since the root clock needs carotenoid-derived signals for LR formation (Ke *et al.*, 2022). Thus, these results suggest a role of ABA and carotenoid biosynthesis in the better capacity to develop longer LRs in Wesway at 29ºC-N, compared to Westar.

Finally, our transcriptomic analysis also reveals a strong suppression of genes related to ribosomal activity in both varieties at 29ºC-N, and to a lesser extent in response to the individual stresses. Genes related to ribosomal activity have shown to alter their expression under N deficiency in some crops like tea, watermelon and citrus (Nawaz *et al.*, 2018; Ruan *et al.*, 2022; Lai *et al.*, 2023), suggesting a role of the regulation of protein translation in the response to N nutrition. Furthermore,

different abiotic stresses alter the expression of ribosomal genes to regulate the properties and function of the ribosome, altering the protein translation rates (Fakih *et al.*, 2023). Since we identified several changes in ribosomal genes, our data suggest a role of ribosomal activity in the root responses to combined warm temperature and N deficiency in *B. napus*, probably via post-transcriptional modifications (Figure 5.1). Different post-transcriptional modification mechanisms, such as messenger RNA (mRNA) processing, stability, localization or protein translation play an important role on plant adaptation to abiotic stresses and organ development (Floris *et al.*, 2009).

To summarize, we have provided new insights into the transcriptional responses of *B. napus* to the combination of warm temperature and N deficiency, and identified new genes and pathways that are specifically up-regulated or down-regulated under this stress combination. Since the stress caused by combined warm temperature and N deficiency will be aggravated by climate change in the future, the identification of these genes/pathways could be useful to select new markers that can be used in genetic improvement programmes to select more efficient and tolerant varieties. Furthermore, these data support the idea that root responses to stress combinations significantly differ from root responses to individual stresses, and highlights the importance of studying abiotic stresses in combination.

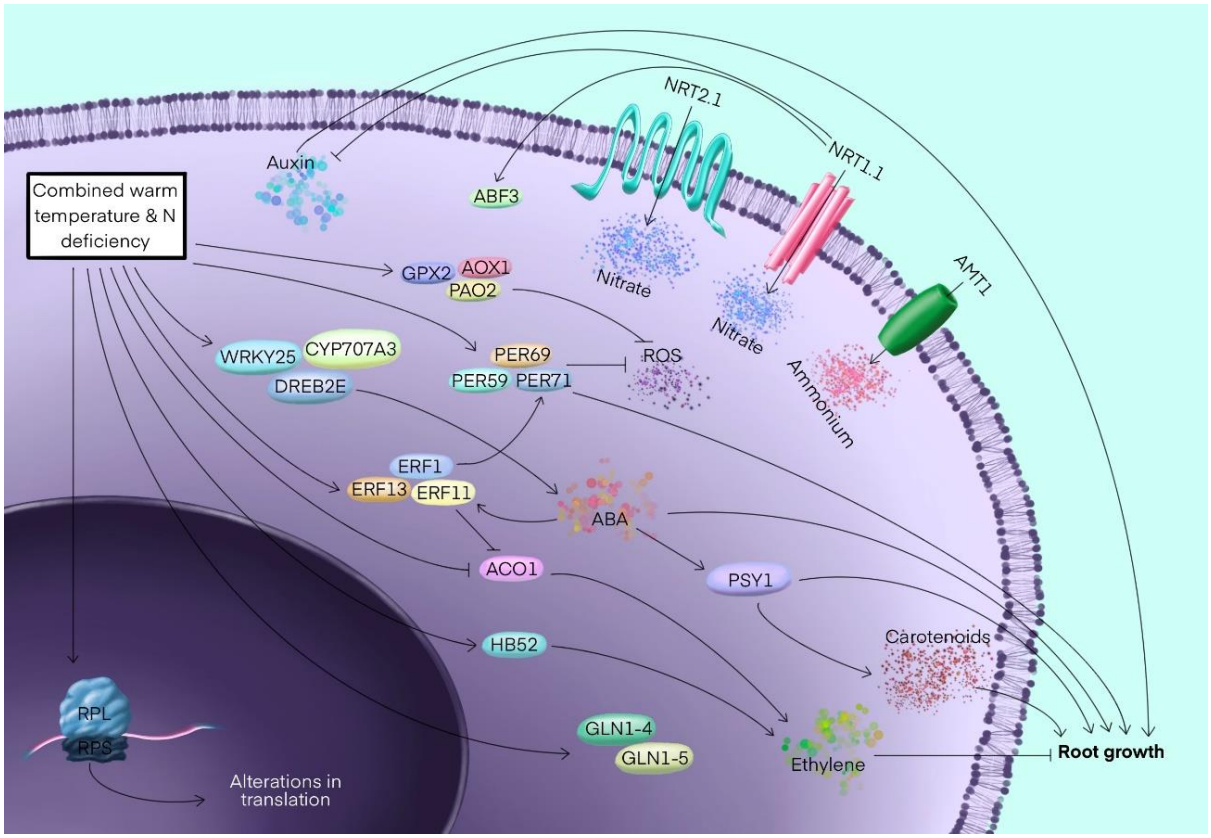


Figure 5.1: Model of the putative molecular pathways controlling the root responses to the combination of warm temperature and N deficiency in *B. napus*. During this response, root cells activate antioxidant enzymes to mitigate the negative effects of ROS, as well as nitrate and ammonium transporters to increase N uptake, and enzymes involved in N metabolism, like GLN1-4 and 1-5, to optimize N use efficiency. The transporter NRT1.1 inhibits root growth in areas with low N levels via inhibition of auxin signalling, and at the same time promotes root growth in areas with higher N levels via ABF3. The combination of warm temperature and N deficiency also activates ABA signalling and represses ethylene signalling, contributing to root growth. Likewise, more sensitive varieties seem to activate ethylene signalling through increased expression of *HB52*, thus reducing root growth. Finally, the combination of warm temperature and N deficiency causes alterations in the transcription of many ribosomal genes, which could cause alterations in protein translation, affecting the overall response to this stress.

## 5.3. Transcriptional changes in shoots are coordinated with morphological root responses to combined warm temperature and N deficiency.

Transcriptomic analysis in shoots of the *B. napus* varieties Westar and Wesway revealed that Westar alters the expression of more genes under N deficiency alone, compared to the other stress treatments, whereas Wesway modifies the expression of a higher number of genes under the combination of N deficiency and warm temperature. This contrasts our previous results in roots, where the number of

DEGs under the stress combination in Westar is higher than under N deficiency. Remarkably, in Westar, the DEGs at 29ºC-N are different from those observed in response to the individual stresses, suggesting an independent and differential regulation of the transcriptional response under the stress combination. In Wesway, on the contrary, we observed that a larger number of DEGs are shared between the 21ºC-N and 29ºC-N treatments, suggesting that the temperature has a lower impact than the N deficiency on the molecular response to the stress combination or that N deficiency partially compensates the effect of warm temperatures. Altogether, these results indicate that, even though the transcriptional changes observed in roots suggest a stronger effect of the stress combination than the effect of the individual stresses, shoots might not follow this tendency and the individual N deficiency stress could cause a strong transcriptional response as well.

We identified several functional processes in shoots that are more enriched in Wesway than in Westar under the stress combination, including calcium-mediated ABA signalling, with genes like *CAM2*, *CAM3*, *CML24* and *CPK32* among others. *CAM2* and *CAM3* have been related to tolerance to different abiotic stresses like drought, salinity and aluminium toxicity (Yoo *et al.*, 2019; Zhu *et al.*, 2022; Zheng *et al.*, 2022: Hau *et al.*, 2024). CML24 is a calcium sensor that functions in ABA signalling under different stresses (Delk *et al.*, 2005). CPK32 has been associated with enhanced ammonium uptake by roots (Qin *et al.*, 2020) and the up-regulation of CPK32 in shoots possibly correlates with the increased levels of the ammonium transporter AMT1-1 observed in Wesway roots at 29ºC-N. These data are also consistent with our results in roots, where we observe increased expression of ABA-related genes in Wesway at 29ºC-N. Taken together, these data suggest that Wesway could activate ABA signalling in shoots to a greater extent than Westar, suggesting that ABA signalling could mediate the enhanced LR growth observed in Wesway compared to Westar in response to the combination of warm temperatures and N deficiency.

Our data also show increased expression of genes involved in long-distance N signalling in Wesway at 29ºC-N, but not in Westar, such as *CEP6*, *CLE26* and *CLE43*. CEP peptides participate in the long-distance response to N deficiency and are directed toward the activation of nitrate transporters in roots (Taleski *et al.*, 2018). This higher level of CEPs correlates with the increased expression of *BnNRT2.1* and *BnNRT1.1* observed in Wesway roots at 29ºC-N. CEP6 positively regulates root nodulation under N deficiency in soybean (Wang *et al.*, 2023d; Wu

*et al.*, 2024). Similarly, CLE peptides are expressed in both roots and shoots and play a role on long-distance signalling under N deficiency, ultimately participating in the modulation of root system architecture (Araya *et al.*, 2016). Particularly, expression of *AtCLE26* in *B. napus* has previously shown to modulate root architecture by inhibiting the primary root growth but enhancing lateral root growth (Czyzewicz *et al.*, 2016). This is consistent with our results, since both Westar and Wesway develop longer lateral roots at 21ºC-N, but only Wesway develops longer lateral roots at 29ºC-N, correlating with the expression patterns of *BnCLE26*. Thus, it would be interesting to analyse the response of *B. napus* lines overexpressing *AtCLE26* to warm temperatures combined with different N regimens in future experiments. In addition, long-distance shoot to root CEP peptide signalling plays an important role in the response to N deficiency by regulating lateral root growth and increasing the expression of N transporters in roots (Mohd-Radzman *et al.*, 2016; Ohkubo *et al.*, 2017). CEP peptides are activated under N deficiency in roots and bind to CEPR receptors in shoots, where they trigger a signalling cascade directed towards the activation of N transporters in roots, as well as the suppression of LR growth in zones with lower N and promotion of LR growth in zones with higher N availability (Tabata *et al.*, 2014; Taleski *et al.*, 2018; Roy *et al.*, 2022). This correlates with our results in root traits, where N deficiency caused an increase in LR growth in the upper parts of the root system but not in the bottom parts.

Furthermore, in response to warm temperatures (independently of the N level), Westar seedlings down-regulated *HYH*, a *HY5* homolog. *HY5* is expressed in shoots and triggers a shoot to root signal to activate *NRT* transporters such as *NRT2.1* in roots under low N levels (Xuan *et al.*, 2017). This correlates with the increased expression of *NRT* transporters observed in Wesway at 29ºC-N but not in Westar. *HY5* participates in the thermomorphogenesis response by positively regulating root architecture and increasing root depth through different pathways, including regulating the expression of auxin and brassinosteroids-regulated genes (Martins *et al.*, 2017; Gaillochet *et al.*, 2020; Lee *et al.*, 2021). This is consistent with our results in roots, since Westar is one of the few genotypes that reduced its root depth under warm temperature. Taken together, our results suggest that Wesway might have enhanced long-distance shoot to root signalling under the stress combination, compared to Westar, thus having a positive effect on root architecture and N uptake by roots. This suggests that varieties that are able to develop a more adapted root system under the stress combination could activate

these molecular responses in shoots, improving their performance and productivity.

## 5.4. Elevated temperatures change the root responses to N deficiency in Arabidopsis.

After studying the root response to combined stresses in *B. napus*, we wanted to investigate the root responses to N deficiency combined with warm temperature or heat stress, using Arabidopsis as a model plant. N deficiency alone, as well as combined with warm temperature cause a decrease in LR density, being consistent with our results in *B. napus*. Combined heat stress and N deficiency also reduce LR density. Even though LR density was reduced by N deficiency and the combination of N deficiency and heat stress, the number of pre-branch sites was similar under N deficiency and control conditions. This suggests that heat stress combined with N deficiency specifically affects some aspects of the development of the root system but not others. Our data suggest that N deficiency negatively affects root growth in the short term, but since the number of PB sites is not affected, a longer N deficiency treatment could result in more LR formation by promoting the emergence of quiescent lateral root primordia (Manzano *et al.*, 2012). The inhibition of root growth caused by N deficiency is abolished when seedlings are grown under N deficiency in combination with warm or high temperatures, suggesting that higher temperatures compensate some of the negative effects of the N scarcity. The fact that this reduction in root length as a response to -N was not observed under warm temperature or high temperature suggests that elevated temperatures could alter the root responses to N deficiency. A possible explanation could be that the plant prioritizes its response to elevated temperature, which can be lethal in the short run, before addressing the additional problem of the N deficiency.

It is worth to mention that the decrease in root length observed under N deficiency alone in Arabidopsis contrasts our previous results in *B. napus*, where root depth increased. The underlying reason might be the severity of the N deficiency treatment, since we used a more severe N deficiency in Arabidopsis (0.05 mM) compared to *B. napus* (0.1 mM). This is consistent with previous data, showing that moderate N deficiency causes an increase in root growth, whereas severe N deficiency causes strong reductions in root growth (Gruber *et al.*, 2013; Giehl & von Wirén, 2014).

At the molecular level, N deficiency strongly induces the expression of *NRT2.4*, while the combination of N deficiency and warm temperature limits the induction of *NRT2.4*. Furthermore, under combined heat stress and N deficiency, the expression of *NRT2.4* was reduced to levels found in seedlings grown under optimal N levels. *NRT2.4* encodes for a high affinity nitrate transporter mainly induced by N deficiency in roots and partially in shoots and is crucial for N uptake and loading into the phloem (Kiba *et al.*, 2012). Several studies have shown that heat stress causes a reduction in the uptake of several nutrients, including nitrogen (Tindall *et al.*, 1990; Giri *et al.*, 2017; Villar *et al.*, 2019). In tomato, heat stress strongly reduced the N and C levels in roots and decreased the levels of the NRT1 and NRT2 proteins, as well as proteins related to the uptake of other nutrients (Mishra *et al.*, 2023). These studies support the hypothesis that heat stress could suppress the expression of genes related to N uptake and/or metabolism and therefore could affect the molecular and physiological responses triggered by N starvation. The expression of *NRT2.4* seems to be differentially modulated in response to various abiotic stresses. Under drought stress, the expression of *NRT2.4* increases in leaves, whereas under salinity stress, the expression of *NRT2.4* strongly decreases in leaves and roots of tomato seedlings (Akbudak *et al.*, 2022). In our conditions, heat stress down-regulates *NRT2.4* regardless of the external N supply, which could have negative consequences on nutrient uptake. Thus, here we show that both warm and high temperatures seem to suppress the root response to N deficiency, since plants grown at -N combined with high temperatures show a similar LR density and *NRT2.4* expression than plants grown under optimal N conditions. These data suggest that changes in the external temperature should be considered when designing new fertilization programs.

## 5.5. Differences in root adaptation to warm temperature and N deficiency correlate with better shoot performance under N deficiency combined with heat stress.

To study shoot responses under the combination of heat stress and N deficiency, we used our previously identified *B. napus* varieties, Westar and Wesway, grown in pots under two different temperature treatments and two different N conditions using the TGRooZ to create a root-zone temperature gradient similar to natural soils. Our results indicate that under N deficiency alone, Westar reduced its biomass, leaf area and hypocotyl length, whereas Wesway showed increases in

those traits. Furthermore, under constant high shoot/root temperature, both varieties suppressed shoot growth regardless of the N concentration. However, in the TGRooZ, Wesway plants had a higher biomass, leaf area and hypocotyl length under the combination of high temperature and N deficiency compared to Westar.

Although studies reporting the effects of combined heat stress and N deficiency are scarce, variation in the response to heat stress among different *B. napus* genotypes has been previously observed (Singh *et al.*, 2008; Koscielny *et al.*, 2018). Heat stress has shown to decrease shoot length and biomass in *B. napus*, being consistent with our results (Ahmad *et al.*, 2021). In *Brassica campestris*, heat stress causes reductions in shoot biomass in both tolerant and sensitive cultivars, but these reductions are smaller in the tolerant cultivars (Yuan *et al.*, 2017). In our experiments, Wesway shows less reductions in shoot biomass under heat stress or under heat stress combined with N deficiency compared to Westar, suggesting that Wesway might be more tolerant. Variation in the shoot responses to N deficiency among different *B. napus* genotypes has been previously observed as well (Ye *et al.*, 2010; Wang *et al.*, 2015). Symptoms of leaf yellowing and senescence caused by N deficiency have also been reported in *B. napus* (Avice & Etienne, 2014; Sorin *et al.*, 2016; Safavi-Rizi *et al.*, 2018; Shen *et al.*, 2022) and in other crops like wheat, maize, rice and soybean (Crafts-Brandner *et al.*, 1998; Schulte auf'm Erley *et al.*, 2007; Zakari *et al.*, 2020; Zhang *et al.*, 2020c). This in consistent with our observations in both varieties in response to N deficiency after four weeks, although future analyses need to be done to precisely compare the senescence levels between varieties.

N deficiency has shown to alter the C/N ratio in leaves in several species like wheat, maize and citrus (Wang *et al.*, 2019; Tamele *et al.*, 2020; Huang *et al.*, 2022). *B. napus* plants submitted to combined boron and N deficiency increased their C/N ratio in leaves due to increased N remobilization from source to sink and increased sugar accumulation in leaves (Wang *et al.*, 2022b). Based on this, our data suggest that the combination of heat stress and N deficiency could increase sugar accumulation in leaves of Wesway as well, since this variety has a higher C/N ratio under the stress combination. Thus, our results indicate that Wesway presents more shoot and root adaptations under the combination of high temperature and N deficiency than Westar. This suggests that Wesway might be a more suitable variety to grow under N deficiency combined with warm temperature or heat stress.

## 5.6. The combination of warm temperature and Pi deficiency produces an additive negative effect on root traits in *B. napus*.

To understand the root responses to the combination of warm temperature and Pi deficiency in *B. napus*, we characterized the root architecture of different *B. napus* varieties grown under low Pi, warm temperature or the combination of both stresses. Our results indicate that whereas Pi deficiency alone had little effect on root architecture in our experimental conditions, Pi deficiency combined with warm temperature caused significant reductions in root depth and in the number and length of the lateral roots. These reductions are more severe than those caused by warm temperature alone, suggesting an additive negative effect of both stresses. In general, we observed a tendency to reduce Pi content in roots and shoots under Pi deficiency alone in several varieties, but under warm temperature or the stress combination, most varieties accumulated more Pi in roots and shoots than under optimal temperature.

There is little information on the effects of combined warm temperature and Pi deficiency in plants. Pi deficiency alone usually causes a reduction in the primary root growth and an increase in LR growth, effects that have been well studied in Arabidopsis (Al-Ghazi *et al.*, 2003; Crombez *et al*, 2019). In crops, however, Pi starvation alone has shown to produce differential effects, such as elongation of the primary root in rice (Shimizu *et al.*, 2004; Wissuwa *et al.*, 2005), whereas in maize the primary root is unaltered and the lateral root growth is suppressed (Mollier & Pellerin, 1999; Li *et al.*, 2012). In *B. oleracea*, different genotypes grown in a hydroponic system showed differential responses to Pi starvation, and several of them showed an unaltered root phenotype, similarly to the results obtained in this thesis (Pongrac *et al.*, 2020). In *B. napus*, a field study using different genotypes showed that long-term Pi starvation does not cause significant reductions in root biomass (Duan *et al.*, 2020), being also consistent with our results. In contrast, another study that monitored the effects of Pi starvation in *B. napus* at different developmental stages found that root length and LR density develop more slowly during the vegetative stage in low Pi conditions compared to high Pi conditions (Yuan *et al.*, 2016b). Thus, a possible explanation for the lack of significant alterations in the root system in our -Pi conditions could be that we measured the root traits only in the first seven days of treatments, but not in later developmental stages. On the other hand, Ren *et al.* (2011) observed a suppression

of the primary root growth and a slight increase in LR root number under Pi starvation in *B. napus*, but they applied a more extreme Pi deficiency (0.001 mM of Pi) compared to our Pi concentration (0.0025 mM of Pi), and they also used a high Pi concentration for the control treatment (1 mM of Pi) compared to us (0.312 mM of Pi). As mentioned above, the information regarding the effects of combined Pi starvation and warm temperature is scarce. In Arabidopsis, overexpression of heat shock factors suppresses the root responses to Pi deficiency, reducing lateral root growth and worsening the negative effects of Pi starvation (Zhao *et al.*, 2022), which is consistent with the phenotype of impaired root growth observed in our stress combination treatment.

Based on the observed root responses to combined -P and warm temperatures, we selected two genotypes with differential root responses to this stress combination: Wesway and Industry. Wesway shows small reductions in root depth and in LR number and length in response to -P, warm temperature or the combination of both stresses. On the other hand, Industry does not show significant alterations under Pi starvation or warm temperature, but experiences a significant reduction in root depth, LR density and LR length under the stress combination, suggesting a specific sensitivity to the stress combination that is not observed in Wesway. Interestingly, Industry shows a similar Pi content in all treatments, whereas Wesway slightly accumulates more Pi under the stress combination treatment. In shoots, Industry accumulates significantly higher Pi levels under the stress combination, whereas Wesway accumulates more Pi under the three stress conditions. Since the root system of Industry was more affected by the stress combination than that of Wesway, Industry could prioritize Pi accumulation in shoots over roots, which could compromise root growth. Previous studies in *B. napus* showed that the amount of free cellular Pi decreased in roots after 18 days of Pi deficiency (Chen *et al.*, 2015a). A possible explanation for the fact that we did not observe significant differences could be because we measured Pi content after 3 days of germination in a medium with optimal Pi followed by 7 days of Pi deficiency and in these conditions, *B. napus* plants might still have enough Pi reserves to develop without showing strong Pi deficiency-related symptoms. Ren *et al.* (2011) also observed a reduction in the free cellular Pi content in *B. napus*, but they applied a more severe Pi starvation treatment than the one applied in this study. Furthermore, the increased free cellular Pi concentrations observed at 29ºC-P could be explained by several reasons, including P mobilization from organic compounds to free cellular Pi or the increased expression of high affinity

Pi transporters, although based on our gene expression analyses this possibility seems to be less plausible. Under Pi starvation, plants can improve their Pi use efficiency by recycling Pi from organic phosphorous via hydrolases and by catabolizing phospholipids via phospholipases (Tran *et al.*, 2010 Nilsson *et al.*, 2010; Plaxton & Tran, 2011). Furthermore, plants grown under Pi starvation could activate APases and PAPs that can hydrolyse Pi from organic compounds and from intracellular Pi monoesters (Plaxton & Tran, 2011). These mechanisms are known to be activated under Pi starvation and could be the reason behind Pi accumulation in shoots and roots of both varieties at 29ºC-P.

Thus, we have characterized the effects of combined warm temperature and Pi deficiency in the root architecture of *B. napus* and found that both stresses have an additive negative effect, causing a suppression of root growth. We have shown that the effects of Pi deficiency on the root system are different when plants are grown under warm temperature than under optimal temperature, which means that plants could respond differently to Pi starvation under a climate change scenario. These results highlight the importance of studying the Pi starvation response under warm temperatures and identifying varieties that are tolerant to the combination of both stresses for crop genetic improvement programs.

## 5.7. The combination of warm temperature and Pi deficiency suppresses root growth by modifying hormonal and nutrient pathways.

To identify genes that are deregulated by the combination of warm temperature and Pi deficiency in *B. napus*, we performed a transcriptomic analysis in roots and shoots of the varieties Industry and Wesway grown under these stresses. In roots, both varieties showed little transcriptomic alterations caused by Pi deficiency alone, being consistent with our results in root traits, where most varieties seemed unaltered by Pi deficiency. The transcriptomic changes caused by the combination of Pi deficiency and warm temperature, however, were much stronger in both varieties, with a higher number of DEGs altered compared to warm temperature or Pi deficiency individually, thus supporting the additive effect observed in root traits.

We observed that both varieties up-regulate many genes involved in the inhibition of the primary root growth under the stress combination, but not under Pi deficiency alone, such as *BnCLE14*, *BnAMLT1* and *BnDTX43* and cytokinin

related genes also involved in the inhibition of the primary root growth, such as *BnARR1*. Induction of *ARR1*, a cytokinin-response gene, causes the repression of *SCR*, leading to a reduction in the primary root growth (Zhang *et al.*, 2013b). The CLE14 peptide is an important component of the Pi starvation response that participates in the inhibition of the primary root growth by blocking the activity of SCR and SHR, which releases WOX5, a negative regulator of the primary root growth (Gutiérrez-Alanís *et al.*, 2017; Figure 5.2). ALMT1 is a malate transporter that plays a role on the Pi starvation response (Mora-Macías *et al.*, 2017), whereas DTX43, also known as FRD3 is a member of the MATE efflux family of citrate transporters (Roschzttardtz *et al.*, 2011). Malate and citrate are secreted into the rhizosphere by roots under Pi starvation, and these compounds can increase soil acidification, which, together with microbe decomposition, increase Pi solubilization in the soil, ultimately leading to diffusion of solubilized Pi to the roots (Kirk *et al.*, 1999; Zhang *et al.*, 2020b). Based on our data, the combination of warm temperatures and Pi deficiency might trigger the exudation of malate and citrate to eventually increase Pi absorption. In addition, accumulation of malate and citrate in the apoplast, together with the accumulation of CLE14 can down-regulate SCR and SHR, thus leading to the inhibition of the primary root growth under Pi starvation (Crombez *et al.*, 2019; Figure 5.2). These data suggest that Pi starvation combined with warm temperature causes an inhibition of the primary root growth, which is consistent with our previous results, where both varieties decreased their root depth at 29ºC-P. We also observed that some of the genes involved in the suppression of the primary root growth are induced only in Industry at 29ºC-N but not in Wesway, suggesting a further reduction in root growth in this variety. Some of these genes are *BnLPR1* and *BnSTOP1*. LPR1 is an enzyme that mediates the conversion of $Fe^{2+}$ to $Fe^{3+}$ under Pi starvation, leading to the accumulation of $Fe^{3+}$ in the apoplast. Then, $Fe^{3+}$ forms a complex with malate that ultimately contributes to the inhibition of the primary root growth (Crombez *et al.*, 2019; Figure 5.2). On top of this, the transcription factor STOP1 directly regulates *LPR1* under Pi starvation (Balzergue *et al.*, 2017; Mora-Macías *et al.*, 2017). These results suggest that under the stress combination, Industry could activate mechanisms that supress the primary root growth to a greater extent than Wesway, leading to specific reductions in root depth at 29ºC-P.

In addition, we observed a down-regulation of genes related to cell wall organization, cell division and elongation at 29ºC-P in both varieties, such as *BnLAC17, BnFK,* or *BnDIM*. FK is crucial for cell division and organization, and

its absence leads to impaired root and shoot growth, with abnormalities in the root structure (Schrick *et al.*, 2000). DIM, also called DWF1, is a protein that participates on brassinosteroid biosynthesis and is crucial for lignin formation, contributing to proper secondary cell wall formation and cell elongation, and its absence leads to impaired root growth (Mussig *et al.*, 2003; Hossain *et al.*, 2012; Figure 5.2). Down-regulation of genes related to brassinosteroid biosynthesis as a consequence of Pi starvation has been previously reported, and contributes to reduced root growth (Singh *et al.*, 2014). Balanced brassinosteroid signalling is necessary for proper root growth, since decreases in brassinosteroid biosynthesis are associated with reductions in cell division and growth in the root meristem (González-García *et al.*, 2011). LAC17 has shown to be crucial for lignification in the root vascular tissue and necessary for proper root growth (Zhao *et al.*, 2013). Altogether, these results suggest that the combination of warm temperatures and Pi deficiency causes a reduction in cell division and an altered cell organization in roots, thus contributing to the observed reductions in overall root growth (Figure 5.2).

We also observed a down-regulation of several genes involved in LR development and auxin signalling and transport in Industry at 29ºC-P, but not in Wesway, such as *BnAUX1, BnPIN3* and *BnMYB77, BnIAA14*. In addition, *BnARF16* and *BnARF19*, which are involved in auxin signalling are down-regulated in both varieties. The phytohormone auxin is a central player in the Pi-starvation mediated suppression of LR growth (Castrillo *et al.*, 2017). Particularly, AUX1, an auxin transporter, is involved in the promotion of root hair development under Pi starvation (Bhosale *et al.*, 2018; Villaécija-Aguilar *et al.*, 2022), suggesting that Industry could reduce root hair formation under the stress combination. PIN auxin transporters are crucial for the development of lateral root primordia under Pi starvation (Xu *et al.*, 2005). *PIN3* is expressed under Pi starvation and can promote root elongation, and has been related to root gravitropism, being also involved in the elongation of the primary root (Lian *et al.*, 2023; Wang *et al.*, 2024a). *ARR1*, a cytokinin related gene, can also down-regulate *PIN3*, thus impairing auxin transport and reducing root growth (Zhu *et al.*, 2015). The transcription factor *MYB77* is a central player in the auxin signal transduction and *myb77* knockout mutants show impaired LR development (Shin *et al.*, 2007). Furthermore, both *ARF16* and *ARF19* are crucial for lateral root initiation and their absence suppresses LR formation (Okushima *et al.*, 2005; Shen *et al.*, 2013). In addition, IAA14 has shown to contribute to LR growth together with ARF19 (Narise *et al.*,

2010; Figure 5.2). In Arabidopsis, a dominant mutation in *IAA14* completely blocks LR formation (Fukaki *et al.*, 2002). These results suggest that the stress combination induces several mechanisms that impair LR development in both varieties, but more significantly in Industry, which is consistent with our results in root traits, where LR number and length was strongly reduced in Industry by the stress combination, but not by the individual stresses.

Finally, we observed that the stress combination causes a strong induction of genes related to ubiquitin activity in both varieties, and this induction is not present under the individual stresses, including genes like *BnUBC7, 11 14* or *17*. Ubiquitination has shown to play a central role in the response to Pi starvation (Iglesias *et al.*, 2013; Rojas-Triana *et al.*, 2013; Pan *et al.*, 2019). The enzymes UBC7 and UBC14 have shown to play a role in the response to multiple stress conditions such as salt, oxidative stress and ABA (Feng *et al.*, 2020). UBC11 seems to impair primary root and LR development via auxin signalling (Han *et al.*, 2023), which is consistent with our results, since both varieties reduced their root depth and LR number and length at 29ºC-P. This suggests that ubiquitination-dependent processes are specifically activated under the stress combination and not under the individual stresses, and could contribute to the observed reductions in root growth (Figure 5.2).

In summary, we have identified several processes that are specifically activated or repressed under the combination of warm temperature and Pi deficiency in *B. napus*. These results demonstrate that the root molecular responses to Pi starvation are significantly influenced by warm temperatures, and this should be considered in future studies due to the current effects of climate change in the global temperature.

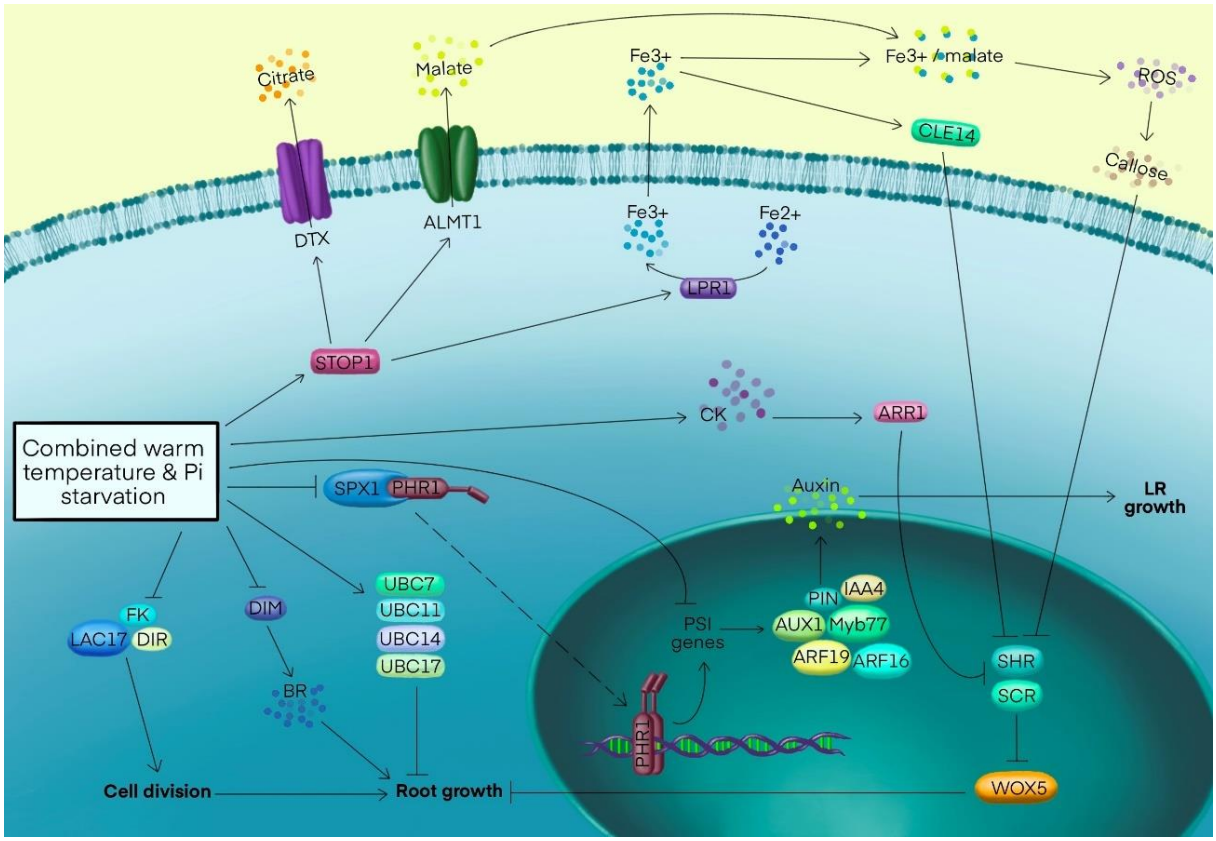


Figure 5.2: Model of the putative molecular responses to the combination of warm temperature and Pi deficiency in roots of *B. napus*. The stress combination causes an activation of *BnSTOP1*, which triggers the excretion of citrate and malate into the apoplast, as well as the activation of *BnLPR1*, which causes an accumulation of $Fe^{3+}$ in the apoplast. This would lead to the formation of callose and the activation of *BnCLE14*, which together suppress the activity of BnSCR and BnSHR, releasing BnWOX5 and negatively regulating root growth. The stress combination could also increase the levels of CK, leading to the induction of *BnARR1*, which has also an inhibitory effect on BnSCR and BnSHR. At the same time, the stress combination could cause a suppression of genes related to the auxin-mediated LR development, thus reducing LR growth, and enhance the activity of ubiquitin related genes associated with a suppression of root growth. Finally, the stress combination might also inhibit *BnDIM*, a BR precursor, and *BnFK*, *BnDIR* and *BnLAC17*, involved in cell division and organization, which ultimately contributes to the suppression of root growth.

## 5.8. The negative root response to combined warm temperature and Pi deficiency affects shoot development.

After identifying two genotypes, Industry and Wesway, with differential root responses to the combination of warm temperatures and Pi starvation, we aimed to study the effects of this variation on shoot performance. Thus, we performed an RNA-sequencing analysis in shoots of these two varieties submitted to the different treatments. RNA-sequencing analysis revealed few transcriptional changes caused

by Pi starvation alone in both varieties, being consistent with our results in roots. We also observe major transcriptional changes under the stress combination than under individual stresses, again being consistent with our results in roots, and supporting the hypothesis that both stresses have an additive effect. However, in shoots we observe a higher number of down-regulated than up-regulated genes at 29ºC-P in both varieties, which is different from our results in roots, where the number of down-regulated and up-regulated genes is similar. This is also observed under warm temperature alone and could indicate that a major number of molecular processes was suppressed in shoots, compared to roots. A speculative explanation is that in response to warm temperatures, plants reduce their growth and biochemical activity in shoots by down-regulating some of their processes. This would help plants to save energy and focus their resources in roots to prioritize Pi search and uptake from the soil.

The combination of warm temperatures and Pi deficiency in shoots down-regulates many genes related to phenylpropanoid metabolism in both varieties, including *BnLDOX, BnLAC10, 11* and *17*, being consistent with our results in roots. *LDOX* is known to promote anthocyanin accumulation under Pi starvation in Arabidopsis and tomato (Liu *et al.*, 2022; Wu *et al.*, 2023), whereas *LAC11* and *LAC17* participate in lignin production and are crucial for proper root and shoot growth (Khandal *et al.*, 2020). Our data indicate that the stress combination causes a reduction in lignin production in shoots of both varieties, which could alter other metabolic pathways and influence anthocyanin biosynthesis (Baxter & Stewart, 2013; Kim *et al.*, 2022). Anthocyanins are crucial compounds in the response to several abiotic and biotic stresses and they provide protection by increasing photosynthetic rates and improving nutrient uptake (Kaur *et al.*, 2023), and they are known to play a role on shoot responses to Pi starvation (Yin *et al.*, 2012). Again, these results suggest that the effects of combined Pi starvation and warm temperature differ from the effects of Pi starvation alone. Lignin plays a crucial role in cell wall stability and participates in water transport along the plant. Several abiotic and biotic stresses can cause alterations in lignin content (Moura *et al.*, 2010; Yadav & Chattopadhyay, 2023), and based on our results, we hypothesize that the combination of warm temperature and Pi deficiency could reduce lignin production and cause potential damage to cell walls. This is supported by the fact that the stress combination down-regulates expansin-related genes such as *BnEXPA1* and *BnEXPB3*. In *B. rapa*, EXPA1 has been related to proper shoot and root elongation (Muthusamy *et al.*, 2020), and in Arabidopsis,

EXPA1 ensures proper cell wall organization under stress conditions (Gao *et al.*, 2010). Based on these data, combined warm temperatures and Pi deficiency could potentially reduce shoot growth and elongation by reducing the expression of genes related to cell wall stability, lignin and anthocyanin accumulation.

Being consistent with our results in roots, the stress combination induces the expression of many genes related to ubiquitination in shoots of both varieties, like *BnUBC4, 11* and *14*, and reduces the expression of genes involved in hormone signalling, such as *BnAUX1, BnPIN3* and *BnIPT3*. UBC4 has been related to reduced sugar accumulation in shoots, as well as to enhanced leaf senescence (Wang *et al.*, 2022a), supporting the hypothesis that the stress combination negatively affects shoot development. Several of these hormone-related genes are also down-regulated in roots of Industry at 29ºC-P, but down-regulated in both varieties in shoots. These results suggest that the stress combination could trigger systemic hormonal changes in shoots that could explain the negative effects previously observed in the root system.

Overall, our results suggest that the combination of warm temperature and Pi deficiency have detrimental effects on shoot development, which correlates with the observed suppression on root growth. This suppression on root growth could impair nutrient uptake and homeostasis in the whole plant, ultimately affecting shoot development and many other processes, and could play a role in the observed suppression of genes related to phenylpropanoid biosynthesis, lignin and anthocyanin accumulation in shoots. At the same time, the possible impairment in shoot growth and anthocyanin accumulation could worsen the effects of Pi starvation in the whole plant, thus contributing to reductions in root growth. These results also suggest that the stress combination could cause a suppression of the auxin-mediated induction of LR growth via impairment of auxin shoot to root transport. Again, these results demonstrate the importance of studying plant responses to Pi deficiency under warm temperature to generate a more realistic environmental context that takes into account the global temperature changes caused by climate change.

## 5.9. The Pi starvation response mediated by the interaction between PHR and SPX proteins is conserved in *B. napus*.

To provide more insights into the Pi starvation responses in *B. napus*, we aimed to study the conserved mechanism that activates the Pi starvation response via the

SPX-PHR1 interaction. Thus, we identified and characterized the subcellular localization and function of one PHR1 (a MYB-CC protein) ortholog in *B. napus*. Our results indicate that the MYB-CC family of transcription factors contains 58 members in *B. napus*, two of them being potential orthologs of *A. thaliana* AtPHR1: BnMYB-CC1 and BnMYB-CC29. We found that BnMYB-CC1, also called BnPHR1 in this thesis, interacts with BnSPX1.1 in the nucleus. At the same time, BnPHR1 can induce the expression of *BnSPX1.1*, and BnSPX1.1 can impair the function of BnPHR1, thus reducing its own transcription in a negative feedback loop.

Recent studies also identified BnMYB-CC1 and BnMYB-CC29 as potential PHR1 orthologs. Overexpression of *BnMYB-CC29* in Arabidopsis and *B. napus* up-regulated several Pi-starvation induced genes and trigged the Pi starvation response (Ren *et al.*, 2012), whereas BnMYB-CC1 (or BnPHR1 in this thesis) can bind to the promoter of *BnPHT1;2* and has been related to enhanced LR development and Pi concentration (Liu *et al.*, 2023). This is consistent with our results, where BnPHR1 induced the expression of *BnSPX1.1*, another PSI gene, and supports the hypothesis that BnPHR1 might act as an activator of PSI genes, thus resembling its function in Arabidopsis and rice (Dong *et al.*, 2019; Zhou *et al.*, 2021). The fact that this molecular regulatory mechanism is conserved in *B. napus* suggests that other known components of this response could be conserved as well. For instance, the interaction between SPX and PHR proteins is mediated by InsP6 in Arabidopsis and InsP8 in rice, and Pi starvation causes a decrease in the levels of these InsPs, leading to a structural change in the SPX protein that de-couples its interaction with PHR proteins (Dong *et al.*, 2019; Zhou *et al.*, 2021). Further research is needed to elucidate the role of InsPs on the interaction between PHR1 and SPX1 in *B. napus*. Furthermore, PHR proteins are known to form dimers to activate the expression of PSI genes (Sega & Pacak, 2019). The fact that this mechanism is conserved in *B. napus* suggests the possibility that they form dimers as well, but more research is needed to confirm this. Our results provide insights into the cellular localization and function of PHR1 in *B. napus* and the identification of this conserved mechanism could facilitate future research oriented toward understanding the Pi starvation response mechanisms in *B. napus*.

## 5.10. The combination of warm temperature and N deficiency represses genes involved in the Pi starvation response.

Our transcriptomic analysis revealed that N deficiency, warm temperature and their combination cause a strong suppression of many genes related to the Pi starvation response in roots of *B. napus*, including *BnSPX3, BnSPX1, BnPHO1, BnPECP2, BnPAP7, 17* and *BnIPS3*. To study their role, we analysed the changes in different root traits in T-DNA mutant seedlings of some of these genes grown under these conditions. The *spx1spx2* double mutant shows a similar LR density than Col-0 under normal conditions, but higher LR density under N deficiency, warm temperatures or the combination of both stresses. The *spx3* mutant shows a different effect, with higher LR density than Col-0 under normal conditions and under the individual stresses, but the same LR density than Col-0 under the stress combination. The fact that these stress treatments alter LR density in the two mutants suggests that these PSI genes might play a role in the root responses to N deficiency, warm temperature or the combination of both stresses, affecting LR growth and having potential effects on nutrient uptake.

Decreases in the expression of genes related to the Pi starvation response as a consequence of high temperatures have been previously reported in Arabidopsis and barley (Pacak *et al.*, 2016; González-García *et al.*, 2023). At the same time, N deficiency alone strongly suppresses the Pi starvation response, causing the down-regulation of many PSI genes in Arabidopsis, rice, wheat and maize (Schlüter *et al.*, 2012; Medici *et al.*, 2019). Furthermore, the regulatory pathways of the N and Pi starvation responses have shown to interact in different ways. NITROGEN LIMITATION ADAPTION (NLA) is involved in the adaptive response to N deficiency (Peng *et al.*, 2007), and encodes a RING E3 ubiquitin ligase that works synergistically with PHO2 to degrade PHT transporters and modulate Pi homeostasis (Lin *et al.*, 2013). Medici *et al.* (2015) identified a GARP transcription factor, *AtNIGT1/HRS1*, that is involved in the suppression of the primary root growth under Pi starvation, but only when nitrate is present, and this transcription factor is controlled by NRT1.1. Another GARP transcription factor, GLK1, positively regulates the Pi starvation response by increasing the activity of PHR1 through direct interaction, and the function of GLK1 strongly depends on the N supply (Li *et al.*, 2022a). This suggests that, since the suppression of the primary root growth is one of the typical mechanisms of the Pi starvation response (Crombez *et al.*, 2019), these mechanisms need to be suppressed under N

starvation to allow the enlargement of the primary root during the adaptation response to this nutritional stress (Gruber *et al.*, 2013; Giehl & von Wirén, 2014). The activation of many PSI genes, including *SPX1, IPS1* and *PHT1-1* depends on N availability, and severe N deficiency has shown to repress the expression of these genes even under Pi starvation (Medici *et al.*, 2019). These studies suggest that the Pi starvation response is only activated when there is a certain level of N availability. Furthermore, NLA can directly degrade PHR1 in response to N deficiency, thus suppressing the Pi starvation response (Park *et al.*, 2023). On the other hand, under Pi starvation and optimal N conditions, the NIGT1 transcription factor can down-regulate *NRT1.1* and *NRT2.1* and simultaneously up-regulate *PHT1.1* and *PHT1.4* to favour phosphate uptake instead of nitrate uptake (Ueda *et al.*, 2020a; Wang *et al.*, 2020b; Wang *et al.*, 2023a). At the same time, Pi starvation alone can promote ammonium uptake via STOP1 (Tian *et al.*, 2021). Pi starvation signalling is known to be affected by other abiotic stresses as well, such as salinity, exogenous ABA or drought (Baek *et al.*, 2017). These studies suggest that many stresses influence the Pi starvation response, and particularly, high temperatures as well as N deficiency seem to suppress this response.

Several studies suggest that N deficiency suppresses the Pi starvation response in favour of the N starvation response under both stresses (Medici *et al.*, 2019; Krouk & Kiba, 2020; Li *et al.*, 2022a; Park *et al.*, 2023). Under this scenario, we could hypothesize that the plant prioritizes the activation of the N starvation response when encountered with both nutritional deficiencies simultaneously, which suggests a preference for nitrogen uptake/usage over phosphate. At the same time, our previous results regarding the effects of high temperature combined with N deficiency (see Discussion: 5.4.) suggest that under heat stress, the plant suppresses the N starvation response in favour of activating the heat stress response. Indeed, some studies show that under heat stress, the plant is unable to acquire N and decreases the activity of proteins involved in N transport (Lahti *et al.*, 2005; Giri *et al.*, 2017). Thus, we can speculate that the plant prioritizes the adaptation to heat stress before addressing any nutrient deficiencies, and when the temperature requirements are met, the plant prioritizes nitrogen over phosphate. This makes sense considering that an excessive and prolonged heat stress can severely compromise plant growth.

# 6. CONCLUSIONS

1. The effect of N deficiency combined with warm temperature in the lateral roots of *B. napus* is compensatory. Whereas N deficiency increases the length of the upper lateral roots, warm temperature suppresses upper LR growth, and the stress combination produces an intermediate phenotype, with significant variability between different *B. napus* varieties.
2. The capacity to develop longer lateral roots under the combination of warm temperature and N deficiency correlates with the induction of genes related to oxidoreductase activity, N metabolism and transport, and the ABA-mediated response to stress.
3. The induction of small peptides that move from shoot to root and genes related to ABA signalling correlate with a better capacity to develop longer lateral roots under the combination of warm temperature and N deficiency.
4. The development of longer lateral roots under the combination of warm temperature and N deficiency results in increased shoot biomass and C/N ratio under the combination of N deficiency and heat stress.
5. Arabidopsis seedlings submitted to N deficiency together with elevated temperature are less responsive to N deficiency and seem to prioritize the response to high temperature. Consequently, N deficiency causes less alterations in LR density and in the expression of nitrate transporters in roots when combined with high temperature.
6. *B. napus* shows mild root morphological alterations in response to Pi deficiency alone. However, when Pi deficiency is combined with warm temperatures, the primary and lateral root growth are severely reduced, suggesting an additive negative effect of both stresses.
7. Reductions in root growth observed under combined warm temperature and Pi deficiency might be caused by the combination of several mechanisms like Fe-dependent inhibition of the primary root growth, reduced expression of genes related to cell division and elongation, reduced expression of auxin-related genes involved in lateral root development and an increased ubiquitin activity.

8. Combined warm temperature and Pi deficiency might cause a reduction in the biosynthesis of phenylpropanoids, anthocyanins and lignin in shoots.
9. The regulatory mechanism of the Pi starvation response mediated by PHR1 and SPX1 is conserved in *B. napus*.
10. The repression of genes related to the Pi starvation response is part of the molecular responses to combined warm temperature and N deficiency.

# References


Aggarwal, S., Kumar, A., Jain, M., Sudan, J., Singh, K., Kumari, S., & Mustafiz, A. (2020). C-terminally encoded peptides (CEPs) are potential mediators of abiotic stress response in plants. *Physiol. Mol. Biol. Plants* 26, 2019-2033. doi: 10.1007/s12298-020-00881-4.

Agnolucci, P., Rapti, C., Alexander, P., De Lipsis, V., Holland, R. A., Eigenbrod, F., & Ekins, P. (2020). Impacts of rising temperatures and farm management practices on global yields of 18 crops. *Nat. Food* 1(9), 562-571. doi: 10.1038/s43016-020-00148-x.

Ahmad, M., Waraich, E. A., Hussain, S., Ayyub, C. M., Ahmad, Z., & Zulfiqar, U. (2021). Improving heat stress tolerance in Camelina sativa and Brassica napus through thiourea seed priming. *J. Plant Growth Regul.* 41, 1-17. doi: 10.1007/s00344-021-10482-4.

Ahmed, I. M., Dai, H., Zheng, W., Cao, F., Zhang, G., Sun, D., & Wu, F. (2013). Genotypic differences in physiological characteristics in the tolerance to drought and salinity combined stress between Tibetan wild and cultivated barley. *Plant Physiol. Biochem.* 63, 49-60. doi: 10.1016/j.plaphy.2012.11.004.

Akbudak, M. A., Filiz, E., & Çetin, D. (2022). Genome-wide identification and characterization of high-affinity nitrate transporter 2 (NRT2) gene family in tomato (Solanum lycopersicum) and their transcriptional responses to drought and salinity stresses. *J. Plant Physiol.* 272, 153684. doi: 10.1016/j.jplph.2022.153684.

Alagarasan, G. (2024). Duality of jacalin-related lectin: Master regulator and chaperone. *Plant Commun.* 5(2). doi: 10.1016/j.xplc.2024.100825.

Alarcón, M. V., Lloret-Salamanca, A., Lloret, P. G., Iglesias, D. J., Talón, M., & Salguero, J. (2009). Effects of antagonists and inhibitors of ethylene biosynthesis on maize root elongation. *Plant Signaling Behav.* 4(12), 1154-1156. doi: 10.4161/psb.4.12.9948.

Al-Ghazi, Y., Muller, B., Pinloche, S., Tranbarger, T. J., Nacry, P., Rossignol, M., ... & Doumas, P. (2003). Temporal responses of Arabidopsis root architecture to phosphate starvation: evidence for the involvement of auxin signalling. *Plant Cell Environ.* 26(7), 1053-1066. doi: 10.1046/j.1365-3040.2003.01030.x.

Alhdad, G. M., Seal, C. E., Al-Azzawi, M. J., & Flowers, T. J. (2013). The effect of combined salinity and waterlogging on the halophyte Suaeda maritima: the role of antioxidants. *Environ. Exp. Bot.* 87, 120-125. doi: 10.1016/j.envexpbot.2012.10.010.

Ali, A. Y. A., Ibrahim, M. E. H., Zhou, G., Nimir, N. E. A., Jiao, X., Zhu, G., et al. (2020). Exogenous jasmonic acid and humic acid increased salinity tolerance of sorghum. *Agron. J.* 112, 871–884. doi: 10.1002/agj2.20072

Ali, A., & Yun, D. J. (2020). Arabidopsis HOS15 is a multifunctional protein that negatively regulate ABA-signaling and drought stress. *Plant Biotechnol. Rep.* 14, 163-167. doi: 10.1007/s11816-020-00600-1.

Al-Mamun, M. H., Cazzonelli, C. I., & Krishna, P. (2024). BZR1 and BES1 transcription factors mediate brassinosteroid control over root system architecture in response to nitrogen availability. *Front. Plant Sci.* 15, 1387321. doi: 10.3389/fpls.2024.1387321.

Aloni, B., Pashkar, T., Karni, L., & Daie, J. (1991). Nitrogen supply influences carbohydrate partitioning of pepper seedlings and transplant development. *J. American Society for Horticultural Science* 116(6), 995-999. doi: 10.21273/JASHS.116.6.995.

Alvarez, J. M., Riveras, E., Vidal, E. A., Gras, D. E., Contreras-López, O., Tamayo, K. P., ... & Gutiérrez, R. A. (2014). Systems approach identifies TGA 1 and TGA 4 transcription factors as important regulatory components of the nitrate response of A rabidopsis thaliana roots. *Plant J.* 80(1), 1-13. doi: 10.1111/tpj.12618.

Ames, B. N. (1966). [10] Assay of inorganic phosphate, total phosphate and phosphatases. *Methods Enzymol.* 8, 115-118. Academic Press. doi: 10.1016/0076-6879(66)08014-5.

Araya, T., von Wirén, N., & Takahashi, H. (2016). CLE peptide signaling and nitrogen interactions in plant root development. *Plant Mol. Biol.* 91, 607-615. doi: 10.1007/s11103-016-0472-9.

Ashapkin, V. V., Kutueva, L. I., Aleksandrushkina, N. I., and Vanyushin, B. F. (2020). Epigenetic Mechanisms of plant adaptation to biotic and abiotic stresses. *Int. J. Mol. Sci*. 21:7457. doi: 10.3390/ijms21207457.

Ashraf, M. J. B. A. (2009). Biotechnological approach of improving plant salt tolerance using antioxidants as markers. *Biotechnol. Adv.* 27(1), 84-93. doi: 10.1016/j.biotechadv.2008.09.003.

Atkinson, J. A., Pound, M. P., Bennett, M. J., and Wells, D. M. (2019). Uncovering the hidden half of plants using new advances in root phenotyping. *Curr. Opin. Biotechnol*. 55, 1–8. doi: 10.1016/j.copbio.2018.06.002.

Atkinson, J. A., Wingen, L. U., Griffiths, M., Pound, M. P., Gaju, O., Foulkes, M. J., ... & Wells, D. M. (2015). Phenotyping pipeline reveals major seedling root growth QTL in hexaploid wheat. *J. Exp. Bot.* 66(8), 2283-2292. doi: 10.1093/jxb/erv006.

Atkinson, N. J., and Urwin, P. E. (2012). The interaction of plant biotic and abiotic stresses: from genes to the field. *J. Exp. Bot*. 63, 3523–3543. doi: 10.1093/jxb/ers100.

Avice, J. C., & Etienne, P. (2014). Leaf senescence and nitrogen remobilization efficiency in oilseed rape (*Brassica napus L.*). *J. Exp. Bot.* 65(14), 3813-3824. doi: 10.1093/jxb/eru177.

Baek, D., Chun, H. J., Yun, D. J., & Kim, M. C. (2017). Cross-talk between phosphate starvation and other environmental stress signaling pathways in plants. *Mol. Cells* 40(10), 697-705. doi: 10.14348/molcells.2017.0192.

Balcerowicz, D., Schoenaers, S., & Vissenberg, K. (2015). Cell fate determination and the switch from diffuse growth to planar polarity in Arabidopsis root epidermal cells. *Front. Plant Sci.* 6, 1163. doi: 10.3389/fpls.2015.01163.

Balzergue, C., Dartevelle, T., Godon, C., Laugier, E., Meisrimler, C., Teulon, J. M., ... & Desnos, T. (2017). Low phosphate activates STOP1-ALMT1 to rapidly inhibit root cell elongation. *Nat. Commun.* 8(1), 15300. doi: 10.1038/ncomms15300.

Bancroft, I. (2011). Genetics and Genomics of the Brassicaceae (pp. 585-596). R. Schmidt (Ed.). New York:: Springer.

Bandara, N., Akbari, A., Esparza, Y., & Wu, J. (2018). Canola protein: A promising protein source for delivery, adhesive, and material applications. *J. Am. Oil Chem. Soc.* 95(8), 1075-1090. doi: 10.1002/aocs.12039.

Bandurska, H. (2005). The effect of salicylic acid on barley response to water deficit. *Acta Physiol. Plant*. 27, 379–386. doi: 10.1007/s11738-005-0015-5.

Bassirirad, H. (2000). Kinetics of nutrient uptake by roots: responses to global change. *New Phytol*. 147, 155–169. doi: 10.1046/j.1469-8137.2000.00682.x

Batool, M., El-Badri, A. M., Hassan, M. U., Haiyun, Y., Chunyun, W., Zhenkun, Y., ... & Zhou, G. (2022). Drought stress in Brassica napus: effects, tolerance mechanisms, and management strategies. *J. Plant Growth Regul.* 1-25. doi: 10.1007/s00344-021-10542-9.

Baxter, H. L., & Stewart Jr, C. N. (2013). Effects of altered lignin biosynthesis on phenylpropanoid metabolism and plant stress. *Biofuels* 4(6), 635-650. doi: 10.4155/bfs.13.56.

Bennett, T., van den Toorn, A., Willemsen, V., & Scheres, B. (2014). Precise control of plant stem cell activity through parallel regulatory inputs. *Development* 141(21), 4055-4064. doi: 10.1242/dev.110148.

Berka, M., Luklová, M., Dufková, H., Berková, V., Novák, J., Saiz-Fernández, I., ... & Černý, M. (2020). Barley root proteome and metabolome in response to cytokinin and abiotic stimuli. *Front. Plant Sci.* 11, 590337. doi: 10.3389/fpls.2020.590337.

Bernstein, N., & Kafkafi, U. (2002). Root growth under salinity stress. In Plant Roots (pp. 1222-1250). CRC Press.

Bhardwaj, H. L., & Hamama, A. A. (2003). Accumulation of glucosinolate, oil, and erucic acid in developing Brassica seeds. *Ind. Crops Prod.* 17(1), 47-51. doi: 10.1016/S0926-6690(02)00058-4.

Bhosale, R., Giri, J., Pandey, B. K., Giehl, R. F., Hartmann, A., Traini, R., ... & Swarup, R. (2018). A mechanistic framework for auxin dependent Arabidopsis root hair elongation to low external phosphate. *Nat. Commun.* 9(1), 1409. doi: 10.1038/s41467-018-03851-3.

Bita, C. E., & Gerats, T. (2013). Plant tolerance to high temperature in a changing environment: scientific fundamentals and production of heat stress-tolerant crops. *Front. Plant Sci.* 4, 273. doi: 10.3389/fpls.2013.00273.

Borgen, B. H., Thangstad, O. P., Ahuja, I., Rossiter, J. T., & Bones, A. M. (2010). Removing the mustard oil bomb from seeds: transgenic ablation of myrosin cells in oilseed rape (Brassica napus) produces MINELESS seeds. *J. Exp. Bot.* 61(6), 1683-1697. doi: 10.1093/jxb/erq039.

Borges, C. E., Von dos Santos Veloso, R., Da Conceição, C. A., Mendes, D. S., Ramirez-Cabral, N. Y., Shabani, F., ... & Da Silva, R. S. (2023). Forecasting Brassica napus production under climate change with a mechanistic species distribution model. *Sci. Rep.* 13(1), 12656. doi: 10.1038/s41598-023-38910-3.

Boter, M., Pozas, J., Jarillo, J. A., Piñeiro, M., & Pernas, M. (2023). Brassica napus roots use different strategies to respond to warm temperatures. *Int. J. Mol. Sci.* 24(2), 1143. doi: 10.3390/ijms24021143.

Bouguyon, E., Perrine-Walker, F., Pervent, M., Rochette, J., Cuesta, C., Benkova, E., ... & Nacry, P. (2016). Nitrate controls root development through posttranscriptional regulation of the NRT1. 1/NPF6. 3 transporter/sensor. *Plant Physiol.* 172(2), 1237-1248. doi: 10.1104/pp.16.01047.

Bowman, M. J., Willis, D. K., & Simon, P. W. (2014). Transcript abundance of phytoene synthase 1 and phytoene synthase 2 is associated with natural variation of storage root carotenoid pigmentation in carrot. *Journal of the American Society for Horticultural Science* 139(1), 63-68. doi: 10.21273/JASHS.139.1.63.

Bravo-F, P., and Uribe, E. G. (1981). Temperature dependence of the concentration kinetics of absorption of phosphate and potassium in corn roots. *Plant Physiol.* 674, 815–819. doi: 10.1104/pp.67.4.815.

Brumos, J., Robles, L. M., Yun, J., Vu, T. C., Jackson, S., Alonso, J. M., & Stepanova, A. N. (2018). Local auxin biosynthesis is a key regulator of plant development. *Dev. Cell* 47(3), 306-318. doi: 10.1016/j.devcel.2018.09.022.

Bustos, R., Castrillo, G., Linhares, F., Puga, M. I., Rubio, V., Pérez-Pérez, J., ... & Paz-Ares, J. (2010). A central regulatory system largely controls transcriptional activation and repression responses to phosphate starvation in Arabidopsis. *PLoS Genet.* 6(9), e1001102. doi: 10.1371/journal.pgen.1001102.

Bybordi, A., & Tabatabaei, J. (2009). Effect of salinity stress on germination and seedling properties in canola cultivars (Brassica napus L.). *Notulae Botanicae Horti Agrobotanici Cluj-Napoca* 37(2), 71-76. doi: 10.15835/nbha3723299.

Caba, J. M., Centeno, M. L., Fernández, B., Gresshoff, P. M., & Ligero, F. (2000). Inoculation and nitrate alter phytohormone levels in soybean roots: differences between a supernodulating mutant and the wild type. *Planta* 211, 98-104. doi: 10.1007/s004250000265.

Calleja-Cabrera, J., Boter, M., Oñate-Sánchez, L., and Pernas, M. (2020). Root growth adaptation to climate change in crops. *Front. Plant Sci*. 11:544. doi:10.3389/fpls.2020.00544.

Campos-García, T., Molina-Torres, J., & Overmyer, K. (2021). Reactive oxygen species signalling is involved in alkamide-induced alterations in root development. *bioRxiv*, 2021-12. doi: 10.1101/2021.12.23.474045.

Canvin, D. T. (1965). The effect of temperature on the oil content and fatty acid composition of the oils from several oil seed crops. *Can. J. Bot.* 43(1), 63-69. doi: 10.1139/b65-008.

Cao, Y., Song, F., Goodman, R. M., and Zheng, Z. (2006). Molecular characterization of four rice genes encoding ethylene-responsive transcriptional factors and their expressions in response to biotic and abiotic stress. *J. Plant Physiol*. 163, 1167–1178. doi: 10.1016/j.jplph.2005.11.004.

Castrillo, G., Teixeira, P. J. P. L., Paredes, S. H., Law, T. F., De Lorenzo, L., Feltcher, M. E., ... & Dangl, J. L. (2017). Root microbiota drive direct integration of phosphate stress and immunity. *Nature*, 543(7646), 513-518. doi: 10.1038/nature21417.

Catlin, P. B. (1996). Root systems and root physiology. *Almond Production Manual* 107-12.

Cavell, A. C., Lydiate, D. J., Parkin, I. A. P., Dean, C., & Trick, M. (1998). Collinearity between a 30-centimorgan segment of Arabidopsis thaliana chromosome 4 and duplicated regions within the *Brassica napus* genome. *Genome* 41(1), 62-69. doi: 10.1139/g97-097.

Chacón-López, A., Ibarra-Laclette, E., Sánchez-Calderón, L., Gutiérrez-Alanís, D., & Herrera-Estrella, L. (2011). Global expression pattern comparison between low phosphorus insensitive 4 and WT Arabidopsis reveals an important role of reactive oxygen species and jasmonic acid in the root tip response to phosphate starvation. *Plant Signaling Behav.* 6(3), 382-392. doi: 10.4161/psb.6.3.14160.

Chai, S., Chen, J., Yue, X., Li, C., Zhang, Q., De Dios, V. R., ... & Tan, W. (2022). Interaction of BES1 and LBD37 transcription factors modulates brassinosteroid-regulated root forging response under low nitrogen in Arabidopsis. *Front. Plant Sci.* 13, 998961. doi: 10.3389/fpls.2022.998961.

Chalhoub, B., Denoeud, F., Liu, S., Parkin, I. A., Tang, H., Wang, X., ... & Wincker, P. (2014). Early allopolyploid evolution in the post-Neolithic *Brassica napus* oilseed genome. *Science*, 345(6199), 950-953. doi: 10.1126/science.1253435.

Chaudhry, S., and Sidhu, G. P. S. (2021). Climate change regulated abiotic stress mechanisms in plants: a comprehensive review. *Plant Cell Rep*. 41, 1–31. doi: 10.1007/s00299-021-02759-5.

Chen, S., Ding, G., Wang, Z., Cai, H., & Xu, F. (2015a). Proteomic and comparative genomic analysis reveals adaptability of *Brassica napus* to phosphorus-deficient stress. *J. Proteomics* 117, 106-119. doi: 10.1016/j.jprot.2015.01.012.

Chen, S., Zhao, H., Ding, G., & Xu, F. (2015b). Genotypic differences in antioxidant response to phosphorus deficiency in *Brassica napus*. *Plant Soil*. 391, 19-32. doi: 10.1007/s11104-015-2395-7.

Chen, D., Wang, S., Xiong, B., Cao, B., & Deng, X. (2015c). Carbon/nitrogen imbalance associated with drought-induced leaf senescence in Sorghum bicolor. *PloS one* 10(8), e0137026. doi: 10.1371/journal.pone.0137026.

Chew, S. C. (2020). Cold-pressed rapeseed (*Brassica napus*) oil: Chemistry and functionality. *Food Res. Int.* 131, 108997. doi: 10.1016/j.foodres.2020.108997.

Choi, K., Khan, R., and Lee, S. W. (2021). Dissection of plant microbiota and plant microbiome interactions. *J. Microbiol*. 59, 281–291. doi: 10.1007/s12275-021-0619-5.

Clifton, R., Millar, A. H., & Whelan, J. (2006). Alternative oxidases in Arabidopsis: a comparative analysis of differential expression in the gene family provides new insights into function of

non-phosphorylating bypasses. *Biochim. Biophys. Acta (BBA)-Bioenergetics* 1757(7), 730-741. doi: 10.1016/j.bbabio.2006.03.009.

Cock, P. J., Fields, C. J., Goto, N., Heuer, M. L., & Rice, P. M. (2010). The Sanger FASTQ file format for sequences with quality scores, and the Solexa/Illumina FASTQ variants. *Nucleic Acids Res.* 38(6), 1767-1771. doi: 10.1093/nar/gkp1137.

Comas, L. H., Becker, S. R., Cruz, V. M. V., Byrne, P. F., & Dierig, D. A. (2013). Root traits contributing to plant productivity under drought. *Front. Plant Sci.* 4, 442. doi: 10.3389/fpls.2013.00442.

Conesa, C. M., Saez, A., Navarro-Neila, S., de Lorenzo, L., Hunt, A. G., Sepúlveda, E. B., ... & Del Pozo, J. C. (2020). Alternative polyadenylation and salicylic acid modulate root responses to low nitrogen availability. *Plants*, 9(2), 251. doi: 10.3390/plants9020251.

Corbesier, L., Bernier, G., & Périlleux, C. (2002). C: N ratio increases in the phloem sap during floral transition of the long-day plants Sinapis alba and Arabidopsis thaliana. *Plant Cell Physiol.* 43(6), 684-688. doi: 10.1093/pcp/pcf071.

Crafts-Brandner, S. J., Hölzer, R., & Feller, U. (1998). Influence of nitrogen deficiency on senescence and the amounts of RNA and proteins in wheat leaves. *Physiol. Plant.* 102(2), 192-200. doi: 10.1034/j.1399-3054.1998.1020206.x.

Crombez, H., Motte, H., & Beeckman, T. (2019). Tackling plant phosphate starvation by the roots. *Dev. Cell*, 48(5), 599-615. doi: 10.1016/j.devcel.2019.01.002.

Cui, Y. N., Li, X. T., Yuan, J. Z., Wang, F. Z., Wang, S. M., & Ma, Q. (2019). Nitrate transporter NPF7. 3/NRT1. 5 plays an essential role in regulating phosphate deficiency responses in Arabidopsis. *Biochem. Biophys. Res. Commun.* 508(1), 314-319. doi: 10.1016/j.bbrc.2018.11.118.

Czyzewicz, N., & De Smet, I. (2016). The Arabidopsis thaliana CLAVATA3/EMBRYO-SURROUNDING REGION 26 (CLE26) peptide is able to alter root architecture of Solanum lycopersicum and *Brassica napus*. *Plant Signaling Behav.* 11(1), e1118598. doi: 10.1080/15592324.2015.1118598.

Dai, Z., Yu, M., Chen, H., Zhao, H., Huang, Y., Su, W., ... & Xu, J. (2020). Elevated temperature shifts soil N cycling from microbial immobilization to enhanced mineralization, nitrification and denitrification across global terrestrial ecosystems. *Global Change Biol.* 26(9), 5267-5276. doi: 10.1111/gcb.15211.

Damiran, D., & McKinnon, J. J. (2018). Evaluation of wheat-based dried distillers grains with solubles or canola meal derived from Brassica napus seed as an energy source for feedlot steers. *Transl. Anim. Sci.* 2(suppl_1), S139-S144. doi: 10.1093/tas/txy051.

Das, K. K., Mohapatra, A., George, A. P., Chavali, S., Witzel, K., & Ramireddy, E. (2023). The proteome landscape of the root cap reveals a role for the jacalin-associated lectin JAL10 in the salt-induced endoplasmic reticulum stress pathway. *Plant Commun.* 4(6). doi: 10.1016/j.xplc.2023.100726.

Dash, M., Yordanov, Y. S., Georgieva, T., Kumari, S., Wei, H., & Busov, V. (2015). A systems biology approach identifies new regulators of poplar root development under low nitrogen. *Plant J.* 84(2), 335-346. doi: 10.1111/tpj.13002.

Datta, S., Prescott, H., & Dolan, L. (2015). Intensity of a pulse of RSL4 transcription factor synthesis determines Arabidopsis root hair cell size. *Nat. Plants* 1, 15138. doi: 10.1038/nplants.2015.138.

Davies, W. J., and Bacon, M. A. (2003). "Adaptation of roots to drought," in Root Ecology, eds H. de Kroon and E. J. W. Visser (Heidelberg: Springer). 173–192.

de Ollas, C., Hernando, B., Arbona, V., and Gómez-Cadenas, A. (2013). Jasmonic,acid transient accumulation is needed for abscisic acid increase in citrus roots under drought stress conditions. *Physiol. Plant.* 147, 296–306. doi: 10.1111/j.1399-3054.2012.01659.x.

De Smet, I., Vassileva, V., De Rybel, B., Levesque, M. P., Grunewald, W., Van Damme, D., ... & Beeckman, T. (2008). Receptor-like kinase ACR4 restricts formative cell divisions in the Arabidopsis root. *Science* 322(5901), 594-597. doi: 10.1126/science.1160158.

Del Gatto, A., Melilli, M. G., Raccuia, S. A., Pieri, S., Mangoni, L., Pacifico, D., ... & Mengarelli, C. (2015). A comparative study of oilseed crops (*Brassica napus* L. subsp. *oleifera* and *Brassica carinata* A. Braun) in the biodiesel production chain and their adaptability to different Italian areas. *Ind. Crops Prod.* 75, 98-107. doi: 10.1016/j.indcrop.2015.04.029.

Delamare, J., Brunel-Muguet, S., Morvan-Bertrand, A., Cantat, O., Firmin, S., Trinsoutrot-Gattin, I., ... & Personeni, E. (2023). Thermopriming effects on root morphological traits and root exudation during the reproductive phase in two species with contrasting strategies: *Brassica napus* (L.) and *Camelina sativa* (L.) Crantz. *Environ. Exp. Bot.* 210, 105318. doi: 10.1016/j.envexpbot.2023.105318.

Delk, N. A., Johnson, K. A., Chowdhury, N. I., & Braam, J. (2005). CML24, regulated in expression by diverse stimuli, encodes a potential $Ca^{2+}$ sensor that functions in responses to abscisic acid, daylength, and ion stress. *Plant Physiol.* 139(1), 240-253. doi: 10.1104/pp.105.062612.

DeLucia, E. H., Heckathorn, S. A., and Day, T. A. (1992). Effects of soil temperature on growth, biomass allocation and resource acquisition of *Andropogon gerardii* Vitman. *New Phytol.* 120, 543–549. doi: 10.1111/j.1469-8137.1992.tb01804.x.

Dempewolf, H., Eastwood, R. J., Guarino, L., Khoury, C. K., Müller, J. V., and Toll, J. (2014). Adapting agriculture to climate change: a global initiative to collect, conserve, and use crop wild relatives. *Agroecol. Sustain. Food Syst.* 38, 369–377. doi: 10.1080/21683565.2013.870629.

Deng, P., Wang, L., Cui, L., Feng, K., Liu, F., Du, X., et al. (2015). Global identification of microRNAs and their targets in barley under salinity stress. *PLoS One* 10 (9) :e0137990. doi: 10.1371/journal.pone.0137990.

Deolu-Ajayi, A. O., Meyer, A. J., Haring, M. A., Julkowska, M. M., & Testerink, C. (2019). Genetic loci associated with early salt stress responses of roots. *IScience* 21, 458-473. doi: 10.1016/j.isci.2019.10.043.

Desikan, R., Cheung, M. K., Bright, J., Henson, D., Hancock, J. T., and Neill, S. J. (2004). ABA, hydrogen peroxide and nitric oxide signalling in stomatal guard cells. *J. Exp. Bot.* 55, 205–212. doi: 10.1093/jxb/erh033.

Ding, L., Li, Y., Wang, Y., Gao, L., Wang, M., Chaumont, F., et al. (2016). Root ABA accumulation enhances rice seedling drought tolerance under ammonium supply: interaction with aquaporins. *Front. Plant Sci.* 7:1206. doi: 10.3389/fpls.2016.01206.

Ding, Y., Liu, N., Virlouvet, L., Riethoven, J. J., Fromm, M., & Avramova, Z. (2013). Four distinct types of dehydration stress memory genes in *Arabidopsis thaliana*. *BMC Plant Biol.* 13, 1-11. doi: 10.1186/1471-2229-13-229.

Dolan, L., Janmaat, K., Willemsen, V., Linstead, P., Poethig, S., Roberts, K., & Scheres, B. (1993). Cellular organisation of the *Arabidopsis thaliana* root. *Development* 119(1), 71-84. doi: 10.1242/dev.119.1.71.

Dong, J., Ma, G., Sui, L., Wei, M., Satheesh, V., Zhang, R., ... & Lei, M. (2019). Inositol pyrophosphate InsP8 acts as an intracellular phosphate signal in Arabidopsis. *Mol. Plant* 12(11), 1463-1473. doi: 10.1016/j.molp.2019.08.002.

Dong, J., Piñeros, M. A., Li, X., Yang, H., Liu, Y., Murphy, A. S., ... & Liu, D. (2017). An Arabidopsis ABC transporter mediates phosphate deficiency-induced remodeling of root architecture by modulating iron homeostasis in roots. *Mol. Plant* 10(2), 244-259. doi: 10.1016/j.molp.2016.11.001.

DoVale, J. C., and Fritsche-Neto, R. (2015). "Root phenomics," in Phenomics, eds R. Fritsche-Neto and A. Borém (Cham: Springer International Publishing). 49–66. doi: 10.1007/978-3-319-13677-6_4.

Du, H., Yang, C., Ding, G., Shi, L., & Xu, F. (2017). Genome-wide identification and characterization of SPX domain-containing members and their responses to phosphate deficiency in *Brassica napus*. *Front. Plant Sci.* 8, 35. doi: 10.3389/fpls.2017.00035.

Du, Y., & Scheres, B. (2018). Lateral root formation and the multiple roles of auxin. *J. Exp. Bot.* 69(2), 155-167. doi: 10.1093/jxb/erx223.

Duan, C. G., Wang, X., Xie, S., Pan, L., Miki, D., Tang, K., ... & Zhu, J. K. (2017). A pair of transposon-derived proteins function in a histone acetyltransferase complex for active DNA demethylation. *Cell Res.* 27(2), 226-240. doi: 10.1038/cr.2016.147.

Duan, X., Jin, K., Ding, G., Wang, C., Cai, H., Wang, S., ... & Shi, L. (2020). The impact of different morphological and biochemical root traits on phosphorus acquisition and seed yield of Brassica napus. *Field Crops Res.* 258, 107960. doi: 10.1016/j.fcr.2020.107960.

Dubrovsky, J. G., Rost, T. L., Colón-Carmona, A., & Doerner, P. (2001). Early primordium morphogenesis during lateral root initiation in *Arabidopsis thaliana*. *Planta* 214, 30-36. doi: 10.1007/s004250100598.

Duda, M. K., O'Shea, K. M., & Stanley, W. C. (2009). ω-3 polyunsaturated fatty acid supplementation for the treatment of heart failure: mechanisms and clinical potential. *Cardiovasc. Res.* 84(1), 33-41. doi: 10.1093/cvr/cvp169.

Eljebbawi, A., Savelli, B., Libourel, C., Estevez, J. M., & Dunand, C. (2022). Class III peroxidases in response to multiple abiotic stresses in *Arabidopsis thaliana* Pyrenean populations. *Int. J. Mol. Sci.* 23(7), 3960. doi: 10.3390/ijms23073960.

Engelsberger, W. R., & Schulze, W. X. (2012). Nitrate and ammonium lead to distinct global dynamic phosphorylation patterns when resupplied to nitrogen-starved Arabidopsis seedlings. *Plant J.* 69(6), 978-995. doi: 10.1111/j.1365-313X.2011.04848.x.

Fahad, S., Bajwa, A. A., Nazir, U., Anjum, S. A., Farooq, A., Zohaib, A., ... & Huang, J. (2017). Crop production under drought and heat stress: plant responses and management options. *Front. Plant Sci.* 8, 1147. doi: 10.3389/fpls.2017.01147.

Fakih, Z., Plourde, M. B., & Germain, H. (2023). Differential participation of plant ribosomal proteins from the small ribosomal subunit in protein translation under stress. *Biomolecules* 13(7), 1160. doi: 10.3390/biom13071160.

Feng, H., Wang, S., Dong, D., Zhou, R., & Wang, H. (2020). Arabidopsis ubiquitin-conjugating enzymes UBC7, UBC13, and UBC14 are required in plant responses to multiple stress conditions. *Plants* 9(6), 723. doi: 10.3390/plants9060723.

Ferreira, L. J., Azevedo, V., Maroco, J., Oliveira, M. M., and Santos, A. P. (2015). Salt tolerant and sensitive rice varieties display differential methylome flexibility under salt stress. *PLoS One* 10: e0124060. doi: 10.1371/journal.pone.0124060.

Ferreyra, M. L. F., Pezza, A., Biarc, J., Burlingame, A. L., & Casati, P. (2010). Plant L10 ribosomal proteins have different roles during development and translation under ultraviolet-B stress. *Plant Physiol.* 153(4), 1878-1894. doi: 10.1104/pp.110.157057.

Fetterman Jr, J. W., & Zdanowicz, M. M. (2009). Therapeutic potential of n-3 polyunsaturated fatty acids in disease. *American Journal of health-system pharmacy*, 66(13), 1169-1179. doi: 10.2146/ajhp080411.

Finco, A., Bentivoglio, D., & Nijkamp, P. (2012). Integrated evaluation of biofuel production options in agriculture: an exploration of sustainable policy scenarios. *International Journal of Foresight and Innovation Policy*, 8(2-3), 173-188. doi: 10.1504/IJFIP.2012.046109.

Fisher, A. P., & Sozzani, R. (2016). Uncovering the networks involved in stem cell maintenance and asymmetric cell division in the Arabidopsis root. *Curr. Opin. Plant Biol.* 29, 38-43. doi: 10.1016/j.pbi.2015.11.002.

Fitter, A. (2002). Characteristics and functions of root systems. In Plant roots (pp. 49-78). CRC Press.

Floris, M., Mahgoub, H., Lanet, E., Robaglia, C., & Menand, B. (2009). Post-transcriptional regulation of gene expression in plants during abiotic stress. *Int. J. Mol. Sci.* 10(7), 3168-3185. doi: 10.3390/ijms10073168.

Fonseca de Lima, C. F., Kleine-Vehn, J., De Smet, I., & Feraru, E. (2021). Getting to the root of belowground high temperature responses in plants. *J. Exp. Bot.* 72(21), 7404-7413. doi: 10.1093/jxb/erab202.

Foyer, C. H., and Noctor, G. (2009). Redox regulation in photosynthetic organisms: signaling, acclimation, and practical implications. *Antioxid. Redox Signal.* 11, 861–905. doi: 10.1089/ars.2008.2177.

Franco, J. A., Bañón, S., Vicente, M. J., Miralles, J., Bañón, S., Vicente, M. J., et al. (2015). Root development in horticultural plants grown under abiotic stress conditions. *J. Hortic. Sci. Biotechnol.* 86, 543–556. doi: 10.1080/14620316.2011.11512802.

Freeborough, W., Gentle, N., & Rey, M. E. (2021). WRKY transcription factors in cassava contribute to regulation of tolerance and susceptibility to cassava mosaic disease through stress responses. *Viruses* 13(9), 1820. doi: 10.3390/v13091820.

Friml, J., Wiśniewska, J., Benková, E., Mendgen, K., & Palme, K. (2002). Lateral relocation of auxin efflux regulator PIN3 mediates tropism in Arabidopsis. *Nature* 415(6873), 806-809. doi: 10.1038/415806a.

Fu, W., Chen, D., Pan, Q., Li, F., Zhao, Z., Ge, X., & Li, Z. (2018). Production of red-flowered oilseed rape via the ectopic expression of O rychophragmus violaceus O v PAP 2. *Plant Biotechnol. J.* 16(2), 367-380. doi: 10.1111/pbi.12777.

Fujita, M., Fujita, Y., Maruyama, K., Seki, M., Hiratsu, K., Ohme-Takagi, M., et al. (2004). A dehydration-inducedNAC protein, RD26, is involved in a novel ABA-dependent stress-signaling pathway. *Plant J.* 39, 863–876. doi: 10.1111/j.1365-313X.2004.02171.x.

Fukaki, H., Tameda, S., Masuda, H., & Tasaka, M. (2002). Lateral root formation is blocked by a gain-of-function mutation in the SOLITARY-ROOT/IAA14 gene of Arabidopsis. *Plant J.* 29(2), 153-168. doi: 10.1046/j.0960-7412.2001.01201.x.

Gaillochet, C., Burko, Y., Platre, M. P., Zhang, L., Simura, J., Willige, B. C., ... & Busch, W. (2020). HY5 and phytochrome activity modulate shoot-to-root coordination during thermomorphogenesis in Arabidopsis. *Development* 147(24), dev192625. doi: 10.1242/dev.192625.

Galassetti, P., & Pontello, A. (2006). Dietary effects on oxidation of low-density lipoprotein and atherogenesis. *Current Atherosclerosis Reports* 8(6), 523-529. doi: 10.1007/s11883-006-0028-6.

Gandullo, J., Ahmad, S., Darwish, E., Karlova, R., & Testerink, C. (2021). Phenotyping tomato root developmental plasticity in response to salinity in soil rhizotrons. *Plant Phenomics* doi: 10.34133/2021/2760532.

Gao, K. U. N., Chen, F., Yuan, L., Zhang, F., & Mi, G. (2015). A comprehensive analysis of root morphological changes and nitrogen allocation in maize in response to low nitrogen stress. *Plant Cell Environ.* 38(4), 740-750. doi: 10.1111/pce.12439.

Gao, R., Zhou, L., Guo, G., Li, Y., Chen, Z., Lu, R., ... & Chen, J. (2023). Comparative analysis of root transcriptome of high-NUE mutant and wild-type barley under low-nitrogen conditions. *Agronomy* 13(3), 806. doi: 10.3390/agronomy13030806.

Gao, X., Liu, K., & Lu, Y. T. (2010). Specific roles of AtEXPA1 in plant growth and stress adaptation. *Russ. J. Plant Physiol.* 57, 241-246. doi: 10.1134/S1021443710020111.

García, M. J., Romera, F. J., Lucena, C., Alcántara, E., & Pérez-Vicente, R. (2015). Ethylene and the regulation of physiological and morphological responses to nutrient deficiencies. *Plant Physiol.* 169(1), 51-60. doi: 10.1104/pp.15.00708.

García-Díaz, A., Bienes, R., Sastre, B., Novara, A., Gristina, L., & Cerda, A. (2017). Nitrogen losses in vineyards under different types of soil groundcover. A field runoff simulator approach in central Spain. *Agric. Ecosyst. Environ.* 236, 256-267. doi: 10.1016/j.agee.2016.12.013.

Gasco, G., Alvarez, M. L., Paz-Ferreiro, J., & Mendez, A. (2019). Combining phytoextraction by Brassica napus and biochar amendment for the remediation of a mining soil in Riotinto (Spain). *Chemosphere* 231, 562-570. doi: 10.1016/j.chemosphere.2019.05.168.

Gaspar, T. H., Penel, C. L., Thorpe, T., & Grappin, H. (1982). Chemistry and biochemistry of peroxidases. Peroxidases, A Survey of Their Biochemical and Physiological Roles in Higher Plants, University de Geneve Press, Geneva, 10-60.

Gastal, F., Lemaire, G., Durand, J. L., & Louarn, G. (2015). Quantifying crop responses to nitrogen and avenues to improve nitrogen-use efficiency. In Crop physiology (pp. 161-206). *Academic Press*. doi: 10.1016/B978-0-12-417104-6.00008-X.

Ghosh, D., and Xu, J. (2014). Abiotic stress responses in plant roots: a proteomics perspective. *Front. Plant Sci.* 5:6. doi: 10.3389/fpls.2014.00006.

Giehl, R. F., & von Wirén, N. (2014). Root nutrient foraging. *Plant Physiol.* 166(2), 509-517. doi: 10.1104/pp.114.245225.

Gifford, M. L., Dean, A., Gutierrez, R. A., Coruzzi, G. M., & Birnbaum, K. D. (2008). Cell-specific nitrogen responses mediate developmental plasticity. *Proc. Natl. Acad. Sci.* 105(2), 803-808. doi: 10.1073/pnas.0709559105.

Giraud, E., Ho, L. H., Clifton, R., Carroll, A., Estavillo, G., Tan, Y. F., ... & Whelan, J. (2008). The absence of ALTERNATIVE OXIDASE1a in Arabidopsis results in acute sensitivity to combined light and drought stress. *Plant Physiol.* 147(2), 595-610. doi: 10.1104/pp.107.115121.

Giri, A., Heckathorn, S., Mishra, S., and Krause, C. (2017). Heat stress decreases levels of nutrient-uptake and -assimilation proteins in tomato roots. *Plants* 6:6. doi: 10.1038/s41598-019-49496-0.

Goncalves, B. X., Lima-Melo, Y., dos Santos Maraschin, F., & Margis-Pinheiro, M. (2020). Phosphate starvation responses in crop roots: from well-known players to novel candidates. *Environ. Exp. Bot.* 178, 104162. doi: 10.1016/j.envexpbot.2020.104162.

González-García, M. P., Conesa, C. M., Lozano-Enguita, A., Baca-González, V., Simancas, B., Navarro-Neila, S., ... & Del Pozo, J. C. (2023). Temperature changes in the root ecosystem affect plant functionality. *Plant Commun.* 4(3). doi: 10.1016/j.xplc.2022.100514.

González-García, M. P., Vilarrasa-Blasi, J., Zhiponova, M., Divol, F., Mora-García, S., Russinova, E., & Caño-Delgado, A. I. (2011). Brassinosteroids control meristem size by promoting cell cycle progression in Arabidopsis roots. *Development* 138(5), 849-859. doi: 10.1242/dev.057331.

Graças, J. P., Lima, J. E., Peres, L. E. P., Jamet, E., Dunand, C., Vitorello, V. A., & Chervin, C. (2021). Ethylene signaling causing tolerance of Arabidopsis thaliana roots to low pH stress is linked to class III peroxidase activity. *J. Plant Growth Regul.* 40, 116-125. doi: 10.1007/s00344-019-10060-9.

Gruber, B. D., Giehl, R. F., Friedel, S., & von Wirén, N. (2013). Plasticity of the Arabidopsis root system under nutrient deficiencies. *Plant Physiol.* 163(1), 161-179. doi: 10.1104/pp.113.218453.

Gulden, R. H., Warwick, S. I., & Thomas, A. G. (2008). The biology of Canadian weeds. 137. Brassica napus L. and B. rapa L. *Can. J. Plant Sci.* 88(5), 951-996. doi: 10.4141/CJPS07203.

Guo, B., Liang, Y., and Zhu, Y. (2009). Does salicylic acid regulate antioxidant defense system, cell death, cadmium uptake and partitioning to acquire cadmium tolerance in rice? J. *Plant Physiol.* 166, 20–31. doi: 10.1016/j.jplph.2008.01.002.

Guo, Q., Love, J., Roche, J., Song, J., Turnbull, M. H., & Jameson, P. E. (2017). A RootNav analysis of morphological changes in Brassica napus L. roots in response to different nitrogen forms. *Plant Growth Regul.* 83, 83-92. doi: 10.1007/s10725-017-0285-0.

Guo, Z. J., Chen, X. J., Wu, X. L., Ling, J. Q., and Xu, P. (2004). Overexpression of the AP2/EREBP transcription factor OPBP1 enhances disease resistance and salt tolerance in tobacco. *Plant Mol. Biol.* 55, 607–618. doi: 10.1007/s11103-004-1521-3.

Gupta, R., Min, C. W., Kim, Y. J., & Kim, S. T. (2019). Identification of Msp1-induced signaling components in rice leaves by integrated proteomic and phosphoproteomic analysis. *Int. J. Mol. Sci.* 20(17), 4135. doi: 10.3390/ijms20174135.

Guseman, J. M., Hellmuth, A., Lanctot, A., Feldman, T. P., Moss, B. L., Klavins, E., ... & Nemhauser, J. L. (2015). Auxin-induced degradation dynamics set the pace for lateral root development. *Development* 142(5), 905-909. doi: 10.1242/dev.117234.

Gutiérrez-Alanís, D., Yong-Villalobos, L., Jimenez-Sandoval, P., Alatorre-Cobos, F., Oropeza-Aburto, A., Mora-Macías, J., ... & Herrera-Estrella, L. (2017). Phosphate starvation-dependent iron mobilization induces CLE14 expression to trigger root meristem differentiation through CLV2/PEPR2 signaling. *Dev. Cell* 41(5), 555-570. doi: 10.1016/j.devcel.2017.05.009.

Habibi, F., Ramezanian, A., Rahemi, M., Eshghi, S., Guillén, F., Serrano, M., et al. (2019). Postharvest treatments with g□aminobutyric acid, methyl jasmonate, or methyl salicylate enhance chilling tolerance of blood orange fruit at prolonged cold storage. *J. Sci. Food Agric.* 99, 6408–6417. doi: 10.1002/jsfa.9920.

Hachiya, T., & Okamoto, Y. (2017). Simple spectroscopic determination of nitrate, nitrite, and ammonium in Arabidopsis thaliana. *Bio-protocol* 7(10), e2280-e2280. doi: 10.21769/BioProtoc.2280.

Hamburger, D., Rezzonico, E., MacDonald-Comber Petétot, J., Somerville, C., & Poirier, Y. (2002). Identification and characterization of the Arabidopsis PHO1 gene involved in phosphate loading to the xylem. *Plant Cell* 14(4), 889-902. doi: 10.1105/tpc.000745.

HAN, P. P., Lu, Q. I. N., LI, Y. S., LIAO, X. S., XU, Z. X., HU, X. J., ... & Xing, L. I. A. O. (2017). Identification of suitable reference genes in leaves and roots of rapeseed (*Brassica napus* L.) under different nutrient deficiencies. *J. Integr. Agric.* 16(4), 809-819. doi: 10.1016/S2095-3119(16)61436-3.

Han, S. H., Park, Y. J., & Park, C. M. (2020). HOS1 activates DNA repair systems to enhance plant thermotolerance. *Nat. Plants* 6(12), 1439-1446. doi: 10.1038/s41477-020-00809-6.

Han, Y., Zhang, C., Sha, H., Wang, X., Yu, Y., Liu, J., ... & Fang, J. (2023). Ubiquitin-Conjugating Enzyme OsUBC11 Affects the Development of Roots via Auxin Pathway. *Rice* 16(1), 9. doi: 10.1186/s12284-023-00626-3.

Hanitzsch, M., Schnitzer, D., Seidel, T., Golldack, D., & Dietz, K. J. (2007). Transcript level regulation of the vacuolar H+-ATPase subunit isoforms VHA-a, VHA-E and VHA-G in *Arabidopsis thaliana*. *Mol. Membr. Biol.* 24(5-6), 507-518. doi: 10.1080/09687680701447393.

Hanzawa, T., Shibasaki, K., Numata, T., Kawamura, Y., Gaude, T., & Rahman, A. (2013). Cellular auxin homeostasis under high temperature is regulated through a SORTING NEXIN1–dependent endosomal trafficking pathway. *Plant Cell* 25(9), 3424-3433. doi: 10.1105/tpc.113.115881.

Hardman, W. E. (2007). Dietary canola oil suppressed growth of implanted MDA-MB 231 human breast tumors in nude mice. *Nutrition and cancer* 57(2), 177-183. doi: 10.1080/01635580701277445.

Hasanuzzaman, M., Nahar, K., Alam, M. M., Roychowdhury, R., & Fujita, M. (2013). Physiological, biochemical, and molecular mechanisms of heat stress tolerance in plants. *Int. J. Mol. Sci.* 14(5), 9643-9684. doi: 10.3390/ijms14059643.

Hau, B., Symonds, K., Teresinski, H., Janssen, A., Duff, L., Smith, M., ... & Snedden, W. A. (2024). Arabidopsis calmodulin-like proteins CML13 and CML14 interact with calmodulin-binding transcriptional activators and function in salinity stress response. *Plant Cell Physiol.* 65(2), 282-300. doi: 10.1093/pcp/pcad152.

He, Z., Zhao, T., Yin, Z., Liu, J., Cheng, Y., & Xu, J. (2020). The phytochrome-interacting transcription factor CsPIF8 contributes to cold tolerance in citrus by regulating superoxide dismutase expression. *Plant Sci.* 298, 110584. doi: 10.1016/j.plantsci.2020.110584.

Hellens, R. P., Allan, A. C., Friel, E. N., Bolitho, K., Grafton, K., Templeton, M. D., ... & Laing, W. A. (2005). Transient expression vectors for functional genomics, quantification of promoter activity and RNA silencing in plants. *Plant Methods* 1, 1-14. doi: 10.1186/1746-4811-1-13.

Ho, C. H., Lin, S. H., Hu, H. C., & Tsay, Y. F. (2009). CHL1 functions as a nitrate sensor in plants. *Cell* 138(6), 1184-1194. doi: 10.1016/j.cell.2009.07.004.

Hossain, A., Syed, M. A., Maitra, S., Garai, S., Mondal, M., Akter, B., ... & Hossain, T. (2022). Genetic regulation, biosynthesis, and the roles of osmoprotective compounds in abiotic stress tolerance in plants. In *Plant Abiotic Stress Physiology* (pp. 61-114). Apple Academic Press. doi: 10.1016/j.plaphy.2020.06.041.

Hossain, M. S., Kawakatsu, T., Kim, K. D., Zhang, N., Nguyen, C. T., Khan, S. M., ... & Stacey, G. (2017). Divergent cytosine DNA methylation patterns in single-cell, soybean root hairs. *New Phytol.* 214(2), 808-819. doi: 10.1111/nph.14421.

Hossain, Z., McGarvey, B., Amyot, L., Gruber, M., Jung, J., & Hannoufa, A. (2012). DIMINUTO 1 affects the lignin profile and secondary cell wall formation in Arabidopsis. *Planta* 235, 485-498. doi: 10.1007/s00425-011-1519-4.

Hsieh, P. H., Kan, C. C., Wu, H. Y., Yang, H. C., & Hsieh, M. H. (2018). Early molecular events associated with nitrogen deficiency in rice seedling roots. *Sci. Rep.* 8(1), 12207. doi: 10.1038/s41598-018-30632-1.

Hu, D., Jing, J., Snowdon, R. J., Mason, A. S., Shen, J., Meng, J., & Zou, J. (2021). Exploring the gene pool of Brassica napus by genomics-based approaches. *Plant Biotechnol. J.* 19(9), 1693-1712. doi: 10.1111/pbi.13636.

Hu, X., Liu, R., Li, Y., Wang, W., Tai, F., Xue, R., & Li, C. (2010a). Heat shock protein 70 regulates the abscisic acid-induced antioxidant response of maize to combined drought and heat stress. *Plant Growth Regul.* 60, 225-235. doi: 10.1007/s10725-009-9436-2.

Hu, Y., Ye, X., Shi, L., Duan, H., & Xu, F. (2010b). Genotypic differences in root morphology and phosphorus uptake kinetics in *Brassica napus* under low phosphorus supply. *J. Plant Nutr.* 33(6), 889-901. doi: 10.1080/01904161003658239.

Hu, Y., Zhang, L., Zhao, L., Li, J., He, S., Zhou, K., et al. (2011). Trichostatin a selectively suppresses the cold-induced transcription of the *ZmDREB1* gene in maize. *PLoS One* 6: e22132. doi: 10.1371/journal.pone.0022132.

Hu, Z., Huang, X., Amombo, E., Liu, A., Fan, J., Bi, A., ... & Fu, J. (2020). The ethylene responsive factor CdERF1 from bermudagrass (*Cynodon dactylon*) positively regulates cold tolerance. *Plant Sci.* 294, 110432. doi: 10.1016/j.plantsci.2020.110432.

Hu, Z., Huang, X., Xia, H., Zhang, Z., Lu, H., Wang, X., ... & Sun, S. (2024). Transcription factor *OsSHR2* regulates rice architecture and yield per plant in response to nitrogen. *Planta* 259(6), 148. doi: 10.1007/s00425-024-04400-7.

Huang, B., and Xu, Q. (2000). Root growth and nutrient element status of creeping bentgrass cultivars differing in heat tolerance as influenced by supraoptimal shoot and root temperatures. *J. Plant Nutr.* 23, 979–990. doi: 10.1080/01904160009382075.

Huang, B., Rachmilevitch, S., & Xu, J. (2012). Root carbon and protein metabolism associated with heat tolerance. *J. Exp. Bot.* 63(9), 3455-3465. doi: 10.1093/jxb/ers003.

Huang, P. Y., Catinot, J., & Zimmerli, L. (2016). Ethylene response factors in Arabidopsis immunity. *J. Exp. Bot.* 67(5), 1231-1241. doi: 10.1093/jxb/erv518.

Huang, W. T., Xie, Y. Z., Chen, X. F., Zhang, J., Chen, H. H., Ye, X., ... & Chen, L. S. (2021). Growth, mineral nutrients, photosynthesis and related physiological parameters of Citrus in response to nitrogen deficiency. *Agronomy* 11(9), 1859. doi: 10.3390/agronomy11091859.

Huang, W. T., Zheng, Z. C., Hua, D., Chen, X. F., Zhang, J., Chen, H. H., ... & Chen, L. S. (2022). Adaptive responses of carbon and nitrogen metabolisms to nitrogen-deficiency in Citrus sinensis seedlings. *BMC Plant Biol.* 22(1), 370. doi: 10.1186/s12870-022-03759-7.

Huerta-Cepas, J., Serra, F., & Bork, P. (2016). ETE 3: reconstruction, analysis, and visualization of phylogenomic data. *Mol. Biol. Evol.* 33(6), 1635-1638. doi: 10.1093/molbev/msw046.

Hungria, M., and Kaschuk, G. (2014). Regulation of N2 fixation and NO3□/NH4+ assimilation in nodulated and N-fertilized Phaseolus vulgaris L. exposed to high temperature stress. *Environ. Exp. Bot.* 98, 32–39. doi: 10.1016/j.envexpbot.2013.10.010.

Hurry, V., Strand, Å., Furbank, R., & Stitt, M. (2000). The role of inorganic phosphate in the development of freezing tolerance and the acclimatization of photosynthesis to low temperature is revealed by the pho mutants of Arabidopsis thaliana. *Plant J.* 24(3), 383-396. doi: 0.1046/j.1365-313x.2000.00888.x.

Iglesias, J., Trigueros, M., Rojas-Triana, M., Fernández, M., Albar, J. P., Bustos, R., ... & Rubio, V. (2013). Proteomics identifies ubiquitin–proteasome targets and new roles for chromatin-remodeling in the Arabidopsis response to phosphate starvation. *J. Proteomics* 94, 1-22. doi: 10.1016/j.jprot.2013.08.015.

Illston, B. G., & Fiebrich, C. A. (2017). Horizontal and vertical variability of observed soil temperatures. *Geosci. Data J.* 4(1), 40-46. doi: 10.1002/gdj3.47.

Inoue, H., Nojima, H., & Okayama, H. (1990). High efficiency transformation of Escherichia coli with plasmids. *Gene* 96(1), 23-28. doi: 10.1016/0378-1119(90)90336-P.

Ishiyama, K., Inoue, E., Watanabe-Takahashi, A., Obara, M., Yamaya, T., & Takahashi, H. (2004). Kinetic properties and ammonium-dependent regulation of cytosolic isoenzymes of glutamine synthetase in Arabidopsis. *J. Biol. Chem.* 279(16), 16598-16605. doi: 10.1074/jbc.M313710200.

Iuchi, S., Koyama, H., Iuchi, A., Kobayashi, Y., Kitabayashi, S., Kobayashi, Y., ... & Kobayashi, M. (2007). Zinc finger protein STOP1 is critical for proton tolerance in Arabidopsis and coregulates a key gene in aluminum tolerance. *Proc. Natl Acad. Sci.* 104(23), 9900-9905. doi: 10.1073/pnas.0700117104.

Iyer, N. J., Tang, Y., and Mahalingam, R. (2013). Physiological, biochemical and molecular responses to a combination of drought and ozone in Medicago truncatula. *Plant Cell Environ.* 36, 706–720. doi: 10.1111/pce.12008.

Jacobsen, S.-E., Liu, F., and Jensen, C. R. (2009). Does root-sourced ABA play a role for regulation of stomata under drought in quinoa (*Chenopodium quinoa* Willd.). *Sci. Hortic.* 122, 281–287. doi: 10.1016/j.scienta.2009.05.019.

Jahreis, G., & Schäfer, U. (2011). Rapeseed (*Brassica napus*) oil and its benefits for human health. In Nuts and seeds in health and disease prevention (pp. 967-974). *Academic Press* doi: 10.1016/B978-0-12-375688-6.10114-8.

Jan, R., Kim, N., Lee, S. H., Khan, M. A., Asaf, S., Lubna, ... & Kim, K. M. (2021). Enhanced flavonoid accumulation reduces combined salt and heat stress through regulation of transcriptional and hormonal mechanisms. *Front. Plant Sci.* 12, 796956. doi: 10.3389/fpls.2021.796956.

Janes, G., Von Wangenheim, D., Cowling, S., Kerr, I., Band, L., French, A. P., & Bishopp, A. (2018). Cellular patterning of Arabidopsis roots under low phosphate conditions. *Front. Plant Sci.* 9, 735. doi: 10.3389/fpls.2018.00735.

Jean-Baptiste, K., McFaline-Figueroa, J. L., Alexandre, C. M., Dorrity, M. W., Saunders, L., Bubb, K. L., ... & Cuperus, J. T. (2019). Dynamics of gene expression in single root cells of *Arabidopsis thaliana*. *Plant Cell*, 31(5), 993-1011. doi: 10.1105/tpc.18.00785.

Ji, J., Lin, S., Xin, X., Li, Y., He, J., Xu, X., ... & Yin, G. (2023). Effects of *OsAOX1a* deficiency on mitochondrial metabolism at critical node of seed viability in rice. *Plants* 12(12), 2284. doi: 10.3390/plants12122284.

Jia, H., Zhang, S., Wang, L., Yang, Y., Zhang, H., Cui, H., ... & Xu, G. (2017). OsPht1; 8, a phosphate transporter, is involved in auxin and phosphate starvation response in rice. *J. Exp. Bot.* 68(18), 5057-5068. doi: 10.1093/jxb/erx317.

Jia, Z., & von Wirén, N. (2020). Signaling pathways underlying nitrogen-dependent changes in root system architecture: from model to crop species. *J. Exp. Bot.* 71(15), 4393-4404. doi: 10.1093/jxb/eraa033.

Jia, Z., Giehl, R. F., & von Wirén, N. (2020). The root foraging response under low nitrogen depends on *DWARF1*-mediated brassinosteroid biosynthesis. *Plant Physiol.* 183(3), 998-1010. doi: 10.1104/pp.20.00440.

Jiang, C., Gao, X., Liao, L., Harberd, N. P., & Fu, X. (2007). Phosphate starvation root architecture and anthocyanin accumulation responses are modulated by the gibberellin-DELLA signaling pathway in Arabidopsis. *Plant Physiol.* 145(4), 1460-1470. doi: 10.1104/pp.107.103788.

Jiang, Y., Yang, B., & Deyholos, M. K. (2009). Functional characterization of the Arabidopsis *bHLH92* transcription factor in abiotic stress. *Mol. Genet. Genomics* 282, 503-516. doi: 10.1007/s00438-009-0481-3.

Jiao, X., Lyu, Y., Wu, X., Li, H., Cheng, L., Zhang, C., ... & Shen, J. (2016). Grain production versus resource and environmental costs: towards increasing sustainability of nutrient use in China. *J. Exp. Bot.* 67(17), 4935-4949. doi: 10.1093/jxb/erw282.

Johnston, A. E., Poulton, P. R., Fixen, P. E., & Curtin, D. (2014). Phosphorus: its efficient use in agriculture. *Adv. Agron.* 123, 177-228. doi: 10.1016/B978-0-12-420225-2.00005-4.

Jonassen, E. M., Lea, U. S., & Lillo, C. (2008). *HY5* and *HYH* are positive regulators of nitrate reductase in seedlings and rosette stage plants. *Planta* 227, 559-564. doi: 10.1007/s00425-007-0638-4.

Jung, I., Ahn, H., Shin, S. J., Kim, J., Kwon, H. B., Jung, W., et al. (2016). Clustering and evolutionary analysis of small RNAs identify regulatory siRNA clusters induced under drought stress in rice. *BMC Syst. Biol.* 10:115. doi: 10.1186/s12918-016-0355-3.

Kamranfar, I., Balazadeh, S., & Mueller-Roeber, B. (2021). NAC transcription factor RD26 is a regulator of root hair morphogenic plasticity. *BioRxiv* 2021-04. doi: 10.1101/2021.04.21.440803.

Kang, Y., & Udvardi, M. (2012). Global regulation of reactive oxygen species scavenging genes in alfalfa root and shoot under gradual drought stress and recovery. *Plant Signaling Behav.* 7(5), 539-543. doi: 10.4161/psb.19780.

Kanno, S., Arrighi, J. F., Chiarenza, S., Bayle, V., Berthome, R., Peret, B., ... & Nussaume, L. (2016). A novel role for the root cap in phosphate uptake and homeostasis. *Elife* 5, e14577. doi: 10.7554/eLife.14577.

Kant, S., Peng, M., & Rothstein, S. J. (2011). Genetic regulation by NLA and microRNA827 for maintaining nitrate-dependent phosphate homeostasis in Arabidopsis. *PLoS Genet.* 7(3), e1002021. doi: 10.1371/journal.pgen.1002021.

Karlova, R., Boer, D., Hayes, S., & Testerink, C. (2021). Root plasticity under abiotic stress. *Plant Physiol.* 187(3), 1057-1070. doi: 10.1093/plphys/kiab392.

Karni, L., Aktas, H., Deveturero, G., and Aloni, B. (2010). Involvement of root ethylene and oxidative stress-related activities in pre-conditioning of tomato transplants by increased salinity. *J. Hortic. Sci. Biotechnol.* 85, 23–29. doi: 10.1080/14620316.2010.11512625.

Karthikeyan, A. S., Varadarajan, D. K., Jain, A., Held, M. A., Carpita, N. C., & Raghothama, K. G. (2007). Phosphate starvation responses are mediated by sugar signaling in Arabidopsis. *Planta* 225, 907-918. doi: 10.1007/s00425-006-0408-8.

Kaur, S., Tiwari, V., Kumari, A., Chaudhary, E., Sharma, A., Ali, U., & Garg, M. (2023). Protective and defensive role of anthocyanins under plant abiotic and biotic stresses: An emerging application in sustainable agriculture. *J. Biotechnol.* 361, 12-29. doi: 10.1016/j.jbiotec.2022.11.009.

Kazan, K., & Lyons, R. (2016). The link between flowering time and stress tolerance. *J. Exp. Bot.* 67(1), 47-60. doi: 10.1093/jxb/erv441.

Ke, D., Guo, J., Li, K., Wang, Y., Han, X., Fu, W., ... & Jia, K. P. (2022). Carotenoid-derived bioactive metabolites shape plant root architecture to adapt to the rhizospheric environments. *Front. Plant Sci.* 13, 986414. doi: 10.3389/fpls.2022.986414.

Khan, M. A., Gemenet, D. C., and Villordon, A. (2016). Root system architecture and abiotic stress tolerance: current knowledge in root and tuber crops. *Front. Plant Sci.* 7:1584. doi: 10.3389/fpls.2016.01584.

Khandal, H., Singh, A. P., & Chattopadhyay, D. (2020). The MicroRNA397b-LACCASE2 module regulates root lignification under water and phosphate deficiency. *Plant Physiol.* 182(3), 1387-1403. doi: 10.1104/pp.19.00921.

Khanzada, H., Wassan, G. M., He, H., Mason, A. S., Keerio, A. A., Khanzada, S., ... & Rasheed, A. (2020). Differentially evolved drought stress indices determine the genetic variation of *Brassica napus* at seedling traits by genome-wide association mapping. *J. Adv. Res.* 24, 447-461. doi: 10.1016/j.jare.2020.05.019.

Kiba, T., Feria-Bourrellier, A. B., Lafouge, F., Lezhneva, L., Boutet-Mercey, S., Orsel, M., ... & Krapp, A. (2012). The Arabidopsis nitrate transporter NRT2. 4 plays a double role in roots and shoots of nitrogen-starved plants. *Plant Cell* 24(1), 245-258. doi: 10.1105/tpc.111.092221.

Kidokoro, S., Watanabe, K., Ohori, T., Moriwaki, T.,Maruyama, K., Mizoi, J., et al. (2015). Soybean DREB 1/CBF-type transcription factors function in heat and drought as well as cold stress-responsive gene expression. *Plant J.* 81, 505–518. doi: 10.1111/tpj.12746.

Kidwai, M., Ahmad, I. Z., & Chakrabarty, D. (2020). Class III peroxidase: an indispensable enzyme for biotic/abiotic stress tolerance and a potent candidate for crop improvement. *Plant Cell Rep.* 39(11), 1381-1393. doi: 10.1007/s00299-020-02588-y.

Kilasi, N. L., Singh, J., Vallejos, C. E., Ye, C., Jagadish, S. K., Kusolwa, P., & Rathinasabapathi, B. (2018). Heat stress tolerance in rice (Oryza sativa L.): identification of quantitative trait loci and candidate genes for seedling growth under heat stress. *Front. Plant Sci.* 9, 1578. doi: 10.3389/fpls.2018.01578.

Kim, D., Jeon, S. J., Yanders, S., Park, S. C., Kim, H. S., & Kim, S. (2022). MYB3 plays an important role in lignin and anthocyanin biosynthesis under salt stress condition in Arabidopsis. *Plant Cell Rep.* 41(7), 1549-1560. doi: 10.1007/s00299-022-02878-7.

Kim, D., Langmead, B., & Salzberg, S. L. (2015). HISAT: a fast spliced aligner with low memory requirements. *Nat. Methods* 12(4), 357-360. doi: 10.1038/nmeth.3317.

Kirk, G. J. D., Santos, E. E., & Santos, M. B. (1999). Phosphate solubilization by organic anion excretion from rice growing in aerobic soil: rates of excretion and decomposition, effects on rhizosphere pH and effects on phosphate solubility and uptake. *New Phytol.* 142(2), 185-200. doi: 10.1046/j.1469-8137.1999.00400.x.

Klay, I., Pirrello, J., Riahi, L., Bernadac, A., Cherif, A., Bouzayen, M., et al. (2014). Ethylene response factor Sl-ERF. B. 3 is responsive to abiotic stresses and mediates salt and cold stress response regulation in tomato. *Sci. World J.* 2014:67681. doi: 10.1155/2014/167681.

Klepper, B. (1992). Development and growth of crop root systems. In Limitations to plant root growth (pp. 1-25). *New York, NY: Springer New York*. doi: 10.1007/978-1-4612-2894-3_1.

Klimenko, S., Peshkova, A., and Dorofeev, N. (2006). Nitrate reductase activity during heat shock in winter wheat. *J. Stress Physiol*. Biochem. 2, 50–55.

Koevoets, I. T., Venema, J. H., Elzenga, J. T. M., and Testerink, C. (2016). Roots withstanding their environment: exploiting root system architecture responses to abiotic stress to improve crop tolerance. *Front. Plant Sci*. 7:1335. doi: 10.3389/fpls.2016.01335.

Konishi, M., & Yanagisawa, S. (2013). Arabidopsis NIN-like transcription factors have a central role in nitrate signalling. *Nat. Commun.* 4(1), 1617. doi: 10.1038/ncomms2621.

Kordrostami, M., & Mafakheri, M. (2020). Rapeseed: biology and physiological responses to drought stress. *The Plant Family Brassicaceae: Biology and Physiological Responses to Environmental Stresses*, 263-276. doi: 10.1007/978-981-15-6345-4_8.

Koscielny, C. B., Hazebroek, J., & Duncan, R. W. (2018). Phenotypic and metabolic variation among spring *Brassica napus* genotypes during heat stress. *Crop Pasture Sci.* 69(3), 284-295. doi: 10.1071/CP17259.

Kotak, S., Larkindale, J., Lee, U., von Koskull-Döring, P., Vierling, E., & Scharf, K. D. (2007). Complexity of the heat stress response in plants. *Curr. Opin. Plant Biol.* 10(3), 310-316. doi: 10.1016/j.pbi.2007.04.011.

Kris-Etherton, P. M. (1999). Monounsaturated fatty acids and risk of cardiovascular disease. *Circulation* 100(11), 1253-1258. doi: 10.1161/01.CIR.100.11.1253.

Kris-Etherton, P. M., Harris, W. S., & Appel, L. J. (2003). Fish consumption, fish oil, omega-3 fatty acids, and cardiovascular disease. *Arterioscler., Thromb., Vasc. Biol.* 23(2), e20-e30. doi: 10.1161/01.ATV.0000038493.65177.94.

Krouk, G., & Kiba, T. (2020). Nitrogen and phosphorus interactions in plants: from agronomic to physiological and molecular insights. *Curr. Opin. Plant Biol.* 57, 104-109. doi: 10.1016/j.pbi.2020.07.002.

Krouk, G., Lacombe, B., Bielach, A., Perrine-Walker, F., Malinska, K., Mounier, E., ... & Gojon, A. (2010). Nitrate-regulated auxin transport by NRT1. 1 defines a mechanism for nutrient sensing in plants. *Dev. Cell* 18(6), 927-937. doi: 10.1016/j.devcel.2010.05.008.

Kumar, K., Raina, S. K., and Sultan, S. M. (2020). Arabidopsis MAPK signaling pathways and their cross talks in abiotic stress response. *J. Plant Biochem. Biotechnol.* 29, 700–714. doi: 10.1007/s13562-020-00596-3.

Kusano, M., Fukushima, A., Redestig, H., & Saito, K. (2011). Metabolomic approaches toward understanding nitrogen metabolism in plants. *J. Exp. Bot.* 62(4), 1439-1453. doi: 10.1093/jxb/erq417.

Lahti, M., Aphalo, P. J., Finer, L., Ryyppo, A., Lehto, T., and Mannerkoski, H. (2005). Effects of soil temperature on shoot and root growth and nutrient uptake of 5-year-old Norway spruce seedlings. *Tree Physiol.* 25, 115–122. doi:10.1093/treephys/25.1.115.

Lai, Y. H., Peng, M. Y., Rao, R. Y., Chen, W. S., Huang, W. T., Ye, X., ... & Chen, L. S. (2023). An Integrated Analysis of Metabolome, Transcriptome, and Physiology Revealed the Molecular and Physiological Response of Citrus sinensis Roots to Prolonged Nitrogen Deficiency. *Plants* 12(14), 2680. doi: 10.3390/plants12142680.

Lamb, C., & Dixon, R. A. (1997). The oxidative burst in plant disease resistance. *Annu. Rev. Plant Biol.* 48(1), 251-275. doi: 10.1146/annurev.arplant.48.1.251.

Lang, Z., Lei, M., Wang, X., Tang, K., Miki, D., Zhang, H., ... & Zhu, J. K. (2015). The methyl-CpG-binding protein MBD7 facilitates active DNA demethylation to limit DNA hyper-methylation and transcriptional gene silencing. *Mol. Cell* 57(6), 971-983. doi: 10.1016/j.molcel.2015.01.009.

Langfelder, P., & Horvath, S. (2008). WGCNA: an R package for weighted correlation network analysis. *BMC Bioinf.* 9, 1-13. doi: 10.1186/1471-2105-9-559.

Langmead, B., & Salzberg, S. L. (2012). Fast gapped-read alignment with Bowtie 2. *Nat. Methods* 9(4), 357-359. doi: 10.1038/nmeth.1923.

Larkindale, J., Hall, J. D., Knight, M. R., & Vierling, E. (2005). Heat stress phenotypes of Arabidopsis mutants implicate multiple signaling pathways in the acquisition of thermotolerance. *Plant Physiol.* 138(2), 882-897. doi: 10.1104/pp.105.062257.

Leblanc, A., Renault, H., Lecourt, J., Etienne, P., Deleu, C., & Le Deunff, E. (2008). Elongation changes of exploratory and root hair systems induced by aminocyclopropane carboxylic acid and aminoethoxyvinylglycine affect nitrate uptake and BnNrt2. 1 and BnNrt1. 1 transporter gene expression in oilseed rape. *Plant Physiol.* 146(4), 1928-1940. doi: 10.1104/pp.107.109363.

Lee, J. W., Kim, I. H., & Woyengo, T. A. (2020). Toxicity of canola-derived glucosinolate degradation products in pigs—A review. *Animals* 10(12), 2337. doi: 10.3390/ani10122337.

Lee, S., Showalter, J., Zhang, L., Cassin-Ross, G., Rouached, H., & Busch, W. (2024). Nutrient levels control root growth responses to high ambient temperature in plants. *Nature Commun.* 15(1), 4689. doi: 10.1038/s41467-024-49180-6.

Lee, S., Wang, W., & Huq, E. (2021). Spatial regulation of thermomorphogenesis by HY5 and PIF4 in Arabidopsis. *Nature Commun.* 12(1), 3656. doi: 10.1038/s41467-021-24018-7.

Lemaire, L., Deleu, C., & Le Deunff, E. (2013). Modulation of ethylene biosynthesis by ACC and AIB reveals a structural and functional relationship between the K15NO3 uptake rate and root absorbing surfaces. *J. Exp. Bot.* 64(10), 2725-2737. doi: 10.1093/jxb/ert124.

Léran, S., Muños, S., Brachet, C., Tillard, P., Gojon, A., & Lacombe, B. (2013). Arabidopsis NRT1. 1 is a bidirectional transporter involved in root-to-shoot nitrate translocation. *Mol. Plant* 6(6), 1984-1987. doi: 10.1093/mp/sst068.

Lewis, D. R., Negi, S., Sukumar, P., & Muday, G. K. (2011). Ethylene inhibits lateral root development, increases IAA transport and expression of PIN3 and PIN7 auxin efflux carriers. *Development* 138(16), 3485-3495. doi: 10.1242/dev.065102.

Li, B., & Dewey, C. N. (2011). RSEM: accurate transcript quantification from RNA-Seq data with or without a reference genome. *BMC Bioinf.* 12, 1-16. doi: 10.1186/1471-2105-12-323.

Li, F., Vallabhaneni, R., & Wurtzel, E. T. (2008). PSY3, a new member of the phytoene synthase gene family conserved in the Poaceae and regulator of abiotic stress-induced root carotenogenesis. *Plant Physiol.* 146(3), 1333-1345. doi: 10.1104/pp.107.111120.

Li, L. X., Chen, B. Y., Yan, G. X., Gao, G. Z., Xu, K., Xie, T., ... & Wu, X. M. (2020a). Proposed strategies and current progress of research and utilization of oilseed rape germplasm in China. *J. Plant Genet. Resour*, 21, 1-19.

Li, L., Yang, H., Liu, P., Ren, W., Wu, X., & Huang, F. (2018). Combined impact of heat stress and phosphate deficiency on growth and photochemical activity of sheepgrass (Leymus chinensis). *J. Plant Physiol.* 231, 271-276. doi: 10.1016/j.jplph.2018.10.008.

Li, N., Euring, D., Cha, J. Y., Lin, Z., Lu, M., Huang, L. J., & Kim, W. Y. (2021). Plant hormone-mediated regulation of heat tolerance in response to global climate change. *Front. Plant Sci.* 11, 627969. doi: 10.3389/fpls.2020.627969.

Li, P., Chen, F., Cai, H., Liu, J., Pan, Q., Liu, Z., ... & Yuan, L. (2015a). A genetic relationship between nitrogen use efficiency and seedling root traits in maize as revealed by QTL analysis. *J. Exp. Bot.* 66(11), 3175-3188. doi: 10.1093/jxb/erv127.

Li, P., Zhuang, Z., Cai, H., Cheng, S., Soomro, A. A., Liu, Z., ... & Chen, F. (2016). Use of genotype-environment interactions to elucidate the pattern of maize root plasticity to nitrogen deficiency. *Journal of Integrative Plant Biology*, 58(3), 242-253. doi: 10.1111/jipb.12384.

Li, Q., Ding, G., Yang, N., White, P. J., Ye, X., Cai, H., ... & Xu, F. (2020b). Comparative genome and transcriptome analysis unravels key factors of nitrogen use efficiency in *Brassica napus* L. *Plant Cell Environ.* 43(3), 712-731. doi: 10.1111/pce.13689.

Li, S., Fu, Q., Huang, W., & Yu, D. (2009). Functional analysis of an Arabidopsis transcription factor *WRKY25* in heat stress. *Plant Cell Rep.* 28, 683-693. doi: 10.1007/s00299-008-0666-y.

Li, X., Zhang, D., Li, H., Wang, Y., Zhang, Y., & Wood, A. J. (2014). *EsDREB2B*, a novel truncated DREB2-type transcription factor in the desert legume Eremosparton songoricum, enhances tolerance to multiple abiotic stresses in yeast and transgenic tobacco. *BMC Plant Biol.* 14, 1-16. doi: 10.1186/1471-2229-14-44.

Li, X.-P., Tian, A.-G., Luo, G.-Z., Gong, Z.-Z., Zhang, J.-S., and Chen, S.-Y. (2005). Soybean DRE-binding transcription factors that are responsive to abiotic stresses. *Theor. Appl. Genet.* 110, 1355–1362. doi: 10.1007/s00122-004-1867-6.

Li, Y., Li, Y., Yao, X., Wen, Y., Zhou, Z., Lei, W., ... & Lin, H. (2022a). Nitrogen-inducible GLK1 modulates phosphate starvation response via the PHR1-dependent pathway. *New Phytol.* 236(5), 1871-1887. doi: 10.1111/nph.18499.

Li, Y., Mukherjee, I., Thum, K. E., Tanurdzic, M., Katari, M. S., Obertello, M., ... & Coruzzi, G. M. (2015b). The histone methyltransferase SDG8 mediates the epigenetic modification of light and carbon responsive genes in plants. *Genome Biol.* 16, 1-15. doi: 10.1186/s13059-015-0640-2.

Li, Y., Yang, X., Li, X., Wang, C., Ding, G., Xu, F., ... & Shi, L. (2023). Jasmonic acid participating in the systemic regulation of phosphate starvation response in *Brassica napus. Plant Soil* 1-18. doi: 10.1007/s11104-023-06355-2.

Li, Y., Yang, X., Liu, H., Wang, W., Wang, C., Ding, G., ... & Shi, L. (2022b). Local and systemic responses conferring acclimation of *Brassica napus* roots to low phosphorus conditions. *J. Exp. Bot.* 73(14), 4753-4777. doi: 10.1093/jxb/erac177.

Li, Z., Xu, C., Li, K., Yan, S., Qu, X., & Zhang, J. (2012). Phosphate starvation of maize inhibits lateral root formation and alters gene expression in the lateral root primordium zone. *BMC Plant Biol.* 12, 1-17. doi: 10.1186/1471-2229-12-89.

Li, Z., Zhang, L., Yu, Y., Quan, R., Zhang, Z., Zhang, H., & Huang, R. (2011). The ethylene response factor AtERF11 that is transcriptionally modulated by the bZIP transcription factor HY5 is a crucial repressor for ethylene biosynthesis in Arabidopsis. *Plant J.* 68(1), 88-99. doi: 10.1111/j.1365-313X.2011.04670.x.

Lian, W., Yu, Q., Zhang, P., Cui, Y., Yin, Z., Cui, H., ... & Jia, H. (2023). NtPIN3 positively regulates low phosphorus tolerance by changing root elongation, Pi concentration and antioxidant capacity in tobacco. *Environ. Exp. Bot.* 208, 105257. doi: 10.1016/j.envexpbot.2023.105257.

Lin, W. Y., Huang, T. K., & Chiou, T. J. (2013). NITROGEN LIMITATION ADAPTATION, a target of microRNA827, mediates degradation of plasma membrane–localized phosphate transporters to maintain phosphate homeostasis in Arabidopsis. *Plant Cell* 25(10), 4061-4074. doi: 10.1105/tpc.113.116012.

Lin, Y. L., & Tsay, Y. F. (2017). Influence of differing nitrate and nitrogen availability on flowering control in Arabidopsis. *J. Exp. Bot.* 68(10), 2603-2609. doi: 10.1093/jxb/erx053.

Linn, J., Ren, M., Berkowitz, O., Ding, W., van der Merwe, M. J., Whelan, J., & Jost, R. (2017). Root cell-specific regulators of phosphate-dependent growth. *Plant Physiol.* 174(3), 1969-1989. doi: 10.1104/pp.16.01698.

Little, D. Y., Rao, H., Oliva, S., Daniel-Vedele, F., Krapp, A., & Malamy, J. E. (2005). The putative high-affinity nitrate transporter NRT2. 1 represses lateral root initiation in response to nutritional cues. *Proc. Natl. Acad. Sci.* 102(38), 13693-13698. doi: 10.1073/pnas.0504219102.

Liu, F., Xu, Y., Chang, K., Li, S., Liu, Z., Qi, S., ... & Wang, Y. (2019a). The long noncoding RNA T5120 regulates nitrate response and assimilation in Arabidopsis. *New Phytol.* 224(1), 117-131. doi: 10.1111/nph.16038.

Liu, H., Pan, Y., Cui, R., Hammond, J. P., White, P. J., Zhang, Y., ... & Shi, L. (2023). Integrating genome-wide association studies with selective sweep reveals genetic loci associated with tolerance to low phosphate availability in Brassica napus. *Mol. Breed.* 43(7), 53. doi: 10.1007/s11032-023-01399-9.

Liu, J., & He, Z. (2020). Small DNA methylation, big player in plant abiotic stress responses and memory. *Front. Plant Sci.* 11, 595603. doi: 10.3389/fpls.2020.595603.

Liu, J., An, X., Cheng, L., Chen, F., Bao, J., Yuan, L., ... & Mi, G. (2010). Auxin transport in maize roots in response to localized nitrate supply. *Ann. Bot.* 106(6), 1019-1026. doi: 10.1093/aob/mcq202.

Liu, L., Yang, D., Xing, B., Zhang, H., & Liang, Z. (2018). *Salvia castanea* hairy roots are more tolerant to phosphate deficiency than *Salvia miltiorrhiza* hairy roots based on the secondary metabolism and antioxidant defenses. *Molecules* 23(5), 1132. doi: 10.3390/molecules23051132.

Liu, Q., Ren, T., Zhang, Y., Li, X., Cong, R., White, P. J., & Lu, J. (2019b). Yield loss of oilseed rape (Brassica napus L.) under nitrogen deficiency is associated with under-regulation of plant population density. *Eur. J. Agron.* 103, 80-89. doi: 10.1016/j.eja.2018.11.006.

Liu, X., Huang, B., & Banowetz, G. (2002). Cytokinin effects on creeping bentgrass responses to heat stress: I. Shoot and root growth. *Crop Sci.* 42(2), 457-465. doi: 10.2135/cropsci2002.4570.

Liu, Y., & von Wirén, N. (2017). Ammonium as a signal for physiological and morphological responses in plants. *J. Exp. Bot.* 68(10), 2581-2592. doi: 10.1093/jxb/erx086.

Liu, Y., Zhao, K., Lü, G. B., Jiang, T. B., & Zhou, B. R. (2020). Transcription factor gene ERF11 response to osmotic stress in *Populus simonii× P. nigra* Poplar. *Bulletin of Botanical Research* 40(3), 433. doi: 10.7525/j.issn.1673-5102.2020.03.015.

Liu, Z., Wu, X., Wang, E., Liu, Y., Wang, Y., Zheng, Q., ... & Zhang, Y. (2022). PHR1 positively regulates phosphate starvation-induced anthocyanin accumulation through direct upregulation of genes F3'H and LDOX in Arabidopsis. *Planta* 256(2), 42. doi: 10.1007/s00425-022-03952-w.

Lohani, N., Singh, M. B., & Bhalla, P. L. (2020). High temperature susceptibility of sexual reproduction in crop plants. *J. Exp. Bot.* 71(2), 555-568. doi: 10.1093/jxb/erz426.

López-Arredondo, D. L., Leyva-González, M. A., González-Morales, S. I., López-Bucio, J., & Herrera-Estrella, L. (2014). Phosphate nutrition: improving low-phosphate tolerance in crops. *Annu. Rev. Plant Biol.* 65(1), 95-123. doi: 10.1146/annurev-arplant-050213-035949.

Lopez-Emparan, A., Quezada-Martinez, D., Zuniga-Bustos, M., Cifuentes, V., Iniguez-Luy, F., & Federico, M. L. (2014). Functional analysis of the *Brassica napus* L. phytoene synthase (PSY) gene family. *PLoS One* 9(12), e114878. doi: 10.1371/journal.pone.0114878.

Louvieaux, J., Spanoghe, M., & Hermans, C. (2020). Root morphological traits of seedlings are predictors of seed yield and quality in winter oilseed rape hybrid cultivars. *Front. Plant Sci.* 11, 568009. doi: 10.3389/fpls.2020.568009.

Love, M. I., Huber, W., & Anders, S. (2014). Moderated estimation of fold change and dispersion for RNA-seq data with DESeq2. *Genome Biol.* 15, 1-21. doi: 10.1186/s13059-014-0550-8.

Lu, K., Wei, L., Li, X., Wang, Y., Wu, J., Liu, M., ... & Li, J. (2019). Whole-genome resequencing reveals *Brassica napus* origin and genetic loci involved in its improvement. *Nat. Commun.* 10(1), 1154. doi: 10.1038/s41467-019-09134-9.

Lukoszek, R., Feist, P., & Ignatova, Z. (2016). Insights into the adaptive response of *Arabidopsis thaliana* to prolonged thermal stress by ribosomal profiling and RNA-Seq. *BMC Plant Biol.* 16, 1-13. doi: 10.1186/s12870-016-0915-0.

Lv, B., Wei, K., Hu, K., Tian, T., Zhang, F., Yu, Z., ... & Ding, Z. (2021). MPK14-mediated auxin signaling controls lateral root development via ERF13-regulated very-long-chain fatty acid biosynthesis. *Mol. Plant* 14(2), 285-297. doi: 10.1016/j.molp.2020.11.011.

Lv, Q., Zhong, Y., Wang, Y., Wang, Z., Zhang, L., Shi, J., ... & Wu, P. (2014). SPX4 negatively regulates phosphate signaling and homeostasis through its interaction with PHR2 in rice. *Plant Cell* 26(4), 1586-1597. doi: 10.1105/tpc.114.123208.

Lynch, J. P. (2011). Root phenes for enhanced soil exploration and phosphorus acquisition: tools for future crops. *Plant Physiol.* 156(3), 1041-1049. doi: 10.1104/pp.111.175414.

M'hamdi, O., Égei, M., Pék, Z., Ilahy, R., Nemeskéri, E., Helyes, L., & Takács, S. (2023). Root Development Monitoring under Different Water Supply Levels in Processing Tomato Plants. *Plants* 12(20), 3517. doi: 10.3390/plants12203517.

Ma, B., Yin, C. C., He, S. J., Lu, X., Zhang, W. K., Lu, T. G., ... & Zhang, J. S. (2014). Ethylene-induced inhibition of root growth requires abscisic acid function in rice (Oryza sativa L.) seedlings. *PLoS Genetics*, 10(10), e1004701. doi: 10.1371/journal.pgen.1004701.

Maass, D., Arango, J., Wüst, F., Beyer, P., & Welsch, R. (2009). Carotenoid crystal formation in Arabidopsis and carrot roots caused by increased phytoene synthase protein levels. *PLoS Genet.* 4(7), e6373. doi: 10.1371/journal.pone.0006373.

Maghiaoui, A., Gojon, A., & Bach, L. (2020). NRT1. 1-centered nitrate signaling in plants. *J. Exp. Bot.* 71(20), 6226-6237. doi: 10.1093/jxb/eraa361.

Maheswari, M., Murthy, A. N. G., & Shanker, A. K. (2017). Nitrogen nutrition in crops and its importance in crop quality. In The Indian nitrogen assessment (pp. 175-186). *Elsevier*. doi: 10.1016/B978-0-12-811836-8.00012-4.

Maksimović, J. D., Zhang, J., Zeng, F., Živanović, B. D., Shabala, L., Zhou, M., & Shabala, S. (2013). Linking oxidative and salinity stress tolerance in barley: can root antioxidant enzyme activity be used as a measure of stress tolerance?. *Plant Soil* 365, 141-155. doi: 10.1007/s11104-012-1366-5.

Mangano, S., Denita-Juarez, S. P., Choi, H. S., Marzol, E., Hwang, Y., Ranocha, P., ... & Estevez, J. M. (2017). Molecular link between auxin and ROS-mediated polar growth. *Proc. Natl Acad. Sci.* 114(20), 5289-5294. doi: 10.1073/pnas.1701536114.

Mansour, M. M. F. (2023). Role of vacuolar membrane transport systems in plant salinity tolerance. *J. Plant Growth Reg.* 42(3), 1364-1401. doi: 10.1007/s00344-022-10655-9.

Manzano, C., Pallero-Baena, M., Casimiro, I., De Rybel, B., Orman-Ligeza, B., Van Isterdael, G., ... & Del Pozo, J. C. (2014). The emerging role of reactive oxygen species signaling during lateral root development. *Plant Physiol.* 165(3), 1105-1119. doi: 10.1104/pp.114.238873.

Marchant, A., Bhalerao, R., Casimiro, I., Eklöf, J., Casero, P. J., Bennett, M., & Sandberg, G. (2002). AUX1 promotes lateral root formation by facilitating indole-3-acetic acid distribution between sink and source tissues in the Arabidopsis seedling. *Plant Cell* 14(3), 589-597. doi: 10.1105/tpc.010354.

Marchive, C., Roudier, F., Castaings, L., Bréhaut, V., Blondet, E., Colot, V., ... & Krapp, A. (2013). Nuclear retention of the transcription factor NLP7 orchestrates the early response to nitrate in plants. *Nat. Commun.* 4(1), 1713. doi: 10.1038/ncomms2650.

Martinez Pacheco, J., Ranocha, P., Kasulin, L., Fusari, C. M., Servi, L., Ferrero, L., ... & Estevez, J. M. (2021). Apoplastic class III peroxidases PRX62 and PRX69 regulate ROS-homeostasis

and cell wall associated extensins linked to root hair growth at low-temperature in *Arabidopsis thaliana*. *bioRxiv* 2021-08. doi: 10.1101/2021.08.20.456256.

Martins, S., Montiel-Jorda, A., Cayrel, A., Huguet, S., Roux, C. P. L., Ljung, K., & Vert, G. (2017). Brassinosteroid signaling-dependent root responses to prolonged elevated ambient temperature. *Nat. Commun.* 8(1), 309. doi: 10.1038/s41467-017-00355-4.

Marzol, E., Borassi, C., Carignani Sardoy, M., Ranocha, P., Aptekmann, A. A., Bringas, M., ... & Estevez, J. M. (2022). Class III peroxidases PRX01, PRX44, and PRX73 control root hair growth in Arabidopsis thaliana. *Int. J. Mol. Sci.* 23(10), 5375. doi: 10.3390/ijms23105375.

Masson-Delmotte, V., Zhai, P., Pirani, A., Connors, S. L., Péan, C., Berger, S., ... & Zhou, B. (2021). Climate change 2021: the physical science basis. Contribution of working group I to the sixth assessment report of the intergovernmental panel on climate change, 2(1), 2391. doi: 10.1017/9781009157896.

Matiolli, C. C., Tomaz, J. P., Duarte, G. T., Prado, F. M., Del Bem, L. E. V., Silveira, A. B., ... & Vincentz, M. (2011). The Arabidopsis bZIP gene AtbZIP63 is a sensitive integrator of transient abscisic acid and glucose signals. *Plant Physiol.* 157(2), 692-705. doi: 10.1104/pp.111.181743.

Matiu, M., Ankerst, D. P., and Menzel, A. (2017). Interactions between temperature and drought in global and regional crop yield variability during 1961-2014. *PLoS One* 12: e0178339. doi: 10.1371/journal.pone.0178339.

Mawson, R., Heaney, R. K., Zdunczyk, Z., & Kozlowska, H. J. F. N. (1993). Rapeseed meal-glucosinolates and their antinutritional effects. Part II. Flavour and palatability. *Food/Nahrung* 37(4), 336-344. doi: 10.1002/food.19930370405.

McMichael, B. L., & Burke, J. J. (1998). Soil temperature and root growth.

Medici, A., Marshall-Colon, A., Ronzier, E., Szponarski, W., Wang, R., Gojon, A., ... & Krouk, G. (2015). AtNIGT1/HRS1 integrates nitrate and phosphate signals at the Arabidopsis root tip. *Nat. Commun.* 6(1), 6274. doi: 10.1038/ncomms7274.

Medici, A., Szponarski, W., Dangeville, P., Safi, A., Dissanayake, I. M., Saenchai, C., ... & Krouk, G. (2019). Identification of molecular integrators shows that nitrogen actively controls the phosphate starvation response in plants. *Plant Cell* 31(5), 1171-1184. doi: 10.1105/tpc.18.00656.

Medici, L. O., Azevedo, R. A., Smith, R. J., & Lea, P. J. (2004). The influence of nitrogen supply on antioxidant enzymes in plant roots. *Funct. Plant Biol.* 31(1), 1-9. doi: 10.1071/FP03130.

Meena, R. P., Ghosh, G., Vishwakarma, H., & Padaria, J. C. (2022). Expression of a Pennisetum glaucum gene DREB2A confers enhanced heat, drought and salinity tolerance in transgenic Arabidopsis. *Mol. Biol. Rep.* 49(8), 7347-7358. doi: 10.1007/s11033-022-07527-6.

Merret, R., Nagarajan, V. K., Carpentier, M. C., Park, S., Favory, J. J., Descombin, J., ... & Bousquet-Antonelli, C. (2015). Heat-induced ribosome pausing triggers mRNA co-translational decay in Arabidopsis thaliana. *Nucleic Acids Res.* 43(8), 4121-4132. doi: 10.1093/nar/gkv234.

Metwally, A., Finkemeier, I., Georgi, M., and Dietz, K. J. (2003). Salicylic acid alleviates the cadmium toxicity in barley seedlings. *Plant Physiol.* 132, 272–281.doi: 10.1104/pp.102.018457.

Mi, G., Chen, F., & Zhang, F. (2008). Multiple signaling pathways controls nitrogen-mediated root elongation in maize. *Plant Signaling Behav.* 3(11), 1030-1032. doi: 10.4161/psb.6800.

Miao, Z. Q., Zhao, P. X., Mao, J. L., Yu, L. H., Yuan, Y., Tang, H., ... & Xiang, C. B. (2018). HOMEOBOX PROTEIN52 mediates the crosstalk between ethylene and auxin signaling during primary root elongation by modulating auxin transport-related gene expression. *Plant Cell* 30(11), 2761-2778. doi: 10.1105/tpc.18.00584.

Miryeganeh, M. (2021). Plants' epigenetic mechanisms and abiotic stress. *Genes* 12:1106. doi: 10.3390/genes12081106.

Mishra, S. K., Tripp, J., Winkelhaus, S., Tschiersch, B., Theres, K., Nover, L., et al. (2002). In the complex family of heat stress transcription factors, HsfA1 has a unique role as master regulator of thermotolerance in tomato. *Genes Dev.* 16, 1555–1567. doi: 10.1101/gad.228802.

Mishra, S., Spaccarotella, K., Gido, J., Samanta, I., & Chowdhary, G. (2023). Effects of heat stress on plant-nutrient relations: An update on nutrient uptake, transport, and assimilation. *Int. J. Mol. Sci.* 24(21), 15670. doi: 10.3390/ijms242115670.

Mittler, R. (2006). Abiotic stress, the field environment and stress combination. *Trends Plant Sci.* 11, 15–19. doi: 10.1016/j.tplants.2005.11.002.

Mittler, R., Finka, A., & Goloubinoff, P. (2012). How do plants feel the heat?. *Trends Biochem. Sci.* 37(3), 118-125. doi: 10.1016/j.tibs.2011.11.007.

Moeder, W., Del Pozo, O., Navarre, D. A., Martin, G. B., & Klessig, D. F. (2007). Aconitase plays a role in regulating resistance to oxidative stress and cell death in Arabidopsis and *Nicotiana benthamiana*. *Plant Mol. Biol.* 63, 273-287. doi: 10.1007/s11103-006-9087-x.

Mohd-Radzman, N. A., Laffont, C., Ivanovici, A., Patel, N., Reid, D., Stougaard, J., ... & Djordjevic, M. A. (2016). Different pathways act downstream of the CEP peptide receptor CRA2 to regulate lateral root and nodule development. *Plant Physiol.* 171(4), 2536-2548. doi: 10.1104/pp.16.00113.

Moller, I. M., Jensen, P. E., and Hansson, A. (2007). Oxidative modifications to cellular components in plants. *Annu. Rev. Plant Biol.* 58, 459–481. doi: 10.1146/ annurev.arplant.58.032806.103946.

Mollier, A., & Pellerin, S. (1999). Maize root system growth and development as influenced by phosphorus deficiency. *J. Exp. Bot.* 50(333), 487-497. doi: 10.1093/jxb/50.333.487.

Moni, A., Lee, A. Y., Briggs, W. R., & Han, I. S. (2015). The blue light receptor Phototropin 1 suppresses lateral root growth by controlling cell elongation. *Plant Biol.* 17(1), 34-40. doi: 10.1111/plb.12187.

Mora-Macías, J., Ojeda-Rivera, J. O., Gutiérrez-Alanís, D., Yong-Villalobos, L., Oropeza-Aburto, A., Raya-González, J., ... & Herrera-Estrella, L. (2017). Malate-dependent Fe accumulation is a critical checkpoint in the root developmental response to low phosphate. *Proc. Natl Acad. Sci.* 114(17), E3563-E3572. doi: 10.1073/pnas.1701952114.

Moreno-Risueño, M. A., Van Norman, J. M., Moreno, A., Zhang, J., Ahnert, S. E., & Benfey, P. N. (2010). Oscillating gene expression determines competence for periodic Arabidopsis root branching. *Science* 329(5997), 1306-1311. doi: 10.1126/science.1191937.

Morere-Le Paven, M. C., Viau, L., Hamon, A., Vandecasteele, C., Pellizzaro, A., Bourdin, C., ... & Limami, A. M. (2011). Characterization of a dual-affinity nitrate transporter MtNRT1. 3 in the model legume *Medicago truncatula*. *J. Exp. Bot.* 62(15), 5595-5605. doi: 10.1093/jxb/err243.

Mounier, E., Pervent, M., Ljung, K., Gojon, A., & Nacry, P. (2014). Auxin-mediated nitrate signalling by NRT 1.1 participates in the adaptive response of A rabidopsis root architecture to the spatial heterogeneity of nitrate availability. *Plant Cell Environ.* 37(1), 162-174. doi: 10.1111/pce.12143.

Moura, J. C. M. S., Bonine, C. A. V., de Oliveira Fernandes Viana, J., Dornelas, M. C., & Mazzafera, P. (2010). Abiotic and biotic stresses and changes in the lignin content and composition in plants. *J. Int. Plant Biol.* 52(4), 360-376. doi: 10.1111/j.1744-7909.2010.00892.x.

Mukhopadhyay, P., Reddy, M. K., Singla-Pareek, S. L., & Sopory, S. K. (2011). Transcriptional downregulation of rice rpL32 gene under abiotic stress is associated with removal of

transcription factors within the promoter region. *PLoS One* 6(11), e28058. doi: 10.1371/journal.pone.0028058.

Müller, J., Toev, T., Heisters, M., Teller, J., Moore, K. L., Hause, G., ... & Abel, S. (2015). Iron-dependent callose deposition adjusts root meristem maintenance to phosphate availability. *Dev. Cell* 33(2), 216-230. doi: 10.1016/j.devcel.2015.02.007.

Müller, R., Nilsson, L., Nielsen, L. K., & Hamborg Nielsen, T. (2005). Interaction between phosphate starvation signalling and hexokinase-independent sugar sensing in Arabidopsis leaves. *Physiol. Plant.* 124(1), 81-90. doi: 10.1111/j.1399-3054.2005.00496.x.

Munns, D. N., Fogle, V. W., & Hallock, B. G. (1977). Alfalfa root nodule distribution and inhibition of nitrogen fixation by heat 1. *Agron. J.* 69(3), 377-380. doi: 10.2134/agronj1977.00021962006900030011x.

Munns, R., Cramer, G. R., & Ball, M. C. (1999). Interactions between rising CO2, soil salinity, and plant growth. In Carbon dioxide and environmental stress (pp. 139-167). *Academic Press*. doi: 10.1016/B978-012460370-7/50006-1.

Muralidhara, P., Weiste, C., Collani, S., Krischke, M., Kreisz, P., Draken, J., ... & Dröge-Laser, W. (2021). Perturbations in plant energy homeostasis prime lateral root initiation via SnRK1-bZIP63-ARF19 signaling. *Proc. Natl Acad. Sci.* 118(37), e2106961118. doi: 10.1073/pnas.210696111.

Mussig, C., Shin, G. H., & Altmann, T. (2003). Brassinosteroids promote root growth in Arabidopsis. *Plant Physiol.* 133(3), 1261-1271. doi: 10.1104/pp.103.028662.

Muthusamy, M., Kim, J. A., Jeong, M. J., & Lee, S. I. (2020). Blue and red light upregulate α-expansin 1 (EXPA1) in transgenic *Brassica rapa* and its overexpression promotes leaf and root growth in Arabidopsis. *Plant Growth Regul.* 91(1), 75-87. doi: 10.1007/s10725-020-00588-2.

Nagaharu, U. J. J. J. B., & Nagaharu, N. J. J. J. B. (1935). Genome analysis in Brassica with special reference to the experimental formation of *B. napus* and peculiar mode of fertilization. *Jpn. J. Bot.* 7(7), 389-452.

Nagel, K. A., Kastenholz, B., Jahnke, S., Van Dusschoten, D., Aach, T., Mühlich, M., ... & Schurr, U. (2009). Temperature responses of roots: impact on growth, root system architecture and implications for phenotyping. *Funct. Plant Biol.* 36(11), 947-959. doi: 10.1071/FP09184.

Nakashima, K., Tran, L. S., Van Nguyen, D., Fujita, M., Maruyama, K., Todaka, D., et al. (2007). Functional analysis of a NAC-type transcription factor OsNAC6 involved in abiotic and biotic stress-responsive gene expression in rice. *Plant J.* 51, 617–630. doi: 10.1111/j.1365-313X.2007.03168.x.

Narise, T., Kobayashi, K., Baba, S., Shimojima, M., Masuda, S., Fukaki, H., & Ohta, H. (2010). Involvement of auxin signaling mediated by IAA14 and ARF7/19 in membrane lipid remodeling during phosphate starvation. *Plant Mol. Biol.* 72, 533-544. doi: 10.1007/s11103-009-9589-4.

Nath, U. K., Kim, H. T., Khatun, K., Park, J. I., Kang, K. K., & Nou, I. S. (2016). Modification of fatty acid profiles of rapeseed (*Brassica napus* L.) oil for using as food, industrial feed-stock and biodiesel. *Plant Breed. Biotechnol.* 4(2), 123-134. doi: 10.9787/PBB.2016.4.2.123.

Nawaz, M. A., Chen, C., Shireen, F., Zheng, Z., Sohail, H., Afzal, M., ... & Huang, Y. (2018). Genome-wide expression profiling of leaves and roots of watermelon in response to low nitrogen. *BMC Genomics* 19, 1-19. doi: 10.1186/s12864-018-4856-x.

Negi, S., Ivanchenko, M. G., & Muday, G. K. (2008). Ethylene regulates lateral root formation and auxin transport in *Arabidopsis thaliana. Plant J.* 55(2), 175-187. doi: 10.1111/j.1365-313X.2008.03495.x.

Nilsson, L., Müller, R., & Nielsen, T. H. (2010). Dissecting the plant transcriptome and the regulatory responses to phosphate deprivation. *Physiol. Plant.* 139(2), 129-143. doi: 10.1111/j.1399-3054.2010.01356.x.

Nussaume, L., Kanno, S., Javot, H., Marin, E., Pochon, N., Ayadi, A., ... & Thibaud, M. C. (2011). Phosphate import in plants: focus on the PHT1 transporters. *Front. Plant Sci.* 2, 83. doi: 10.3389/fpls.2011.00083.

Ohashi-Ito, K., Iwamoto, K., Nagashima, Y., Kojima, M., Sakakibara, H., & Fukuda, H. (2019). A positive feedback loop comprising LHW–TMO5 and local Auxin biosynthesis regulates initial vascular development in Arabidopsis roots. *Plant Cell Physiol.* 60(12), 2684-2691. doi: 10.1093/pcp/pcz156.

Ohkubo, Y., Tanaka, M., Tabata, R., Ogawa-Ohnishi, M., & Matsubayashi, Y. (2017). Shoot-to-root mobile polypeptides involved in systemic regulation of nitrogen acquisition. *Nat. Plants* 3: 17029. doi: 10.1038/nplants.2017.29.

Okushima, Y., Overvoorde, P. J., Arima, K., Alonso, J. M., Chan, A., Chang, C., ... & Theologis, A. (2005). Functional genomic analysis of the AUXIN RESPONSE FACTOR gene family members in Arabidopsis thaliana: unique and overlapping functions of ARF7 and ARF19. *Plant Cell* 17(2), 444-463. doi: 10.1105/tpc.104.028316.

Ondzighi-Assoume, C. A., Chakraborty, S., & Harris, J. M. (2016). Environmental nitrate stimulates abscisic acid accumulation in Arabidopsis root tips by releasing it from inactive stores. *Plant Cell* 28(3), 729-745. doi: 10.1105/tpc.15.00946.

Orman-Ligeza, B., Parizot, B., De Rycke, R., Fernandez, A., Himschoot, E., Van Breusegem, F., ... & Draye, X. (2016). RBOH-mediated ROS production facilitates lateral root emergence in Arabidopsis. *Development* 143(18), 3328-3339. doi: 10.1242/dev.136465.

Orosa-Puente, B., Leftley, N., Von Wangenheim, D., Banda, J., Srivastava, A. K., Hill, K., ... & Bennett, M. J. (2018). Root branching toward water involves posttranslational modification of transcription factor ARF7. *Science* 362(6421), 1407-1410. doi: 10.1126/science.aau3956.

Orsel, M., Moison, M., Clouet, V., Thomas, J., Leprince, F., Canoy, A. S., ... & Masclaux-Daubresse, C. (2014). Sixteen cytosolic glutamine synthetase genes identified in the Brassica napus L. genome are differentially regulated depending on nitrogen regimes and leaf senescence. *J. Exp. Bot.* 65(14), 3927-3947. doi: 10.1093/jxb/eru041.

Ortiz-Bobea, A., Wang, H., Carrillo, C. M., & Ault, T. R. (2019). Unpacking the climatic drivers of US agricultural yields. *Environ. Res. Lett.* 14(6), 064003. doi: 10.1088/1748-9326/ab1e75.

Otomaru, D., Ooi, N., Monden, K., Suzuki, T., Noguchi, K., Nakagawa, T., & Hachiya, T. (2024). Alternative oxidase alleviates mitochondrial oxidative stress during limited nitrate reduction in Arabidopsis thaliana. *Biomolecules* 14(8), 989. doi: 10.3390/biom14080989.

Ozturk, Z. N., Talamé, V., Deyholos, M., Michalowski, C. B., Galbraith, D. W., Gozukirmizi, N., et al. (2002). Monitoring large-scale changes in transcript abundance in drought-and salt-stressed barley. *Plant Mol. Biol.* 48, 551–573. doi: 10.1023/a:1014875215580

Pacak, A., Barciszewska-Pacak, M., Swida-Barteczka, A., Kruszka, K., Sega, P., Milanowska, K., ... & Szweykowska-Kulinska, Z. (2016). Heat stress affects Pi-related genes expression and inorganic phosphate deposition/accumulation in barley. *Front. Plant Sci.* 7, 926. doi: 10.3389/fpls.2016.00926.

Pacheco, J. M., Gabarain, V. B., Lopez, L. E., Lehuedé, T. U., Ocaranza, D., & Estevez, J. M. (2023). Understanding signaling pathways governing the polar development of root hairs in low-temperature, nutrient-deficient environments. *Curr. Opin. Plant Biol.* 75, 102386. doi: 10.1016/j.pbi.2023.102386.

Pacifici, E., Polverari, L., & Sabatini, S. (2015). Plant hormone cross-talk: the pivot of root growth. *J. Exp. Bot.* 66(4), 1113-1121. doi: 10.1093/jxb/eru534.

Pan, W., Wu, Y., & Xie, Q. (2019). Regulation of ubiquitination is central to the phosphate starvation response. *Trends Plant Sci.* 24(8), 755-769. doi: 10.1016/j.tplants.2019.05.002.

Pandey, B. K., Mehra, P., & Giri, J. (2013). Phosphorus starvation response in plants and opportunities for crop improvement. *Climate change and plant abiotic stress tolerance* 991-1012. doi: 10.1002/9783527675265.ch37.

Pandey, P., Ramegowda, V., and Senthil-kumar, M. (2015). Shared and unique responses of plants to multiple individual stresses and stress combinations: physiological and molecular mechanisms. *Front. Plant Sci.* 6:723. doi: 10.3389/fpls.2015.00723.

Park, C. H., Roh, J., Youn, J. H., Son, S. H., Park, J. H., Kim, S. Y., ... & Kim, S. K. (2018). Arabidopsis ACC oxidase 1 coordinated by multiple signals mediates ethylene biosynthesis and is involved in root development. *Mol. Cells* 41(10), 923-932. doi: 10.14348/molcells.2018.0092.

Park, C. H., Seo, C., Park, Y. J., Youn, J. H., Roh, J., Moon, J., & Kim, S. K. (2020). BES1 directly binds to the promoter of the ACC oxidase 1 gene to regulate gravitropic response in the roots of Arabidopsis thaliana. *Plant Signaling Behav.* 15(1), 1690724. doi: 10.1080/15592324.2019.1690724.

Park, M. R., Baek, S. H., de Los Reyes, B. G., Yun, S. J., & Hasenstein, K. H. (2012). Transcriptome profiling characterizes phosphate deficiency effects on carbohydrate metabolism in rice leaves. *J. Plant Physiol.* 169(2), 193-205. doi: 10.1016/j.jplph.2011.09.002.

Park, S. H., Jeong, J. S., Huang, C. H., Park, B. S., & Chua, N. H. (2023). Inositol polyphosphates-regulated polyubiquitination of PHR1 by NLA E3 ligase during phosphate starvation response in Arabidopsis. *New Phytol.* 237(4), 1215-1228. doi: 10.1111/nph.18621.

Parthasarathi, T., Firdous, S., David, E. M., Lesharadevi, K., & Djanaguiraman, M. (2022). Effects of high temperature on crops. In Advances in plant defense mechanisms. *IntechOpen* doi: 10.5772/intechopen.105945.

Passaia, G., Queval, G., Bai, J., Margis-Pinheiro, M., & Foyer, C. H. (2014). The effects of redox controls mediated by glutathione peroxidases on root architecture in *Arabidopsis thaliana*. *J. Exp. Bot.* 65(5), 1403-1413. doi: 10.1093/jxb/ert486.

Pastuszewska, B., Ochtabinska, A., & Morawski, A. (2000). A note on the nutritional adequacy of stock diets for laboratory rats and mice. *J. Anim. Feed Sci.* 9(3), 533-542.

Paula, E. M., Broderick, G. A., & Faciola, A. P. (2020). Effects of replacing soybean meal with canola meal for lactating dairy cows fed 3 different ratios of alfalfa to corn silage. *J. Dairy Sci.* 103(2), 1463-1471. doi: 10.3168/jds.2019-16947.

Peleg, Z., and Blumwald, E. (2011). Hormone balance and abiotic stress tolerance in crop plants. *Curr. Opin. Plant Biol.* 14, 290–295. doi: 10.1016/j.pbi.2011.02.001.

Peng, M., Hannam, C., Gu, H., Bi, Y. M., & Rothstein, S. J. (2007). A mutation in NLA, which encodes a RING-type ubiquitin ligase, disrupts the adaptability of Arabidopsis to nitrogen limitation. *Plant J.* 50(2), 320-337. doi: 10.1111/j.1365-313X.2007.03050.x.

Peng, X. X., Tang, X. K., Zhou, P. L., Hu, Y. J., Deng, X. B., Yan, H., et al. (2011). Isolation and expression patterns of rice WRKY82 transcription factor gene responsive to both biotic and abiotic stresses. *Agric. Sci. China* 10, 893–901. doi: 10.1016/S1671-2927(11)60074-6.

Pérez-López, U., Miranda-Apodaca, J., Muñoz-Rueda, A., & Mena-Petite, A. (2013). Lettuce production and antioxidant capacity are differentially modified by salt stress and light intensity under ambient and elevated CO2. *J. Plant Physiol.* 170(17), 1517-1525. doi: 10.1016/j.jplph.2013.06.004.

Pérez-Torres, C. A., Lopez-Bucio, J., Cruz-Ramírez, A., Ibarra-Laclette, E., Dharmasiri, S., Estelle, M., & Herrera-Estrella, L. (2008). Phosphate availability alters lateral root development in Arabidopsis by modulating auxin sensitivity via a mechanism involving the TIR1 auxin receptor. *Plant Cell* 20(12), 3258-3272. doi: 10.1105/tpc.108.058719.

Perianez-Rodriguez, J., Rodriguez, M., Marconi, M., Bustillo-Avendaño, E., Wachsman, G., Sanchez-Corrionero, A., ... & Moreno-Risueño, M. A. (2021). An auxin-regulable oscillatory circuit drives the root clock in Arabidopsis. *Sci. Adv.* 7(1), eabd4722. doi: 10.1126/sciadv.abd4722.

Petricka, J. J., Winter, C. M., & Benfey, P. N. (2012). Control of Arabidopsis root development. *Annu. Rev. Plant Biol.* 63(1), 563-590. doi: 10.1146/annurev-arplant-042811-105501.

Plaxton, W. C., & Tran, H. T. (2011). Metabolic adaptations of phosphate-starved plants. *Plant Physiol.* 156(3), 1006-1015. doi: 10.1104/pp.111.175281.

Poitout, A., Crabos, A., Petřík, I., Novák, O., Krouk, G., Lacombe, B., & Ruffel, S. (2018). Responses to systemic nitrogen signaling in Arabidopsis roots involve trans-zeatin in shoots. *Plant Cell* 30(6), 1243-1257. doi: 10.1105/tpc.18.00011.

Pongrac, P., Castillo-Michel, H., Reyes-Herrera, J., Hancock, R. D., Fischer, S., Kelemen, M., ... & White, P. J. (2020). Effect of phosphorus supply on root traits of two *Brassica oleracea* L. genotypes. *BMC Plant Biol.* 20, 1-17. doi: 10.1186/s12870-020-02558-2.

Pospíšilová, H., Jiskrova, E., Vojta, P., Mrizova, K., Kokáš, F., ˇCudejková, M. M., et al. (2016). Transgenic barley overexpressing a cytokinin dehydrogenase gene shows greater tolerance to drought stress. *New Biotechnol.* 33, 692–705. doi:10.1016/j.nbt.2015.12.005.

Prerostova, S., Dobrev, P. I., Kramna, B., Gaudinova, A., Knirsch, V., Spichal, L., ... & Vankova, R. (2020). Heat acclimation and inhibition of cytokinin degradation positively affect heat stress tolerance of Arabidopsis. *Front. Plant Sci.* 11, 87. doi: 10.3389/fpls.2020.00087.

Price, M. N., Dehal, P. S., & Arkin, A. P. (2010). FastTree 2–approximately maximum-likelihood trees for large alignments. *PloS one* 5(3), e9490. doi: 10.1371/journal.pone.0009490.

Puga, M. I., Mateos, I., Charukesi, R., Wang, Z., Franco-Zorrilla, J. M., de Lorenzo, L., ... & Paz-Ares, J. (2014). SPX1 is a phosphate-dependent inhibitor of Phosphate Starvation Response 1 in Arabidopsis. *Proc. Natl Acad. Sci.* 111(41), 14947-14952. doi: 10.1073/pnas.1404654111.

Qiao, S., Fang, Y., Wu, A., Xu, B., Zhang, S., Deng, X., et al. (2019). Dissecting root trait variability in maize genotypes using the semi-hydroponic phenotyping platform. *Plant Soil* 439, 75–90. doi: 10.1007/s11104-018-3803-6.

Qin, D. B., Liu, M. Y., Yuan, L., Zhu, Y., Li, X. D., Chen, L. M., ... & Wang, Y. (2020). CALCIUM-DEPENDENT PROTEIN KINASE 32-mediated phosphorylation is essential for the ammonium transport activity of AMT1; 1 in Arabidopsis roots. *J. Exp. Bot.* 71(16), 5087-5097. doi: 10.1093/jxb/eraa249.

Qin, L., Walk, T. C., Han, P., Chen, L., Zhang, S., Li, Y., ... & Liao, H. (2019). Adaption of roots to nitrogen deficiency revealed by 3D quantification and proteomic analysis. *Plant Physiol.* 179(1), 329-347. doi: 10.1104/pp.18.00716.

Qiu, Y., and Yu, D. (2009). Over-expression of the stress-induced *OsWRKY45* enhances disease resistance and drought tolerance in Arabidopsis. *Environ. Exp. Bot.* 65, 35–47. doi: 10.1016/j.envexpbot.2008.07.002.

Quadrana, L. (2020). The contribution of transposable elements to transcriptional novelty in plants: the FLC affair. *Transcription* 11(3-4), 192-198. doi: 10.1080/21541264.2020.1803031.

Raboanatahiry, N., Li, H., Yu, L., & Li, M. (2021). Rapeseed (*Brassica napus*): Processing, utilization, and genetic improvement. *Agronomy* 11(9), 1776. doi: 10.3390/agronomy11091776.

Ranty, B., Aldon, D., Cotelle, V., Galaud, J.-P., Thuleau, P., and Mazars, C. (2016). Calcium sensors as key hubs in plant responses to biotic and abiotic stresses. *Front. Plant Sci.* 7:327. doi: 10.3389/fpls.2016.00327.

Rashid, M., Hampton, J. G., Rolston, M. P., Khan, K. M., & Saville, D. J. (2018). Heat stress during seed development affects forage brassica (*Brassica napus* L.) seed quality. *J. Agron. Crop Sci.* 204(2), 147-154. doi: 10.1111/jac.12251.

Remans, T., Nacry, P., Pervent, M., Girin, T., Tillard, P., Lepetit, M., & Gojon, A. (2006). A central role for the nitrate transporter NRT2. 1 in the integrated morphological and physiological responses of the root system to nitrogen limitation in Arabidopsis. *Plant Physiol.* 140(3), 909-921. doi: 10.1104/pp.105.075721.

Ren, F., Chen, L., Guo, Q. Q., Zhong, H., Wu, Y., Chang, L. L., & Li, X. B. (2011). Identification and expression analysis of genes induced by phosphate starvation in leaves and roots of *Brassica napus. Plant Growth Regul.* 65, 65-81. doi: 10.1007/s10725-011-9575-0.

Ren, F., Guo, Q. Q., Chang, L. L., Chen, L., Zhao, C. Z., Zhong, H., & Li, X. B. (2012). *Brassica napus* PHR1 gene encoding a MYB-like protein functions in response to phosphate starvation. *PLoS one*. doi: 10.1371/journal.pone.0044005.

Ren, F., Zhao, C. Z., Liu, C. S., Huang, K. L., Guo, Q. Q., Chang, L. L., ... & Li, X. B. (2014). A Brassica napus PHT1 phosphate transporter, BnPht1; 4, promotes phosphate uptake and affects roots architecture of transgenic Arabidopsis. *Plant Mol. Biol.* 86, 595-607. doi: 10.1007/s11103-014-0249-y.

Rennenberg, H., Loreto, F., Polle, A., Brilli, F., Fares, S., Beniwal, R. S., & Gessler, A. J. P. B. (2006). Physiological responses of forest trees to heat and drought. *Plant Biol.* 8(05), 556-571. doi: 10.1055/s-2006-924084.

Reymond, M., Svistoonoff, S., Loudet, O., Nussaume, L., & Desnos, T. (2006). Identification of QTL controlling root growth response to phosphate starvation in *Arabidopsis thaliana. Plant Cell Environ.* 29(1), 115-125. doi: 10.1111/j.1365-3040.2005.01405.x.

Reynolds-Henne, C. E., Langenegger, A., Mani, J., Schenk, N., Zumsteg, A., and Feller, U. (2010). Interactions between temperature, drought and stomatal opening in legumes. *Environ. Exp. Bot*. 68, 37–43. doi: 10.1016/j.envexpbot.2009.11.002.

Ried, M. K., Wild, R., Zhu, J., Pipercevic, J., Sturm, K., Broger, L., ... & Hothorn, M. (2021). Inositol pyrophosphates promote the interaction of SPX domains with the coiled-coil motif of PHR transcription factors to regulate plant phosphate homeostasis. *Nat. Commun.* 12(1), 384. doi: 10.1038/s41467-020-20681-4.

Rivera, D., Rommi, K., Fernandes, M. M., Lantto, R., & Tzanov, T. (2015). Biocompounds from rapeseed oil industry co-stream as active ingredients for skin care applications. *Int. J. Cosmet. Sci.* 37(5), 496-505. doi: 10.1111/ics.12222.

Rivero, R. M., Ruiz, J. M., & Romero, L. M. (2004). Importance of N source on heat stress tolerance due to the accumulation of proline and quaternary ammonium compounds in tomato plants. *Plant Biol.* 6(06), 702-707. doi: 10.1055/s-2004-821293.

Rizhsky, L., Liang, H., Shuman, J., Shulaev, V., Davletova, S., and Mittler, R. (2004). When defense pathways collide. the response of Arabidopsis to a combination of drought and heat stress. *Plant Physiol*. 134, 1683–1696. doi: 10.1104/pp.103.033431

Rojas-Triana, M., Bustos, R., Espinosa-Ruiz, A., Prat, S., Paz-Ares, J., & Rubio, V. (2013). Roles of ubiquitination in the control of phosphate starvation responses in plants F. *J. Int. Plant Biol.* 55(1), 40-53. doi: 10.1111/jipb.12017.

Roschzttardtz, H., Séguéla-Arnaud, M., Briat, J. F., Vert, G., & Curie, C. (2011). The FRD3 citrate effluxer promotes iron nutrition between symplastically disconnected tissues throughout Arabidopsis development. *Plant Cell*, 23(7), 2725-2737. doi: 10.1105/tpc.111.088088.

Rouached, H., Stefanovic, A., Secco, D., Bulak Arpat, A., Gout, E., Bligny, R., & Poirier, Y. (2011). Uncoupling phosphate deficiency from its major effects on growth and transcriptome via PHO1 expression in Arabidopsis. *Plant J.* 65(4), 557-570. doi: 10.1111/j.1365-313X.2010.04442.x.

Roy, S. J., Negrão, S., & Tester, M. (2014). Salt resistant crop plants. *Curr. Opin. Biotechnol.* 26, 115-124. doi: 10.1016/j.copbio.2013.12.004.

Roy, S., Griffiths, M., Torres-Jerez, I., Sanchez, B., Antonelli, E., Jain, D., ... & Udvardi, M. (2022). Application of synthetic peptide CEP1 increases nutrient uptake rates along plant roots. *Front. Plant Sci.* 12, 793145. doi: 10.3389/fpls.2021.793145.

Royo, B., Moran, J. F., Ratcliffe, R. G., & Gupta, K. J. (2015). Nitric oxide induces the alternative oxidase pathway in Arabidopsis seedlings deprived of inorganic phosphate. *J. Exp. Bot.* 66(20), 6273-6280. doi: 10.1093/jxb/erv338.

Ruan, L., Wei, K., Li, J., He, M., Wu, L., Aktar, S., ... & Cheng, H. (2022). Responses of tea plants (Camellia sinensis) with different low-nitrogen tolerances during recovery from nitrogen deficiency. *J. Sci. Food Agric.* 102(4), 1405-1414. doi: 10.1002/jsfa.11473.

Rubin, G., Tohge, T., Matsuda, F., Saito, K., & Scheible, W. R. (2009). Members of the LBD family of transcription factors repress anthocyanin synthesis and affect additional nitrogen responses in Arabidopsis. *Plant Cell* 21(11), 3567-3584. doi: 10.1105/tpc.109.067041.

Rubio, V., Linhares, F., Solano, R., Martín, A. C., Iglesias, J., Leyva, A., & Paz-Ares, J. (2001). A conserved MYB transcription factor involved in phosphate starvation signaling both in vascular plants and in unicellular algae. *Genes & Development* 15(16), 2122-2133. doi: 10.1101/gad.204401.

Sabatini, S., Beis, D., Wolkenfelt, H., Murfett, J., Guilfoyle, T., Malamy, J., ... & Scheres, B. (1999). An auxin-dependent distal organizer of pattern and polarity in the Arabidopsis root. *Cell* 99(5), 463-472. doi: 10.1016/S0092-8674(00)81535-4.

Safavi-Rizi, V., Franzaring, J., Fangmeier, A., & Kunze, R. (2018). Divergent N deficiency-dependent senescence and transcriptome response in developmentally old and young Brassica napus leaves. *Front. Plant Sci.* 9, 48. doi: 10.3389/fpls.2018.00048.

Sailaja, B., Voleti, S., Subrahmanyam, D., Sarla, N., Prasanth, V. V., Bhadana, V., et al. (2014). Prediction and expression analysis of miRNAs associated with heat stress in Oryza sativa. *Rice Sci.* 21, 3–12. doi: 10.1016/S1672-6308(13)60164-X

Sakuma, Y., Liu, Q., Dubouzet, J. G., Abe, H., Shinozaki, K., & Yamaguchi-Shinozaki, K. (2002). DNA-binding specificity of the ERF/AP2 domain of Arabidopsis DREBs, transcription factors involved in dehydration-and cold-inducible gene expression. *Biochem. Biophys. Res. Commun.* 290(3), 998-1009. doi: 10.1006/bbrc.2001.6299.

Salazar-Henao, J. E., Lin, W. D., & Schmidt, W. (2016). Discriminative gene co-expression network analysis uncovers novel modules involved in the formation of phosphate deficiency-induced root hairs in Arabidopsis. *Sci. Rep.* 6(1), 26820. doi: 10.1038/srep26820.

Sales, C. R., Ribeiro, R. V., Silveira, J. A., Machado, E. C., Martins, M. O., & Lagôa, A. M. M. (2013). Superoxide dismutase and ascorbate peroxidase improve the recovery of photosynthesis in sugarcane plants subjected to water deficit and low substrate temperature. *Plant Physiol. Biochem.* 73, 326-336. doi: 10.1016/j.plaphy.2013.10.012.

Sánchez-Bermúdez, M., Del Pozo, J. C., & Pernas, M. (2022). Effects of combined abiotic stresses related to climate change on root growth in crops. *Front. Plant Sci.* 13, 918537. doi: 10.3389/fpls.2022.918537.

Sánchez-Calderón, L., López-Bucio, J., Chacón-López, A., Cruz-Ramírez, A., Nieto-Jacobo, F., Dubrovsky, J. G., & Herrera-Estrella, L. (2005). Phosphate starvation induces a determinate developmental program in the roots of Arabidopsis thaliana. *Plant Cell Physiol.* 46(1), 174-184. doi: 10.1093/pcp/pci011.

Sassi, M., Lu, Y., Zhang, Y., Wang, J., Dhonukshe, P., Blilou, I., ... & Xu, J. (2012). COP1 mediates the coordination of root and shoot growth by light through modulation of PIN1-and PIN2-dependent auxin transport in Arabidopsis. *Development* 139(18), 3402-3412.

Sato, A., & Miura, K. (2011). Root architecture remodeling induced by phosphate starvation. *Plant Signaling Behav.* 6(8), 1122-1126. doi: 10.4161/psb.6.8.15752.

Schenke, D., Boettcher, C., and Scheel, D. (2011). Crosstalk between abiotic ultraviolet-B stress and biotic (flg22) stress signalling in Arabidopsis prevents flavonol accumulation in favor of pathogen defence compound production. *Plant Cell Environ.* 34, 1849–1864. doi:10.1111/j.1365-3040.2011.02381.x.

Schlüter, U., Mascher, M., Colmsee, C., Scholz, U., Bräutigam, A., Fahnenstich, H., & Sonnewald, U. (2012). Maize source leaf adaptation to nitrogen deficiency affects not only nitrogen and carbon metabolism but also control of phosphate homeostasis. *Plant Physiol.* 160(3), 1384-1406. doi: 10.1104/pp.112.204420.

Schrick, K., Mayer, U., Horrichs, A., Kuhnt, C., Bellini, C., Dangl, J., ... & Jürgens, G. (2000). FACKEL is a sterol C-14 reductase required for organized cell division and expansion in Arabidopsis embryogenesis. *Genes & development* 14(12), 1471-1484. doi: 10.1101/gad.14.12.1471.

Schulte auf'm Erley, G., Begum, N., Worku, M., Bänziger, M., & Horst, W. J. (2007). Leaf senescence induced by nitrogen deficiency as indicator of genotypic differences in nitrogen efficiency in tropical maize. *J. Plant Nutr. Soil Sci.* 170(1), 106-114. doi: 10.1002/jpln.200625147.

Secco, D., Wang, C., Arpat, B. A., Wang, Z., Poirier, Y., Tyerman, S. D., ... & Whelan, J. (2012). The emerging importance of the SPX domain-containing proteins in phosphate homeostasis. *New Phytol.* 193(4), 842-851. doi: 10.1111/j.1469-8137.2011.04002.x.

Sega, P., & Pacak, A. (2019). Plant PHR transcription factors: put on a map. *Genes* 10(12), 1018. doi: 10.3390/genes10121018.

Sega, P., Kruszka, K., Szewc, Ł., Szweykowska-Kulińska, Z., & Pacak, A. (2020). Identification of transcription factors that bind to the 5′-UTR of the barley PHO2 gene. *Plant Mol. Biol.* 102(1), 73-88. doi: 10.1007/s11103-019-00932-9.

Selote, D. S., & Khanna-Chopra, R. (2010). Antioxidant response of wheat roots to drought acclimation. *Protoplasma* 245, 153-163. doi: 10.1007/s00709-010-0169-x.

Seo, P. J., Kim, M. J., Park, J. Y., Kim, S. Y., Jeon, J., Lee, Y. H., et al. (2010). Cold activation of a plasma membrane-tethered NAC transcription factor induces a pathogen resistance response in Arabidopsis. *Plant J.* 61, 661–671. doi: 10.1111/j.1365-313X.2009.04091.x.

Seo, P. J., Lee, S. B., Suh, M. C., Park, M. J., Go, Y. S., and Park, C. M. (2011). The MYB96 transcription factor regulates cuticular wax biosynthesis under drought conditions in Arabidopsis. *Plant Cell* 23, 1138–1152. doi: 10.1105/tpc.111.083485.

Shaheen, M. R., Ayyub, C. M., Amjad, M., & Waraich, E. A. (2016). Morpho-physiological evaluation of tomato genotypes under high temperature stress conditions. *J. Sci. Food Agric.* 96(8), 2698-2704. doi: 10.1002/jsfa.7388.

Sheibanirad, A., Haghighi, M., & Pessarakli, M. (2023). The effect of root zone temperature at low nitrogen level of nutrient solution on sweet pepper. *J. Plant Nutr.* 46(16), 3983-4000. doi: 10.1080/01904167.2023.2220725.

Shekhar, V., Stckle, D., Thellmann, M., and Vermeer, J. E. M. (2019). The role of plant root systems in evolutionary adaptation. *Curr. Top. Dev. Biol.* 131, 55–80. doi: 10.1016/bs.ctdb.2018.11.011.

Shen, C., Wang, S., Zhang, S., Xu, Y., Qian, Q., Qi, Y., & Jiang, D. A. (2013). OsARF16, a transcription factor, is required for auxin and phosphate starvation response in rice (Oryza sativa L.). *Plant Cell Environ.* 36(3), 607-620. doi: 10.1111/pce.12001.

Shen, X., Yang, L., Han, P., Gu, C., Li, Y., Liao, X., & Qin, L. (2022). Metabolic profiles reveal changes in the leaves and roots of rapeseed (Brassica napus L.) seedlings under nitrogen deficiency. *Int. J. Mol. Sci.* 23(10), 5784. doi: 10.3390/ijms23105784.

Shen, Y. G., Zhang, W. K., He, S. J., Zhang, J. S., Liu, Q., and Chen, S. Y. (2003). An EREBP/AP2-type protein in Triticum aestivum was a DRE-binding transcription factor induced by cold, dehydration and ABA stress. *Theor. Appl. Genet.* 106, 923–930. doi: 10.1007/s00122002-1131-x.

Shen, Y., McLaughlin, N., Zhang, X., Xu, M., & Liang, A. (2018). Effect of tillage and crop residue on soil temperature following planting for a Black soil in Northeast China. *Sci. Rep.* 8(1), 4500. doi: 10.1038/s41598-018-22822-8.

Shi ZhengJun, S. Z., Fan XiaoLin, F. X., Klaus, D., & Sattemacher, B. (2005). Effect of localized nitrogen supply on root morphology in rice and its mechanism. *Chinese Journal of Rice Science*. 19(2), 147-152.

Shi, X., Jiang, F., Wen, J., & Wu, Z. (2019). Overexpression of Solanum habrochaites microRNA319d (sha-miR319d) confers chilling and heat stress tolerance in tomato (S. lycopersicum). *BMC Plant Biol.* 19, 1-17. doi: 10.1186/s12870-019-1823-x.

Shimizu, A., Yanagihara, S., Kawasaki, S., & Ikehashi, H. (2004). Phosphorus deficiency-induced root elongation and its QTL in rice (*Oryza sativa* L.). *Theor. Appl. Genet.* 109, 1361-1368. doi: 10.1007/s00122-004-1751-4.

Shin, H., Shin, H. S., Dewbre, G. R., & Harrison, M. J. (2004). Phosphate transport in Arabidopsis: Pht1; 1 and Pht1; 4 play a major role in phosphate acquisition from both low-and high-phosphate environments. *Plant J.* 39(4), 629-642. doi: 10.1111/j.1365-313X.2004.02161.x.

Shin, R., Burch, A. Y., Huppert, K. A., Tiwari, S. B., Murphy, A. S., Guilfoyle, T. J., & Schachtman, D. P. (2007). The Arabidopsis transcription factor MYB77 modulates auxin signal transduction. *Plant Cell* 19(8), 2440-2453. doi: 10.1105/tpc.107.050963.

Shinohara, T., Martin, E. A., and Leskovar, D. I. (2017). Ethylene regulators influence germination and root growth of globe artichoke seedlings exposed to heat stress conditions. *Seed Sci. Technol.* 45, 167–178. doi: 10.15258/sst.2017.45.1.07.

Silva-Navas, J., Conesa, C. M., Saez, A., Navarro-Neila, S., Garcia-Mina, J. M., Zamarreño, A. M., ... & Del Pozo, J. C. (2019). Role of cis-zeatin in root responses to phosphate starvation. *New Phytol.* 224(1), 242-257. doi: 10.1111/nph.16020.

Silva-Navas, J., Moreno-Risueno, M. A., Manzano, C., Pallero-Baena, M., Navarro-Neila, S., Téllez-Robledo, B., ... & del Pozo, J. C. (2015). D-Root: a system for cultivating plants with the roots in darkness or under different light conditions. *Plant J.* 84(1), 244-255. doi: 10.1111/tpj.12998.

Silva-Navas, J., Moreno-Risueno, M. A., Manzano, C., Téllez-Robledo, B., Navarro-Neila, S., Carrasco, V., ... & Del Pozo, J. C. (2016). Flavonols mediate root phototropism and growth through regulation of proliferation-to-differentiation transition. *Plant Cell* 28(6), 1372-1387. doi: 10.1105/tpc.15.00857.

Simon, N. M., Graham, C. A., Comben, N. E., Hetherington, A. M., & Dodd, A. N. (2020). The circadian clock influences the long-term water use efficiency of Arabidopsis. *Plant Physiol.* 183(1), 317-330. doi: 10.1104/pp.20.00030.

Singh, A. P., Fridman, Y., Friedlander-Shani, L., Tarkowska, D., Strnad, M., & Savaldi-Goldstein, S. (2014). Activity of the brassinosteroid transcription factors BRASSINAZOLE RESISTANT1 and BRASSINOSTEROID INSENSITIVE1-ETHYL METHANESULFONATE-SUPPRESSOR1/BRASSINAZOLE RESISTANT2 blocks developmental reprogramming in response to low phosphate availability. *Plant Physiol.* 166(2), 678-688. doi: 10.1104/pp.114.245019.

Singh, A. P., Fridman, Y., Holland, N., Ackerman-Lavert, M., Zananiri, R., Jaillais, Y., ... & Savaldi-Goldstein, S. (2018). Interdependent nutrient availability and steroid hormone signals facilitate root growth plasticity. *Dev. Cell* 46(1), 59-72. doi: 10.1016/j.devcel.2018.06.002.

Singh, S. K., Kakani, V. G., Brand, D., Baldwin, B., & Reddy, K. R. (2008). Assessment of cold and heat tolerance of winter-grown canola (Brassica napus L.) cultivars by pollen-based parameters. *J. Agron. Crop Sci.* 194(3), 225-236. doi: 10.1111/j.1439-037X.2008.00309.x.

Singh, S., Yadav, S., Singh, A., Mahima, M., Singh, A., Gautam, V., & Sarkar, A. K. (2020). Auxin signaling modulates LATERAL ROOT PRIMORDIUM 1 (LRP 1) expression during lateral root development in Arabidopsis. *Plant J.* 101(1), 87-100. doi: 10.1111/tpj.14520.

Smith, S., & De Smet, I. (2012). Root system architecture: insights from Arabidopsis and cereal crops. *Phil. Trans. R. Soc. B: Biological Sciences*, 367(1595), 1441-1452. doi: 10.1098/rstb.2011.0234.

Song, H., Cai, Z., Liao, J., Tang, D., & Zhang, S. (2019). Sexually differential gene expressions in poplar roots in response to nitrogen deficiency. *Tree Physiol.* 39(9), 1614-1629. doi: 10.1093/treephys/tpz057.

Song, L., Yu, H., Dong, J., Che, X., Jiao, Y., & Liu, D. (2016). The molecular mechanism of ethylene-mediated root hair development induced by phosphate starvation. *PLoS Genet.* 12(7), e1006194. doi: 10.1371/journal.pgen.1006194.

Song, Z., Fan, N., Jiao, G., Liu, M., Wang, X., & Jia, H. (2019). Overexpression of OsPT8 increases auxin content and enhances tolerance to high-temperature stress in Nicotiana tabacum. *Genes* 10(10), 809. doi: 10.3390/genes10100809.

Sorin, C., Leport, L., Cambert, M., Bouchereau, A., Mariette, F., & Musse, M. (2016). Nitrogen deficiency impacts on leaf cell and tissue structure with consequences for senescence associated processes in *Brassica napus*. *Bot. Stud.* 57(1), 11. doi: 10.1186/s40529-016-0125-y.

St. Clair, S. B., and Lynch, J. P. (2010). The opening of pandora's box: climate change impacts on soil fertility and crop nutrition in developing countries. *Plant Soil* 335, 101–115. doi: 10.1007/s11104-010-0328-z.

Steffens, B., & Rasmussen, A. (2016). The physiology of adventitious roots. *Plant Physiol.* 170(2), 603-617. doi: 10.1104/pp.15.01360.

Stevens, J., Senaratna, T., and Sivasithamparam, K. (2006). Salicylic acid induces salinity tolerance in tomato (Lycopersicon esculentum cv. Roma): associated changes in gas exchange, water relations and membrane stabilisation. *Plant Growth Regul.* 49, 77–83. doi: 10.1007/s10725-006-0019-1.

Stührwohldt, N., Bühler, E., Sauter, M., & Schaller, A. (2020). Precursor processing by SBT3. 8 and phytosulfokine signaling contribute to drought stress tolerance in Arabidopsis. *bioRxiv* 2020-10. doi: 10.1101/2020.10.21.349779.

Sun, G., Luan, M., Xue, S., Yan, J., & Lan, W. (2024). Vacuolar H+-ATPase Is Required for Efficient Vacuolar Phosphate Storage and Systemic Pi Homeostasis in Arabidopsis. *Plant Cell Environ.* 48(1), 587-598. doi: 10.1111/pce.15166.

Sun, M. M., Tian, Y., Chun, M., & Chen, Y. F. (2022). The ubiquitin E3 ligase PRU2 modulates phosphate uptake in Arabidopsis. *Int. J. Mol. Sci.* 23(4), 2273. doi: 10.3390/ijms23042273.

Sun, X., Chen, F., Yuan, L., & Mi, G. (2020). The physiological mechanism underlying root elongation in response to nitrogen deficiency in crop plants. *Planta* 251, 1-14. doi: 10.1007/s00425-020-03376-4.

Sunkar, R., Chinnusamy, V., Zhu, J., and Zhu, J. K. (2007). Small RNAs as big players in plant abiotic stress responses and nutrient deprivation. *Trends Plant Sci.* 12, 301–309. doi: 10.1016/j.tplants.2007.05.001.

Sunseri, F., Aci, M. M., Mauceri, A., Caldiero, C., Puccio, G., Mercati, F., & Abenavoli, M. R. (2023). Short-term transcriptomic analysis at organ scale reveals candidate genes involved in low N responses in NUE-contrasting tomato genotypes. *Front. Plant Sci.* 14, 1125378. doi: 10.3389/fpls.2023.1125378.

Suzuki, N., Rivero, R. M., Shulaev, V., Blumwald, E., and Mittler, R. (2014). Tansley review abiotic and biotic stress combinations. *New Phytol.* 203, 32–43. doi:10.1111/nph.12797.

Svistoonoff, S., Creff, A., Reymond, M., Sigoillot-Claude, C., Ricaud, L., Blanchet, A., ... & Desnos, T. (2007). Root tip contact with low-phosphate media reprograms plant root architecture. *Nat. Genet.* 39(6), 792-796. doi: 10.1038/ng2041.

Swarbreck, S. M., Wang, M., Wang, Y., Kindred, D., Sylvester-Bradley, R., Shi, W., ... & Griffiths, H. (2019). A roadmap for lowering crop nitrogen requirement. *Trends Plant Sci.* 24(10), 892-904. doi: 10.1016/j.tplants.2019.06.006.

Szklarczyk, D., Franceschini, A., Wyder, S., Forslund, K., Heller, D., Huerta-Cepas, J., ... & Von Mering, C. (2015). STRING v10: protein–protein interaction networks, integrated over the tree of life. *Nucleic Acids Res.* 43(D1), D447-D452. doi: 10.1093/nar/gku1003.

Tabata, R., Sumida, K., Yoshii, T., Ohyama, K., Shinohara, H., & Matsubayashi, Y. (2014). Perception of root-derived peptides by shoot LRR-RKs mediates systemic N-demand signaling. *Science* 346(6207), 343-346. doi: 10.1126/science.1257800.

Takatsuka, H., & Umeda, M. (2014). Hormonal control of cell division and elongation along differentiation trajectories in roots. *J. Exp. Bot.* 65(10), 2633-2643. doi: 10.1093/jxb/ert485.

Takeno, K. (2016). Stress-induced flowering: the third category of flowering response. *J. Exp. Bot.* 67(17), 4925-4934. doi: 10.1093/jxb/erw272.

Talanova, V., Akimova, T., and Titov, A. (2003). Effect of whole plant and local heating on the ABA content in cucumber seedling leaves and roots and on their heat tolerance. *Russ. J. Plant Physiol.* 50, 90–94. doi: 10.1023/A:1021996703940.

Taleski, M., Imin, N., & Djordjevic, M. A. (2018). CEP peptide hormones: key players in orchestrating nitrogen-demand signalling, root nodulation, and lateral root development. *J. Exp. Bot.* 69(8), 1829-1836. doi: 10.1093/jxb/ery037.

Taleski, M., Jin, M., Chapman, K., Taylor, K., Winning, C., Frank, M., ... & Djordjevic, M. A. (2024). CEP hormones at the nexus of nutrient acquisition and allocation, root development, and plant–microbe interactions. *J. Exp. Bot.* 75(2), 538-552. doi: 10.1093/jxb/erad444.

Tamele, R. A., Ueno, H., Toma, Y., & Morita, N. (2020). Nitrogen recoveries and nitrogen use efficiencies of organic fertilizers with different C/N ratios in maize cultivation with low-fertile soil by 15N method. *Agriculture* 10(7), 272. doi: 10.3390/agriculture10070272.

Teng, R. M., Yang, N., Li, J. W., Liu, C. F., Chen, Y., Li, T., ... & Zhuang, J. (2022). Isolation and characterization of an LBD transcription factor CsLBD39 from tea plant (Camellia sinensis) and its roles in modulating nitrate content by regulating nitrate-metabolism-related genes. *Int. J. Mol. Sci.* 23(16), 9294. doi: 10.3390/ijms23169294.

Teves, S. S., & Henikoff, S. (2011). Heat shock reduces stalled RNA polymerase II and nucleosome turnover genome-wide. *Genes & Development* 25(22), 2387-2397. doi: 10.1101/gad.177675.111.

Tian, Q. Y., Sun, P., & Zhang, W. H. (2009). Ethylene is involved in nitrate-dependent root growth and branching in Arabidopsis thaliana. *New Phytol.* 184(4), 918-931. doi: 10.1111/j.1469-8137.2009.03004.x.

Tian, Q., Chen, F., Zhang, F., & Mi, G. (2005). Possible involvement of cytokinin in nitrate-mediated root growth in maize. *Plant Soil*, 277, 185-196. doi: 10.1007/s11104-005-6837-5.

Tian, W. H., Ye, J. Y., Cui, M. Q., Chang, J. B., Liu, Y., Li, G. X., ... & Zheng, S. J. (2021). A transcription factor STOP1-centered pathway coordinates ammonium and phosphate acquisition in Arabidopsis. *Mol. Plant* 14(9), 1554-1568. doi: 10.1016/j.molp.2021.06.024.

Tian, Z., Liu, X., Yu, J., Gu, S., Zhang, L., Jiang, D., ... & Dai, T. (2020). Early nitrogen deficiency favors high nitrogen recovery efficiency by improving deeper soil root growth and reducing nitrogen loss in wheat. *Arch. Agron. Soil Sci.* 66(10), 1384-1398. doi: 10.1080/03650340.2019.1671972.

Tindall, J. A., Mills, H. A., and Radcliffe, D. E. (1990). The effect of root zone temperature on nutrient uptake of tomato. *J. Plant Nutr.* 13, 939–956. doi:10.1080/01904169009364127.

Tiwari, M., Singh, B., Yadav, M., Pandey, V., & Bhatia, S. (2021). High throughput identification of miRNAs reveal novel interacting targets regulating chickpea-rhizobia symbiosis. *Environ. Exp. Bot.* 186, 104469. doi: 10.1016/j.envexpbot.2021.104469.

Tokizawa, M., Enomoto, T., Chandnani, R., Mora-Macías, J., Burbridge, C., Armenta-Medina, A., ... & Kochian, L. V. (2023). The transcription factors, STOP1 and TCP20, are required for root system architecture alterations in response to nitrate deficiency. *Proc. Nat. Acad. Sci.* 120(35), e2300446120. doi: 10.1073/pnas.2300446120.

Tong, J., Walk, T. C., Han, P., Chen, L., Shen, X., Li, Y., ... & Qin, L. (2020). Genome-wide identification and analysis of high-affinity nitrate transporter 2 (NRT2) family genes in rapeseed (*Brassica napus* L.) and their responses to various stresses. *BMC Plant Biol.* 20, 1-16. doi: 10.1186/s12870-020-02648-1.

Tran, H. T., Hurley, B. A., & Plaxton, W. C. (2010). Feeding hungry plants: the role of purple acid phosphatases in phosphate nutrition. *Plant Sci.* 179(1-2), 14-27. doi: 10.1016/j.plantsci.2010.04.005.

Trapeznikov, V. K., Ivanov, I. I., and Kudoyarova, G. R. (2003). Effect of heterogeneous distribution of nutrients on root growth, ABA content and drought resistance of wheat plants. *Plant Soil* 252, 207–214. doi: 10.1023/A:1024734310214.

Tripathy, M. K., Deswal, R., & Sopory, S. K. (2021). Plant RABs: role in development and in abiotic and biotic stress responses. *Curr. Genomics* 22(1), 26-40. doi: 10.2174/1389202922666210114102743.

Trumbo, P., Schlicker, S., Yates, A. A., & Poos, M. (2002). Dietary reference intakes for energy, carbohydrate, fiber, fat, fatty acids, cholesterol, protein and amino acids. (Commentary). *Journal of the American dietetic association* 102(11), 1621-1631.

Tsai, S. S., & Chang, Y. C. A. (2022). Plant maturity affects flowering ability and flower quality in phalaenopsis, focusing on their relationship to carbon-to-nitrogen ratio. *HortScience*, 57(2), 191-196. doi: 10.21273/HORTSCI16273-21.

Tuteja, N. (2007). Abscisic Acid and abiotic stress signaling. *Plant Signal. Behav.* 2, 135–138. doi: 10.4161/psb.2.3.4156.

Ueda, Y., Kiba, T., & Yanagisawa, S. (2020a). Nitrate-inducible NIGT1 proteins modulate phosphate uptake and starvation signalling via transcriptional regulation of SPX genes. *Plant J.* 102(3), 448-466. doi: 10.1111/tpj.14637.

Ueda, Y., Ohtsuki, N., Kadota, K., Tezuka, A., Nagano, A. J., Kadowaki, T., ... & Yanagisawa, S. (2020b). Gene regulatory network and its constituent transcription factors that control nitrogen-deficiency responses in rice. *New Phytol.* 227(5), 1434-1452. doi: 10.1111/nph.16627.

Ullah, A., Romdhane, L., Rehman, A., & Farooq, M. (2019). Adequate zinc nutrition improves the tolerance against drought and heat stresses in chickpea. *Plant Physiol. Biochem.* 143, 11-18. doi: 10.1016/j.plaphy.2019.08.020.

Umezawa, T., Okamoto, M., Kushiro, T., Nambara, E., Oono, Y., Seki, M., ... & Shinozaki, K. (2006). CYP707A3, a major ABA 8′-hydroxylase involved in dehydration and rehydration response in Arabidopsis thaliana. *Plant J.* 46(2), 171-182. doi: 10.1111/j.1365-313X.2006.02683.x.

VALDÉS-LÓPEZ, O. S. W. A. L. D. O., ARENAS-HUERTERO, C. A. T. A. L. I. N. A., Ramirez, M., Girard, L., Sanchez, F., Vance, C. P., ... & Hernandez, G. (2008). Essential role of MYB transcription factor: PvPHR1 and microRNA: PvmiR399 in phosphorus-deficiency signalling in common bean roots. *Plant Cell Environ.* 31(12), 1834-1843. doi: 10.1111/j.1365-3040.2008.01883.x.

Valdés-López, O., Batek, J., Gomez-Hernandez, N., Nguyen, C. T., Isidra-Arellano, M. C., Zhang, N., ... & Stacey, G. (2016). Soybean roots grown under heat stress show global changes in their transcriptional and proteomic profiles. *Front. Plant Sci.* 7, 517. doi: 10.3389/fpls.2016.00517.

Van der Werf, A., & Nagel, O. W. (1996). Carbon allocation to shoots and roots in relation to nitrogen supply is mediated by cytokinins and sucrose: opinion. *Plant Soil* 185, 21-32. doi: 10.1007/BF02257562.

Vannini, C., Campa, M., Iriti, M., Genga, A., Faoro, F., Carravieri, S., et al. (2007). Evaluation of transgenic tomato plants ectopically expressing the rice Osmyb4 gene. *Plant Sci.* 173, 231–239. doi: 10.1016/j.plantsci.2007.05.007.

Vaseva, I. I., Simova-Stoilova, L., Kirova, E., Mishev, K., Depaepe, T., Van Der Straeten, D., & Vassileva, V. (2021). Ethylene signaling in salt-stressed Arabidopsis thaliana ein2-1 and ctr1-1 mutants–a dissection of molecular mechanisms involved in acclimation. *Plant Physiol. Biochem.* 167, 999-1010. doi: 10.1016/j.plaphy.2021.09.029.

Vazquez-Carrasquer, V., Laperche, A., Bissuel-Bélaygue, C., Chelle, M., & Richard-Molard, C. (2021). Nitrogen uptake efficiency, mediated by fine root growth, early determines temporal and genotypic variations in nitrogen use efficiency of winter oilseed rape. *Front. Plant Sci.* 12, 641459. doi: 10.3389/fpls.2021.641459.

Velasquez, S. M., Barbez, E., Kleine-Vehn, J., & Estevez, J. M. (2016). Auxin and cellular elongation. *Plant Physiol.* 170(3), 1206-1215. doi: 10.1104/pp.15.01863.

Veljović Jovanović, S., Kukavica, B., Vidović, M., Morina, F., & Menckhoff, L. (2018). Class III peroxidases: functions, localization and redox regulation of isoenzymes. *Antioxidants and antioxidant enzymes in higher plants*, 269-300. doi: 10.1007/978-3-319-75088-0_13.

Verslues, P. E., & Longkumer, T. (2022). Size and activity of the root meristem: a key for drought resistance and a key model of drought-related signaling. *Physiol. Plant.* 174(1), e13622. doi: 10.1111/ppl.13622.

Vidal, E. A., Álvarez, J. M., & Gutiérrez, R. A. (2014). Nitrate regulation of AFB3 and NAC4 gene expression in Arabidopsis roots depends on NRT1. 1 nitrate transport function. *Plant Signaling Behav.* 9(6), e28501. doi: 10.4161/psb.28501.

Vidal, E. A., Araus, V., Lu, C., Parry, G., Green, P. J., Coruzzi, G. M., & Gutiérrez, R. A. (2010). Nitrate-responsive miR393/AFB3 regulatory module controls root system architecture in Arabidopsis thaliana. *Proc. Natl. Acad. Sci.* 107(9), 4477-4482. doi: 10.1073/pnas.0909571107.

Vijayakumar, P., Datta, S., & Dolan, L. (2016). ROOT HAIR DEFECTIVE SIX-LIKE 4 (RSL 4) promotes root hair elongation by transcriptionally regulating the expression of genes required for cell growth. *New Phytol.* 212(4), 944-953. doi: 10.1111/nph.14095.

Villaécija-Aguilar, J. A., Körösy, C., Maisch, L., Hamon-Josse, M., Petrich, A., Magosch, S., ... & Gutjahr, C. (2022). KAI2 promotes Arabidopsis root hair elongation at low external phosphate by controlling local accumulation of AUX1 and PIN2. *Curr. Biol.* 32(1), 228-236. doi: 10.1016/j.cub.2021.10.044.

Villar, N., Aranguren, M., Castellón, A., Besga, G., & Aizpurua, A. (2019). Soil nitrogen dynamics during an oilseed rape (*Brassica napus* L.) growing cycle in a humid Mediterranean climate. *Sci. Rep.* 9(1), 13864. doi: 10.1038/s41598-019-50347-1.

Villordon, A. Q., Ginzberg, I., and Firon, N. (2014). Root architecture and root and tuber crop productivity. *Trends Plant Sci.* 19, 419–425. doi: 10.1016/j.tplants.2014.02.002.

Voss-Fels, K. P., Snowdon, R. J., and Hickey, L. T. (2018). Designer roots for future crops. *Trends Plant Sci.* 23, 957–960. doi: 10.1016/j.tplants.2018.08.004.

Wahid, A., & Shabbir, A. (2005). Induction of heat stress tolerance in barley seedlings by pre-sowing seed treatment with glycinebetaine. *Plant Growth Regul.* 46, 133-141. doi: 10.1007/s10725-005-8379-5.

Wahid, A., Gelani, S., Ashraf, M., & Foolad, M. R. (2007). Heat tolerance in plants: an overview. *Environ. Exp. Bot.* 61(3), 199-223. doi: 10.1016/j.envexpbot.2007.05.011.

Waidmann, S., Sarkel, E., and Kleine-Vehn, J. (2020). Same same, but different: growth responses of primary and lateral roots. *J. Exp. Bot.* 71, 2397–2411. doi: 10.1093/jxb/eraa027.

Waititu, J. K., Zhang, C., Liu, J., and Wang, H. (2020). Plant non-coding RNAs: origin, biogenesis, mode of action and their roles in abiotic stress. *Int. J. Mol.* Sci. 21:8401. doi: 10.3390/ijms21218401.

Wallace, H., Knutsen, H. K., Alexander, J., Barregård, L., Bignami, M., Brüschweiler, B., ... & Vleminckx, C. (2016). Erucic acid in feed and food. *EFSA J.* doi: 10.2903/j.efsa.2016.4593.

Wang XiaoWu, W. X., Wang HanZhong, W. H., Wang Jun, W. J., Sun RiFei, S. R., Wu Jian, W. J., Liu ShengYi, L. S., ... & Li Bo, L. B. (2011). The genome of the mesopolyploid crop species *Brassica rapa*. *Nat. Genet.* 43(10), 1035-1039. doi: 10.1038/ng.919.

Wang, F., Wang, Y., Ying, L., Lu, H., Liu, Y., Liu, Y., ... & Mao, C. (2023a). Integrated transcriptomic analysis identifies coordinated responses to nitrogen and phosphate deficiency in rice. *Front. Plant Sci.* 14, 1164441. doi: 10.3389/fpls.2023.1164441.

WANG, F., XUE, K., & FU, W. (2019). Effects of soil nitrogen and phosphorus contents on ecological stoichiometry of wheat leaf. *Chinese Journal of Eco-Agriculture*, 27(1), 60-71. doi: 10.13930/j.cnki.cjea.180133.

Wang, G. L., Ding, G. D., Xu, F. S., Cai, H. M., Zou, J., & Ye, X. S. (2015). Genotype differences in photosynthetic characteristics and nitrogen efficiency of new-type oilseed rape responding to low nitrogen stress. *J. Agric. Sci.* 153(6), 1030-1043. doi: 10.1017/S0021859614000744.

Wang, J. R., Hu, H., Wang, G. H., Li, J., Chen, J. Y., & Wu, P. (2009). Expression of PIN genes in rice (Oryza sativa L.): tissue specificity and regulation by hormones. *Mol. Plant* 2(4), 823-831. doi: 10.1093/mp/ssp023.

Wang, J., Sun, J., Miao, J., Guo, J., Shi, Z., He, M., ... & Li, Z. (2013). A phosphate starvation response regulator Ta-PHR1 is involved in phosphate signalling and increases grain yield in wheat. *Ann. Bot.* 111(6), 1139-1153. doi: 10.1093/aob/mct080.

Wang, J., Sun, N., Zheng, L., Zhang, F., Xiang, M., Chen, H., ... & Wei, N. (2023b). Brassinosteroids promote etiolated apical structures in darkness by amplifying the ethylene response via the EBF-EIN3/PIF3 circuit. *Plant Cell* 35(1), 390-408. doi: 10.1093/plcell/koac316.

Wang, K., Zhang, X., & Ervin, E. (2012). Antioxidative responses in roots and shoots of creeping bentgrass under high temperature: Effects of nitrogen and cytokinin. *J. Plant Physiol.* 169(5), 492-500. doi: 10.1016/j.jplph.2011.12.007.

Wang, K., Zhang, X., Goatley, M., & Ervin, E. (2014a). Heat shock proteins in relation to heat stress tolerance of creeping bentgrass at different N levels. *PLoS One* 9(7), e102914. doi: 10.1371/journal.pone.0102914.

Wang, Q., Guan, Y., Wu, Y., Chen, H., Chen, F., and Chu, C. (2008). Overexpression of a rice OsDREB1F gene increases salt, drought, and low temperature tolerance in both Arabidopsis and rice. *Plant Mol. Biol.* 67, 589–602. doi: 10.1007/s11103-008-9340-6.

Wang, R., Zhang, Y., Kieffer, M., Yu, H., Kepinski, S., & Estelle, M. (2016). HSP90 regulates temperature-dependent seedling growth in Arabidopsis by stabilizing the auxin co-receptor F-box protein TIR1. *Nat. Commun.* 7(1), 10269. doi: 10.1038/ncomms10269.

Wang, S., Cao, L., Willick, I. R., Wang, H., & Tanino, K. K. (2022a). Arabidopsis ubiquitin-conjugating enzymes UBC4, UBC5, and UBC6 have major functions in sugar metabolism and leaf senescence. *Int. J. Mol. Sci.* 23(19), 11143. doi: 10.3390/ijms231911143.

Wang, W., Ding, G., White, P. J., Wang, M., Zou, J., Xu, F., ... & Shi, L. (2020a). Genetic dissection of the shoot and root ionomes of Brassica napus grown with contrasting phosphate supplies. *Ann. Bot.* 126(1), 119-140. doi: 10.1093/aob/mcaa055.

Wang, X., Altaf, M. A., Hao, Y., Wang, Z., & Zhu, G. (2023c). Effect of heat stress on root architecture, photosynthesis, and antioxidant profile of water spinach (Ipomoea aquatica Forsk) seedlings. *Horticulturae* 9(8), 923. doi: 10.3390/horticulturae9080923.

Wang, X., Qin, J., Tian, W., Wang, M., Du, W., & Wang, L. (2023d). The soybean CEP6 signaling peptides positively regulates nodulation. doi: 10.21203/rs.3.rs-2794767/v1.

Wang, X., Wang, H. F., Chen, Y., Sun, M. M., Wang, Y., & Chen, Y. F. (2020b). The transcription factor NIGT1. 2 modulates both phosphate uptake and nitrate influx during phosphate starvation in Arabidopsis and maize. *Plant Cell* 32(11), 3519-3534. doi: 10.1105/tpc.20.00361.

Wang, X., Yuan, Y., Charrier, L., Deng, Z., Geisler, M., Deng, X. W., & Chen, H. (2024a). Light-stabilized GIL1 suppresses PIN3 activity to inhibit hypocotyl gravitropism. *J. Integr. Plant Biol.* 66(9), 1886-1897. doi: 10.1111/jipb.13736.

Wang, X., Zhao, C., Müller, C., Wang, C., Ciais, P., Janssens, I., ... & Piao, S. (2020c). Emergent constraint on crop yield response to warmer temperature from field experiments. *Nat. Sustainability* 3(11), 908-916. doi: 10.1038/s41893-020-0569-7.

Wang, Y., Yuan, Z., Wang, J., Xiao, H., Wan, L., Li, L., ... & Zhang, J. (2023e). The nitrate transporter NRT2. 1 directly antagonizes PIN7-mediated auxin transport for root growth adaptation. *Proc. Nat. Acad. Sci.* 120(25), e2221313120. doi: 10.1073/pnas.2221313120.

Wang, Y., Zhao, Z., Wang, S., Shi, L., Ding, G., & Xu, F. (2022b). Boron mediates nitrogen starvation-induced leaf senescence by regulating ROS production and C/N balance in Brassica napus. *Environ. Exp. Bot.* 200, 104905. doi: 10.1016/j.envexpbot.2022.104905.

Wang, Z., Ruan, W., Shi, J., Zhang, L., Xiang, D., Yang, C., ... & Wu, P. (2014b). Rice SPX1 and SPX2 inhibit phosphate starvation responses through interacting with PHR2 in a phosphate-dependent manner. *PNAS* 111(41), 14953-14958. doi: 10.1073/pnas.1404680111.

Wang, Z., Zheng, Z., & Liu, D. (2024b). Comparative functional analyses of PHR1, PHL1, and PHL4 transcription factors in regulating Arabidopsis responses to phosphate starvation. *Front. Plant Sci.* 15, 1379562. doi: 10.3389/fpls.2024.1379562.

Wani, I. A., ul Ashraf, Z., & Muzzaffar, S. (2022). Erucic acid. In Handbook of plant and animal toxins in food (pp. 169-176). CRC Press.

Watts, N., Amann, M., Arnell, N., Ayeb-Karlsson, S., Beagley, J., Belesova, K., et al. (2021). The 2020 report of the lancet countdown on health and climate change: responding to converging crises. *Lancet* 397, 129–170. doi: 10.1016/ S0140-6736(20)32290-X.

Weber, K., & Burow, M. (2018). Nitrogen–essential macronutrient and signal controlling flowering time. *Physiol. Plant.* 162(2), 251-260. doi: 10.1111/ppl.12664.

Wei, L., Zhang, D., Xiang, F., and Zhang, Z. (2009). Differentially expressed miRNAs potentially involved in the regulation of defense mechanism to drought stress in maize seedlings. *Int. J. Plant Sci.* 170, 979–989. doi: 10.1086/605122.

Wei, T., Simko, V., Levy, M., Xie, Y., Jin, Y., Zemla, J., ... & Protivinsky, T. (2021). R package" corrplot": Visualization of a Correlation Matrix (Version Version 0.92).

Wells, C. E., and Eissenstat, D. M. (2002). Beyond the roots of young seedlings: the influence of age and order on fine root physiology. *J. Plant Growth Regul.* 21, 324–334. doi: 10.1007/s00344-003-0011-1.

Welsch, R., Wust, F., Bar, C., Al-Babili, S., & Beyer, P. (2008). A third phytoene synthase is devoted to abiotic stress-induced abscisic acid formation in rice and defines functional diversification of phytoene synthase genes. *Plant Physiol.* 147(1), 367-380. doi: 10.1104/pp.108.117028.

West, G., Inzé, D., & Beemster, G. T. (2004). Cell cycle modulation in the response of the primary root of Arabidopsis to salt stress. *Plant Physiol.* 135(2), 1050-1058. doi: 10.1104/pp.104.040022.

Wirth, J., Chopin, F., Santoni, V., Viennois, G., Tillard, P., Krapp, A., ... & Gojon, A. (2007). Regulation of root nitrate uptake at the NRT2. 1 protein level in Arabidopsis thaliana. *J. Biol. Chem.* 282(32), 23541-23552. doi: 10.1074/jbc.M700901200.

Wissuwa, M., Gamat, G., & Ismail, A. M. (2005). Is root growth under phosphorus deficiency affected by source or sink limitations?. *J. Exp. Bot.* 56(417), 1943-1950. doi: 10.1093/jxb/eri189.

Won, S. K., Lee, Y. J., Lee, H. Y., Heo, Y. K., Cho, M., & Cho, H. T. (2009). Cis-element-and transcriptome-based screening of root hair-specific genes and their functional characterization in Arabidopsis. *Plant Physiol.* 150(3), 1459-1473. doi: 10.1104/pp.109.140905.

Wu, P., Ma, L., Hou, X., Wang, M., Wu, Y., Liu, F., & Deng, X. W. (2003). Phosphate starvation triggers distinct alterations of genome expression in Arabidopsis roots and leaves. *Plant Physiol.* 132(3), 1260-1271. doi: 10.1104/pp.103.021022.

Wu, S., Wang, X., Qin, J., Tian, W., Wang, M., Yue, A., ... & Zhao, J. (2024). Soybean CEP6 Signaling Peptides Positively Regulate Nodulation. *Agronomy* 14(5), 988. doi: 10.3390/agronomy14050988.

Wu, T. Y., Krishnamoorthi, S., Goh, H., Leong, R., Sanson, A. C., & Urano, D. (2020a). Crosstalk between heterotrimeric G protein-coupled signaling pathways and WRKY transcription factors modulating plant responses to suboptimal micronutrient conditions. *J. Exp. Bot.* 71(10), 3227-3239. doi: 10.1093/jxb/eraa108.

Wu, W., Shah, F., Duncan, R. W., & Ma, B. L. (2020b). Grain yield, root growth habit and lodging of eight oilseed rape genotypes in response to a short period of heat stress during flowering. *Agric. For. Meteorol.* 287, 107954. doi: 10.1016/j.agrformet.2020.107954.

Wu, X., Liu, Z., Liu, Y., Wang, E., Zhang, D., Huang, S., ... & Zhang, Y. (2023). SlPHL1 is involved in low phosphate stress promoting anthocyanin biosynthesis by directly upregulation of genes SlF3H, SlF3′ H, and SlLDOX in tomato. *Plant Physiol. Biochem.* 200, 107801. doi: 10.1016/j.plaphy.2023.107801.

Xia, N., Zhang, G., Liu, X. Y., Deng, L., Cai, G. L., Zhang, Y., et al. (2010). Characterization of a novel wheat NAC transcription factor gene involved in defense response against stripe rust pathogen infection and abiotic stresses. *Mol. Biol. Rep.* 37, 3703–3712. doi: 10.1007/s11033-010-0023-4.

Xia, Z., Zhang, S., Wang, Q., Zhang, G., Fu, Y., & Lu, H. (2021). Effects of root zone warming on maize seedling growth and photosynthetic characteristics under different phosphorus levels. *Front. Plant Sci.* 12, 746152. doi: 10.3389/fpls.2021.746152.

Xiao, X., Zhang, J., Satheesh, V., Meng, F., Gao, W., Dong, J., ... & Lei, M. (2022). SHORT-ROOT stabilizes PHOSPHATE1 to regulate phosphate allocation in Arabidopsis. *Nat. Plants* 8(9), 1074-1081. doi: 10.1038/s41477-022-01231-w.

Xu, C., & Huang, B. (2008). Root proteomic responses to heat stress in two Agrostis grass species contrasting in heat tolerance. *J. Exp. Bot.* 59(15), 4183-4194. doi: 10.1093/jxb/ern258.

Xu, M., Zhu, L., Shou, H., & Wu, P. (2005). A PIN1 family gene, OsPIN1, involved in auxin-dependent adventitious root emergence and tillering in rice. *Plant Cell Physiol.* 46(10), 1674-1681. doi: 10.1093/pcp/pci183.

Xu, P., Zhao, P. X., Cai, X. T., Mao, J. L., Miao, Z. Q., & Xiang, C. B. (2020). Integration of jasmonic acid and ethylene into auxin signaling in root development. *Front. Plant Sci.* 11, 271. doi: 10.3389/fpls.2020.00271.

Xu, Y., Burgess, P., & Huang, B. (2015). Root antioxidant mechanisms in relation to root thermotolerance in perennial grass species contrasting in heat tolerance. *PLoS One* 10(9), e0138268. doi: 10.1371/journal.pone.0138268.

Xu, Y., Liu, F., Han, G., & Cheng, B. (2018). Genome-wide identification and comparative analysis of phosphate starvation-responsive transcription factors in maize and three other gramineous plants. *Plant Cell Rep.* 37, 711-726. doi: 10.1007/s00299-018-2262-0.

Xu, Z. S., Ni, Z. Y., Li, Z. Y., Li, L. C., Chen, M., Gao, D. Y., et al. (2009). Isolation and functional characterization of HvDREB1-a gene encoding a dehydrationresponsive element binding protein in *Hordeum vulgare. J. Plant Res*. 122,121–130. doi: 10.1007/s10265-008-01953.

Xuan, W., Beeckman, T., & Xu, G. (2017). Plant nitrogen nutrition: sensing and signaling. *Curr. Opin. Plant Biol.* 39, 57-65. doi: 10.1016/j.pbi.2017.05.010.

Xue, G.-P., Sadat, S., Drenth, J., and McIntyre, C. L. (2014). The heat shock factor family from Triticum aestivum in response to heat and other major abiotic stresses and their role in regulation of heat shock protein genes. *J. Exp. Bot*. 65, 539–557. doi: 10.1093/jxb/ert399.

Xue, Y. B., Xiao, B. X., Zhu, S. N., Mo, X. H., Liang, C. Y., Tian, J., & Liao, H. (2017). GmPHR25, a GmPHR member up-regulated by phosphate starvation, controls phosphate homeostasis in soybean. *J. Exp. Bot.* 68(17), 4951-4967. doi: 10.1093/jxb/erx292.

Yadav, S., & Chattopadhyay, D. (2023). Lignin: the building block of defense responses to stress in plants. *J. Plant Growth Regul.* 42(10), 6652-6666. doi: 10.1007/s00344-023-10926-z.

Yan, Y., Wang, H., Hamera, S., Chen, X., & Fang, R. (2014). miR444a has multiple functions in the rice nitrate-signaling pathway. *Plant J.* 78(1), 44-55. doi: 10.1111/tpj.12446.

Yang, X., Dong, G., Palaniappan, K., Mi, G., & Baskin, T. I. (2017). Temperature-compensated cell production rate and elongation zone length in the root of Arabidopsis thaliana. *Plant Cell Environ*. 40(2), 264-276. doi: 10.1111/pce.12855.

Ye, L., Wang, X., Lyu, M., Siligato, R., Eswaran, G., Vainio, L., ... & Mähönen, A. P. (2021). Cytokinins initiate secondary growth in the Arabidopsis root through a set of LBD genes. *Curr. Biol.* 31(15), 3365-3373. doi: 10.1016/j.cub.2021.05.036.

Ye, X., Hong, J., Shi, L., & Xu, F. (2010). Adaptability mechanism of nitrogen-efficient germplasm of natural variation to low nitrogen stress in *Brassica napus*. *J. Plant Nutr.* 33(13), 2028-2040. doi: 10.1080/01904167.2010.512211.

Yi, K., Menand, B., Bell, E., & Dolan, L. (2010). A basic helix-loop-helix transcription factor controls cell growth and size in root hairs. *Nat. Genet.* 42(3), 264-267. doi: 10.1038/ng.529.

Yi, Z., Li, S., Liang, Y., Zhao, H., Hou, L., Yu, S., & Ahammed, G. J. (2018). Effects of exogenous spermidine and elevated CO 2 on physiological and biochemical changes in tomato plants under iso-osmotic salt stress. *J. Plant Growth Regul.* 37, 1222-1234. doi: 10.1007/s00344-018-9856-1.

Yin, W. A. N. G., Tao, L. I. U., LI, X. K., Tao, R. E. N., CONG, R. H., & LU, J. W. (2015). Nutrient deficiency limits population development, yield formation, and nutrient uptake of direct sown winter oilseed rape. *J. Int. Agric.* 14(4), 670-680. doi: 10.1016/S2095-3119(14)60798-X.

Yin, Y., Borges, G., Sakuta, M., Crozier, A., & Ashihara, H. (2012). Effect of phosphate deficiency on the content and biosynthesis of anthocyanins and the expression of related genes in suspension-cultured grape (Vitis sp.) cells. *Plant Physiol. Biochem.* 55, 77-84. doi: 10.1016/j.plaphy.2012.03.009.

Yokawa, K., Kagenishi, T., Kawano, T., Mancuso, S., & Baluška, F. (2011). Illumination of Arabidopsis roots induces immediate burst of ROS production. *Plant Signaling Behav.* 6(10), 1460-1464. doi: 10.4161/psb.6.10.18165.

Yong, Z., Kotur, Z., & Glass, A. D. (2010). Characterization of an intact two-component high-affinity nitrate transporter from Arabidopsis roots. *Plant J.* 63(5), 739-748. doi: 10.1111/j.1365-313X.2010.04278.x.

Yoo, C. Y., Mano, N., Finkler, A., Weng, H., Day, I. S., Reddy, A. S., ... & Mickelbart, M. V. (2019). A Ca2+/CaM-regulated transcriptional switch modulates stomatal development in response to water deficit. *Sci. Rep.* 9(1), 12282. doi: 10.1038/s41598-019-47529-2.

You, Y., Li, W., Chen, Y., Zhang, Q., & Zhang, K. (2024). Soil carbon and nitrogen accumulation during long-term natural vegetation restoration following agricultural abandonment in Qingling Mountains. *Ecol. Eng.* 201, 107212. doi: 10.1016/j.ecoleng.2024.107212.

Yu, X., Yang, J., Li, X., Liu, X., Sun, C., Wu, F., et al. (2013). Global analysis of cisnatural antisense transcripts and their heat-responsive nat-siRNAs in Brassica rapa. *BMC Plant Biol.* 13:208. doi: 10.1186/1471-2229-13-208

Yu, Z., Qu, X., Lv, B., Li, X., Sui, J., Yu, Q., & Ding, Z. (2024). MAC3A and MAC3B mediate degradation of the transcription factor ERF13 and thus promote lateral root emergence. *Plant Cell* koae047. doi: 10.1093/plcell/koae047.

Yuan, L., Gu, R., Xuan, Y., Smith-Valle, E., Loqué, D., Frommer, W. B., & von Wirén, N. (2013). Allosteric regulation of transport activity by heterotrimerization of Arabidopsis ammonium transporter complexes in vivo. *Plant Cell* 25(3), 974-984. doi: 10.1105/tpc.112.108027.

Yuan, L., Liu, S., Zhu, S., Chen, G., Liu, F., Zou, M., & Wang, C. (2016a). Comparative response of two wucai (Brassica campestris L.) genotypes to heat stress on antioxidative system and cell ultrastructure in root. *Acta Physiol. Plant.* 38, 1-8. doi: 10.1007/s11738-016-2246-z.

Yuan, L., Tang, L., Zhu, S., Hou, J., Chen, G., Liu, F., ... & Wang, C. (2017). Influence of heat stress on leaf morphology and nitrogen–carbohydrate metabolisms in two wucai (Brassica campestris L.) genotypes. *Acta Societatis Botanicorum Poloniae* 86(2). doi: 10.5586/asbp.3554.

Yuan, P., Ding, G. D., Cai, H. M., Jin, K. M., Broadley, M. R., Xu, F. S., & Shi, L. (2016b). A novel Brassica–rhizotron system to unravel the dynamic changes in root system architecture of oilseed rape under phosphorus deficiency. *Ann. Bot.* 118(2), 173-184. doi: 10.1093/aob/mcw083.

Yun, W., Jinping, Z., Yong, S., Jauhar, A., Jianlong, X., and Zhikang, L. (2012). Identification of genetic overlaps for salt and drought tolerance using simple sequence repeat markers on an advanced backcross population in rice. *Crop Sci.* 52, 1583–1592. doi:10.2135/cropsci2011.12.0628.

Zakari, S. A., Asad, M. A. U., Han, Z., Zhao, Q., & Cheng, F. (2020). Relationship of nitrogen deficiency-induced leaf senescence with ROS generation and ABA concentration in rice flag leaves. *J. Plant Growth Regul.* 39, 1503-1517. doi: 10.1007/s00344-020-10128-x.

Zandalinas, S. I., Sengupta, S., Fritschi, F. B., Azad, R. K., Nechushtai, R., and Mittler, R. (2021). The impact of multifactorial stress combination on plant growth and survival. *New Phytol.* 230, 1034–1048. doi: 10.1111/nph.17232.

Zeng, H., Wu, H., Wang, G., Dai, S., Zhu, Q., Chen, H., ... & Du, L. (2022). Arabidopsis CAMTA3/SR1 is involved in drought stress tolerance and ABA signaling. *Plant Sci.* 319, 111250. doi: 10.1016/j.plantsci.2022.111250.

Zhang, C., Li, H., Yuan, C., Liu, S., Li, M., Zhu, J., ... & Guo, X. (2020a). CKB 1 regulates expression of ribosomal protein L10 family gene and plays a role in UV-B response. *Plant Biol.* 22, 143-152. doi: 10.1111/plb.12954.

Zhang, G., Chen, M., Li, L., Xu, Z., Chen, X., Guo, J., et al. (2009). Overexpression of the soybean GmERF3 gene, an AP2/ERF type transcription factor for increased tolerances to salt, drought, and diseases in transgenic tobacco. *J. Exp. Bot.* 60, 3781–3796. doi:10.1093/jxb/erp214.

Zhang, H., He, X., Munyaneza, V., Zhang, G., Ye, X., Wang, C., ... & Ding, G. (2024). Acid phosphatase involved in phosphate homeostasis in Brassica napus and the functional analysis of BnaPAP10s. *Plant Physiol. Biochem.* 208, 108389. doi: 10.1016/j.plaphy.2024.108389.

Zhang, H., Huang, Y., Ye, X., & Xu, F. (2011). Genotypic variation in phosphorus acquisition from sparingly soluble P sources is related to root morphology and root exudates in *Brassica napus*. *Sci. China Life Sci.* 54, 1134-1142. doi: 10.1007/s11427-011-4254-y.

Zhang, H., Yue, M., Zheng, X., Gautam, M., He, S., & Li, L. (2018a). The role of promoter-associated histone acetylation of Haem Oxygenase-1 (HO-1) and Giberellic Acid-Stimulated Like-1 (GSL-1) genes in heat-induced lateral root primordium inhibition in maize. *Front. Plant Sci.* 9, 1520. doi: 10.3389/fpls.2018.01520.

Zhang, H., Zhang, X., & Xiao, J. (2023a). Epigenetic regulation of nitrogen signaling and adaptation in plants. *Plants* 12(14), 2725. doi: 10.3390/plants12142725.

Zhang, J. C., Wang, X. N., Sun, W., Wang, X. F., Tong, X. S., Ji, X. L., ... & Hao, Y. J. (2020b). Phosphate regulates malate/citrate-mediated iron uptake and transport in apple. *Plant Sci.* 297, 110526. doi: 10.1016/j.plantsci.2020.110526.

Zhang, J., Yuan, H., Yang, Y., Fish, T., Lyi, S. M., Thannhauser, T. W., ... & Li, L. (2016). Plastid ribosomal protein S5 is involved in photosynthesis, plant development, and cold stress tolerance in Arabidopsis. *J. Exp. Bot.* 67(9), 2731-2744. doi: 10.1093/jxb/erw106.

Zhang, J., Zhao, P., Chen, S., Sun, L., Mao, J., Tan, S., & Xiang, C. (2023b). The ABI3-ERF1 module mediates ABA-auxin crosstalk to regulate lateral root emergence. *Cell Rep.* 42(7). doi: 10.1016/j.celrep.2023.112809.

Zhang, L., Chen, B., Zhang, G., Li, J., Wang, Y., Meng, Y., & Zhou, Z. (2013a). Effect of soil salinity, soil drought, and their combined action on the biochemical characteristics of cotton roots. *Acta Physiol. Plant.* 35, 3167-3179. doi: 10.1007/s11738-013-1350-6.

Zhang, N. N., Zou, H., Lin, X. Y., Pan, Q., Zhang, W. Q., Zhang, J. H., ... & Chen, J. (2020c). Hydrogen sulfide and rhizobia synergistically regulate nitrogen (N) assimilation and remobilization during N deficiency-induced senescence in soybean. *Plant Cell Environ.* 43(5), 1130-1147. doi: 10.1111/pce.13736.

Zhang, R., Xu, C., Bao, Z., Xiao, R., Chen, X., Xiao, W., et al. (2021). Auxin alters sodium ion accumulation and nutrient accumulation by playing protective role in salinity challenged strawberry. *Plant Physiol. Biochem*. 164, 1–9. doi: 10.1016/j.plaphy.2021.04.008.

Zhang, W., Swarup, R., Bennett, M., Schaller, G. E., & Kieber, J. J. (2013b). Cytokinin induces cell division in the quiescent center of the Arabidopsis root apical meristem. *Curr. Biol.* 23(20), 1979-1989. doi: 10.1016/j.cub.2013.08.008.

Zhang, X., Cui, Y., Yu, M., Su, B., Gong, W., Balu¡ ka, F. E., ... & Lin, J. (2019). Phosphorylation-mediated dynamics of nitrate transceptor NRT1. 1 regulate auxin flux and nitrate signaling in lateral root growth. *Plant Physiol.* 181(2), 480-498. doi: 10.1104/pp.19.00346.

Zhang, Y., Liu, Q., & Rempel, C. (2018b). Processing and characteristics of canola protein-based biodegradable packaging: A review. *Critical Reviews in Food Science and Nutrition* 58(3), 475-485. doi: 10.1080/10408398.2016.1193463.

Zhao, C., Liu, B., Piao, S., Wang, X., Lobell, D. B., Huang, Y., et al. (2017). Temperature increase reduces global yields of major crops in four independent estimates. *Proc. Natl. Acad. Sci.* U.S.A 114, 9326–9331. doi: 10.1073/pnas.1701762114.

Zhao, L., Liu, F., Xu, W., Di, C., Zhou, S., Xue, Y., ... & Su, Z. (2009). Increased expression of OsSPX1 enhances cold/subfreezing tolerance in tobacco and Arabidopsis thaliana. *Plant Biotechnol. J.* 7(6), 550-561. doi: 10.1111/j.1467-7652.2009.00423.x.

Zhao, M., Ding, H., Zhu, J. K., Zhang, F., & Li, W. X. (2011). Involvement of miR169 in the nitrogen-starvation responses in Arabidopsis. *New Phytol.* 190(4), 906-915. doi: 10.1111/j.1469-8137.2011.03647.x.

Zhao, Q., Nakashima, J., Chen, F., Yin, Y., Fu, C., Yun, J., ... & Dixon, R. A. (2013). Laccase is necessary and nonredundant with peroxidase for lignin polymerization during vascular development in Arabidopsis. *Plant Cell* 25(10), 3976-3987. doi: 10.1105/tpc.113.117770.

Zhao, Y., Miao, J., He, J., Tian, X., Gao, K., Ma, C., ... & Liu, W. (2022). Wheat heat shock factor TaHsfA2d contributes to plant responses to phosphate deficiency. *Plant Physiol. Biochem.* 185, 178-187. doi: 10.1016/j.plaphy.2022.05.035.

Zheng, D., Han, X., An, Y. I., Guo, H., Xia, X., & Yin, W. (2013). The nitrate transporter NRT2. 1 functions in the ethylene response to nitrate deficiency in A rabidopsis. *Plant Cell Environ.* 36(7), 1328-1337. doi: 10.1111/pce.12062.

Zheng, M., Zheng, H., Wu, Y., Xiao, Y., Du, Y., Xu, W., ... & Ouyang, Z. (2015). Changes in nitrogen budget and potential risk to the environment over 20 years (1990–2010) in the agroecosystems of the Haihe Basin, China. *J. Environ. Sci.* 28, 195-202. doi: 10.1016/j.jes.2014.05.053.

Zheng, Q., & Liu, K. (2022). Worldwide rapeseed (*Brassica napus* L.) research: A bibliometric analysis during 2011–2021. *Oil Crop Sci.* 7(4), 157-165. doi: 10.1016/j.ocsci.2022.11.004.

Zheng-jun, S. H. I., Xiao-lin, F. A. N., & D KLAUS, B. S. (2005). Effect of localized nitrogen supply on root morphology in rice and its mechanism. *Chinese Journal OF Rice Science*, 19(2), 147.

Zhong, Y., Wang, Y., Guo, J., Zhu, X., Shi, J., He, Q., ... & Mao, C. (2018). Rice SPX6 negatively regulates the phosphate starvation response through suppression of the transcription factor PHR2. *New Phytol.* 219(1), 135-148. doi: 10.1111/nph.15155.

Zhou, J., Hu, Q., Xiao, X., Yao, D., Ge, S., Ye, J., ... & Xing, W. (2021). Mechanism of phosphate sensing and signaling revealed by rice SPX1-PHR2 complex structure. *Nat. Commun.* 12(1), 7040. doi: 10.1038/s41467-021-27391-5.

Zhou, J., Jiao, F., Wu, Z., Li, Y., Wang, X., He, X., ... & Wu, P. (2008). OsPHR2 is involved in phosphate-starvation signaling and excessive phosphate accumulation in shoots of plants. *Plant Physiol.* 146(4), 1673-1686. doi: 10.1104/pp.107.111443.

Zhou, X., He, F., Liu, F., Zheng, X., Di, C., Zhou, S., ... & Su, Z. (2007). Integration of cold signal transduction pathway related to ABA 8'-hydroxylase in Arabidopsis. In Biotechnology and Sustainable Agriculture 2006 and Beyond: Proceedings of the 11th IAPTC&B Congress, August 31-18, 2006 Beijing, China (pp. 471-474). *Springer Netherlands*. doi: 10.1007/978-1-4020-6635-1_78.

Zhu, B., Ye, C., Lu, H., Chen, X., Chai, G., Chen, J., et al. (2006). Identification and characterization of a novel heat shock transcription factor gene, *GmHsfA1*, in soybeans (*Glycine max*). *J. Plant Res*. 119, 247–256. doi: 10.1007/s10265-006-0267-1.

Zhu, J. K. (2016). Abiotic stress signaling and responses in plants. *Cell* 167(2), 313-324. doi: 10.1016/j.cell.2016.08.029.

Zhu, J., Zhang, K. X., Wang, W. S., Gong, W., Liu, W. C., Chen, H. G., ... & Lu, Y. T. (2015). Low temperature inhibits root growth by reducing auxin accumulation via ARR1/12. *Plant Cell Physiol.* 56(4), 727-736. doi: 10.1093/pcp/pcu217.

Zhu, L., Liu, L., Sun, H., Zhang, Y., Liu, X., Wang, N., ... & Li, C. (2022). The responses of lateral roots and root hairs to nitrogen stress in cotton based on daily root measurements. *J. Agron. Crop Sci.* 208(1), 89-105. doi: 10.1111/jac.12525.

Zhu, X., Wang, P., Bai, Z., Herde, M., Ma, Y., Li, N., ... & Yang, Z. B. (2022). Calmodulin-like protein CML24 interacts with CAMTA2 and WRKY46 to regulate ALMT1-dependent Al resistance in Arabidopsis thaliana. *New Phytol.* 233(6), 2471-2487. doi: 10.1111/nph.17812.

Zhu, Y., Zhong, L., Huang, X., Su, W., Liu, H., Sun, G., ... & Chen, R. (2023). BcAMT1; 5 mediates nitrogen uptake and assimilation in flowering Chinese cabbage and improves plant growth when overexpressed in Arabidopsis. *Horticulturae*, 9(1), 43. doi: 10.3390/horticulturae9010043.

Zhuo, M., Sakuraba, Y., & Yanagisawa, S. (2024). Dof1. 7 and NIGT1 transcription factors mediate multilayered transcriptional regulation for different expression patterns of nitrate transporter2 genes under nitrogen deficiency stress. *New Phytol.* 242(5), 2132-2147. doi: 10.1111/nph.19695.

Zong, W., Yang, J., Fu, J., and Xiong, L. (2020). Synergistic regulation of drought responsive genes by transcription factor OsbZIP23 and histone modification in rice. *J. Int. Plant Biol.* 62, 723–729. doi: 10.1111/jipb.12850.

# Annex A – Supplementary Figures

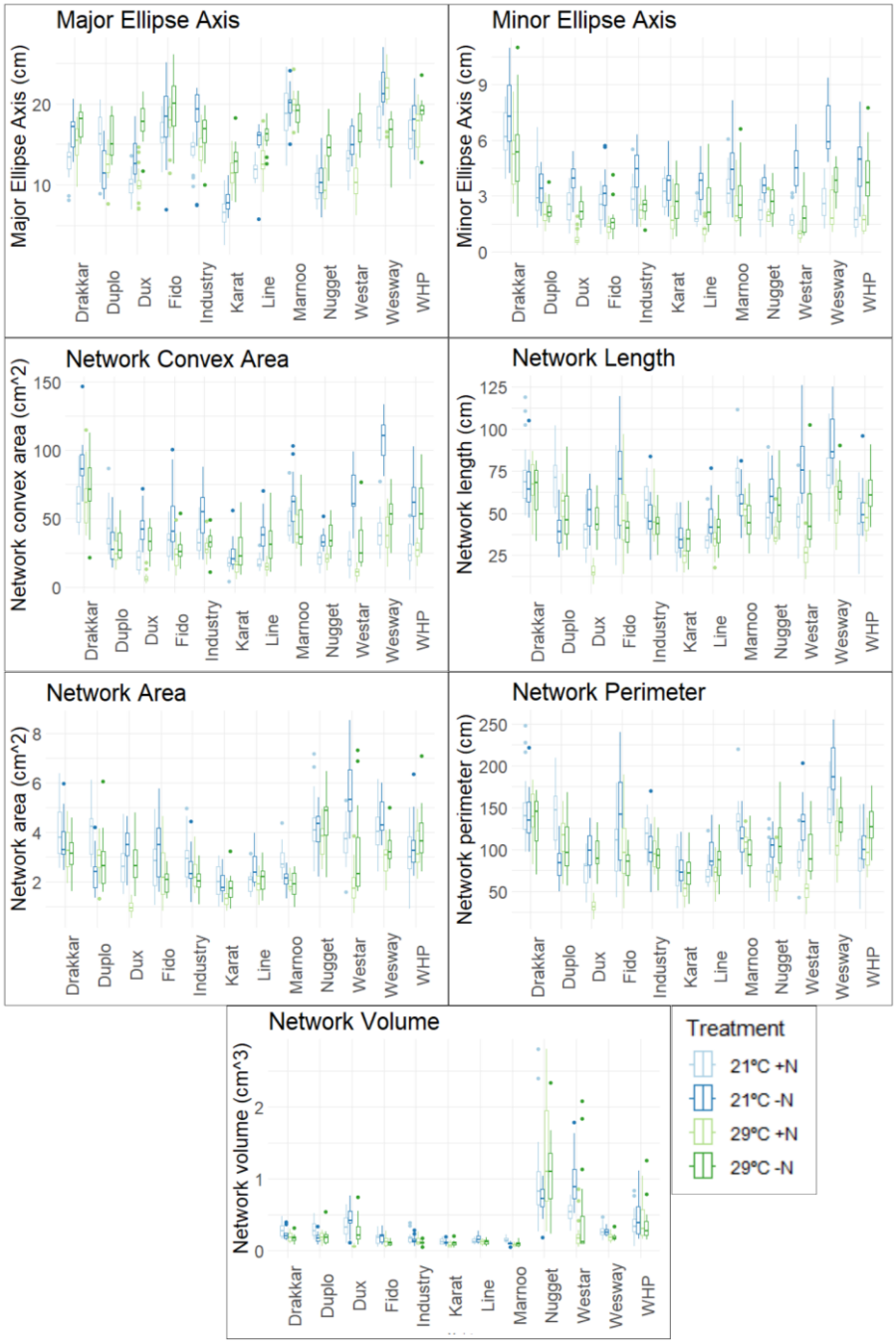


Supplementary Figure 1: Boxplots showing the distribution of the values from different root traits across *B. napus* individuals submitted to different temperature and N treatments. The X-axis indicates the different varieties. The legend shows the different temperature and N treatments: 21°C+N (21°C and optimal nitrogen), 21°C-N (21°C and nitrogen deficiency), 29°C+N (29°C and optimal nitrogen) and 29°C-N (29°C and nitrogen deficiency).

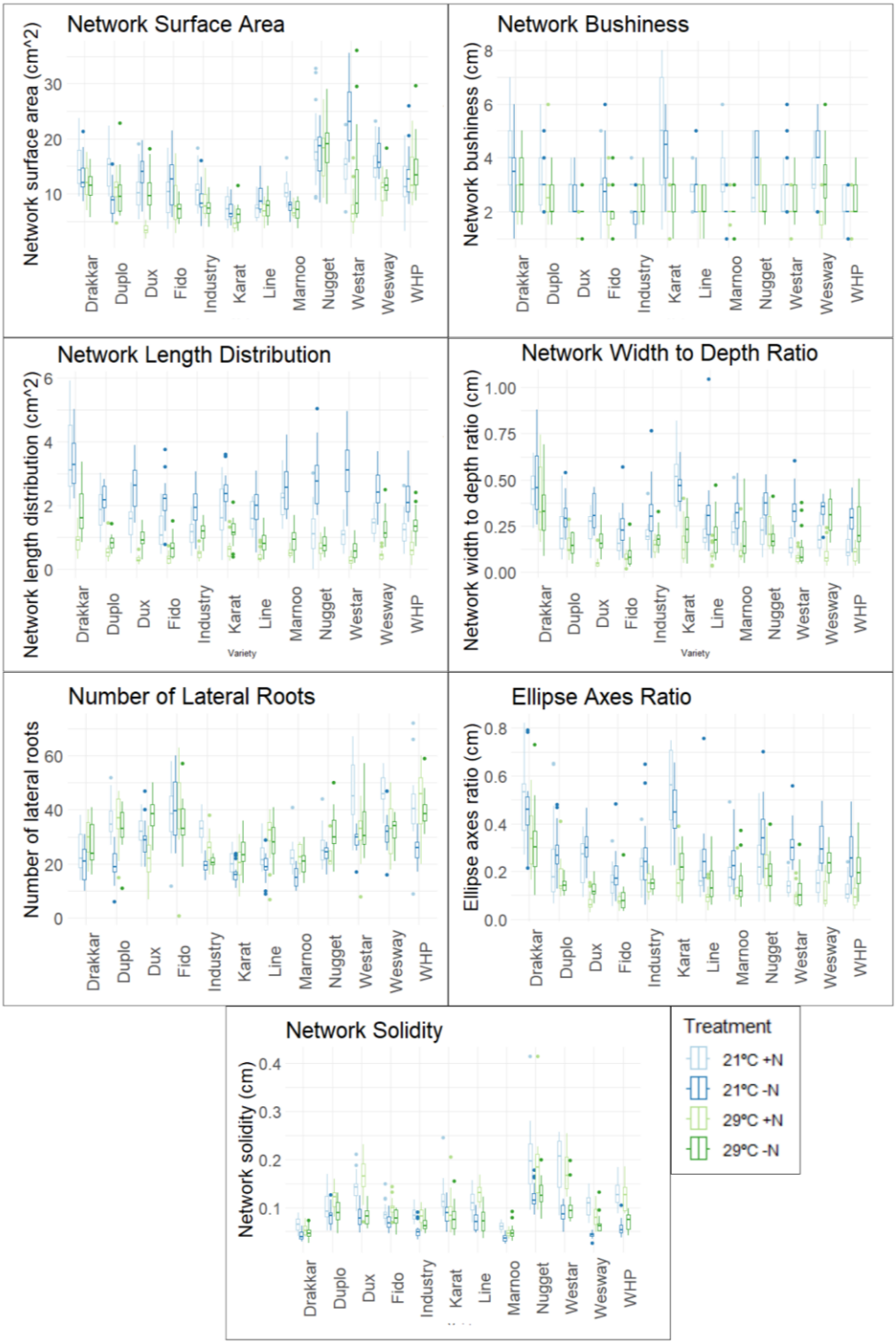


Supplementary Figure 2: Boxplots showing the distribution of the values from different root traits across *B. napus* individuals submitted to different temperature and N treatments. The X-axis indicates the different cultivars. The legend shows the different temperature and N treatments: 21ºC+N (21ºC and optimal nitrogen), 21ºC-N (21ºC and nitrogen deficiency), 29ºC+N (29ºC and optimal nitrogen) and 29ºC-N (29ºC and nitrogen deficiency).

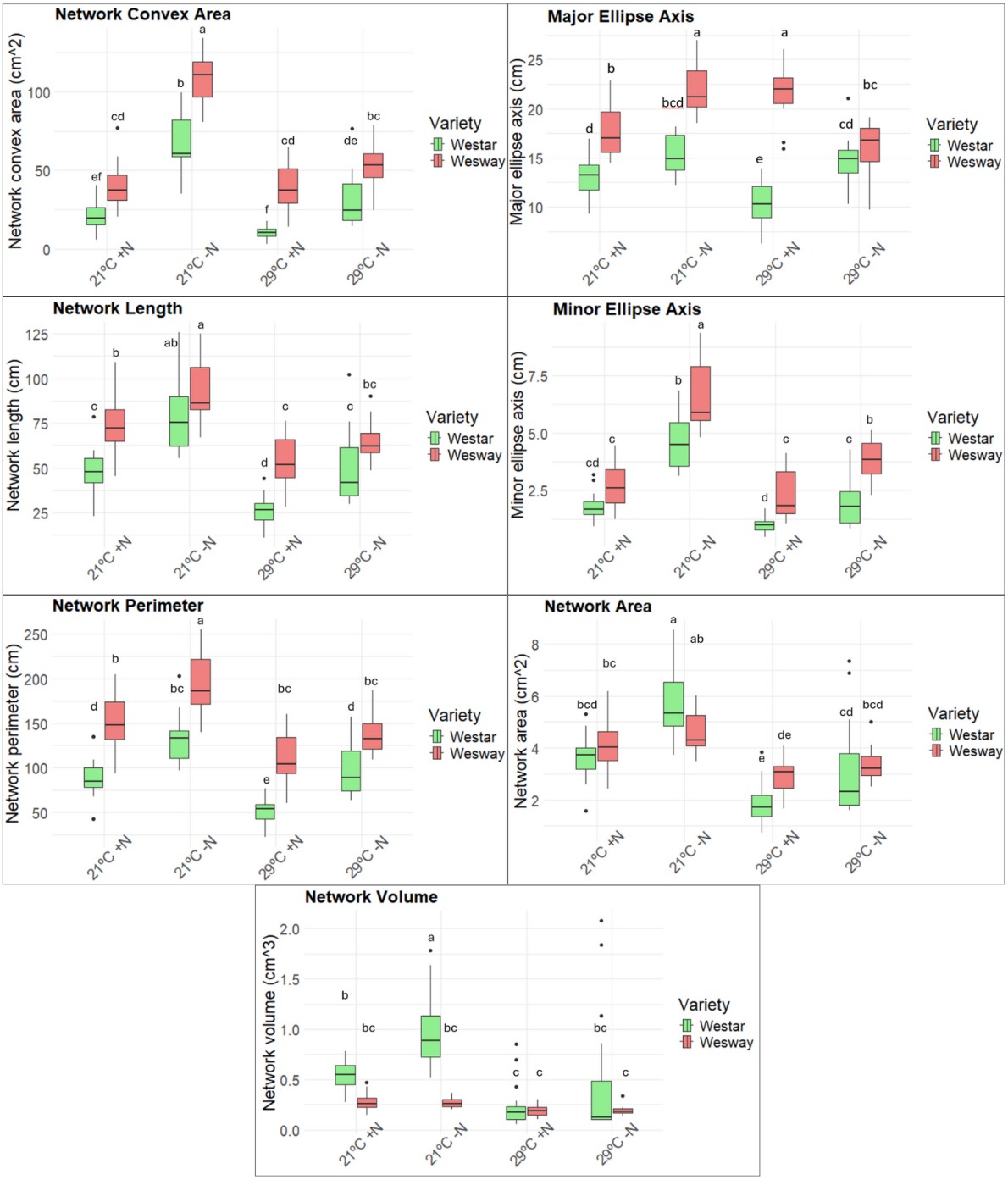


Supplementary Figure 3: Boxplots representing the distribution of the values from different root traits across *B. napus* individuals from the varieties Westar (green) and Wesway (red) submitted to different temperature and nitrogen treatments. X-axis indicates the different treatments: 21ºC+N (21ºC and optimal nitrogen), 21ºC-N (21ºC and nitrogen deficiency), 29ºC+N (29ºC and optimal nitrogen) and 29ºC-N (29ºC and nitrogen deficiency). Error bars represent the standard deviation between 20 independent seedlings. Letters indicate significant differences between groups (p-value < 0.05). Groups that are significantly different do not share any letter.

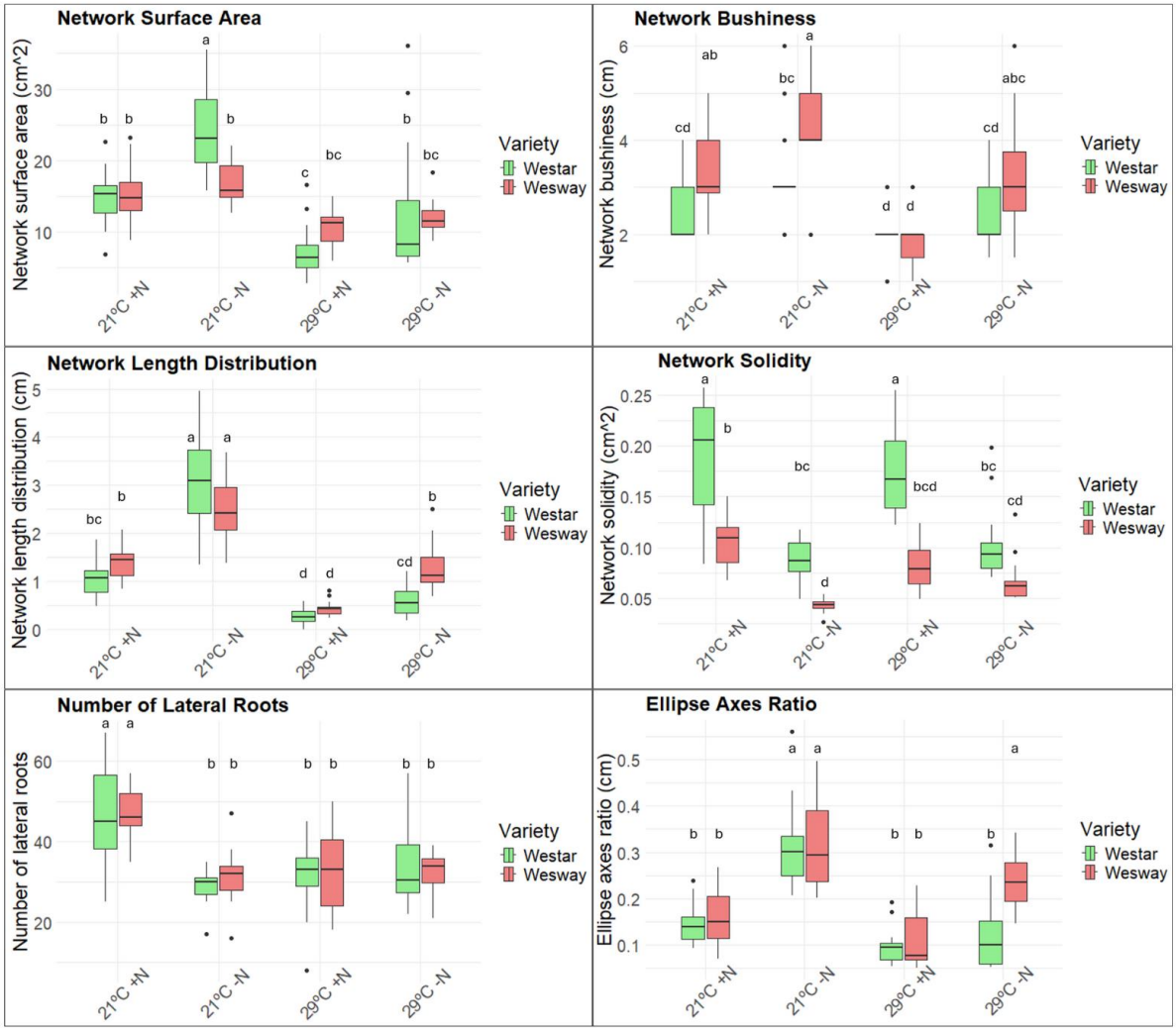


Supplementary Figure 4: Boxplots representing the distribution of the values from different root traits across *B. napus* individuals from the varieties Westar (green) and Wesway (red) submitted to different temperature and nitrogen treatments. X-axis indicates the different treatments: 21ºC+N (21ºC and optimal nitrogen), 21ºC-N (21ºC and nitrogen deficiency), 29ºC+N (29ºC and optimal nitrogen) and 29ºC-N (29ºC and nitrogen deficiency). Error bars represent the standard deviation between 20 independent seedlings. Letters indicate significant differences between groups (p-value < 0.05). Groups that are significantly different do not share any letter.

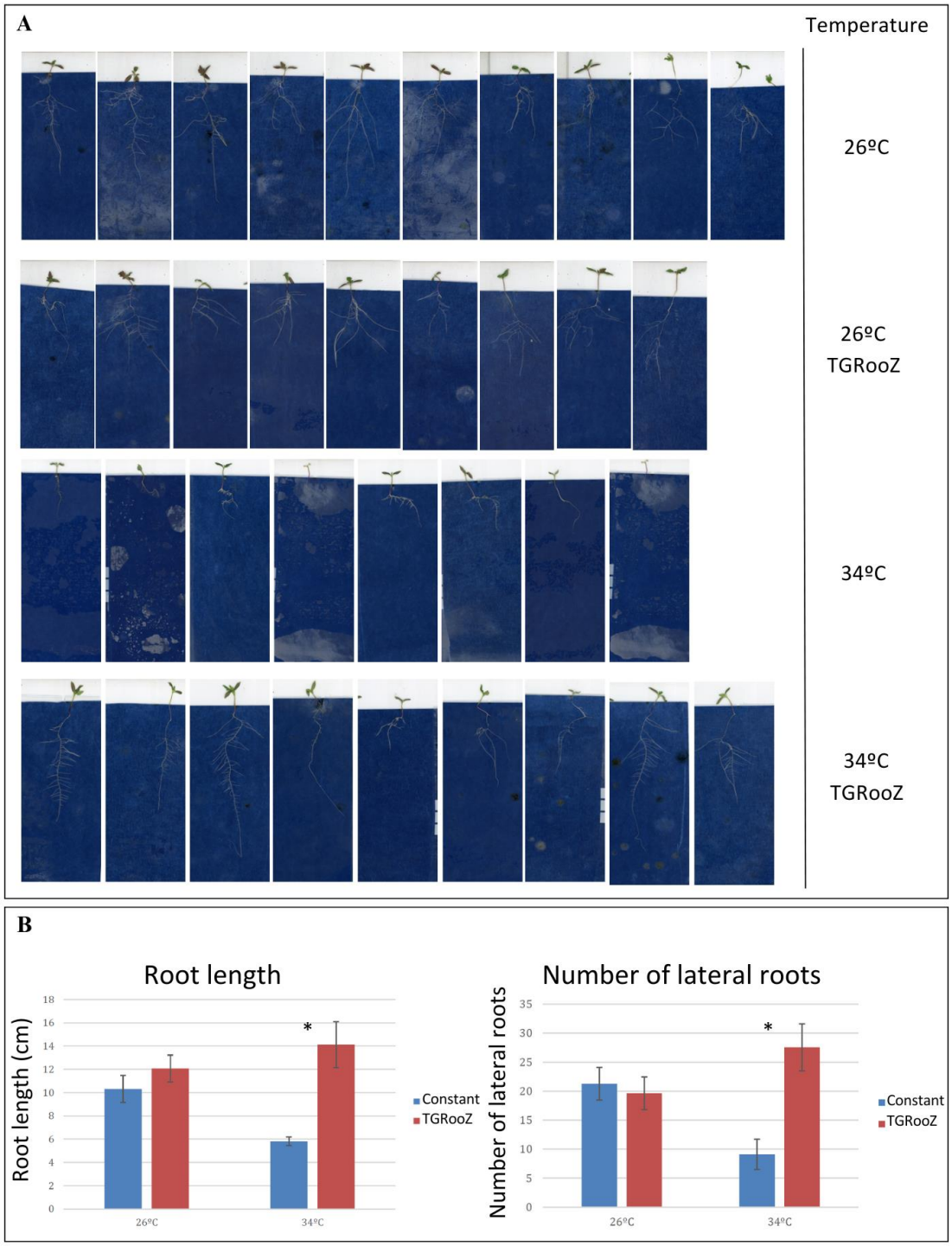


Supplementary Figure 5: 7-day old tomato seedlings (variety Moneymaker) grown in germination paper with the roots in the dark and submitted to two different temperature treatments (26ºC and 34ºC) and grown either on the TGRooZ system (TGRooZ) or in a chamber with a constant root temperature (Constant). A) Images of the root system of tomato seedlings submitted to the different treatments after 7 days. B) Measurements of the primary root length (left) and the number of lateral roots (right). X-axis shows the different temperatures. The color legend indicates whether the invididuals were grown at a constant root temperature or in the TGRooZ system. Asterisks indicate significant differences between groups (p-value < 0.05).

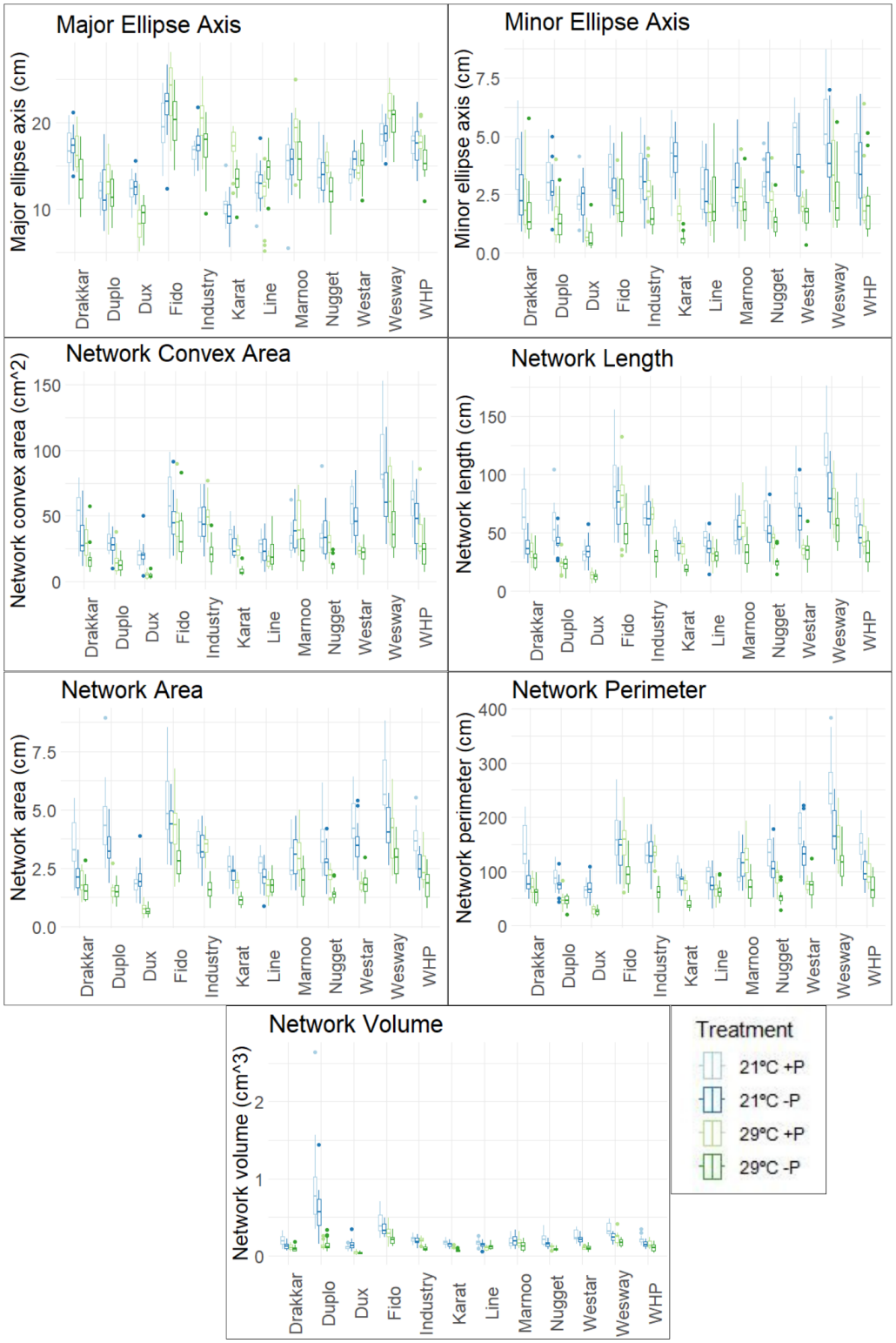


Supplementary Figure 6: Boxplots showing the distribution of the values from different root traits across *B. napus* individuals submitted to different temperature and Pi treatments. The X-axis indicates the different cultivars. The legend shows the different temperature and Pi treatments: 21ºC+P, 21ºC-P, 29ºC+P and 29ºC-P.

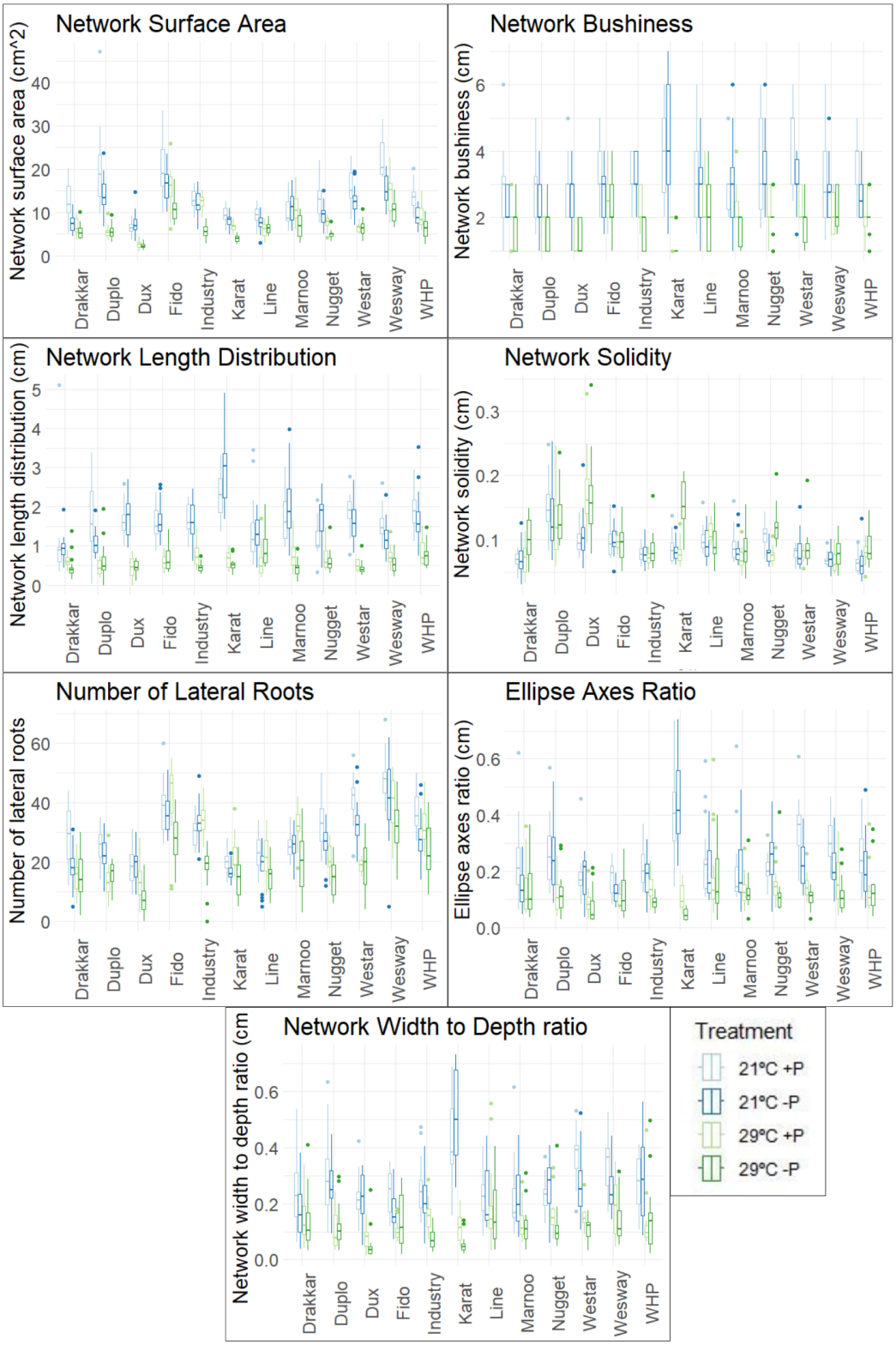


Supplementary Figure 7: Boxplots showing the distribution of the values from different root traits across *B. napus* individuals submitted to different temperature and Pi treatments. The X-axis indicates the different cultivars. The legend shows the different temperature and Pi treatments: 21ºC+P, 21ºC-P, 29ºC+P and 29ºC-P.

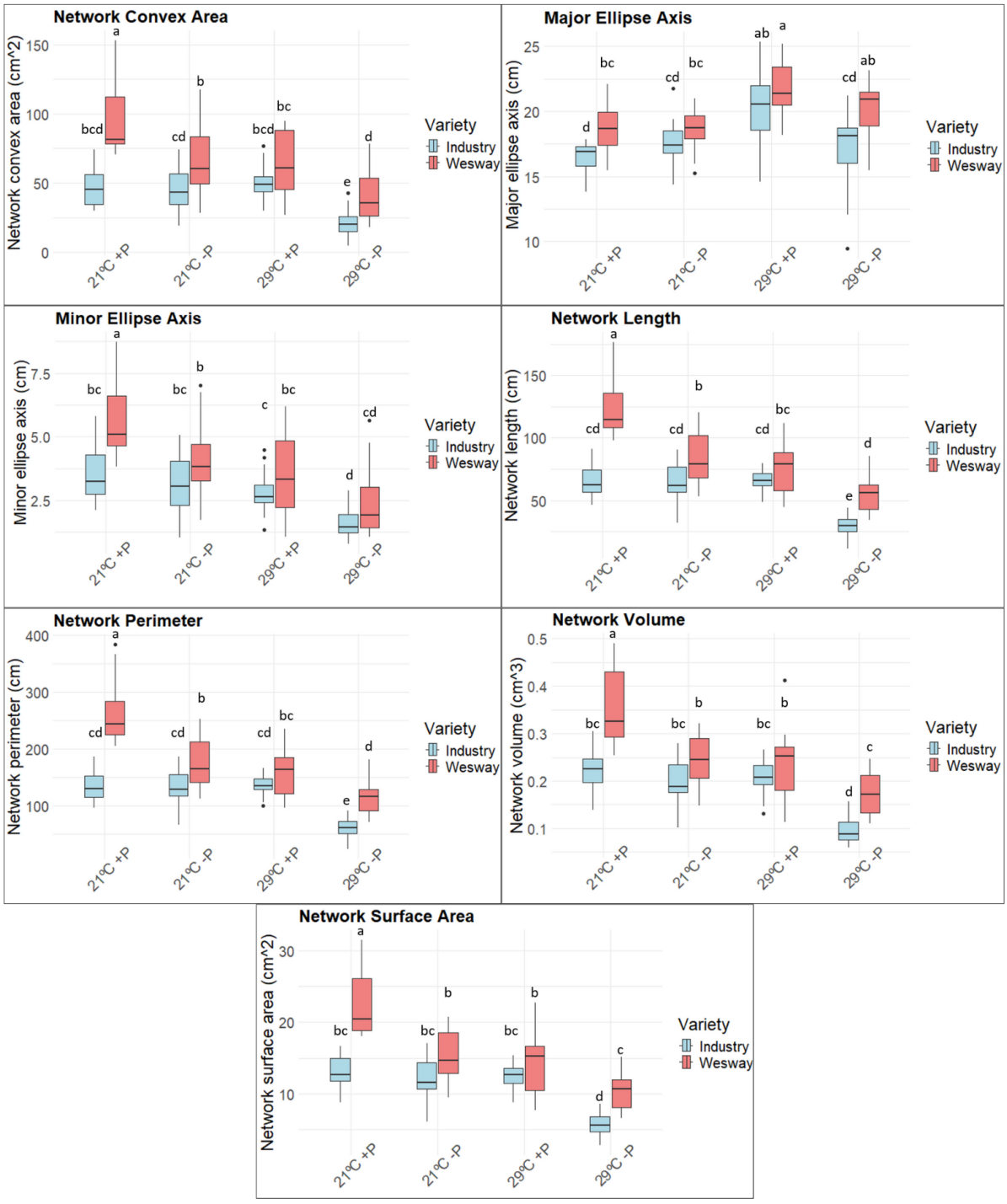


Supplementary Figure 8: Boxplots representing the distribution of the values from different root traits across *B. napus* individuals from the varieties Industry (blue) and Wesway (red) submitted to different temperature and nitrogen treatments. X-axis indicates the different treatments: 21ºC+P, 21ºC-P, 29ºC+P and 29ºC-P. Error bars represent the standard deviation between 20 independent seedlings. Letters indicate significant differences between groups (p-value < 0.05). Groups that are significantly different from each other do not share any letter.

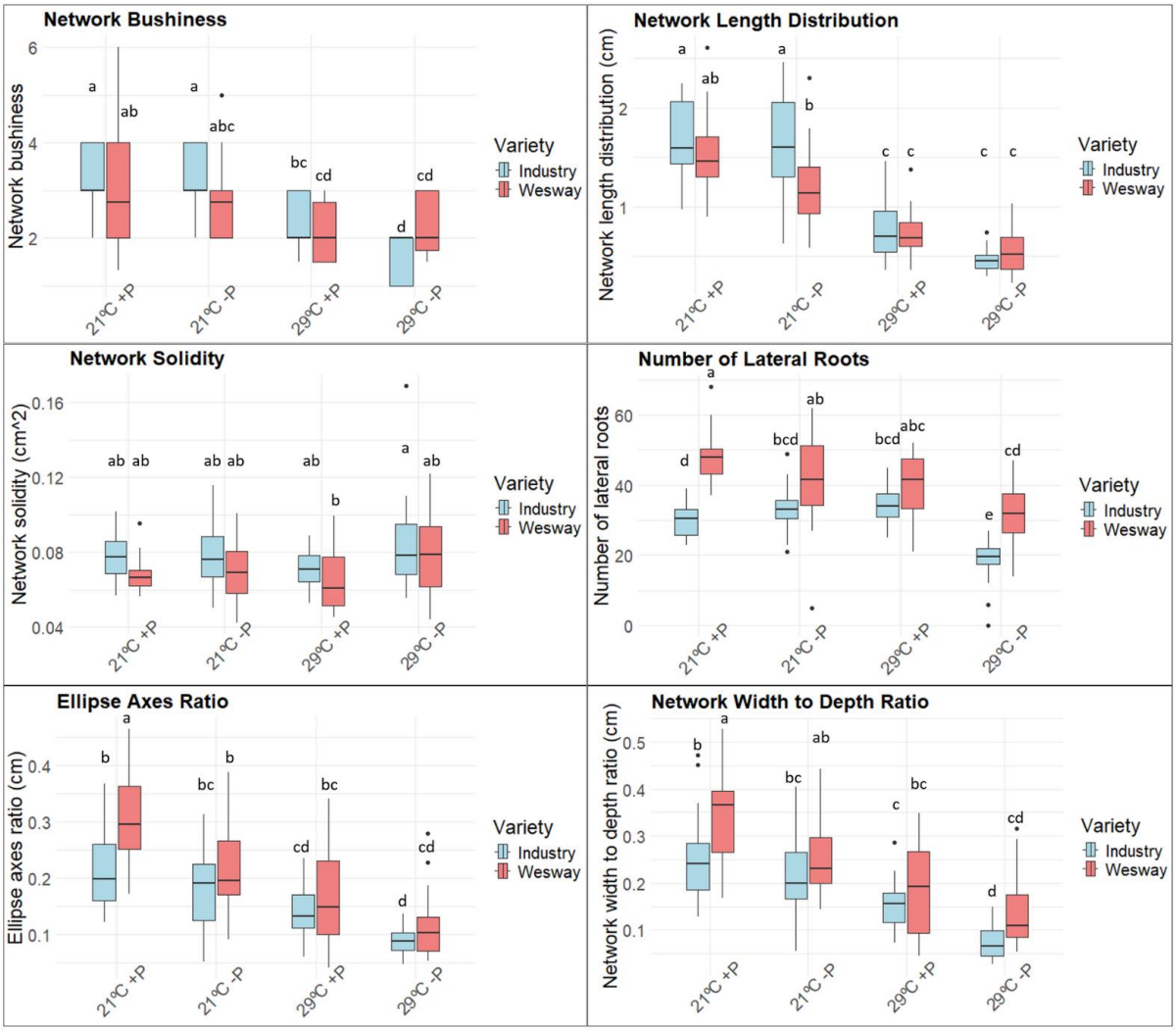


Supplementary Figure 9: Boxplots representing the distribution of the values from different root traits across *B. napus* individuals from the varieties Industry (blue) and Wesway (red) submitted to different temperature and nitrogen treatments. X-axis indicates the different treatments: 21°C+P, 21°C-P, 29°C+P and 29°C-P. Error bars represent the standard deviation between 20 independent seedlings. Letters indicate significant differences between groups (p-value < 0.05). Groups that are significantly different from each other do not share any letter.

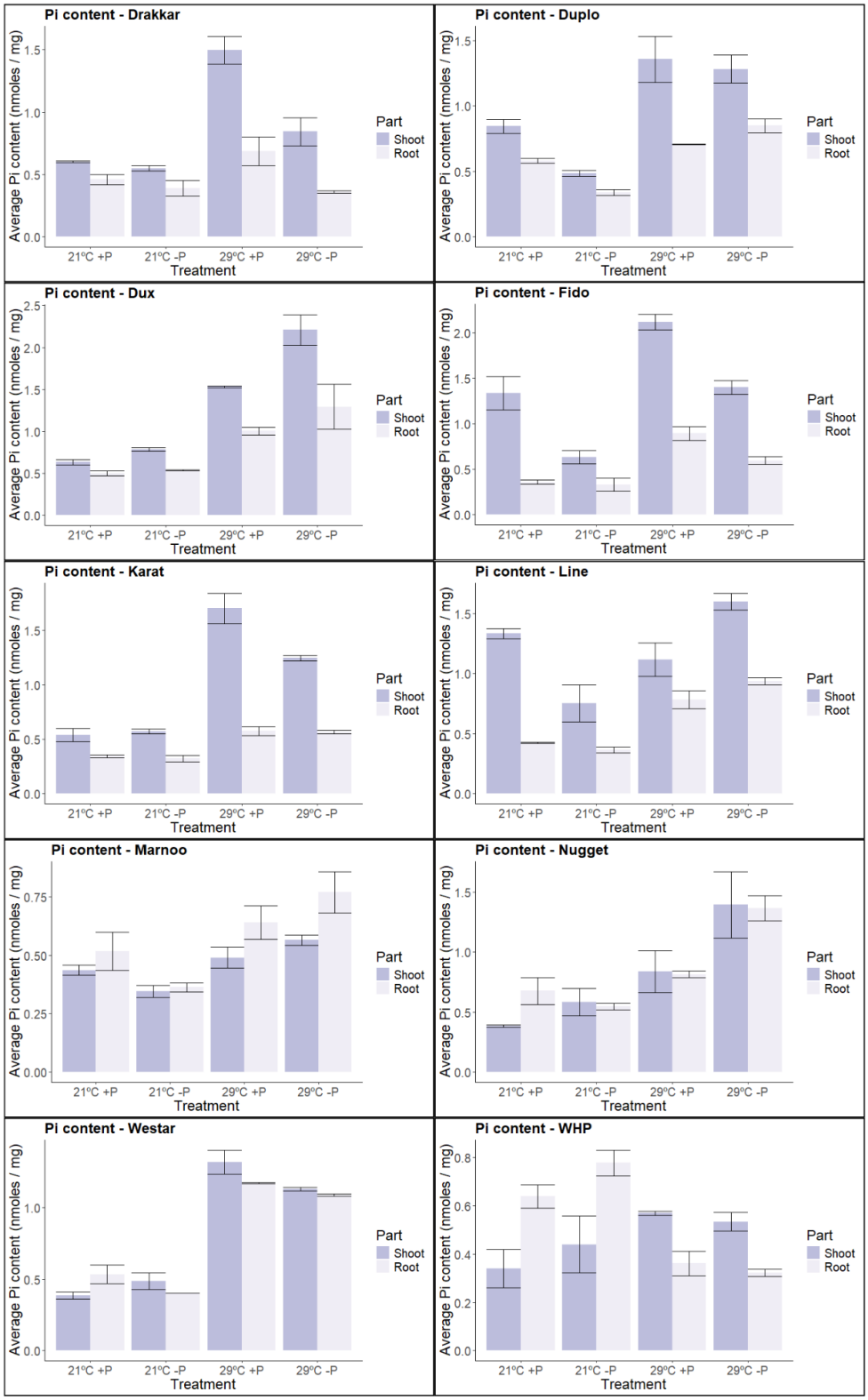


Supplementary Figure 10: Phosphate (Pi) content in whole roots and shoots of different *B. napus* varieties grown under different temperature and phosphate treatments. Y-axis indicates the average Pi content (nmol / mg). X-axis shows the different treatments: 21ºC+P, 21ºC-P, 29ºC+P or 29ºC-P. The colour legend indicates the sample type: either root or shoot. Error bars represent the standard deviation between two biological replicates and three technical replicates each.

# Annex B – Supplementary Tables

- Supplementary Table 1: A) List of *B. napus* varieties with their respective genotype code, name, type of germplasm and country of origin. B) List of the different root traits measured. The list includes all traits with their respective categories, the abbreviation used for the grahps and analyses, a description of each trait as described in the GiaRoots manual, and a graphical representation of each trait.
- Supplementary Table 2: A) Table depicting the values of all the individual measurements of different root traits in 7-day old *B. napus* seedlings from 12 different varieties, grown under different temperature and/or nitrogen conditions. B) Table depicting the values of the average, standard deviation and number of samples (count) for each trait measured in 7-day old *B. napus* individuals from 12 varieties grown under different temperature and/or nitrogen conditions.
- Supplementary Table 3: Principal component analysis (PCA) of root traits from *B. napus* individuals grown under different temperature and/or nitrogen conditions. A) Table with the correlation coefficients between all the variables. Correlation coefficients were calculated using the Pearson correlation method. B) Contribution of each variable to the main 5 principal components. The contribution values are provided as a percentage. C) Cos2 values for all the variables in the main 5 principal components.
- Supplementary Table 4: A) List of the DEGs in roots of *B. napus* individuals from two varieties (Westar and Wesway) and grown under four different temperature and/or nitrogen treatments (21ºC +N, 21ºC -N, 29ºC +N and 29ºC -N). B) Gene Ontology (GO) analysis of DEGs in roots of *B. napus* individuals from two varieties (Westar and Wesway) and grown under four different temperature and/or nitrogen treatments (21ºC +N, 21ºC -N, 29ºC +N and 29ºC -N).
- Supplementary Table 5: A) Table depicting the values from all the individual measurements of different root traits in 7-day old *B. napus* seedlings from 12 different varieties, grown under different temperature and/or phosphate (Pi) conditions. B) Table depicting the values for the average, standard deviation

and number of samples (count) for each trait measured in 7-day old *B. napus* individuals from 12 varieties grown under different temperature and/or phosphate (Pi) conditions.

- Supplementary Table 6: Principal component analysis (PCA) of root traits from *B. napus* individuals grown under different temperature and/or phosphate conditions. A) Table with the correlation coefficients between all the variables. Correlation coefficients were calculated using the Pearson correlation method. B) Contribution of each variable to the main 5 principal components. The contribution values are provided as a percentage. C) Cos2 values for all the variables in the main 5 principal components.
- Supplementary Table 7: Genomic information on the MYB-CC protein members identified in *B. napus*. The table displays the number of exons in each gene, as well as the coding sequence start and end positions for each exon, and the length of the coding sequence.
- Supplementary Table 8: A) List of the DEGs in roots of *B. napus* individuals from two varieties (Industry and Wesway) and grown under four different temperature and/or Pi treatments (21ºC +P, 21ºC -P, 29ºC +P and 29ºC -P). B) Gene Ontology (GO) analysis of DEGs in roots of *B. napus* individuals from two varieties (Industry and Wesway) grown under four different temperature and/or Pi treatments (21ºC +P, 21ºC -P, 29ºC +P and 29ºC -P).
- Supplementary Table 9: A) List of the DEGs in shoots of *B. napus* individuals from two varieties (Westar and Wesway) and grown under four different temperature and/or N treatments (21ºC +N, 21ºC -N, 29ºC +N and 29ºC -N). B) Gene Ontology (GO) analysis of DEGs in shoots of *B. napus* individuals from two varieties (Westar and Wesway) grown under four different temperature and/or N treatments (21ºC +N, 21ºC -N, 29ºC +N and 29ºC -N).
- Supplementary Table 10: A) List of the DEGs in shoots of *B. napus* individuals from two varieties (Industry and Wesway) and grown under four different temperature and/or Pi treatments (21ºC +P, 21ºC -P, 29ºC +P and 29ºC -P). B) Gene Ontology (GO) analysis of DEGs in shoots of *B. napus* individuals from two varieties (Industry and Wesway) grown under four different temperature and/or Pi treatments (21ºC +P, 21ºC -P, 29ºC +P and 29ºC -P).

All supplementary tables can be found in the external storage unit that is attached to this manuscript.